



ARMY TM 5-1300
NAVY NAVFAC P-397
AIR FORCE AFR 88-22

STRUCTURES TO RESIST **THE EFFECTS OF ACCIDENTAL** **EXPLOSIONS**

"Approved for public release; distribution is unlimited"

DEPARTMENTS OF THE ARMY, THE NAVY, AND THE AIR FORCE
NOVEMBER 1990

FOREWORD

**"STRUCTURES TO RESIST THE EFFECTS OF ACCIDENTAL EXPLOSIONS"
Revision 1**

Revision 1 is a significant change to this tri-Service manual. It supersedes Change 1 of 17 March 1971 and provides design criteria for a wide assortment of construction materials. Blast resistant capacities of selected, pre-engineered facilities and suppressive shields are now formally recognized. Significant changes are made in design criteria for stirrups. Single leg stirrups with 135 degree bends are permitted for rotations up to eight degrees for Category 2 protection. Membrane stresses are recognized for the reserve strength they provide as dynamic rotations increase. Capacities and design procedures for blast resistant windows are addressed.

Many individuals contributed to this manual and all such contributions are appreciated. Contributions from Mr. Norval Dobbs, Dr. Wilfred Baker and Dr. Thomas Zaker are particularly worthy of note.

Design procedures in this manual are recognized by DOD 6055.9-STD, "Ammunition and Explosives Safety Standards" and are intended for use in the design and analysis of protective constructions intended to control the effects of accidental explosions. The design procedures provide a basis for quantitative protection against propagation of explosions, damage to facilities, and loss of life. Nevertheless, in a work of this magnitude it is expected that there may be points which require further verification or modification as a result of future tests and experience. Recommendations for change or comments with regard to the usefulness of the manual may be submitted to:

Chairman
Department of Defense Explosives Safety Board
2461 Eisenhower Avenue
Room 856C, Hoffman Building #1
Alexandria, VA 22331-0600

REPRODUCTION AUTHORIZATION/RESTRICTIONS

This manual has been prepared by or for the Government and, except to the extent indicated below, is public property and not subject to copyright.

Reprints or republications of this manual should include a credit substantially as follows: "Joint Departments of the Army, the Navy, and the Air Force, Structures to Resist the Effects of Accidental Explosions, TM 5-1300/NAVFAC P-397/AFR 88-22."

If the reprint or republication contains copyrighted material, the credit should also state: "Anyone wishing to make further use of copyrighted material, by itself and apart from this text, should seek necessary permission directly from the proprietors."

ARMY MANUAL
No. 5-1300
NAVY MANUAL
No. NAVFAC P-397
AIR FORCE REGULATION
No. 88-22

HEADQUARTERS
DEPARTMENTS OF THE ARMY, THE
NAVY, AND THE AIR FORCE
WASHINGTON, DC, 19 NOVEMBER 1990

STRUCTURES TO RESIST THE EFFECTS OF ACCIDENTAL EXPLOSIONS

CHAPTER 1. INTRODUCTION

SECTION	PAGE
1-1 Purpose	1-1
1-2 Objective	1-1
1-3 Background	1-1
1-4 Scope	1-2
1-5 Format	1-3
1-6 General	1-4
1-7 Safety Factor	1-4
1-8 System Components	1-4
1-8.1 General	1-4
1-8.2 Donor System	1-4
1-8.3 Acceptor System	1-6
1-9 Protection Categories	1-8
1-10 Protective Systems	1-9
1-10.1 Protective Structures	1-9
1-10.2 Containment Type Structures	1-10
1-10.3 Shelters	1-11
1-10.4 Barriers	1-11
1-11 Human Tolerance	1-11
1-11.1 Blast Pressures	1-11
1-11.2 Structural Motion	1-12
1-11.3 Fragments	1-14
1-12 Equipment Tolerance	1-14
1-12.1 Blast Pressures	1-14
1-12.2 Structural Motion and Shock	1-15
1-12.3 Fragments	1-16
1-13 Tolerance of Explosives	1-16
1-13.1 General	1-16
1-13.2 Blast Pressures	1-16
1-13.3 Structural Motions	1-17
1-13.4 Fragments	1-17
1-14 Structural Response	1-29
1-14.1 General	1-29
1-14.2 Pressure Design Ranges	1-29
1-14.3 Analyzing Blast Environment	1-30
APPENDIX 1A List of Symbols	
APPENDIX 1B Bibliography	

"Approved for public release; distribution is unlimited"

*This manual supersedes TM 5-1300/NAVFAC P-397/AFM 88-22, dated 15 June 1969.

CHAPTER 2. BLAST, FRAGMENT, AND SHOCK LOADS

Section	PAGE
2-1 Purpose	2-1
2-2 Objective	2-1
2-3 Background	2-1
2-4 Scope	2-2
2-5 Format	2-3
2-6 General	2-4
2-7 Effects of Explosive Output	2-5
2-8 Blast Phenomena	2-6
2-8.1 General	2-6
2-8.2 Explosive Materials	2-6
2-9 TNT Equivalency	2-7
2-10 Blast-Loading Categories	2-8
2-10.1 Unconfined Explosion	2-8
2-10.2 Confined Explosion	2-8
2-11 Blast Loading Protection	2-9
2-12 Blast-Wave Phenomena	2-10
2-13 Unconfined Explosions	2-11
2-13.1 Free Air Burst	2-11
2-13.2 Air Burst	2-12
2-13.3 Surface Burst	2-13
2-13.4 Multiple Explosions	2-14
2-14 Confined Explosions	2-15
2-14.1 Effects of Confinement	2-15
2-14.2 Shock Pressures	2-17
2-14.3 Gas Pressures	2-23
2-14.4 Leakage Pressures	2-26
2-15 External Blast Loads on Structures	2-29
2-15.1 General	2-29
2-15.2 Forces Acting on Structure	2-30
2-15.3 Above-Ground Rectangular Structure Without Openings	2-31
2-15.4 Above Ground Rectangular Structures with Openings.	2-35
2-15.5 Pressure Buildup In Structures	2-41
2-16 General	2-287
2-17 Primary Fragments	2-287
2-17.1 General	2-287
2-17.2 Initial Fragment Velocity	2-288
2-17.3 Fragment Mass Distribution	2-289
2-17.4 Variation of Fragment Velocity with Distance	2-292
2-17.5 Primary Fragments - Shape, Caliber Density and Impact Angle	2-294
2-18 Secondary Fragments	2-296
2-18.1 General	2-296
2-18.2 Velocity of Unconstrained Secondary Fragments	2-297
2-18.3 Velocity of Constrained Secondary Fragments	2-300
2-19 Fragment Trajectories	2-301
2-20 Introduction	2-326
2-21 Ground Shock	2-326
2-21.1 Introduction	2-326
2-21.2 Air Blast-Induced Ground Shock	2-327
2-21.3 Direct-Induced Ground Motion	2-329
2-22 Air Shock	2-330
2-22.1 Introduction	2-330
2-22.2 Method of Analysis	2-330

2-23	Structure Motions	2-332
2-23.1	Introduction	2-332
2-23.2	Net Ground Shock	2-332
2-23.3	Maximum Structure Motion	2-333
2-24	Shock Response Spectra	2-334
2-24.1	Introduction	2-334
2-24.2	Definition of Shock Spectra Grid	2-334
2-24.3	Response Spectra	2-335
APPENDIX 2A Illustrative Examples		
APPENDIX 2B List of Symbols		
APPENDIX 2C Bibliography		

CHAPTER 3. PRINCIPLES OF DYNAMIC ANALYSIS

3-1	Purpose	3-1
3-2	Objective	3-1
3-3	Background	3-1
3-4	Scope	3-2
3-5	Format	3-3
3-6	General	3-4
3-7	General	3-5
3-8	Introduction	3-7
3-9	Ultimate Resistance	3-8
3-9.1	General	3-8
3-9.2	One-Way Elements	3-8
3-9.3	Two-Way Elements	3-9
3-9.4	Openings in Two-Way Elements	3-13
3-10	Post-Ultimate Resistance	3-14
3-11	Partial Failure and Ultimate Deflection	3-14
3-12	Elasto-Plastic Resistance	3-15
3-13	Elasto-Plastic Stiffnesses and Deflections	3-16
3-14	Resistance-Deflection Functions for Design	3-17
3-14.1	General	3-17
3-14.2	Limited Deflections	3-18
3-14.3	Large Deflections	3-18
3-15	Support Shears or Reactions	3-18
3-16	Introduction	3-72
3-17	Dynamic Design Factors	3-73
3-17.1	Introduction	3-73
3-17.2	Load, Mass, and Resistance Factors	3-74
3-17.3	Load-Mass Factor	3-77
3-17.4	Natural Period of Vibration	3-79
3-18	Introduction	3-85
3-19	Elements Which Respond to Pressure Only and Pressure-Time Relationship.	3-85
3-19.1	General	3-85
3-19.2	Analysis by Numerical Methods	3-85
3-19.3	Design Charts for Idealized Loadings	3-90
3-20	Elements Which Respond to Impulse	3-98
3-20.1	General	3-98
3-20.2	Determination of Time to Reach Maximum Deflection	3-101
APPENDIX 3A Illustrative Examples		
APPENDIX 3B List of Symbols		
APPENDIX 3C Bibliography		

CHAPTER 4. REINFORCED CONCRETE DESIGN

4-1	Purpose	4-1
4-2	Objective	4-1
4-3	Background	4-1
4-4	Scope	4-2
4-5	Format	4-3
4-6	General	4-4
4-7	General	4-5
4-8	Modes of Structural Behavior	4-5
4-9	Structural Behavior of Reinforced Concrete	4-5
	4-9.1 General	4-5
	4-9.2 Ductile Mode of Behavior in the Far Design Range	4-6
	4-9.3 Ductile Mode of Behavior in the Close-in Design Range	4-7
	4-9.4 Brittle Mode of Behavior	4-7
4-10	Introduction	4-16
4-11	Stress-Strain Curve	4-16
4-12	Allowable Material Strengths	4-17
	4-12.1 General	4-17
	4-12.2 Reinforcement	4-17
	4-12.3 Concrete	4-18
4-13	Dynamic Design Stresses for Reinforced Concrete	4-18
	4-13.1 General	4-18
	4-13.2 Dynamic Increase Factor	4-18
	4-13.3 Dynamic Design Stresses	4-20
4-14	Modulus of Elasticity	4-27
	4-14.1 Concrete	4-27
	4-14.2 Reinforcing Steel	4-27
	4-14.3 Modular Ratio	4-27
4-15	Moment of Inertia	4-27
4-16	Introduction	4-32
4-17	Ultimate Moment Capacity	4-33
	4-17.1 Cross Section Type I	4-33
	4-17.2 Cross Section Types II and III	4-34
	4-17.3 Minimum Flexural Reinforcement	4-35
4-18	Ultimate Shear (Diagonal Tension) Capacity	4-35
	4-18.1 Ultimate Shear Stress	4-35
	4-18.2 Shear Capacity of Unreinforced Concrete	4-36
	4-18.3 Design of Shear Reinforcement	4-37
	4-18.4 Minimum Shear Reinforcement	4-38
4-19	Direct Shear Capacity	4-39
	4-19.1 General	4-39
	4-19.2 Direct Shear Capacity of Concrete	4-39
	4-19.3 Design of Diagonal Bars	4-40
4-20	Punching Shear	4-40
	4-20.1 Ultimate Punching Shear Stress	4-40
	4-20.2 Punching Shear Capacity of Concrete	4-40
4-21	Development of Reinforcement	4-41
	4-21.1 General	4-41
4-21.2	Provisions for Conventionally Reinforced Concrete Elements	4-41
	4-21.3 Provisions for Laced Reinforced Concrete Elements	4-42
	4-21.4 Development Length for Reinforcement in Tension	4-43
	4-21.5 Development Length for Reinforcement in Compression	4-43
	4-21.6 Development Length of Hooked Bars	4-44
	4-21.7 Lap Splices of Reinforcement	4-44
	4-21.8 Mechanical Splices of Reinforcement	4-45

4-21.9	Welding of Reinforcement	4-45
4-21.10	Bundled Reinforcing Bars	4-45
4-22	Introduction	4-52
4-23	Distribution of Flexural Reinforcement	4-53
4-23.1	General	4-53
4-23.2	Optimum Reinforcement Distribution	4-53
4-23.3	Optimum Total Percentage of Reinforcement	4-54
4-24	Flexural Design for Small Deflections	4-54
4-25	Design for Large Deflections	4-55
4-25.1	Introduction	4-55
4-25.2	Lateral Restraint	4-55
4-25.3	Resistance-Deflection Curve	4-56
4-25.4	Ultimate Tensile Membrane Capacity	4-56
4-25.5	Flexural Design	4-57
4-26	Dynamic Analysis	4-58
4-26.1	Design for Shock Load	4-58
4-26.2	Design for Rebound	4-59
4-27	Design for Shear	4-60
4-27.1	General	4-60
4-27.2	Ultimate Shear Stress at d_v from the Support	4-60
4-27.3	Ultimate Support Shear	4-62
4-28	Introduction	4-69
4-29	Distribution of Flexural Reinforcement	4-70
4-29.1	General	4-70
4-29.2	Elastic Distribution of Moments According to the ACI Building Code	4-70
4-29.3	Design for Small Deflections	4-73
4-29.4	Design for Large Deflections	4-73
4-29.5	Minimum Reinforcement	4-74
4-30	Dynamic Analysis	4-74
4-30.1	General	4-74
4-30.2	Ultimate Flexural Resistance	4-75
4-30.3	Ultimate Tension Membrane Capacity	4-78
4-30.4	Elastic Deflections	4-79
4-30.5	Load-Mass Factors	4-80
4-30.6	Dynamic Response	4-81
4-31	Dynamic Design	4-82
4-31.1	Flexural Capacity	4-82
4-31.2	Shear Capacity	4-82
4-31.3	Columns	4-83
4-32	Introduction	4-94
4-33	Flexural Design for Large Deflections	4-95
4-33.1	General	4-95
4-33.2	Impulse Coefficients	4-96
4-33.3	Design Equations for Deflections X_1 and X_u	4-99
4-33.4	Optimum Reinforcement	4-99
4-33.5	Design Equation for Deflections Less than X_1 or X_u	4-102
4-33.6	Design Equations for Unspalled Cross Sections	4-103
4-34	Flexural Design for Limited Deflections	4-103
4-35	Design for Shear	4-104
4-35.1	General	4-104
4-35.2	Ultimate Shear Stress	4-105
4-35.3	Ultimate Support Shears	4-106
4-36	Composite Construction	4-143
4-36.1	General	4-143

4-36.2	Blast Attenuation Ability of Sand Fill	4-143
4-36.3	Procedure for Design of Composite Elements	4-145
4-37	Introduction	4-149
4-38	Ultimate Moment Capacity	4-150
4-38.1	Tension Reinforcement Only	4-150
4-38.2	Tension and Compression Reinforcement	4-151
4-38.3	Minimum Flexural Reinforcement	4-152
4-39	Ultimate Shear (Diagonal Tension) Capacity	4-152
4-39.1.	Ultimate Shear Stress	4-152
4-39.2	Shear Capacity of Unreinforced Concrete	4-153
4-39.3	Design of Shear Reinforcement	4-153
4-39.4	Minimum Shear Reinforcement	4-153
4-40	Direct Shear	4-154
4-41	Ultimate Torsion Capacity	4-155
4-41.1	General	4-155
4-41.2	Ultimate Torsional Stress	4-155
4-41.3	Capacity of Unreinforced Concrete for Combined Shear and Torsion	4-156
4-41.4	Design of Torsion Reinforcement	4-157
4-41.5	Minimum Torsion Reinforcement	4-159
4-42	Flexural Design	4-160
4-42.1	Introduction	4-160
4-42.2	Small Deflections	4-160
4-42.3	Large Deflections	4-160
4-43	Dynamic Analysis	4-162
4-43.1	Design for Shock Load	4-162
4-43.2	Design for Rebound	4-163
4-44	Introduction	4-166
4-45	Strength of Compression Members (P-M Curve)	4-166
4-45.1	General	4-166
4-45.2	Pure Compression	4-166
4-45.3	Pure Flexure	4-167
4-45.4	Balanced Conditions	4-167
4-45.5	Compression Controls	4-168
4-45.6	Tension Controls	4-169
4-46	Slenderness Effects	4-170
4-46.1	General	4-170
4-46.2	Slenderness Ratio	4-170
4-46.3	Moment Magnification	4-171
4-47	Dynamic Analysis	4-173
4-48	Design of Tied Columns	4-174
4-48.1	General	4-174
4-48.2	Minimum Eccentricity	4-175
4-48.3	Longitudinal Reinforcement Requirements	4-175
4-48.4	Closed Ties Requirements	4-175
4-49	Design of Spiral Columns	4-176
4-49.1	General	4-176
4-49.2	Minimum Eccentricity	4-176
4-49.3	Longitudinal Reinforcement Requirements	4-176
4-49.4	Spiral Reinforcing Requirements	4-176
4-50	Introduction	4-180
4-51	Design of Exterior Columns	4-180
4-52	Introduction	4-181
4-53	Direct Spalling	4-181
4-54	Scabbing	4-182

4-55	Prediction of Concrete Spalling	4-182
4-56	Minimization of Effects of Spalling and Scabbing	4-183
	4-56.1 Design parameters	4-184
	4-56.2 Composite Construction	4-184
	4-56.3 Fragment Shields	4-185
4-57	Post-Failure Concrete Fragments	4-187
4-58	Post-Failure Impulse Capacity	4-188
	4-58.1 General	4-188
	4-58.2 Laced Elements	4-188
4-59	Introduction	4-205
	4-59.1 Fragment Characteristics	4-205
	4-59.2 Velocity and Impact Limitations	4-205
4-60	Fragment Impact on Concrete	4-205
	4-60.1. General	4-205
	4-60.2 Penetration by Armor-Piercing Fragments	4-206
	4-60.3 Penetration of Fragments Other than Armor-Piercing	4-207
	4-60.4 Perforation of Concrete	4-208
	4-60.5 Spalling due to Fragment Impact	4-209
4-61	Fragment Impact on Composite Construction	4-209
	4-61.1 General	4-209
	4-61.2 Penetration of Composite Barriers	4-210
4-62	Introduction	4-219
4-63	Concrete	4-219
4-64	Flexural Reinforcement	4-220
4-65	Construction Details for "Far Range" Design	4-221
	4-65.1 General	4-221
	4-65.2 Elements Designed for Limited Deflections	4-221
	4-65.3 Elements Designed for Large Deflections	4-222
	4-65.4 Column Details	4-222
4-66	Construction Details for "Close-In Design"	4-223
	4-66.1 General	4-223
	4-66.2 Laced Elements	4-224
	4-66.3 Elements Reinforced with Single Leg Stirrups	4-227
4-67	Composite Construction	4-229
4-68	Single and Multicubicle Structures	4-230
4-69	Sequence of Construction	4-231
	APPENDIX 4A Illustrative Examples	
	APPENDIX 4B List of Symbols	
	APPENDIX 4C Bibliography	

CHAPTER 5. STRUCTURAL STEEL DESIGN

5-1	Purpose	5-1
5-2	Objective	5-1
5-3	Background	5-1
5-4	Scope	5-2
5-5	Format	5-3
5-6	General	5-4
5-7	Differences Between Steel and Concrete Structures in Protective Design	5-5
5-8	Economy of Design of Protective Structures in the Inelastic Range	5-6
5-9	Applications of Steel Elements and Structures In Protective Design	5-6
5-10	Application of Dynamic Analysis	5-6
5-11	General	5-8

5-12	Mechanical Properties	5-8
5-12.1	Mechanical Properties Under Static Loading, Static Design Stresses	5-8
5-12.2	Mechanical Properties Under Dynamic Loading, Dynamic Increase Factors	5-9
5-13	Recommended Dynamic Design Stresses	5-10
5-13.1	General	5-10
5-13.2	Dynamic Design Stress for Ductility Ratio $\mu \leq 10$	5-10
5-13.3	Dynamic Design Stress for Ductility Ratio, $\mu > 10$	5-11
5-13.4	Dynamic Design Stress for Shear	5-11
5-14	Plastic Behavior of Steel Structures	5-16
5-15	Relationship Between Structure Function and Deformations	5-16
5-15.1	General	5-16
5-15.2	Acceptor-type Structures in the Low Pressure Ranges	5-16
5-15.3	Acceptor- or Donor-type Structures in the High Pressure Range	5-16
5-16	Deformation Criteria	5-17
5-16.1	General	5-17
5-16.2	Structural Response Quantities	5-17
5-16.3	Ductility Ratio, μ	5-17
5-16.4	Support Rotation, θ	5-18
5-16.5	Limiting Deformations for Beams	5-18
5-16.6	Application of Deformation Criteria to a Frame Structure	5-18
5-16.7	Limiting Deformations for Plates	5-19
5-17	Rebound	5-20
5-18	Secondary Modes of Failure	5-20
5-18.1	General	5-20
5-18.2	Instability Modes of Failure	5-20
5-18.3	Brittle Modes of Failure	5-21
5-19	General	5-26
5-20	Dynamic Flexural Capacity	5-26
5-20.1	General	5-26
5-20.2	Moment-curvature Relationship for Beams	5-27
5-20.3	Design Plastic Moment, M_p	5-27
5-21	Resistance and Stiffness Functions	5-28
5-21.1	General	5-28
5-21.2	Single-span Beams	5-28
5-21.3	Multi-span Beams	5-28
5-22	Design for Flexure	5-29
5-22.1	General	5-29
5-22.2	Response Charts	5-29
5-22.3	Preliminary Dynamic Load Factors	5-29
5-22.4	Additional Considerations in Flexural Design	5-30
5-23	Design for Shear	5-30
5-24	Local Buckling	5-31
5-25	Web Crippling	5-32
5-26	Lateral Bracing	5-32
5-26.1	General	5-32
5-26.2	Requirements for Members with $\mu \leq 3$	5-33
5-26.3	Requirements for Members with $\mu > 3$	5-33
5-26.4	Requirements for Elements Subjected to Rebound	5-34
5-26.5	Requirements for Bracing Members	5-34
5-27	General	5-39
5-28	Dynamic Flexural Capacity	5-39

5-29	Resistance and Stiffness Functions	5-39
5-30	Design for Flexure	5-40
5-31	Design for Shear	5-40
5-32	Unsymmetrical Bending	5-44
	5-32.1 General	5-44
	5-32.2 Elastic and Plastic Section Modulus	5-44
	5-32.3 Equivalent Elastic Stiffness	5-45
	5-32.4 Lateral Bracing and Recommended Design Criteria	5-45
	5-32.5 Torsion and Unsymmetrical Bending	5-45
5-33	Steel Joists and Joist Girders (Open-web Steel Joists)	5-46
5-34	Blast Resistant Design of Cold-Formed Steel Panels	5-48
	5-34.1 General	5-48
	5-34.2 Resistance in Flexure	5-48
	5-34.3 Equivalent Elastic Deflection	5-50
	5-34.4 Design for Flexure	5-50
	5-34.5 Recommended Ductility Ratios	5-50
	5-34.6 Recommended Support Rotations	5-51
	5-34.7 Rebound	5-51
	5-34.8 Resistance in Shear	5-51
	5-34.9 Web Crippling	5-52
5-35	Summary of Deformation Criteria for Structural Elements	5-54
5-36	Blast Door Design	5-64
	5-36.1 General	5-64
	5-36.2 Functions and Methods of Opening	5-64
	5-36.3 Design Considerations	5-64
	5-36.4 Examples of Blast Door Designs	5-66
	5-36.5 Blast Door Rebound	5-67
	5-36.6 Methods of Design	5-68
5-37	Plastic Design Criteria	5-76
	5-37.1 General	5-76
	5-37.2 In-plane Loads	5-76
	5-37.3 Combined Axial Loads and Biaxial Bending	5-76
5-38	Effective Length Ratios for Beam-columns	5-77
5-39	Effective Length Factor, K	5-78
5-40	General	5-81
5-41	Trial Design of Single-Story Rigid Frames	5-82
	5-41.1 Collapse Mechanisms	5-82
	5-41.2 Dynamic Deflections and Rotations	5-83
	5-41.3 Dynamic Load Factors	5-83
	5-41.4 Loads in Frame Members	5-83
	5-41.5 Sizing of Frame Members	5-83
	5-41.6 Stiffness and Deflection	5-84
5-42	Trial Design of Single-Story Frames with Supplementary Bracing	5-85
	5-42.1 General	5-85
	5-42.2 Collapse Mechanisms	5-85
	5-42.3 Bracing Ductility Ratio	5-85
	5-42.4 Dynamic Load Factor	5-86
	5-42.5 Loads in Frame Members	5-86
	5-42.6 Stiffness and Deflection	5-87
	5-42.7 Slenderness Requirements for Diagonal Braces	5-87
	5-42.8 Sizing of Frame Members	5-87
5-43	General	5-96
5-44	Types of Connections	5-96
5-45	Requirements for Main Framing Connections	5-97
5-46	Design of Connections	5-97

5-47	Dynamic Design Stresses for Connections	5-98
5-48	Requirements for Floor and Wall Panel Connections	5-98
5-49	Penetration of Fragments into Steel	5-102
5-49.1	Failure Mechanisms	5-102
5-49.2	Primary Fragment Penetration Equations	5-102
5-49.3	Residual Velocity After Perforation of Steel Plate	5-103
5-50	General	5-107
5-51	Steel Framed Buildings	5-107
5-52	Cold-formed, Light Gage Steel Panels	5-107
5-53	Blast Doors	5-108
APPENDIX 5A Illustrative Examples		
APPENDIX 5B List of Symbols		
APPENDIX 5C Bibliography		

CHAPTER 6. SPECIAL CONSIDERATIONS IN EXPLOSIVE FACILITY DESIGN

6-1	Purpose	6-1
6-2	Objective	6-1
6-3	Background	6-1
6-4	Scope	6-2
6-5	Format	6-3
6-6	General	6-4
6-7	Application	6-5
6-8	Design Criteria for Reinforced Masonry Walls	6-6
6-8.1	Static Capacity of Reinforced Masonry Units	6-6
6-8.2	Dynamic Strength of Material	6-7
6-8.3	Ultimate Strength of Reinforced Concrete Masonry Walls	6-7
6-8.4	Dynamic Analysis	6-9
6-8.5	Rebound	6-10
6-9	Non-Reinforced Masonry Walls	6-10
6-9.1	Rigid Supports	6-10
6-9.2	Non-rigid Supports	6-12
6-9.3	Simply Supported Walls	6-13
6-10	Applications	6-26
6-11	Static Strength of Materials	6-26
6-11.1	Concrete	6-26
6-11.2	Reinforcing Bars	6-26
6-11.3	Welded Wire Fabric	6-27
6-11.4	Prestressing Tendons	6-27
6-12	Dynamic Strength of Materials	6-27
6-13	Ultimate Strength of Precast Elements	6-27
6-13.1	Ultimate Dynamic Moment Capacity of Prestressed Beams	6-28
6-13.2	Diagonal Tension and Direct Shear of Prestressed Elements	6-31
6-14	Dynamic Analysis	6-31
6-15	Rebound	6-32
6-15.1	Non-prestressed elements	6-32
6-15.2	Prestressed elements	6-32
6-16	Connections	6-33
6-16.1	General	6-33
6-16.2	Column-to-Foundation Connection	6-34
6-16.3	Roof Slab-to-Girder Connection	6-34
6-16.4	Wall Panel-to-Roof Slab Connection	6-34
6-16.5	Wall Panel-to-Foundation Connection	6-34
6-16.6	Panel Splice	6-34

6-16.7	Reinforcement Around Door Openings	6-34
6-17	General	6-42
6-18	General Layout	6-42
6-18.1	Structural Steel	6-42
6-18.2	Foundations	6-43
6-18.3	Roof and Walls	6-43
6-18.4	Connections for Roof and Wall Coverings	6-43
6-19	Preparation of Partial Blast Analysis	6-44
6-20	Pre-Engineered Building Design	6-44
6-21	Blast Evaluation of the Structure	6-45
6-22	Recommended Specification for Pre-Engineered Buildings	6-45
6-23	General	6-55
6-24	Application	6-55
6-24.1	Safety Approved Suppressive Shields	6-56
6-24.2	New Shield Design	6-56
6-25	Design Criteria	6-57
6-26	Design Procedures	6-58
6-26.1	Space Requirements	6-58
6-26.2	Charge Parameters	6-58
6-26.3	Fragment Parameters	6-58
6-26.4	Structural Details	6-59
6-26.5	Access Penetrations	6-59
6-27	Introduction	6-73
6-28	Background	6-73
6-29	Design Criteria for Glazing	6-74
6-29.1	Specified Glazing	6-74
6-29.2	Design Stresses	6-75
6-29.3	Dynamic Response to Blast Load	6-75
6-29.4	Design Charts	6-75
6-29.5	Alternate Design Procedure	6-76
6-30	Design Criteria for Frames	6-78
6-30.1	Sealants, Gaskets, and Beads	6-78
6-30.2	Glazing Setting	6-78
6-30.3	Frame Loads	6-78
6-30.4	Rebound	6-80
6-31	Acceptance Test Specification	6-80
6-31.1	Test Procedure - Window Assembly Test	6-80
6-31.2	Acceptance Criteria	6-81
6-31.3	Certification for Rebound	6-82
6-32	Installation Inspection	6-82
6-33	Introduction	6-134
6-34	Design Loads for Underground Structures	6-134
6-34.1	General	6-134
6-34.2	Roof Loads	6-135
6-34.3	Wall Loads	6-135
6-35	Structural Design	6-136
6-35.1	Wall and Roof Slabs	6-136
6-35.2	Burster Slab	6-136
6-36	Structure Motions	6-137
6-36.1	Shock Spectra	6-137
6-36.2	Shock Isolation Systems	6-137
6-37	General	6-142
6-38	Description of Earth-Covered Arch-Type Magazines	6-142
6-39	Separation Distances of Standard Magazines	6-143
6-40	Design	6-143

6-41	Construction	6-144
6-42	Non-Standard Magazines	6-144
6-43	General	6-147
6-43.1	Applications	6-147
6-43.2	Remote-Actuated valves	6-147
6-43.3	Blast-Actuated Valves	6-148
6-43.4	Plenums	6-148
6-43.5	Fragment Protection	6-149
6-44	Types of Blast Valves	6-149
6-44.1	General	6-149
6-44.2	Blast Shield	6-149
6-44.3	Sand Filter	6-149
6-44.4	Blast Resistant Louvers	6-150
6-44.5	Poppet Valves	6-150
6-45	Introduction	6-164
6-46	Objectives	6-164
6-47	Structure Motions	6-165
6-48	Shock Tolerance of Personnel and Equipment	6-165
6-48.1	Personnel	6-165
6-48.2	Equipment	6-165
6-49	Shock Isolation Principles	6-166
6-49.1	General Concepts	6-166
6-49.2	Single-Mass Dynamic Systems	6-167
6-49.3	Shock Isolation Arrangements	6-169
6-50	Shock Isolation Devices	6-173
6-50.1	Introduction	6-173
6-50.2	Helical Coil Springs	6-174
6-50.3	Torsion Springs	6-175
6-50.4	Pneumatic Springs	6-175
6-50.5	Liquid Springs	6-176
6-50.6	Other Devices	6-177
6-51	Hardmounted Systems	6-178
6-52	Attachments	6-178
6-52.1	Introduction	6-178
6-52.2	Design Loads	6-179
	APPENDIX 6A Illustrative Examples	
	APPENDIX 6B List of Symbols	
	APPENDIX 6C Bibliography	

LIST OF TABLES

TABLE		PAGE
1-1	Blast Effects in Man Applicable to Fast-Rising Air Blasts of Short Duration (3-5 ms.)	1-23
1-2	50 Percent Probability of Penetrating Human Skin	1-23
1-3	Threshold of Serious Injury to Personnel Due to Fragment Impact . .	1-24
1-4	Examples of Equipment Shock Tolerances	1-24
1-5	Safe Separation Distance (bulk explosives)	1-25
1-6	Safe Separation Distance (munitions)	1-26
2-1	Heat of Detonation and Heat of Combustion	2-278
2-2	List of Illustrations of Peak Incident Pressure and Impulse Produced by Surface Detonation of Various Explosives	2-279
2-3	List of Illustrations for Average Peak Reflected Pressure and Scaled Average Unit Reflected Impulse	2-285
2-4	List of Illustrations for Interior Side Wall Idealized Times T_3 and T_4	2-286
2-5	Specific Weight and Gurney Energy Constant for Various Explosives	2-321
2-6	Initial Velocity of primary fragments for various geometries. . .	2-322
2-7	Mott Scaling Constants for Mild Steel Casings and Various Explosives	2-323
2-8	Drag Coefficient, C_D , for various shapes	2-324
2-9	Steel Toughness	2-325
2-10	Mass Density for Typical Soils and Rocks	2-338
2-11	Typical Seismic Velocities for Soils and Rocks	2-338
2-12	Coefficient of Friction for Concrete Foundation and Underlying Soils	2-339
3-1	Ultimate Unit Resistance for One-Way Elements	3-61
3-2	Ultimate Unit Resistance for Two-Way Elements (Symmetrical Yield Lines)	3-62
3-3	Ultimate Unit Resistance for Two-Way Elements (Unsymmetrical Yield Lines)	3-63
3-4	Post Ultimate Unit Resistances for Two-Way Elements	3-64
3-5	General and Ultimate Deflections for One-Way Elements	3-65
3-6	General, Partial Failure, and Ultimate Deflections for Two-Way Elements	3-66
3-7	Elastic and Elasto-Plastic Unit Resistances for One-Way Elements .	3-67
3-8	Elastic, Elasto-Plastic and Equivalent Elastic Stiffnesses for One-Way Elements	3-68
3-9	Support Shears for One-Way Elements	3-69
3-10	Ultimate Support Shears for Two-Way Elements (Symmetrical Yield Lines)	3-70
3-11	Ultimate Support Shears for Two-Way Elements (Unsymmetrical Yield Lines)	3-71
3-12	Transformation Factors for One-Way Elements	3-83
3-13	Load-Mass Factors in the Elastic and Elasto-Plastic Ranges for Two-Way Elements	3-84
3-14	Details of computation by acceleration impulse extrapolation method	3-328
3-15	Figure numbers corresponding to various combinations of C_1 and C_2	3-329
3-16	Response Chart Interpolation	3-330
4-1	Dynamic Increase Factor (DIF) for Design of Reinforced Concrete Elements	4-25

4-2	Dynamic Design Stresses for Design of Reinforced Concrete Elements	4-26
4-3	Minimum Area of Flexural Reinforcement	4-50
4-4	Minimum Design Shear Stresses for Slabs	4-51
4-5	Restraint and Aspect Ratio Requirements of Tension Membrane Behavior	4-66
4-6	Ultimate Shear Stress at Distance d_o from Face of Support for One-Way Elements	4-67
4-7	Ultimate Shear Stress at Distance d_o from Face of Support for Two-Way Elements	4-68
4-8	Deflection Coefficients for Interior Panels of Flat Slabs	4-93
4-9	Impulse Coefficient C_1 for Two-Way Elements	4-136
4-10	Impulse Coefficient C_u for Two-Way Elements	4-137
4-11	Impulse Coefficient C_u for One-Way Elements	4-138
4-12	Shear Coefficients for Ultimate Shear Stress at Distance d_c from the Support for One-Way Elements (Cross Section Type II and III)	4-139
4-13	Shear Coefficients for Ultimate Shear Stress at Distance d_c from the Support for Two-Way Elements (Cross Sections Type II and III)	4-140
4-14	Shear Coefficients for Ultimate Shear for One-Way Elements (Cross Section Type II and III)	4-141
4-15	Shear Coefficients for Ultimate Support Shear for Two-Way Elements (Cross Section Type II and III)	4-142
4-16	Relative Penetrability Coefficients for Various Missile Materials	4-218
5-1	Static Design Stresses for Materials	5-14
5-2	Dynamic Increase Factor, c , for Yield Stress of Structural Steels	5-15
5-3	Dynamic Increase Factor, c , for Ultimate Stress of Structural Steels	5-15
5-4	Preliminary Dynamic Load Factors for Plates	5-43
5-5	Dynamic Design Shear Stress for Webs of Cold-formed Members ($f_{ds} = 44$ ksi)	5-60
5-6	Dynamic Design Shear Stress for Webs of Cold-formed Members ($f_{ds} = 66$ ksi)	5-61
5-7	Dynamic Design Shear Stress for Webs of Cold-formed Members ($f_{ds} = 88$ ksi)	5-62
5-8	Summary of Deformation Criteria	5-63
5-9	Design Requirements for Sample Blast Doors	5-75
5-12	Effective Length Factors for Columns and Beam-Columns.	5-80
5-13	Collapse Mechanisms for Rigid Frames with Fixed and Pinned Bases.	5-92
5-14	Stiffness Factors for Single Story, Multi-Bay Rigid Frames Subjected to Uniform Horizontal Loading.	5-93
5-15	Collapse Mechanisms for Rigid Frames with Supplementary Bracing and Pinned Bases.	5-94
5-16	Collapse Mechanisms for Frames with Supplementary Bracing, Nonrigid Girder-to-Column Connections and Pinned Bases.	5-95
6-1	Properties of Hollow Masonry Units	6-24
6-2	Deflection Criteria for Masonry Walls	6-24
6-3	Moment of Inertia of Masonry Walls	6-25
6-4	Summary of Suppressive Shield Groups	6-71
6-5	Charge Parameters for Safety Approved Shields	6-72
6-6	Static Design Strength r_u (psi), for Tempered Glass* [a = long dimension of glass pane (in.); b = short dimension of glass pane (in.)]	6-109
6-7	Minimum Design Thickness, Clearances, and Bite Requirements	6-116

6-8	Maximum (b/t) Ratio for Linear Plate Behavior Under Blast Load and Coefficients for Resistance and Deflection and Fundamental Period of Simply Supported Glass Plates Based on Small Deflection Theory (No Tensile Membrane Behavior)	6-117
6-9	Coefficients for Frame Loading	6-118
6-10	Statistical Acceptance and Rejection Coefficients	6-119
6-11	Fundamental Period of Vibration, T_n , for Monolithic Tempered Glass	6-120
6-12	Effective Elastic Static Resistance, r_{eff}	6-127
6-13	Blast Valves	6-163

LIST OF FIGURES

FIGURE		PAGE
1-1	Explosive Protection System	1-7
1-2	Survival curves for lung damage	1-19
1-3	Human ear damage due to blast pressure	1-20
1-4	Example of safe separation tests	1-21
1-5	Safe separation test shields	1-22
1-6	Variation of structural response and blast loads	1-32
1-7	Parameters defining pressure design ranges	1-33
1-8	Design ranges corresponding to location of the structural elements relative to an explosion	1-34
2-1	Blast loading categories	2-43
2-2	Free-field pressure-time variation	2-44
2-3	Peak incident pressure versus peak dynamic pressure, density of air behind shock front and particle velocity	2-45
2-4	Free-air burst environment	2-46
2-5	Pressure-time variation for a free-air burst	2-47
2-6	Peak incident pressure versus the ratio of normal reflected pressure/incident pressure for a free air burst	2-48
2-7	Positive phase shock wave parameters for a spherical TNT explosion in free air at sea level	2-49
2-8	Negative phase shock wave parameters for a spherical TNT explosion in free air at sea level	2-50
2-9	Variation of reflected pressure as a function of angle of in- cidence	2-51
2-10	Variation of scaled reflected impulse as a function of angle of incidence	2-52
2-11	Air burst environment	2-53
2-12	Pressure-time variation for air burst	2-54
2-13	Scaled height of triple point	2-55
2-14	Surface burst blast environment	2-56
2-15	Positive phase shock wave parameters for a hemispherical TNT explosion on the surface at sea level	2-57
2-16	Negative phase shock wave parameters for a hemispherical TNT explosion on the surface at sea level	2-58
2-17	Explosive shapes	2-59
2-18	Peak positive incident pressure and scaled impulse for an explo- sion on the surface at sea level	2-60
2-19	Peak positive incident pressure and scaled impulse for an explo- sion on the surface at sea level	2-61
2-20	Peak positive incident pressure and scaled impulse for an explo- sion on the surface at sea level	2-62
2-21	Peak positive incident pressure and scaled impulse for an explo- sion on the surface at sea level	2-63
2-22	Peak positive incident pressure and scaled impulse for an explo- sion on the surface at sea level	2-64
2-23	Peak positive incident pressure and scaled impulse for an explo- sion on the surface at sea level	2-65
2-24	Peak positive incident pressure and scaled impulse for an explo- sion on the surface at sea level	2-66
2-25	Peak positive incident pressure and scaled impulse for an explo- sion on the surface at sea level	2-67
2-26	Peak positive incident pressure and scaled impulse for an explo- sion on the surface at sea level	2-68

2-27 Peak positive incident pressure and scaled impulse for an explosion on the surface at sea level 2-69

2-28 Peak positive incident pressure and scaled impulse for an explosion on the surface at sea level 2-70

2-29 Peak positive incident pressure and scaled impulse for an explosion on the surface at sea level 2-71

2-30 Peak positive incident pressure and scaled impulse for an explosion on the surface at sea level 2-72

2-31 Peak positive incident pressure and scaled impulse for an explosion on the surface at sea level 2-73

2-32 Peak positive incident pressure and scaled impulse for an explosion on the surface at sea level 2-74

2-33 Peak positive incident pressure and scaled impulse for an explosion on the surface at sea level 2-75

2-34 Peak positive incident pressure and scaled impulse for an explosion on the surface at sea level 2-76

2-35 Peak positive incident pressure and scaled impulse for an explosion on the surface at sea level 2-77

2-36 Peak positive incident pressure and scaled impulse for an explosion on the surface at sea level 2-78

2-37 Peak positive incident pressure and scaled impulse for an explosion on the surface at sea level 2-79

2-38 Peak positive incident pressure and scaled impulse for an explosion on the surface at sea level 2-80

2-39 Peak positive incident pressure and scaled impulse for an explosion on the surface at sea level 2-81

2-40 Peak positive incident pressure and scaled impulse for an explosion on the surface at sea level 2-82

2-41 Peak positive incident pressure and scaled impulse for an explosion on the surface at sea level 2-83

2-42 Peak positive incident pressure and scaled impulse for an explosion on the surface at sea level 2-84

2-43 Peak positive incident pressure and scaled impulse for an explosion on the surface at sea level 2-85

2-44 Peak positive incident pressure and scaled impulse for an explosion on the surface at sea level 2-86

2-45 Peak positive incident pressure and scaled impulse for an explosion on the surface at sea level 2-87

2-46 Peak positive incident pressure and scaled impulse for an explosion on the surface at sea level 2-88

2-47 Peak positive incident pressure and scaled impulse for an explosion on the surface at sea level 2-89

2-48 Peak positive incident pressure and scaled impulse for an explosion on the surface at sea level 2-90

2-49 Peak positive incident pressure and scaled impulse for an explosion on the surface at sea level 2-91

2-50 Confined explosion structures 2-92

2-51 Barrier and cubicle configurations and parameters 2-93

2-52 Average peak reflected pressure ($N = 1$, $P/L = 0.10$, $h/H = 0.10$) 2-94

2-53 Average peak reflected pressure ($N = 1$, $P/L = 0.25$ and 0.75 , $h/H = 0.10$) 2-95

2-54 Average peak reflected pressure ($N = 1$, $P/L = 0.50$, $h/H = 0.10$) 2-96

2-55 Average peak reflected pressure ($N = 1$, $P/L = 0.10$, $h/H = 0.25$) 2-97

2-56 Average peak reflected pressure ($N = 1$, $P/L = 0.25$ and 0.75 , $h/H = 0.25$) 2-98

2-57	Average peak reflected pressure	(N = 1, P/L = 0.50, h/H = 0.25)	2-99
2-58	Average peak reflected pressure	(N = 1, P/L = 0.10, h/H = 0.50)	2-100
2-59	Average peak reflected pressure	(N = 1, P/L = 0.25 and 0.75, h/H = 0.50)	2-101
2-60	Average peak reflected pressure	(N = 1, P/L = 0.50, h/H = 0.50)	2-102
2-61	Average peak reflected pressure	(N = 1, P/L = 0.10, h/H = 0.75)	2-103
2-62	Average peak reflected pressure	(N = 1, P/L = 0.25 and 0.75, h/H = 0.75)	2-104
2-63	Average peak reflected pressure	(N = 1, P/L = 0.50, h/H = 0.75)	2-105
2-64	Average peak reflected pressure	(N = 2, P/L = 0.10, h/H = 0.10)	2-106
2-65	Average peak reflected pressure	(N = 2, P/L = 0.25, h/H = 0.10)	2-107
2-66	Average peak reflected pressure	(N = 2, P/L = 0.50, h/H = 0.10)	2-108
2-67	Average peak reflected pressure	(N = 2, P/L = 0.75, h/H = 0.10)	2-109
2-68	Average peak reflected pressure	(N = 2, P/L = 0.10, h/H = 0.25)	2-110
2-69	Average peak reflected pressure	(N = 2, P/L = 0.25, h/H = 0.25)	2-111
2-70	Average peak reflected pressure	(N = 2, P/L = 0.50, h/H = 0.25)	2-112
2-71	Average peak reflected pressure	(N = 2, P/L = 0.75, h/H = 0.25)	2-113
2-72	Average peak reflected pressure	(N = 2, P/L = 0.10, h/H = 0.50)	2-114
2-73	Average peak reflected pressure	(N = 2, P/L = 0.25, h/H = 0.50)	2-115
2-74	Average peak reflected pressure	(N = 2, P/L = 0.50, h/H = 0.50)	2-116
2-75	Average peak reflected pressure	(N = 2, P/L = 0.75, h/H = 0.50)	2-117
2-76	Average peak reflected pressure	(N = 2, P/L = 0.10, h/H = 0.75)	2-118
2-77	Average peak reflected pressure	(N = 2, P/L = 0.25, h/H = 0.75)	2-119
2-78	Average peak reflected pressure	(N = 2, P/L = 0.50, h/H = 0.75)	2-120
2-79	Average peak reflected pressure	(N = 2, P/L = 0.75, h/H = 0.75)	2-121
2-80	Average peak reflected pressure	(N = 3, P/L = 0.10, h/H = 0.10)	2-122
2-81	Average peak reflected pressure	(N = 3, P/L = 0.25 and 0.75, h/H = 0.10)	2-123
2-82	Average peak reflected pressure	(N = 3, P/L = 0.50, h/H = 0.10)	2-124
2-83	Average peak reflected pressure	(N = 3, P/L = 0.10, h/H = 0.25)	2-125
2-84	Average peak reflected pressure	(N = 3, P/L = 0.25 and 0.75, h/H = 0.25)	2-126
2-85	Average peak reflected pressure	(N = 3, P/L = 0.50, h/H = 0.25)	2-127
2-86	Average peak reflected pressure	(N = 3, P/L = 0.10, h/H = 0.50)	2-128
2-87	Average peak reflected pressure	(N = 3, P/L = 0.25 and 0.75, h/H = 0.50)	2-129
2-88	Average peak reflected pressure	(N = 3, P/L = 0.50, h/H = 0.50)	2-130
2-89	Average peak reflected pressure	(N = 3, P/L = 0.10, h/H = 0.75)	2-131
2-90	Average peak reflected pressure	(N = 3, P/L = 0.25 and 0.75, h/H = 0.75)	2-132
2-91	Average peak reflected pressure	(N = 3, P/L = 0.50, h/H = 0.75)	2-133
2-92	Average peak reflected pressure	(N = 4, P/L = 0.10, h/H = 0.10)	2-134
2-93	Average peak reflected pressure	(N = 4, P/L = 0.25 and 0.75, h/H = 0.10)	2-135
2-94	Average peak reflected pressure	(N = 4, P/L = 0.50, h/H = 0.10)	2-136
2-95	Average peak reflected pressure	(N = 4, P/L = 0.10, h/H = 0.25 and 0.75)	2-137
2-96	Average peak reflected pressure	(N = 4, P/L = 0.25 and 0.75, h/H = 0.25 and 0.75)	2-138
2-97	Average peak reflected pressure	(N = 4, P/L = 0.50, h/H = 0.25 and 0.75)	2-139
2-98	Average peak reflected pressure	(N = 4, P/L = 0.10, h/H = 0.50)	2-140
2-99	Average peak reflected pressure	(N = 4, P/L = 0.25 and 0.75, h/H = 0.50)	2-141
2-100	Average peak reflected pressure	(N = 4, P/L = 0.50, h/H = 0.50)	2-142

2-101	Scaled average unit reflected impulse (N = 1, P/L = 0.10, h/H = 0.10)	2-143
2-102	Scaled average unit reflected impulse (N = 1, P/L = 0.25 and 0.75, h/H = 0.10)	2-144
2-103	Scaled average unit reflected impulse (N = 1, P/L = 0.50, h/H = 0.10)	2-145
2-104	Scaled average unit reflected impulse (N = 1, P/L = 0.10, h/H = 0.25)	2-146
2-105	Scaled average unit reflected impulse (N = 1, P/L = 0.25 and 0.75, h/H = 0.25)	2-147
2-106	Scaled average unit reflected impulse (N = 1, P/L = 0.50, h/H = 0.25)	2-148
2-107	Scaled average unit reflected impulse (N = 1, P/L = 0.10, h/H = 0.50)	2-149
2-108	Scaled average unit reflected impulse (N = 1, P/L = 0.25 and 0.75, h/H = 0.50)	2-150
2-109	Scaled average unit reflected impulse (N = 1, P/L = 0.50, h/H = 0.50)	2-151
2-110	Scaled average unit reflected impulse (N = 1, P/L = 0.10, h/H = 0.75)	2-152
2-111	Scaled average unit reflected impulse (N = 1, P/L = 0.25 and 0.75, h/H = 0.75)	2-153
2-112	Scaled average unit reflected impulse (N = 1, P/L = 0.50, h/H = 0.75)	2-154
2-113	Scaled average unit reflected impulse (N = 2, P/L = 0.10, h/H = 0.10)	2-155
2-114	Scaled average unit reflected impulse (N = 2, P/L = 0.25, h/H = 0.10)	2-156
2-115	Scaled average unit reflected impulse (N = 2, P/L = 0.50, h/H = 0.10)	2-157
2-116	Scaled average unit reflected impulse (N = 2, P/L = 0.75, h/H = 0.10)	2-158
2-117	Scaled average unit reflected impulse (N = 2, P/L = 0.10, h/H = 0.25)	2-159
2-118	Scaled average unit reflected impulse (N = 2, P/L = 0.25, h/H = 0.25)	2-160
2-119	Scaled average unit reflected impulse (N = 2, P/L = 0.50, h/H = 0.25)	2-161
2-120	Scaled average unit reflected impulse (N = 2, P/L = 0.75, h/H = 0.25)	2-162
2-121	Scaled average unit reflected impulse (N = 2, P/L = 0.10, h/H = 0.50)	2-163
2-122	Scaled average unit reflected impulse (N = 2, P/L = 0.25, h/H = 0.50)	2-164
2-123	Scaled average unit reflected impulse (N = 2, P/L = 0.50, h/H = 0.50)	2-165
2-124	Scaled average unit reflected impulse (N = 2, P/L = 0.75, h/H = 0.50)	2-166
2-125	Scaled average unit reflected impulse (N = 2, P/L = 0.10, h/H = 0.75)	2-167
2-126	Scaled average unit reflected impulse (N = 2, P/L = 0.25, h/H = 0.75)	2-168
2-127	Scaled average unit reflected impulse (N = 2, P/L = 0.50, h/H = 0.75)	2-169

2-128 Scaled average unit reflected impulse (N = 2, P/L = 0.75, h/H = 0.75)	2-170
2-129 Scaled average unit reflected impulse (N = 3, P/L = 0.10, h/H = 0.10)	2-171
2-130 Scaled average unit reflected impulse (N = 3, P/L = 0.25 and 0.75, h/H = 0.10)	2-172
2-131 Scaled average unit reflected impulse (N = 3, P/L = 0.50, h/H = 0.10)	2-173
2-132 Scaled average unit reflected impulse (N = 3, P/L = 0.10, h/H = 0.25)	2-174
2-133 Scaled average unit reflected impulse (N = 3, P/L = 0.25 and 0.75, h/H = 0.25)	2-175
2-134 Scaled average unit reflected impulse (N = 3, P/L = 0.50, h/H = 0.25)	2-176
2-135 Scaled average unit reflected impulse (N = 3, P/L = 0.10, h/H = 0.50)	2-177
2-136 Scaled average unit reflected impulse (N = 3, P/L = 0.25 and 0.75, h/H = 0.50)	2-178
2-137 Scaled average unit reflected impulse (N = 3, P/L = 0.50, h/H = 0.50)	2-179
2-138 Scaled average unit reflected impulse (N = 3, P/L = 0.10, h/H = 0.75)	2-180
2-139 Scaled average unit reflected impulse (N = 3, P/L = 0.25 and 0.75, h/H = 0.75)	2-181
2-140 Scaled average unit reflected impulse (N = 3, P/L = 0.50, h/H = 0.75)	2-182
2-141 Scaled average unit reflected impulse (N = 4, P/L = 0.10, h/H = 0.10)	2-183
2-142 Scaled average unit reflected impulse (N = 4, P/L = 0.25 and 0.75, h/H = 0.10)	2-184
2-143 Scaled average unit reflected impulse (N = 4, P/L = 0.50, h/H = 0.10)	2-185
2-144 Scaled average unit reflected impulse (N = 4, P/L = 0.10, h/H = 0.25 and 0.75)	2-186
2-145 Scaled average unit reflected impulse (N = 4, P/L = 0.25 and 0.75, h/H = 0.25 and 0.75)	2-187
2-146 Scaled average unit reflected impulse (N = 4, P/L = 0.50, h/H = 0.25 and 0.75)	2-188
2-147 Scaled average unit reflected impulse (N = 4, P/L = 0.10, h/H = 0.50)	2-189
2-148 Scaled average unit reflected impulse (N = 4, P/L = 0.25 and 0.75, h/H = 0.50)	2-190
2-149 Scaled average unit reflected impulse (N = 4, P/L = 0.50, h/H = 0.50)	2-191
2-150 Reflection factor for shock loads on frangible elements.	2-192
2-151 Pressure-time variation for a partially vented explosion.	2-193
2-152 Peak gas pressure produced by a TNT detonation in a partially contained chamber.	2-194
2-153 Scaled gas impulse ($W/V_f = 0.002, i_r/W^{1/3} = 20$)	2-195
2-154 Scaled gas impulse ($W/V_f = 0.002, i_r/W^{1/3} = 100$)	2-196
2-155 Scaled gas impulse ($W/V_f = 0.002, i_r/W^{1/3} = 600$)	2-197
2-156 Scaled gas impulse ($W/V_f = 0.015, i_r/W^{1/3} = 20$)	2-198
2-157 Scaled gas impulse ($W/V_f = 0.015, i_r/W^{1/3} = 100$)	2-199
2-158 Scaled gas impulse ($W/V_f = 0.015, i_r/W^{1/3} = 600$)	2-200
2-159 Scaled gas impulse ($W/V_f = 0.15, i_r/W^{1/3} = 20$)	2-201

2-160	Scaled gas impulse ($W/V_f = 0.15, i_r/W^{1/3} = 100$)	2-202
2-161	Scaled gas impulse ($W/V_f = 0.15, i_r/W^{1/3} = 600$)	2-203
2-162	Scaled gas impulse ($W/V_f = 1.0, i_r/W^{1/3} = 100$)	2-204
2-163	Scaled gas impulse ($W/V_f = 1.0, i_r/W^{1/3} = 600$)	2-205
2-164	Scaled gas impulse ($W/V_f = 1.0, i_r/W^{1/3} = 2000$)	2-206
2-165	Combined shock and gas pressures.	2-207
2-166	TNT conversion factor for charges.	2-208
2-167	Fully vented three-wall cubicles and direction of blast wave propagation.	2-209
2-168	Envelope curves for peak positive pressure outside three-wall cubicles without a roof	2-210
2-169	Envelope curves for peak positive pressure outside three-wall cubicles with a roof	2-211
2-170	Envelope curves for maximum peak pressure outside three-wall cubicles	2-212
2-171	Scaled peak positive impulse out the open front of cubic three-wall cubicle without a roof	2-213
2-172	Scaled peak positive impulse out the open front of rectangular three-wall cubicle without a roof	2-214
2-173	Scaled peak positive impulse behind sidewall of cubic three-wall cubicle without a roof	2-215
2-174	Scaled peak positive impulse behind sidewall of rectangular three-wall cubicle without a roof	2-216
2-175	Scaled peak positive impulse behind backwall of cubic three-wall cubicle without a roof	2-217
2-176	Scaled peak positive impulse behind backwall of rectangular three-wall cubicle without a roof	2-218
2-177	Scaled peak positive impulse out the open front of cubic three-wall cubicle with a roof	2-219
2-178	Scaled peak positive impulse out the open front of rectangular three-wall cubicle with a roof	2-220
2-179	Scaled peak positive impulse behind sidewall of cubic three-wall cubicle with a roof	2-221
2-180	Scaled peak positive impulse behind sidewall of rectangular three-wall cubicle with a roof	2-222
2-181	Scaled peak positive impulse behind backwall of cubic three-wall cubicle with a roof	2-223
2-182	Scaled peak positive impulse behind backwall of rectangular three-wall cubicle with a roof	2-224
2-183	Four wall cubicle vented through its roof	2-225
2-184	Peak positive pressure outside of a four-wall cubicle vented through its roof	2-226
2-185	Scaled positive impulse outside of a four-wall cubicle vented through its roof	2-227
2-186	Four wall cubicle vented through a wall and direction of blast wave propagation	2-228
2-187	Peak positive pressure at the front of a partially vented four-wall cubicle	2-229
2-188	Peak positive pressure at the side of a partially vented four-wall cubicle	2-230
2-189	Peak positive pressure at the back of a partially vented four wall cubicle	2-231
2-190	Idealized pressure-time variation.	2-232
2-191	Front wall loading.	2-233

2-192	Velocity of sound in reflected overpressure region versus peak incident overpressure.	2-234
2-193	Reflected pressure coefficient versus angle of incidence.	2-235
2-194	Reflected scaled impulse versus angle of incidence.	2-236
2-195	Roof and side wall loading.	2-237
2-196	Peak equivalent uniform roof pressures.	2-238
2-197	Scaled rise time of equivalent uniform positive roof pressures.	2-239
2-198	Scaled duration of equivalent uniform roof pressures.	2-240
2-199	Rear wall loading.	2-241
2-200	Idealized structure configuration for interior blast loads.	2-242
2-201	Idealized interior blast loads.	2-243
2-202	Sub-division of typical front wall with openings.	2-244
2-203	Maximum average pressure on interior face of front wall (W/H = 3/4).	2-245
2-204	Maximum average pressure on interior face of front wall (W/H = 3/2).	2-246
2-205	Maximum average pressure on interior face of front wall (W/H = 3).	2-247
2-206	Maximum average pressure on interior face of front wall (W/H = 6).	2-248
2-207	Arrival time, T_1 , for interior front wall blast load (W/H = 3/4 and 3/2)	2-249
2-208	Arrival time, T_1 , for interior front wall blast load (W/H = 3 and 6)	2-250
2-209	Idealized rise time, $T_2 - T_1$, for interior front wall blast load (W/H = 3/4 and 3/2)	2-251
2-210	Idealized rise time, $T_2 - T_1$, for interior front wall blast load (W/H = 3 and 6)	2-252
2-211	Idealized duration, $T_3 - T_1$, for interior front wall blast load (W/H = 3/4 and 3/2)	2-253
2-212	Idealized duration, $T_3 - T_1$, for interior front wall blast load (W/H = 3 and 6)	2-254
2-213	Idealized times T_1 and T_2 for interior side wall blast load	2-255
2-214	Idealized times T_3 and T_4 for interior side wall blast load (L/H = 1, W/H = 3/4)	2-256
2-215	Idealized times T_3 and T_4 for interior side wall blast load (L/H = 1, W/H = 3/2)	2-257
2-216	Idealized times T_3 and T_4 for interior side wall blast load (L/H = 1, W/H = 3)	2-258
2-217	Idealized times T_3 and T_4 for interior side wall blast load (L/H = 1, W/H = 6)	2-259
2-218	Idealized times T_3 and T_4 for interior side wall blast load (L/H = 2, W/H = 3/4)	2-260
2-219	Idealized times T_3 and T_4 for interior side wall blast load (L/H = 2, W/H = 3/2)	2-261
2-220	Idealized times T_3 and T_4 for interior side wall blast load (L/H = 2, W/H = 3)	2-262
2-221	Idealized times T_3 and T_4 for interior side wall blast load (L/H = 2, W/H = 6)	2-263
2-222	Idealized times T_3 and T_4 for interior side wall blast load (L/H = 4, W/H = 3/4)	2-264
2-223	Idealized times T_3 and T_4 for interior side wall blast load (L/H = 4, W/H = 3/2)	2-265
2-224	Idealized times T_3 and T_4 for interior side wall blast load (L/H = 4, W/H = 3)	2-266

2-225	Idealized times T_3 and T_4 for interior side wall blast load ($L/H = 4, W/H = 6$)	2-267
2-226	Idealized times T_3 and T_4 for interior side wall blast load ($L/H = 8, W/H = 3/4$)	2-268
2-227	Idealized times T_3 and T_4 for interior side wall blast load ($L/H = 8, W/H = 3/2$)	2-269
2-228	Idealized times T_3 and T_4 for interior side wall blast load ($L/H = 8, W/H = 3$)	2-270
2-229	Idealized times T_3 and T_4 for interior side wall blast load ($L/H = 8, W/H = 6$)	2-271
2-230	Idealized pressure coefficient for back wall interior blast load ($L/H = 1$ and 2)	2-272
2-231	Idealized pressure coefficient for back wall interior blast load ($L/H = 4$ and 8)	2-273
2-232	Arrival time, T_1 , for interior back wall blast load ($W/H = 3/4$ and $3/2$)	2-274
2-233	Arrival time, T_1 , for interior back wall blast load ($W/H = 3$ and 6)	2-275
2-234	Idealized time T_2 and T_1 for interior back wall blast load	2-276
2-235	Leakage pressure coefficient vs. pressure differential	2-277
2-236	Explosive outer casing separated by incompressible fluid	2-304
2-237	Initial velocity of primary fragments for various geometries	2-305
2-238	M_A/B versus cylindrical casing geometry	2-306
2-239	Design fragment weight versus design confidence level ($0.3 < C_L < 1$)	2-307
2-240	Design fragment weight versus design confidence level ($0.986 < C_L < 1$)	2-308
2-241	$B^2/N_T/W_c$ versus casing geometry	2-309
2-242	Equivalent cylindrical explosive casings	2-310
2-243	Variation of primary fragment velocity with distance	2-311
2-244	Primary fragment shapes	2-312
2-245	Relationship between fragment weight and fragment diameter	2-313
2-246	Interaction of blast wave with an irregular object	2-314
2-247	Idealized pressure-time loading in an irregular fragment	2-315
2-248	Nondimensional object velocity, V , as a function of pressure and impulse	2-316
2-249	Target shape factor for unconstrained fragments	2-317
2-250	Specific acquired impulse versus distance	2-318
2-251	Scaled fragment velocities for constrained fragments	2-319
2-252	Fragment range prediction	2-320
2-253	Net ground motions produced by an explosion at the ground surface	2-336
2-254	Typical response shock spectra	2-337
3-1	Typical resistance-deflection for two-way element	3-20
3-2	Idealized yield line locations for several two-way elements	3-21
3-3	Determination of ultimate unit resistance	3-22
3-4	Location of yield lines for two-way element with two adjacent edges supported and two edges free (values of x)	3-23
3-5	Location of yield lines for two-way element with two adjacent edges supported and two edges free (values of y)	3-24
3-6	Location of symmetrical yield lines for two-way element with three edges supported and one edge free (values of y)	3-25
3-7	Location of unsymmetrical yield lines for two-way element with three edges supported and one edge free ($x_2/x_1 = 0.1$)	3-26
3-8	Location of unsymmetrical yield lines for two-way element with three edges supported and one edge free ($x_2/x_1 = 0.3$)	3-27

3-9 Location of unsymmetrical yield lines for two-way element with three edges supported and one edge free ($x_2/x_1 = 0.5$) 3-28

3-10 Location of unsymmetrical yield lines for two-way element with three edges supported and one edge free ($x_2/x_1 = 0.75$) 3-29

3-11 Location of unsymmetrical yield lines for two-way element with three edges supported and one edge free ($x_2/x_1 = 1.0$) 3-30

3-12 Location of unsymmetrical yield lines for two-way element with three edges supported and one edge free ($x_2/x_1 = 1.25$) 3-31

3-13 Location of unsymmetrical yield lines for two-way element with three edges supported and one edge free ($x_2/x_1 = 1.5$) 3-32

3-14 Location of unsymmetrical yield lines for two-way element with three edges supported and one edge free ($x_2/x_1 = 1.75$) 3-33

3-15 Location of unsymmetrical yield lines for two-way element with three edges supported and one edge free ($x_2/x_1 = 2.0$) 3-34

3-16 Location of unsymmetrical yield lines for two-way element with three edges supported and one edge free (values of y) 3-35

3-17 Location of symmetrical yield lines for two-way element with four edges supported 3-36

3-18 Location of unsymmetrical yield lines for two-way element with four edges supported (values of x_1) 3-37

3-19 Location of unsymmetrical yield lines for two-way element with four edges supported (values of y_1) 3-38

3-20 Location of unsymmetrical yield lines for two-way element with four edges supported values of x/L and y/H) 3-39

3-21 Effects of openings on yield lines locations 3-40

3-22 Deflection of two-way element 3-41

3-23 Graphical summary of two-way elements 3-42

3-24 Moment and deflection coefficients for uniformly loaded, two-way element with two adjacent edges fixed and two edges free 3-43

3-25 Moment and deflection coefficients for uniformly loaded, two-way element with one edge fixed, an adjacent edge simply supported and two edges free 3-44

3-26 Moment and deflection coefficients for uniformly loaded, two-way element with two adjacent edges simply supported and two edges free 3-45

3-27 Moment and deflection coefficients for uniformly loaded, two-way element with three edges fixed and one edge free 3-46

3-28 Moment and deflection coefficients for uniformly loaded, two-way element with two opposite edges fixed, one edge simply supported and one edge free 3-47

3-29 Moment and deflection coefficients for uniformly loaded, two-way element with two opposite edges simply supported, one edge fixed, and one edge free 3-48

3-30 Moment and deflection coefficients for uniformly loaded, two-way element with three edges simply supported and one edge free 3-49

3-31 Moment and deflection coefficients for uniformly loaded, two-way element with two adjacent edges fixed, one edge simply supported, and one edge free 3-50

3-32 Moment and deflection coefficients for uniformly loaded, two-way element with two adjacent edges simply supported, one edge fixed, and one edge free 3-51

3-33 Moment and deflection coefficients for uniformly loaded, two-way element with all edges fixed 3-52

3-34 Moment and deflection coefficients for uniformly loaded, two-way element with two opposite edges fixed and two edges simply supported 3-53

3-35 Moment and deflection coefficients for uniformly loaded, two-way element with three edges fixed and one edge simply supported 3-54

3-36 Moment and deflection coefficients for uniformly loaded, two-way element with all edges simply supported 3-55

3-37 Moment and deflection coefficients for uniformly loaded, two-way element with two adjacent edges fixed, and two edges simply supported 3-56

3-38 Moment and deflection coefficients for uniformly loaded, two-way element with three edges simply supported and one edge fixed 3-57

3-39 Resistance-deflection functions for limited deflections 3-58

3-40 Resistance-deflection functions for large deflections 3-59

3-41 Determination of ultimate support shear 3-60

3-42 Typical single-degree-of-freedom system 3-80

3-43 Determination of load-mass factor in the plastic range 3-81

3-44 Load-mass factors in plastic range for two-way elements 3-82

3-45 Acceleration-impulse extrapolation method 3-102

3-46 Discontinuities in the acceleration curve 3-103

3-47 Pressure-time function with two different time intervals 3-104

3-48 A two-degrees-of-freedom system 3-105

3-49 Maximum response of elastic, one-degree-of-freedom system for triangular load 3-106

3-50 Maximum response of elastic, one-degree-of-freedom system for rectangular load 3-107

3-51 Maximum response of elastic, one-degree-of-freedom system for gradually applied load 3-108

3-52 Maximum response of elastic, one-degree-of-freedom system for triangular pulse load 3-109

3-53 Maximum response of elastic, one-degree-of-freedom system for sinusoidal pulse load 3-110

3-54 Maximum deflection of elasto-plastic, one-degree-of-freedom system for triangular load 3-111

3-55 Maximum response time of elasto-plastic, one-degree-of-freedom system for triangular load 3-112

3-56 Maximum deflection of elasto-plastic, one-degree-of-freedom system for rectangular load 3-113

3-57 Maximum response time of elasto-plastic, one-degree-of-freedom system for rectangular load 3-114

3-58 Maximum deflection of elasto-plastic, one-degree-of-freedom system for gradually applied load 3-115

3-59 Maximum response time of elasto-plastic, one-degree-of-freedom system for gradually applied load 3-116

3-60 Maximum deflection of elasto-plastic, one-degree-of-freedom system for triangular pulse load 3-117

3-61 Maximum response time of elasto-plastic, one-degree-of-freedom system for triangular pulse load 3-118

3-62 Various bilinear-triangular loads 3-119

3-63 Regions of figures 3-64 through 3-266, labeling of axis and curves. 3-120

3-64a Maximum response of elasto-plastic, one-degree-of-freedom system for bilinear-triangular pulse ($C_1 = 1.000$, $C_2 = 1.0$) 3-121

3-64b Maximum response of elasto-plastic, one-degree-of-freedom system for bilinear-triangular pulse ($C_1 = 1.000$, $C_2 = 1.0$) 3-122

3-65	Maximum response of elasto-plastic, one-degree-of-freedom system for bilinear-triangular pulse ($C_1 = 0.681, C_2 = 1.7$)	3-123
3-66	Maximum response of elasto-plastic, one-degree-of-freedom system for bilinear-triangular pulse ($C_1 = 0.464, C_2 = 1.7$)	3-124
3-67	Maximum response of elasto-plastic, one-degree-of-freedom system for bilinear-triangular pulse ($C_1 = 0.316, C_2 = 1.7$)	3-125
3-68	Maximum response of elasto-plastic, one-degree-of-freedom system for bilinear-triangular pulse ($C_1 = 0.215, C_2 = 1.7$)	3-126
3-69	Maximum response of elasto-plastic, one-degree-of-freedom system for bilinear-triangular pulse ($C_1 = 0.147, C_2 = 1.7$)	3-127
3-70	Maximum response of elasto-plastic, one-degree-of-freedom system for bilinear-triangular pulse ($C_1 = 0.100, C_2 = 1.7$)	3-128
3-71	Maximum response of elasto-plastic, one-degree-of-freedom system for bilinear-triangular pulse ($C_1 = 0.056, C_2 = 1.7$)	3-129
3-72	Maximum response of elasto-plastic, one-degree-of-freedom system for bilinear-triangular pulse ($C_1 = 0.032, C_2 = 1.7$)	3-130
3-73	Maximum response of elasto-plastic, one-degree-of-freedom system for bilinear-triangular pulse ($C_1 = 0.018, C_2 = 1.7$)	3-131
3-74	Maximum response of elasto-plastic, one-degree-of-freedom system for bilinear-triangular pulse ($C_1 = 0.010, C_2 = 1.7$)	3-132
3-75	Maximum response of elasto-plastic, one-degree-of-freedom system for bilinear-triangular pulse ($C_1 = 0.681, C_2 = 3.0$)	3-133
3-76	Maximum response of elasto-plastic, one-degree-of-freedom system for bilinear-triangular pulse ($C_1 = 0.464, C_2 = 3.0$)	3-134
3-77	Maximum response of elasto-plastic, one-degree-of-freedom system for bilinear-triangular pulse ($C_1 = 0.316, C_2 = 3.0$)	3-135
3-78	Maximum response of elasto-plastic, one-degree-of-freedom system for bilinear-triangular pulse ($C_1 = 0.215, C_2 = 3.0$)	3-136
3-79	Maximum response of elasto-plastic, one-degree-of-freedom system for bilinear-triangular pulse ($C_1 = 0.147, C_2 = 3.0$)	3-137
3-80	Maximum response of elasto-plastic, one-degree-of-freedom system for bilinear-triangular pulse ($C_1 = 0.100, C_2 = 3.0$)	3-138
3-81	Maximum response of elasto-plastic, one-degree-of-freedom system for bilinear-triangular pulse ($C_1 = 0.056, C_2 = 3.0$)	3-139
3-82	Maximum response of elasto-plastic, one-degree-of-freedom system for bilinear-triangular pulse ($C_1 = 0.032, C_2 = 3.0$)	3-140
3-83	Maximum response of elasto-plastic, one-degree-of-freedom system for bilinear-triangular pulse ($C_1 = 0.018, C_2 = 3.0$)	3-141
3-84	Maximum response of elasto-plastic, one-degree-of-freedom system for bilinear-triangular pulse ($C_1 = 0.010, C_2 = 3.0$)	3-142
3-85	Maximum response of elasto-plastic, one-degree-of-freedom system for bilinear-triangular pulse ($C_1 = 0.750, C_2 = 5.5$)	3-143
3-86	Maximum response of elasto-plastic, one-degree-of-freedom system for bilinear-triangular pulse ($C_1 = 0.562, C_2 = 5.5$)	3-144
3-87	Maximum response of elasto-plastic, one-degree-of-freedom system for bilinear-triangular pulse ($C_1 = 0.422, C_2 = 5.5$)	3-145
3-88	Maximum response of elasto-plastic, one-degree-of-freedom system for bilinear-triangular pulse ($C_1 = 0.316, C_2 = 5.5$)	3-146
3-89	Maximum response of elasto-plastic, one-degree-of-freedom system for bilinear-triangular pulse ($C_1 = 0.237, C_2 = 5.5$)	3-147
3-90	Maximum response of elasto-plastic, one-degree-of-freedom system for bilinear-triangular pulse ($C_1 = 0.178, C_2 = 5.5$)	3-148
3-91	Maximum response of elasto-plastic, one-degree-of-freedom system for bilinear-triangular pulse ($C_1 = 0.133, C_2 = 5.5$)	3-149

3-92	Maximum response of elasto-plastic, one-degree-of-freedom system for bilinear-triangular pulse ($C_1 = 0.100, C_2 = 5.5$)	3-150
3-93	Maximum response of elasto-plastic, one-degree-of-freedom system for bilinear-triangular pulse ($C_1 = 0.068, C_2 = 5.5$)	3-151
3-94	Maximum response of elasto-plastic, one-degree-of-freedom system for bilinear-triangular pulse ($C_1 = 0.046, C_2 = 5.5$)	3-152
3-95	Maximum response of elasto-plastic, one-degree-of-freedom system for bilinear-triangular pulse ($C_1 = 0.032, C_2 = 5.5$)	3-153
3-96	Maximum response of elasto-plastic, one-degree-of-freedom system for bilinear-triangular pulse ($C_1 = 0.022, C_2 = 5.5$)	3-154
3-97	Maximum response of elasto-plastic, one-degree-of-freedom system for bilinear-triangular pulse ($C_1 = 0.015, C_2 = 6.$)	3-155
3-98	Maximum response of elasto-plastic, one-degree-of-freedom system for bilinear-triangular pulse ($C_1 = 0.010, C_2 = 6.$)	3-156
3-99	Maximum response of elasto-plastic, one-degree-of-freedom system for bilinear-triangular pulse ($C_1 = 0.750, C_2 = 10.$)	3-157
3-100	Maximum response of elasto-plastic, one-degree-of-freedom system for bilinear-triangular pulse ($C_1 = 0.648, C_2 = 10.$)	3-158
3-101	Maximum response of elasto-plastic, one-degree-of-freedom system for bilinear-triangular pulse ($C_1 = 0.562, C_2 = 10.$)	3-159
3-102	Maximum response of elasto-plastic, one-degree-of-freedom system for bilinear-triangular pulse ($C_1 = 0.422, C_2 = 10.$)	3-160
3-103	Maximum response of elasto-plastic, one-degree-of-freedom system for bilinear-triangular pulse ($C_1 = 0.316, C_2 = 10.$)	3-161
3-104	Maximum response of elasto-plastic, one-degree-of-freedom system for bilinear-triangular pulse ($C_1 = 0.237, C_2 = 10.$)	3-162
3-105	Maximum response of elasto-plastic, one-degree-of-freedom system for bilinear-triangular pulse ($C_1 = 0.178, C_2 = 10.$)	3-163
3-106	Maximum response of elasto-plastic, one-degree-of-freedom system for bilinear-triangular pulse ($C_1 = 0.133, C_2 = 10.$)	3-164
3-107	Maximum response of elasto-plastic, one-degree-of-freedom system for bilinear-triangular pulse ($C_1 = 0.100, C_2 = 10.$)	3-165
3-108	Maximum response of elasto-plastic, one-degree-of-freedom system for bilinear-triangular pulse ($C_1 = 0.068, C_2 = 10.$)	3-166
3-109	Maximum response of elasto-plastic, one-degree-of-freedom system for bilinear-triangular pulse ($C_1 = 0.046, C_2 = 10.$)	3-167
3-110	Maximum response of elasto-plastic, one-degree-of-freedom system for bilinear-triangular pulse ($C_1 = 0.032, C_2 = 10.$)	3-168
3-111	Maximum response of elasto-plastic, one-degree-of-freedom system for bilinear-triangular pulse ($C_1 = 0.022, C_2 = 10.$)	3-169
3-112	Maximum response of elasto-plastic, one-degree-of-freedom system for bilinear-triangular pulse ($C_1 = 0.015, C_2 = 10.$)	3-170
3-113	Maximum response of elasto-plastic, one-degree-of-freedom system for bilinear-triangular pulse ($C_1 = 0.010, C_2 = 10.$)	3-171
3-114	Maximum response of elasto-plastic, one-degree-of-freedom system for bilinear-triangular pulse ($C_1 = 0.909, C_2 = 30.$)	3-172
3-115	Maximum response of elasto-plastic, one-degree-of-freedom system for bilinear-triangular pulse ($C_1 = 0.866, C_2 = 30.$)	3-173
3-116	Maximum response of elasto-plastic, one-degree-of-freedom system for bilinear-triangular pulse ($C_1 = 0.825, C_2 = 30.$)	3-174
3-117	Maximum response of elasto-plastic, one-degree-of-freedom system for bilinear-triangular pulse ($C_1 = 0.750, C_2 = 30.$)	3-175
3-118	Maximum response of elasto-plastic, one-degree-of-freedom system for bilinear-triangular pulse ($C_1 = 0.715, C_2 = 30.$)	3-176

3-119	Maximum response of elasto-plastic, one-degree-of-freedom system for bilinear-triangular pulse ($C_1 = 0.681, C_2 = 30.$)	3-177
3-120	Maximum response of elasto-plastic, one-degree-of-freedom system for bilinear-triangular pulse ($C_1 = 0.648, C_2 = 30.$)	3-178
3-121	Maximum response of elasto-plastic, one-degree-of-freedom system for bilinear-triangular pulse ($C_1 = 0.619, C_2 = 30.$)	3-179
3-122	Maximum response of elasto-plastic, one-degree-of-freedom system for bilinear-triangular pulse ($C_1 = 0.562, C_2 = 30.$)	3-180
3-123	Maximum response of elasto-plastic, one-degree-of-freedom system for bilinear-triangular pulse ($C_1 = 0.511, C_2 = 30.$)	3-181
3-124	Maximum response of elasto-plastic, one-degree-of-freedom system for bilinear-triangular pulse ($C_1 = 0.464, C_2 = 30.$)	3-182
3-125	Maximum response of elasto-plastic, one-degree-of-freedom system for bilinear-triangular pulse ($C_1 = 0.383, C_2 = 30.$)	3-183
3-126	Maximum response of elasto-plastic, one-degree-of-freedom system for bilinear-triangular pulse ($C_1 = 0.316, C_2 = 30.$)	3-184
3-127	Maximum response of elasto-plastic, one-degree-of-freedom system for bilinear-triangular pulse ($C_1 = 0.261, C_2 = 30.$)	3-185
3-128	Maximum response of elasto-plastic, one-degree-of-freedom system for bilinear-triangular pulse ($C_1 = 0.215, C_2 = 30.$)	3-186
3-129	Maximum response of elasto-plastic, one-degree-of-freedom system for bilinear-triangular pulse ($C_1 = 0.178, C_2 = 30.$)	3-187
3-130	Maximum response of elasto-plastic, one-degree-of-freedom system for bilinear-triangular pulse ($C_1 = 0.147, C_2 = 30.$)	3-188
3-131	Maximum response of elasto-plastic, one-degree-of-freedom system for bilinear-triangular pulse ($C_1 = 0.121, C_2 = 30.$)	3-189
3-132	Maximum response of elasto-plastic, one-degree-of-freedom system for bilinear-triangular pulse ($C_1 = 0.100, C_2 = 30.$)	3-190
3-133	Maximum response of elasto-plastic, one-degree-of-freedom system for bilinear-triangular pulse ($C_1 = 0.075, C_2 = 30.$)	3-191
3-134	Maximum response of elasto-plastic, one-degree-of-freedom system for bilinear-triangular pulse ($C_1 = 0.056, C_2 = 30.$)	3-192
3-135	Maximum response of elasto-plastic, one-degree-of-freedom system for bilinear-triangular pulse ($C_1 = 0.042, C_2 = 30.$)	3-193
3-136	Maximum response of elasto-plastic, one-degree-of-freedom system for bilinear-triangular pulse ($C_1 = 0.032, C_2 = 30.$)	3-194
3-137	Maximum response of elasto-plastic, one-degree-of-freedom system for bilinear-triangular pulse ($C_1 = 0.026, C_2 = 30.$)	3-195
3-138	Maximum response of elasto-plastic, one-degree-of-freedom system for bilinear-triangular pulse ($C_1 = 0.018, C_2 = 30.$)	3-196
3-139	Maximum response of elasto-plastic, one-degree-of-freedom system for bilinear-triangular pulse ($C_1 = 0.013, C_2 = 30.$)	3-197
3-140	Maximum response of elasto-plastic, one-degree-of-freedom system for bilinear-triangular pulse ($C_1 = 0.010, C_2 = 30.$)	3-198
3-141	Maximum response of elasto-plastic, one-degree-of-freedom system for bilinear-triangular pulse ($C_1 = 0.909, C_2 = 100.$)	3-199
3-142	Maximum response of elasto-plastic, one-degree-of-freedom system for bilinear-triangular pulse ($C_1 = 0.866, C_2 = 100.$)	3-200
3-143	Maximum response of elasto-plastic, one-degree-of-freedom system for bilinear-triangular pulse ($C_1 = 0.825, C_2 = 100.$)	3-201
3-144	Maximum response of elasto-plastic, one-degree-of-freedom system for bilinear-triangular pulse ($C_1 = 0.787, C_2 = 100.$)	3-202
3-145	Maximum response of elasto-plastic, one-degree-of-freedom system for bilinear-triangular pulse ($C_1 = 0.750, C_2 = 100.$)	3-203

3-146 Maximum response of elasto-plastic, one-degree-of-freedom system for bilinear-triangular pulse ($C_1 = 0.715, C_2 = 100.$) 3-204

3-147 Maximum response of elasto-plastic, one-degree-of-freedom system for bilinear-triangular pulse ($C_1 = 0.681, C_2 = 100.$) 3-205

3-148 Maximum response of elasto-plastic, one-degree-of-freedom system for bilinear-triangular pulse ($C_1 = 0.648, C_2 = 100.$) 3-206

3-149 Maximum response of elasto-plastic, one-degree-of-freedom system for bilinear-triangular pulse ($C_1 = 0.619, C_2 = 100.$) 3-207

3-150 Maximum response of elasto-plastic, one-degree-of-freedom system for bilinear-triangular pulse ($C_1 = 0.590, C_2 = 100.$) 3-208

3-151 Maximum response of elasto-plastic, one-degree-of-freedom system for bilinear-triangular pulse ($C_1 = 0.562, C_2 = 100.$) 3-209

3-152 Maximum response of elasto-plastic, one-degree-of-freedom system for bilinear-triangular pulse ($C_1 = 0.511, C_2 = 100.$) 3-210

3-153 Maximum response of elasto-plastic, one-degree-of-freedom system for bilinear-triangular pulse ($C_1 = 0.464, C_2 = 100.$) 3-211

3-154 Maximum response of elasto-plastic, one-degree-of-freedom system for bilinear-triangular pulse ($C_1 = 0.422, C_2 = 100.$) 3-212

3-155 Maximum response of elasto-plastic, one-degree-of-freedom system for bilinear-triangular pulse ($C_1 = 0.365, C_2 = 100.$) 3-213

3-156 Maximum response of elasto-plastic, one-degree-of-freedom system for bilinear-triangular pulse ($C_1 = 0.316, C_2 = 100.$) 3-214

3-157 Maximum response of elasto-plastic, one-degree-of-freedom system for bilinear-triangular pulse ($C_1 = 0.274, C_2 = 100.$) 3-215

3-158 Maximum response of elasto-plastic, one-degree-of-freedom system for bilinear-triangular pulse ($C_1 = 0.261, C_2 = 100.$) 3-216

3-159 Maximum response of elasto-plastic, one-degree-of-freedom system for bilinear-triangular pulse ($C_1 = 0.237, C_2 = 100.$) 3-217

3-160 Maximum response of elasto-plastic, one-degree-of-freedom system for bilinear-triangular pulse ($C_1 = 0.215, C_2 = 100.$) 3-218

3-161 Maximum response of elasto-plastic, one-degree-of-freedom system for bilinear-triangular pulse ($C_1 = 0.178, C_2 = 100.$) 3-219

3-162 Maximum response of elasto-plastic, one-degree-of-freedom system for bilinear-triangular pulse ($C_1 = 0.147, C_2 = 100.$) 3-220

3-163 Maximum response of elasto-plastic, one-degree-of-freedom system for bilinear-triangular pulse ($C_1 = 0.121, C_2 = 100.$) 3-221

3-164 Maximum response of elasto-plastic, one-degree-of-freedom system for bilinear-triangular pulse ($C_1 = 0.100, C_2 = 100.$) 3-222

3-165 Maximum response of elasto-plastic, one-degree-of-freedom system for bilinear-triangular pulse ($C_1 = 0.075, C_2 = 100.$) 3-223

3-166 Maximum response of elasto-plastic, one-degree-of-freedom system for bilinear-triangular pulse ($C_1 = 0.056, C_2 = 100.$) 3-224

3-167 Maximum response of elasto-plastic, one-degree-of-freedom system for bilinear-triangular pulse ($C_1 = 0.042, C_2 = 100.$) 3-225

3-168 Maximum response of elasto-plastic, one-degree-of-freedom system for bilinear-triangular pulse ($C_1 = 0.032, C_2 = 100.$) 3-226

3-169 Maximum response of elasto-plastic, one-degree-of-freedom system for bilinear-triangular pulse ($C_1 = 0.026, C_2 = 100.$) 3-227

3-170 Maximum response of elasto-plastic, one-degree-of-freedom system for bilinear-triangular pulse ($C_1 = 0.018, C_2 = 100.$) 3-228

3-171 Maximum response of elasto-plastic, one-degree-of-freedom system for bilinear-triangular pulse ($C_1 = 0.013, C_2 = 100.$) 3-229

3-172 Maximum response of elasto-plastic, one-degree-of-freedom system for bilinear-triangular pulse ($C_1 = 0.010, C_2 = 100.$) 3-230

3-173	Maximum response of elasto-plastic, one-degree-of-freedom system for bilinear-triangular pulse ($C_1 = 0.909, C_2 = 300.$)	3-231
3-174	Maximum response of elasto-plastic, one-degree-of-freedom system for bilinear-triangular pulse ($C_1 = 0.866, C_2 = 300.$)	3-232
3-175	Maximum response of elasto-plastic, one-degree-of-freedom system for bilinear-triangular pulse ($C_1 = 0.825, C_2 = 300.$)	3-233
3-176	Maximum response of elasto-plastic, one-degree-of-freedom system for bilinear-triangular pulse ($C_1 = 0.787, C_2 = 300.$)	3-234
3-177	Maximum response of elasto-plastic, one-degree-of-freedom system for bilinear-triangular pulse ($C_1 = 0.750, C_2 = 300.$)	3-235
3-178	Maximum response of elasto-plastic, one-degree-of-freedom system for bilinear-triangular pulse ($C_1 = 0.715, C_2 = 300.$)	3-236
3-179	Maximum response of elasto-plastic, one-degree-of-freedom system for bilinear-triangular pulse. ($C_1 = 0.681, C_2 = 300.$)	3-237
3-180	Maximum response of elasto-plastic, one-degree-of-freedom system for bilinear-triangular pulse ($C_1 = 0.648, C_2 = 300.$)	3-238
3-181	Maximum response of elasto-plastic, one-degree-of-freedom system for bilinear-triangular pulse ($C_1 = 0.619, C_2 = 300.$)	3-239
3-182	Maximum response of elasto-plastic, one-degree-of-freedom system for bilinear-triangular pulse ($C_1 = 0.590, C_2 = 300.$)	3-240
3-183	Maximum response of elasto-plastic, one-degree-of-freedom system for bilinear-triangular pulse ($C_1 = 0.562, C_2 = 300.$)	3-241
3-184	Maximum response of elasto-plastic, one-degree-of-freedom system for bilinear-triangular pulse ($C_1 = 0.536, C_2 = 300.$)	3-242
3-185	Maximum response of elasto-plastic, one-degree-of-freedom system for bilinear-triangular pulse ($C_1 = 0.511, C_2 = 300.$)	3-243
3-186	Maximum response of elasto-plastic, one-degree-of-freedom system for bilinear-triangular pulse ($C_1 = 0.487, C_2 = 300.$)	3-244
3-187	Maximum response of elasto-plastic, one-degree-of-freedom system for bilinear-triangular pulse ($C_1 = 0.464, C_2 = 300.$)	3-245
3-188	Maximum response of elasto-plastic, one-degree-of-freedom system for bilinear-triangular pulse ($C_1 = 0.422, C_2 = 300.$)	3-246
3-189	Maximum response of elasto-plastic, one-degree-of-freedom system for bilinear-triangular pulse ($C_1 = 0.383, C_2 = 300.$)	3-247
3-190	Maximum response of elasto-plastic, one-degree-of-freedom system for bilinear-triangular pulse ($C_1 = 0.365, C_2 = 300.$)	3-248
3-191	Maximum response of elasto-plastic, one-degree-of-freedom system for bilinear-triangular pulse ($C_1 = 0.348, C_2 = 300.$)	3-249
3-192	Maximum response of elasto-plastic, one-degree-of-freedom system for bilinear-triangular pulse ($C_1 = 0.316, C_2 = 300.$)	3-250
3-193	Maximum response of elasto-plastic, one-degree-of-freedom system for bilinear-triangular pulse ($C_1 = 0.287, C_2 = 300.$)	3-251
3-194	Maximum response of elasto-plastic, one-degree-of-freedom system for bilinear-triangular pulse ($C_1 = 0.274, C_2 = 300.$)	3-252
3-195	Maximum response of elasto-plastic, one-degree-of-freedom system for bilinear-triangular pulse ($C_1 = 0.261, C_2 = 300.$)	3-253
3-196	Maximum response of elasto-plastic, one-degree-of-freedom system for bilinear-triangular pulse ($C_1 = 0.237, C_2 = 300.$)	3-254
3-197	Maximum response of elasto-plastic, one-degree-of-freedom system for bilinear-triangular pulse ($C_1 = 0.215, C_2 = 300.$)	3-255
3-198	Maximum response of elasto-plastic, one-degree-of-freedom system for bilinear-triangular pulse ($C_1 = 0.198, C_2 = 300.$)	3-256
3-199	Maximum response of elasto-plastic, one-degree-of-freedom system for bilinear-triangular pulse ($C_1 = 0.178, C_2 = 300.$)	3-257

3-200	Maximum response of elasto-plastic, one-degree-of-freedom system for bilinear-triangular pulse ($C_1 = 0.162, C_2 = 300.$)	3-258
3-201	Maximum response of elasto-plastic, one-degree-of-freedom system for bilinear-triangular pulse ($C_1 = 0.147, C_2 = 300.$)	3-259
3-202	Maximum response of elasto-plastic, one-degree-of-freedom system for bilinear-triangular pulse ($C_1 = 0.133, C_2 = 300.$)	3-260
3-203	Maximum response of elasto-plastic, one-degree-of-freedom system for bilinear-triangular pulse ($C_1 = 0.121, C_2 = 300.$)	3-261
3-204	Maximum response of elasto-plastic, one-degree-of-freedom system for bilinear-triangular pulse ($C_1 = 0.110, C_2 = 300.$)	3-262
3-205	Maximum response of elasto-plastic, one-degree-of-freedom system for bilinear-triangular pulse ($C_1 = 0.100, C_2 = 300.$)	3-263
3-206	Maximum response of elasto-plastic, one-degree-of-freedom system for bilinear-triangular pulse ($C_1 = 0.091, C_2 = 300.$)	3-264
3-207	Maximum response of elasto-plastic, one-degree-of-freedom system for bilinear-triangular pulse ($C_1 = 0.083, C_2 = 300.$)	3-265
3-208	Maximum response of elasto-plastic, one-degree-of-freedom system for bilinear-triangular pulse ($C_1 = 0.075, C_2 = 300.$)	3-266
3-209	Maximum response of elasto-plastic, one-degree-of-freedom system for bilinear-triangular pulse ($C_1 = 0.068, C_2 = 300.$)	3-267
3-210	Maximum response of elasto-plastic, one-degree-of-freedom system for bilinear-triangular pulse ($C_1 = 0.056, C_2 = 300.$)	3-268
3-211	Maximum response of elasto-plastic, one-degree-of-freedom system for bilinear-triangular pulse ($C_1 = 0.046, C_2 = 300.$)	3-269
3-212	Maximum response of elasto-plastic, one-degree-of-freedom system for bilinear-triangular pulse ($C_1 = 0.042, C_2 = 300.$)	3-270
3-213	Maximum response of elasto-plastic, one-degree-of-freedom system for bilinear-triangular pulse ($C_1 = 0.032, C_2 = 300.$)	3-271
3-214	Maximum response of elasto-plastic, one-degree-of-freedom system for bilinear-triangular pulse ($C_1 = 0.026, C_2 = 300.$)	3-272
3-215	Maximum response of elasto-plastic, one-degree-of-freedom system for bilinear-triangular pulse ($C_1 = 0.022, C_2 = 300.$)	3-273
3-216	Maximum response of elasto-plastic, one-degree-of freedom system for bilinear-triangular pulse ($C_1 = 0.018, C_2 = 300.$)	3-274
3-217	Maximum response of elasto-plastic, one-degree-of-freedom system for bilinear-triangular pulse ($C_1 = 0.015, C_2 = 300.$)	3-275
3-218	Maximum response of elasto-plastic, one-degree-of-freedom system for bilinear-triangular pulse ($C_1 = 0.013, C_2 = 300.$)	3-276
3-219	Maximum response of elasto-plastic, one-degree-of-freedom system for bilinear-triangular pulse ($C_1 = 0.010, C_2 = 300.$)	3-277
3-220	Maximum response of elasto-plastic, one-degree-of-freedom system for bilinear-triangular pulse ($C_1 = 0.909, C_2 = 1000.$)	3-278
3-221	Maximum response of elasto-plastic, one-degree-of-freedom system for bilinear-triangular pulse ($C_1 = 0.866, C_2 = 1000.$)	3-279
3-222	Maximum response of elasto-plastic, one-degree-of-freedom system for bilinear-triangular pulse ($C_1 = 0.825, C_2 = 1000.$)	3-280
3-223	Maximum response of elasto-plastic, one-degree-of-freedom system for bilinear-triangular pulse ($C_1 = 0.787, C_2 = 1000.$)	3-281
3-224	Maximum response of elasto-plastic, one-degree-of-freedom system for bilinear-triangular pulse ($C_1 = 0.750, C_2 = 1000.$)	3-282
3-225	Maximum response of elasto-plastic, one-degree-of-freedom system for bilinear-triangular pulse ($C_1 = 0.715, C_2 = 1000.$)	3-283
3-226	Maximum response of elasto-plastic, one-degree-of-freedom system for bilinear-triangular pulse ($C_1 = 0.681, C_2 = 1000.$)	3-284

3-227	Maximum response of elasto-plastic, one-degree-of-freedom system for bilinear-triangular pulse ($C_1 = 0.648, C_2 = 1000.$)	3-285
3-228	Maximum response of elasto-plastic, one-degree-of-freedom system for bilinear-triangular pulse ($C_1 = 0.619, C_2 = 1000.$)	3-286
3-229	Maximum response of elasto-plastic, one-degree-of-freedom system for bilinear-triangular pulse ($C_1 = 0.590, C_2 = 1000.$)	3-287
3-230	Maximum response of elasto-plastic, one-degree-of-freedom system for bilinear-triangular pulse ($C_1 = 0.562, C_2 = 1000.$)	3-288
3-231	Maximum response of elasto-plastic, one-degree-of-freedom system for bilinear-triangular pulse ($C_1 = 0.536, C_2 = 1000.$)	3-289
3-232	Maximum response of elasto-plastic, one-degree-of-freedom system for bilinear-triangular pulse ($C_1 = 0.511, C_2 = 1000.$)	3-290
3-233	Maximum response of elasto-plastic, one-degree-of-freedom system for bilinear-triangular pulse ($C_1 = 0.487, C_2 = 1000.$)	3-291
3-234	Maximum response of elasto-plastic, one-degree-of-freedom system for bilinear-triangular pulse ($C_1 = 0.464, C_2 = 1000.$)	3-292
3-235	Maximum response of elasto-plastic, one-degree-of-freedom system for bilinear-triangular pulse ($C_1 = 0.422, C_2 = 1000.$)	3-293
3-236	Maximum response of elasto-plastic, one-degree-of-freedom system for bilinear-triangular pulse ($C_1 = 0.383, C_2 = 1000.$)	3-294
3-237	Maximum response of elasto-plastic, one-degree-of-freedom system for bilinear-triangular pulse ($C_1 = 0.365, C_2 = 1000.$)	3-295
3-238	Maximum response of elasto-plastic, one-degree-of-freedom system for bilinear-triangular pulse ($C_1 = 0.348, C_2 = 1000.$)	3-296
3-239	Maximum response of elasto-plastic, one-degree-of-freedom system for bilinear-triangular pulse ($C_1 = 0.316, C_2 = 1000.$)	3-297
3-240	Maximum response of elasto-plastic, one-degree-of-freedom system for bilinear-triangular pulse ($C_1 = 0.287, C_2 = 1000.$)	3-298
3-241	Maximum response of elasto-plastic, one-degree-of-freedom system for bilinear-triangular pulse ($C_1 = 0.274, C_2 = 1000.$)	3-299
3-242	Maximum response of elasto-plastic, one-degree-of-freedom system for bilinear-triangular pulse ($C_1 = 0.261, C_2 = 1000.$)	3-300
3-243	Maximum response of elasto-plastic, one-degree-of-freedom system for bilinear-triangular pulse ($C_1 = 0.237, C_2 = 1000.$)	3-301
3-244	Maximum response of elasto-plastic, one-degree-of-freedom system for bilinear-triangular pulse ($C_1 = 0.215, C_2 = 1000.$)	3-302
3-245	Maximum response of elasto-plastic, one-degree-of-freedom system for bilinear-triangular pulse ($C_1 = 0.198, C_2 = 1000.$)	3-303
3-246	Maximum response of elasto-plastic, one-degree-of-freedom system for bilinear-triangular pulse ($C_1 = 0.178, C_2 = 1000.$)	3-304
3-247	Maximum response of elasto-plastic, one-degree-of-freedom system for bilinear-triangular pulse ($C_1 = 0.162, C_2 = 1000.$)	3-305
3-248	Maximum response of elasto-plastic, one-degree-of-freedom system for bilinear-triangular pulse ($C_1 = 0.147, C_2 = 1000.$)	3-306
3-249	Maximum response of elasto-plastic, one-degree-of-freedom system for bilinear-triangular pulse ($C_1 = 0.133, C_2 = 1000.$)	3-307
3-250	Maximum response of elasto-plastic, one-degree-of-freedom system for bilinear-triangular pulse ($C_1 = 0.121, C_2 = 1000.$)	3-308
3-251	Maximum response of elasto-plastic, one-degree-of-freedom system for bilinear-triangular pulse ($C_1 = 0.110, C_2 = 1000.$)	3-309
3-252	Maximum response of elasto-plastic, one-degree-of-freedom system for bilinear-triangular pulse ($C_1 = 0.100, C_2 = 1000.$)	3-310
3-253	Maximum response of elasto-plastic, one-degree-of-freedom system for bilinear-triangular pulse ($C_1 = 0.091, C_2 = 1000.$)	3-311

3-254	Maximum response of elasto-plastic, one-degree-of-freedom system for bilinear-triangular pulse ($C_1 = 0.083, C_2 = 1000.$)	3-312
3-255	Maximum response of elasto-plastic, one-degree-of-freedom system for bilinear-triangular pulse ($C_1 = 0.075, C_2 = 1000.$)	3-313
3-256	Maximum response of elasto-plastic, one-degree-of-freedom system for bilinear-triangular pulse ($C_1 = 0.068, C_2 = 1000.$)	3-314
3-257	Maximum response of elasto-plastic, one-degree-of-freedom system for bilinear-triangular pulse ($C_1 = 0.056, C_2 = 1000.$)	3-315
3-258	Maximum response of elasto-plastic, one-degree-of-freedom system for bilinear-triangular pulse ($C_1 = 0.046, C_2 = 1000.$)	3-316
3-259	Maximum response of elasto-plastic, one-degree-of-freedom system for bilinear-triangular pulse ($C_1 = 0.042, C_2 = 1000.$)	3-317
3-260	Maximum response of elasto-plastic, one-degree-of-freedom system for bilinear-triangular pulse ($C_1 = 0.032, C_2 = 1000.$)	3-318
3-261	Maximum response of elasto-plastic, one-degree-of-freedom system for bilinear-triangular pulse ($C_1 = 0.026, C_2 = 1000.$)	3-319
3-262	Maximum response of elasto-plastic, one-degree-of-freedom system for bilinear-triangular pulse ($C_1 = 0.022, C_2 = 1000.$)	3-320
3-263	Maximum response of elasto-plastic, one-degree-of-freedom system for bilinear-triangular pulse ($C_1 = 0.018, C_2 = 1000.$)	3-321
3-264	Maximum response of elasto-plastic, one-degree-of-freedom system for bilinear-triangular pulse ($C_1 = 0.015, C_2 = 1000.$)	3-322
3-265	Maximum response of elasto-plastic, one-degree-of-freedom system for bilinear-triangular pulse ($C_1 = 0.013, C_2 = 1000.$)	3-323
3-266	Maximum response of elasto-plastic, one-degree-of-freedom system for bilinear-triangular pulse ($C_1 = 0.010, C_2 = 1000.$)	3-324
3-267	Graphical interpolation	3-325
3-268	Elastic rebound of simple spring-mass system	3-326
3-269	Pressure-time and resistance-time curves for elements which respond to impulse	3-327
4-1	Typical resistance-deflection curve for flexural response of concrete elements	4-9
4-2	Single leg stirrups	4-10
4-3	Lacing reinforcement	4-11
4-4	Typical resistance-deflection curve for tension membrane response of concrete	4-12
4-5	Typical laced wall	4-13
4-6	Failure of a laced element	4-14
4-7	Failure of an unlaced element	4-15
4-8	Typical stress-strain curves for concrete and reinforcing steel	4-22
4-9	Design curve for DIF for ultimate compressive strength of concrete	4-23
4-10	Design curve for DIF for yield stress of ASTM A 615 grade 60 reinforcing steel	4-24
4-11	Coefficient for moment of inertia of cracked sections with tension reinforcement only	4-30
4-12	Coefficient for moment of inertia of cracked sections with equal reinforcement on opposite faces	4-31
4-13	Typical reinforced concrete cross sections	4-46
4-14	Location of critical sections for diagonal tension	4-47
4-15	Angle of inclination of lacing bars	4-48
4-16	Geometry for standard hooked reinforcement	4-49
4-17	Relationship between design parameters for unlaced elements	4-63
4-18	Idealized resistance-deflection curve for large deflections	4-64

4-19 Determination of ultimate shears 4-65

4-20 Typical flat slab structure 4-84

4-21 Relationship between design parameters for flat slabs 4-85

4-22 Unit moments 4-86

4-23 Typical resistance-deflection functions for flat slabs 4-87

4-24 Yield line pattern for multi-panel flat slab 4-88

4-25 Quarter panel of flat slab 4-89

4-26 Dynamic resistance-deflection curve 4-90

4-27 Critical locations for shear stresses 4-91

4-28 Typical column loads 4-92

4-29 Relationship between design parameters for laced elements 4-108

4-30 Impulse coefficient C_1 for an element with two adjacent edges fixed and two edges free 4-109

4-31 Impulse coefficient C_1 for an element with three edges fixed and one edge free 4-110

4-32 Impulse coefficient C_1 for an element with four edges fixed 4-111

4-33 Impulse coefficient C_u for an element with two adjacent edges fixed and two edges free 4-112

4-34 Impulse coefficient C_u for an element with three edges fixed and one edge free 4-113

4-35 Impulse coefficient C_u for an element with four edges fixed 4-114

4-36 Determination of optimum ratio of p_v/p_H for maximum impulse capacity 4-115

4-37 Optimum ratio of p_v/p_H for maximum capacity at partial failure deflection, X_1 4-116

4-38 Optimum ratio of p_v/p_H for maximum capacity at incipient failure, X_u 4-117

4-39 Vertical shear coefficients for ultimate shear stress at distance d_c from the support (cross section type II and III) 4-118

4-40 Horizontal shear coefficients for ultimate shear stress at distance d_c from the support (cross section type II and III) 4-119

4-41 Vertical shear parameters for ultimate shear stress at distance d_c from the support (cross section type II and III) 4-120

4-42 Vertical shear coefficient ratios for ultimate shear stress at distance d_c from the support (cross section type II and III) 4-121

4-43 Horizontal shear parameters for ultimate shear stress at distance d_c from the support (cross section type II and III) 4-122

4-44 Horizontal shear coefficient ratios for ultimate shear stress at distance d_c from the support (cross section type II and III) 4-123

4-45 Vertical shear parameters for ultimate shear stress at distance d_c from the support (cross section type II and III) 4-124

4-46 Vertical shear coefficient ratios for ultimate shear stress at distance d_c from the support (cross section type II and III) 4-125

4-47 Horizontal shear parameters for ultimate shear stress at distance d_c from the support (cross section type II and III) 4-126

4-48 Horizontal shear coefficient ratios for ultimate shear stress at distance d_c from the support (cross section type II and III) 4-127

4-49 Vertical shear parameters for ultimate shear stress at distance d_c from the support (cross section type II and III) 4-128

4-50 Vertical shear coefficient ratios for ultimate shear stress at distance d_c from the support (cross section type II and III) 4-129

4-51 Horizontal shear parameters for ultimate shear stress at distance d_c from the support (cross section type II and III) 4-130

4-52 Horizontal shear coefficient ratios for ultimate shear stress at distance d_c from the support (cross section type II and III) 4-131

4-53	Shear coefficients for ultimate support shear (cross section type II and III)	4-132
4-54	Shear coefficients for ultimate support shear (cross section type II and III)	4-133
4-55	Shear coefficients for ultimate support shear (cross section type II and III)	4-134
4-56	Shear coefficients for ultimate support shear (cross section type II and III)	4-135
4-57	Attenuation of blast impulse in sand and concrete, $w_s = 85$ pcf	4-147
4-58	Attenuation of blast impulse in sand and concrete, $w_s = 100$ pcf	4-148
4-59	Relationship between design parameters for beams	4-164
4-60	Arrangement of reinforcement for combined flexure and torsion	4-165
4-61	Column interaction diagram	4-178
4-62	Typical interior column sections	4-179
4-63	Direct spalled element	4-192
4-64	Scabbed element	4-193
4-65	Spall threshold for blast waves loading walls	4-194
4-66	Unspalled panel of composite panel	4-195
4-67	Shielding systems for protection against concrete fragments	4-196
4-68	Rigid attachment of fragment shield to barrier	4-197
4-69	Failure of an unlaced element	4-198
4-70	Failure at plastic hinges of laced elements	4-199
4-71	Backwall failure of cubicle with laced reinforcement	4-200
4-72	Idealized curves for determination of post-failure fragment velocities	4-201
4-73	Post-failure coefficient C_f for an element fixed on two adjacent edges and two edges free	4-202
4-74	Post-failure coefficient C_f for an element fixed on three edges and one edge free	4-203
4-75	Post-failure coefficient C_f for an element fixed on four edges	4-204
4-76	Perforation and spalling of concrete due to primary fragments	4-212
4-77	Shape of standard primary fragments	4-213
4-78	Concrete penetration chart for armor-piercing steel fragments	4-214
4-79	Residual fragment velocity upon perforation of concrete barriers (for cases where $x < 2d$)	4-215
4-80	Residual fragment velocity upon perforation of: (1) Concrete barriers (for cases where $x > 2d$) (2) Sand layers	4-216
4-81	Depth of penetration into sand by standard primary fragments	4-217
4-82	Typical flexural reinforcement splice pattern for close-in effects	4-234
4-83	Typical section through conventionally reinforced concrete wall	4-235
4-84	Floor slab-wall intersections	4-236
4-85	Typical horizontal corner details of conventionally reinforced concrete walls	4-237
4-86	Preferred location of lap splices for a two-way element fixed on four edges	4-238
4-87	Splice locations for multi-span slab	4-239
4-88	Section through column of flat slab	4-240
4-89	Laced reinforced element	4-241
4-90	Typical lacing bend details	4-242
4-91	Typical methods of lacing	4-243
4-92	Typical location of continuous and discontinuous lacing	4-244
4-93	Typical details for splicing of lacing bars	4-245
4-94	Length of lacing bars	4-246
4-95	Reinforcement details of laced concrete walls	4-247

4-96	Typical detail at intersection of two continuous laced walls . . .	4-248
4-97	Typical detail at intersection of continuous and discontinuous laced walls	4-249
4-98	Typical detail at corner of laced walls	4-250
4-99	Intersection of continuous and discontinuous laced walls without wall extensions	4-251
4-100	Corner details for laced walls without wall extensions	4-252
4-101	Element reinforced with single leg stirrups	4-253
4-102	Typical detail at corner for walls reinforced with single leg stirrups	4-254
4-103	Reinforcement detail of wall with single leg stirrups	4-255
4-104	Typical composite wall details	4-256
4-105	Typical single-cell structures	4-257
4-106	Typical multicubicle structures	4-258
4-107	Pouring sequence	4-259
5-1	Typical stress-strain curves for steel.	5-12
5-2	Dynamic increase factors for yield stresses at various strain rates for ASTM A-36 and A-514 steels.	5-13
5-3	Member end rotations for beams and frames.	5-23
5-4	Relationships between design parameters for beams.	5-24
5-5	Relationships between design parameters for plates.	5-25
5-6	Theoretical stress distribution for pure bending at various stages of dynamic loading.	5-35
5-7	Moment-curvature diagram for simple-supported, dynamically loaded, I-shaped beams.	5-36
5-8	Values of β for use in equations 5-20 and 5-21.	5-37
5-9	Typical lateral bracing details.	5-38
5-10	Moment-curvature diagram for dynamically loaded plates and rectangular cross section beams.	5-41
5-11	Biaxial bending of a doubly-symmetric section.	5-42
5-12	Resistance-deflection curve for a typical cold-formed section.	5-55
5-13	Elastic rebound of single-degree-of-freedom system.	5-56
5-14	Allowable dynamic (design) shear stresses for webs of cold-	5-57
5-15	Maximum end support reaction for cold-formed steel sections	5-58
5-16	Maximum interior support reaction for cold-formed steel	5-59
5-17	Gasket detail for blast door.	5-69
5-18	Built-up double-leaf blast door with frame built into concrete.	5-70
5-19	Horizontal sliding blast door.	5-71
5-20	Single-leaf blast door with fragment shield (very high pressure).	5-72
5-21	Single-leaf blast door (high pressure).	5-73
5-22	Bilinear blast load and single-degree-of-freedom response for determining rebound resistance.	5-74
5-23	Orientation of roof purlins with respect to blast load direction for frame blast loading.	5-89
5-24	Estimates of peak shears and axial loads in rigid frames due to horizontal loads.	5-90
5-25	Estimates of peak shears and axial loads in braced frames due to horizontal loads.	5-91
5-26	Corner connection behavior.	5-100
5-27	Typical connections for cold-formed steel panels.	5-101
5-28	Steel penetration design chart - AP steel fragments penetrating mild steel plates.	5-104
5-29	Steel penetration design chart - mild steel fragments penetrating mild steel plates.	5-105

5-30	Residual fragment velocity upon perforation of steel barriers. . .	5-106
5-31	Typical framing plan for a single-story blast-resistant steel structure.	5-109
5-32	Typical framing detail at interior Column 2-C.	5-110
5-33	Typical framing detail at end Column 1-C.	5-111
5-34	Typical framing detail at side column 2-D.	5-112
5-35	Typical framing detail at corner Column 1-D.	5-113
5-36	Typical details for cold-formed, light gage steel paneling. . . .	5-114
5-37	Typical welded connections for attaching cold-formed steel panels to supporting members.	5-115
5-38	Typical bolted connections for attaching cold-formed steel panels to supporting members.	5-116
5-39	Details of typical fasteners for cold-formed steel panels. . . .	5-117
5-40	Single-leaf blast door installed in a steel structure.	5-118
5-41	Double-leaf blast door installed in a concrete structure.	5-119
5-42	Compression-arch and tension-arch blast doors.	5-120
6-1	Masonry wall with flexible support	6-14
6-2	Masonry wall with rigid support	6-15
6-3	Concrete masonry walls	6-16
6-4	Typical joint reinforced masonry construction	6-17
6-5	Special masonry unit for use with reinforcing bars	6-18
6-6	Arching action of non-reinforced masonry wall	6-19
6-7	Typical concrete masonry units	6-20
6-8	Connection details for rebound and/or negative overpressures . . .	6-21
6-9	Deflection of non-reinforced masonry walls	6-22
6-10	Structural behavior of non-reinforced solid masonry panel with rigid supports	6-23
6-11	Common precast elements	6-36
6-12	Typical stress-strain curve for high strength wire	6-37
6-13	Roof slab-to-girder connection	6-38
6-14	Typical wall panel-to-roof slab connection	6-39
6-15	Wall panel-to foundation connection	6-40
6-16	Typical panel splice	6-41
6-17	General layout of pre-engineered building	6-53
6-18	Recommended pre-engineered building design loads	6-54
6-19a	General configuration of suppressive shield groups	6-62
6-19b	General configuration of suppressive shield groups (continued) . . .	6-63
6-20	Typical utility penetration	6-64
6-21	Typical location of utility penetration in shield groups 4, 5, and 81 mm	6-65
6-22	Typical location of utility penetrations in shield group 3	6-66
6-23	Typical vacuum line penetration	6-67
6-24	Sliding personnel door	6-68
6-25	Door - group 3 shield	6-69
6-26	Rotating product door	6-70
6-27	Characteristic Parameters for Glass Pane, Blast Loading, Resistance Function and Response Model	6-83
6-28	Peak Blast Pressure Capacity for Tempered Glass Panes (a/b = 1.00, t = 1/4 and 5/16 in)	6-84
6-29	Peak Blast Pressure Capacity for Tempered Glass Panes (a/b = 1.00, t = 3/8 and 1/2 in)	6-85
6-30	Peak Blast Pressure Capacity for Tempered Glass Panes (a/b = 1.00, t = 5/8 and 3/4 in)	6-86

6-31	Peak Blast Pressure Capacity for Tempered Glass Panes (a/b = 1.25, t = 1/4 and 5/16 in)	6-87
6-32	Peak Blast Pressure Capacity for Tempered Glass Panes (a/b = 1.25, t = 3/8 and 1/2 in)	6-88
6-33	Peak Blast Pressure Capacity for Tempered Glass Panes (a/b = 1.25, t = 5/8 and 3/4 in)	6-89
6-34	Peak Blast Pressure Capacity for Tempered Glass Panes (a/b = 1.50, t = 1/4 and 5/16 in)	6-90
6-35	Peak Blast Pressure Capacity for Tempered Glass Panes (a/b = 1.50, t = 3/8 and 1/2 in)	6-91
6-36	Peak Blast Pressure Capacity for Tempered Glass Panes (a/b = 1.50, t = 5/8 and 3/4 in)	6-92
6-37	Peak Blast Pressure Capacity for Tempered Glass Panes (a/b = 1.75, t = 1/4 and 5/16 in)	6-93
6-38	Peak Blast Pressure Capacity for Tempered Glass Panes (a/b = 1.75, t = 3/8 and 1/2 in)	6-94
6-39	Peak Blast Pressure Capacity for Tempered Glass Panes (a/b = 1.75, t = 5/8 and 3/4 in)	6-95
6-40	Peak Blast Pressure Capacity for Tempered Glass Panes (a/b = 2.00, t = 1/4 and 5/16 in)	6-96
6-41	Peak Blast Pressure Capacity for Tempered Glass Panes (a/b = 2.00, t = 3/8 and 1/2 in)	6-97
6-42	Peak Blast Pressure Capacity for Tempered Glass Panes (a/b = 2.00, t = 5/8 and 3/4 in)	6-98
6-43	Peak Blast Pressure Capacity for Tempered Glass Panes (a/b = 3.00, t = 1/4 and 5/16 in)	6-99
6-44	Peak Blast Pressure Capacity for Tempered Glass Panes (a/b = 3.00, t = 3/8 and 1/2 in)	6-100
6-45	Peak Blast Pressure Capacity for Tempered Glass Panes (a/b = 3.00, t = 5/8 and 3/4 in)	6-101
6-46	Peak Blast Pressure Capacity for Tempered Glass Panes (a/b = 4.00, t = 1/4 and 5/16 in)	6-102
6-47	Peak Blast Pressure Capacity for Tempered Glass Panes (a/b = 4.00, t = 3/8 and 1/2 in)	6-103
6-48	Peak Blast Pressure Capacity for Tempered Glass Panes (a/b = 4.00, t = 5/8 and 3/4 in)	6-104
6-49	Nondimensional Static Load-Stress Relationships for Simply Supported Tempered Glass	6-105
6-50	Nondimensional Static Load-Crater Deflection Relationships for Simply Supported Tempered Glass	6-106
6-51	Edge, Face, and Bite Requirements	6-107
6-52	Distribution of Lateral Load Transmitted by Glass Pane to the Window Frame	6-108
6-53	Geometry of a buried structure	6-138
6-54	Typical roof panel load	6-139
6-55	Contribution of three pressure waves on a wall	6-140
6-56	Spall plate	6-141
6-57	Typical earth-covered steel-arch magazine	6-145
6-58	Minimum separation distances of standard magazine	6-146
6-59	Sketch of 300 cfm sand filter	6-157
6-60	Blast-actuated louver	6-158
6-61	Arrangement of multiple louvers for a large volume of air	6-159
6-62	Typical blast-actuated poppet valve	6-160
6-63	Time delay path	6-161

6-64	Idealized model of shock isolated mass	6-162
6-65	Shock isolation system	6-180
6-66	Base-mounted isolation systems configuration	6-181
6-67	Overhead pendulum shock isolation systems using platforms	6-182
6-68	Helical compression spring mounts	6-183
6-69	Typical torsion spring shock isolation system	6-184
6-70	Schematic of single and double action pneumatic cylinders	6-185
6-71	Schematic of liquid springs	6-186
6-72	Belleville springs	6-187

"STRUCTURES TO RESIST THE EFFECTS OF ACCIDENTAL EXPLOSIONS"

CHAPTER 1. INTRODUCTION

CHAPTER 1

INTRODUCTION

INTRODUCTION**1-1. Purpose**

The purpose of this manual is to present methods of design for protective construction used in facilities for development, testing, production, storage, maintenance, modification, inspection, demilitarization, and disposal of explosive materials.

1-2. Objective

The primary objectives are to establish design procedures and construction techniques whereby propagation of explosion (from one structure or part of a structure to another) or mass detonation can be prevented and to provide protection for personnel and valuable equipment.

The secondary objectives are to:

- (1) Establish the blast load parameters required for design of protective structures.
- (2) Provide methods for calculating the dynamic response of structural elements including reinforced concrete, and structural steel.
- (3) Establish construction details and procedures necessary to afford the required strength to resist the applied blast loads.
- (4) Establish guidelines for siting explosive facilities to obtain maximum cost effectiveness in both the planning and structural arrangements, providing closures, and preventing damage to interior portions of structures because of structural motion, shock, and fragment perforation.

1-3. Background

For the first 60 years of the 20th century, criteria and methods based upon results of catastrophic events were used for the design of explosive facilities. The criteria and methods did not include a detailed or reliable quantitative basis for assessing the degree of protection afforded by the protective facility. In the late 1960's quantitative procedures were set forth in the first edition of the present manual, "Structures to Resist the Effects of Accidental Explosions". This manual was based on extensive research and development programs which permitted a more reliable approach to current and future design requirements. Since the original publication of this manual, more extensive testing and development programs have taken place. This additional research included work with materials other than reinforced concrete which was the principal construction material referenced in the initial version of the manual.

Modern methods for the manufacture and storage of explosive materials, which include many exotic chemicals, fuels, and propellants, require less space for a given quantity of explosive material than was previously needed. Such concentration of explosives increases the possibility of the propagation of accidental explosions. (One accidental explosion causing the detonation of

other explosive materials.) It is evident that a requirement for more accurate design techniques is essential. This manual describes rational design methods to provide the required structural protection.

These design methods account for the close-in effects of a detonation including the high pressures and the nonuniformity of blast loading on protective structures or barriers. These methods also account for intermediate and far-range effects for the design of structures located away from the explosion. The dynamic response of structures, constructed of various materials, or combination of materials, can be calculated, and details are given to provide the strength and ductility required by the design. The design approach is directed primarily toward protective structures subjected to the effects of a high explosive detonation. However, this approach is general, and it is applicable to the design of other explosive environments as well as other explosive materials as mentioned above.

The design techniques set forth in this manual are based upon the results of numerous full- and small-scale structural response and explosive effects tests of various materials conducted in conjunction with the development of this manual and/or related projects.

1-4. Scope

It is not the intent of this manual to establish safety criteria. Applicable documents should be consulted for this purpose. Response predictions for personnel and equipment are included for information.

In this manual an effort is made to cover the more probable design situations. However, sufficient general information on protective design techniques has been included in order that application of the basic theory can be made to situations other than those which were fully considered.

This manual is applicable to the design of protective structures subjected to the effects associated with high explosive detonations. For these design situations, the manual will apply for explosive quantities less than 25,000 pounds for close-in effects. However, this manual is also applicable to other situations such as far- or intermediate-range effects. For these latter cases the design procedures are applicable for explosive quantities in the order of 500,000 pounds which is the maximum quantity of high explosive approved for aboveground storage facilities in the Department of Defense manual, "Ammunition and Explosives Safety Standards", DOD 6055.9-STD. Since tests were primarily directed toward the response of structural steel and reinforced concrete elements to blast overpressures, this manual concentrates on design procedures and techniques for these materials. However, this does not imply that concrete and steel are the only useful materials for protective construction. Tests to establish the response of wood, brick blocks, and plastics, as well as the blast attenuating and mass effects of soil are contemplated. The results of these tests may require, at a later date, the supplementation of these design methods for these and other materials.

Other manuals are available to design protective structures against the effects of high explosive or nuclear detonations. The procedures in these manuals will quite often complement this manual and should be consulted for specific applications.

Computer programs, which are consistent with procedures and techniques contained in the manual, have been approved by the appropriate representative of the US Army, the US Navy, the US Air Force and the Department of Defense Explosives Safety Board (DDESB). These programs are available through the following repositories:

- (1) Department of the Army
Commander and Director
U.S. Army Engineer
Waterways Experiment Station
Post Office Box 631
Vicksburg, Mississippi 39180-0631
Attn: WESKA
- (2) Department of the Navy
Commanding Officer
Naval Civil Engineering Laboratory
Port Hueneme, California 93043
Attn: Code L51
- (3) Department of the Air Force
Aerospace Structures
Information and Analysis Center
Wright Patterson Air Force Base
Ohio 45433
Attn: AFFDL/FBR

If any modifications to these programs are required, they will be submitted for review by DDESB and the above services. Upon concurrence of the revisions, the necessary changes will be made and notification of the changes will be made by the individual repositories.

1-5. Format

This manual is subdivided into six specific chapters dealing with various aspects of design. The titles of these chapters are as follows:

Chapter 1	Introduction
Chapter 2	Blast, Fragment, and Shock Loads
Chapter 3	Principles of Dynamic Analysis
Chapter 4	Reinforced Concrete Design
Chapter 5	Structural Steel Design
Chapter 6	Special Considerations in Explosive Facility Design

When applicable, illustrative examples are included in the Appendices.

Commonly accepted symbols are used as much as possible. However, protective design involves many different scientific and engineering fields, and, therefore, no attempt is made to standardize completely all the symbols used. Each symbol is defined where it is first used, and in the list of symbols at the end of each chapter.

CHAPTER CONTENTS

1-6. General

This chapter presents a qualitative description of an explosive protective system, and addresses acceptor system tolerances, and the basis for structural design.

SAFETY FACTOR

1-7. Safety Factor

Simplifications leading to safety conservative structural designs are made in the design procedures of this manual. However, unknown factors can still cause an overestimation of a structure's capacity to resist the effects of an explosion. Unexpected shock wave reflections, construction methods, quality of construction materials, etc., vary for each facility. To compensate for such unknowns it is recommended that the TNT equivalent weight be increased by 20 percent. This increased charge weight is the "effective charge weight" to be used for design. Departures from this recommendation must be approved by the responsible agency.

All charts pertaining to explosive output in this manual are for readings at sea level.

EXPLOSION PROTECTION SYSTEM

1-8. System Components

1-8.1. General

Explosive manufacturing and storage facilities are constructed so that they provide a predetermined level of protection against the hazards of accidental explosions. These facilities consist of three components: (1) the donor system (amount, type and location of the potentially detonating explosive) which produces the damaging output, (2) the acceptor system (personnel, equipment, and "acceptor" explosives) which requires protection, and (3) the protection system (protective structure, structural components or distance) necessary to shield against or attenuate the hazardous effects to levels which are tolerable to the acceptor system. The flow chart in Figure 1-1 briefly summarizes the protective system and relates the individual components to each other.

1-8.2. Donor System

The donor system includes the type and amount of the potentially detonating explosive as well as materials which, due to their proximity to the explosive, become part of the damaging output. The output of the donor explosive includes blast overpressures (hereafter referred to as blast pressures or pressures), primary fragments resulting from cased explosives and secondary fragments resulting from materials in the immediate vicinity of the donor explosive. Other effects from the donor include ground shock, fire, heat, dust, electromagnetic pulse, etc. For the quantities of explosives considered in this manual, blast pressures constitute the principal parameter governing the design of protective structures. However, in some situations, primary

and/or secondary fragments and ground shock may assume equal importance in the planning of the protection system. The other effects mentioned are usually of concern in specific types of facilities, and their influence on the overall design can usually be met with the use of standard engineering design procedures. Except for very large quantities of explosives, ground shock effects will usually be small and, in most cases, will be of concern when dislodging of components within the protective structure is possible.

The chemical and physical properties of the donor explosive determine the magnitude of the blast pressures whereas the distribution of the pressure pattern is primarily a function of the location of the donor explosive relative to the components of the protective facility. The mass-velocity properties of the primary fragments depend upon the properties of the donor explosive and the explosive casing, while, for secondary fragments, their mass-velocity properties are functions of the type of fragment materials (equipment, frangible portions of the structure, etc.), their relative position to the donor explosive, and the explosive itself.

The explosive properties, including the molecular structure (monomolecular, bimolecular, etc.) of the explosive, shape and dimensional characteristics, and the physical makeup (solid, liquid, gas) of the charge, determine the limitation of the detonation process. These limitations result in either a high- or low-order detonation. With a high-order detonation, the process is generally complete and results in the maximum pressure output for the given type and amount of material. On the other hand, if the detonation is incomplete with the initial reaction not proceeding through the material mass, then a large quantity of the explosive is consumed by deflagration and the blast pressure is reduced.

Primary fragments are produced by the explosion of a cased donor charge. They result from the shattering of a container which is in direct contact with the explosive material. The container may be the casing of conventional munitions, the kettles, hoppers, and other metal containers used in the manufacture of explosives, the metal housing of rocket engines, etc. Primary fragments are characterized by very high initial velocities (in the order of thousands of feet per second), large numbers of fragments, and relatively small sizes. The heavier fragments may penetrate a protective element depending upon its composition and thickness. The lighter fragments seldom achieve perforation. However, in certain cases, primary fragments may ricochet into the protected area and cause injury to personnel, damage to equipment, or propagation of acceptor explosives. For protection against primary fragments, sufficient structural mass must be provided to prevent full penetration, and the configuration of the components of the protective facility must prevent fragments from ricocheting into protected areas.

Secondary fragments are produced by the blast wave impacting objects located in the vicinity of the explosive source. At these close distances, the magnitude of the shock load is very high and objects can be broken up and/or torn loose from their supports.

Pieces of machinery, tools, materials such as pipes and lumber, parts of the structure (donor structure) enclosing the donor explosive, large pieces of equipment, etc. may be propelled by the blast. Secondary fragments are characterized by large sizes (up to hundreds of pounds) and comparatively low velocities (hundreds of feet per second). These fragments may cause the same

damage as primary fragments, that is, injury to personnel, damage to equipment or detonation of acceptor explosives. However, protection against secondary fragments is slightly different than for primary fragments. While preventing perforation by primary fragments is important, secondary fragments pose additional problems due to their increased weight. The protective structure must be capable of resisting the large impact force (momentum) associated with a large mass travelling at a relatively high velocity.

1-8.3. Acceptor System

The acceptor system is composed of the personnel, equipment, or explosives that require protection. Acceptable injury to personnel or damage to equipment, and sensitivity of the acceptor explosive(s), establishes the degree of protection which must be provided by the protective structure. The type and capacity of the protective structure are selected to produce a balanced design with respect to the degree of protection required by the acceptor and the hazardous output of the donor.

Protection in the immediate vicinity of the donor explosive is difficult because of high pressures, ground shock, fire, heat, and high speed fragments generally associated with a detonation. Protection can be afforded through the use of distance and/or protective structures. Personnel may be subjected to low blast pressures and/or small ground motions without direct injury. However, injury can be sustained by falling and impacting hard surfaces.

In most explosive processing facilities, equipment is expendable and does not require protection. Equipment which is very expensive, difficult to replace in a reasonable period of time, and/or must remain functional to insure the continuous operation of a vital service may require protection. The degree of protection will vary depending upon the type and inherent strength of the equipment. In general, equipment and personnel are protected in a similar manner. However, equipment can usually sustain higher pressures than personnel, certain types of equipment may be able to withstand fragment impact whereas personnel can not, and lastly, equipment can sustain larger shock loads since it can be shock isolated and/or secured to the protective structure.

The degree of protection for acceptor explosives range from full protection to allowable partial or total collapse of the protective structure. In order to prevent detonation, sensitive acceptor explosives must be protected from blast pressures, fragment impact, and ground shock whereas "insensitive" explosives may be subjected to these effects in amounts consistent with their tolerance. The tolerances of explosives to initial blast pressures, structural motions, and impact differ for each type of explosive material with pressure being the lesser cause of initiation. Impact loads are the primary causes of initiation of acceptor explosives. They include primary and secondary fragment impact as well as impact of the explosive against a hard surface in which the explosive is dislodged from its support by pressure or ground shock and/or propelled by blast pressures.

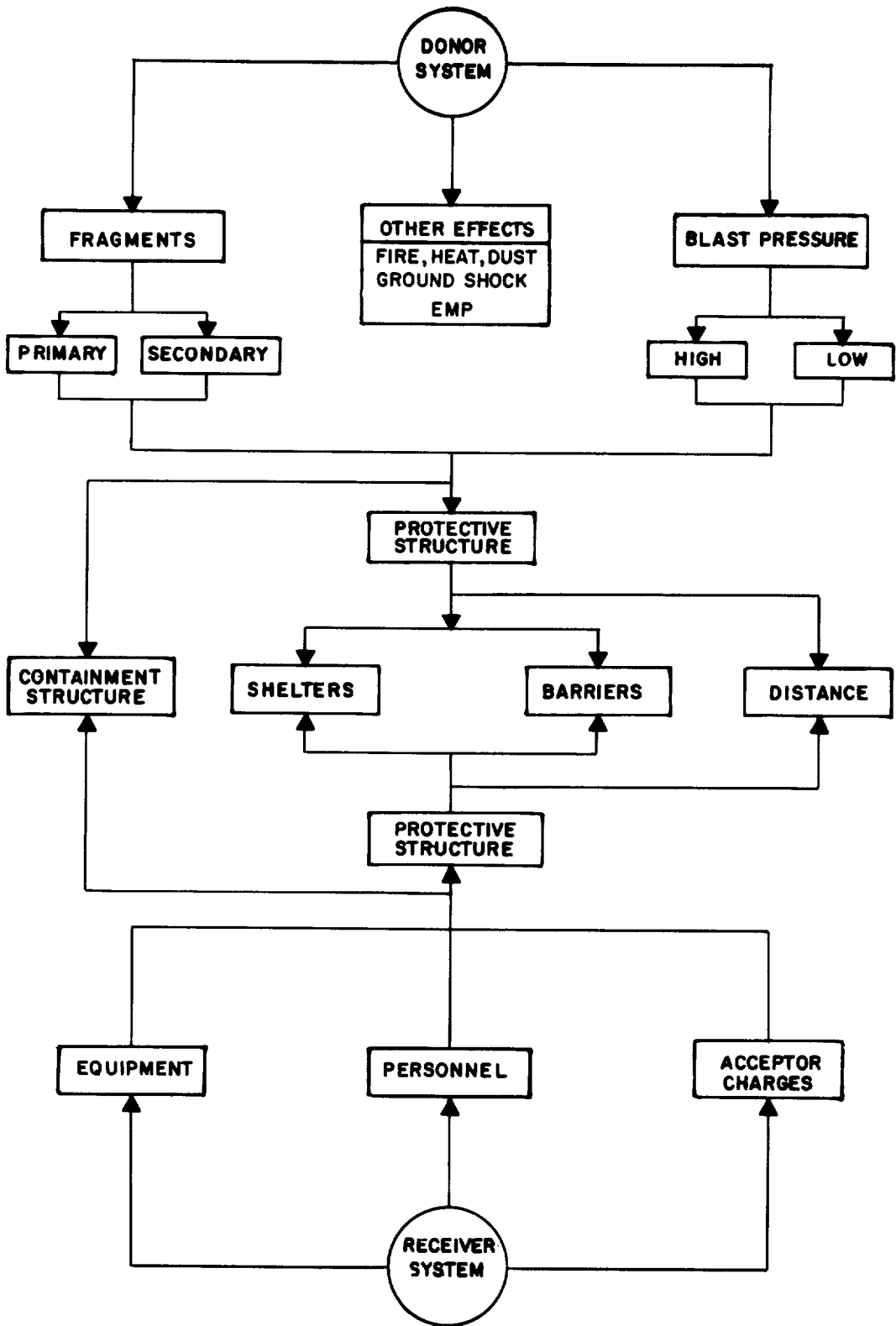


Figure 1-1 Explosive protective system

PROTECTION CATEGORIES

1-9. Protection Categories

For the purpose of analysis, the protection afforded by a facility or its components can be subdivided into four protection categories as described below:

1. Protection Category 1 - Protect personnel against the uncontrolled release of hazardous materials, including toxic chemicals, active radiological and/or biological materials; attenuate blast pressures and structural motion to a level consistent with personnel tolerances; and shield personnel from primary and secondary fragments and falling portions of the structure and/or equipment;

2. Protection Category 2 - Protect equipment, supplies and stored explosives from fragment impact, blast pressures and structural response;

3. Protection Category 3 - Prevent communication of detonation by fragments, high-blast pressures, and structural response; and

4. Protection Category 4 - Prevent mass detonation of explosives as a result of subsequent detonations produced by communication of detonation between two adjoining areas and/or structures. This category is similar to Category 3 except that a controlled communication of detonation is permitted between defined areas.

ACCEPTOR SYSTEMS TOLERANCES

1-10. Protective Systems

1-10.1. Protective Structures

Personnel, equipment or explosives are protected from the effects of an accidental explosion by the following means: (1) sufficient distance between the donor and acceptor systems to attenuate the hazardous effects of the donor to a level tolerable to the acceptor, (2) a structure to directly protect the acceptor system from the hazardous output of the donor system, (3) a structure to fully contain or confine the hazardous output of the donor system, and (4) a combination of the above means. While large distances may be used to protect acceptor systems, a protective facility is the most common method employed when limited area is available. In general, separation distances are used as a means of attenuating the hazardous effects of the donor to a level which makes the design of a protective facility feasible, practical and cost effective.

Protective structures can be classified as shelters, barriers or containment structures. Protection is provided by each structure in three distinct manners. Shelters are structures that fully enclose the acceptor system with hardened elements. These elements provide direct protection against the effects of blast pressures, primary and secondary fragments and ground shock. Containment structures are buildings which fully or near fully enclose the donor system with hardened elements. They protect the acceptor system by confining or limiting the damaging output of the donor system. A barrier acts as a shield between the donor and acceptor systems. They attenuate the damaging output of the donor system to a level which is tolerable to the acceptor system.

Shelters are fully enclosed structures and are used to protect personnel from injury, prevent damage to valuable equipment, and prevent detonation of sensitive explosives. The exterior of the structure is composed of hardened elements which must be designed to resist the effects of blast pressures and both primary and secondary fragment impact and the interior must be arranged to shock isolate the acceptor system. Entrances must be sealed by blast doors, and depending upon the amount of usage and/or the potential explosive hazard, may also require blast locks (an entrance containing a blast door followed by a second blast door; one of which is always closed). Other openings required for facility operations, such as ventilation passages, equipment access openings, etc., may be sealed by blast valves or blast shields. Design criteria for these protective closures are governed by their size and location and the magnitude of the blast pressure and fragment effects acting on them. Small openings may be permitted if the magnitude and rate of pressure buildup within the structure is tolerable to the occupants and contents of the shelter. Specific provisions may also be necessary to insure that partitions, hung ceilings, lighting fixtures, equipment, mechanical and electrical fixtures, piping, conduits, etc., are not dislodged as a result of structure motions or leakage pressures and become a hazard to the building's occupants and contents.

Barriers are generally used to prevent propagation of explosions. They act as a shield between two or more potentially detonating explosives. Their main purpose is to stop high speed fragments from impacting acceptor explosives.

In addition, they reduce secondary fragments striking the acceptor. They can also reduce blast pressures in the near range (at a distance up to ten times barrier height) but have little or no effect on the far range. Barriers can be either barricades (revetted or unrevetted earth barricades), simple cantilever walls, etc., or cubicle-type structures where one or more sides and/or the roof are open to the atmosphere or enclosed by frangible elements. Igloos (earth covered magazines), below ground silos, and other similar structures with open or frangible surfaces can also be classified as barriers. They are usually used in storage, manufacturing, or processing of explosives or explosive materials. The explosives are usually located close to the protective element. Consequently, the barrier is subjected to high intensity blast loads and the acceptor explosive is subjected to comparatively high leakage pressures.

Containment structures are generally used for high hazard operations and/or operations involving toxic materials. These operations must be remotely controlled since operating personnel should not be located within the structure during hazardous operation. All entrances must be sealed with blast doors. Other openings required for facility operations such as ventilation passages, equipment and/or product access openings, etc., must be sealed by blast valves or blast shields. For operations not involving toxic materials, blast pressures may be released to the atmosphere. However, this pressure release must be controlled both in magnitude and direction either by mechanical means (through blast valves or shields) or by limiting the size of the openings and/or directing the leakage pressures to areas where personnel, equipment and acceptor explosives will be protected.

The various components of a protective facility must be designed to resist the effects of an explosion. The exterior walls and roof are the primary protective elements. These elements are said to be "hardened" if they are designed to resist all the effects associated with an explosion (blast pressures, primary and secondary fragments, structure motions). On the other hand, a blast resistant element is designed to resist blast pressure only. While a blast resistant element is not designed specifically to resist fragments, the element has inherent fragment resistance properties which increases with increasing blast resistant capabilities. In many parts of this manual, the term "blast resistant" is used synonymously with "hardened."

1-10.2. Containment Type Structures

The first three protection categories can apply to structures classified as containment structures when these structures are designed to prevent or limit the release of toxic or other hazardous materials to a level consistent with the tolerance of personnel. These structures generally are designed as donor structures and can resist the effects of "close-in" detonations (detonations occurring close to the protective structures). Added protection is accomplished by minimizing the pressure leakage to the structures exteriors, by preventing penetration to the exterior of the structure by primary fragments and/or formation of fragments from the structure itself. Quite often, containment structures may serve as a shelter as described below. Procedures for designing reinforced concrete containment structures are contained in Chapter 4. A design ratio of weight to volume of $W/V < .15 \text{ lb/ft}^3$ is a practical range for reinforced concrete containment structures.

1-10.3. Shelters

The first three protection categories apply to shelters which provide protection for personnel, valuable equipment, and/or extremely sensitive explosives. Shelters, which are usually located away from the explosion, accomplish this protection by minimizing the pressure leakage into a structure, providing adequate support for the contents of the structure, and preventing penetration to the interior of the structure by high-speed primary fragments, and/or by the impact of fragments formed by the breakup of the donor structure. Protection against the uncontrolled spread of hazardous material is provided by limiting the flow of the dangerous materials into the shelter using blast valves, filters, and other means. Procedures for designing concrete and structural steel buildings are contained in Chapters IV and V, respectively.

1-10.4. Barriers

Although the first three protection categories of protection can be achieved with the use of a shelter, the last two protection categories (para. 1-9) pertain to the design of barriers where protection of explosives from the effects of blast pressures and impact by fragments must be provided. For the third protection category, the explosion must be confined to a donor cell, whereas in the fourth protection category, propagation between two adjoining areas is permitted. However, the communication of detonation must not extend to other areas of the facility. This situation may arise in the event of the dissimilarity of construction and/or explosive content of adjacent areas. Procedures for designing reinforced concrete barriers are contained in Chapter 4.

1-11. Human Tolerance

1-11.1. Blast Pressures

Human tolerance to the blast output of an explosion is relatively high. However, the orientation of a person (standing, sitting, prone, face-on or side-on to the pressure front), relative to the blast front, as well as the shape of the pressure front (fast or slow rise, stepped loading), are significant factors in determining the amount of injury sustained. Shock tube and explosive tests have indicated that human blast tolerance varies with both the magnitude of the shock pressure as well as the shock duration, i.e., the pressure tolerance for short-duration blast loads is significantly higher than that for long-duration blast loads.

Tests have indicated that the air-containing tissues of the lungs can be considered as the critical target organ in blast pressure injuries. The release of air bubbles from disrupted alveoli of the lungs into the vascular system probably accounts for most deaths. Based on present data, a tentative estimate of man's response to fast rise pressures of short duration (3 to 5 ms.) is presented in Figure 1-2. The threshold and severe lung-hemorrhage pressure levels are 30 to 40 psi and above 80 psi, respectively, while the threshold for lethality due to lung damage is approximately 100 to 120 psi (Table 1-1). On the other hand, the threshold pressure level for petechial hemorrhage resulting from long-duration loads may be as low as 10 to 15 psi, or approximately one-third that for short duration blast loads. Since survival is dependent on the mass of the human, the survival for babies will be different than the survival for small children which will be different from

that for women and men. These differences have been depicted in Figure 1-2 which indicates that the survival scaled impulse depends on the weight of the human. It is recommended that 11 lb. be used for babies, 55 lb. for small children, 121 lb. for adult women and 154 lb. for adult males.

A direct relationship has been established between the percentage of ruptured eardrums and maximum pressure, i.e., 50 percent of exposed eardrums rupture at a pressure of 15 psi for fast rising pressures while the threshold of eardrums rupture for fast rising pressure is 5 psi. Temporary hearing loss can occur at pressure levels less than that which will produce onset of eardrum rupture. This temporary hearing loss is a function of the pressure and impulse of a blast wave advancing normal to the eardrum. The curve which represents the case where 90 percent of those exposed are not likely to suffer an excessive degree of hearing loss, is referred to as the temporary threshold shift. The pressures referred to above are the maximum effective pressures, that is, the highest of either the incident pressure, the incident pressure plus the dynamic pressures, or the reflected pressure. The type of pressure which will be the maximum effective depends upon the orientation of the individual relative to the blast as well as the proximity of reflecting surfaces and the occurrence of jetting effects which will cause pressure amplification as the blast wave passes through openings. As an example, consider the pressure level which will cause the onset of lung injury to personnel in various positions and locations. The threshold would be 30 to 40 psi reflected pressure for personnel against a reflector (any position), 30 to 40 psi incident plus dynamic pressure; 20 to 25 psi would be the incident pressure plus 10 to 15 psi dynamic pressure for personnel in the open, either standing or prone-side-on, and 30 to 40 psi incident pressure for personnel in the open in a prone-end-on position.

However, the above pressure level assumes that an individual is supported and will not be injured due to being thrown off balance and impacting a hard and relatively non-yielding surface. In this case, pressure levels which humans can withstand are generally much lower than those causing eardrum or lung damage. For this case, one publication has recommended that tolerable pressure level of humans not exceed 2.3 psi which is higher than temporary threshold shift of temporary hearing loss (Figure 1-3) and probably will cause personnel, which are located in the open, to be thrown off balance.

Structures can be designed to control the build-up of internal pressure, however, jetting effect produced by pressure passing through an opening can result in amplification of the pressures at the interior side of the opening. The magnitude of this increased pressure can be several times as large as the maximum average pressure acting on the interior of the structure during the passage of the shock wave. Therefore, openings where jetting will occur should not be directed into areas where personnel and valuable equipment will be situated.

1-11.2. Structural Motion

It is necessary that human tolerance to two types of shock exposure be considered:

1. Impacts causing body acceleration/deceleration, and

2. Body vibration as a result of the vibratory motion of the structure.

If a subject is not attached to the structure, he may be vulnerable to impact resulting from collision with the floor due to the structure dropping out beneath him and/or the structure rebounding upward towards him. However, the more plausible means of impact injury results from the subject being thrown off balance because of the horizontal motions of the structure, causing him to be thrown bodily against other persons, equipment, walls and other hard surfaces.

Studies have indicated that a probable safe impact tolerance velocity is 10 fps. At 18 fps there is a 50 percent probability of skull fracture and at 23 fps, the probability is nearly 100 percent. This applies to impact with hard, flat surfaces in various body postures. However, if the line of thrust for head impact with a hard surface is directly along the longitudinal axis of the body (a subject falling head first), the above velocity tolerance does not apply since the head would receive the total kinetic energy of the entire body mass. Impacts with corners or edges are also extremely critical even at velocities less than 10 fps. An impact velocity of 10 fps is considered to be generally safe for personnel who are in a fairly rigid posture; therefore, greater impact velocities can be tolerated if the body is in a more flexible position or if the area of impact is large.

The effect of horizontal motion on the stability of personnel (throwing them off balance or hurling them laterally) depends on the body stance and position, the acceleration intensity and duration, and the rate of onset of the acceleration. An investigation of data concerning sudden stops in automobiles and passenger trains indicates that personnel can sustain horizontal accelerations less than 0.44 g without being thrown off balance. These accelerations have durations of several seconds; hence, the accelerations considered in this manual required to throw personnel off balance are probably greater because of their shorter durations. Therefore, the tolerable horizontal acceleration of 0.50 g required to provide protection against ground-shock effects resulting from nuclear detonations should be safe for non-restrained personnel (standing, sitting, or reclining).

If the vertical downward acceleration of the structure is greater than 1 g, relative movement between the subject and the structure is produced. As the structure drops beneath him, the subject begins to fall until such time that the structure slows down and the free falling subject overtakes and impacts with the structure. The impact velocity is equal to the relative velocity between the structure and the subject at the time of impact, and to assure safety, it should not exceed 10 fps.

To illustrate this vertical impact, a body which free falls for a distance equal to 1.5 feet has a terminal or impact velocity of approximately 10 fps against another stationary body. If the impacted body has a downward velocity of 2 fps at the time of impact, then the impact velocity between the two bodies would be 8 fps.

Based on the available personnel vibration data, the following vibrational tolerances for restrained personnel are considered acceptable: 2g for less than 10 Hz, 5g for 10-20 Hz, 7g for 20-40 Hz, and 10g above 40 Hz. However, the use of acceleration tolerances greater than 2g usually requires restrain-

ing devices too elaborate for most explosive manufacturing and testing facilities.

1-11.3. Fragments

Overall, human tolerance to fragment impact is very low; however, certain protection can be provided with shelter type structures. Fragments can be classified based on their size, velocity, material and source, i.e.:

1. Primary fragments, which are small, high-speed missiles usually formed from casing and/or equipment located immediately adjacent to the explosion, and
2. Secondary fragments, which are generated from the breakup of the donor building, equipment contained within the donor structure and/or acceptor buildings which are severely damaged by an explosion.

Discussion of human tolerance of both of these types of fragment overlap, since the basic differences between these fragments are their size and velocity. Impact of primary fragments can be related to an impact by bullets where the fragment is generally small, usually of metal and traveling at high velocities. A great deal of research has been conducted for the military; however, most of the data from these tests is not available. Some fragment-velocity penetration data of humans has been developed for fragment weights equal to or less than 0.033 pounds, and indicates that, as the ratio of the fragment area to weight increases, the velocity which corresponds to a 50 percent probability of penetrating human skin will increase. This trend is illustrated in Table 1-2 where the increase in velocity coincides with the increase of area of the fragment.

Secondary fragments, because they have a large mass, will cause more serious injuries at velocities significantly less than caused by primary fragments. Table 1-3 indicates the velocity which corresponds to the threshold of serious human injury. As mentioned in 1-11.2 above, the impact of a relatively large mass with a velocity less than 10 fps against a human can result in serious bodily injury. Also, the impact of smaller masses (Table 1-3) with higher velocities can result in injuries as severe as those produced by larger masses. See applicable Safety Manual for fragment criteria.

1-12. Equipment Tolerance

1-12.1. Blast Pressures

Unless the equipment is of the heavy-duty type (motor, generators, air handlers, etc.), equipment to be protected from blast pressures must be housed in shelter-type structures similar to those required for the protection of personnel. Under these circumstances, the equipment will be subjected to blast pressures which are permitted to leak into the shelter through small openings. If the magnitude of these leakage pressures is minimized to a level consistent with that required for personnel protection, then in most cases protection from the direct effects of the pressures is afforded to the equipment. However, in some instances, damage to the equipment supports may occur which, in turn, can result in damage to the equipment as a result of falling. Also, if the equipment is located immediately adjacent to the shelter open-

ings, the jetting effects of the pressures entering the structure can have adverse effects on the equipment. In general, equipment should be positioned away from openings and securely supported. However, in some cases, equipment such as air handling units must be positioned close to the exterior openings. In this event, the equipment must be strong enough to sustain the leakage pressures (pressures leaking in or out of openings) or protective units such as blast valves must be installed.

1-12.2. Structural Motion and Shock

Damage to equipment can result in failures which can be divided into two classes; temporary and permanent. Temporary failures, often called "malfunctions," are characterized by temporary disruption of normal operation, whereas permanent failures are associated with breakage, resulting in damage so severe that the ability of the equipment to perform its intended function is impaired permanently or at least over a period of time.

The capacity of an item of equipment to withstand shock and vibration is conventionally expressed in terms of its "fragility level" which is defined as the magnitude of shock (acceleration) that the equipment can tolerate and still remain operational. The fragility level for a particular equipment item is dependent upon the strength of the item (frame, housing, and components) and, to some extent, the nature of the excitation to which it is subjected. An equipment item may sustain a single peak acceleration due to a transient input load, but may fail under a vibration-type input having the same peak acceleration amplitude. Also the effects of the occurrence of resonance may be detrimental to the item functioning. For these reasons, fragility data should be considered in connection with such factors as the natural frequencies and damping characteristics of the equipment and its components, as well as the characteristics of the input used to determine the tolerance as compared to the motion of the structure which will house the equipment.

The maximum shock tolerances for equipment vary considerably more than those for personnel. To establish the maximum shock tolerance for a particular item, it is necessary to perform tests and/or analyses. Only selected items of equipment have been tested to determine shock tolerances applicable for protection from the damage which may be caused by structural motions.

Most of this data resulted from tests to sustain ground-shock motions due to a nuclear environment, which will have a duration considerably longer than that associated with a HE explosion. However, the data which are available concerning shock effects indicate strength and ruggedness or sensitivity of equipment. These data, which are based primarily on transportation and conventional operational shock requirements, indicate that most commercially available mechanical and electrical equipment are able to sustain at least 3g's, while fragile equipment (such as electronic components) can sustain approximately 1.5g's.

The above tolerances are safe values, and actual tolerances are, in many cases, higher than 3g's, as indicated in Table 1-4. However, the use of such acceleration values for particular equipment require verification by shock testing with the induced motions (input) consistent with expected structural motions.

The above tolerances are applicable to equipment which is mounted directly to the sheltering structure. For the equipment to sustain shock accelerations in the order of magnitude of their tolerances, the equipment item must be "tied" down to the structure, that is, the equipment stays attached to the structure and does not impact due to its separation. In most cases, shock isolation systems will be needed to protect the equipment items. The shock isolation systems will consist of platforms which are supported by a spring assembly for large motion and/or cushioning material when the motions are small. These systems should be designed to attenuate the input accelerations to less than 1g in order that separation between the equipment and support system does not occur. If the spring systems are designed to be "soft" (less than 1/2 g) then, depending on the mass of the equipment, vibratory action of the system could occur due to individuals walking on the platforms.

1-12.3. Fragments

Susceptibility of an item of equipment to damage from fragment impact depends upon the ruggedness of its components, its container, if any, and upon the size and velocity of the fragment at the time of impact.

Some heavy equipment (motors, generators, etc.) may sustain malfunctions as a result of the severing of electrical or mechanical connections, but seldom are destroyed by the impact of primary fragments. On the other hand, this heavy equipment can be rendered useless by secondary fragment impact. Fragile equipment (electronic equipment, etc.) will generally be inoperable after the impact of either primary or secondary fragments. The impact force and penetration capability of light fragments may perforate sensitive portions of heavy equipment (fuel tank of generators, etc.). Low-velocity light fragments seldom result in severe damage. These fragments usually ricochet beyond the equipment unless the component part of the equipment it strikes is glass or other fragile material, in which case, some damage may be inflicted.

Although the damage to the equipment of a structure can be great as a result of falling or flying debris, the increased cost of strengthening walls and other portions of the protective shelter is usually not warranted unless personnel or acceptor charge protection is also required and/or the cost of the equipment item lost exceeds the increased construction costs. Even in this latter situation, a probability analysis of the occurrence of an incident should be made prior to incurring additional construction costs.

1-13. Tolerance of Explosives

1-13.1. General

The tolerances of explosives to blast pressure, structural motion, and impact by fragments differ for each type of explosive material and/or item. Generally, fragment impact is the predominant cause of detonation propagation.

1-13.2. Blast Pressures

Except in regions of extremely high pressure, most explosive materials are insensitive to the effects of blast pressures. In many instances, however, the secondary effects, such as dislodgement of the explosive from its support and propulsion of the explosive against hard surfaces, can result in a possible detonation depending upon the tolerance of the explosive to impact.

Results of several different types of sensitivity tests (drop test, card gap tests, friction tests, etc.) are presently available which will aid in the establishment of the tolerances of most explosive materials to impact.

1-13.3. Structural Motions

Structural motion effects on explosives are similar to the impact effects produced by blast pressures. The movement of the structure tends to dislodge the explosive from its support, resulting in an impact of the explosive with the floor or other parts of the structure. The distance the explosive falls and its sensitivity to impact and friction determine whether or not propagation occurs.

1-13.4. Fragments

Although blast pressures and structural motions can produce explosive propagation, the main source of communication of explosions is by fragments, principally primary fragments from the breakup of the donor charge casing, fragments produced by the fracture of equipment close to the explosion, disengagement of interior portions of the structure, and/or failure of the structure proper.

In recent years, an extensive test program has been performed which has provided a significant amount of information regarding explosive propagation by primary fragment impact. This program was conducted primarily to determine safe separation criteria for bulk explosives and munitions, mainly for the design and operation of conveyance systems. The individual test programs were predicated upon given manufacturing operations where improved safety criteria would lessen the probability of a catastrophic event. Individual test programs were performed in two stages, exploratory and confirmatory, where the safe separation was determined during the exploratory phase and confirmation was established on a 95 percent confidence level.

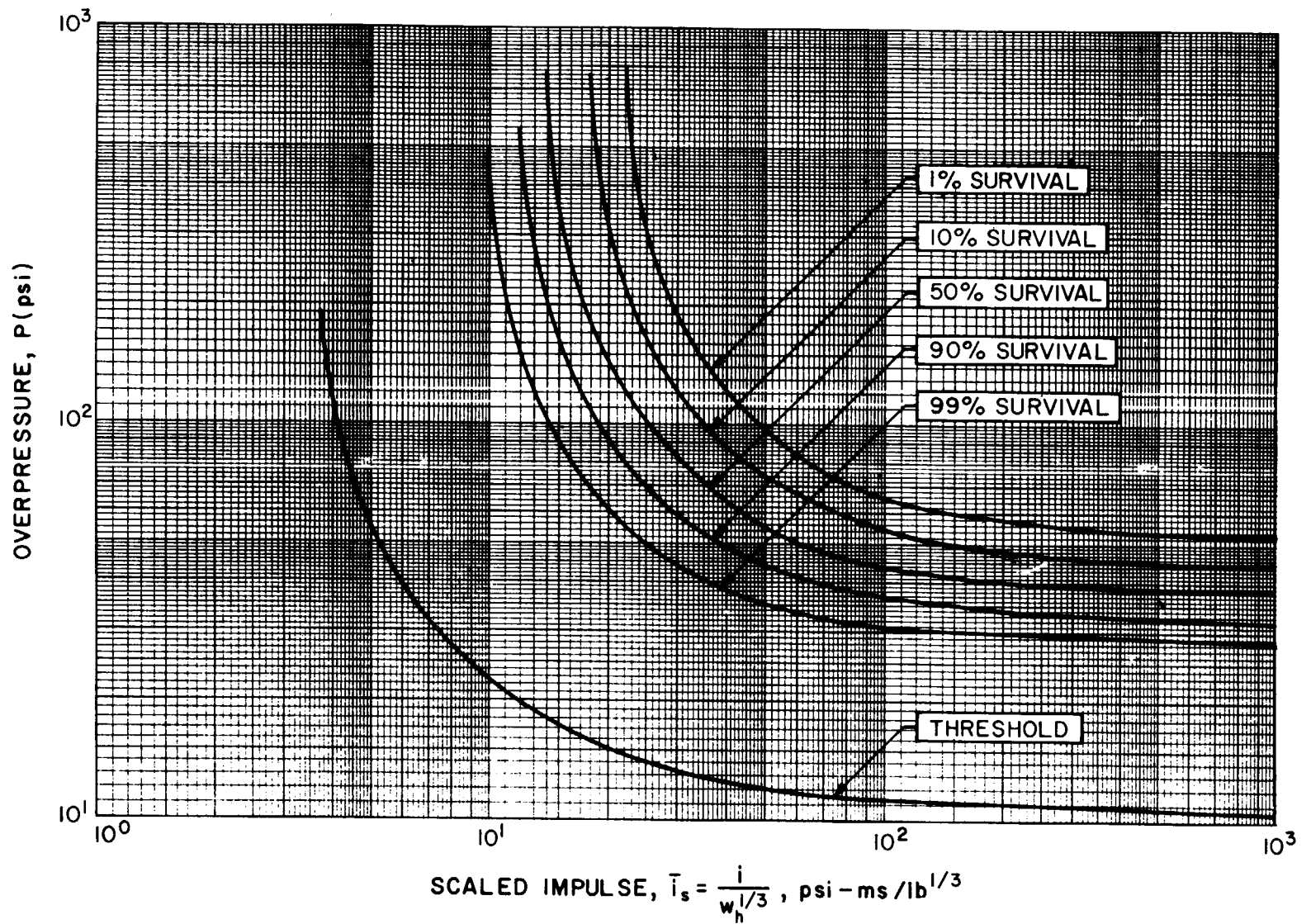
A typical test set-up is illustrated in Figure 1-4, while the results of the various test programs are listed in Table 1-5 for bulk explosives and in Table 1-6 for munitions. These Tables list the bulk explosives and munition types, the configurations examined and the established safe separation distances. For all items/configurations examined, unless specified, the test conditions were: 1) in free air (without tunnels), 2) open spaced (no shields), 3) in a vertical orientation, and 4) measured edge-to-edge. Inspection of Tables 1-5 and 1-6 reveal that minimum safe separation distances have not been established for some of the items listed. If specific safe separation distances are required, as will be for other items not listed, further tests will be required. A detailed compilation of the items and test procedures and methods are listed in the bibliography.

Several testing methods have been developed to determine the sensitivity of explosives to impact by secondary fragments. In one series of tests which utilized a catapult method for propelling approximately 70 pounds of concrete fragments, sand and gravel rubble, against lightly cased Composition B acceptor explosives indicated a boundary velocity on the order of approximately 400 fps. A second series of tests, which propelled concrete fragments as large as 1000 pounds against 155 mm projectiles (thick steel wall projectile), indicated that the projectile would not detonate with striking velocities of 500 fps. This latter test series also included acceptor items consisting of 155 projectiles with thin wall riser funnels, which detonated upon impact with the

concrete. Another series of fragment testing included the propelling of large concrete fragments against thin wall containers with molten explosive simulating typical melt-pour kettles in a loading plant. In all cases, the contents of the simulated kettle detonated. Although the results of these test series indicated that thick wall containers of explosive will prevent propagation, while thin wall containers will not, the number of tests performed in each series was relatively few. Additional tests are required to determine the extent that the variation of container thickness has on the magnitude of the mass/velocity boundary established to date.

Figure 1-2 Survival curves for lung damage

1-19



w_h = Weight of human being (lbs)

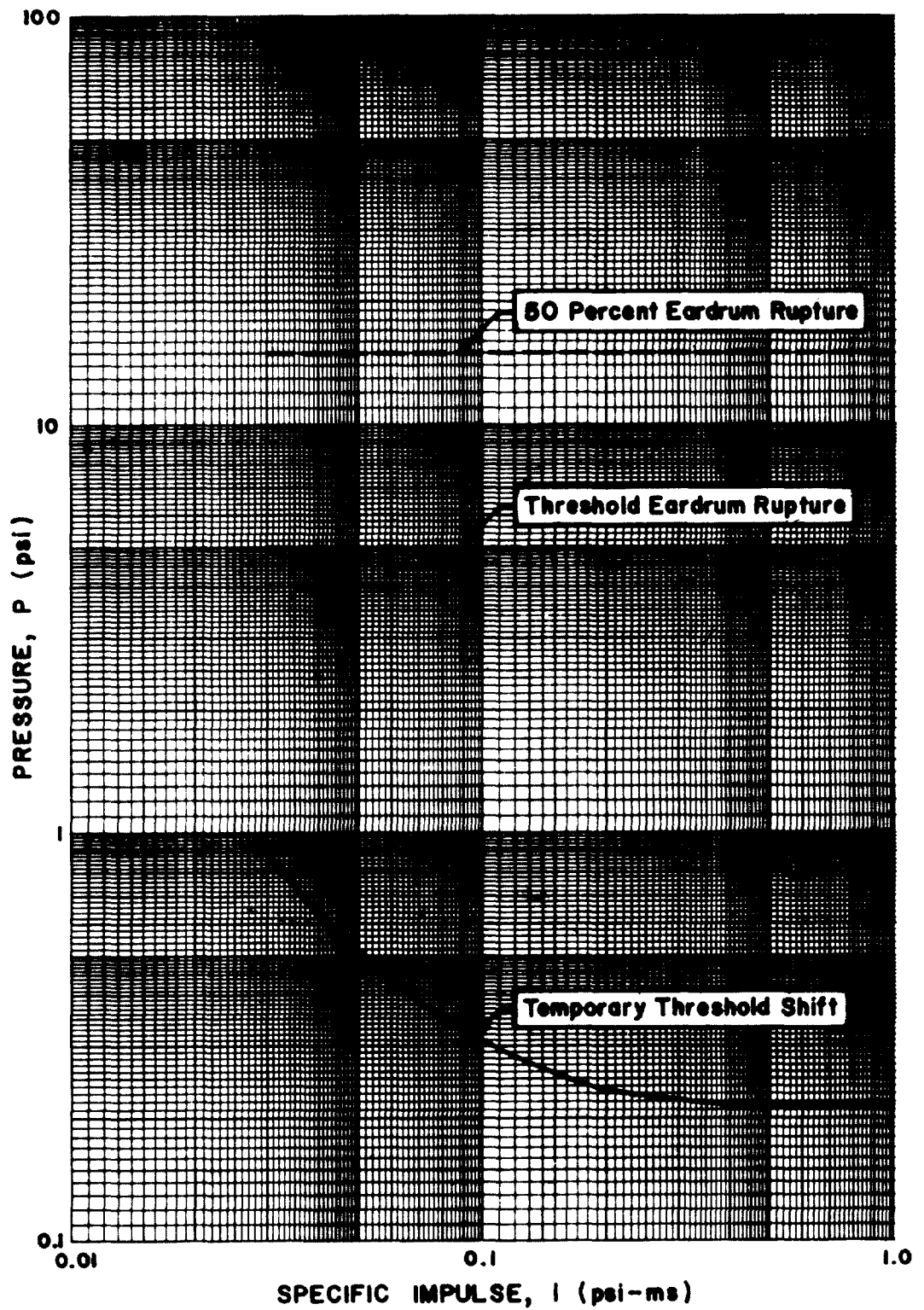


Figure 1-3 Human ear damage due to blast pressures

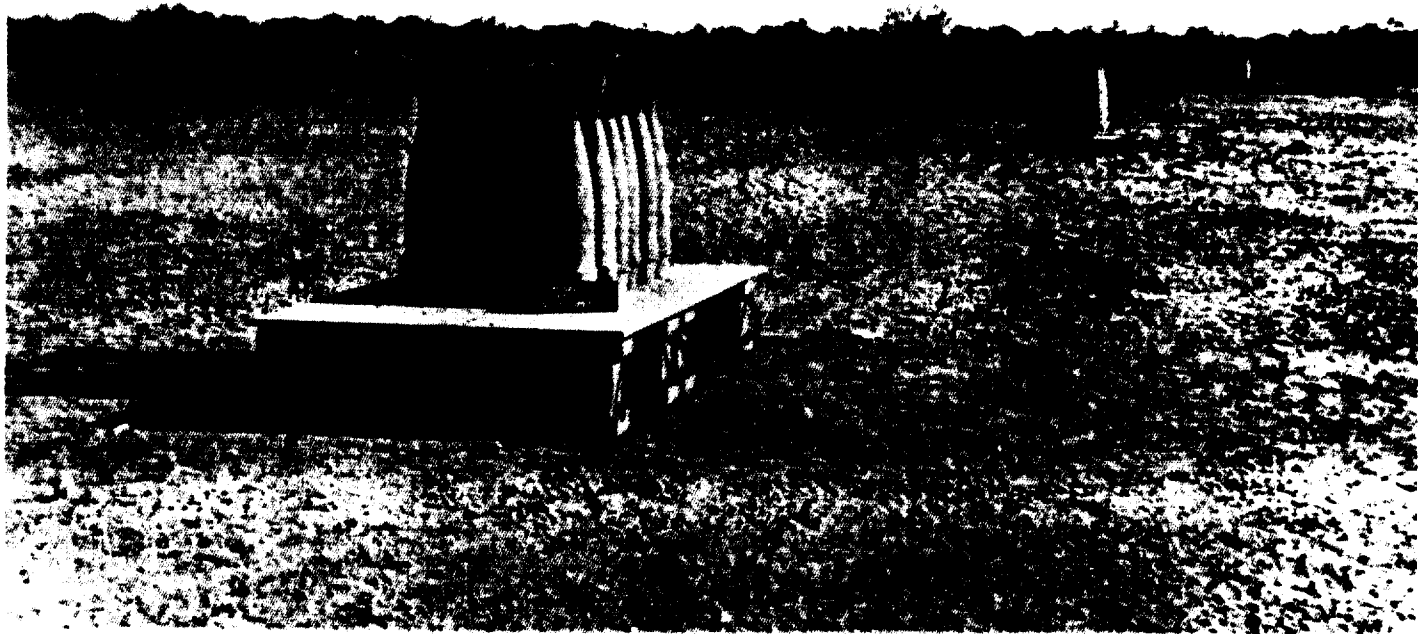
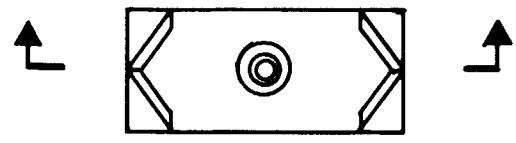


Figure 1-4 Example of safe separation tests

Figure 1-5 Safe separation test shields

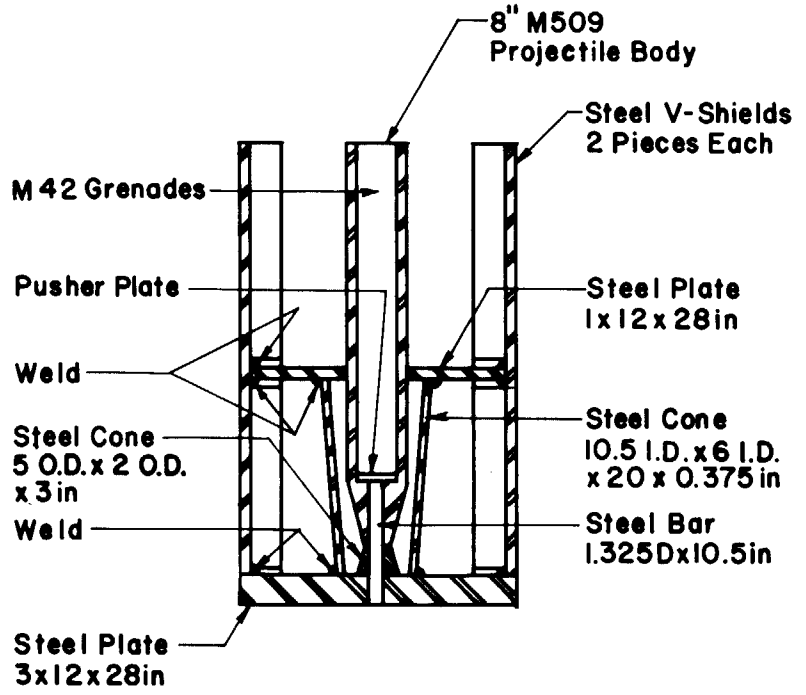
1-22



TOP VIEW

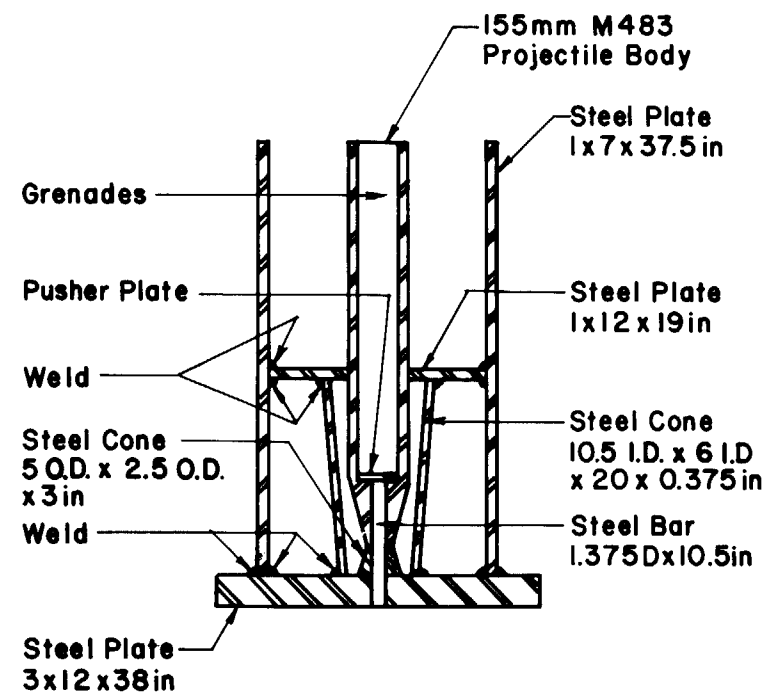


TOP VIEW



SECTION

a. VEE SHIELD TRANSFER PALLET



SECTION

b. MSAAP PALLET

Table 1-1 Blast Effects in Man Applicable to Fast-Rising Air Blasts of Short Duration (3-5 ms.)

Critical Organ or Event	Maximum Effective Pressure (psi)*
Eardrum Rupture	
Threshold	5
50 percent	15
Lung Damage:	
Threshold	30-40
50 percent	80 and above
Lethality	
Threshold	100-120
50 percent	130-180
Near 100 percent	200-250

* Maximum effective pressure is the highest of incident pressure, incident pressure plus dynamic pressure, or reflected pressure.

Table 1-2 50 Percent Probability of Penetrating Human Skin

Ratio of Fragment area/weight (ft ² /lb)	Fragment Area Based on 0.033 lb. fragment weight (ft ²)	Velocity (fps)	Threshold Energy (ft-lb.)
0.03	.00099	100	5
0.10	.00330	165	14
0.20	.00660	250	32
0.30	.00990	335	58
0.40	.01320	425	93

Table 1-3 Threshold of Serious Injury to Personnel Due to Fragment Impact

Critical Organ	Weight (lbs.)	Fragment Velocity(fps)	Energy (ft-lb.)
Thorax	>2.5	10	4
	0.1	80	10
	0.001	400	2.5
Abdomen and limbs	>6.0	10	9
	0.1	75	9
	0.001	550	5
Head	>8.0	10	12
	0.1	100	16
	0.001	450	3

Table 1-4 Examples of Equipment Shock Tolerances

Equipment	Peak Accelerations
Fluorescent light fixtures (with lamps)	20 to 30g
Heavy machinery (motor, generators, transformers, etc. > 4,000 lbs.)	10 to 30g
Medium-weight machinery (pumps, condensers, AC equipment, 1,000 to 4,000 lbs.)	15 to 45g
Light machinery (small motors <1,000 lbs.)	30 to 70g

Table 1-5 Safe Separation Distance (bulk explosives)

Bulk Explosive	Explosive Weight (lbs)	Test Configuration	Safe Separation (ft)
Composition A-5	10	Rubber buckets in tunnel	6.0
	15	Aluminum buckets in tunnel	20.0
Composition B	---	Flake, depth on 15 inch Serpentix conveyor	.17 (1)
	2.5	Riser scrap:2 pieces	1.5
	2.5	4 pieces	3.0
	2.5	2 pieces within funnels	2.0
	2.5	4 pieces within funnels	3.0
	60	Cardboard container in tunnel	12.0
Composition C-4	60	Plastic buckets	12.0 (2)
	35	Aluminum buckets in tunnel	20.0 (2)
Cyclotol (75/25)	50	Aluminum buckets in tunnel	25.0 (2)
	60	Aluminum box in tunnel & 0.38-in Kevlar shield.	24.0
Guanidine Nitrate	60	Cardboard box in tunnel.	18.0
	20	DOT-21C-60 Containers with tops on	3.8
	40	DOT-21C-60 Containers with tops on	4.8
Nitro-Guanidine (Powder)	80	DOT-21C-60 Containers with tops on	5.5
	25	DOT-21C-60 Containers with tops on	5.5
	50	DOT-21C-60 Containers with tops on	7.0
TNT, Type 1 Flake	450	DOT-21C-60 Containers with tops on	16.0
	---	Depth on 2-foot Serpentix conveyor	.08 (1)
	55	Cardboard box	12.0
	168	Aluminum tote bin, w/steel fiberglass in tunnel	60.0
	168	Aluminum tote bin in wooden tunnel	50.0

(1)Depth of material at which propagation is prevented is less than or equal to the value shown.

(2)Minimum distance tested. Actual safe separation distance less than or equal to that indicated. Further tests required to establish minimum safe separation distance.

Table 1-6 Safe Separation Distance (munitions)

Munition	Test Configuration	Safe Separation (ft)
8-inch M106 HE Projectile	Single round with 3-inch diameter aluminum bar shield	1.0
8 inch M509 HE Projectile	Single round with "VEE" shield Figure 1-5a)	2.7
155 mm M107 HE Projectile	Single round with one-inch thick aluminum or 1/2-inch thick steel plate shield	1.5
	24 per pallet	110.0
155 mm M483 HE Projectile	Single round with MS shield (Fig. 1-5b)	0
155 mm M795 HE Projectile (TNT, TYPE 1)	Single round	15.0
105 mm M1 HE Projectile	16 per pallet	30.0
	16 per pallet, with funnel and 3/4-inch thick steel plate shield	20.0
105 mm M456 HEAT-T Projectile	Primed cartridge cases	0
	Single round with 3-inch diameter aluminum bar shield	1.6
	Single round, horizontal with 3-inch diameter aluminum bar shield	0.91
81 mm M374A2E1 HE Cartridge	Single round with 1/4-inch thick Lexan plate extension to 2-inch thick aluminum brick shield	0.73 (1)

Table 1-6 (Cont'd.)

Munition	Test Configuration	Safe Separation (ft)
81mm M374 HE Projectile	Single round	2.0
	Single round with 2-inch thick aluminum brick shield	0.73 (1)
	72 per pallet	30.0
30 mm XM789 HEDP Projectile	2 each. PBXN-5 pellets	0.08
	Shell body with 2 pellets	0.08
	Loaded body assembly	0.08
	Heated loaded body assembly	0.25
	Fuzed projectile	0.25
	25 mm XM792 HEI-T Cartridge	Type I pellets
Type II pellets		0.04
Loaded body assembly		0.17
Fuzed projectile		0.17
Complete cartridge		0.17
BLU-63 A/B Bomblet	Hemispheres	0.04
	Hemispheres in fixtures	0
	Hemispheres, 16 per tray	0
	Bomblet	0.17

Table 1-6 (Cont'd.)

Munition	Test Configuration	Safe Separation (ft)
BLU-97/B Submunition	16 per pallet with 1/2-inch thick aluminum plate shield	4.0
	16 per pallet with "airflow" shield (1/2-inch thick aluminum plates, cut in open "picket fence" design with one plate's spaces covered by the second plate's columns).	5.0
	Single bomblet with either 100% or 75% shield (1/2-inch thick aluminum plate).	0.75
M42/M46 GP Grenades (w/o fuzes)	Single grenade	0.17
	64 per tray	7.0
	768 per carrier, in tunnel	40.0
	8 per M483 Ring Pack	1.0
	15 per M509 Ring Pack	1.5
	32/64 per single/dual cluster tray	0
M56 Mine	Single mine	0.50 (1)
	2-mine canister	0.50 (1)
M74AP and M75 ATAV mines(w/o fuzes)	Single mine with 3-inch thick aluminum brick shield	0.25

(1) Minimum distance tested. Actual safe separation distance less than or equal to that indicated. Further tests required to establish minimum safe separation distance.

BASIS FOR STRUCTURAL DESIGN**1-14. Structural Response****1-14.1. General**

Dynamic response criteria to be used in the design of a protective structure and its elements depend on: (1) the properties (type, weight, shape, casing, etc.) and location of the donor explosive, (2) the sensitivity (tolerance) of the acceptor system, and (3) the physical properties and configuration of the protective structure. In many situations, the acceptor system will control the overall required structural response.

1-14.2. Pressure Design Ranges**1-14.2.1. General**

An engineering analysis of the blast pressure and fragments associated with high explosive detonations acting on protective structures must be made to describe the response of the protective structures to donor output. The response to the blast output is expressed in terms of design ranges according to the pressure intensity, namely, (1) high pressure, and (2) low pressure. As subsequently shown, these design ranges are related to the relative location of the protective structure to the explosion.

1-14.2.2. High-Pressure Design Range

At the high-pressure design range, the initial pressure acting on the protective structure are extremely high and further amplified by their reflections on the structure. Also the durations of the applied loads are short, particularly where complete venting of the explosion products of the detonation occurs. These durations are also short in comparison to the response time (time to reach maximum deflection) of the individual elements of the structures. Therefore, structures subjected to blast effects in the high-pressure range can, in certain cases, be designed for the impulse (area under the pressure-time curve, Chapter 2) rather than the peak pressure associated with longer duration blast pressures. If the acceptor system is comprised exclusively of explosives, the protective donor structure may be permitted to exceed incipient failure and produce "post failure" fragments provided that the fragment velocities are less than that which will initiate detonation of acceptor charges. This latter range of response is referred to as the "brittle mode of failure."

In the event personnel and/or expensive equipment is being protected or where containment type structures are providing the protection, then incipient failure design is not permitted. Here, the effects of the high pressure and the long duration pressures associated with contained products of the explosion must be accounted for in determining the protective structure response.

Fragments associated with the high-pressure range usually consist of high velocity missiles associated with casing breakup or acceleration of equipment positioned close to the explosion. For acceptors containing explosives, the velocities of primary fragments which penetrate the protective structure must be reduced to a level below the velocity which will cause detonation of the acceptor charges. For personnel or expensive equipment, the possibility of

fragment impact on the acceptor must be completely eliminated. Also associated with the "close-in" effects of a high-pressure design range are the possible occurrence of spalling of concrete elements. Spalling is generally associated with the disengagement of the concrete cover over reinforcement at the acceptor side of a protective element. Spalling can be a hazard to personnel and sometimes to equipment but seldom will result in propagation of explosion of an acceptor system.

1-14.2.3. Low-Pressure Design Range

Structures subjected to blast pressures associated with the low-pressure range sustain peak pressures of smaller intensity than those associated with the high-pressure range. However, the duration of the load can even exceed the response time of the structure. Structural elements designed for the low-pressure range depend on both pressure and impulse.

In cases where the peak pressure is relatively low and the explosive charge is very large (several hundred thousand pounds of explosive) the duration of blast pressures will be extremely long in comparison to those of smaller explosive weights. Here the structure responds primarily to the peak pressure in a manner similar to those structures designed to resist the effects of nuclear detonations. This latter case, although seldom encountered, is sometimes referred to as the "very low-pressure range."

Since the low-pressure design range is involved in the design of shelter type structures, donor fragmentation is of concern. Secondary fragments formed from the break-up of donor structures can produce minor damage to a shelter. These fragments generally have a large mass but their velocities are generally much less than those of primary fragments.

1-14.3. Analyzing Blast Environment

Although each design pressure range is distinct, no clear-cut divisions between the ranges exist; therefore, each protective structure must be analyzed to determine its response.

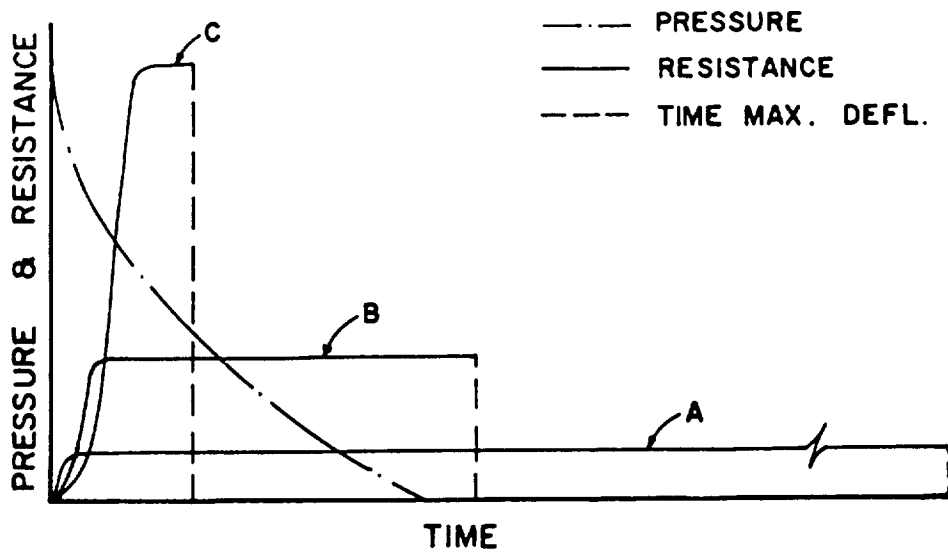
Structural response depends on design and load. Three possible designs, resulting in three distinct resistance-time responses are illustrated in Figure 1-6. Curve A represents the resistance-time function of an element which responds to the impulse; the time to reach maximum deflection is very long in comparison to the load duration. The low-pressure range is represented by Curve B where the element's response depends on both pressure and impulse. Here and dependent on design, the response time of an element can be less than, equal to, or greater than the load duration (Figure 1-6). Curve C illustrates the very low-pressure design range where the element responds to pressure. The required peak resistance is in the order of magnitude of the peak pressure, while the duration of the load is extremely long compared to the time to reach maximum deflection. Although the required maximum resistance will vary in comparison to the peak pressure, the variation will be slight and, in general, the required maximum resistance of an element to resist long duration loads will be only slightly larger (5 to 10 percent) than the peak pressure.

Figure 1-7 indicates semi-quantitatively the parameters which define the design ranges (including the very low range) of an element, along with the

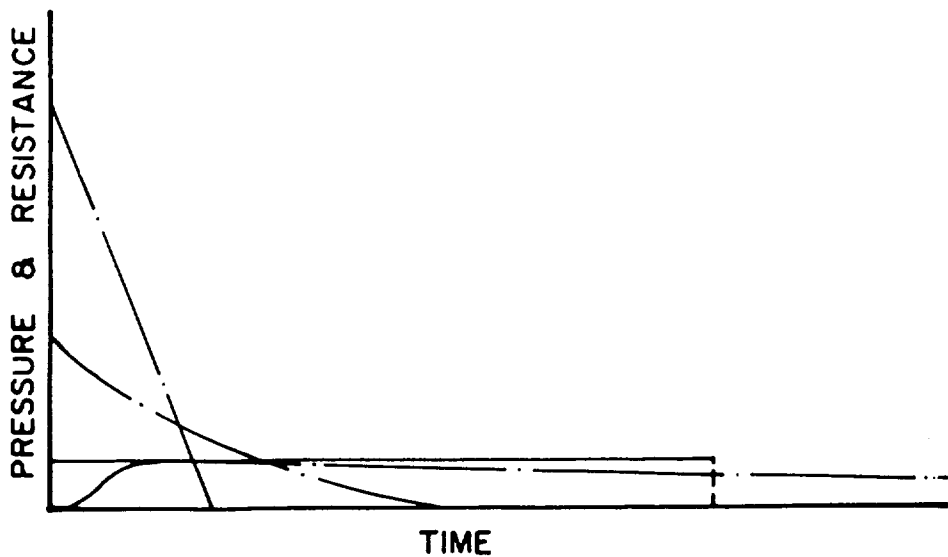
approximate relationship between the time to reach maximum deflection and the load duration.

It was indicated earlier that the design range of an element is related to the location of the element relative to the explosion. For the quantity of explosives considered in this manual, an element designed for the high-pressure range is usually situated immediately adjacent to the explosion, and its exposed surfaces facing the explosion are oriented normal or nearly normal to the propagation of the initial pressure wave (Figure 1-8, cases I through IV). On the other hand, elements which are located close to the explosion and are positioned parallel to the path of the wave propagation may respond to the blast effects associated with the low pressure design range. Elements located close to a detonation seldom respond solely to a peak pressure.

Certain elements of a protective structure located a distance from the explosion may respond to the impulse (high-pressure range) even though they are located at the low-pressure range while other structures located near the explosion will respond to the low-pressure design range. In the former case, the structure will not contain personnel or expensive equipment and will primarily serve as a barrier structure. In the latter case, the structure will serve as a shelter (Case I, Figure 1-8).



a) VARIABLE RESISTANCE - TIME CURVES



b) VARIABLE PRESSURE - TIME CURVES

Figure 1-6 Variation of structural response and blast loads

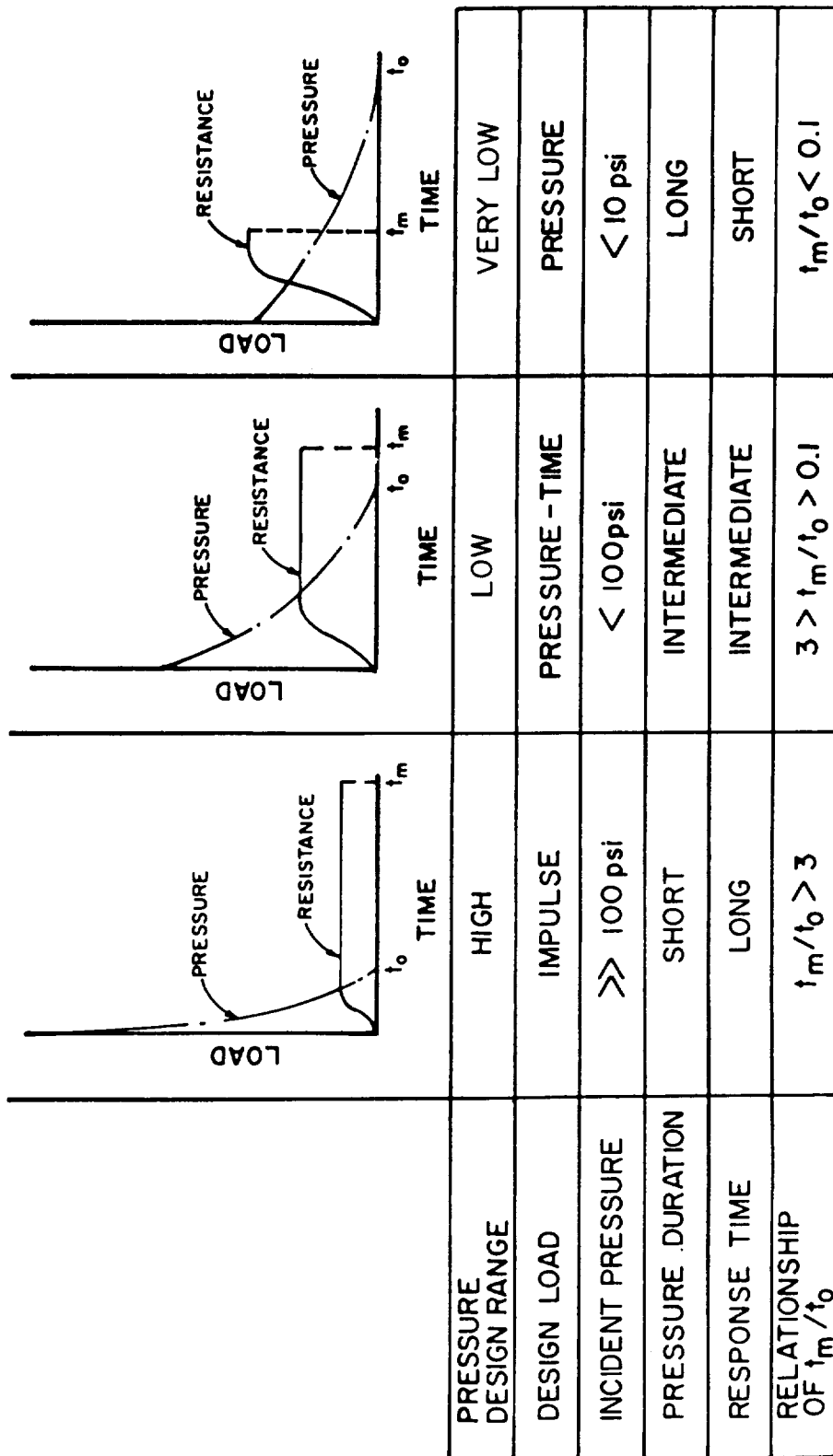
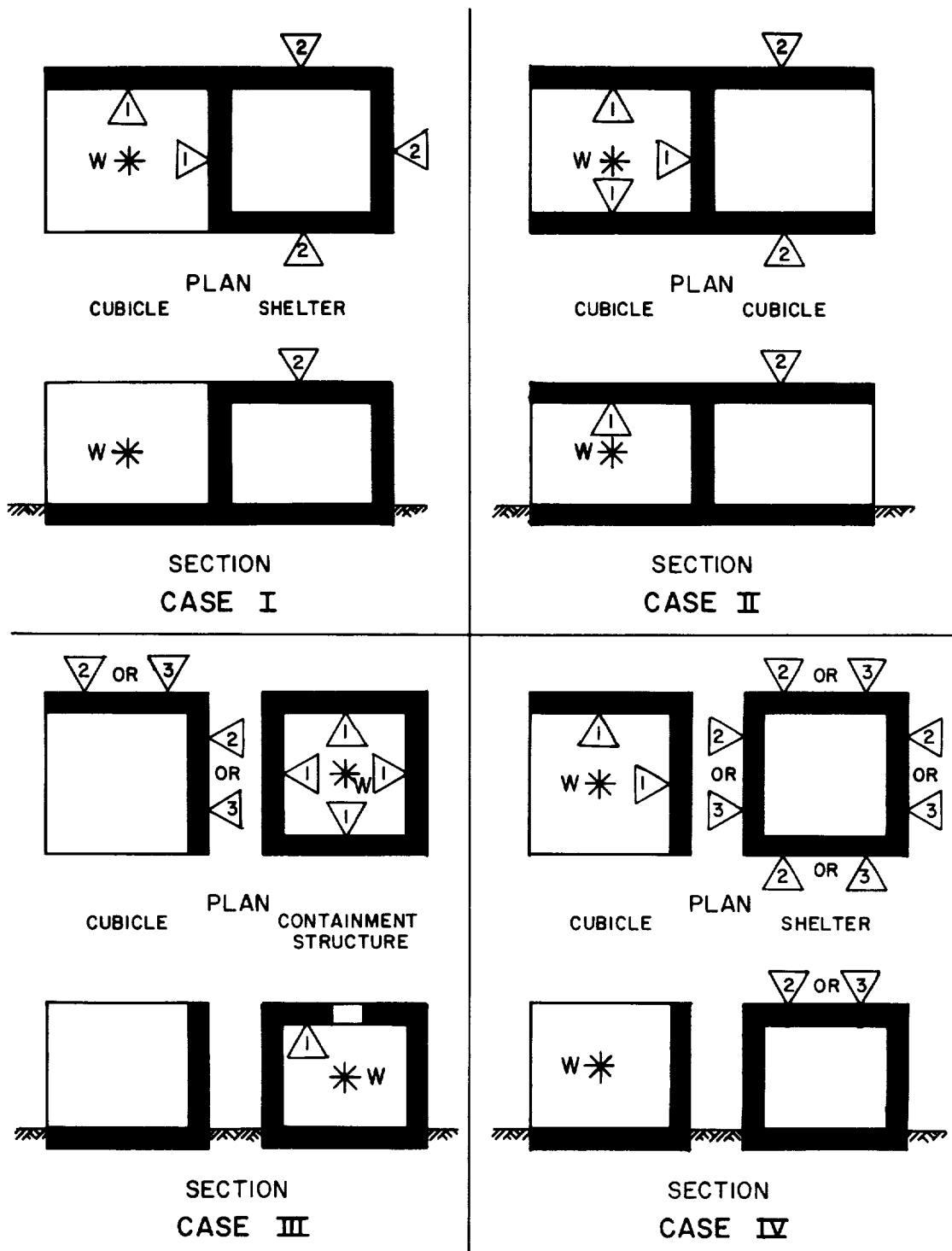


Figure 1-7 Parameters defining pressure design ranges



- LEGEND:**
- ▽1 HIGH-PRESSURE RANGE
 - ▽2 LOW-PRESSURE RANGE
 - ▽3 VERY LOW-PRESSURE RANGE

Figure 1-8 Design ranges corresponding to location of the structural elements relative to an explosion

APPENDIX 1A
LIST OF SYMBOLS

g	acceleration due to gravity (ft/sec ²)
i	unit positive impulse (psi-ms)
i_s^-	unit scaled impulse for use in figure 1-2 (psi-ms/lb ^{1/3})
p	pressure (psi)
t_m	time at which maximum deflection occurs (ms)
t_o	duration of positive phase of blast pressure (ms)
V	volume of containment structure (ft ³)
w_h	weight of human being (lbs)
W	charge weight (lbs)

APPENDIX 1B

BIBLIOGRAPHY

1. Structures to Resist the Effects of Accidental Explosions (with Addenda), Department of the Army Technical Manual (TM5-1300), Department of the Navy Publication (NAVFAC P-397), Department of the Air Force Manual (AFM 88-22), Washington, D.C., June 1969.
2. Dobbs, N., Structures to Resist the Effects of Accidental Explosions, Volume I, Introduction, Special Publication ARLCD-SP-84001, Prepared by Ammann & Whitney Consulting Engineers, New York, N.Y., for U.S. Army Armament Research, Development and Engineering Center, Armament Engineering Directorate, Picatinny Arsenal, Dover, New Jersey, December 1987.
3. Ayvazyan, H., et al., Structures to Resist the Effects of Accidental Explosions, Volume II, Blast, Fragment, and Shock Loads, Special Publication ARLCD-SP-84001, Prepared by Ammann & Whitney Consulting Engineers, New York, N.Y., in association with Southwest Research Institute, San Antonio, TX, for U.S. Army Armament Engineering Directorate, Picatinny Arsenal, Dover, New Jersey, December 1986.
4. Dede, M., et al., Structures to Resist the Effects of Accidental Explosions, Volume III, Principles of Dynamic Analysis, Special Publication ARLCD-SP-84001, Prepared by Ammann & Whitney Consulting Engineers, New York, N.Y., for U.S. Army Armament Research and Development Center, Large Caliber Weapon systems Laboratory, Dover, New Jersey, June 1984.
5. Dede, M., and Dobbs, N., Structures to Resist the Effects of Accidental Explosions, Volume IV, Reinforced Concrete Design, Special Publication ARLCD-SP-84001, Prepared by Ammann & Whitney Consulting Engineers, New York, N.Y., for U.S. Army Armament Research, Development and Engineering Center, Armament Engineering Directorate, Picatinny Arsenal, Dover, New Jersey, April 1987.
6. Kossover, D., and Dobbs, N., Structures to Resist the Effects of Accidental Explosions, Volume V, Structural Steel Design, Special Publication ARLCD-SP-84001, Prepared by Ammann & Whitney Consulting Engineers, New York, N.Y., for U.S. Army Armament Research, Development and Engineering Center, Armament Engineering Directorate, Picatinny Arsenal, Dover, New Jersey, May 1987.
7. Dede, M., Lipvin-Schramm, S., and Dobbs, N. Structures to Resist the Effects of Accidental Explosions, Volume VI, Special Conditions in Explosive Facility Design, Special Publication ARLCD-SP-84001, Prepared by Ammann & Whitney Consulting Engineers, New York, N.Y. for U.S. Army Armament Research and Development Center, Large Caliber Weapon System Laboratory, Dover, New Jersey, April 1985.
8. Safety Manual, AMC-R 385-100, Department of the Army, Headquarters U.S. Army Materiel Command, Alexandria, Virginia, August 1985.
9. A Manual for the Prediction of Blast and Fragment Loadings on Structures, DOE/TIC-11268, Prepared by Southwest Research Institute, San Antonio, TX, for U.S. Department of Energy, Albuquerque Operations Office, Amarillo Area Office, Pantex Plant, Amarillo, Texas, November 1980.
10. White, C.S., The Scope of Blast and Shock Biology and Problem Areas in Relating Physical and Biological Parameters, Lovelace Foundation for Medical Education and Research, Albuquerque, New Mexico, 1968.
11. Richmond, D.R., et al., The Relationship Between Selected Blast Wave Parameters and the Response of Mammals Exposed to Air Blast, Lovelace Foundation for Medical Education and Research, Albuquerque, New Mexico 1968.

12. Hirsch, F.G., Effects of Overpressure on the Ear - A Review, Lovelace Foundation for Medical Education and Research, Albuquerque, New Mexico, 1968.
13. Clemedson, C., Hellstrom, G. and Lingren, S., The Relative Tolerance of the Head, Thorax and Abdomen to Blunt Trauma, Defense Medical Board, Stockholm and Research Institute of National Defense, Sundbyberg, Sweden; Department of Surgery, University of Uppsala, Uppsala, Sweden; Department of Neurosurgery, University of Gothenburg, Gothenburg, Sweden, 1968.
14. Zaker, T.A., Fragment and Debris Hazards, Technical Paper No. 12, Department of Defense Explosives Safety Board, July 1975.
15. Zaker, T.A., Computer Program for Predicting Casualties and Damage from Accidental Explosions, Technical Paper No. 11, Department of Defense Explosives Safety Board, May 1975.
16. Cohen, and Dobbs, Prevention of and Protection Against Accidental Explosion of Munitions, Fuels and Other Hazardous Mixtures, Annals of the New York Academy of Science, October 1968.
17. Stirrat W., Compilation of Safe Separation Data on Bulk Explosives and Munitions, Technical Report ARAED-TR-87033, U.S. Army Armament Research, Development and Engineering Center, Dover, N.J., October, 1987.

"STRUCTURES TO RESIST THE EFFECTS OF ACCIDENTAL EXPLOSIONS"

CHAPTER 2. BLAST, FRAGMENT, AND SHOCK LOADS

CHAPTER 2

BLAST, FRAGMENT, AND SHOCK LOADS

INTRODUCTION

2-1. Purpose

The purpose of this manual is to present methods of design for protective construction used in facilities for development, testing, production, storage, maintenance, modification, inspection, demilitarization, and disposal of explosive materials.

2-2. Objective

The primary objectives are to establish design procedures and construction techniques whereby propagation of explosion (from one structure or part of a structure to another) or mass detonation can be prevented and to provide protection for personnel and valuable equipment.

The secondary objectives are to:

- (1) Establish the blast load parameters required for design of protective structures.
- (2) Provide methods for calculating the dynamic response of structural elements including reinforced concrete, and structural steel.
- (3) Establish construction details and procedures necessary to afford the required strength to resist the applied blast loads.
- (4) Establish guidelines for siting explosive facilities to obtain maximum cost effectiveness in both the planning and structural arrangements, providing closures, and preventing damage to interior portions of structures because of structural motion, shock, and fragment perforation.

2-3. Background

For the first 60 years of the 20th century, criteria and methods based upon results of catastrophic events were used for the design of explosive facilities. The criteria and methods did not include a detailed or reliable quantitative basis for assessing the degree of protection afforded by the protective facility. In the late 1960's quantitative procedures were set forth in the first edition of the present manual, "Structures to Resist the Effects of Accidental Explosions". This manual was based on extensive research and development programs which permitted a more reliable approach to current and future design requirements. Since the original publication of this manual, more extensive testing and development programs have taken place. This additional research included work with materials other than reinforced concrete which was the principal construction material referenced in the initial version of the manual.

Modern methods for the manufacture and storage of explosive materials, which include many exotic chemicals, fuels, and propellants, require less space for a given quantity of explosive material than was previously needed. Such concentration of explosives increases the possibility of the propagation of accidental explosions. (One accidental explosion causing the detonation of

other explosive materials.) It is evident that a requirement for more accurate design techniques is essential. This manual describes rational design methods to provide the required structural protection.

These design methods account for the close-in effects of a detonation including the high pressures and the nonuniformity of blast loading on protective structures or barriers. These methods also account for intermediate and far-range effects for the design of structures located away from the explosion. The dynamic response of structures, constructed of various materials, or combination of materials, can be calculated, and details are given to provide the strength and ductility required by the design. The design approach is directed primarily toward protective structures subjected to the effects of a high explosive detonation. However, this approach is general, and it is applicable to the design of other explosive environments as well as other explosive materials as mentioned above.

The design techniques set forth in this manual are based upon the results of numerous full- and small-scale structural response and explosive effects tests of various materials conducted in conjunction with the development of this manual and/or related projects.

2-4. Scope

It is not the intent of this manual to establish safety criteria. Applicable documents should be consulted for this purpose. Response predictions for personnel and equipment are included for information.

In this manual an effort is made to cover the more probable design situations. However, sufficient general information on protective design techniques has been included in order that application of the basic theory can be made to situations other than those which were fully considered.

This manual is applicable to the design of protective structures subjected to the effects associated with high explosive detonations. For these design situations, the manual will apply for explosive quantities less than 25,000 pounds for close-in effects. However, this manual is also applicable to other situations such as far- or intermediate-range effects. For these latter cases the design procedures are applicable for explosive quantities in the order of 500,000 pounds which is the maximum quantity of high explosive approved for aboveground storage facilities in the Department of Defense manual, "Ammunition and Explosives Safety Standards", DOD 6055.9-STD. Since tests were primarily directed toward the response of structural steel and reinforced concrete elements to blast overpressures, this manual concentrates on design procedures and techniques for these materials. However, this does not imply that concrete and steel are the only useful materials for protective construction. Tests to establish the response of wood, brick blocks, and plastics, as well as the blast attenuating and mass effects of soil are contemplated. The results of these tests may require, at a later date, the supplementation of these design methods for these and other materials.

Other manuals are available to design protective structures against the effects of high explosive or nuclear detonations. The procedures in these manuals will quite often complement this manual and should be consulted for specific applications.

Computer programs, which are consistent with procedures and techniques contained in the manual, have been approved by the appropriate representative of the US Army, the US Navy, the US Air Force and the Department of Defense Explosives Safety Board (DDESB). These programs are available through the following repositories:

- (1) Department of the Army
Commander and Director
U.S. Army Engineer
Waterways Experiment Station
Post Office Box 631
Vicksburg, Mississippi 39180-0631
Attn: WESKA
- (2) Department of the Navy
Commanding Officer
Naval Civil Engineering Laboratory
Port Hueneme, California 93043
Attn: Code L51
- (3) Department of the Air Force
Aerospace Structures
Information and Analysis Center
Wright Patterson Air Force Base
Ohio 45433
Attn: AFFDL/FBR

If any modifications to these programs are required, they will be submitted for review by DDESB and the above services. Upon concurrence of the revisions, the necessary changes will be made and notification of the changes will be made by the individual repositories.

2-5. Format

This manual is subdivided into six specific chapters dealing with various aspects of design. The titles of these chapters are as follows:

Chapter 1	Introduction
Chapter 2	Blast, Fragment, and Shock Loads
Chapter 3	Principles of Dynamic Analysis
Chapter 4	Reinforced Concrete Design
Chapter 5	Structural Steel Design
Chapter 6	Special Considerations in Explosive Facility Design

When applicable, illustrative examples are included in the Appendices.

Commonly accepted symbols are used as much as possible. However, protective design involves many different scientific and engineering fields, and, therefore, no attempt is made to standardize completely all the symbols used. Each symbol is defined where it is first used, and in the list of symbols at the end of each chapter.

CHAPTER CONTENTS

2-6. General

This chapter contains the procedures for determining explosive output and associated structure loadings, fragment effects, and the structural motion effects associated with accidental explosions. These procedures are contained in the following sections: Sections 2-8 through 2-15 deals with the loadings associated with the blast phenomena. These data include, in addition to the determination of the effects of the explosive output, methods for determining blast loads acting on the exterior of and within structures. Sections 2-16 through 2-19 cover the formation of fragments which can be projected by an explosion and include both primary and secondary fragments effects. Sections 2-20 to 2-24 present the method for determining the structural motions, including both ground and air shock effects.

EXPLOSION EFFECTS

2-7. Effects of Explosive Output

In the design of protective structures to resist the effects of accidental explosions, the principal effects of the explosive output to be considered are blast overpressures (hereafter referred to as blast pressures or pressures), fragments generated by the explosion and the shock loads produced by the shock wave transmitted through the air or ground. Of these three parameters, the blast pressures are usually the governing factor in the determination of the structure response. However, in some situations, fragments and/or shock loads may be just as important as the pressures in determining the configuration of the facility.

Although the quantitative data presented pertain to the blast output of bare trinitrotoluene (TNT) spherical or hemispherical charges considered as point source explosions, and other explosives which have been specifically tested. These data can be extended by appropriate means including testing to include other potentially mass-detonating materials (solid, liquid, or gas) of varying shape.

BLAST LOADS

2-8. Blast Phenomena

2-8.1. General

Bare, solid explosives must detonate to produce any explosive effect other than a fire. The term detonation refers to a very rapid and stable chemical reaction which proceeds through the explosive material at a speed, called the detonation velocity, which is supersonic in the unreacted explosive. Detonation velocities range from 22,000 to 28,000 feet per second for most high explosives. The detonation wave rapidly converts the solid or liquid explosive into a very hot, dense, high-pressure gas, and the volume of this gas which had been the explosive material is then the source of strong blast waves in air. Pressures immediately behind the detonation front range from 2,700,000 to 4,900,000 psi. Only about one-third of the total chemical energy available in most high explosives is released in the detonation process. The remaining two-thirds is released more slowly in explosions in air as the detonation products mix with air and burn. This afterburning process has only a slight effect on blast wave properties because it is so much slower than detonation.

The blast effects of an explosion are in the form of a shock wave composed of a high-intensity shock front which expands outward from the surface of the explosive into the surrounding air. As the wave expands, it decays in strength, lengthens in duration, and decreases in velocity. This phenomena is caused by spherical divergence as well as by the fact that the chemical reaction is completed, except for some afterburning associated with the hot explosion products mixing with the surrounding atmosphere.

As the wave expands in air, the front impinges on structures located within its path and then the entire structure is engulfed by the shock pressures. The magnitude and distribution of the blast loads on the structure arising from these pressures are a function of the following factors: (1) explosive properties, namely type of explosive material, energy output (high or low order detonation), and weight of explosive; (2) the location of the detonation relative to the protective structures; and (3) the magnitude and reinforcement of the pressure by its interaction with the ground barrier, or the structure itself. The first of these three factors are discussed in Sections 2-8.2 and 2-9 below and the latter two factors are discussed throughout the remainder of this section.

2-8.2. Explosive Materials

Explosive materials may be classified according to their physical state: solids, liquids, or gases. Solid explosives are primarily high explosives; however, other materials such as flammable chemicals and propellants may also be classified as potentially explosive materials. Liquid and gaseous explosives encompass a wide variety of substances used in the manufacture of chemicals, fuels, and propellants. The blast pressure environment produced will vary not only among the different materials but may also differ for a particular material. Such factors as methods and procedures used in manufacturing, storage, and handling, in addition to specific individual physical and chemical characteristics, may alter the blast effects of an explosive material.

The blast effects of solid materials are best known. This is particularly true for high-explosive materials. The blast pressures, impulses, durations, and other blast effects of an explosion have been well established. These effects are contained in this chapter.

Unlike high-explosive materials, other solid, liquid, and gaseous explosive materials will exhibit a variation of their blast pressure output. An explosion of these materials is in many cases incomplete, and only a portion of the total mass of the explosive (effective charge weight) is involved in the detonation process. The remainder of the mass is usually consumed by deflagration resulting in a large amount of the material's chemical energy being dissipated as thermal energy which, in turn, may cause fires or thermal radiation damage.

2-9. TNT Equivalency

The major quantity of blast effects data presented in this manual pertains to the blast pressures output of bare spherical TNT explosive. These data can be extended to include other potentially mass-detonating materials (Class 1.1) by relating the explosive energy of the "effective charge weight" of those materials to that of an equivalent weight of TNT. In addition to the energy output, other factors may affect the equivalency of material compared to TNT. These factors include the material shape (flat, square, round, etc.), the number of explosive items, explosive confinement (casing, containers, etc.), and the pressure range being considered (close-in, intermediate or far ranges). These other factors will be discussed later in this manual.

For blast resistant design, the effects of the energy output on explosive material, of a specific shape, relative to that of TNT, of similar shape, can be expressed as function of the heat of detonation of the various materials as follows:

$$W_E = \frac{H_{EXP}^d}{H_{TNT}^d} W_{EXP} \quad 2-1$$

where

W_E = effective charge weight

W_{EXP} = weight of the explosive in question

H_{EXP}^d = heat of detonation of explosive in question

H_{TNT}^d = heat of detonation of TNT

The heat of detonation of some of the more commonly used explosives are listed in Table 2-1.

The above equation for the effective charge weight is related primarily to the blast output associated with the shock effects of unconfined detonations (Section 2-13). The effective charge weight produced by the confinement effects

of explosions (Section 2-14) will differ. These differences will be discussed later in this manual.

2-10. Blast-Loading Categories

Blast loads on structures can be divided into two main groups based on the confinement of the explosive charge (unconfined and confined explosions) and can be subdivided based on the blast loading produced within the donor structure or acting on acceptor structures. These blast loading categories are illustrated in Figure 2-1. Figure 2-1 gives the six blast loading categories possible. Figure 2-1 also shows the five possible pressure loads associated with the blast load categories, the location of the explosive charge which would produce these pressure loads, and the protective structures subjected to these loads.

The blast load categories and the resulting pressure loads listed in Figure 2-1 are qualitatively and, quantitatively defined below and in subsequent sections, respectively.

2-10.1. Unconfined Explosion

2-10.1.1. Free Air Burst Explosion

An explosion, which occurs in free air, produces an initial output whose shock wave propagates away from the center of the detonation, striking the protective structure without intermediate amplification of its wave.

2-10.1.2. Air Burst Explosion

An explosion which is located at a distance from and above the protective structure so that the ground reflections of the initial wave occur prior to the arrival of the blast wave at the protective structure. As used in this manual, an air burst is limited to an explosion which occurs at two to three times the height of a one or two-story building.

2-10.1.3. Surface Burst Explosion

A surface burst explosion will occur when the detonation is located close to or on the ground so that the initial shock is amplified at the point of detonation due to the ground reflections.

2-10.2. Confined Explosion

2-10.2.1. Fully Vented Explosion

A fully vented explosion will be produced within or immediately adjacent to a barrier or cubicle type structure with one or more surfaces open to the atmosphere. The initial wave, which is amplified by the nonfrangible portions of the structure, and the products of detonation are totally vented to the atmosphere forming a shock wave (leakage pressures) which propagates away from the structure.

2-10.2.2. Partially Confined Explosion

A partially confined explosion will be produced within a barrier or cubicle type structure with limited size openings and/or frangible surfaces. The initial wave, which is amplified by the frangible and nonfrangible portion of the structure, and the products of detonation are vented to the atmosphere after a finite period of time. The confinement of the detonation products, which consist of the accumulation of high temperatures and gaseous products, is associated with a buildup of quasi-static pressure (hereafter referred to as gas pressure). This pressure has a long duration in comparison to that of the shock pressure.

2-10.2.3. Fully Confined Explosions

Full confinement of an explosion is associated with either total or near total containment of the explosion by a barrier structure. Internal blast loads will consist of unvented shock loads and very long duration gas pressures which are a function of the degree of containment. The magnitude of the leakage pressures will usually be small and will only affect those facilities immediately outside the containment structure.

2-11. Blast Loading Protection

Protection of personnel and valuable equipment (acceptor system) will usually involve protective shelters located away from the detonation. Their design may involve one or more of the following blast-loading categories: free-air burst, air burst, surface burst, and exterior or leakage pressures from either vented or partially confined explosions. These shelters are usually enclosed buildings located at pressure ranges of a few hundred pounds per square inch (psi) or less. Depending on the shelter design pressures, these structures can be either above, below, or at ground surface. In this manual, primary consideration is given to above-ground shelters. However, some consideration is given in Chapter VI regarding shelters positioned at other locations. For the third type of pressure loading of Figure 2-1 (interior shock pressure), protection is required when the shelter is located immediately adjacent to the explosion. The reflected pressure there may be in thousands of psi, but with pressure durations usually small. The acceptor portion of such an explosive system may include other explosive materials and/or personnel. The structure associated with the fifth pressure-loading type is a containment type building and is usually used to prevent escape of toxic chemicals, radiological and/or biological materials, or to limit blast pressures at the exterior to a level consistent with personnel protection.

Of the six categories, those from air bursts are seldom encountered and the free air burst is the least likely to occur. The possibility of such blast environments exists where potentially explosive materials are stored at heights adjacent to or away from protective structures such as in manufacturing (process or storage tanks) or missile sites. In the latter, the rocket propellant would be a source of explosive danger to the ground crew and control facilities.

The other four blast-loading categories can occur in most explosive manufacturing and storage facilities. In such installations, transportation of explosive materials between buildings either by rail, vehicle, or in the case of

liquid or gases, through piping, is a possibility. Also, storage and handling of explosives within buildings are common occurrences.

Although the blast-loading categories can be separated and classified individually, no clear-cut limits differentiate each category. In most explosive facilities, the various blast environments will overlap, and judgement should be used in the application of the following recommendations for determining the blast parameters consistent with the various blast-loading categories.

2-12. Blast-Wave Phenomena

The violent release of energy from a detonation converts the explosive material into a very high pressure gas at very high temperatures. A pressure front associated with the high pressure gas propagates radially into the surrounding atmosphere as a strong shock wave, driven and supported by the hot gases. The shock front, termed the blast wave, is characterized by an almost instantaneous rise from ambient pressure to a peak incident pressure P_{s0} (Figure 2-2).

This pressure increase or shock front travels radially from the burst point with a diminishing shock velocity U which is always in excess of the sonic velocity of the medium. Gas molecules behind the front move at lower flow velocities, termed particle velocities u . These latter particle velocities are associated with the dynamic pressures, whose maximum values are denoted q_0' or the pressures formed by the winds produced by the passage of the shock front. As the shock front expands into increasingly larger volumes of the medium, the peak incident pressures at the fronts decrease and the durations of the pressures increase. Those parameters which vary as the peak incident pressure varies are presented in Figure 2-3.

At any point away from the burst, the pressure disturbance has the shape shown in Figure 2-2. The shock front arrives at a given location at time t_A and, after the rise to the peak value, P_{s0} the incident pressure decays to the ambient value in time t_0^+ which is the positive phase duration. This is followed by a negative phase with a duration t_0^- that is usually much longer than the positive phase and characterized by a negative pressure (below ambient pressure) having a maximum value of P_{s0}^- as well as a reversal of the particle flow. The negative phase is usually less important in a design than is the positive phase, and its amplitude P_s^- must, in all cases, be less than ambient atmosphere pressure p_0 . The incident impulse density associated with the blast wave is the integrated area under the pressure-time curve and is denoted as i_s^+ for the positive phase and i_s^- for the negative phase.

An additional parameter of the blast wave, the wave length, is sometimes required in the analysis of structures. The positive wave length L_w^+ is that length at a given distance from the detonation which, at a particular instant of time, is experiencing positive pressure. The negative wave length L_w^- is similarly defined for negative pressures.

The above treatment of the blast wave phenomena is general. In subsequent sections of this chapter, the magnitude of the various parameters is presented depending upon the category of the detonation as previously described: free air burst, surface burst, exterior or leakage pressures, or interior or high pressure blast loading.

2-13. Unconfined Explosions

2-13.1. Free Air Burst

When a detonation occurs adjacent to and above a protective structure such that no amplification of the initial shock wave occurs between the explosive source and the protective structure, then the blast loads acting on the structure are free-air blast pressures (Fig. 2-4).

As the incident wave moves radially away from the center of the explosion, it will impact with the structure, and, upon impact, the initial wave (pressure and impulse) is reinforced and reflected (Fig. 2-5). The reflected pressure pulse of Figure 2-5 is typical for infinite plane reflectors.

When the shock wave impinges on a surface oriented so that a line which describes the path of travel of the wave is normal to the surface, then the point of initial contact is said to sustain the maximum (normal reflected) pressure and impulse. Figure 2-6 presents the ratios of the normal reflected pressures to the incident pressures as a function of the incident pressures.

The peak pressure and impulse patterns on the structure vary with distance from a maximum at the normal distance R_A to a minimum (incident pressure) where the plane of the structure's surface is perpendicular to the shock front. The positive phase pressures, impulses, durations, and other parameters of this shock environment for a spherical TNT explosions are given in Figure 2-7 versus the scaled distance ($Z = R/W^{1/3}$).

The smallest scaled distance of $0.136 \text{ ft/lb}^{1/3}$ represents the radius of the spherical TNT explosive and, therefore, represents the surface of the explosive. Some parameters have been extrapolated to the charge surface which are shown as dashed portions of the curves. These dashed curves represent an upper limit of scatter in experimental data and variation in theoretical predictions, giving for design purposes conservative limits for these parameters.

In some blast loading situations, negative blast wave parameters (Fig. 2-8) are needed to predict the loading-time function of the blast wave acting on a structure. This is particularly true in flexible type protective structures (usually steel-frame structures) where the overall motion of the structure will be affected by the phasing of the blast loads acting on the various structure surfaces. The effects of the negative phase parameters are usually not important for the design of the more rigid type structures (reinforced concrete).

The curves presented in Figures 2-7 and 2-8 which give the blast wave parameters as a function of scaled distance, extend only to a scaled distance $Z = 100 \text{ ft/lb}^{1/3}$. For most protective structures, or even light structures, damage is relatively superficial beyond this scaled distance, consisting at most of broken windows or deformation of light panels or blow-out walls. But, the curves are also not extended beyond these levels because the blast wave properties start to be seriously affected by atmospheric conditions so that overpressures are very much less or very much more than the "ideal" parameters transmitted through a homogeneous atmosphere.

In the low pressure region, the pressure varies as a function of sound velocity with altitude above the ground surface. At very far distances from an explosion ($Z = 1000 \text{ ft}/lb^{1/3}$, the peak pressures (really sound pressures at these levels) can be ten times greater or more than ten times less than the ideal pressures for a homogenous atmosphere.

Even with enhancement caused by real atmospheric conditions (also called blast focusing), the pressures are still quite low and structural damage should be superficial. If it is necessary to predict such low levels, one should obtain and study more detailed reports listed in the bibliography.

The variation of the pressure and impulse patterns on the surface of a structure between the maximum and minimum values is a function of the angle of incidence. This angle is formed by the line which defines the normal distance R_A between the point of detonation and the structure, and line R (slant distance) which defines the path of shock propagation between the center of the explosion and any other point in question on the structure surface (Fig. 2-4).

The effects of the angle of incidence on the peak reflected pressure $P_{r\alpha}$ and the reflected impulse $i_{r\alpha}$ are shown in Figures 2-9 and 2-10, respectively. The figures are plots of the angle of incidence versus the peak reflected pressure or the reflected impulse as a function of the scaled normal distance between the charge and the surface in question. The usual load condition involves the ground surface and, therefore, this normal scaled distance is referred to as the scaled height of charge above the ground ($H_C/W^{1/3}$). All other blast parameters are obtained from Figures 2-7 and 2-8 for the scaled slant distance $R/W^{1/3}$ to the point in question.

2-13.2. Air Burst

The air burst environment is produced by detonations which occur above the ground surface and at a distance away from the protective structure so that the initial shock wave, propagating away from the explosion, impinges on the ground surface prior to arrival at the structure. As the shock wave continues to propagate outward along the ground surface, a front known as the Mach front (Fig. 2-11) is formed by the interaction of the initial wave (incident wave) and the reflected wave. This reflected wave is the result of the reinforcement of the incident wave by the ground surface.

Some variation of the pressures over the height of the Mach front occurs, but for design purposes, this variation can be neglected and the shock considered as a plane wave over the full height of the front. The blast parameters in the Mach front are calculated at the ground surface. The pressure-time variation of the Mach front (Fig. 2-12a) is similar to that of the incident wave except that the magnitude of the blast parameters are somewhat larger.

The height of the Mach front increases as the wave propagates away from the center of the detonation. This increase in height is referred to as the path of the triple point and is formed by the intersection of the initial, reflected, and Mach waves. A protected structure is considered to be subjected to a plane wave (uniform pressure) when the height of the triple point exceeds the height of the structure. The scaled height of the triple point $H_T/W^{1/3}$ versus scaled ground distance Z_G and scaled charge height $H_C/W^{1/3}$ is plotted in Figure 2-13.

If the height of the triple point does not extend above the height of the structure, then the magnitude of the applied loads will vary with the height of the point being considered. Above the triple point, the pressure-time variation consists of an interaction of the incident and reflected incident wave pressures resulting in a pressure-time variation (Fig. 2-12b) different from that of the Mach incident wave pressures. The magnitude of pressures above the triple point is smaller than that of the Mach front. In most practical design situations, the location of the detonation will be far enough away from the structure so as not to produce this pressure variation. An exception may exist for multistory buildings even though these buildings are usually located at very low-pressure ranges where the triple point is high.

In determining the magnitude of the air blast loads acting on the surface of an above-ground protective structure, the peak incident blast pressures in the Mach wave acting on the ground surface immediately before the structure are calculated first. The peak incident pressure $P_{r\alpha}$ is determined for this point from Figure 2-9 using the scaled height of charge above the ground $H_c/W^{1/3}$ and the angle of incidence α .

A similar procedure is used with Figure 2-10 to determine the impulse $i_{r\alpha}$ of the blast wave acting on the ground surface immediately before the structure. An estimate of the other blast parameters may be obtained from Figures 2-7 and 2-8 by setting the values of $P_{r\alpha}$ and $i_{r\alpha}$ equal to the values of the peak incident pressure P_{so} and incident impulse i_s of the mach wave, respectively. The scaled distances corresponding to P_{so} and i_s are determined from Figure 2-7. The scaled distance corresponding to P_{so} is used to obtain values of P_r , P_{so}^- , $t_A/W^{1/3}$, U , $L_W/W^{1/3}$ and $L_W^-/W^{1/3}$ while the scaled distance corresponding to i_s is used to obtain values of i_r , i_s^- , i_r^- , $t_o/W^{1/3}$ and $t_o^-/W^{1/3}$.

2-13.3. Surface Burst

A charge located on or very near the ground surface is considered to be a surface burst. The initial wave of the explosion is reflected and reinforced by the ground surface to produce a reflected wave. Unlike the air burst, the reflected wave merges with the incident wave at the point of detonation to form a single wave, similar in nature to the mach wave of the air burst but essentially hemispherical in shape (Fig. 2-14).

The positive phase parameters of the surface burst environment for hemispherical TNT explosions are given in Figure 2-15 while the negative phase parameters are given in Figure 2-16. A comparison of these parameters with those of free-air explosions (Fig. 2-7 and 2-8) indicate that, at a given distance from a detonation of the same weight of explosive, all of the parameters of the surface burst environment are larger than those for the free-air environment.

As for the case of air bursts, protected structures subjected to the explosive output of a surface burst will usually be located in the pressure range where the plane wave (Fig. 2-14) concept can be applied. Therefore, for a surface burst, the blast loads acting on structure surface are calculated as described for an air burst except that the incident pressures and other positive phase parameters of the free-field shock environment are obtained from Figure 2-15, and theoretical negative phase blast parameters are shown in Figure 2-16.

As for the case of an air burst, the curves presented in Figures 2-15 and 2-16 which give the blast wave parameters as a function of scaled distance, extend only to a scaled distance $Z = 100 \text{ ft/lb}^{1/3}$ (see section 2-13.1).

Blast parameters for explosives detonated on the ground surface other than hemispherical TNT are listed in Table 2-2. These explosives include both uncased and cased high explosives, propellants and propelling charges as well as pyrotechnic mixtures. The various shapes of the explosive materials are given in Figure 2-17. The blast parameters for the various explosives are illustrated in Figures 2-18 through 2-49. For each explosive material considered, the peak incident pressure P_{so} and scaled incident impulse $i_s/W^{1/3}$ is presented as a function of the scaled ground distance $Z_G = R_G/W^{1/3}$ from the point of detonation. The charge weight W is equal to the actual weight of the explosive material under consideration increased by the required factor of safety (20 percent).

An estimate of the blast parameters other than incident pressure and impulse, may be obtained from Figures 2-15 and 2-16. The scaled ground distance corresponding to the incident pressure P_{so} is used to obtain the values of P_r , P_{so}^- , P_r^- , $t_A/W^{1/3}$, U , $L_w/W^{1/3}$ and $L_w^-/W^{1/3}$. In addition, this scaled ground distance $Z_G = R_G/W^{1/3}$ is used to calculate the equivalent TNT design charge weight W for pressure using the actual ground distance R_G . The absolute values of the scaled blast parameters are obtained by multiplying the scaled values by the equivalent TNT design charge weight.

The scaled ground distance corresponding to the incident impulse requires a graphical solution. The point corresponding to the scaled incident impulse and scaled ground distance for the explosive material in question is plotted on Figure 2-15. A 45 degree line is drawn through this point. The point where the line intersects the scaled impulse curve corresponds to the scaled impulse and scaled ground distance for the equivalent TNT charge. This scaled ground distance is then used to obtain the values of $i_r/W^{1/3}$, $i_s^-/W^{1/3}$, $i_r^-/W^{1/3}$, $t_o/W^{1/3}$ and $t_o^-/W^{1/3}$. In addition, this scaled ground distance and the actual ground distance is used to calculate the equivalent TNT design charge weight for impulse. The absolute values of the scaled blast parameters are obtained by multiplying the scaled values by the equivalent TNT design charge weight.

It may be noted that the above data for explosives other than TNT is limited to surface bursts with container shapes indicated in Figure 2-17. This data should not be extrapolated for scaled distances less than those indicated on Figures 2-18 through 2-49. In addition, the blast pressure and impulse for propellants and, in particular, the pyrotechnic mixtures were obtained from tests which utilized booster charges to initiate the explosive material. Therefore, the blast parameters for both of these materials should be considered as upper limits.

2-13.4. Multiple Explosions

When two or more explosions of similar material occur several milliseconds apart, the blast wave of the initial explosion will propagate ahead of the waves resulting from the subsequent explosions, with the phasing of the propagation of these latter waves being governed by the initiation time and orientation of the individual explosives. If the time delay between explosions is not too large, the blast waves produced by the subsequent explosions will

eventually overtake and merge with that of the initial detonation. The distance from the explosion at which this merger occurs will depend on: (1) the magnitude of the individual explosions, (2) the time delays between the initiation of the explosions, (3) the separation distances between and orientation of the explosives, and (4) obstructions between the explosives themselves and other obstructions between the explosives and other parts of the facility (buildings, walls, barricades, terrain, etc.) which will distort, hinder, and generally interfere with wave propagation.

The pressure time relationships associated with the wave propagation will depend upon the interaction of the individual waves themselves. After all the waves have merged, the pressures associated with the common or merged wave will have a pressure-time relationship which is similar to that produced by a single explosion (Fig. 2-12). However, at closer distances to the explosion, the pressure-time relationship will be more closely represented by a pressure-time curve with multiple peak pressures (similar to that occurring above the triple point (Fig. 2-12)). The multiple peak pressures represent the interaction as the various waves reach the point in question. At distances even closer to the explosion, the time history of the pressures acting on the ground surface may consist of a series of completely separate blast loads. This loading condition is a result of the arrival of the subsequent blast waves at a particular point during or after the occurrence of the negative phase pressures produced by the initial wave at that point.

The latter pressure-time relationship is probably most likely to occur at high pressures close to the explosions while the multiple peak pressure pulse is normally associated with low pressures at far distances. However, in many instances, the multiple peak pressure pulse will occur at high pressures, in particular where the individual explosives are positioned close together, e.g., in a cubicle or other storage facility.

2-14. Confined Explosions

2-14.1. Effects of Confinement

When an explosion occurs within a structure, the peak pressures associated with the initial shock front (free-air pressures) will be extremely high and, in turn, will be amplified by their reflections within the structure. In addition, and depending upon the degree of confinement, the effects of the high temperatures and accumulation of gaseous products produced by the chemical process involved in the explosion will exert additional pressures and increase the load duration within the structure. The combined effects of these pressures may eventually destroy the structure unless the structure is designed to sustain the effects of the internal pressures. Provisions for venting of these pressures will reduce their magnitude as well as their duration.

The use of cubicle-type structures (Fig. 2-50a) or other similar barriers with one or more surfaces either sufficiently frangible or open to the atmosphere will provide some degree of venting depending on the opening size. This type of structure will permit the blast wave from an internal explosion to spill over onto the surrounding ground surface, thereby, significantly reducing the magnitude and duration of the internal pressures. The exterior pressures are quite often referred to as "leakage" pressures while the pressures reflected and reinforced within the structure are termed interior "shock pressures". The pressures associated with the accumulation of the gaseous products and

temperature rise are identified as "gas" pressures. For the design of most fully vented cubicle type structures, the effects of the gas pressure may be neglected.

Detonation in an enclosed structure with relatively small openings (Fig. 2-50b) is associated with both shock and gas pressures whose magnitudes are a maximum. The duration of the gas pressure and, therefore, the impulse of the gas pressure is a function of the size of the opening. It should be noted that the onset of the gas pressure does not necessarily coincide with the onset of the shock pressure. Further, it takes a finite length of time after the onset for the gas pressure to reach its maximum value. However, these times are very small and, for design purposes of most confined structures, they may be treated as instantaneous.

The term "frangible" pertains to those elements of a protective structure which fail and whose strength and mass are such as to reduce the amplification of the shock pressures and the confinement of the explosive gases. To reduce the amplification of the shock pressures, frangible elements must fail so as to relieve quickly the interior pressures acting on those surfaces and minimize their reflection to the nonfrangible elements of the structure. Blast tests of glass panels have shown that a true frangible material does not exist and that some reflection of the initial blast pressures may be expected from very weak and light elements. Further, the buildup of gas pressures is a function of the ratio of the weight of the charge to the volume of the confining structure and the venting area. As stated, this pressure buildup will not begin until sometime after the onset of the shock pressures. Therefore, an element which is not considered frangible for the shock pressure may be frangible for gas pressures.

In addition to being dependent upon the physical properties of an element, frangibility will also be a function of the magnitude of the applied blast loads and, therefore, a function of the quantity of explosive being contained and the distance from the frangible element. Although frangibility is imperfectly understood and difficult to measure, in general, it can be assumed that if a closure's resistance to outward motion is equal to or less than 25 pounds per square foot of surface area, the resistance can be neglected since the time to reach failure is practically zero. In this case, frangibility can be stated solely in terms of the weight (inertial force) of the vent area closure. For resistances greater than 25 psf, the evaluation of frangibility must include the effects of resistance in addition to the weight of an element. The combined effects of the inertial force and the resistance can be accounted for by performing a dynamic analysis and determining the time to reach failure. However, if the blast pressure is very large in comparison to the resistance of the element, the effects of the resistance can be neglected without introducing significant errors. Therefore, it is advantageous to use vent closures that are light and inherently weak and/or weakly supported; such as, corrugated metal decking supported on steel joists, metal panels for walls, plexiglass or thin fiberglass panels supported by wood or lightweight steel frames or gypsum board panels.

In the following paragraphs of this section, a simple cantilever barrier as well as cubicle-type and containment type structures will be discussed. The cubicles are assumed to have one or more surfaces which are open or frangible while the containment structures are either totally enclosed or have small

size openings. The effects of the inertia of frangible elements of these structures will be discussed in subsequent sections.

2-14.2. Shock Pressures

2-14.2.1. Blast Loadings

When an explosion occurs within a cubicle or containment-type structure, the peak pressures as well as the impulse associated with the shock front will be extremely high and will be amplified by the confining structure. Because of the close-in effects of the explosion and the reinforcement of blast pressures due to the reflections within the structure, the distribution of the shock loads on any one surface will be nonuniform with the structural surface closest to the explosion subjected to the maximum load.

An approximate method for the calculation of the internal shock pressures has been developed using theoretical procedures based on semi-empirical blast data and on the results of response tests on slabs. The calculated average shock pressures have been compared with those obtained from the results of tests of a scale-model steel cubicle and have shown good agreement for a wide range of cubicle configurations. This method consists of the determination of the peak pressures and impulses acting at various points of each interior surface and then integrating to obtain the total shock load. In order to simplify the calculation of the response of a protective structure wall to these applied loads, the peak pressures and total impulses are assumed to be uniformly distributed on the surface. The peak average pressure and the total average impulse are given for any wall surface. The actual distribution of the blast loads is highly irregular, because of the multiple reflections and time phasing and results in localized high shear stresses in the element. The use of the average blast loads, when designing, is predicated on the ability of the element to transfer these localized loads to regions of lower stress. Reinforced concrete with properly designed shear reinforcement and steel plates exhibit this characteristic.

The parameters which are necessary to determine the average shock loads are the structure's configuration and size, charge weight, and charge location. Figure 2-51 shows many possible simple barriers, cubicle configurations, and containment type structures as well as the definition of the various parameters pertaining to each. Surfaces depicted are not frangible for determining the shock loadings. The effects of frangibility will be discussed later.

Because of the wide range of required parameters, the procedure for the determination of the shock loads was programmed for solutions on a digital computer. The results of these calculations are presented in Figures 2-52 through 2-100 for the average peak reflected pressures p_r and Figures 2-101 through 2-149 for the average scaled unit impulse $i^-/W^{1/3}$. These shock loads are presented as a function of the parameters defining the configurations presented in Figure 2-51. Each illustration is for a particular combination of values of h/H , l/L , and N reflecting surfaces adjacent to the surface for which the shock loads are being calculated. The wall (if any) parallel and opposite to the surface in question has a negligible contribution to the shock loads for the range of parameters used and was therefore not considered.

The general procedure for use of the above illustrations is as follows:

1. From Figure 2-51, select the particular surface of the structure which conforms to the protective structure given and note N of adjacent reflecting surfaces as indicated in parenthesis.

2. Determine the values of the parameters indicated for the selected surface of the structure in Item 1 above and calculate the following quantities:

$$h/H, l/L, L/H, L/R_A, \text{ and } Z_A = R_A/W^{1/3}.$$

3. Refer to Table 2-3 for the proper peak reflected pressure and impulse charts conforming to the number of adjacent reflected surfaces and the values of l/L and h/H of Item 2 above, and enter the charts to determine the values of p_r and $i_r/W^{1/3}$.

In most cases, the above procedure will require interpolation for one or more of the parameters which define a given situation, in order to obtain the correct average reflected pressure and average reflected impulse. Examples of this interpolation procedure are given in Appendix 2A.

Because of the limitations in the range of the test data and the limited number of values of the parameters given in the above shock load charts, extrapolation of the data given in Figures 2-52 through 2-149 may be required for some of the parameters involved. However, the limiting values as given in the charts for other parameters will not require extrapolation. The values of the average shock loads corresponding to the values of the parameters, which exceed their limiting values (as defined by the charts), will be approximately equal to those corresponding to the limiting values. The following are recommended procedures which will be applicable in most cases for either extrapolation or establishing the limits of impulse loads corresponding to values of the various parameter which exceed the limits of the charts:

1. To extrapolate beyond the limiting values of Z_A , plot a curve of values of p_r versus Z_A for constant values of L/R_A , L/H , h/H and l/L . Extrapolate curve to include the value of p_r corresponding to the value of Z_A required. Repeat similarly for value of $i_r/W^{1/3}$.
2. To extrapolate beyond the limiting values of L/R_A , extrapolate the given curve of p_r versus L/R_A for constant values of Z_A , L/H , h/H and l/L to include the value of p_r corresponding to the value of L/R_A required. Repeat this extrapolation for value of $i_r/W^{1/3}$.
3. Values of p_r and $i_r/W^{1/3}$ corresponding to values of L/H greater than 5 shall be taken as equal to those corresponding to $L/H = 6$ for actual values of Z_A , h/H , and l/L but with a fictitious value of L/R_A in which R_A is the actual value and L is a fictitious value equal to $5H$.
4. Values of p_r and $i_r/W^{1/3}$ corresponding to values of l/L less than 0.10 and greater than 0.75 shall be taken as equal to those corresponding to $l/L = 0.10$ and 0.75 , respectively.
5. Values of p_r and $i_r/W^{1/3}$ corresponding to values of h/H less than 0.10 and greater than 0.75 shall be taken as equal to those corresponding to $h/H = 0.10$ and 0.75 , respectively.

A computer program is available which executes the interpolation procedure using numerical tables equivalent to Figure 2-52 through 2-149. Availability of this program is listed in Section 2-4.

A protective element subjected to high intensity shock pressures may be designed for the impulse rather than the pressure pulse only if the duration of the applied pressure acting on the element is short in comparison to its response time. However, if the time to reach maximum displacement is equal to or less than three times the load duration, then the pressure pulse should be used for these cases. The actual pressure-time relationship resulting from a pressure distribution on the element is highly irregular because of the multiple reflections and time phasing. For these cases, the pressure-time relationship may be approximated by a fictitious peak triangular pressure pulse. The average peak reflected pressure of the pulse is obtained from Figures 2-52 through 2-100 and the average impulse from Figure 2-101 through 2-149 and a fictitious duration is established as a function of the reflected pressure p_r and impulse i_r acting on the element.

$$t_o = 2i_r / p_r \qquad 2-2$$

The above solution for the average shock load does not account for increased blast effects produced by contact charges. Therefore, if the values of the average shock loads given in Figures 2-52 through 2-149 are to be applicable, a separation distance between the element and explosive must be maintained. This separation is measured between the surface of the element and the surface of either the actual charge or the spherical equivalent, whichever results in the larger normal distance between the element's surface and the center of the explosive (the radius of a spherical TNT charge is $r = 0.136 W^{1/3}$). For the purposes of design, the following separation distances are recommended for various charge weights:

Weight of Explosive (lb)	Separation Distance
up to 500	1.0
501 to 1,000	1.5
1,001 to 2,000	2.0
2,001 to 3,000	2.5
above 3,000	3.0

The above separation distances do not apply to floor slabs or other similar structural elements placed on grade. However, a separation distance of at least one foot should be maintained to minimize the size of craters associated with contact explosions.

It should be noted that these separation distances do not necessarily conform to those specified by other government regulations; their use in a particular design must be approved by the cognizant military construction agency.

Average shock loads over entire wall or roof slabs were discussed above. An approximate method may be used to calculate shock loads over surfaces other than an entire wall. These surfaces might include a blast door, panel, column, or other such items found inside any shaped structure.

The method assumes a fictitious strip centered in front of the charge having a width equal to the normal distance R_A and a height equal to that of the struc-

ture. This is the maximum representative area that may be considered. Average shock loads can be determined on entire area or any surface falling within the boundaries of the representative area.

The procedure for determining the shock loads consists of partitioning the surface under consideration into subareas. These subareas do not need to be the same size. The angle of incidence to the center of each subarea is calculated. The reflected pressure and scaled impulse are determined for each subarea using Figures 2-9 and 2-10 respectively. A weighted average with respect to area is taken for both pressure and scaled impulse.

Both the pressure and the impulse are multiplied by a factor of 1.75 to account for secondary shocks. Idealized duration is calculated using Equation 2-2.

2-14.2.2. Frangibility

A frangible element, as defined here, is an element that exhibits a resistance to internal shock loads equal to or less than 25 pounds per square foot and will undergo significant displacement during the loading time of the shock pressures and, thereby, reduce the effects of the shock pressures acting on both the frangible panel itself and reflections to other elements of the structure.

The following are design procedures for determining the magnitude of applied shock pressures which will contribute to the displacement of the frangible element:

- (1) Determine the peak average reflected pressure P_r and average impulse i_r acting on the frangible element assuming that the element is rigid (Figures 2-52 through 2-149).
- (2) Calculate the unit weight of the frangible element and divide this weight by the sixth root of charge weight, $W_F/W^{1/6}$.
- (3) Determine the fictitious scaled distance Z from Figure 2-7, which corresponds to the average impulse determined in Step 1.
- (4) Determine the value of the factor f_r , of average impulse by using the value of $W_F/W^{1/6}$ from Step 2 and the fictitious scaled distance of Step 3 and utilizing Figure 2-150, contributing to the translation of the frangible element (may require interpolation).
- (5) Calculate the value of the average impulse contributing to the translation of the frangible element by multiplying the values of i_r and f_r of steps 1 and 4 respectively.
- (6) Contribute the value of the peak average pressure to the translation of the frangible element that is assumed to be equal to the value of P_r of Step 1.

The step by step procedure for determining the shock loads being reflected from a frangible element to an adjacent element is to:

- (1) Determine the average peak reflected pressure P_r and the average reflected impulse i_r acting on the element in question, assuming that the adjoining frangible element will remain in place (figs. 2-52 through 2-149).
- (2) Determine the average impulse acting on the element in question assuming that the adjoining frangible element is removed (figs. 2-52 through 2-149).
- (3) Subtract the average impulse determined in Step 2 from the average impulse determined in Step 1.
- (4) Calculate the unit weight of the frangible element and divide this weight by the sixth root of the charge weight, $W_F/W^{1/6}$.
- (5) Calculate the normal scaled distance Z between the center of the charge and the surface of the frangible element.
- (6) Utilize Figure 2-150 to determine the value of the fraction f_r of the average impulse reflected to the element in question using the scaled weight density and scaled distance of Steps 4 and 5, respectively (may require interpolation).
- (7) Determine the magnitude of the impulse load reflected to the element in question from the frangible element by multiplying the value of the average impulse of Step 3 by the value of f_r of Step 6.
- (8) Determine the total impulse load acting on the element in question by adding the impulse loads determined in Steps 2 and 7.
- (9) Calculate the peak average reflected pressure of the shock loads acting on the element in question making it equal to the value of P_r of Step 1.

In the above procedure, it is assumed that the frangible element will remain intact while being displaced away from the structure. If the element fails while being translated, then the portion of the shock pressure impulse displacing the element as well as that portion of the impulse being reflected to other elements will be reduced because of additional venting area produced by the element's "break up".

2-14.2.3. TNT Equivalency

The shock loads presented in Figure 2-52 through 2-149 pertain to the blast effects of bare spherical TNT explosives and must be extended to include other potentially mass-detonating materials. However, only a limited amount of testing has been performed to determine the TNT equivalency of confined explosives. Therefore, as an interim procedure, it is suggested that the determination of shock pressures for confined explosives other than TNT utilize equivalencies based on Equation 2-1.

The above relationship assumes that the explosive in question is a bare charge and spherical in shape. If the charge is not spherical, then it is suggested that the explosive be subdivided into several segments which will have approx-

imately equal dimensions and that the reflected impulse for any segment be calculated, as previously discussed. The reflected impulse of the total charge is then determined by multiplying the impulse of the individual segments by the total number of segments. The peak average reflected pressure is calculated by assuming the total charge as having a spherical shape. The impulse load for multiple explosives is obtained in a similar manner except that the locations of the individual charges are considered in calculating their individual impulse load. The impulse load of the total charge is determined by adding together the individual impulse loads. The average peak reflected pressure is calculated using the total weight of the explosive located at the centroid of the individual charges.

The explosive casing will have an effect on the magnitude of the shock pressures. These effects are dependent on the properties of the casing such as material, thickness, shape, etc. A review of a limited amount of surface detonated test data has indicated that the effects of the casing are not severe and, therefore, for design purposes it is recommended that casing effects be neglected.

2-14.2.4. Multiple Explosions

The blast pressures and impulse loads, acting on various elements of cubicle or other similar structures, which are produced by multiple explosions, will usually differ from those produced by a single explosion of the same amount of explosives.

Although the magnitude of the total combined impulse produced by the multiple explosions will usually be larger than that produced by the single explosion, the damage to a protective element due to the impulse of the multiple detonation may be either greater, equal to, or less than that produced by the impulse of the single explosion. For a given total impulse, the degree of damage to a protective element will be defined by the duration of the entire load relative to the response time of the element (time to reach maximum deflection).

A minimum amount of theoretical and experimental data is available concerning the degree of damage sustained by structural elements due to multiple explosions. However, results of response tests of reinforced concrete slabs have indicated that if the total combined duration of the blast loads produced by simultaneously or near simultaneously exploded charges is equal to or less than one-third the response time (time to reach maximum deflection) of the element, then the total combined impulse acting on the element can be estimated by numerically adding the impulse loads produced by the individual explosions. However, if the total combined duration of the blast loads is greater than one-third the response time, the actual pressure-time relationship of the combined loads approximated by a fictitious peaked triangular pressure pulse (similar to that of a single explosion) should be considered. The blast loads produced by charges that are not simultaneously or near simultaneously exploded may be considered as two or more impulse loads, two or more pressure-time loads, or a combination of impulse and pressure-time loads depending on the time delay and the duration of the individual loads compared to the response time of the element. A load or group of loads should be treated as an impulse load if the duration (one load or the combined duration of two or more loads) of the loading is less than one-third the time interval between the on-set of the load or group of loads and the response time of the member.

The duration of the blast loads due to multiple explosions may be approximated by considering the interrelationship between (a) the time intervals between individual explosions, (b) arrival times of the blast waves of the individual explosions at the element and (c) the fictitious duration of the pressure load from individual explosions. Because of the many variables involved, a relationship cannot be given to obtain the duration of the blast loads due to multiple explosions. Each situation will require a series of computations involving the time increments outlined above.

2-14.3. Gas Pressures

2-14.3.1. Blast Loadings

When an explosion occurs within a confined area, gaseous products will accumulate and a temperature within the structure will rise, thereby forming blast pressures whose magnitude is generally less than that of the shock pressure but whose duration is significantly longer. The magnitude of the gas pressures as well as their durations is a function of the size of the vent openings in the structure. For very small openings or no openings at all, the duration of the gas pressures will be very long in comparison to the fundamental periods of the structure's elements and, therefore, may be considered as a long duration load similar to that associated with a nuclear event.

These conditions usually occur in total or near containment type structures. In the former, the internal blast pressures must be contained because of the presence of toxic or other harmful materials in the structure. In near containment structures, the leakage of pressure flow out of the structure usually must be limited because of either personnel or frangible structure are located immediately adjacent to the donor structure. In other cases, however, openings in structures may be quite large, thereby minimizing the products' accumulation and limiting the temperature rise, hence producing gas pressures with limited duration or no duration at all. The structures without gas pressure buildup are referred to as fully vented structures.

A typical pressure-time record at a point on the interior surface of a partially vented chamber is shown in Figure 2-151. The high peaks are the multiple reflections associated with shock pressures. The gas pressure, denoted as p_g , is used as the basis for design and is a function of the charge weight and the contained net volume of the chamber.

Figure 2-152 shows an experimentally fitted curve based upon test results of partially vented chambers with small venting areas where the vent properties ranged between:

$$0 \leq A_f/V^{2/3} \leq 0.022$$

2-3

The values of A and V_f are the chamber's total vent area and free volume which is equal to the total volume minus the volume of all interior equipment, structural elements, etc. The maximum gas pressure, P_g , is plotted against the charge weight to free volume ratio.

Figures 2-153 through 2-164 provide the relationship of the gas pressure scaled impulse $i_g/W^{1/3}$ as a function of the charge weight to free volume ratio

W/V_f , scaled value of the vent opening $A/V_f^{2/3}$, the scaled unit weight of the cover $W_f/W^{1/3}$ over the opening, and the scaled average reflected impulse $i_r/W^{1/3}$ of the shock pressures acting on the frangible wall (Section 2-14.2.2) or a non-frangible wall with a vent opening. (The curves in figures 2-153 through 2-164 for $W_f/W^{1/3} = 0$ were obtained from data with $A/V_f^{2/3} \leq 1.0$. Extrapolated values, for which there is less confidence, are dashed. Curves for $W_f/W^{1/3} > 0$ are not dashed at $A/V_f^{2/3} > 1.0$ because they are not strongly dependent on the extrapolated portion of the curve for $W_f/W^{1/3} = 0$. Even light-weight frangible panels displace slowly enough that the majority of the gas impulse is developed before significant venting ($A/V_f^{2/3} > 1$) can occur.) For a full containment type structure the impulse of the gas pressure will be infinite in comparison to the response time of the elements (long duration load). For near containment type structures where venting is permitted through vent openings without covers, then the impulse loads of the gas pressures are determined using the scaled weight of the cover equal to zero. The impulse loads of the gas pressures corresponding to scaled weight of the cover greater than zero relates to frangible covers and will be discussed later. The effects on the gas pressure impulse caused by the shock impulse loads will vary. The gas impulse loads will have greater variance at lower shock impulse loads than at higher loads. Interpolation will be required for the variation of gas impulse as a function of the shock impulse loads. This interpolation can be performed in a manner similar to the interpolation for the shock pressures.

A computer program is available which executes the interpolation procedure. Availability of this program is listed in Section 2-4.

The actual duration and the pressure-time variation of the gas pressures is not required for the analysis of most structural elements. Similar to the shock pressures, the actual pressure-time relationship can be approximated by a fictitious peak triangular pulse. The peak gas pressure is obtained from Figure 2-152 and the impulse from Figures 2-153 through 2-164 and the fictitious duration is calculated from the following:

$$t_g = 2i_g / P_g \quad 2-4$$

Figure 2-165a illustrates an idealized pressure-time curve considering both the shock and gas pressures. As the duration of the gas pressures approach that of the shock pressures, the effects of the gas pressures on the response of the elements diminishes until the duration of both the shock and gas pressures are equal and the structure is said to be fully vented.

If a chamber is relatively small and/or square in plan area then the magnitude of the gas pressure acting on an individual element will not vary significantly. For design purposes the gas pressures may be considered to be uniform on all members. When the chamber is quite long in one direction and the explosion occurs at one end of the structure, the magnitude of the gas pressures will initially vary along the length of the structure. At the end where the explosion occurs, the peak gas pressure is P_{g1} (Fig. 2-165b) which after a finite time decays to P_{g2} , and finally decays to zero. The gas pressure P_{g2} is based on the total volume of the structure and is obtained from Figure 2-152 while the time for this pressure to decay to zero is calculated from Equation 2-4 where the impulse is obtained from Figures 2-153 through 2-164 again for the total volume of the structure. The peak gas pressure P_{g1} is obtained from Figure 2-152 based on a pseudo volume (Fig. 2-165b) whose length is equal to

its width and the height is the actual height of the structure. The time t_p for the gas pressure to decay from P_{g1} to P_{g2} is taken as the actual length^p of the structure minus the width divided by the velocity of sound (1.12 fpm). At the end where the explosion occurs, the peak gas pressures (P_{g1} , Figure 2-165b) will be a maximum and, after a finite time, they will decay to a value (P_{g2} , Figure 2-165b) which is consistent with full volume of the structure; after which they will decay to zero. The magnitude of the peak gas pressures (P_{g1}) may be evaluated by utilizing Figure 2-152 and a pseudo volume whose length is equal to its width and the height is the actual height of the chamber. The length of time t_p between the two peak gas pressures may be taken as the length minus the width^p of the structure divided by the velocity of sound (1 fpm).

2-14.3.2. Frangibility

Similar to shock pressures, an element can be considered frangible if it is designed such that its resistance to internal blast forces does not exceed 25 psf and that it will undergo significant displacement during the shock and gas loading phases. Figures 2-153 through 2-164 present the method for determining the gas pressure impulse acting on the interior surfaces of the donor structure. These impulse loads will vary as the mass of the cover over the vent opening varies; that is, the heavier the vent opening cover, the larger the gas pressure impulse. Like the vented structures, the internal gas pressure impulse loads produced by a frangible cover must be interpolated as a function of the shock pressure impulse loads.

2-14.3.3. TNT Equivalency

The data presented in Figure 2-152 and Figures 2-153 to 2-164 are for TNT only and must be extended to include other potentially mass-detonating materials. Similar to the shock pressures, only a limited amount of data is available regarding the TNT equivalency of confined explosions and in particular the effects produced on gas pressures. It has been suggested that the TNT equivalency of explosives relating to gas pressures is a function of both the heat of detonation as well as the heat of combustion, while for the shock pressures, the TNT equivalency is a function of the former only. A relationship has been developed based on a limited amount of testing as follows:

$$W_{Eg} = \frac{\phi [H_{EXP}^c - H_{EXP}^d] + H_{EXP}^d}{\phi [H_{TNT}^c - H_{TNT}^d] + H_{TNT}^d} W_{EXP} \quad 2-5$$

where

- W_{Eg} - effective charge weight for gas pressure
- H_{TNT}^c - heat of combustion of TNT
- H_{EXP}^c - heat of combustion of explosive in question

- ϕ - TNT conversion factor (Figure 2-166)
- H_{TNT}^d - heat of detonation of TNT
- H_{EXP}^d - heat of detonation of explosive in question
- W_{EXP} - weight of explosive in question

Gas pressures will be increased because of casings, in particular, if the casing is combustible. Since only unrelated data are available concerning the effects on gas pressures by the casing, a method of compensating for these effects is to adjust the heat of combustion of the given explosive material in Equation 2-5 to account for the heat of combustion of the casing material. This adjustment should be made by chemically combining the heat of combustion of the explosive and casing.

2-14.3.4. Multiple Explosions

The gas pressure produced by the release of the gaseous products of multiple explosions in a confined area may be approximated by considering the explosion to be produced by a single explosive whose weight is equal to the combined weights of the individual charges. This approximation is accurate if the individual charges are positioned in the immediate vicinity of one another and if near simultaneous detonation of the individual charges occurs. If the individual charges are not close to one another and/or positioned at one end of the structure, the magnitude of the gas pressures will initially vary along the length or width of the structure. This variation may be determined in a manner similar to that described in Section 2-14.3.1.

2-14.4. Leakage Pressures

2-14.4.1. Introduction

When an explosion occurs inside a vented chamber, shock pressures escape to the outside along with venting of the gas pressures. Trailing shocks overrun and coalesce with the lead shock at some distance to form a single diverging shock wave. Close to the structure, the blast pressures are affected by the structure itself as the shock pressures spill around the edges of the structure and form highly turbulent vortices. At further distances, this effect is no longer present and the shock pressure decreases with increasing distances. The leakage pressures are enhanced in the direction of venting (front) and reduced to the side and rear. The enhancement of pressures in the front and reduction of pressures to the side and rear are less extreme as the distance away from the structure is increased.

The blast environment outside of cubicle containing fully and partially vented explosions is presented in this section. Pressures and impulses acting on the ground surface are provided as a function of distance from the explosion, direction (front, side, back) relative to the vent opening in the structure, area of the vent opening and volume of the structure. For design purposes, the remaining blast parameters corresponding to the pressure and impulse acting on the ground surface may be obtained from Figure 2-15 and 2-16 in exactly the same manner as a surface burst of an explosive other than TNT.

Explosions in three and four wall cubicles are considered. Three wall cubicles are fully vented structures. The blast environment is furnished for cubicles with or without roofs. Four wall cubicles with a vent opening located either in the roof or one wall are considered. The size of the vent opening is varied from that of a fully vented cubicle through a full range of partially vented structures.

The data presented is based on tests in which the vent openings were completely open. There were no frangible covers over the vent area which might inhibit the pressure flow. Vent openings in protective structures are normally covered with frangible panels for weather protection, separation of operations, etc. These panels will affect the leakage pressures. However, it is assumed that these frangible panels will reduce the shock pressures leaking through the opening to a greater extent than the increase in the internal gas pressure buildup. Therefore, use of this data will predict conservative leakage pressures from cubicles with frangible covers.

2-14.4.2. Fully Vented Three Wall Cubicles

For cubicle-type structures where full venting is provided through the frangible or open portion of the structure, the resulting blast wave exterior of the cubicle will be appreciably modified as compared to an unbarricaded detonation. As the blast wave propagates out from the center of the explosion, the shock front will collide with the interior surfaces of the structure. These collisions will reflect and reinforce the initial loads (pressure and impulse). Eventually these pressures will spill over and around the blast walls, and in the event of rapid collapse of frangible walls, through the structure to the surrounding area. The exterior pressures will not initially have a definite shock front but will, at some distance from the structure, shock-up with frontal pressures similar to those produced by a surface burst. The pressure distance gradients away from the explosion will vary in all directions. This variation is defined by the configuration (shape, openings, etc.) of the protective structure containing the explosion.

A series of tests have been performed on three wall cubicle type structures illustrated in Figure 2-167. Cubic and rectangular three wall cubicles with and without a roof were tested. The results indicated that several parameters were important:

- (1) Direction. Three directions illustrated in Figure 2-167 are considered. The direction normal to the open wall is called the front. The directions perpendicular to the front normal are called the sides. The direction opposite the normal to the open wall is called the back. The blast pressures out the front are greater than that to the side which, in turn, are greater than that to the back.
- (2) Structure geometry. Differences were found in the blast environment depending upon whether the shape of the structure was cubic or rectangular. This was true for pressure and impulse measurements to the side and back, and only impulse to the front. There were no differences in pressure out the front for the cubicle and rectangular structures. The difference in pressures to the side and back occur only close to the structure. Far from the structure, there is no effect on pressure in any direction due to

structure shape. However, impulse does not converge with distance for differences in cubicle shape.

- (3) Charge weight to volume ratio W/V and distance. The ratio W/V does not have an effect on the pressure to the front of any cubicle. There is an effect of W/V on pressure to the side and back of all cubicles, but only close to the structure. For a particular W/V , the pressure is affected differently for a cubic or rectangular structure. Thus, the effect on pressure close in depends both on structure size and W/V . But, for further out, neither affect the pressures. For all values of Z , there is a measured effect of W/V on impulse.
- (4) Venting through the roof. For any direction, cubicle shape, and W/V value, there are differences in blast pressure and impulse based solely on whether or not venting could occur through the roof.
- (5) Scaled distance Z . Both blast pressure and scaled impulse are affected by scaled distance from the explosion. This parameter is not independent of other factors.

The pressure variation in the front, side, and back direction of any three wall cubicle without a roof is given in Figure 2-168 while for a three wall cubicle with a roof the pressure variation is given in Figure 2-169. Due to interferences from the side and back walls which cause complex vortices near the structure and coalescence of shock waves in close, there is a maximum pressure produced in the side and back directions. These pressures are a function of the charge weight to cubicle volume ratio, W/V , and the configuration of the cubicle. The maximum peak pressure in the side or back direction of three wall cubicles with or without a roof are given in Figure 2-170.

The scaled peak positive impulse in the front, side, and back direction of three wall cubicles is given in Figures 2-171 through 2-182. The scaled impulse is given as a function of scaled distance from the explosion for various values of charge weight to structure volume ratio. The curves are presented in two groups; three wall cubicles without roofs and then cubicles with roofs. For each direction, the impulse is given for explosions in cubic and rectangular cubicles, respectively.

2-14.4.3. Partially vented four wall cubicles - vent opening in roof

Four wall cubicles with a vent openings located in the roof will produce blast pressures on the ground surface which are symmetric about the vent opening. Leakage pressures were determined for a below ground cubicle with its roof flush with the ground surface (Fig. 2-183a). Figure 2-183b shows the above-ground four wall cubicle. The vent opening was centrally located in the roof, and various vent areas were considered. The blast pressure was determined to be a strong function of the vent area divided by the structure volume to the two-thirds power ($A/V^{2/3}$) and the scaled distance, and a very weak function of the charge weight to volume ratio W/V which can be ignored with negligible error.

The leakage pressures resulting from an explosion in a partially vented below-ground cubicle with a vent opening in its roof is given in Figure 2-184, and

the impulse is given in Figure 2-185. The scaled ground distance as indicated in Figure 2-183a is used in these charts for the below-ground structures.

Figures 2-184 and 2-185 may also be used to determine the pressure and impulse acting on the ground surface for above-ground four wall cubicles (Fig. 2-183b). For an above-ground structure, the shock front must travel a longer distance than a below-ground structure. Therefore, the scaled distance that must be used in Figures 2-184 and 2-185 is approximated by the addition of the slant and horizontal distances indicated in Figure 2-183b.

The figures are useful in selecting the degree of venting required to limit leakage pressures outside roof-vented four wall cubicles to a specified safe level at safe given distance. From a knowledge of the pressure and impulse on the ground surface, the blast load acting on a structure may be obtained from the procedures given in this report. Thus, an adjacent structure may be designed to resist a blast load resulting from a given vent opening or the vent opening may be varied to suit the capacity of an adjacent structure.

2-14.4.4. Partially vented four wall cubicle - vent opening through wall

Leakage pressures resulting from an explosion in a partially vented four wall cubicle where the vent opening is located in a wall (Fig. 2-186) have not been documented. These leakage pressures have a variation in direction similar to a three wall cubicle with a roof and a variation with vent opening similar to a roof vented four wall cubicle. Extrapolation of the data for these types of cubicles have resulted in Figures 2-187 through 2-189. These figures present a reasonable estimate of the pressures produced in the front, side, and back directions (Fig. 2-186). In addition to direction, these pressures are a function of scaled distance and the vent area divided by the volume to the two-thirds power ($A/V^{2/3}$).

2-15. External Blast Loads on Structures

2-15.1. General

The blast loading on a structure caused by a high-explosive detonation is dependent upon several factors:

- (1) The magnitude of the explosion.
- (2) The location of the explosion relative to the structure in question (unconfined or confined).
- (3) The geometrical configuration of the structure.
- (4) The structure orientation with respect to the explosion and the ground surface (above, flush with, or below the ground).

The procedures presented here for the determination of the external blast loads on structures are restricted to rectangular structures positioned above the ground surface where the structure will be subjected to a plane wave shock front. The procedures can be extended to include structures of other shapes (cylindrical, arch, spherical, etc.) as well as structures positioned at and below the ground surface.

2-15.2. Forces Acting on Structure

The forces acting on a structure associated with a plane shock wave are dependent upon both the peak pressure and the impulse of the incident and dynamic pressures acting in the free-field. The peak pressures and impulses associated with the free-field shock wave have been presented for various explosives.

For each pressure range there is a particle or wind velocity associated with the blast wave that causes a dynamic pressure on objects in the path of the wave. In the free field, these dynamic pressures are essentially functions of the air density and particle velocity. For typical conditions, standard relationships have been established between the peak incident pressure (P_{s0}), the peak dynamic pressure (q_0), the particle velocity, and the air density behind the shock front. The magnitude of the dynamic pressures, particle velocity and air density is solely a function of the peak incident pressure, and, therefore, independent of the explosion size. Figure 2-3 gives the values of the parameters versus the peak incident pressure. Of the three parameters, the dynamic pressure is the most important for determining the loads on structures.

For design purposes, it is necessary to establish the variation or decay of both the incident and dynamic pressures with time since the effects on the structure subjected to a blast loading depend upon the intensity-time history of the loading as well as on the peak intensity. The form of the incident blast wave (Fig. 2-190) is characterized by an abrupt rise in pressure to a peak value, a period of decay to ambient pressure and a period in which the pressure drops below ambient (negative pressure phase).

The rate of decay of the incident and dynamic pressures, after the passage of the shock front, is a function of the peak pressure (both positive and negative phases) and the size of the detonation. For design purposes, the actual decay of the incidental pressure may be approximated by the rise of an equivalent triangular pressure pulse. The actual positive duration is replaced by a fictitious duration which is expressed as a function of the total positive impulse and peak pressure:

$$t_{of} = 2i/p \quad 2-6$$

The above relationship for the equivalent triangular pulse is applicable to the incident as well as the reflected pressures; however, in the case of the latter, the value of the pressure and impulse used with Equation 2-6 is equivalent to that associated with the reflected wave. The fictitious duration of the dynamic pressure may be assumed to be equal to that of the incident pressure.

For determining the pressure-time data for the negative phase, a similar procedure as used in the evaluation of the idealized positive phase may be utilized. The equivalent negative pressure-time curve will have a time of rise equal to 0.25 t_{of} whereas the fictitious duration t_{of}^- is given by the triangular equivalent pulse equation:

$$t_{of}^- = 2i^-/p^- \quad 2-7$$

where i^- and p^- are the total impulse and peak pressure of the negative pulse of either the incident or reflected waves. The effects of the dynamic pressure in the magazine phase region usually may be neglected.

Since the fictitious duration of the positive phase will be smaller in magnitude than the actual duration, a time gap will occur between the fictitious duration and the onset of the negative phase. This time gap, which is illustrated in Figure 2-190, should be maintained in an analysis for consistency of the onset of the various load phasings.

2-15.3. Above-Ground Rectangular Structure Without Openings

2-15.3.1. General

For any given set of free-field incident and dynamic pressure pulses, the forces imparted to an above-ground structure can be divided into four general components: (a) the force resulting from the incident pressure, (b) the force associated with the dynamic pressures, (c) the force resulting from the reflection of the incident pressure impinging upon an interfering surface, and (d) the pressures associated with the negative phase of the shock wave. The relative significance of each of these components is dependent upon the geometrical configuration and size of the structure, the orientation of the structure relative to the shock front, and the design purpose of the blast loads.

The interaction of the incident blast wave with a structure is a complicated process. To reduce the complex problem of blast to reasonable terms, it will be assumed that (a) the structure is generally rectangular in shape, (b) the incident pressure of interest is 200 psi or less, (c) the structure being loaded is in the region of the Mach stem, and (d) the Mach stem extends above the height of the building.

2-15.3.2. Front Wall Loads

For a rectangular above-ground structure at low pressure ranges, the variation with time on the side facing the detonation (front face) when this side is parallel to the shock front (normal reflection) is illustrated in Figure 2-191a. At the moment the incident shock front strikes the front wall, the pressure immediately rises from zero to the normal reflected pressure, P_r , which is a function of the incident pressure (Fig. 2-15). The clearing time, t_c , required to relieve the reflected pressure is represented as:

$$t_c = \frac{4S}{(1 + R) C_r} \quad 2-8$$

where

- S - clearing distance and is equal to H or W/2 (Fig. 2-191a) whichever is the smallest
- H - height of the structure
- R - ratio of S/G where G is equal to H or W/2 (Fig. 2-191) whichever is larger

C_r = sound velocity in reflected region (Fig. 2-192)

The pressure acting on the front wall after time t_c is the algebraic sum of the incident pressure P_s and the drag pressure $C_D q$ or:

$$P = P_s + C_D q \quad 2-9$$

The drag coefficient C_D gives the relationship between the dynamic pressure and the total translational pressure in the direction of the wind produced by the dynamic pressure and varies with the Mach number (or with the Reynold's number at low incident pressures) and the relative geometry of the structure. A value of $C_D=1$ for the front wall is considered adequate for the pressure ranges considered in this manual. At higher pressure ranges, the above procedure may yield a fictitious pressure-time curve because of the extremely short pressure pulse durations involved. Therefore, the pressure-time curve constructed must be checked to determine its accuracy. The comparison is made by constructing a second curve (dotted triangle as indicated in Fig. 2-191a) using the total reflected pressure impulse i_r from Figure 2-15 for a normal reflected shock wave (Fig. 2-191a). The fictitious duration t_{rf} for the normal reflected wave is calculated from:

$$t_{rf} = 2i_r / P_r \quad 2-10$$

where P_r is the peak normal reflected pressure (Fig. 2-15). Whichever curve (Fig. 2-191a) gives the smallest value of the impulse (area under curve), that curve should be used in calculating the wall loading.

If the shock front approaches the structure at an oblique angle (Fig. 2-191b), then the peak pressure will be a function of the incident pressure and the incident angle between the front and the front wall and is obtained from Figure 2-193.

An equation similar to that used for the normal shock front may be used when the angle of obliquity is greater than zero as follows:

$$t_{rf} = 2i_{r\alpha} / P_{r\alpha} \quad 2-11$$

where peak reflected impulse $i_{r\alpha}$ is obtained from Figure 2-194.

Usually only the positive pulse of the pressure-time relationship of Figure 2-191b is utilized for the front wall design since the negative pulse seldom affects the design. For determining the overall motion of the structure, the effects of negative pressures should be included. The peak negative reflected pressure (Fig. 2-190) and reflected impulse are obtained from Figure 2-16 and correspond to the peak incident pressure (Fig. 2-15) acting on the front wall. The rise time and decay of the negative pressures are similarly calculated as described in Section 2-15.2.

2-15.3.3. Roof and Side Walls

As the shock front traverses a structure a pressure is imparted to the roof slab, and side walls equal to the incident pressure at a given time at any specified point reduced by a negative drag pressure. The portion of the sur-

face loaded at a particular time is dependent upon the magnitude of the shock front incident pressure, the location of the shock front and the wavelength (L_w and L_w^-) of the positive and negative pulses.

To determine accurately the overall loading on a surface, a step-by-step analysis of the wave propagation across the surface should be made. This analysis includes an integration of the pressures at various points (Fig. 2-195a) on the surface and at various times to determine the equivalent uniform incident pressure acting on a span L as a function of time (Fig. 2-195b). Since the point of inflection of the element will vary as the shock front traverses the surface, in order to make the assumption of the uniform pressure valid, the reinforcement on both faces must be continuous across the span length.

As the shock wave traverses the roof, the peak value of the incident pressure decays and the wave length increases. As illustrated in Figure 2-195b, the equivalent uniform pressure will increase linearly from time t_f when the blast wave reaches the beginning of the element (point f) to time t_d when the peak equivalent uniform pressure is reached when the shock front arrives at point d. The equivalent uniform pressure will then decrease to zero where the blast load at point b on the element decreases to zero.

To simplify the calculations, the equivalent uniform pressure has been expressed as a function of the blast wave parameters at point f. The equivalent load factor C_E , the rise time, and duration of the equivalent uniform pressure are obtained from Figures 2-196, 2-197, and 2-198, as a function of the wave length-span ratio L_{wf}/L .

The peak value of the pressure acting on the roof P_R is the sum of contribution of the equivalent uniform pressure and drag pressure:

$$P_R = C_E P_{sof} + C_D q_{of} \tag{2-12}$$

where P_{sof} is the incident pressure occurring at point f and q_{of} is the dynamic pressure corresponding to $C_E P_{sof}$.

The drag coefficient C_D for the roof and side walls is a function of the peak dynamic pressure. Recommended values are as follows:

Peak dynamic pressure	Drag coefficient
0-25 psi	-0.40
25-50 psi	-0.30
50-130 psi	-0.20

The data presented above for the equivalent uniform roof and side wall blast pressures are used principally for the design of individual elements. For overall motions of a structure, the effects of the negative phase pressures should be included. The equivalent load factor C_E for the peak equivalent uniform negative pressure is obtained from Figure 2-196 as a function of the wavelength span ratio L_{wf}/L . The value of the negative pressure acting on the roof, P_R^- is equal to $C_E^- P_{sof}$ where the value of C_E^- is a minus value. The value of the equivalent negative pressure duration t_{of} is obtained from Figure 2-198. The value is not a function of the peak incident pressure at point f. The rise time of the negative phase is equal to $0.25 t_{of}$.

If a side wall is positioned at an oblique angle to the shock front, then blast loads acting on the side wall are calculated in the same manner as that described for front walls.

2-15.3.4. Rear Wall

As the shock front passes over the rear edges of the roof and/or side walls the pressure front will expand, forming secondary waves which propagate over the rear wall. In the case of long buildings, the secondary wave enveloping the back wall essentially results from the spillover from the roof, and the side walls. In both cases, the secondary waves are reinforced due to their impingement with reflecting surfaces. The reinforcement of the spillover wave from the roof is produced by its reflection from the ground surface at the base of the rear wall, and the reinforcement of the secondary waves from the side walls is produced by their collision near the center of the wall and/or their interaction with the wave from the roof. Little information is available on the overall effects on the rear wall loading produced by the reflections of the secondary waves.

In most design cases, the primary reason for determining the blast loads acting on the rear wall is to determine the overall drag effects (both front and rear wall loadings) on the building. For this purpose, a procedure may be used where the blast loading on the rear wall Figure (2-199a) is calculated using the equivalent uniform method used for computing the blast loads on the roof and side walls. Here the peak pressure of the equivalent uniform pressure-time curve (Fig. 2-199b) is calculated using the peak pressure that would accrue at the back edge of the roof slab P_{sob} . The equivalent uniform load factors C_E and C_E^- are based on the wave length of the peak pressure above and the height of the rear wall H_s as are the time rises and duration of both the positive and negative phases.

Like the roof and side walls, the blast loads acting on the rear wall are a function of the drag pressures in addition to the incident pressure. The dynamic pressure of the drag corresponds to that associated with the equivalent pressure $C_E P_{sob}$, while the recommended drag coefficients are the same as used for the roof and side walls.

In the event that the back wall is positioned at an oblique angle to the shock front, peak incident pressure at point b should be calculated at the mid width.

2-15.3.5. Multiple Explosions

As previously mentioned, the blast loads, produced by multiple explosions, acting on structures located far from an explosion may consist of a series of separate pressure pulses rather than a single pulse blast load. However, the multiple pressure-pulse loading is usually associated with weights of explosives which are very small (several pounds) and, therefore, will not be the usual design situation. For large charge weights, however, the single pressure pulse loading with multiple peak pressures will occur. At the present time no specific method has been devised which will enable one to evaluate this type of blast loading. In the interim, it is suggested that the multiple peak pressure type loading be replaced by the pressure-pulse which is associated with the merged shock wave. The parameters of this shock wave and cor-

responding pressures are determined assuming a single explosion, the explosive weight of which is equal to the combined weight of the individual charges.

2-15.4. Above Ground Rectangular Structures with Openings.

2-15.4.1. General

Two structural configurations are usually encountered when blast loads are determined on structures with unsealed or unprotected openings in its exterior. The first configuration includes windows, doors or other openings located in both the front and rear walls as well as along the side walls of the structure. The second would include openings located only in the front face of the structure. The remaining surfaces are void of openings. The second configuration is the one most likely to be encountered since interior partitions will restrict the flow of the blast wave through the structure. Increased interior blast loads are produced due to the reflection of the blast wave on interior components. The blast loads associated with the second configuration are primarily discussed in this section with comments regarding the loads pertaining to the first configuration.

When a shock front strikes the front wall of a structure, the incident pressure is amplified. Windows and doors will fail almost immediately (approximately one millisecond) after the onset of the shock front unless they were designed to resist the applied load. As a result, blast pressures will flow into the structure through these openings. This sudden release of high pressure will cause a shock front to form inside of each opening. Each individual front will expand and tend to combine into a single front which will further expand throughout the structure's interior. This interior shock is initially weaker than the incident pressure at the building's exterior. However, the interior pressure will tend to get stronger due to reflections off interior building components.

An idealized structure configuration is shown in Figure 2-200. The incident shock front arriving at the front wall of the structure has an incident pressure P_{so} and wave length L_w . As the shock front sweeps across the structure, blast pressures enter the interior of the building through the opening in the front wall of area A_o . The area of multiple openings are added to obtain a fictitious single opening located at the center of the front wall. The blast pressures entering the building first load the interior surface of the front wall, followed by the interior surface of the side walls and roof, and finally the interior surface of the back wall. The idealized pressure-time load curves for these surfaces are presented in Figure 2-201. The procedures necessary to obtain the magnitude of the parameters given on the idealized load curves for a particular explosion are presented in the remainder of this section. Except for the front wall, the blast pressures acting on the exterior of the structure are not affected by the opening and are determined according to the procedures of the previous section.

The primary purpose of this section is to provide the blast loading on the interior surface of an exterior wall so that the maximum outward motion of the wall may be determined. It is not the intent to use these interior loads to reduce the exterior positive phase loading. Except for the front wall, accurate phasing of the interior and exterior blast loads are not possible. The interior loads will always lag the exterior positive phase loading and, due to reflections off interior components, the duration of the interior load is al-

ways longer. For design, the interior blast loads should be added to the negative phase exterior loading to obtain the maximum outward motion (negative response) of a side wall, roof or back wall. The maximum positive response should be determined for the exterior positive phase loading without any reductions due to internal pressures. In most instances, interior partitions are required to withstand the blast pressures leaking into a structure. The procedures presented in this section may be used to determine the design blast load acting on these elements. An interior partition located parallel to the front wall will reflect the shock front and, therefore, is considered as a back wall. The length of the side wall would then be taken as the distance between the front wall and this partition. An interior partition(s) perpendicular to and framing into the front wall may be considered as a side wall(s). The length of the front wall would then be taken as the distance between an interior partition and a side wall or between two interior partitions. In both cases, only the openings located between these partition walls would be considered as the vent opening.

The procedures presented in this section to determine interior blast loads acting on a structure with an opening in the front wall were developed for a shock front striking the front wall head-on. For the same size opening in a front wall, this orientation of the approaching shock front results in the most severe interior shock wave effects. The use of these procedures for shock fronts approaching at all other angles will result in conservative estimates of the blast loadings acting on the interior of the structure.

2-15.4.2. Exterior Front Wall Loads

The time required for reflected pressures to clear a solid front wall is expressed in multiples of the time necessary for a rarefaction wave to sweep the wall. When walls with openings are considered, clearing takes place around the edges of the opening in addition to the edges of the wall. Depending upon the size of the overall wall and the openings, the clearing time of the reflected pressures may be significantly reduced.

The pressure-time relationship of the applied blast load acting on the front wall of a structure with openings is the same as that of a solid front wall (Fig. 2-191) except the clearing time will be reduced. To evaluate this reduced time, the value of S' is introduced into Equation 2-8. This value is the weighted average distance that the rarefaction wave must travel to cover the wall assuming immediate access of the incident shock to the interior of the structure. If frangible covers (windows, doors) do not fail immediately, the clearing time should not be reduced.

The method for evaluating S' is illustrated in Figure 2-202 where the face of the front wall is divided into rectangular areas. These areas are determined by the location and dimensions of the openings in the wall, and by consideration of the direction along which the reflected pressure clears around the area in the shortest possible time. The individual areas are labeled depending upon the number and location of the clearing sides of the individual areas. Clearing factors δ_n are established for these areas as follows:

Area	δ_n	Number of Clearing Sides
1	1.0	Two adjacent sides
2	0.5	Two opposite sides
3	1.0	One side
4	1.0	None

The weighted average clearing distance S' is expressed as:

$$S' = \frac{\sum \delta_n h_n A_n}{A_f} \leq S \quad 2-13$$

where

S' - weighted average clearing distance with openings

δ_n - clearing factor

h_n - average clearing distance for individual areas as follows:

Area 1 - width or height of area whichever is smaller

Area 2 - distance between opposite sides where clearing occurs

Area 3 - distance between side where clearing occurs and opposite side

Area 4 - same as Area 1

A_n - area of individual wall subdivision

A_f - net area of the wall excluding openings

The clearing time t'_c for a front wall with opening is calculated from Equation 2-8 in which S' is substituted for S or

$$t'_c = \frac{4S'}{(1 + R) C_r} \quad 2-14$$

where all components of Equation 2-14 have been previously defined. It should be realized that the load acting on the front wall with openings is still the same as that shown in Figure 2-191 except with the reduced clearing time, t'_c . The curve which represents the wall loading is still the curve which gives the lower impulse.

As previously stated, window breakage will require a finite length of time. This time may be evaluated using the resisting functions of Chapter VI and the dynamic procedures of Chapter 3. This time must be accounted for in determining the window contribution to the blast pressures acting on the wall.

2-15.4.3. Interior Front Wall Loads

The average pressure acting on the interior face of the front wall will initially build up in a similar manner as the average pressure on the exterior back wall of a closed structure. However, vortices are located all around the interior edges of all openings in the front wall. The effect of these vortices, which tend to reduce the blast load, has been neglected.

The shock front entering through the opening in the front wall travels along the interior face of the front wall, thereby subjecting the wall to incident pressures. When the front reaches the side wall, it is reflected back. The length of wall loaded by this reflected wave is a function of the wave length, L_w . The average pressure acting on the wall is determined assuming a single opening of area A_o located at the center of the wall. In the case of multiple openings, a single opening equal to the combined area of all openings is located in the center of the front wall.

The idealized pressure-time blast load acting on the interior face of the front wall is shown in Figure 2-201a. The time at which the shock front arrives at the exterior surface of the front wall is taken as zero ($T_o = 0$). The blast load acting on the wall begins at time T_1 . This time represents the time it takes for the shock front to enter the structure through the opening A_o . The pressure buildup is linear from time T_1 to a maximum pressure P_{max} at time T_2 , and then it decays linearly to zero at time T_3 .

The maximum average pressure P_{max} acting on the interior face of the front wall varies as a function of the incident pressure P_{so} and the wavelength L_w corresponding to that pressure, and the geometry of the wall. Figure 2-203 through 2-206 give the maximum pressure P_{max} acting on front walls having width to height ratios (W/H) equal to 3/4, 3/2, 3 and 6, respectively.

The idealized times T_1 , T_2 and T_3 are also obtained from plots of front walls having width to height ratios W/H equal to 3/4, 3/2, 3 and 6. The arrival time T_1 of the load is given in Figures 2-207 and 2-208 as a function of the incident pressure acting on the exterior surface of the front wall P_{so} for various opening to wall area ratios A_o/A_w . The rise time of the load, $T_2 - T_1$ is given in Figures 2-209 and 2-210 as a function of P_{so} and various wave length to width of front ratios L_w/W . Finally, the duration of the load $T_3 - T_1$ is given in Figures 2-211 and 2-212 again as a function of P_{so} and L_w/W . The times T_2 and T_3 are obtained from subtracting T_1 from the rise time and duration, respectively.

Failure of the cover sealing openings in a building (windows, doors) will affect the onset of the blast load acting on the interior surface of the front wall. Due to the time required to cause failure of the covers, the onset of the interior pressures may not be in phase with the onset of the exterior blast load. Therefore, care must be taken to arrive at a combined loading for the structural element.

2-15.4.4. Interior Side Wall and Roof Loads

The blast pressures entering the interior of the building through the opening in the front wall (multiple openings are combined to form a single opening) must travel along the interior face of the front wall before arriving at the side wall. The incident pressures arriving at the side wall are increased due to reflection off the wall itself. The front expands and travels across the side wall until it reaches the back wall. It is then reflected off the back wall, and the reflected wave travels back across the side wall towards the front wall. The length of side wall loaded by this reflected wave is a function of the wave length L_w .

The idealized pressure-time blast load acting on the interior face of the side wall and roof is shown on Figure 2-201b. The same assumption is made for the

side wall and roof as for the interior front wall. That is, the time at which the shock front arrives at the front wall of the structure is taken as zero ($T_0 = 0$). The time T_1 represents the time it takes the shock front to travel from the opening across the interior face of the front wall to the side wall (or roof). The pressure build up is linear from time T_1 to a maximum pressure P_{max} at time T_2 , remains constant until time T_3 and decays linearly to zero at time T_4 . This idealized curve applies to both the side walls and roof. The structure configuration parameters as given in Figure 2-200 apply for side wall loadings. However, to determine the roof loading, the structure must be rotated 90 degrees so that the roof takes the position of a side wall. The width and height of the structure must be interchanged. All other parameters are not effected.

The maximum average pressure P_{max} acting on the interior face of the side wall (or roof) varies as a function of the incident pressure P_{so} acting on the exterior face of the front wall, the wavelength L_w corresponding to P_{so} , and the geometry of the structure. Since a large number of plots would be required to describe P_{max} for the blast and geometric parameters involved, an equation has been developed. The value of P_{max} is given by:

$$P_{max} = K / (L_w / L) \tag{2-15}$$

For $6 \geq W/H \leq 3/2$

$$K = (A + [B \times (L_w / L)^C]) \times D \times E \times P_{so}^{1.025} \tag{2-16}$$

where

$$A = [0.002 (W/H)^{1.4467}] - 0.0213 \tag{2-17}$$

$$B = 2.2075 - [1.902 (W/H)^{-0.085}] \tag{2-18}$$

$$C = 1.231 + [0.0008 (W/H)^{2.678}] \tag{2-19}$$

$$D = [2.573 (L/H)^{-0.444}] - 0.3911 \tag{2-20}$$

$$E = 0.4221 + [1.241 (A_o/A_w)^{0.367}] \tag{2-21}$$

For $W/H = 3/4$

$$K = A \times B \times C^E \times F^H \times P_{so}^{0.9718} \tag{2-22}$$

where

$$A = [0.5422 (L_w/L)^{1.2944}] - 0.001829 \tag{2-23}$$

$$B = [0.654 + 2.616 (A_o/A_w) - 4.928 (A_o/A_w)^2] \tag{2-24}$$

$$[2.209 (L/H)^{-0.3451} - 0.739]$$

$$C = 0.829 + 0.104 (L_w/L)^{1.6} \tag{2-25}$$

$$+ [0.00124 + 0.00414 (L_w/L)^{3.334}] [L/H]^D$$

$$D = 2.579 - 0.0534 (L_w/L)^{3.891} \tag{2-26}$$

$$E = 999 (A_o/A_w)^{9.964} \quad 2-27$$

$$F = 1.468 - 1.6627 (A_o/A_w)^{0.7801} \quad 2-28$$

$$+ [1.8692 - 1.1735 (A_o/A_w)^{-0.2226}] [L_w/L]^G$$

$$G = 0.2979 (A_o/A_w)^{-1.4872} - 0.8351 \quad 2-29$$

$$H = (5.425 \times 10^{-4}) + (1.001 \times 10^{-9}) (L/H)^{9.965} \quad 2-30$$

For $3/2 > W/H > 3/4$, graphical interpolation is required to determine P_{\max} . Several values of P_{\max} are determined from Equation 2-15 for values of W/H equal to $3/4$, $3/2$, and preferably two values greater than $3/2$. A plot of P_{\max} versus W/H is prepared and the value of P_{\max} is read for the required W/H .

The idealized times T_1 and T_2 are determined from Figure 2-213. These times are presented as a function of the incident pressure P_{so} arriving at the exterior of the building and the width to height ratio W/H of the front wall. Since the distance that the shock front must travel across the front wall is taken from the center of the opening, times T_1 and T_2 are not a function of the area of the opening. This assumption will not result in significant errors since the openings considered are comparatively small.

The idealized times T_3 and T_4 are determined from Figures 2-214 through 2-229. Each figure is prepared for a given structure configuration defined by the length to height ratio of the side wall L/H and the width to height ratio of the front wall W/H . The times T_3 and T_4 are given on each figure as a function of the incident pressure P_{so} and various values of the wave length to side wall length ratio L_w/L . As explained above, these times are not a function of the area of the opening. For ease of reference, these figures are listed in table 2-4 for the various L/H and W/H ratios provided. In most cases, interpolation will be required to obtain the correct values of T_3 and T_4 for the given structure configuration.

2-15.4.5. Interior Back Wall

The blast pressures entering the interior of the building through the opening in the front wall must travel the full length of the building before arriving at the back wall. The incident pressure arriving at the back wall is essentially uniform over the wall. This pressure is immediately increased to the normal reflected pressure when it strikes the back wall.

The idealized pressure-time blast load acting on the interior face of the back wall is shown in Figure 2-201c. Again, the time at which the shock front arrives at the front wall of the structure is taken as zero ($T_o = 0$). The time T_1 represents the time it takes the shock front to travel from the opening to the back wall. The pressure buildup is instantaneous to P_{RIB} due to the normal reflection of the shock front and then decays to zero at time T_2 . This loading is similar to the loading of an exterior front wall except that clearing is not possible.

The maximum average pressure P_{RIB} acting on the back wall is obtained from Figures 2-230 and 2-231. Each figure is prepared for a given value of L/H . The ratio of the maximum average pressure on the back wall to the incident

pressure P_{RIB}/P_{s0} is given as a function of P_{s0} for various values of A_o/A_w . Interpolation between figures may be necessary for a given structural configuration.

The idealized time T_1 is determined from Figures 2-232 and 2-233. Each figure is prepared for a given value of the width to height ratio of the wall W/H . The time T_1 is given as a function of the incident pressure P_{s0} for various values of the wall length to height ratio L/H and the ratio of the opening area to the wall area A_o/A_w . The duration of the load T_2-T_1 is determined from Figure 2-234. The time is given as a function of the incident pressure P_{s0} for various values of A_o/A_w . Since the back wall is located at the greatest distance from the front wall, the area of the opening has a significant effect on these times and must be considered.

2-15.5. Pressure Buildup In Structures

2-15.5.1. General

The procedures in Section 2-15.4 are for determining the net effects of shock loads entering openings in structures from windows or doors which are not designed to withstand the applied blast loads. In certain cases, structures may have closures which are designed to resist the blast loading, but have very small openings due to vents and ducts, which will not withstand the blast. In this case, the small opening will not allow the shock front to develop inside the structure. However, the structure experiences an increase in its ambient pressure (a "filling" pressure) in a time that is a function of the structure volume, area of the openings, and applied exterior pressure and duration. Since personnel exhibit a tolerance limit to such pressure increases, a method of determining the average pressure inside the structure is needed. It should be noted that the interior pressures immediately adjacent to the openings will be higher than the average pressure.

2-15.5.2. Method of Calculation

The following procedure is applicable for structures with small area-volume ratios and applied blast pressures less than 150 psi. The change in pressure δP_i inside the structure within a time interval δt is a function of the pressure difference at the openings, $P-P_i$, and the area-volume ratio, A_o/V_o :

$$\delta P_i = C_L (A_o / V_o) \delta t \quad 2-31$$

where

C_L - leakage pressure coefficient and a function of the pressure difference $P-P_i$ and is obtained from Figure 2-235

P - applied exterior pressure

P_i - interior pressure

δP_i - interior pressure increment

A_o - area of openings

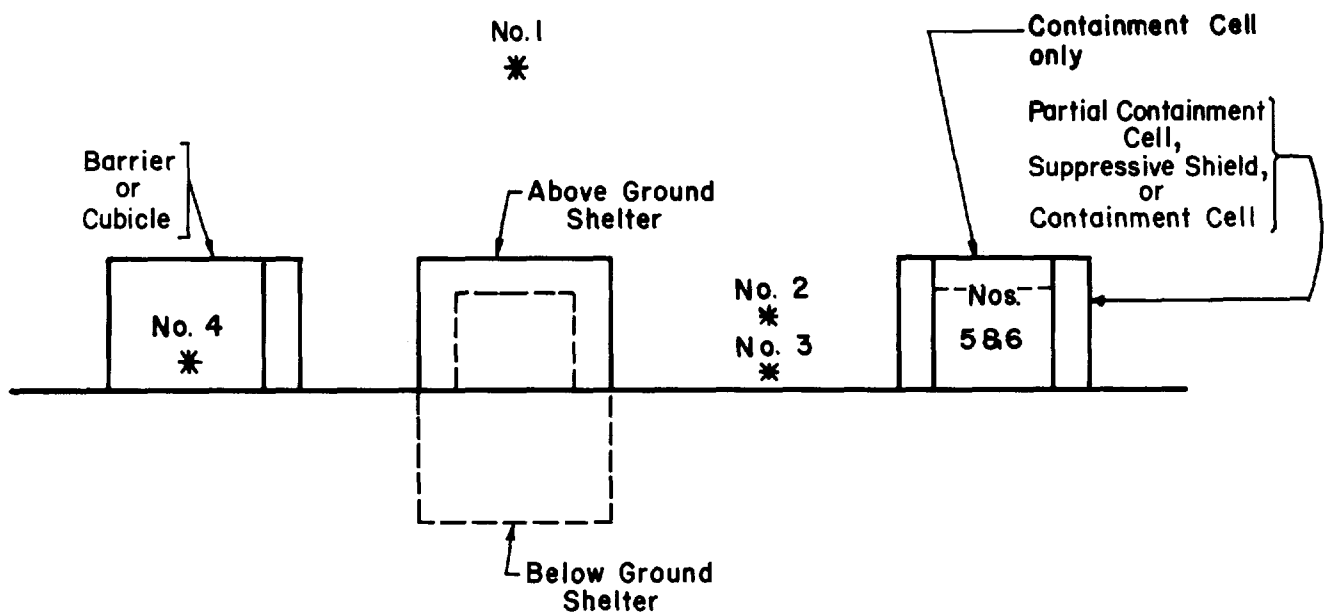
V_o - structure volume

δt - time increment

The interior pressure-time curve is calculated as follows:

- (1) Determine the pressure-time history of the applied blast pressures P acting on the surface surrounding the opening as presented in Section 2-15.3.
- (2) Divide the duration of the applied pressure into n equal intervals (δt), each interval being approximately $t_o/10$ to $t_o/20$, and determine the pressures at the end of each interval.
- (3) Compute the pressure differential $P - P_i$ for each time interval, determine the corresponding value of C_L from Figure 2-235, and calculate δP_i from Equation 2-31 using the proper values of A_o/V_o and δt . Add δP_i to P_i for the interval being considered to obtain the new value of P_i for the next interval.
- (4) Repeat for each interval using the proper values of P and P_i . When $P - P_i$ becomes negative during the analysis, the value of C_L must also be taken as negative.

The above procedure is most easily accomplished by using a tabular arrangement for the required computations. An illustrative example is presented in Appendix 2A.



BLAST LOADING CATEGORIES			
CHARGE CONFINEMENT	CATEGORY	PRESSURE LOADS	PROTECTIVE STRUCTURE
Unconfined Explosions	1. Free Air Burst	a. Unreflected	Shelter
	2. Air Burst	b. Reflected	
	3. Surface Burst	b. Reflected	
Confined Explosions	4. Fully Vented	c. Internal Shock d. Leakage	Cubicle
	5. Partially Confined	c. Internal Shock e. Internal Gas d. Leakage	Partial Containment Cell or Suppressive Shield
	6. Fully Confined	c. Internal Shock e. Internal Gas	Full Containment Cell

Figure 2-1 Blast loading categories

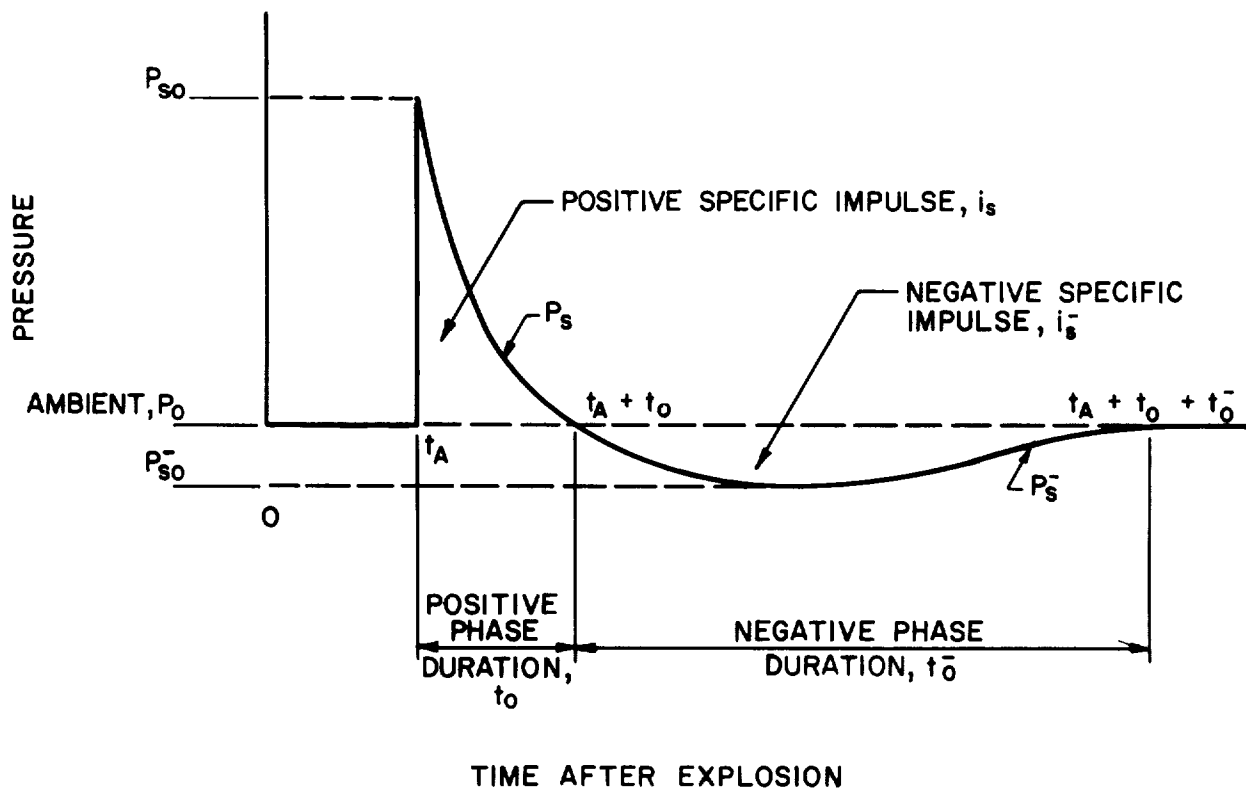


Figure 2-2 Free-field pressure-time variation

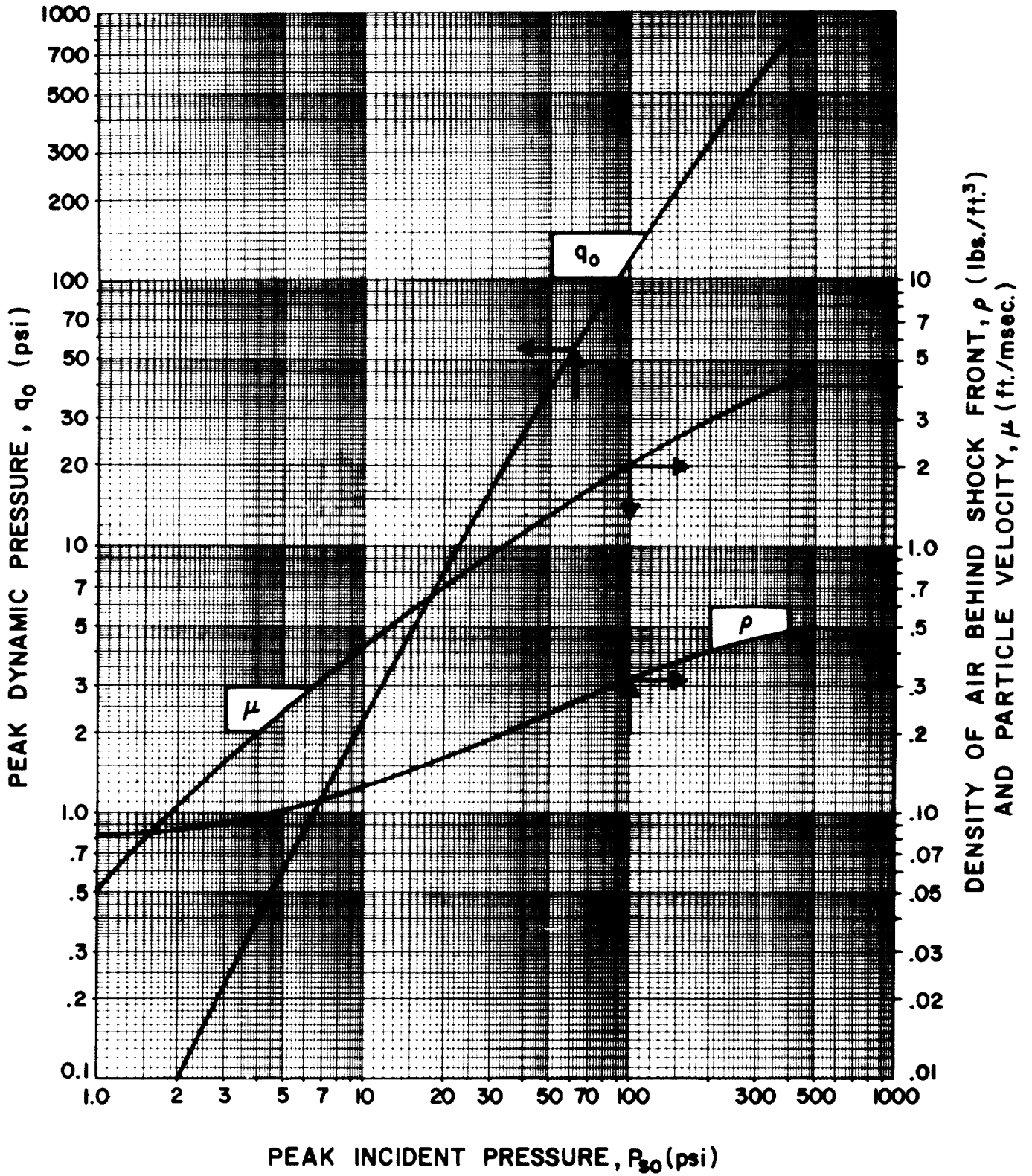
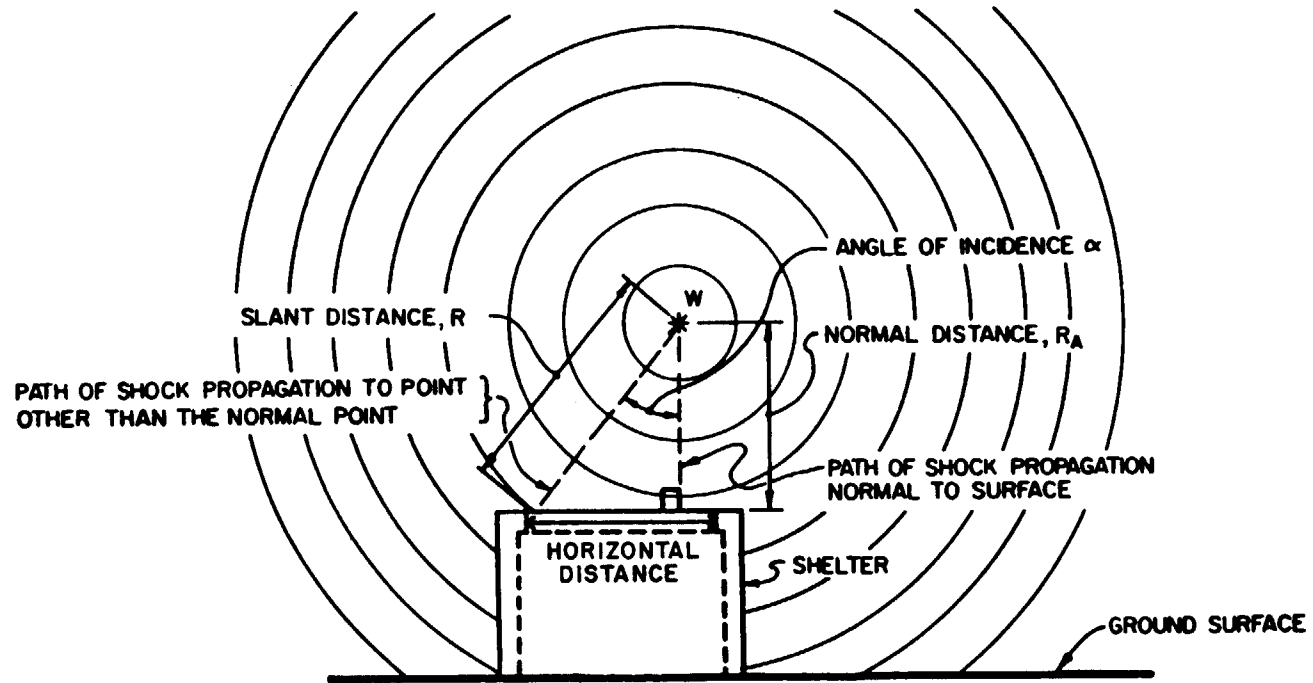


Figure 2-3 Peak incident pressure versus peak dynamic pressure density of air behind the shock front and particle velocity

Figure 2-4 Free-air burst blast environment



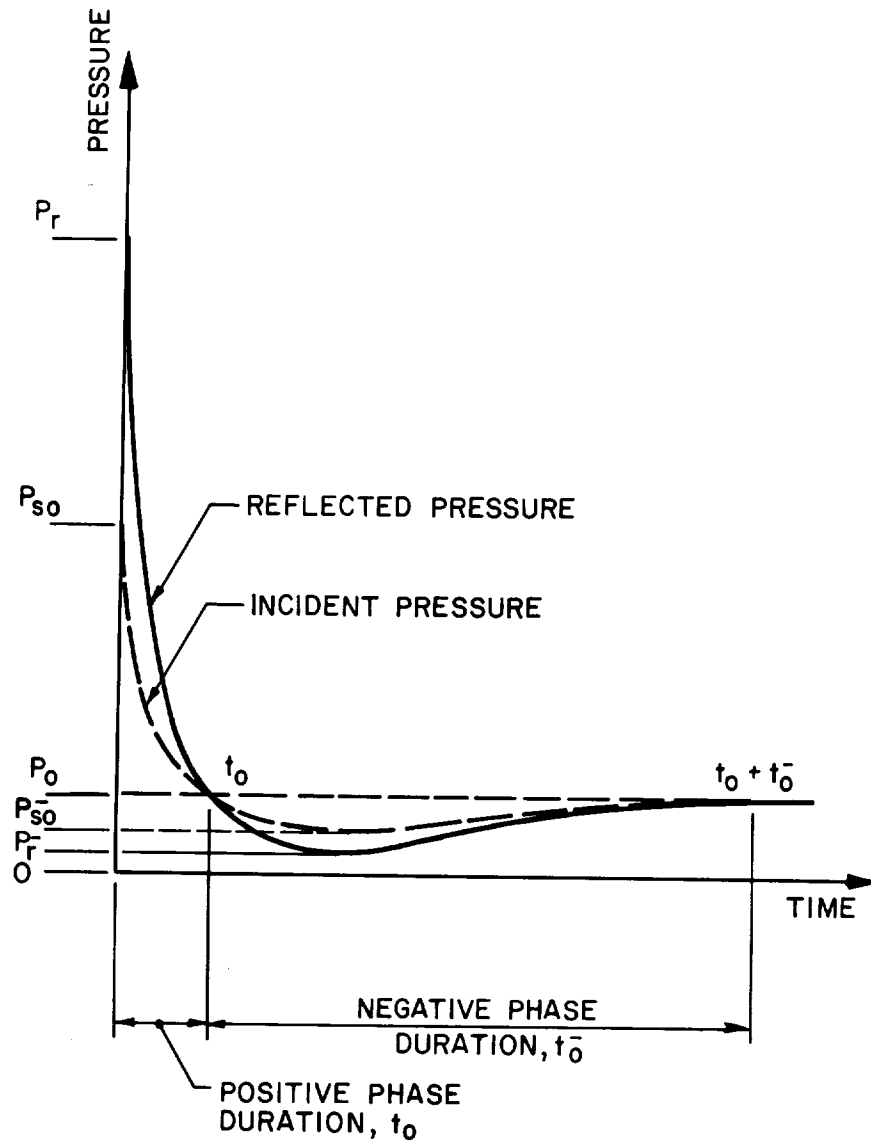


Figure 2-5 Pressure-time variation for a free-air burst

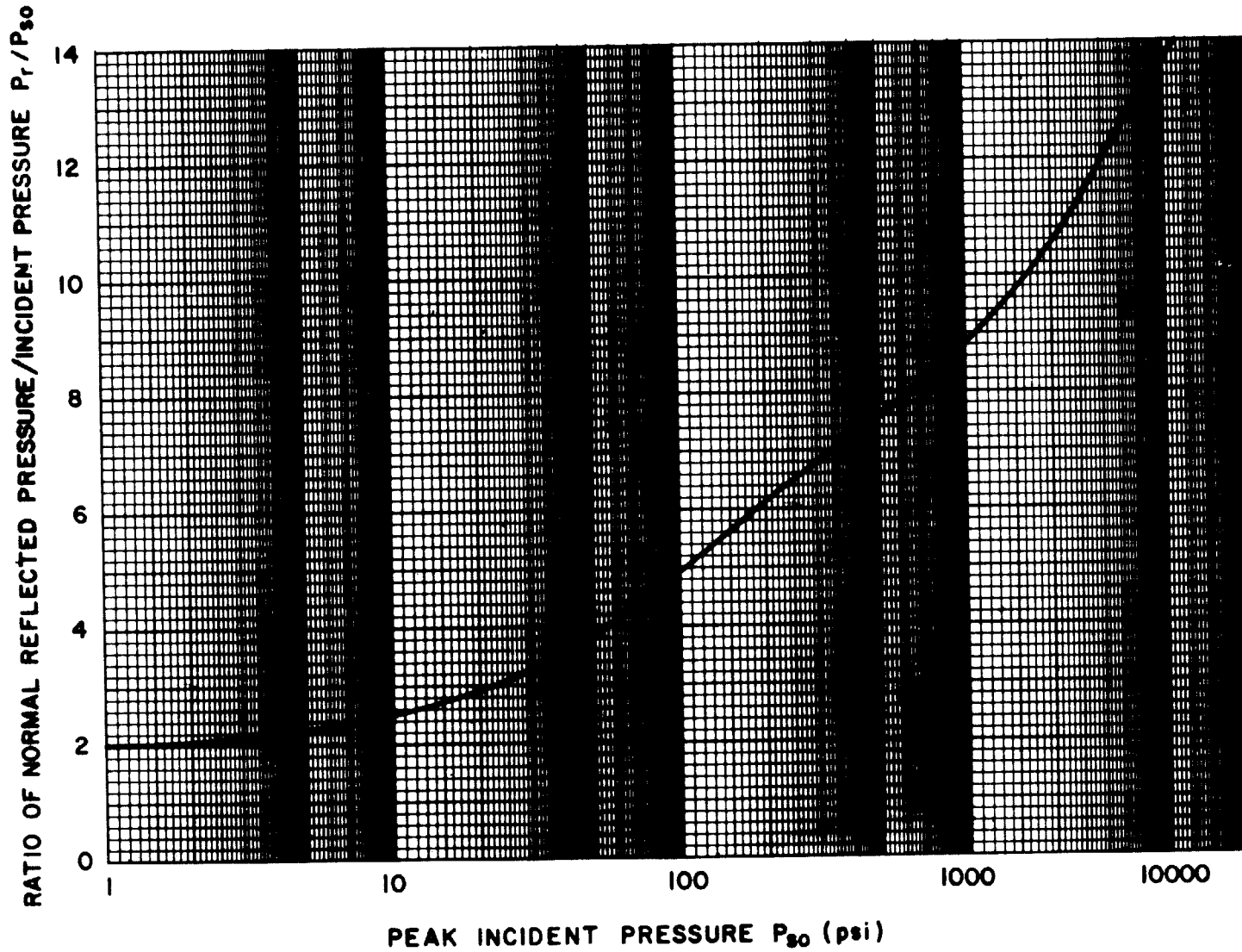
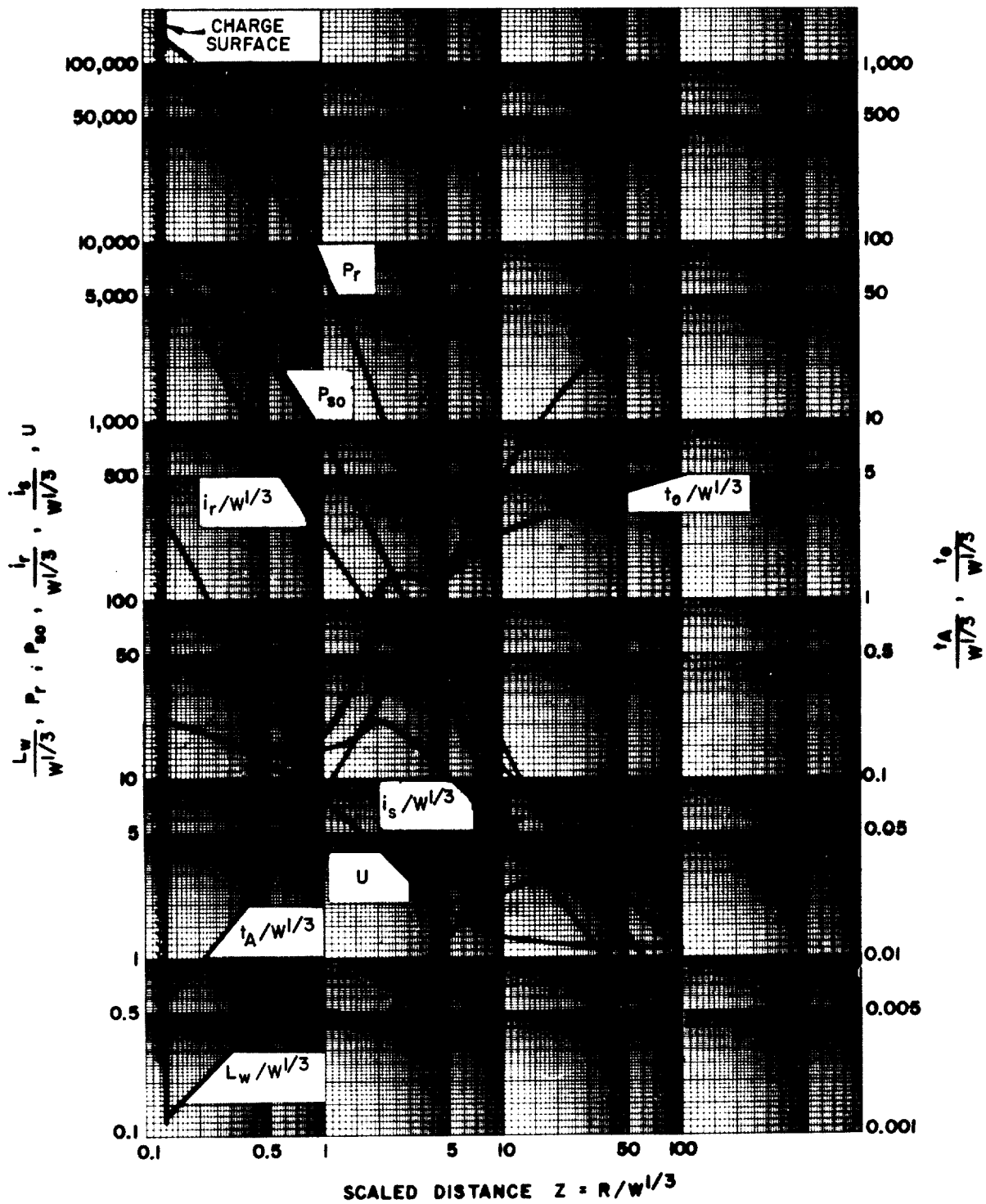
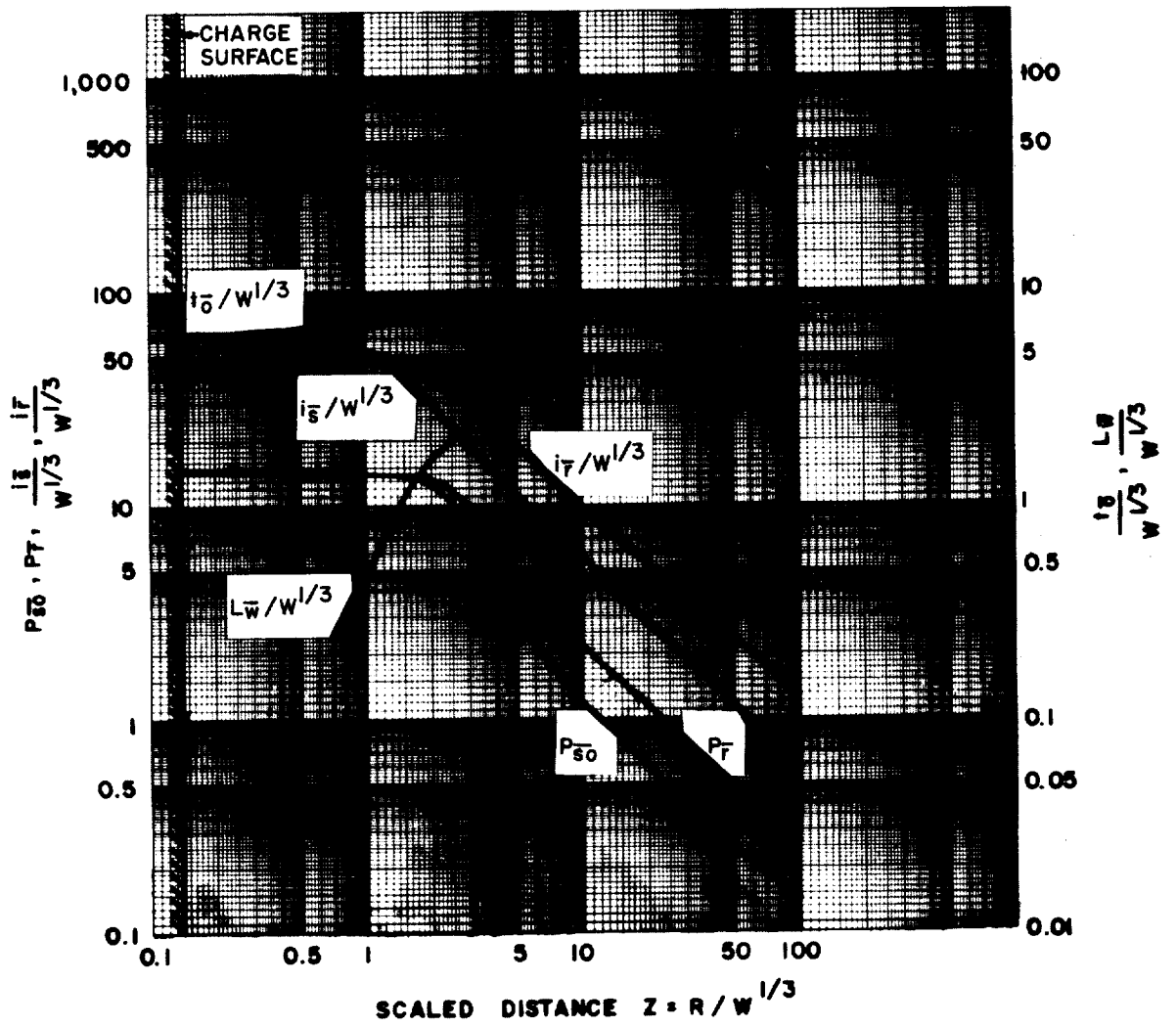


Figure 2-6 Peak incident pressure versus the ratio of normal reflected pressure/ incident pressure for a free air burst



- P_{so} = PEAK POSITIVE INCIDENT PRESSURE, psi
- P_r = PEAK POSITIVE NORMAL REFLECTED PRESSURE, psi
- $i_s/W^{1/3}$ = SCALED UNIT POSITIVE INCIDENT IMPULSE, psi-ms/lb^{1/3}
- $i_r/W^{1/3}$ = SCALED UNIT POSITIVE NORMAL REFLECTED IMPULSE, psi-ms/lb^{1/3}
- $t_A/W^{1/3}$ = SCALED TIME OF ARRIVAL OF BLAST WAVE, ms/lb^{1/3}
- $t_o/W^{1/3}$ = SCALED POSITIVE DURATION OF POSITIVE PHASE, ms/lb^{1/3}
- U = SHOCK FRONT VELOCITY, ft/ms
- W = CHARGE WEIGHT, lbs
- $L_w/W^{1/3}$ = SCALED WAVE LENGTH OF POSITIVE PHASE, ft/lb^{1/3}

Figure 2-7 Positive phase shock wave parameters for a spherical TNT explosion in free air at sea level



- P_{s0} = PEAK NEGATIVE INCIDENT PRESSURE, psi
- P_r = PEAK NEGATIVE NORMAL REFLECTED PRESSURE, psi
- $i_s/W^{1/3}$ = SCALED UNIT NEGATIVE INCIDENT IMPULSE, psi-ms/lb^{1/3}
- $i_r/W^{1/3}$ = SCALED UNIT NEGATIVE NORMAL REFLECTED IMPULSE, psi-ms/lb^{1/3}
- $t_0/W^{1/3}$ = SCALED DURATION OF NEGATIVE PHASE, ms/lb^{1/3}
- $L_w/W^{1/3}$ = SCALED WAVE LENGTH OF NEGATIVE PHASE, ft/lb^{1/3}

Figure 2-8 Negative phase shock wave parameters for a spherical TNT explosion in free air at sea level

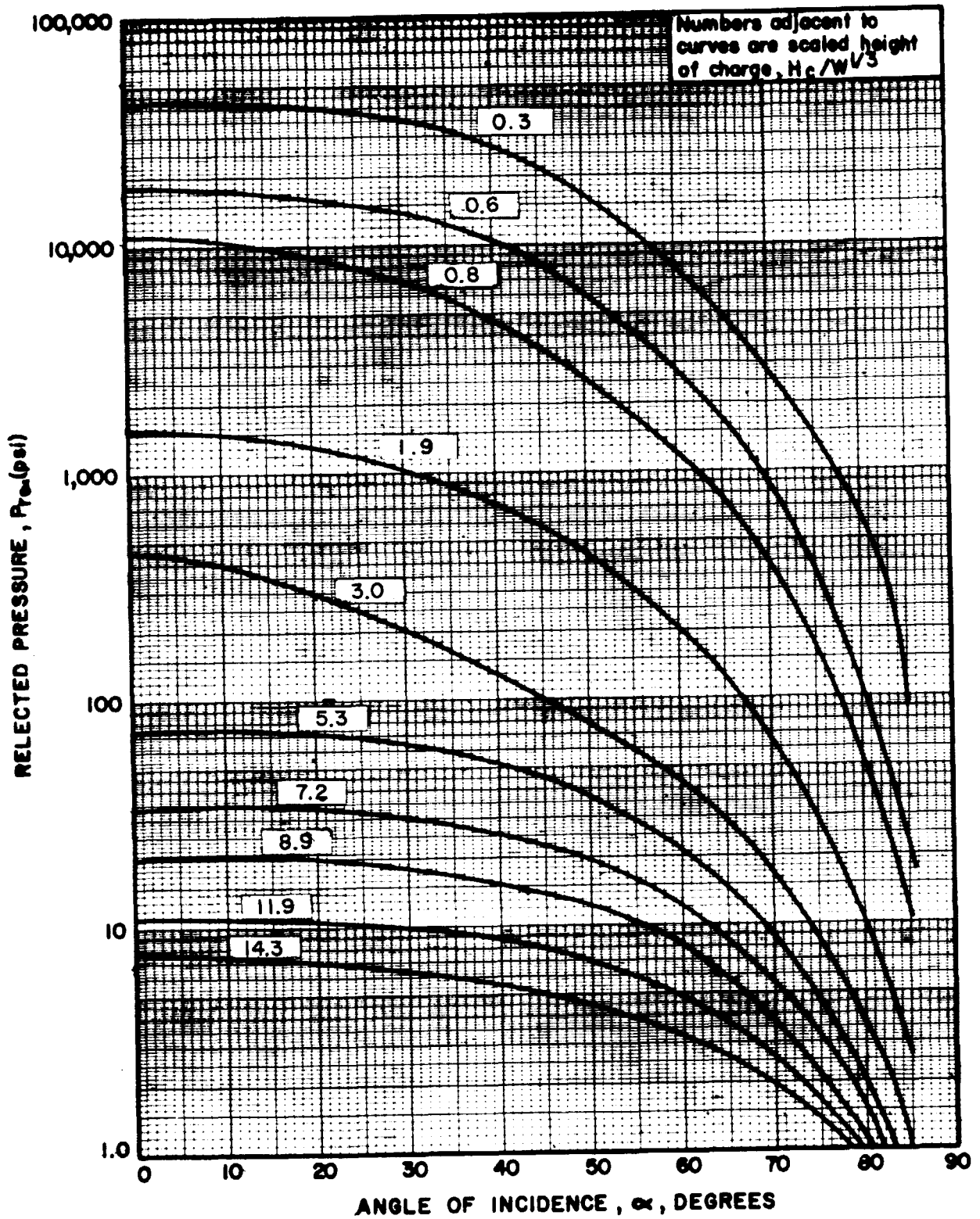


Figure 2-9 Variation of reflected pressure as a function of angle of incidence

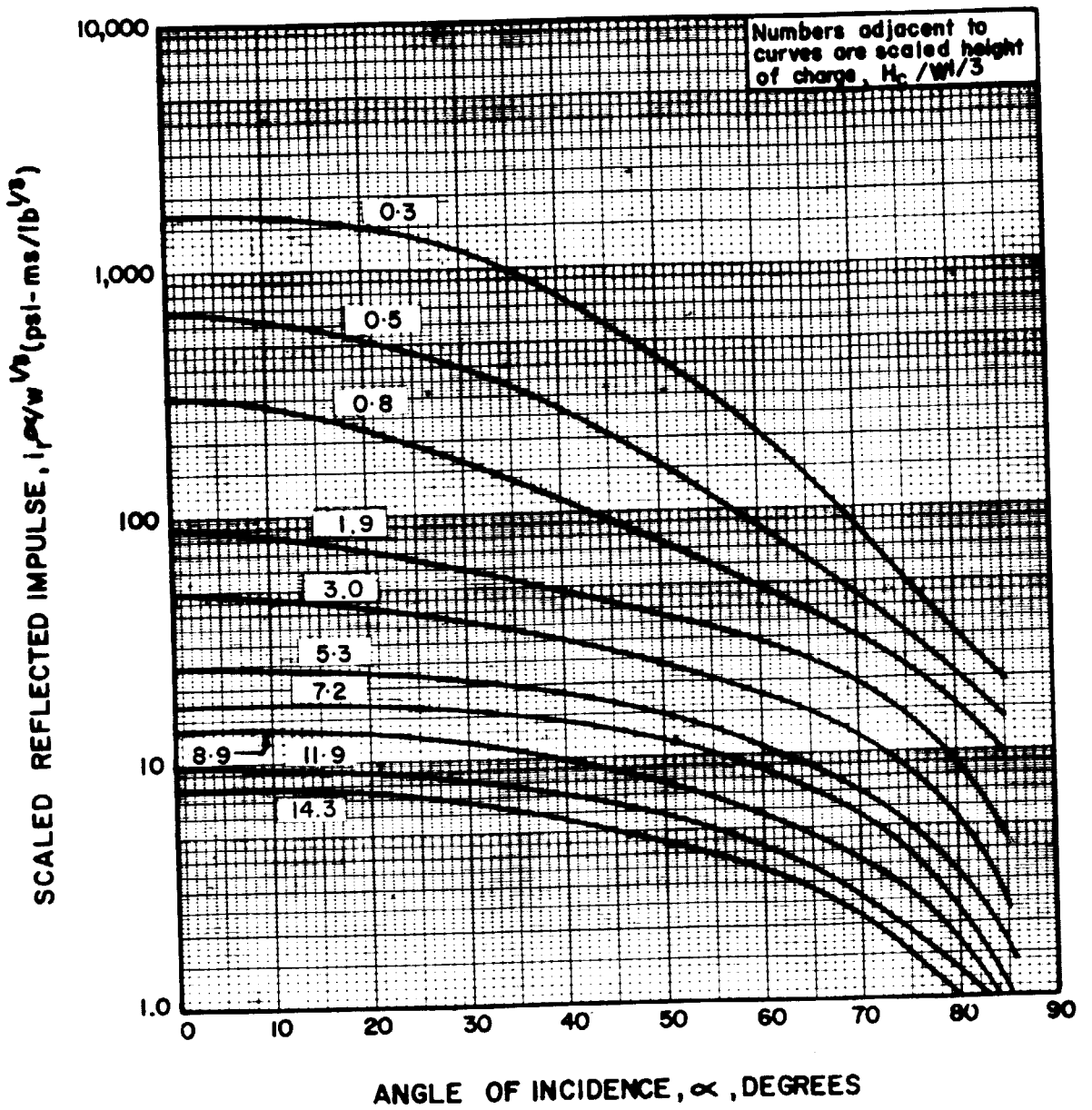


Figure 2-10 Variation of scaled reflected impulse as a function of angle of incidence

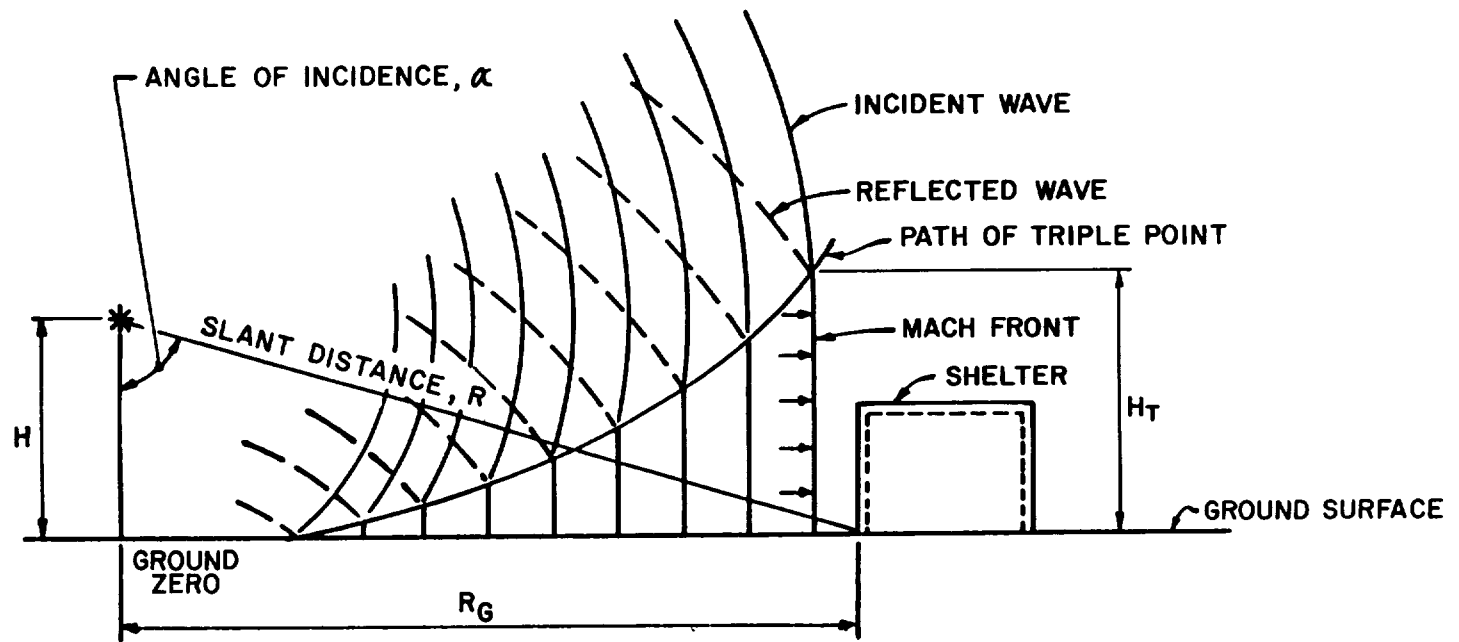


Figure 2-11 Air burst blast environment

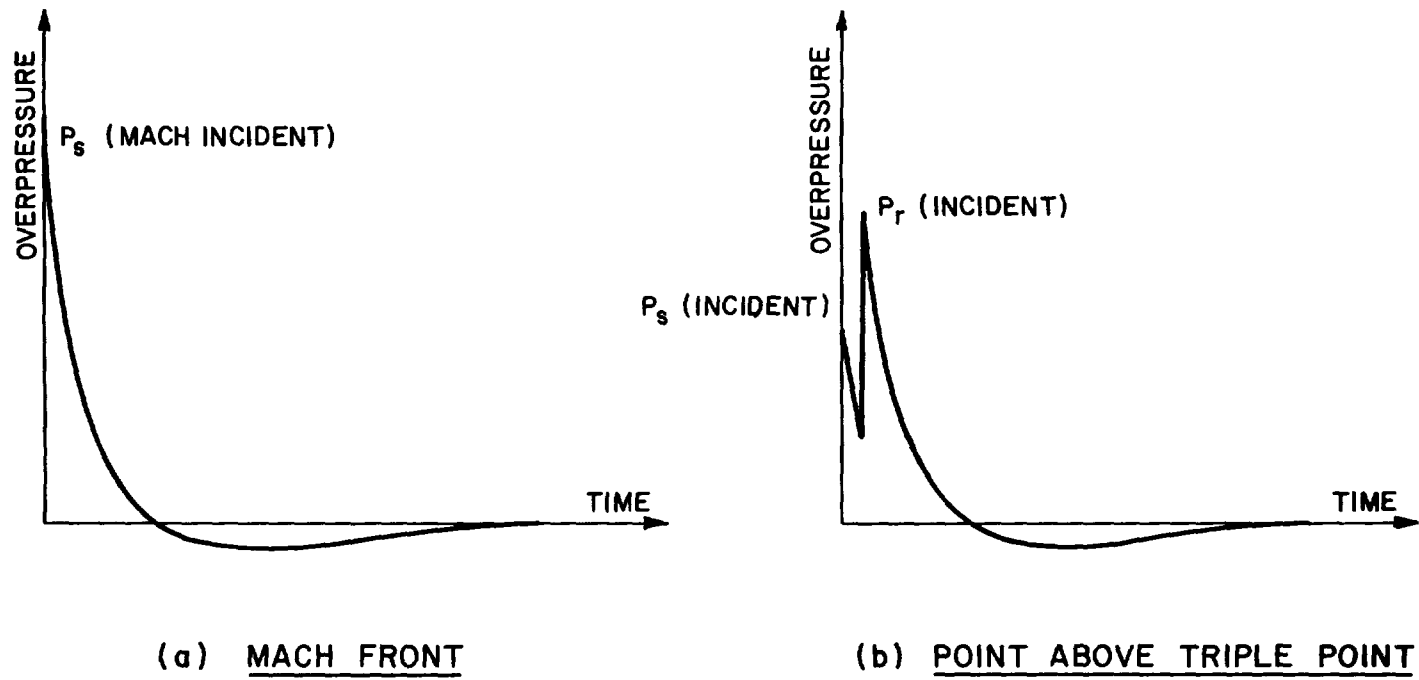


Figure 2-12 Pressure-time variation for air burst

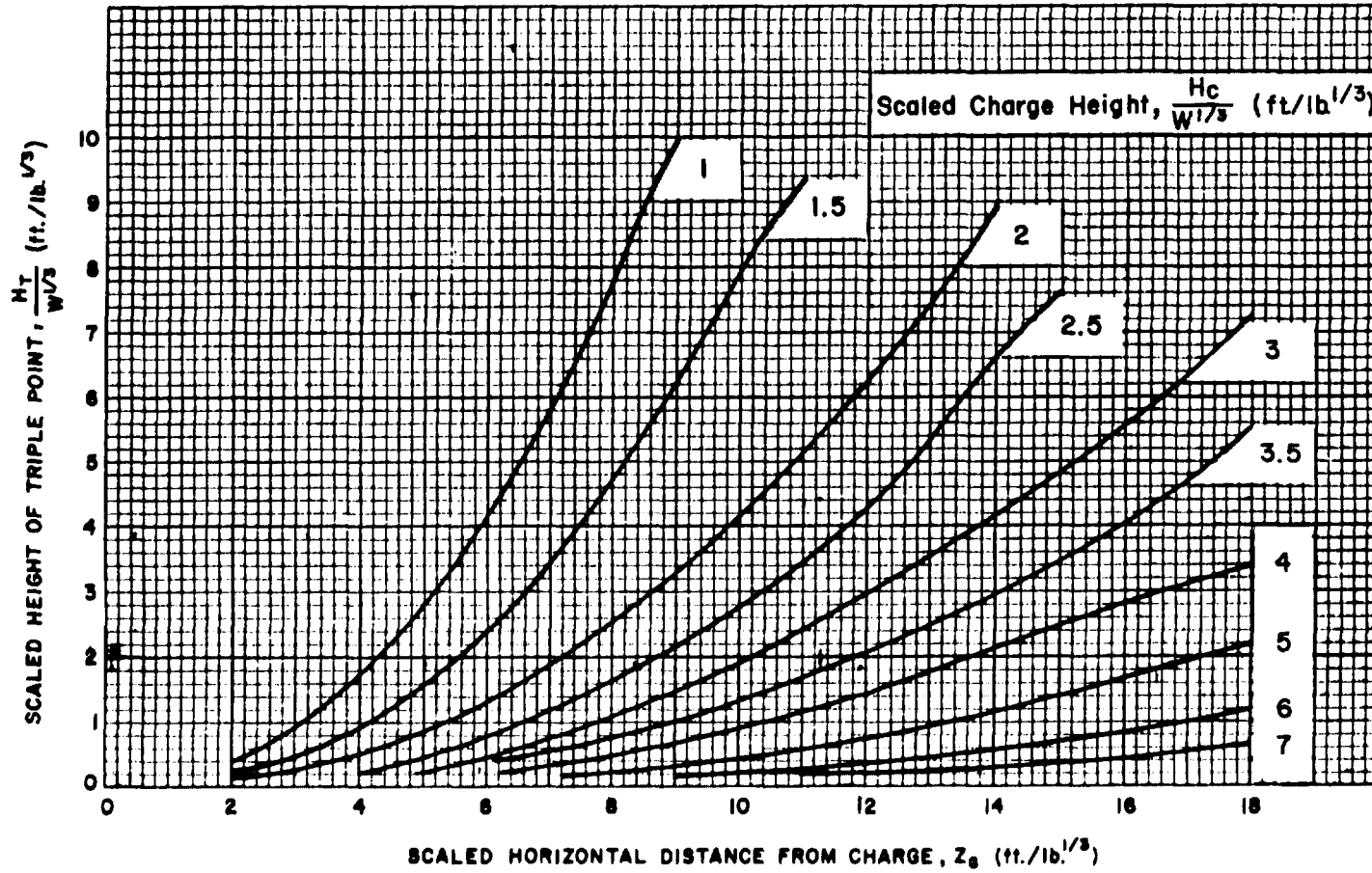


Figure 2-13 Scaled height of triple point

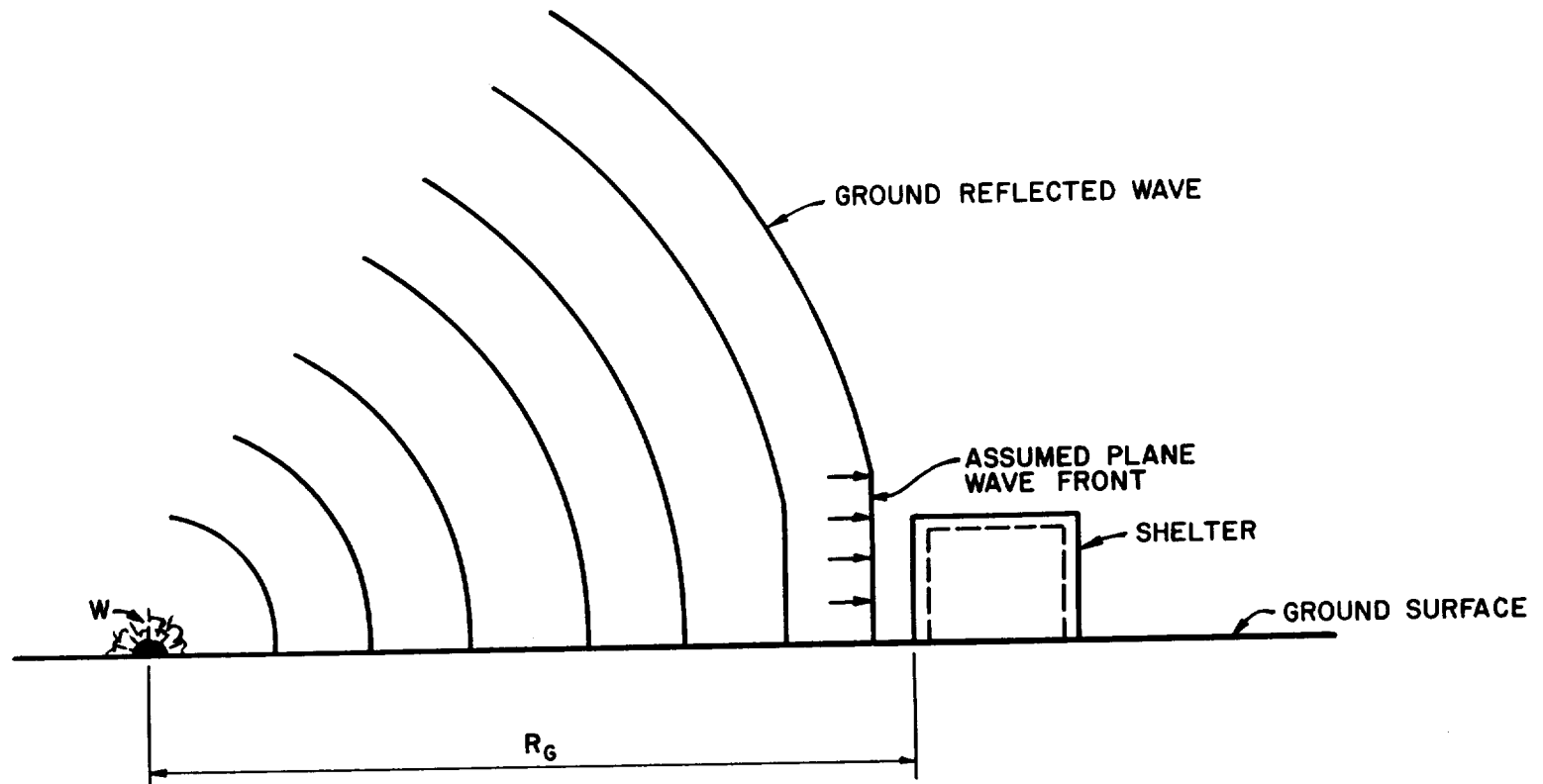
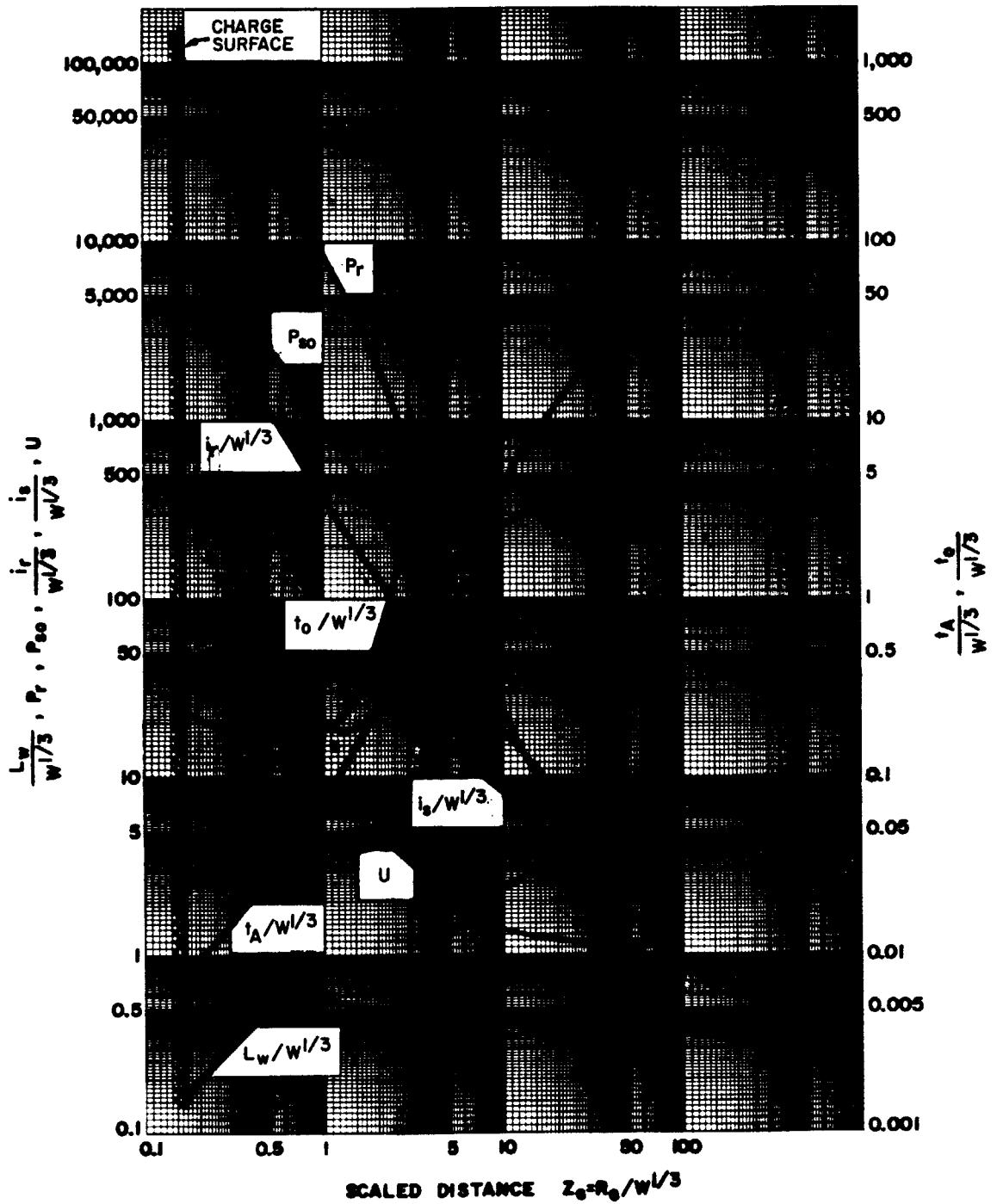
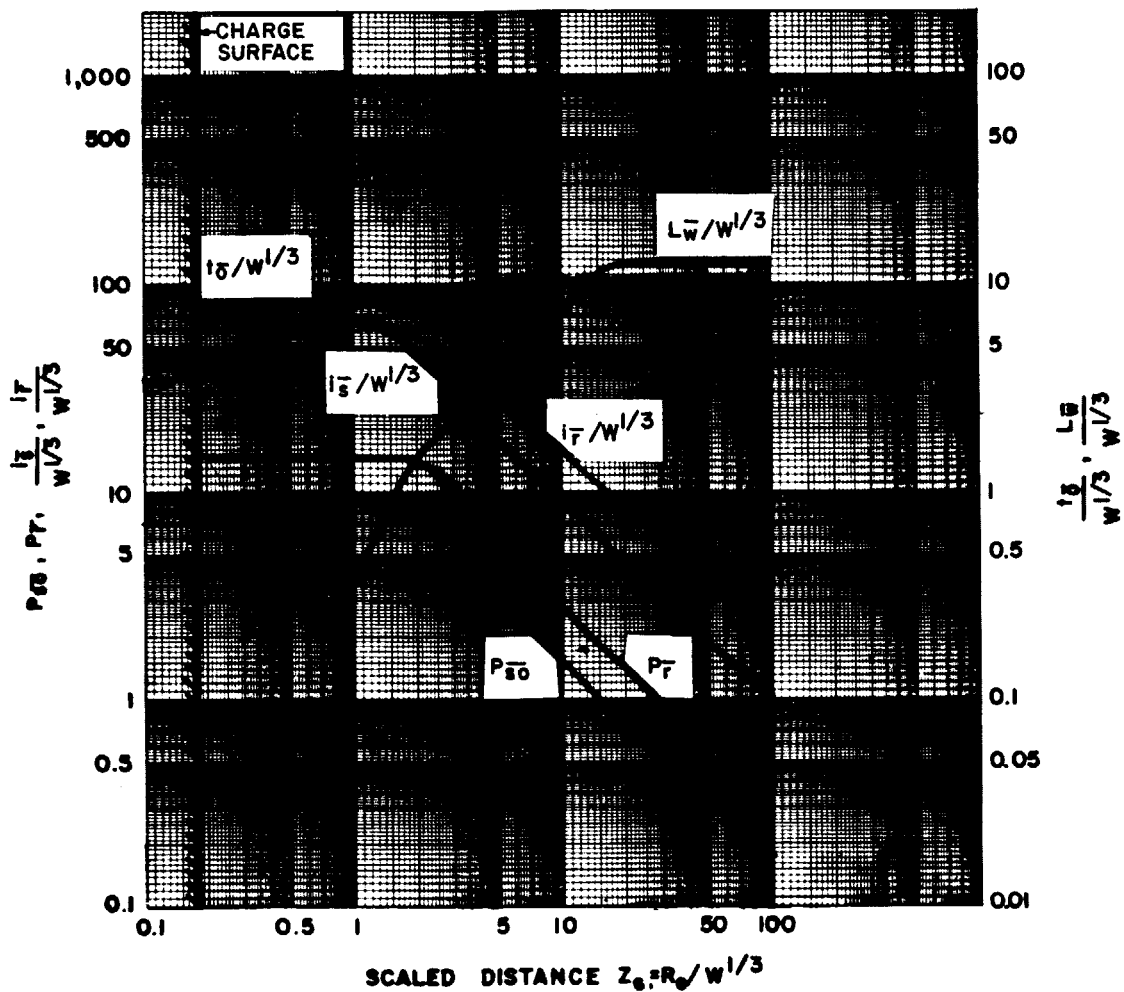


Figure 2-14 Surface burst blast environment



- P_{s0} = PEAK POSITIVE INCIDENT PRESSURE, psi
 P_r = PEAK POSITIVE NORMAL REFLECTED PRESSURE, psi
 $i_s/W^{1/3}$ = SCALED UNIT POSITIVE INCIDENT IMPULSE, psi-ms/lb^{1/3}
 $i_r/W^{1/3}$ = SCALED UNIT POSITIVE NORMAL REFLECTED IMPULSE, psi-ms/lb^{1/3}
 $t_A/W^{1/3}$ = SCALED TIME OF ARRIVAL OF BLAST WAVE, ms/lb^{1/3}
 $t_0/W^{1/3}$ = SCALED POSITIVE DURATION OF POSITIVE PHASE, ms/lb^{1/3}
 U = SHOCK FRONT VELOCITY, ft/ms
 W = CHARGE WEIGHT, lbs
 $L_w/W^{1/3}$ = SCALED WAVE LENGTH OF POSITIVE PHASE, ft/lb^{1/3}

Figure 2-15 Positive phase shock wave parameters for a hemispherical TNT explosion on the surface at sea level



- $P_{\bar{e}0}$ = PEAK NEGATIVE INCIDENT PRESSURE, psi
- $P_{\bar{e}r}$ = PEAK NEGATIVE NORMAL REFLECTED PRESSURE, psi
- $I_{\bar{e}}/W^{1/3}$ = SCALED UNIT NEGATIVE INCIDENT IMPULSE, psi-ms/lb^{1/3}
- $I_{\bar{e}r}/W^{1/3}$ = SCALED UNIT NEGATIVE NORMAL REFLECTED IMPULSE, psi-ms/lb^{1/3}
- $t_{\bar{e}}/W^{1/3}$ = SCALED DURATION OF NEGATIVE PHASE, ms/lb^{1/3}
- $L_{\bar{e}}/W^{1/3}$ = SCALED WAVE LENGTH OF NEGATIVE PHASE, ft/lb^{1/3}

Figure 2-16 Negative phase shock wave parameters for a hemispherical TNT explosion on the surface at sea level

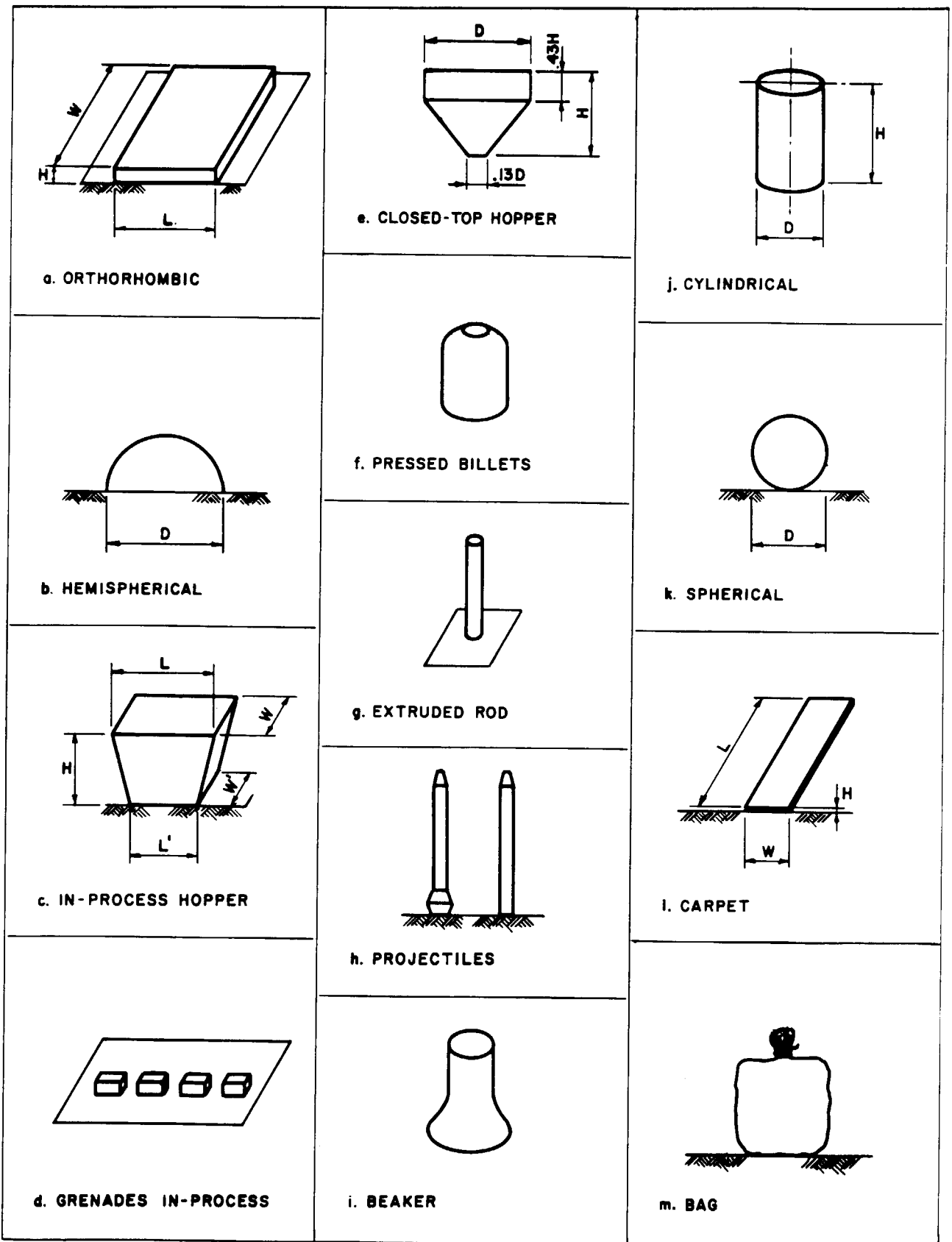
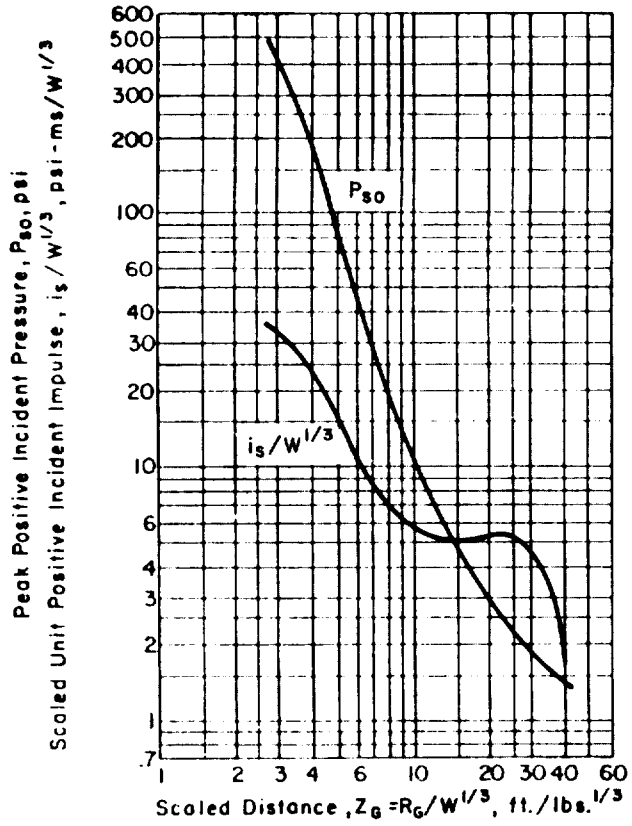
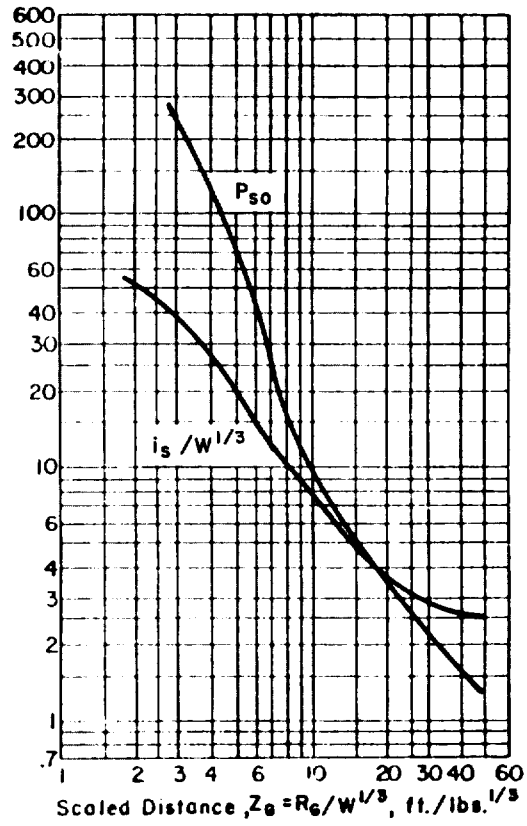


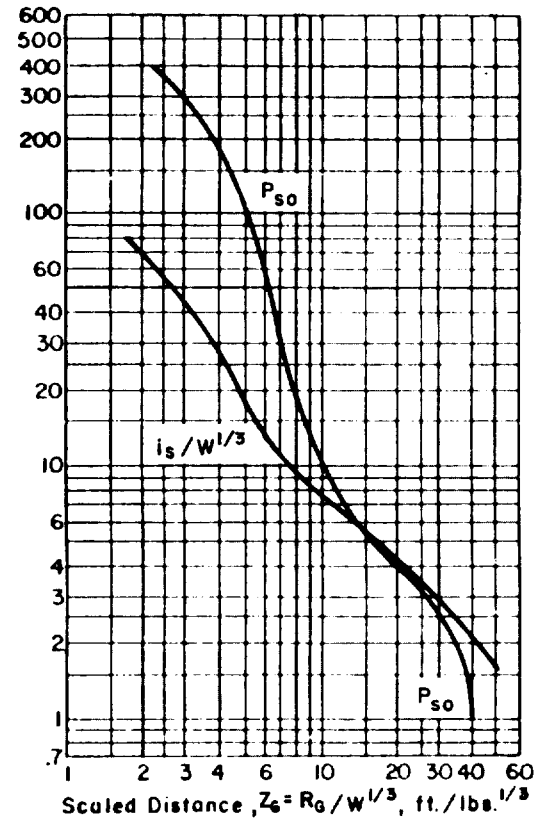
Figure 2-17 Explosive shapes



a. Composition A-3
Rectangular Shape

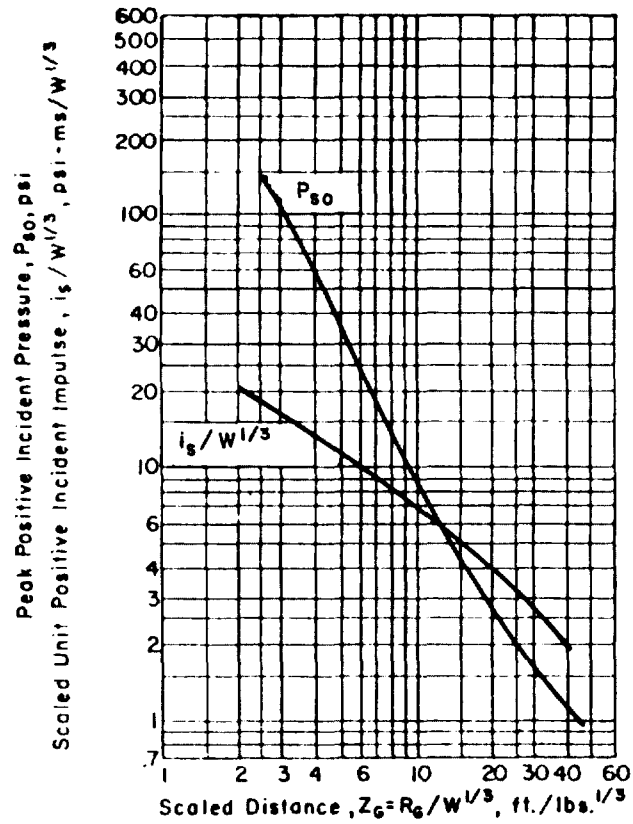


b. Composition A-5
Rectangular Shape

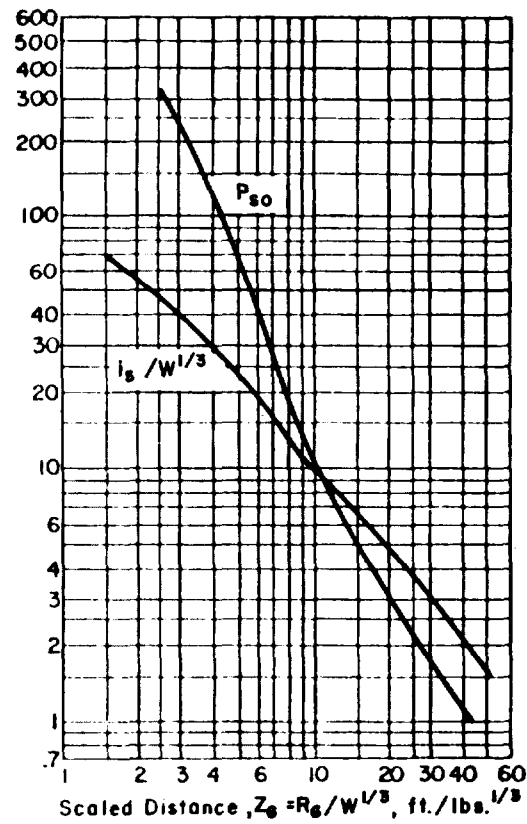


c. Composition A-5
Cylindrical Shape

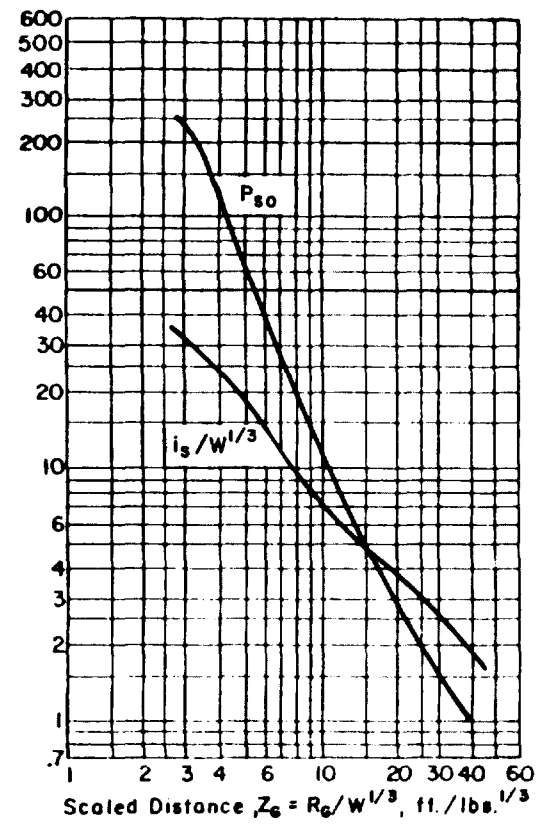
Figure 2-18 Peak positive incident pressure and scaled impulse for an explosion on the surface at sea level



a. Composition B
Hemispherical

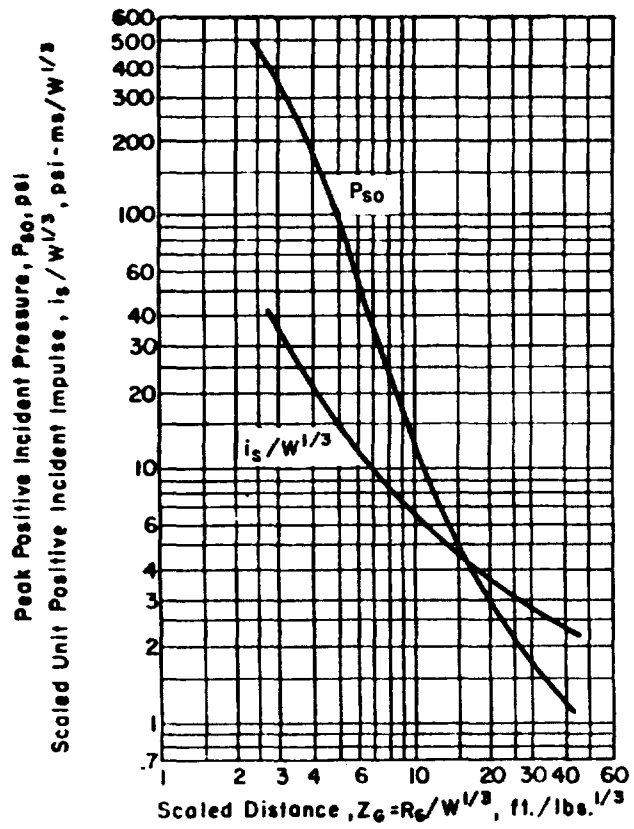


b. Composition B
Cast Spherical

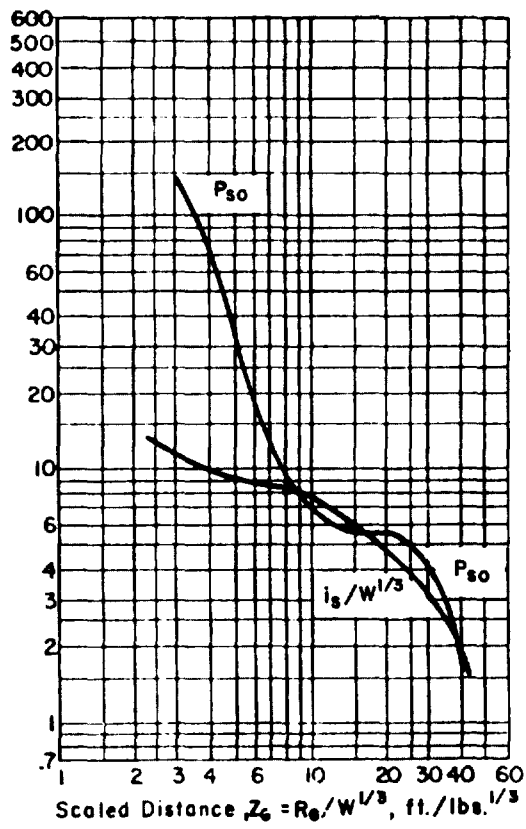


c. Composition B
Cylindrical

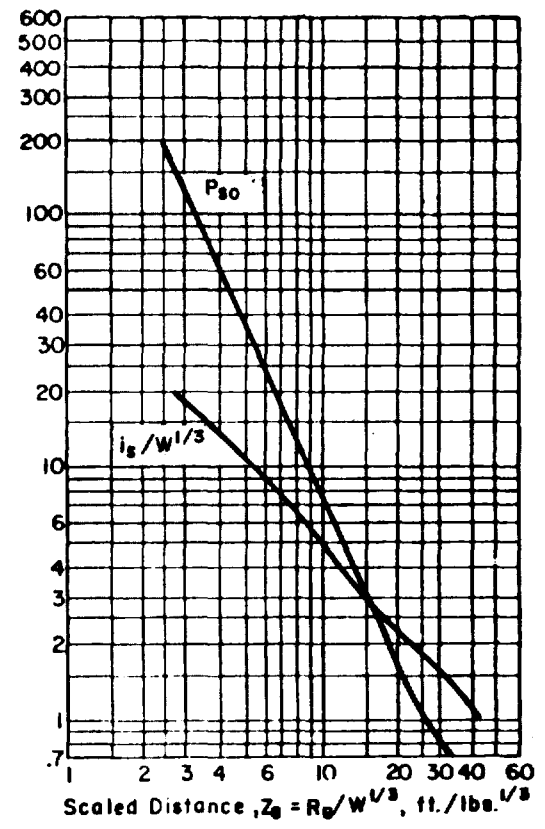
Figure 2-19 Peak positive incident pressure and scaled impulse for an explosion on the surface at sea level



a. Composition C-4
Orthorhombic

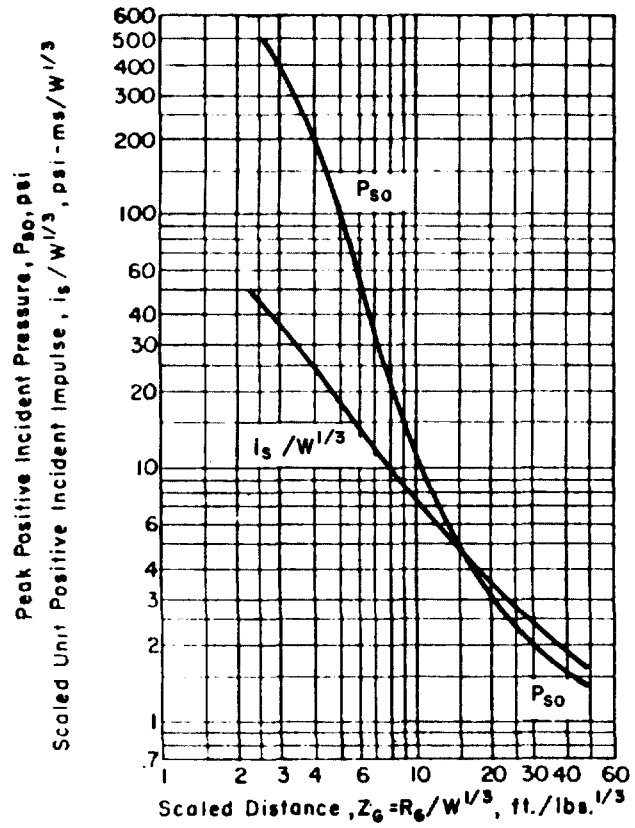


b. Composition C-4
Orthorhombic

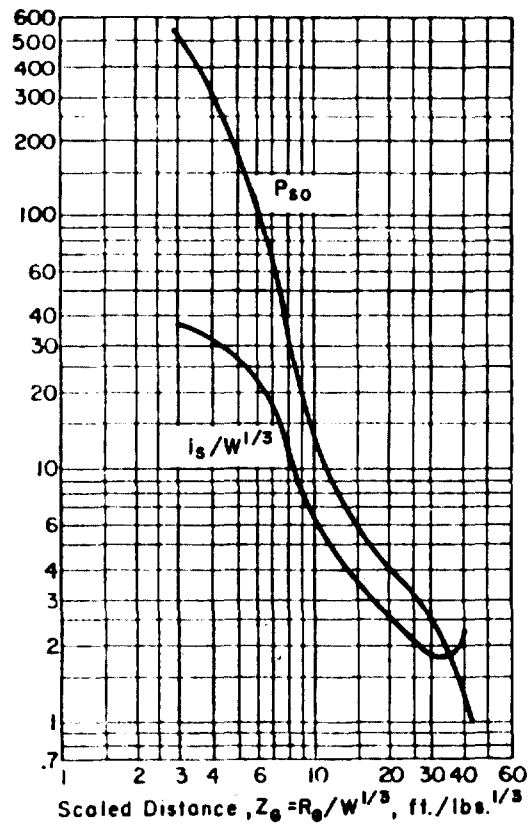


c. Guanidine Nitrate
Orthorhombic

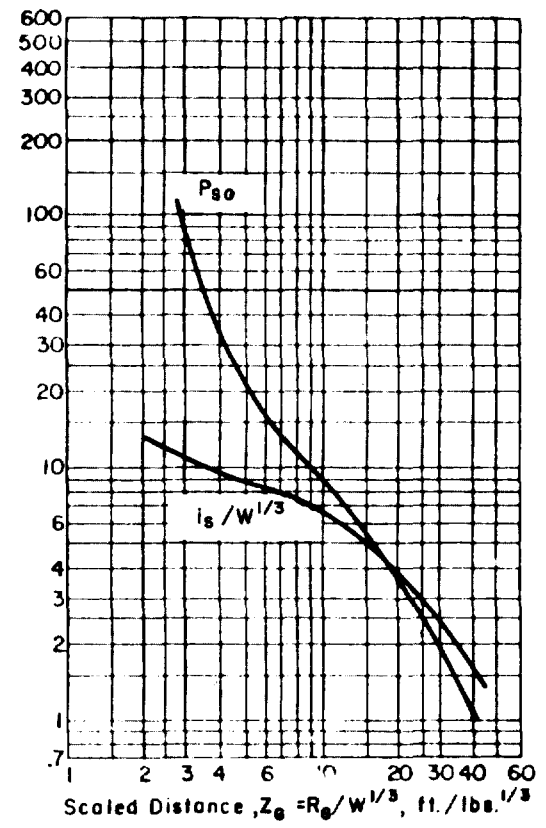
Figure 2-20 Peak positive incident pressure and scaled impulse for an explosion on the surface at sea level



a. Cyclotol 70/30 Orthorhomic

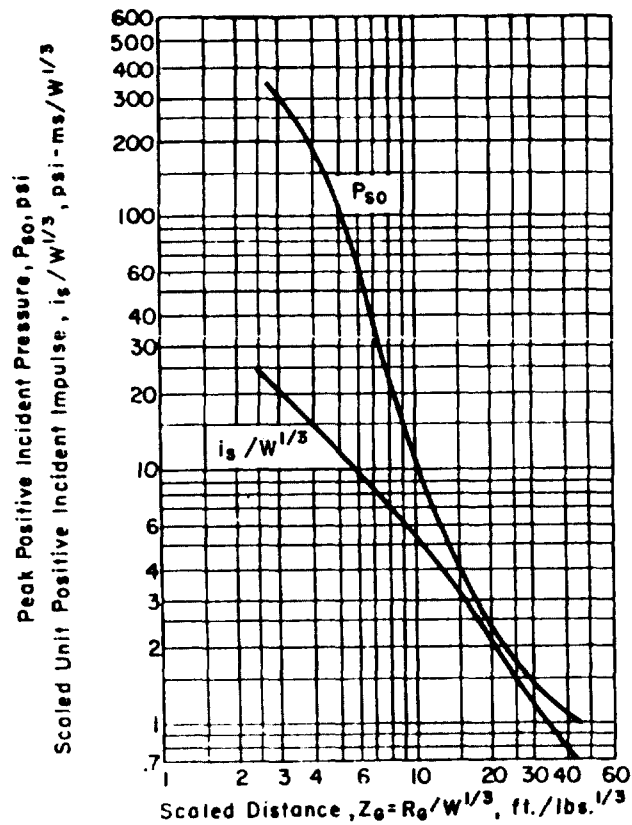


b. Cyclotol 70/30 Hoppers

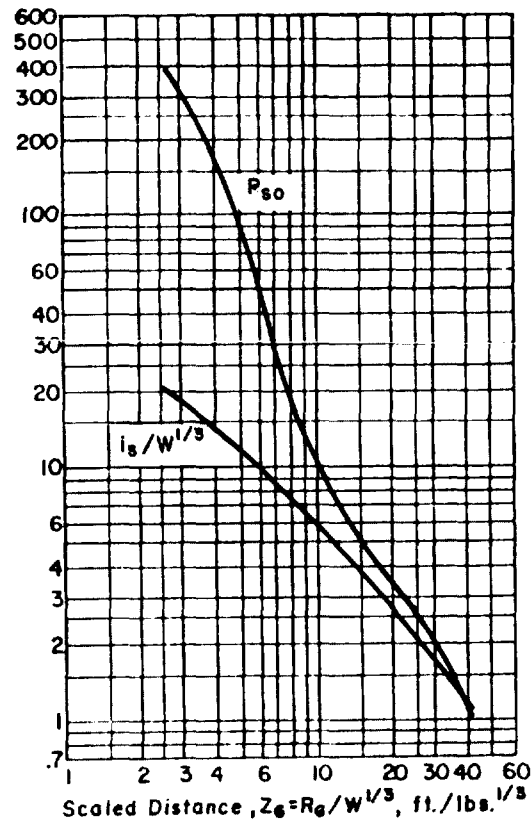


c. 64 M42 Grenades Tray of 64

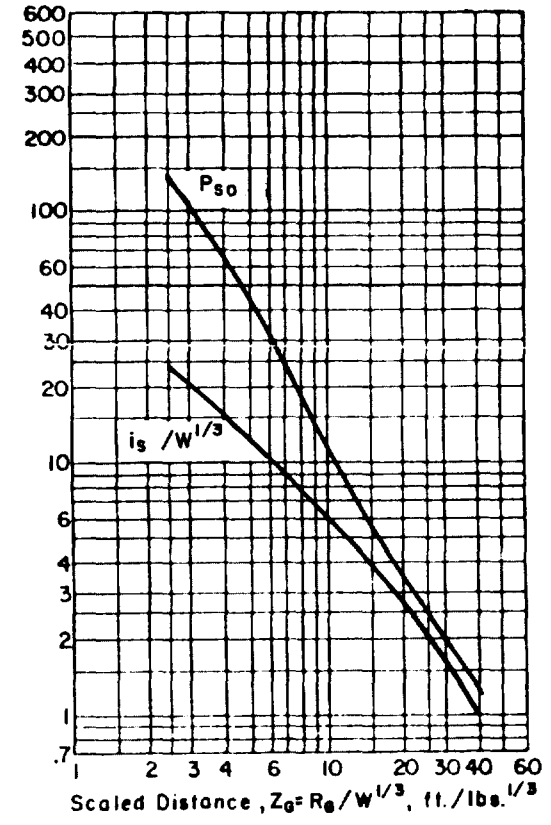
Figure 2-21 Peak positive incident pressure and scaled impulse for an explosion on the surface at sea level



a. HMX
Orthorhombic

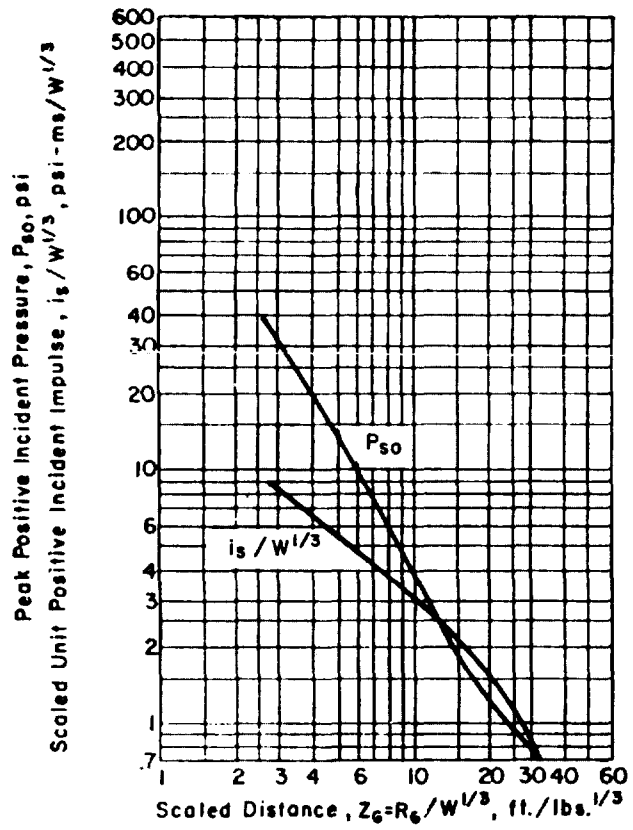


b. HMX
Cylindrical

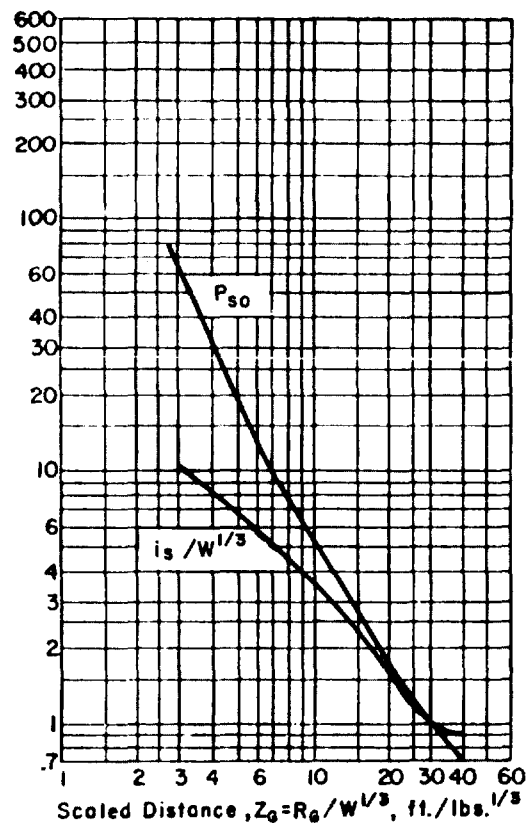


c. M483 155mm ICM Projectile
Single Round

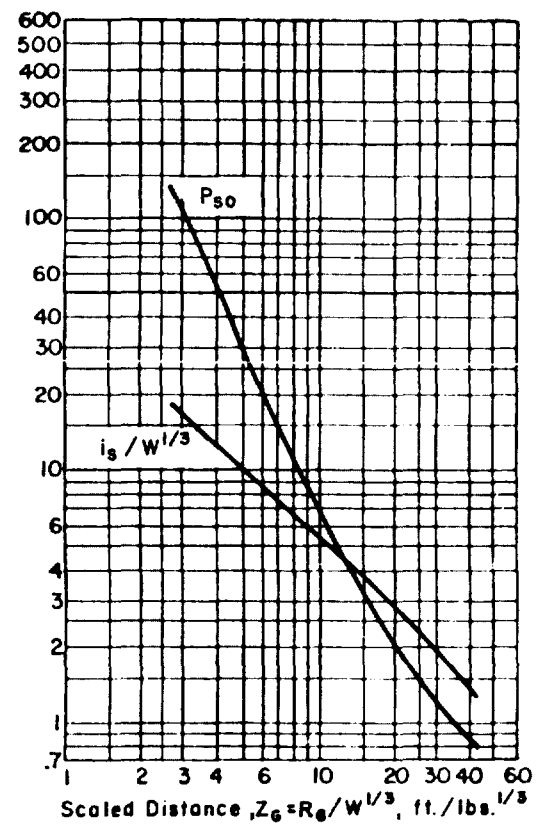
Figure 2-22 Peak positive incident pressure and scaled impulse for an explosion on the surface at sea level



a. Lead Azide (dextrinated)

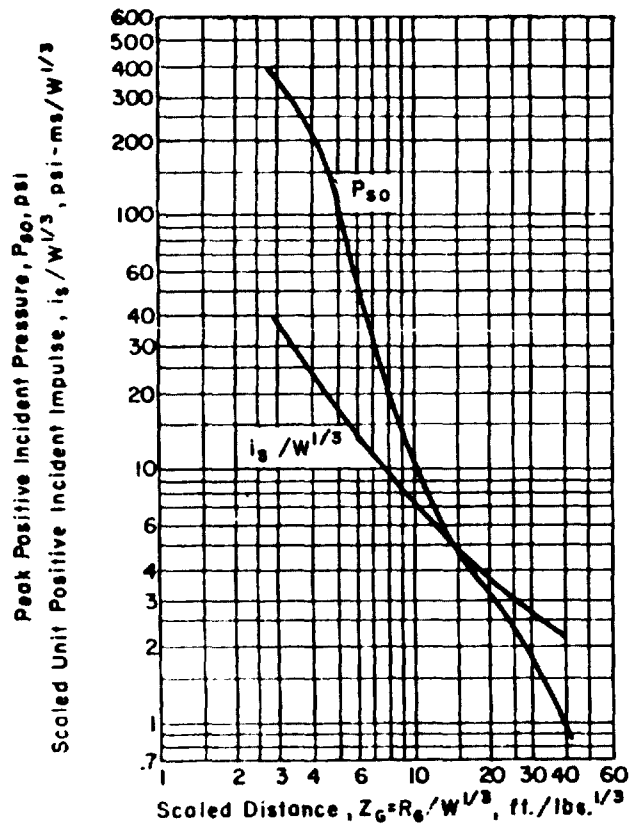


b. Lead Styphnate

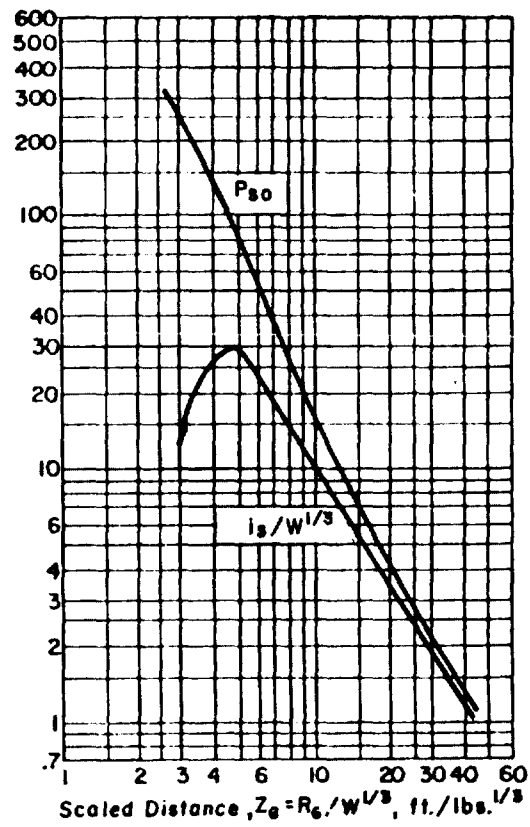


c. Lead Styphnate

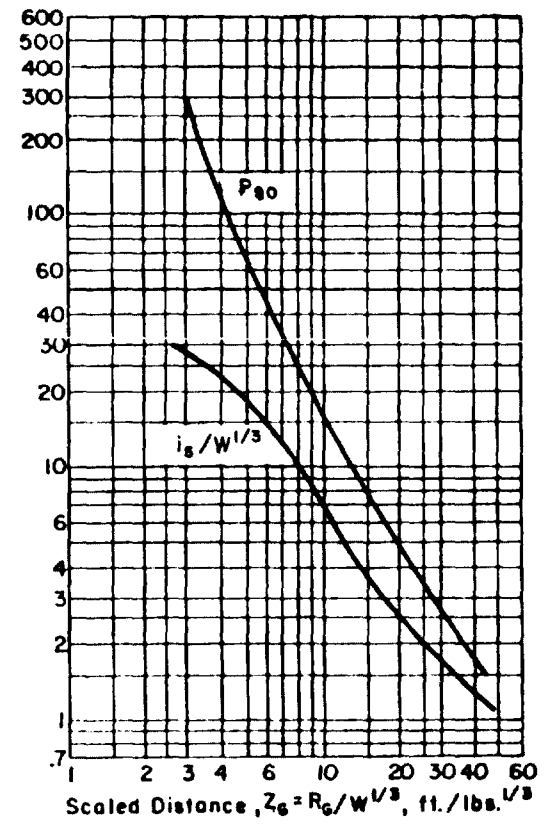
Figure 2-23 Peak positive incident pressure and scaled impulse for an explosion on the surface at sea level



a. LX-14
Orthorhombic

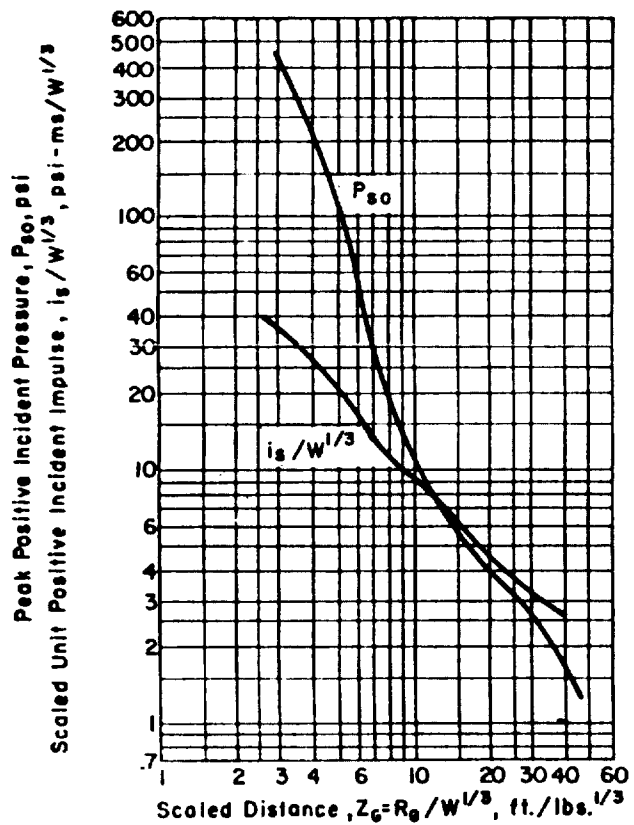


b. LX-14
Pressed billets

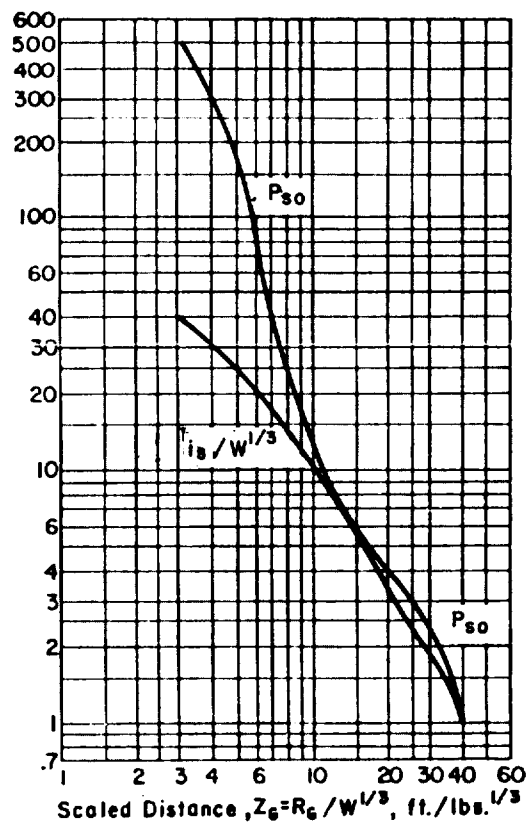


c. LX-14
Orthorhombic

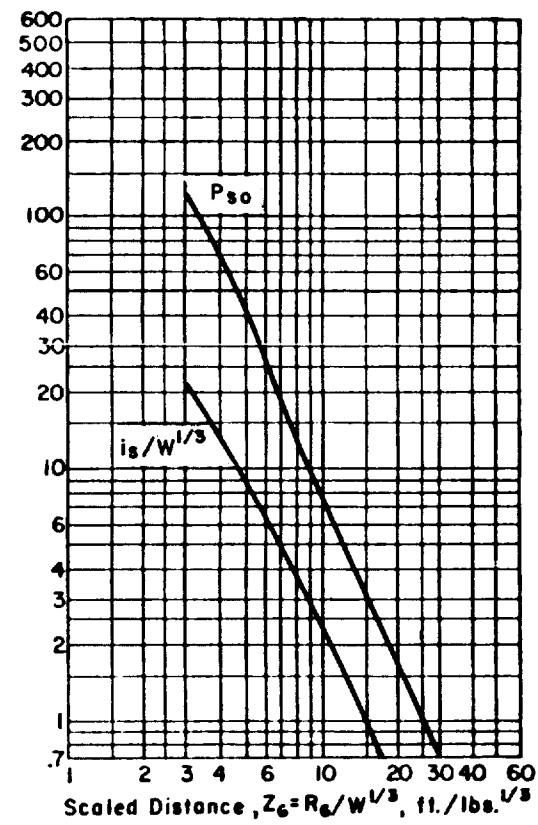
Figure 2-24 Peak positive incident pressure and scaled impulse for an explosion on the surface at sea level



a. Octol 75/25 Orthorhombic

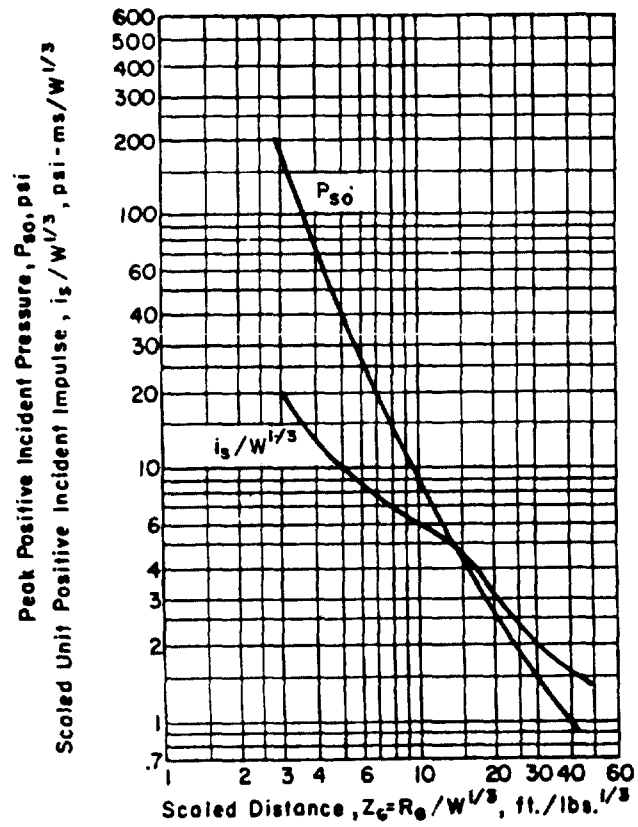


b. Octol 75/25 Hopper

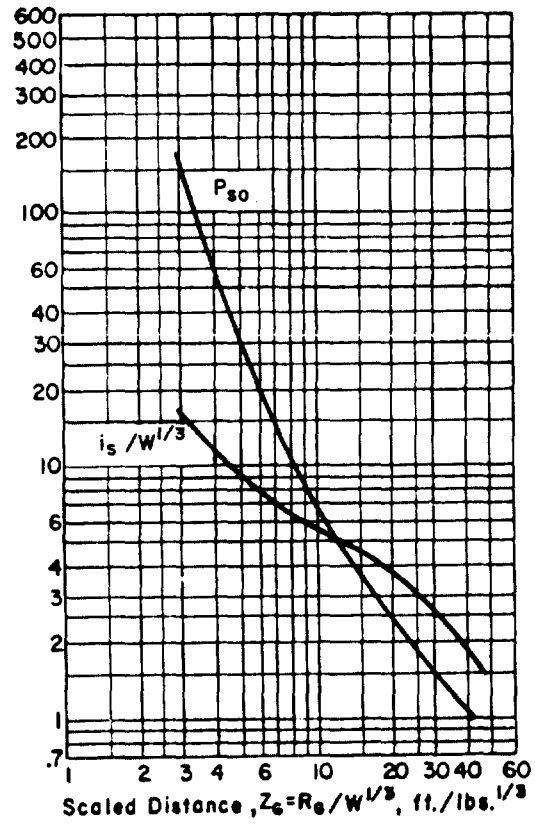


c. M718/741 RAAM Pallet of eight rounds

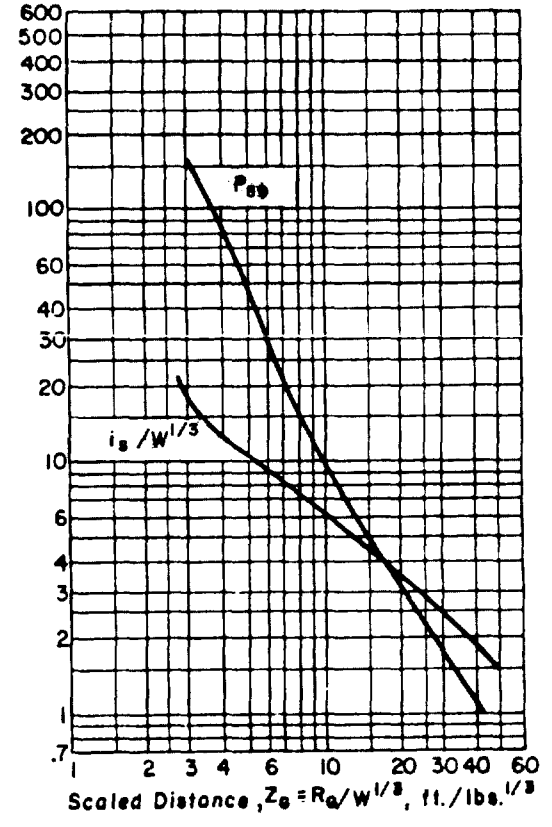
Figure 2-25 Peak positive incident pressure and scaled impulse for an explosion on the surface at sea level



a. Nitrocellulose Cylindrical

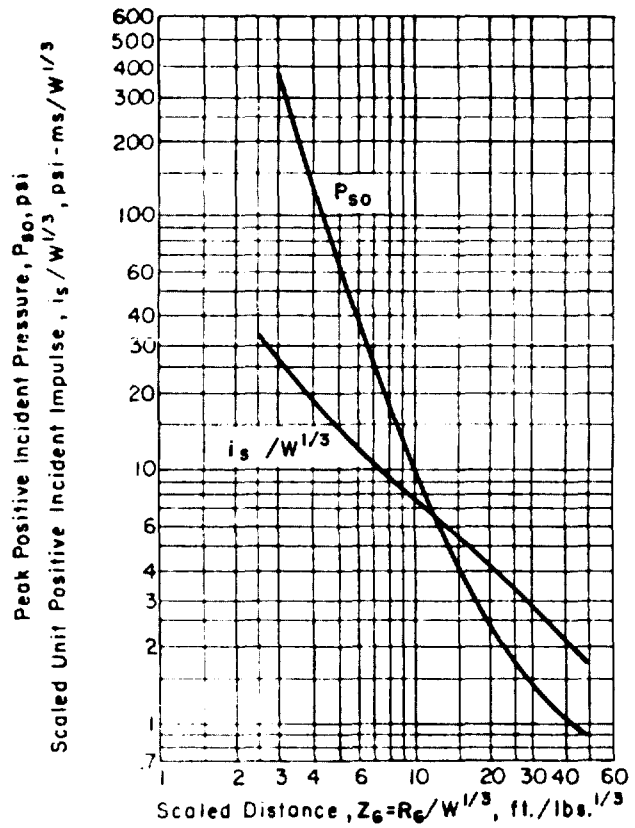


b. Nitrocellulose Dry bed

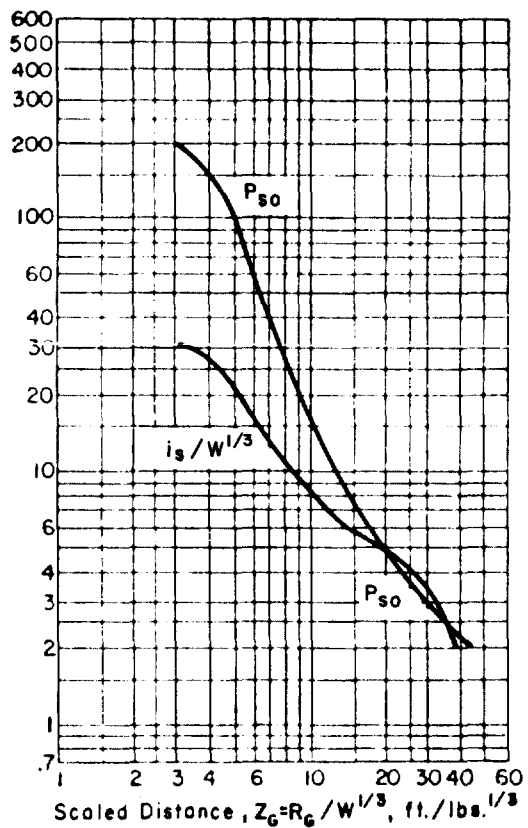


c. Nitrocellulose Orthorhombic

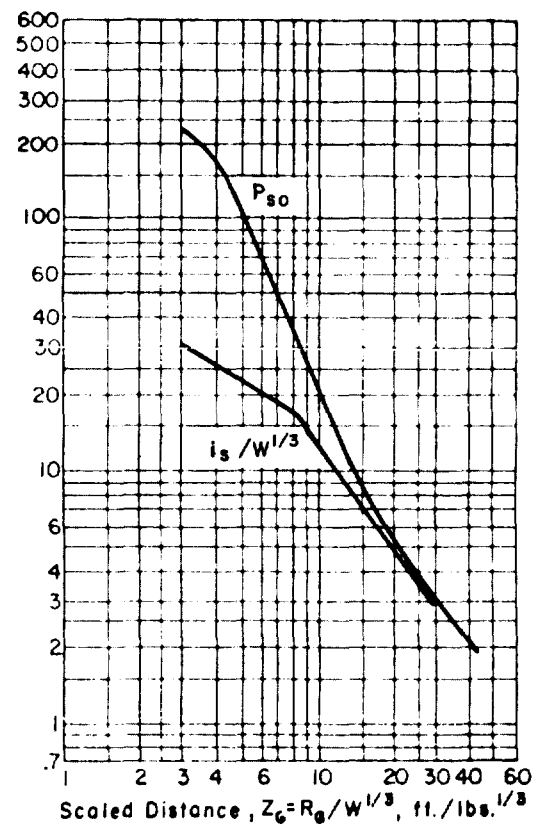
Figure 2-26 Peak positive incident pressure and scaled impulse for an explosion on the surface at sea level



a. Nitroglycerine
Cylindrical

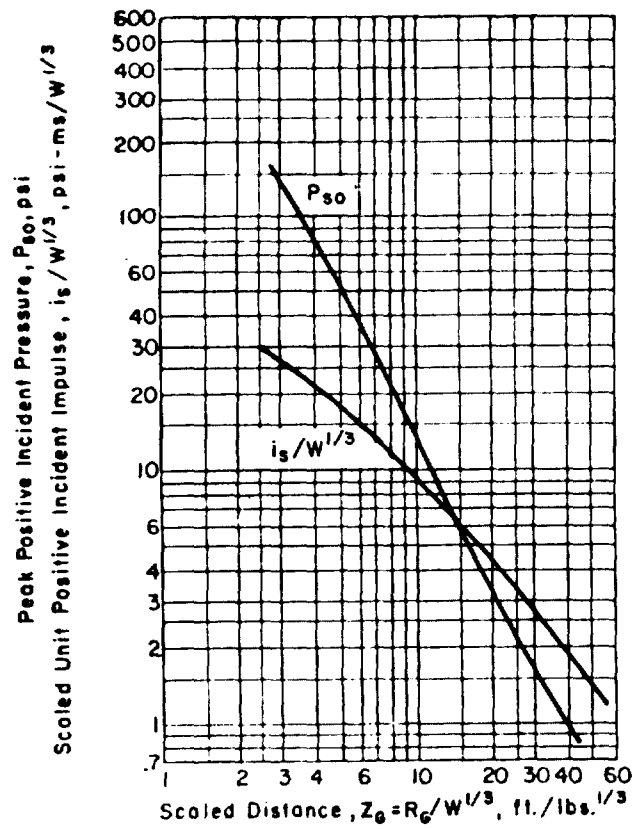


b. PBXC-203
Cylindrical

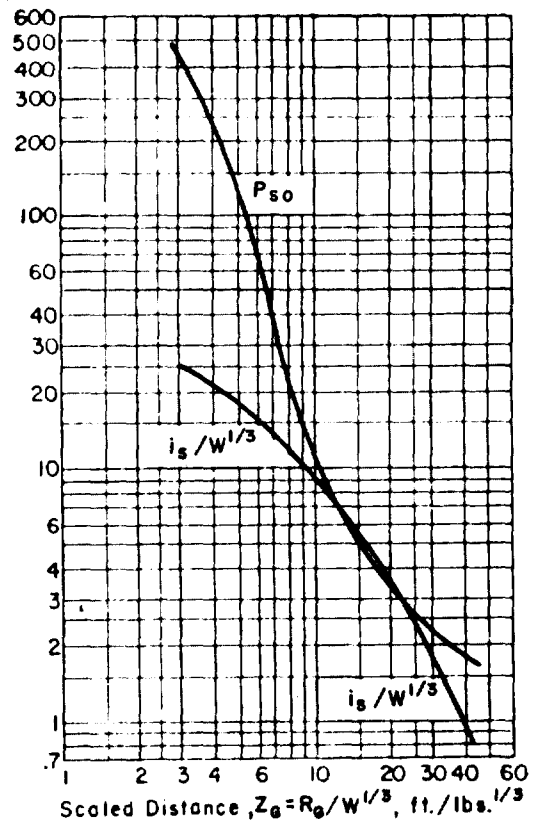


c. PBXC-203
Extruded rod

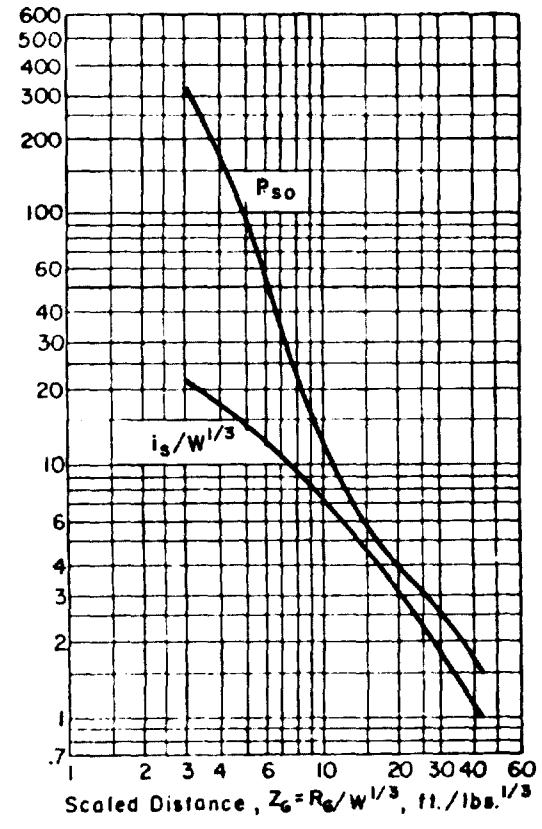
Figure 2-27 Peak positive incident pressure and scaled impulse for an explosion on the surface at sea level



a. RDX Slurry
Cylindrical

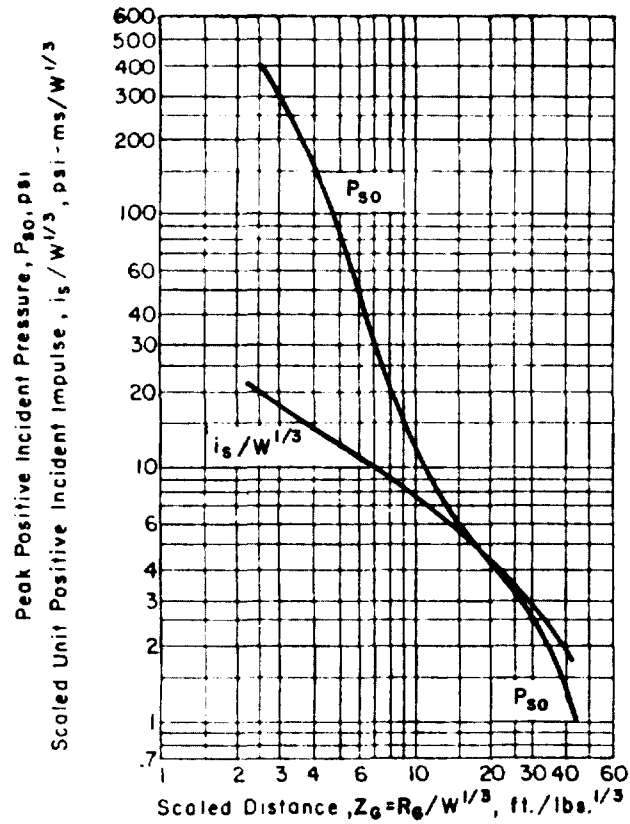


b. RDX 98/2
Orthorhombic

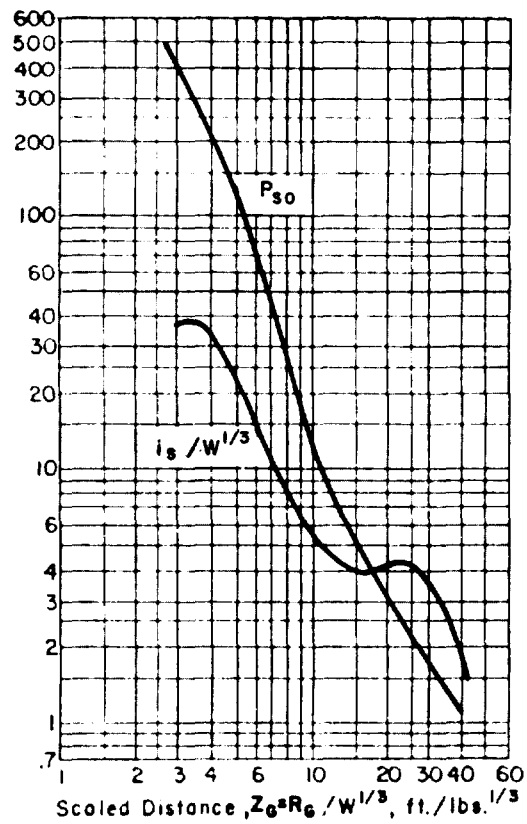


c. RDX 98/2
Cylindrical

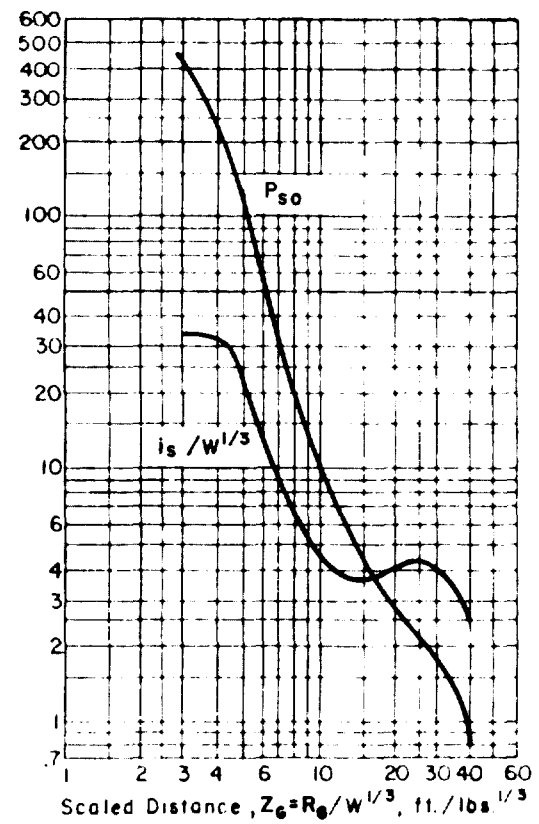
Figure 2-28 Peak positive incident pressure and scaled impulse for an explosion on the surface at sea level



a. TNT
Cylindrical

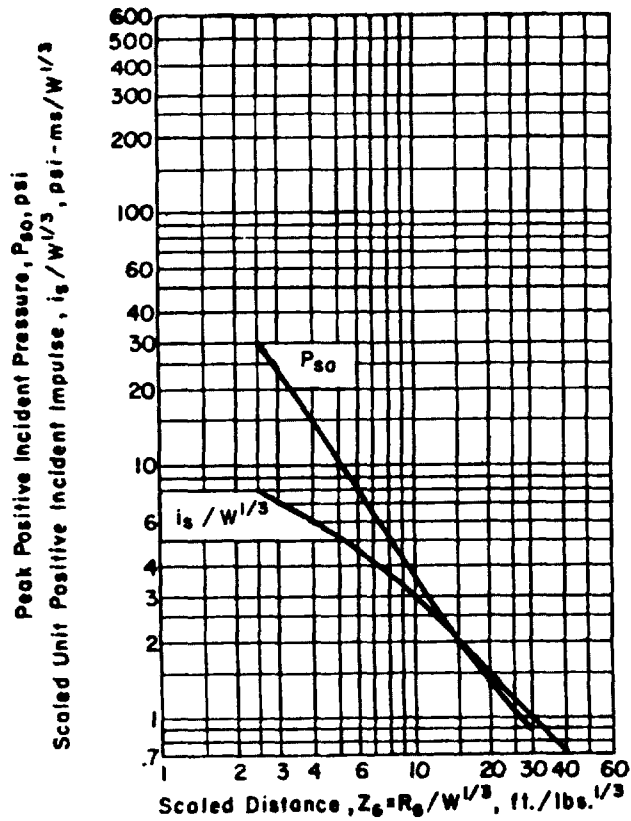


b. TNT
Orthorhombic

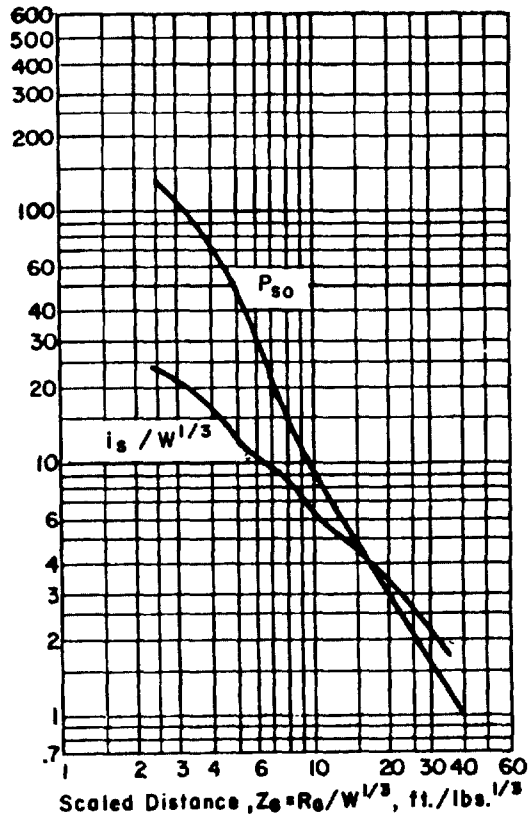


c. TNT
Hopper

Figure 2-29 Peak positive incident pressure and scaled impulse for an explosion on the surface at sea level



a. Tetracene



b. Nitroguanidine
Cylindrical

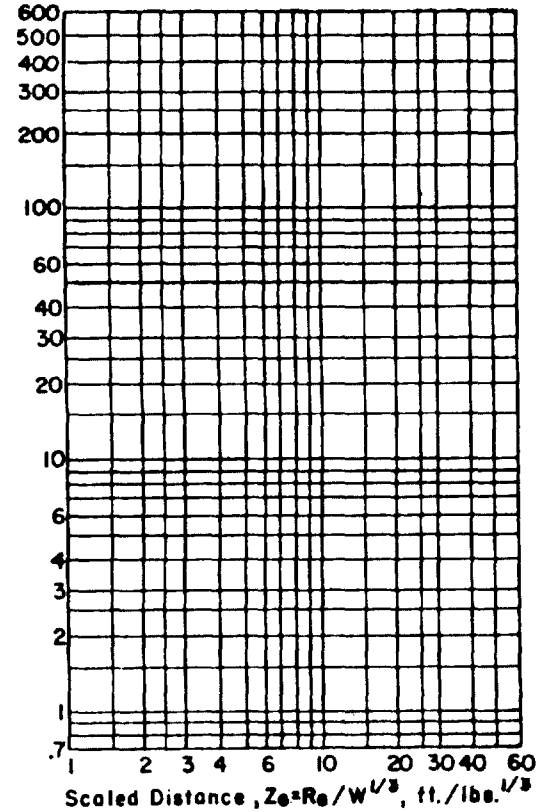
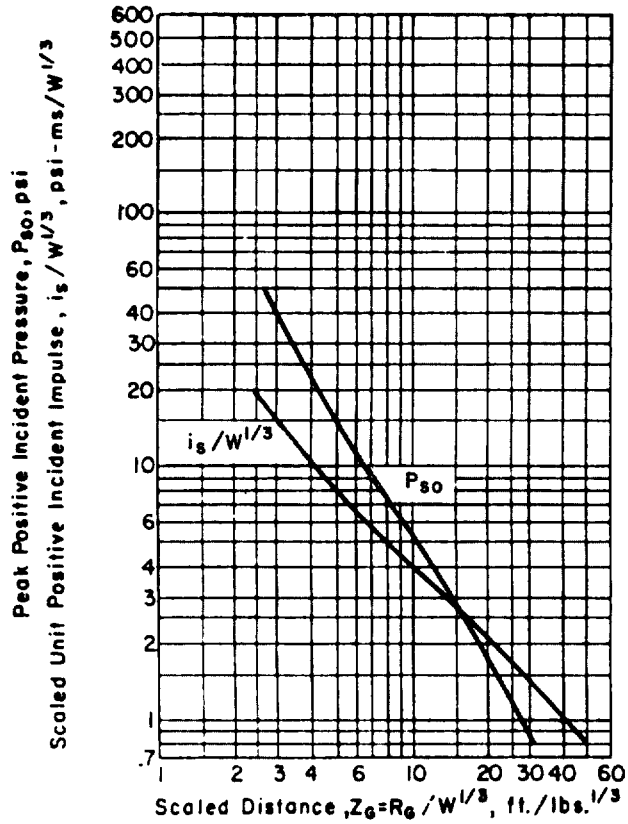
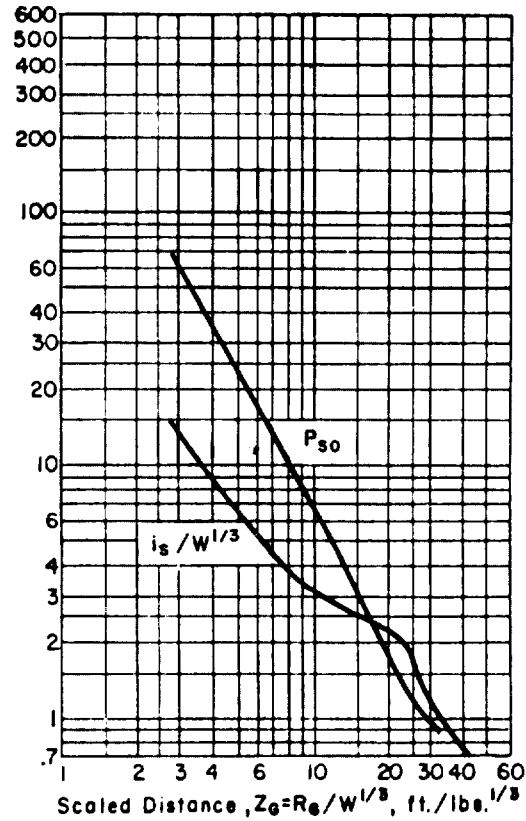


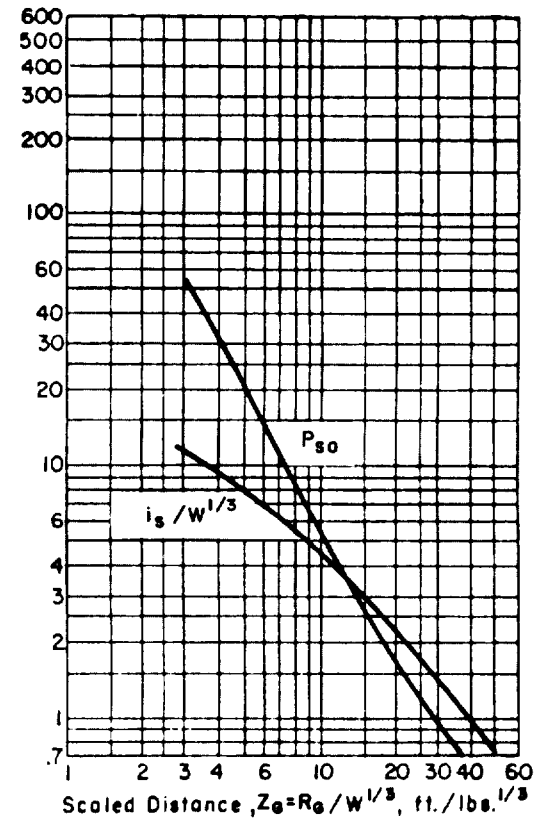
Figure 2-30 Peak positive incident pressure and scaled impulse for an explosion on the surface at sea level



a. Benite Propellant Orthorhombic

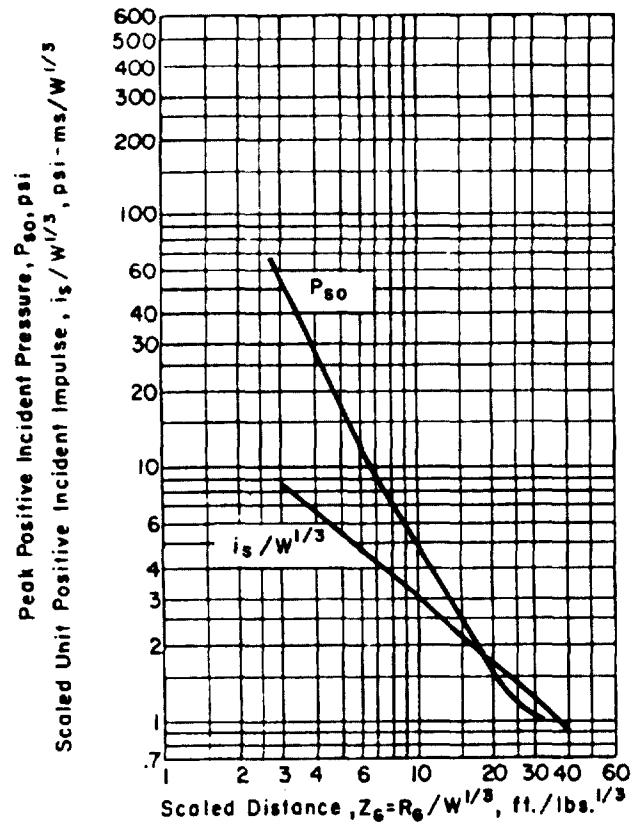


b. Benite Propellant Orthorhombic

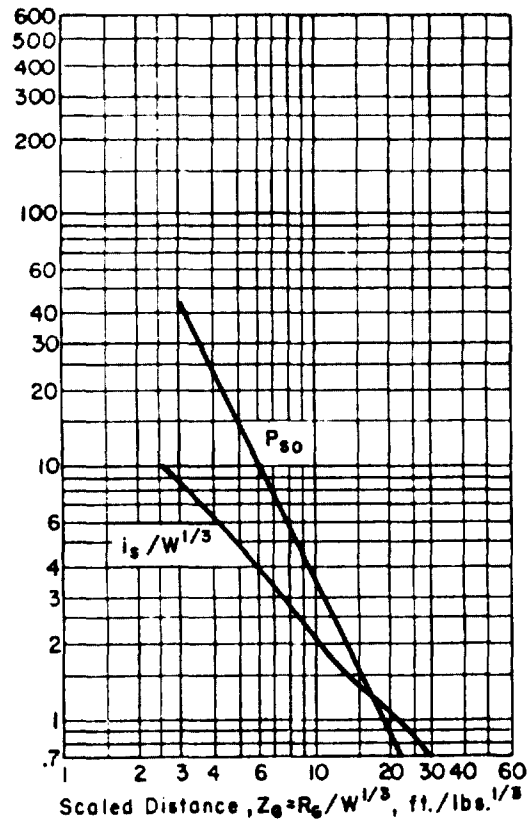


c. Black Powder

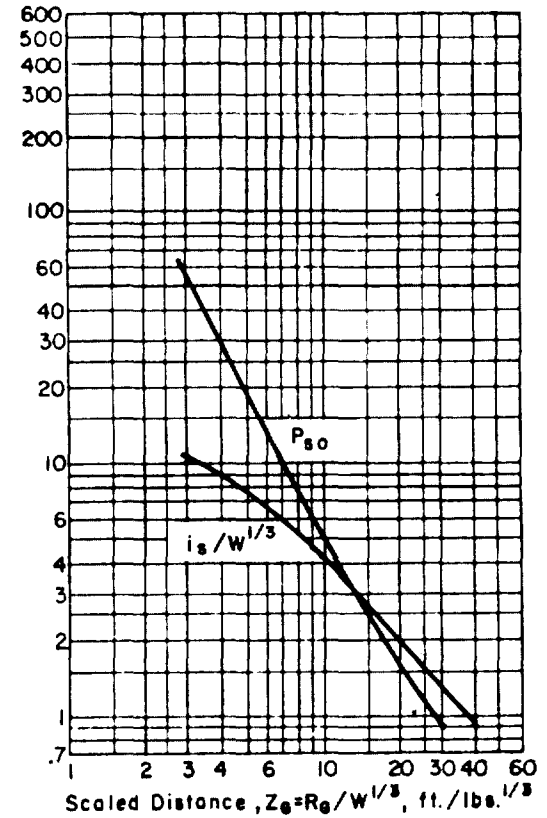
Figure 2-31 Peak positive incident pressure and scaled impulse for an explosion on the surface at sea level



a. BS-NACO Propellant
Cylindrical

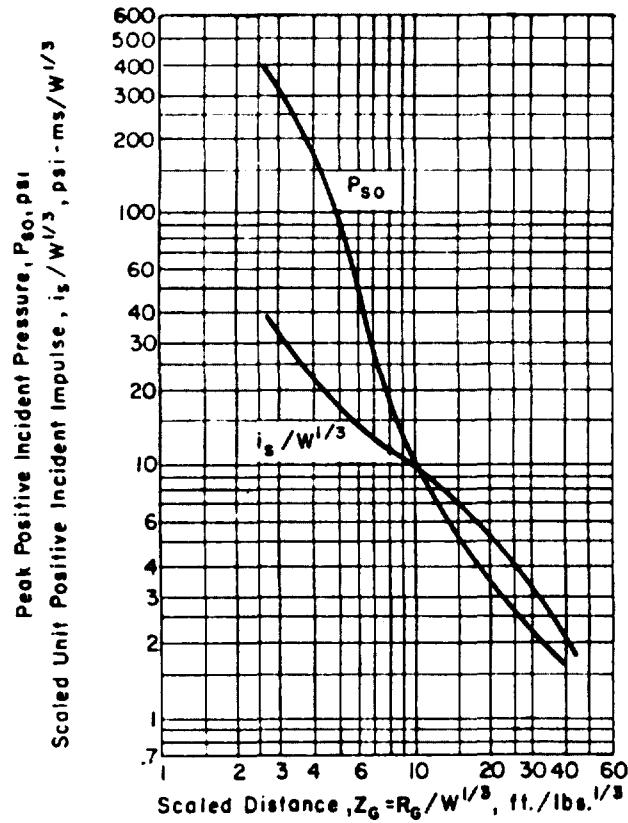


b. BS-NACO Propellant
Orthorhombic

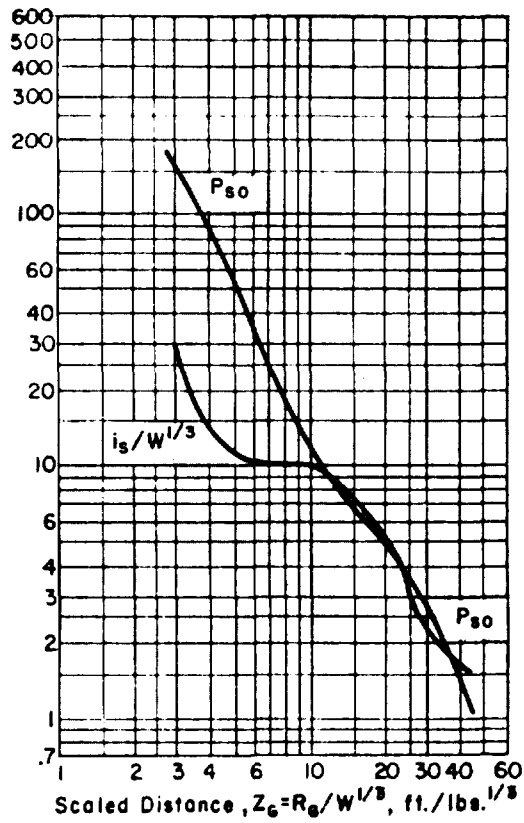


c. BS-NACO Propellant
Hoppers

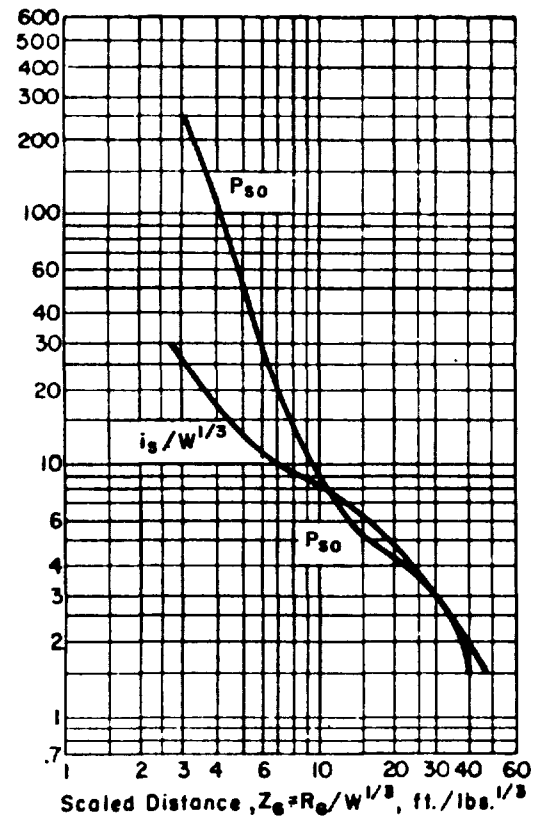
Figure 2-32 Peak positive incident pressure and scaled impulse for an explosion on the surface at sea level



a. DIGL - RP I5420 Propellant Orthorhombic

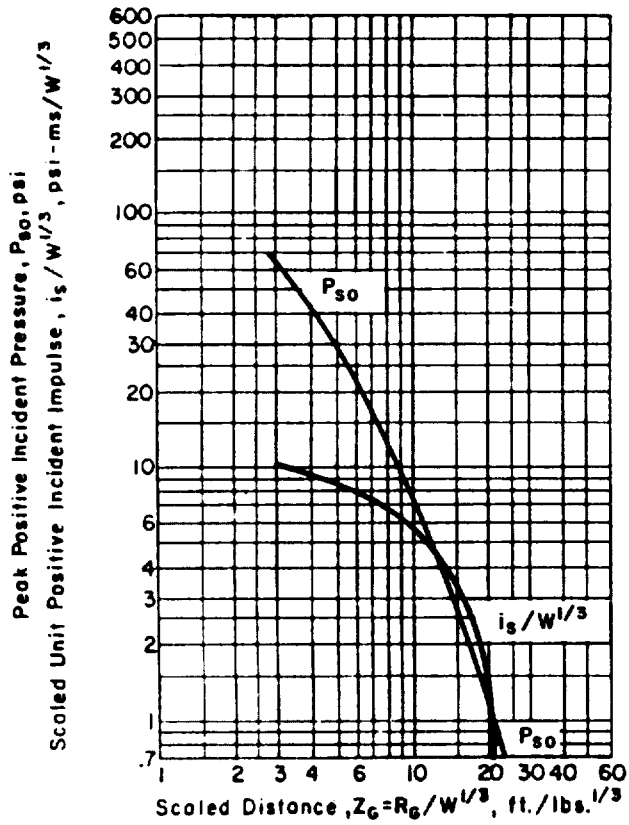


b. DIGL - RP I5421 Propellant Cylindrical

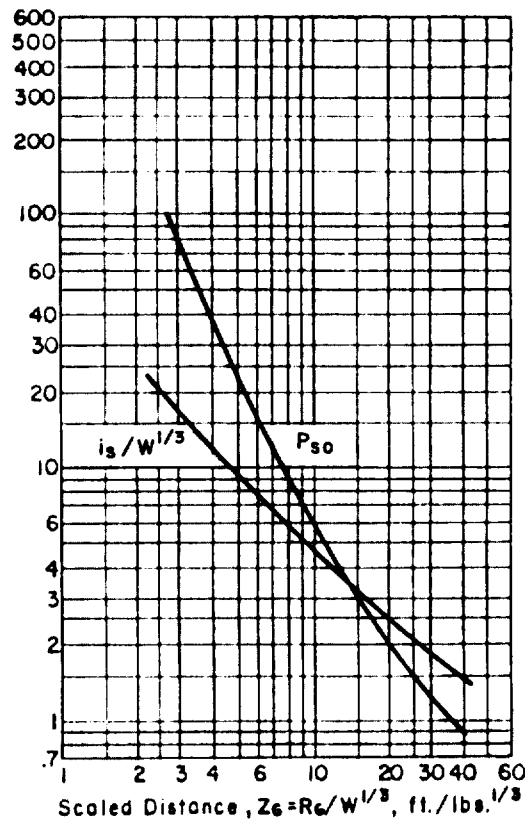


c. DIGL - RP I5422 Propellant Orthorhombic

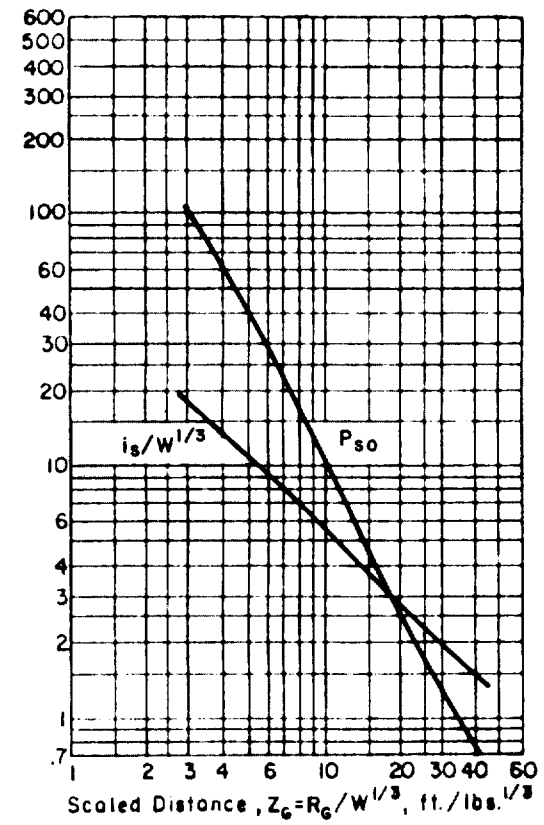
Figure 2-33 Peak positive incident pressure and scaled impulse for an explosion on the surface at sea level



a. MI Propellant
(Single perforated)

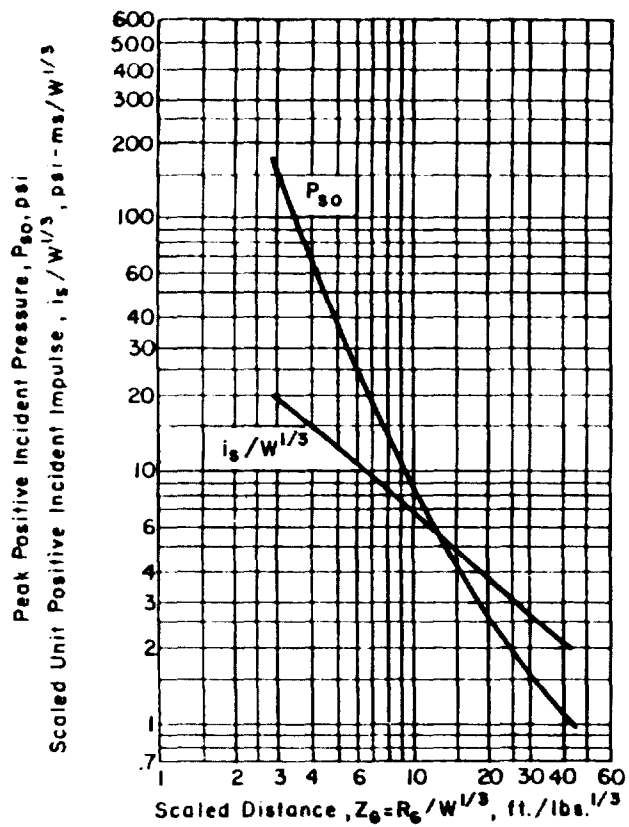


b. MI Propellant
(Multi-perforated)

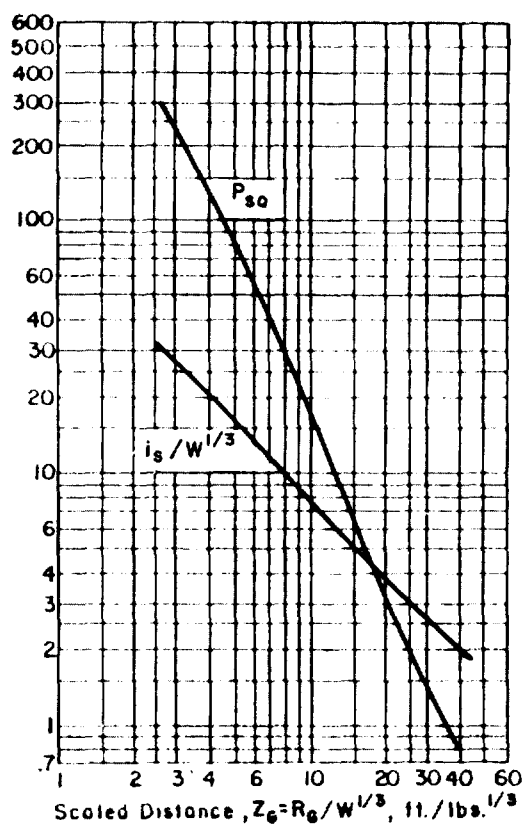


c. M26 EI Propellant
(Multi-perforated)
Blender barrel

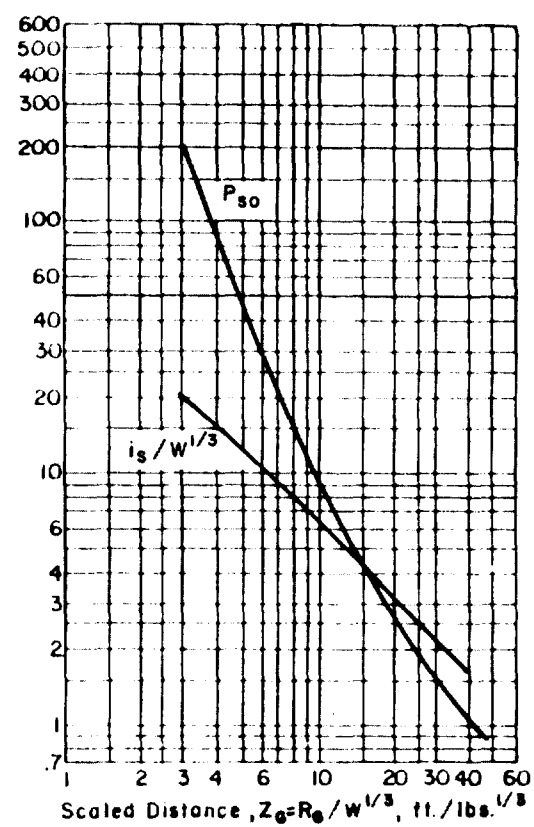
Figure 2-34 Peak positive incident pressure and scaled impulse for an explosion on the surface at sea level



a. M26 E1 Propellant
(Multi-perforated)
Orthorhombic dryer bed



b. M26 E1 Propellant
(Multi-perforated)
Orthorhombic drop buggy



c. M26 E1 Propellant
(Multi-perforated)
Cylindrical

Figure 2-35 Peak positive incident pressure and scaled impulse for an explosion on the surface at sea level

Peak Positive Incident Pressure, P_{s0} , psi
 Scaled Unit Positive Incident Impulse, $i_s/W^{1/3}$, psi-ms/ $W^{1/3}$

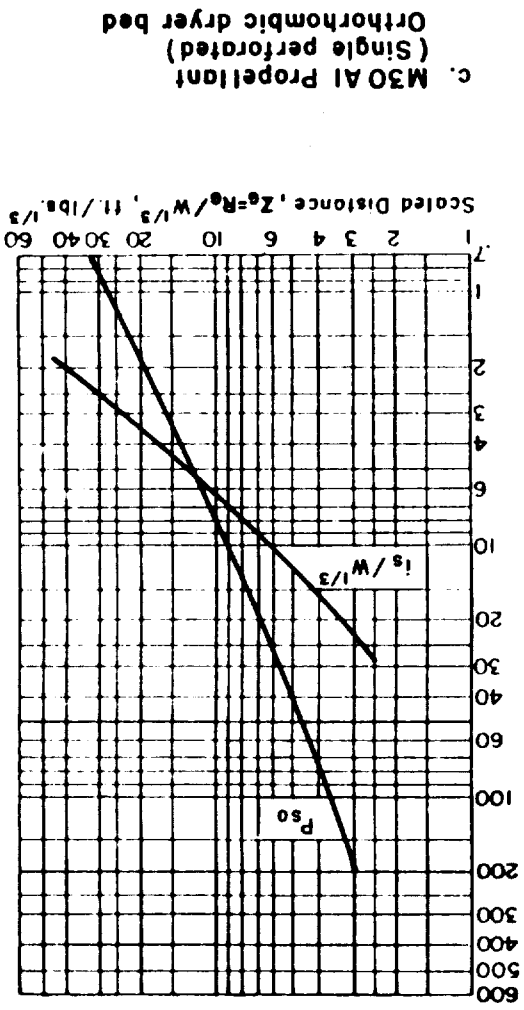
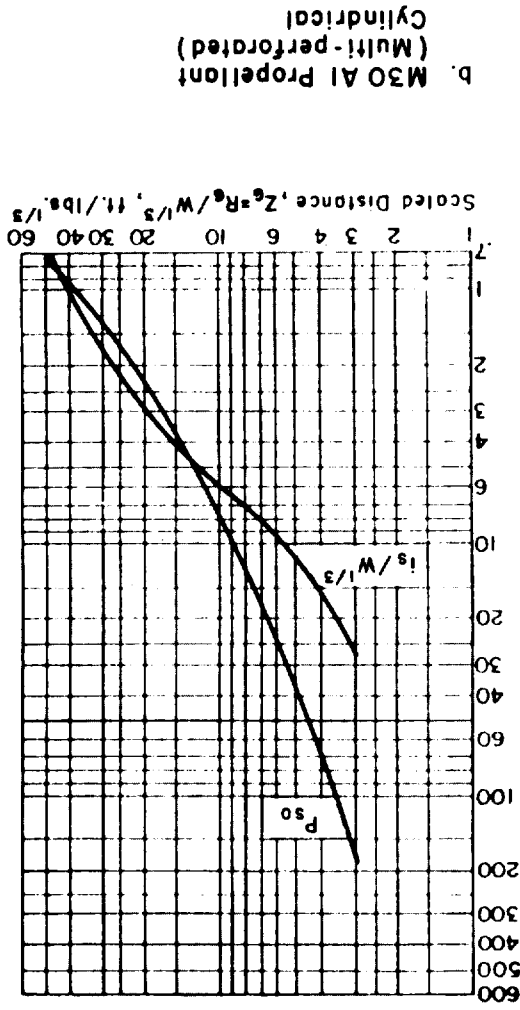
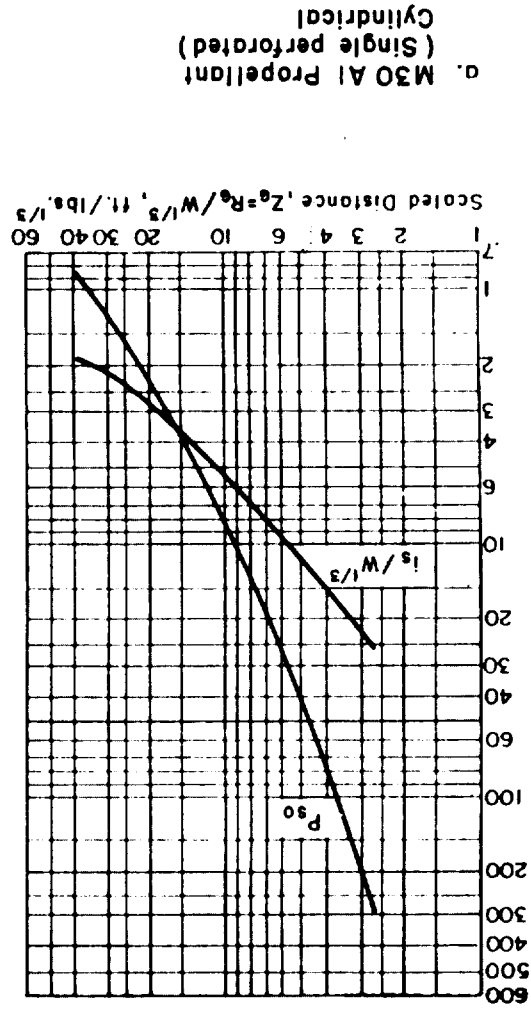
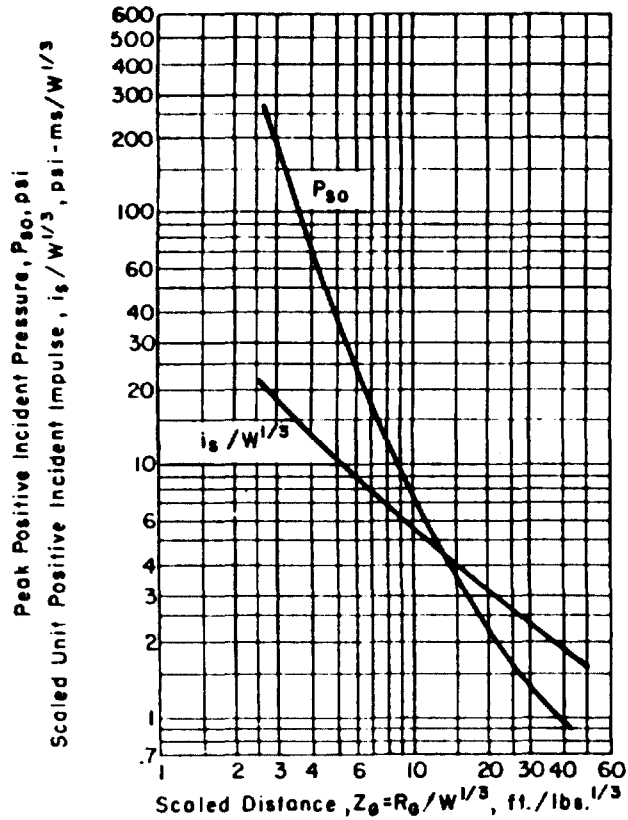
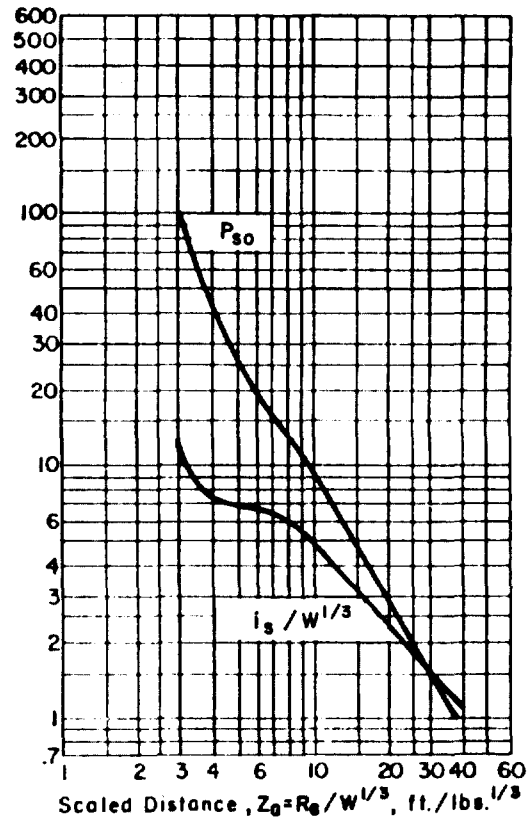


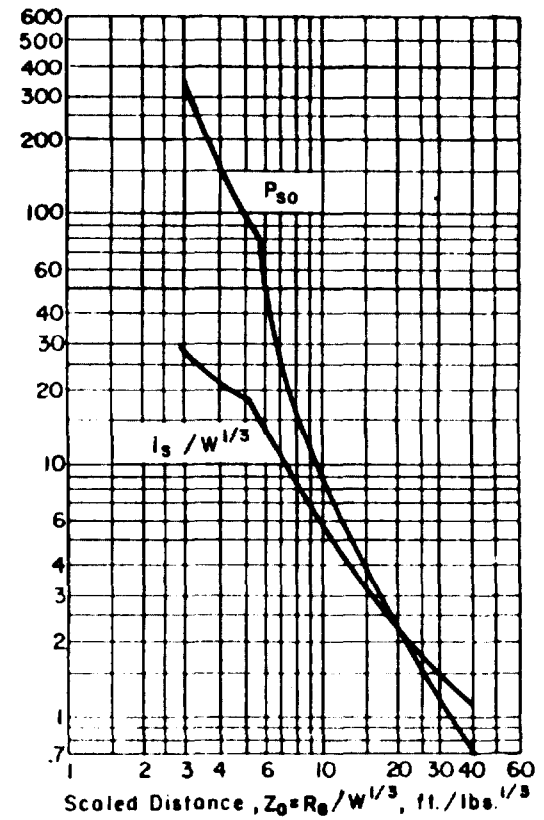
Figure 2-36 Peak positive incident pressure and scaled impulse for an explosion on the surface at sea level



a. M30 Al Propellant
(Multi-perforated)
Orthorhombic dryer-bed

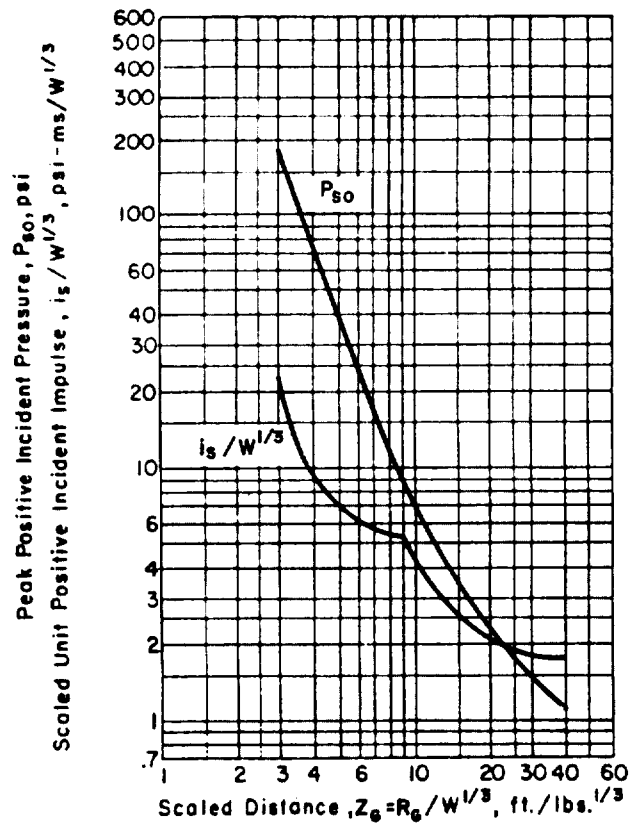


b. M3I Al EI Slotted Stick Propellant
Orthorhombic
(Short Side)

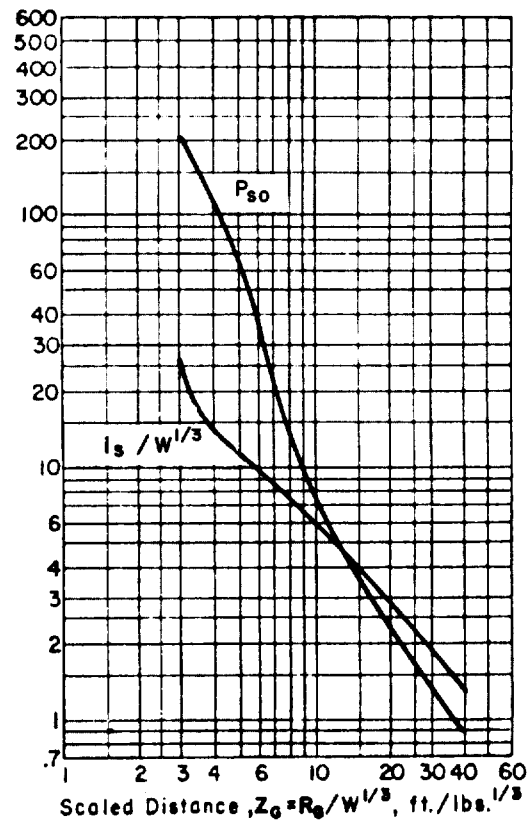


c. M3I Al EI Slotted Stick Propellant
Orthorhombic
(Long Side)

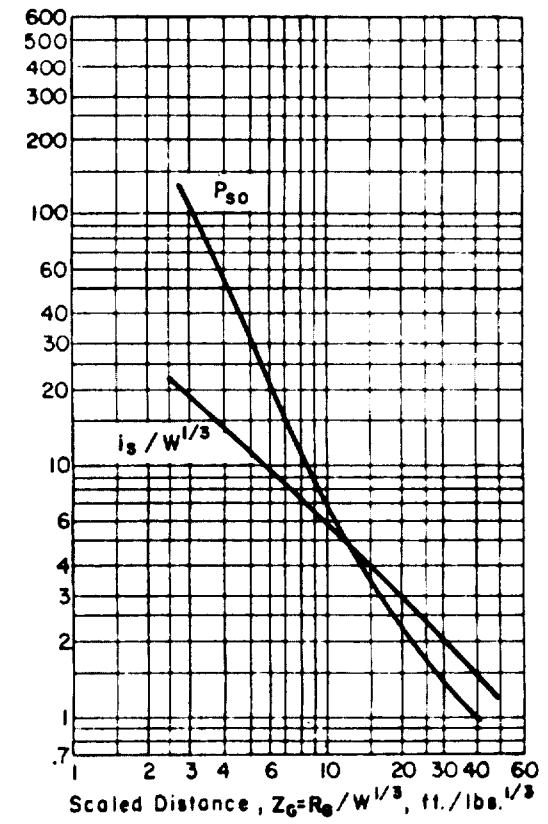
Figure 2-37 Peak positive incident pressure and scaled impulse for an explosion on the surface at sea level



a. M3IAIEI Slotted Stick Propellant
Orthorhombic
(Short Side)

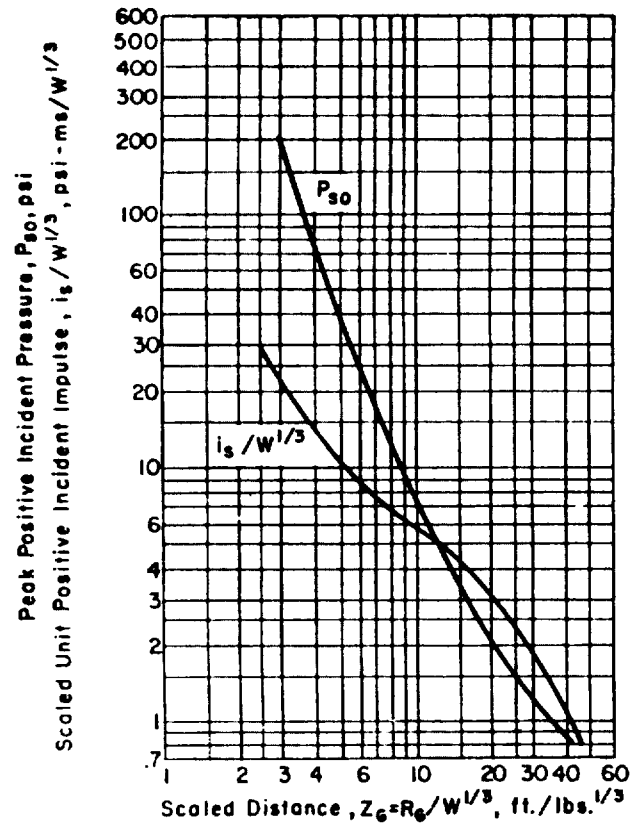


b. M3IAIEI Slotted Stick Propellant
Orthorhombic
(Long Side)

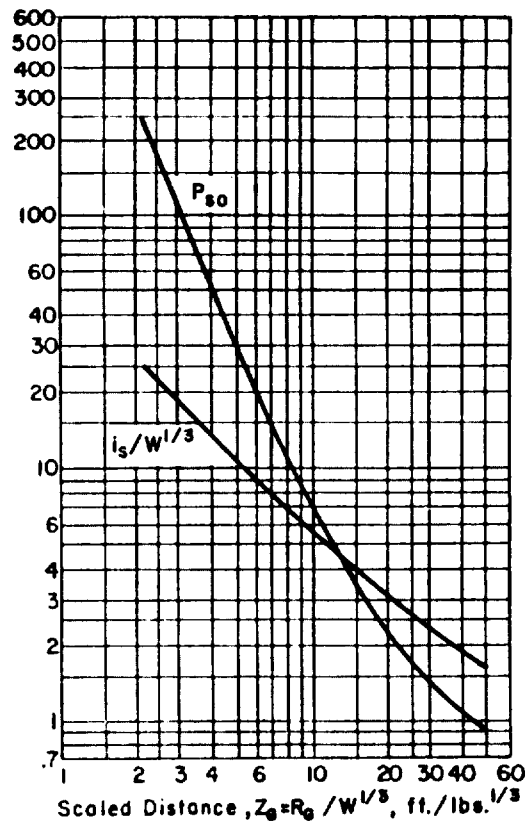


c. N5 Propellant
Shipping containers

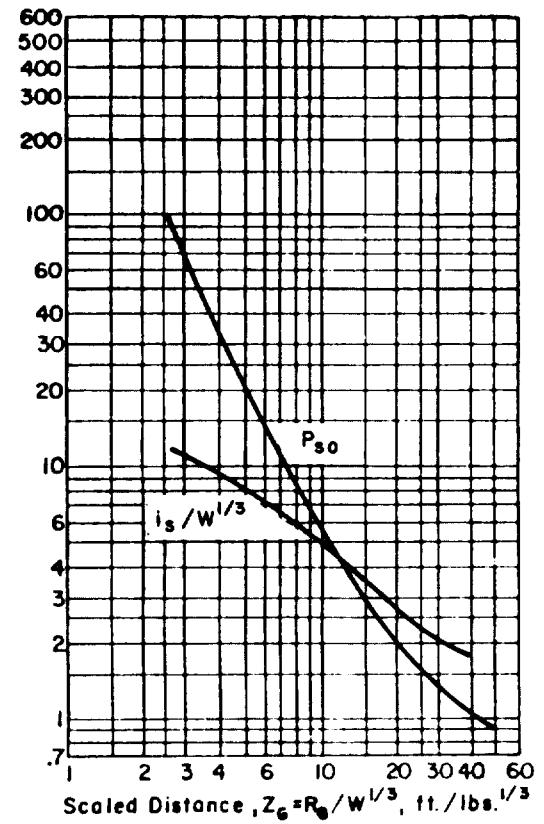
Figure 2-38 Peak positive incident pressure and scaled impulse for an explosion on the surface at sea level



a. N5 Propellant Carpet rolls

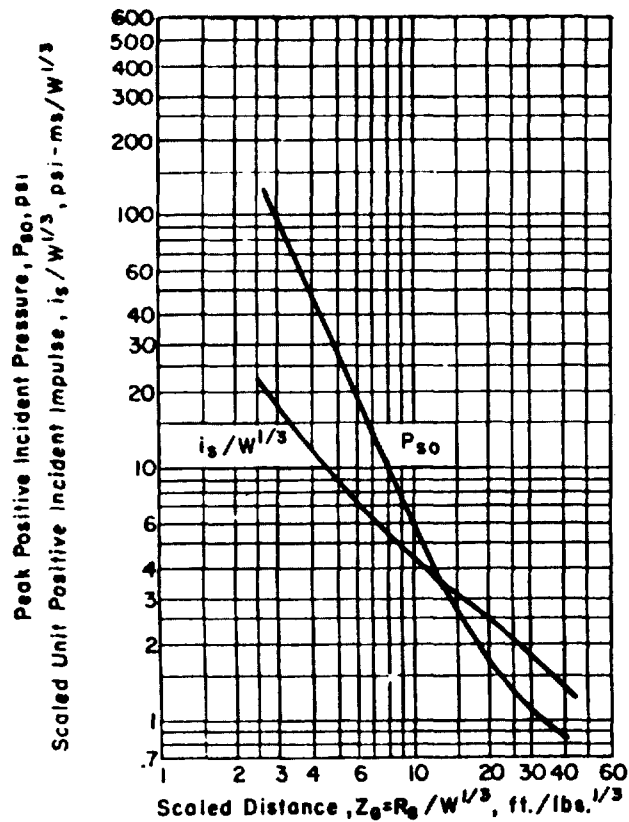


b. N5 Propellant Charge buckets

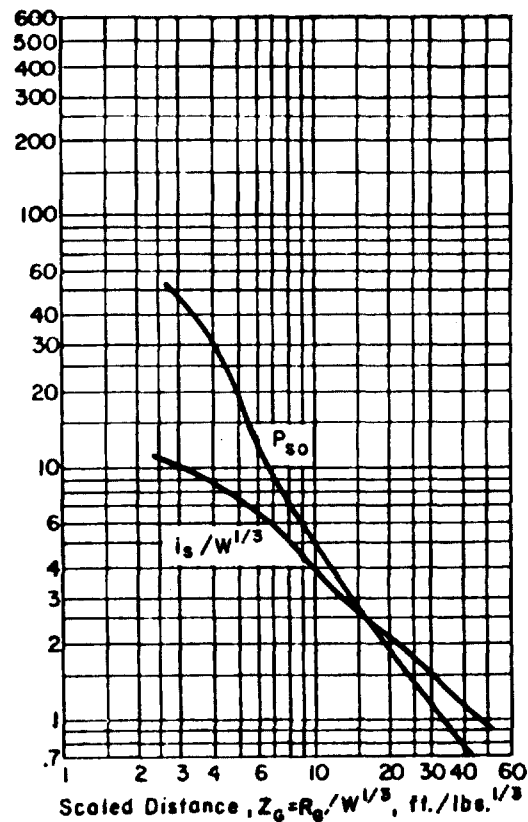


c. N5 Propellant Conveyor belt configuration

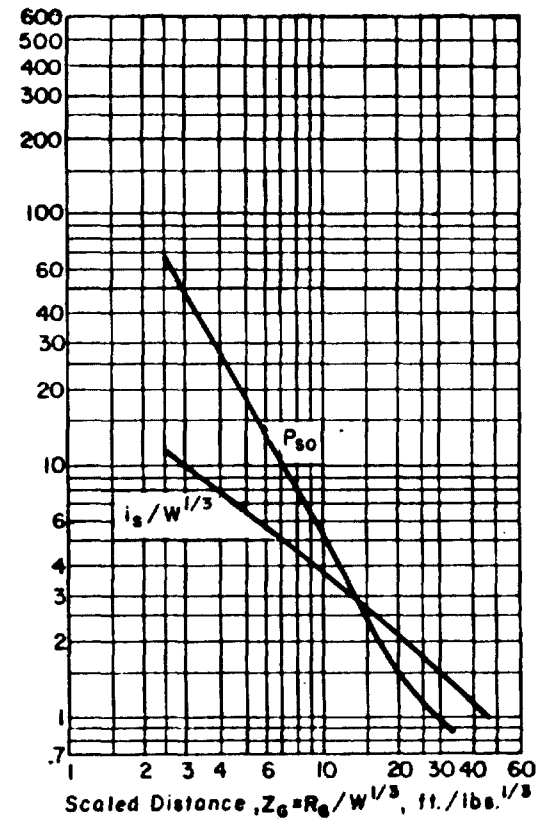
Figure 2-39 Peak positive incident pressure and scaled impulse for an explosion on the surface at sea level



a. M6 Propellant Shipping drums

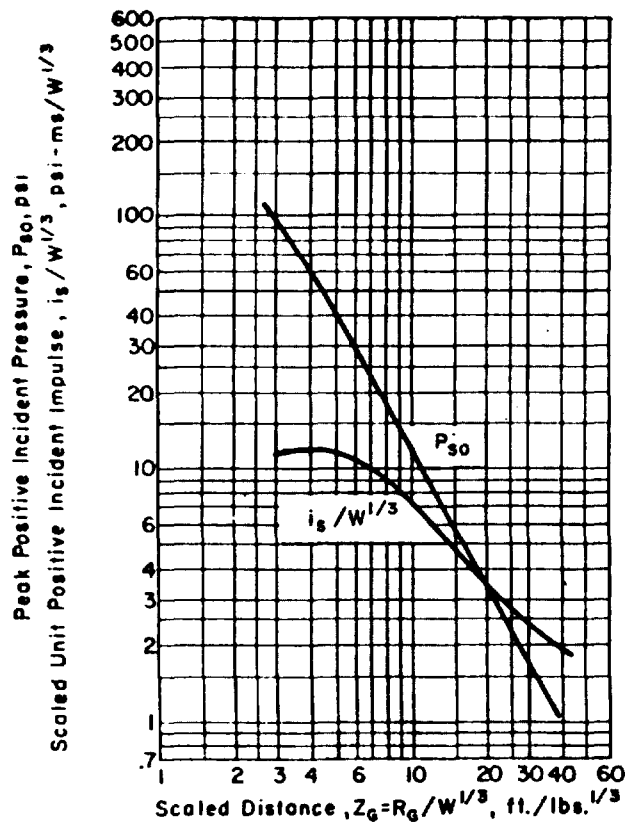


b. M6 Propellant Closed hopper

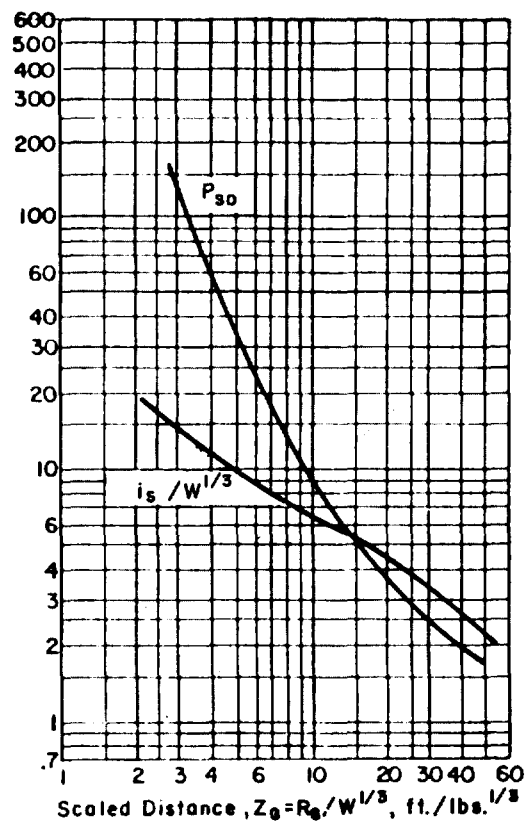


c. M6 Propellant Open hopper

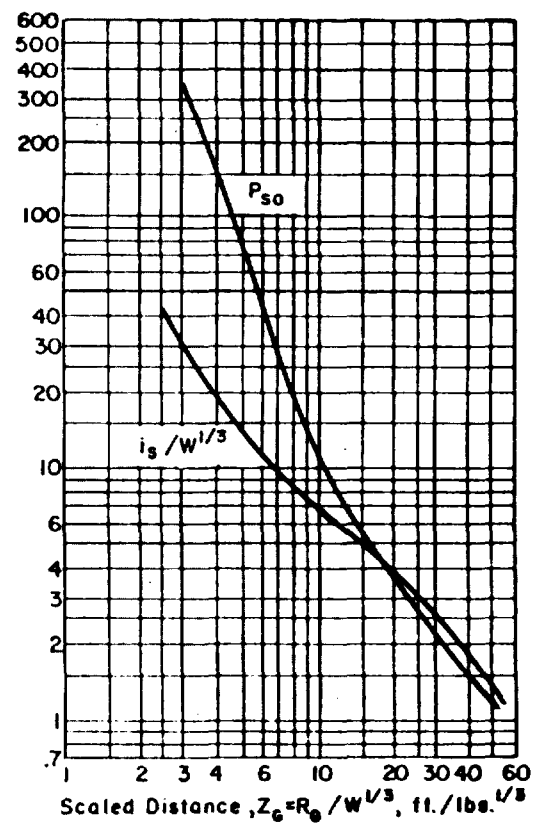
Figure 2-40 Peak positive incident pressure and scaled impulse for an explosion on the surface at sea level



a. 2.75 in. Rocket Grain
MK 43-1

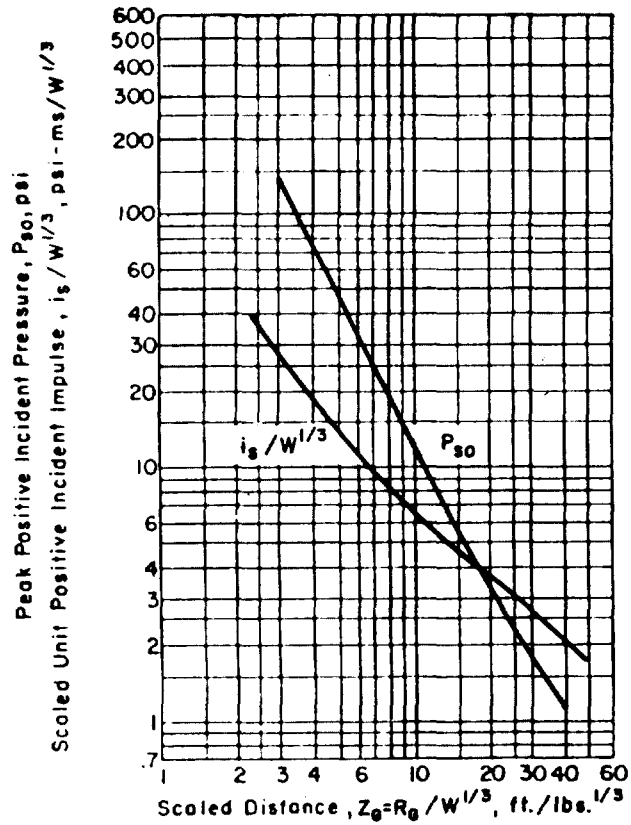


b. WC844 Ball Powder
Orthorhombic

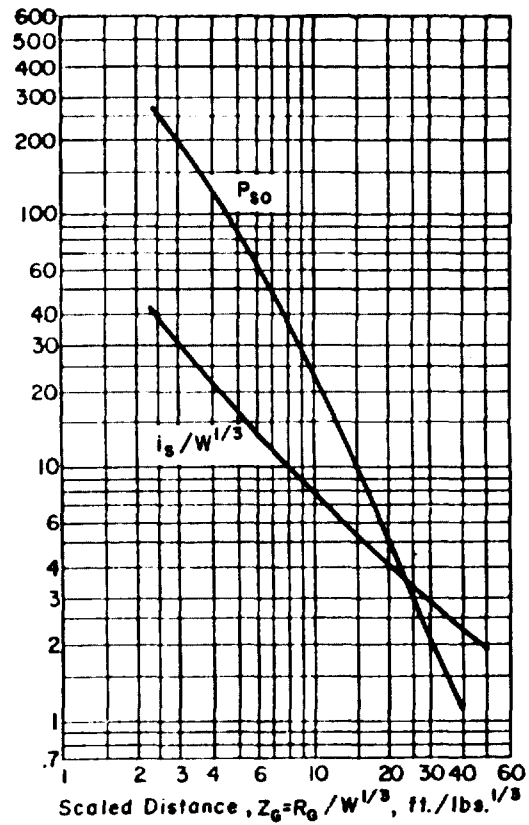


c. WC844 Ball Powder
Cylindrical

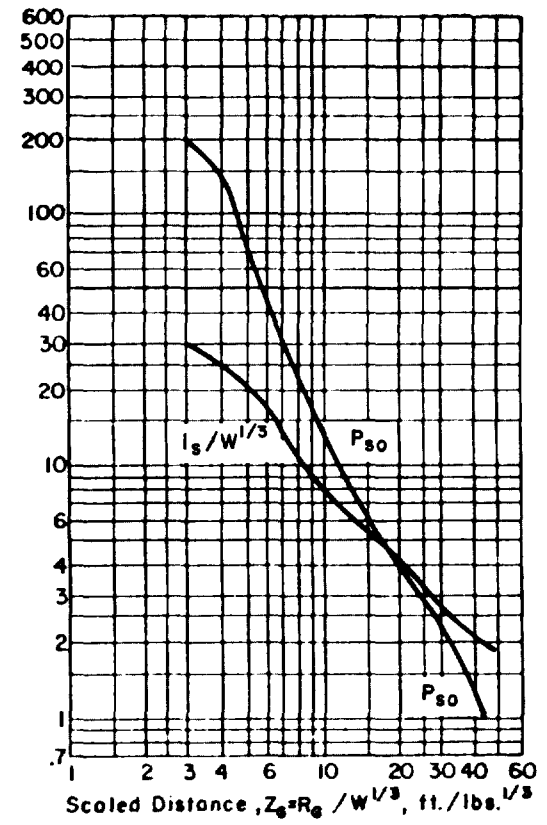
Figure 2-41 Peak positive incident pressure and scaled impulse for an explosion on the surface at sea level



a. XM37 RAP Propellant
(Single forward grain)

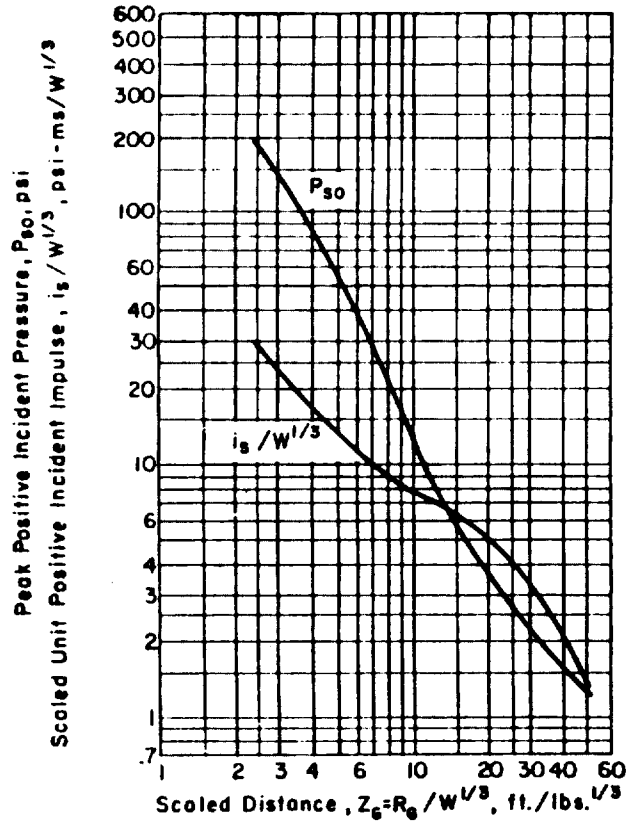


b. XM37 RAP Propellant
(Forward grains)
Extruded billet

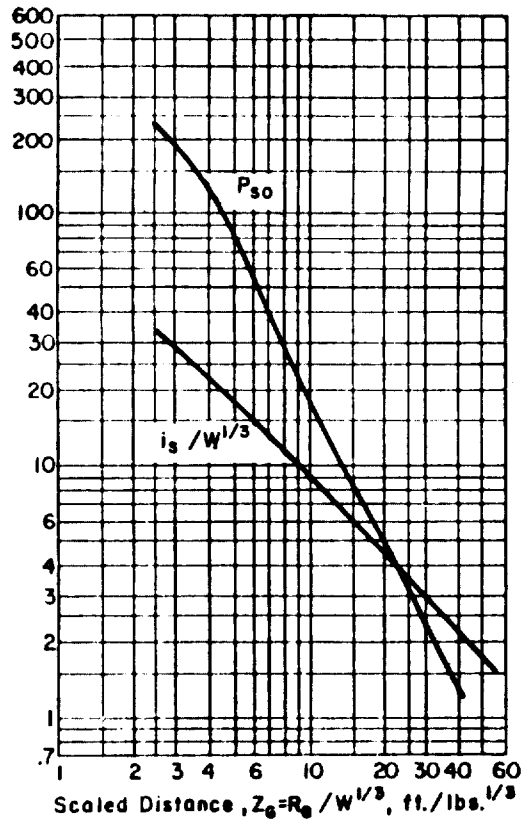


c. XM37 RAP Propellant
(Forward grains)
Ro Con shipping containers

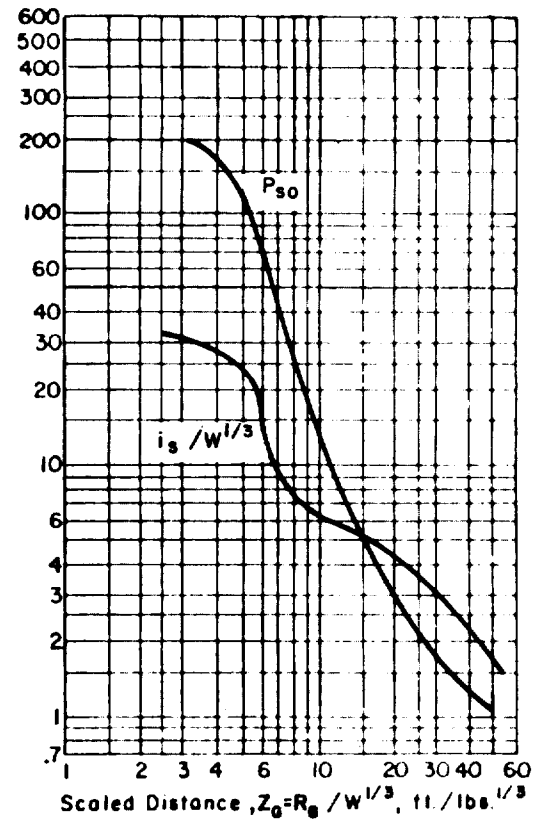
Figure 2-42 Peak positive incident pressure and scaled impulse for an explosion on the surface at sea level



a. XM37 RAP Propellant
(Single aft grain)

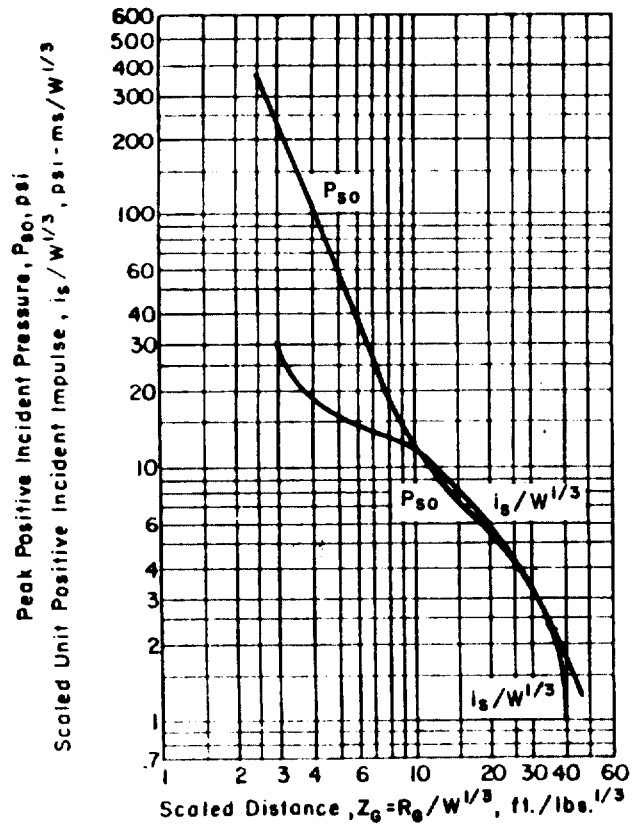


b. XM37 RAP Propellant
(Aft grain)
Extruded billets

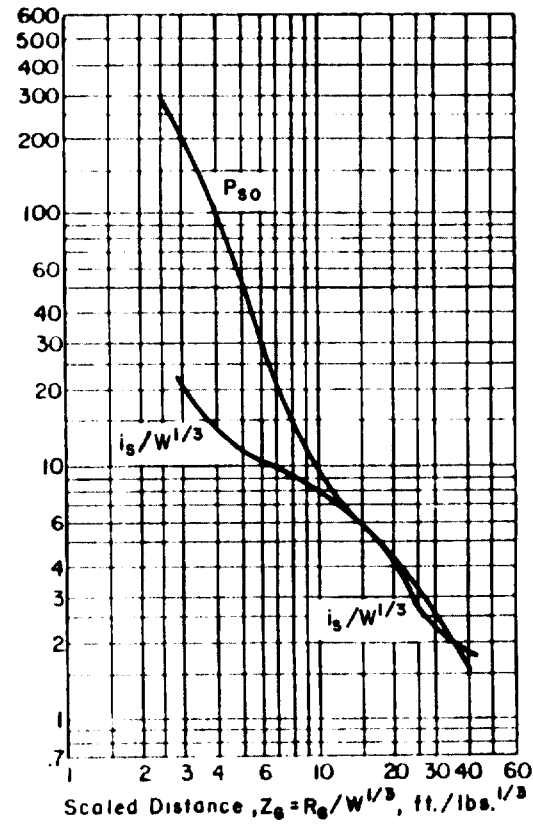


c. XM37 RAP Propellant
(Aft grains)
Ro Con shipping containers

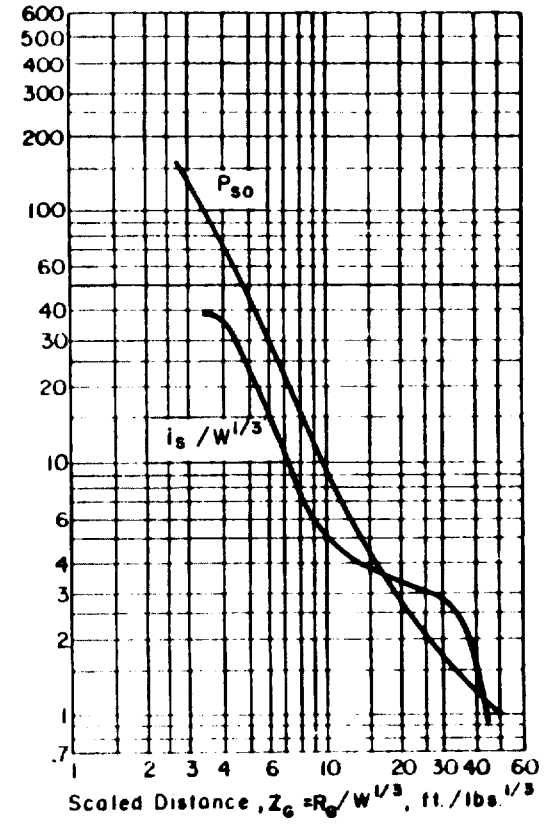
Figure 2-43 Peak positive incident pressure and scaled impulse for an explosion on the surface at sea level



a. JA-2 (L5460) Propellant
Cylindrical

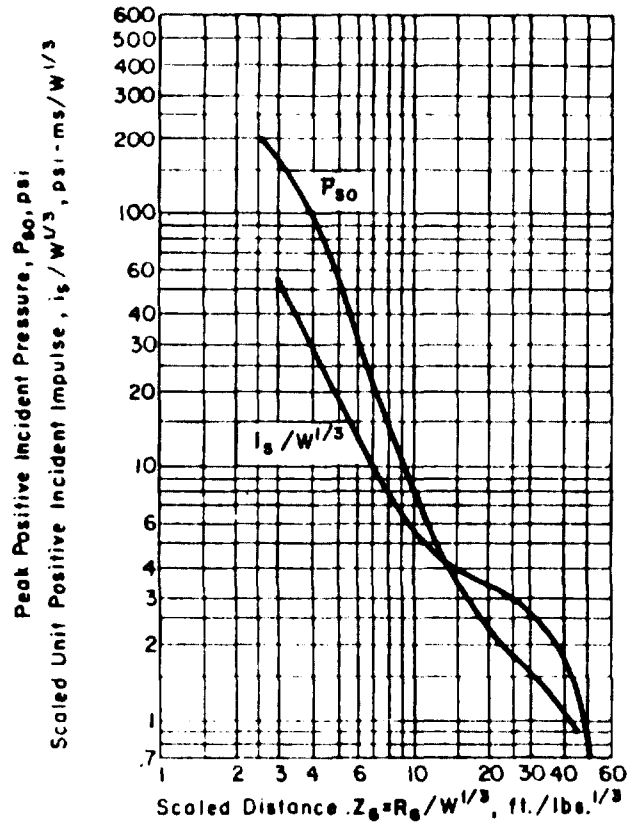


b. JA-2 (L5460) Propellant
Orthorhombic

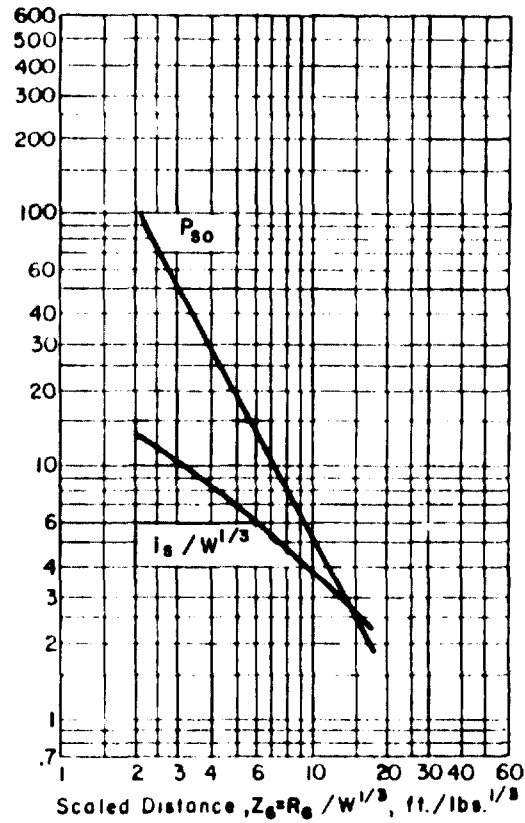


c. MIO Propellant
Orthorhombic
($H/W > 1$)

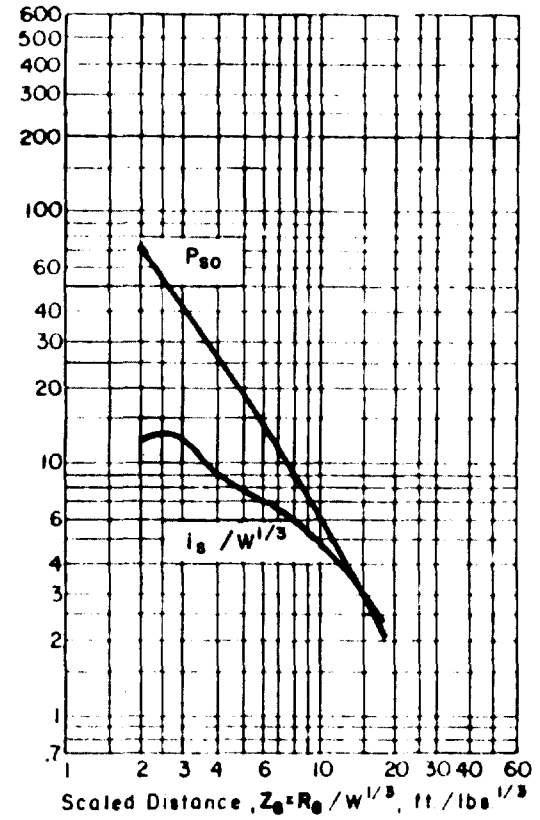
Figure 2-44 Peak positive incident pressure and scaled impulse for an explosion on the surface at sea level



a. MIO Propellant Orthorhombic ($H/W < 1$)

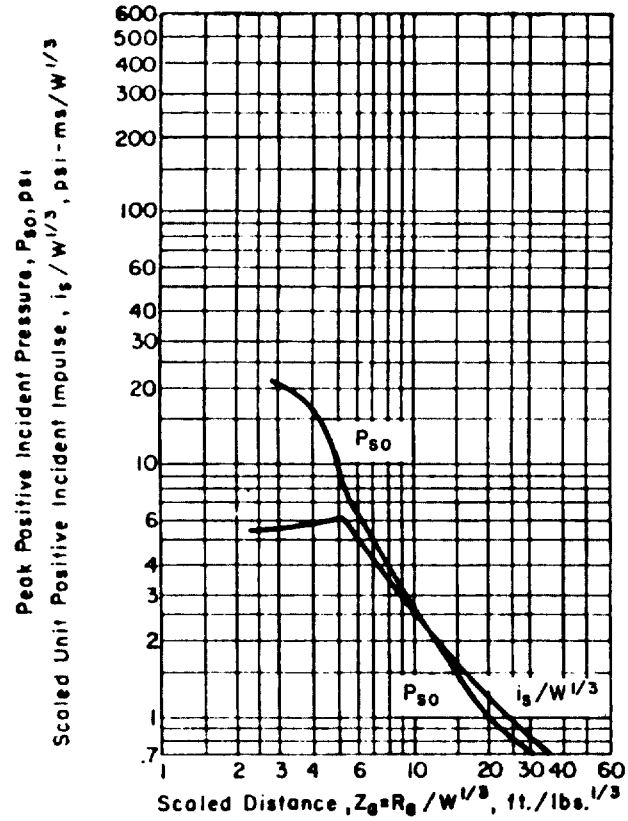


b. 105mm M314-A3 Illuminated Composition (Cylindrical)

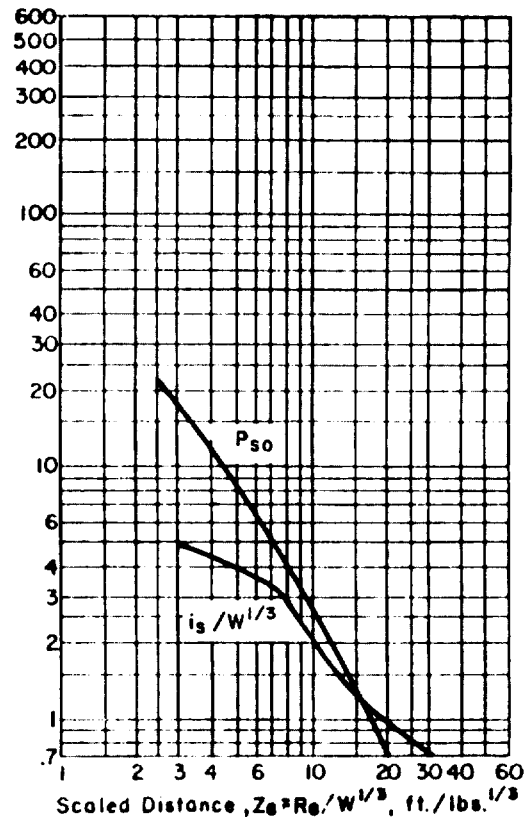


c. 105mm M314-A3 Illuminated Composition (Cylindrical)

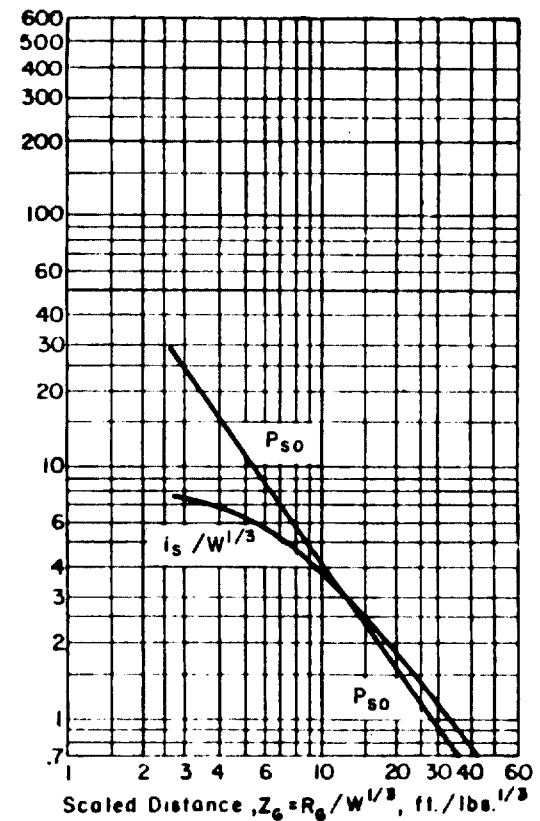
Figure 2-45 Peak positive incident pressure and scaled impulse for an explosion on the surface at sea level



a. I559 Igniter Mixture Cylinder

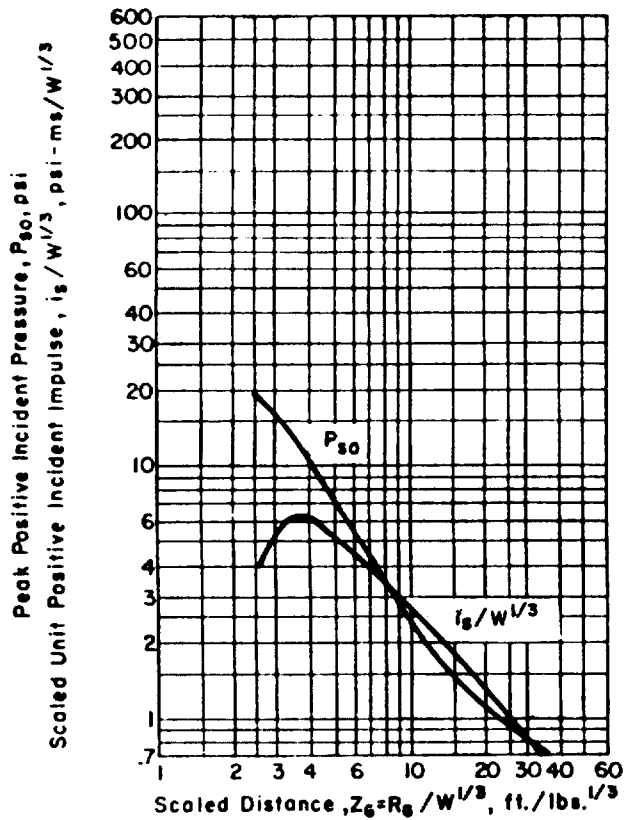


b. I559 Igniter Mixture Cylinder

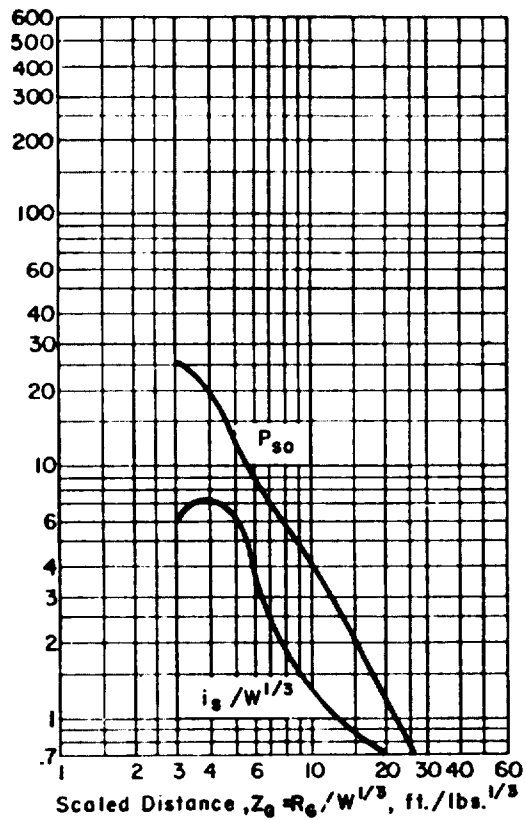


c. I560 Subigniter Mixture Cylinder

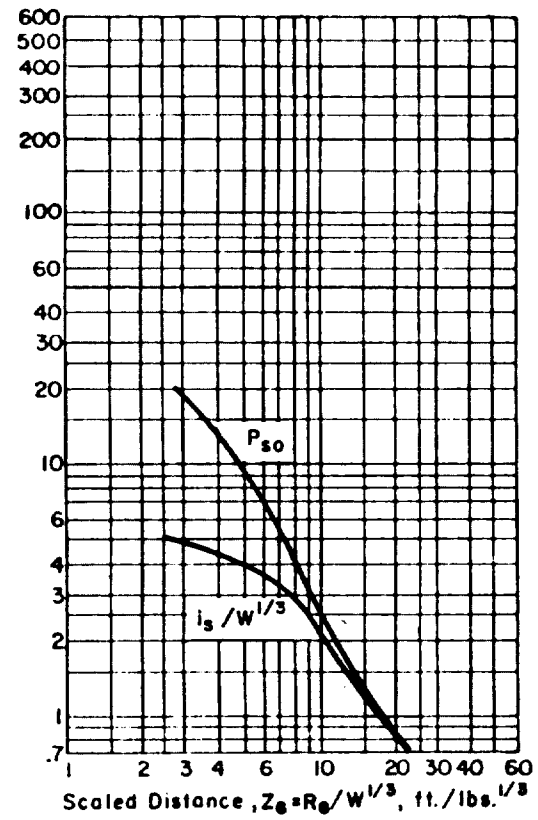
Figure 2-46 Peak positive incident pressure and scaled impulse for an explosion on the surface at sea level



a. I560 Subigniter Mixture Cylinder

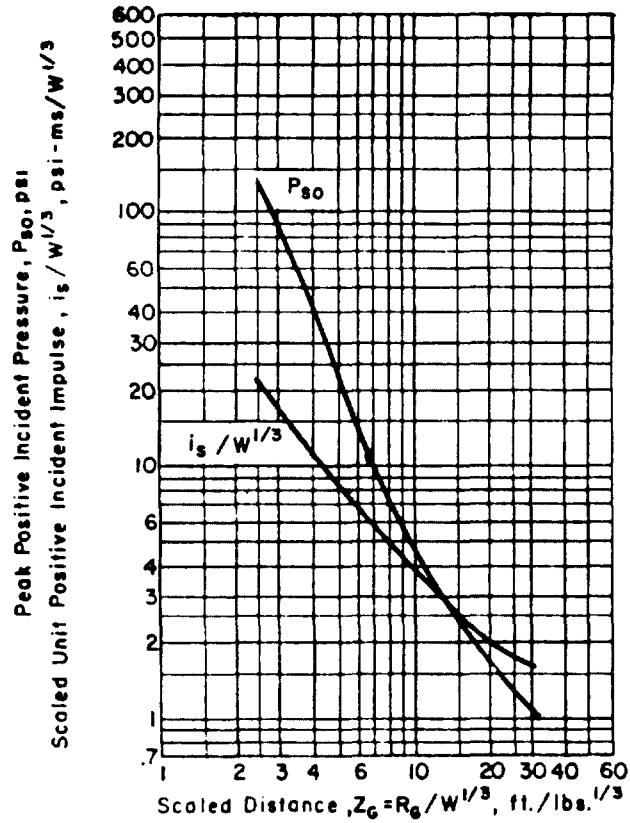


b. R284 Tracer Mixture Cylinder

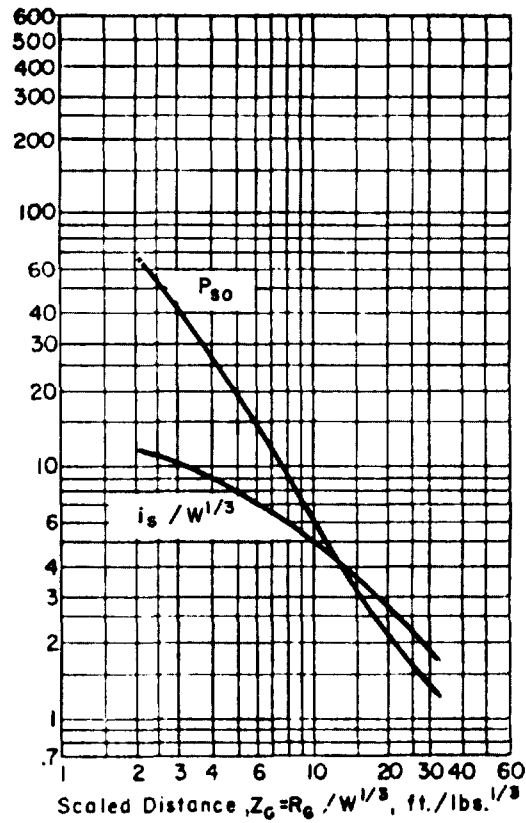


c. R284 Tracer Mixture Cylinder

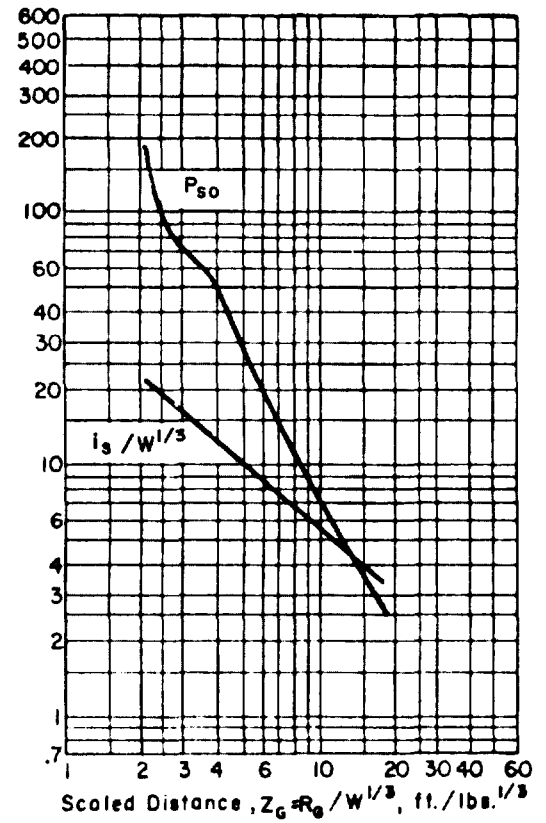
Figure 2-47 Peak positive incident pressure and scaled impulse for an explosion on the surface at sea level



a. M314-A3 First Fire Composition Orthorhombic

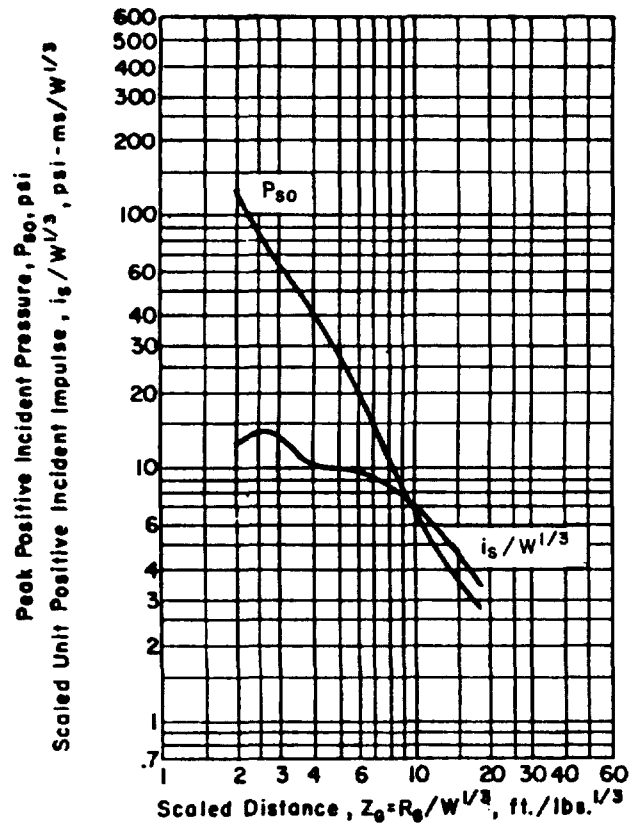


b. M314-A3 First Fire Composition Cylinder

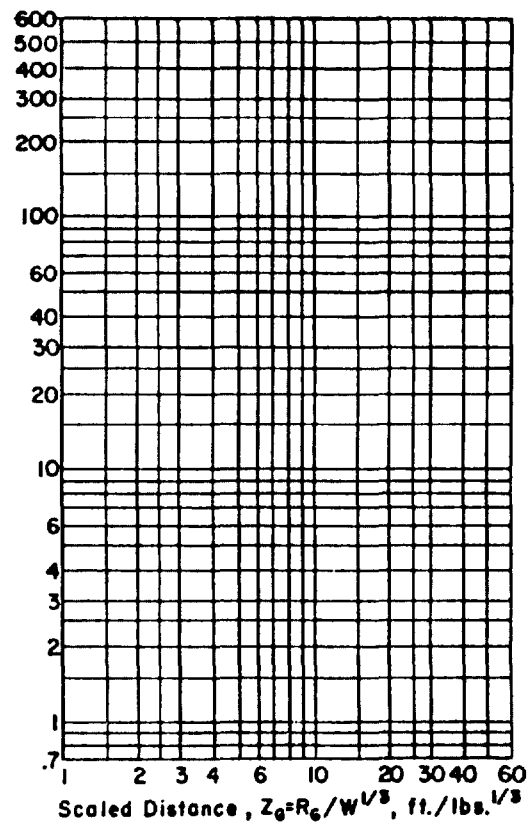


c. M49-A1 Trip Flare Composition Cylinder

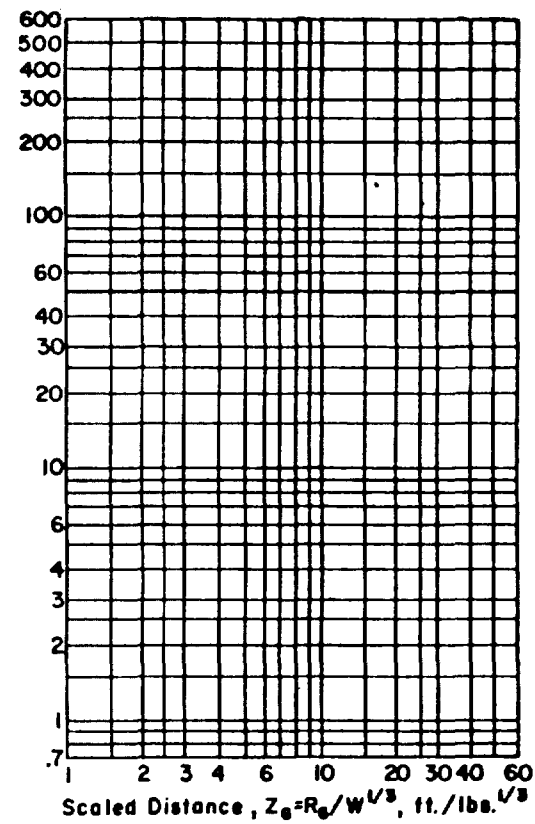
Figure 2-48 Peak positive incident pressure and scaled impulse for an explosion on the surface at sea level



a. M49-AI Trip Flare Composition Cylindrical



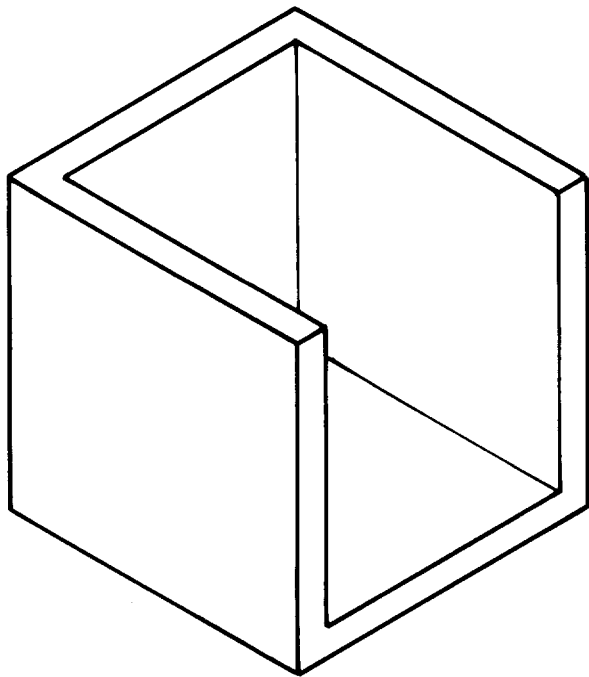
b.



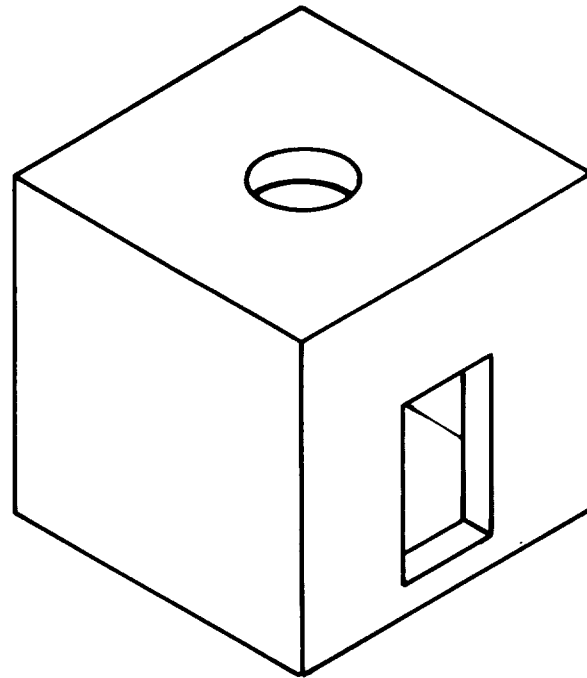
c.

Figure 2-49 Peak positive incident pressure and scaled impulse for an explosion on the surface at sea level

2-92

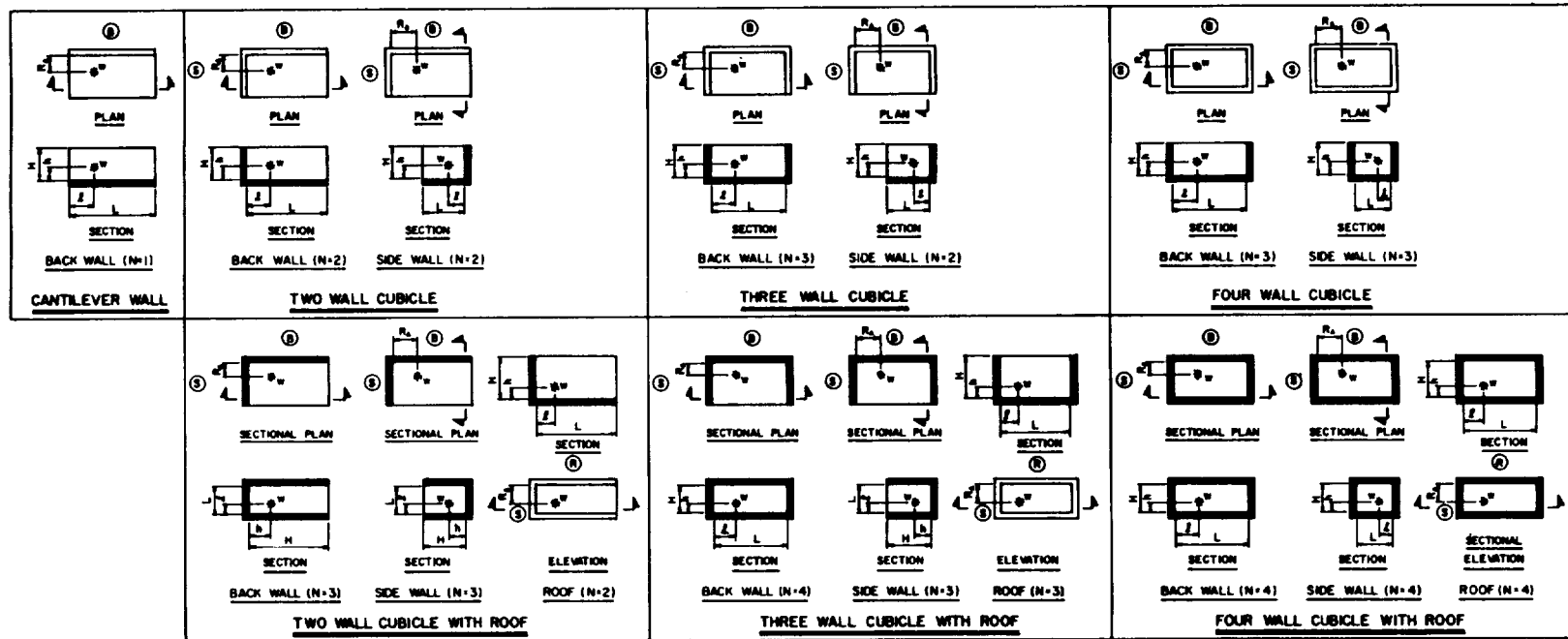


a. Cubicle Structure



b. Enclosed Structure with Openings

Figure 2-50 Confined explosion structures



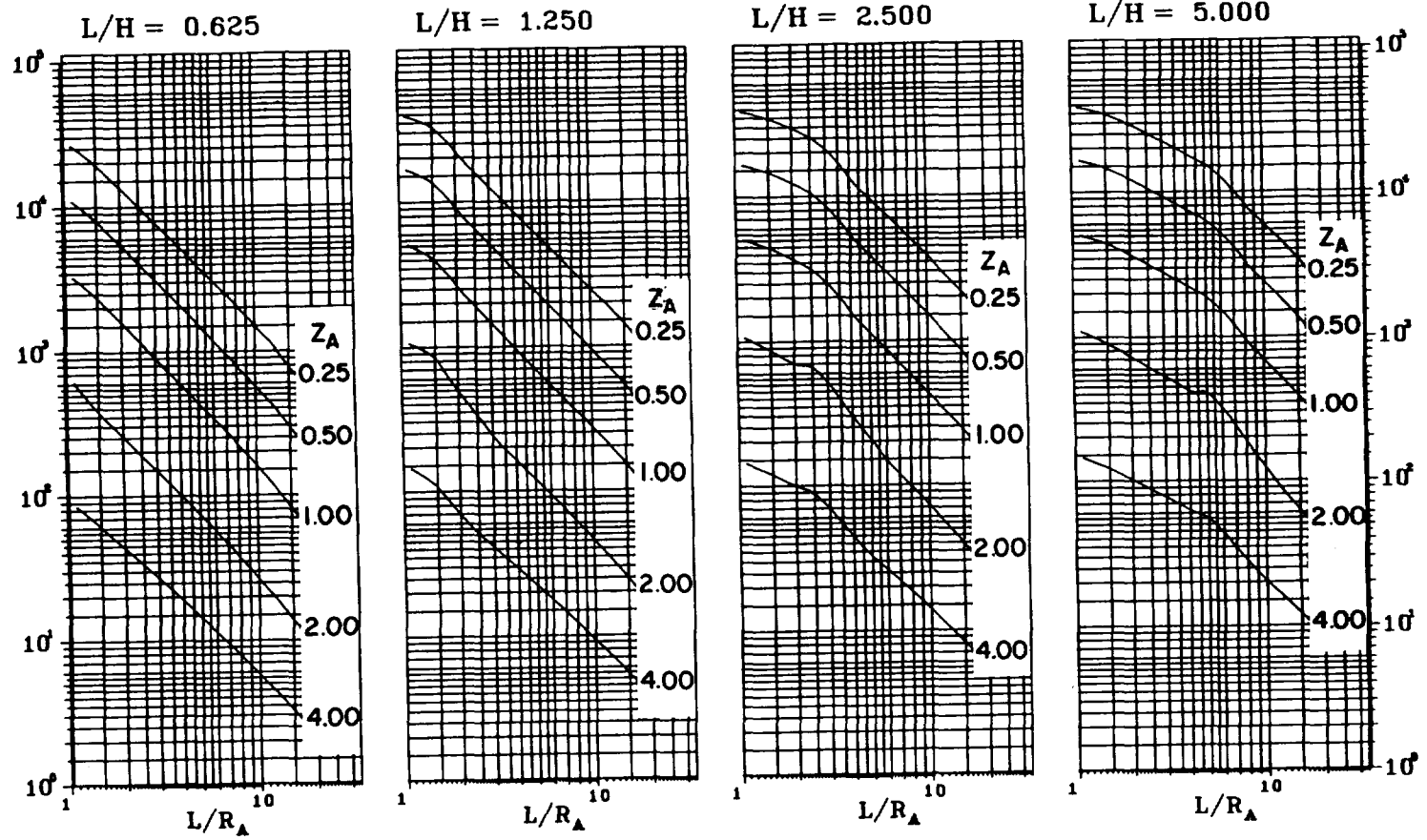
Notes:

1. B denotes Back Wall, S denotes Side Wall and R denotes Roof.
2. Numbers in parentheses indicate number, N, of reflecting surfaces adjacent to surface in question.
3. h is always measured to the nearest reflecting surface.
4. l is always measured to the nearest reflecting surface except for the cantilever wall where it is measured to the nearest free edge.
5. For values of average peak pressures for barrier and cubicle arrangements shown, see Figures 2-52 to 2-100.
For respective scaled average reflected impulses, see Figures 2-101 to 2-149.
For reference list of above Figures for particular values of required parameters in Note 6, see Figure 2-3.
6. Required parameters: N , l/L , h/H , L/H , L/R_A , $Z_A = R_A/W^{1/3}$

Figure 2-51 Barrier and cubicle configurations and parameters

AVERAGE PEAK REFLECTED

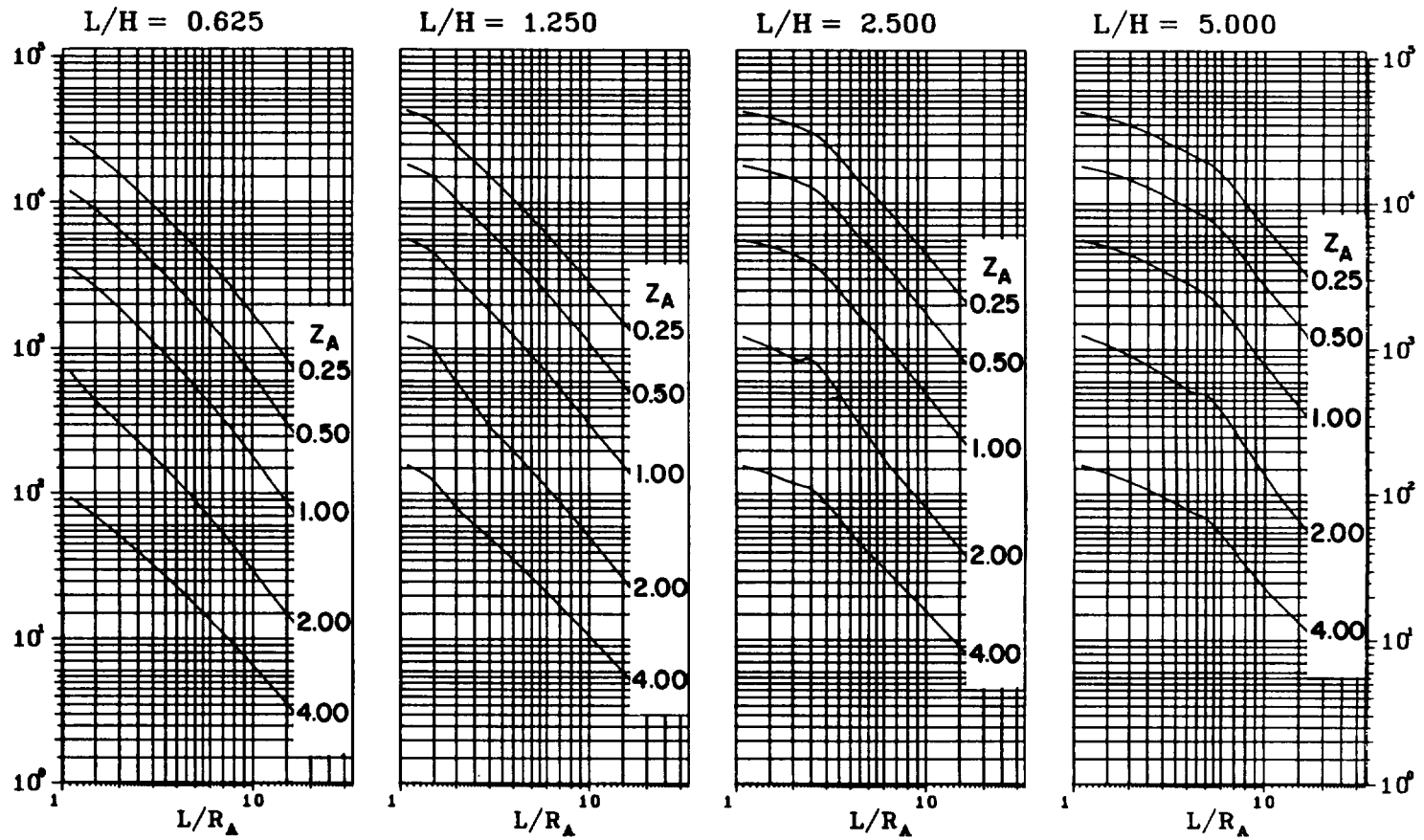
PRESSURE, p_r (psi)



01B

Figure 2-52 Average peak reflected pressure ($N = 1$, $\lambda/L = 0.10$, $h/H = 0.10$)

AVERAGE PEAK REFLECTED

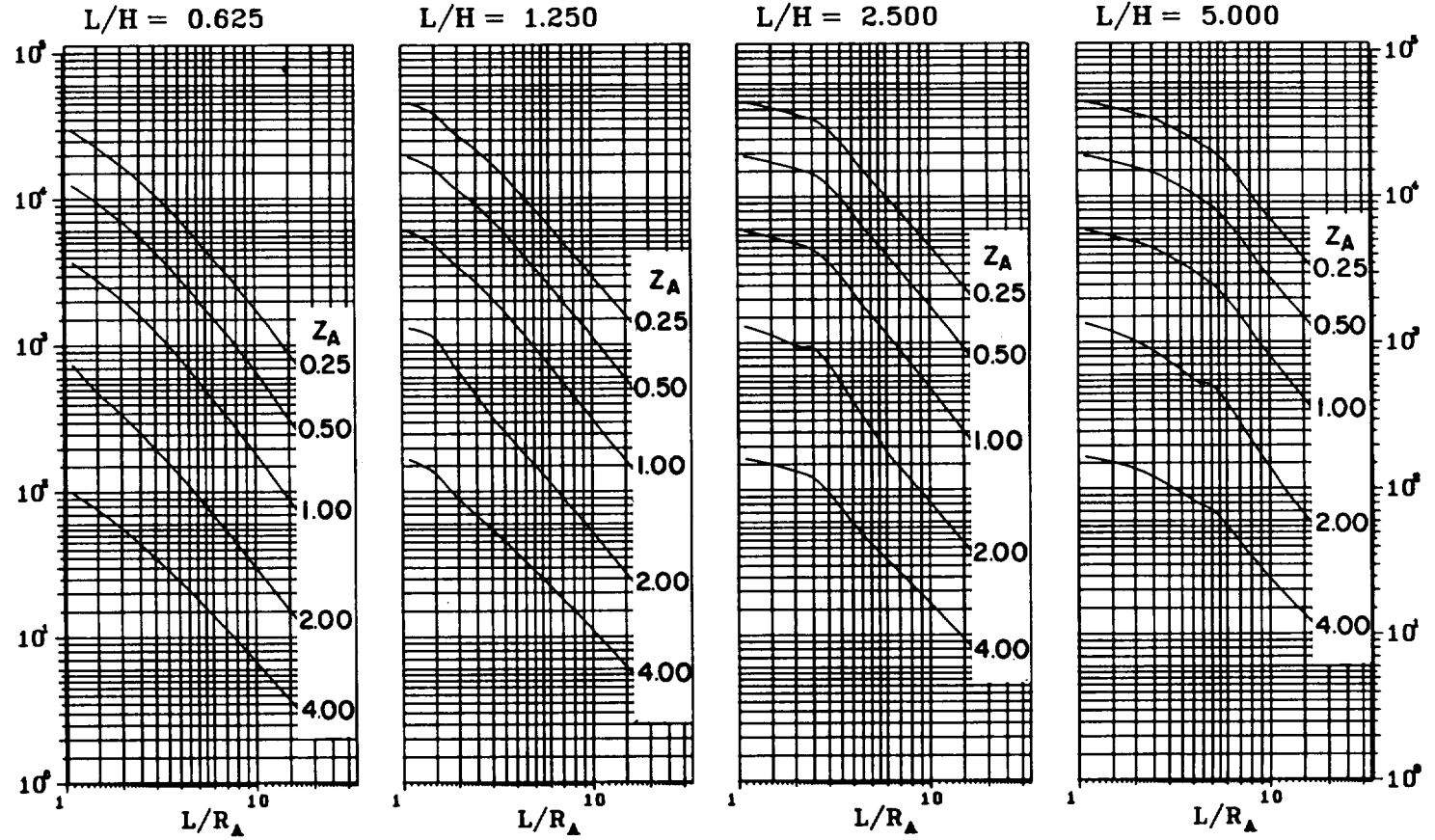
PRESSURE, P_r (psi)

02B

Figure 2-53 Average peak reflected pressure ($N = 1$, $h/H = 0.10$)

AVERAGE PEAK REFLECTED

PRESSURE, p_r (psi)

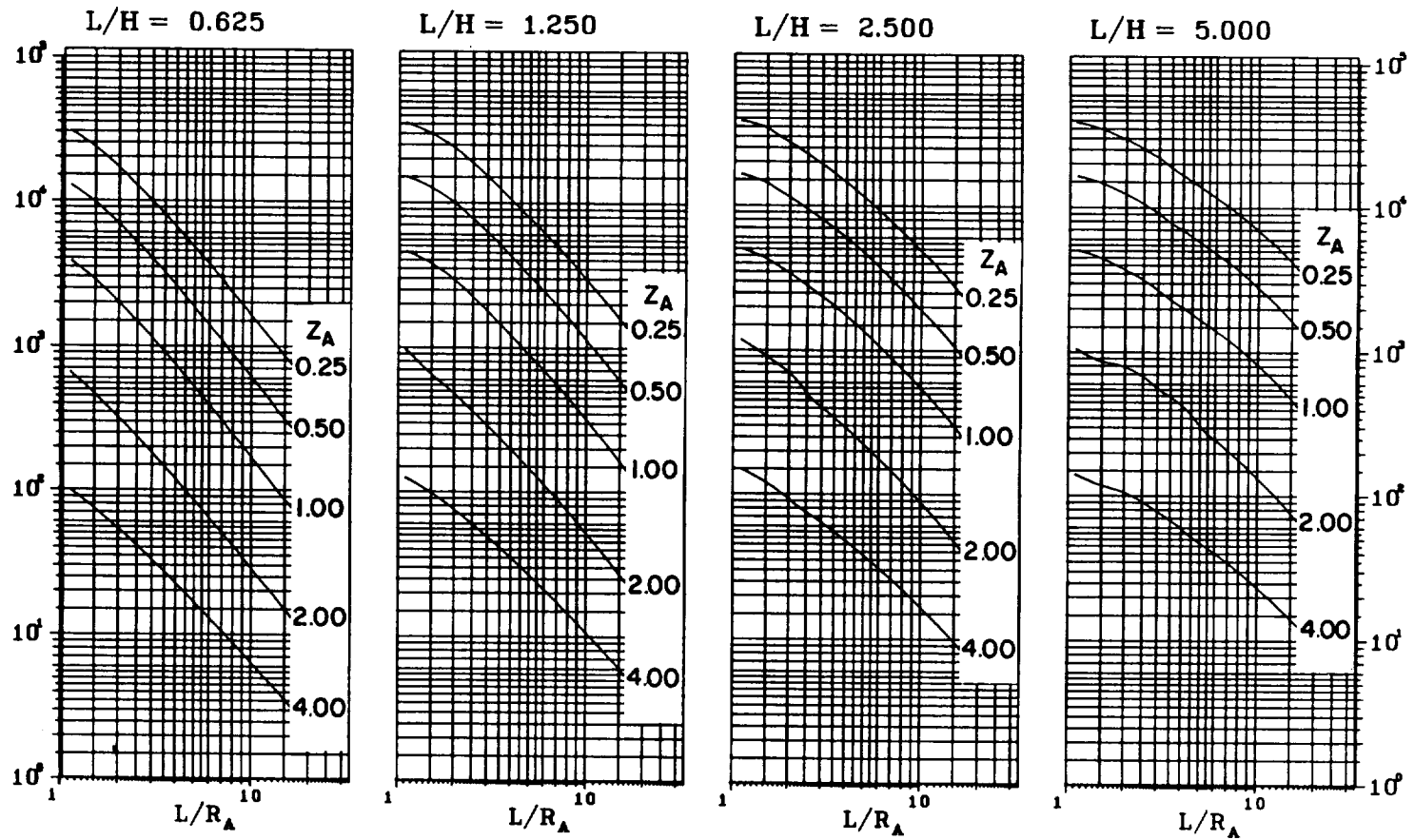


03B

Figure 2-54 Average peak reflected pressure ($N = 1$, $\lambda/L = 0.50$, $h/H = 0.10$)

AVERAGE PEAK REFLECTED

PRESSURE, P_r (psi)

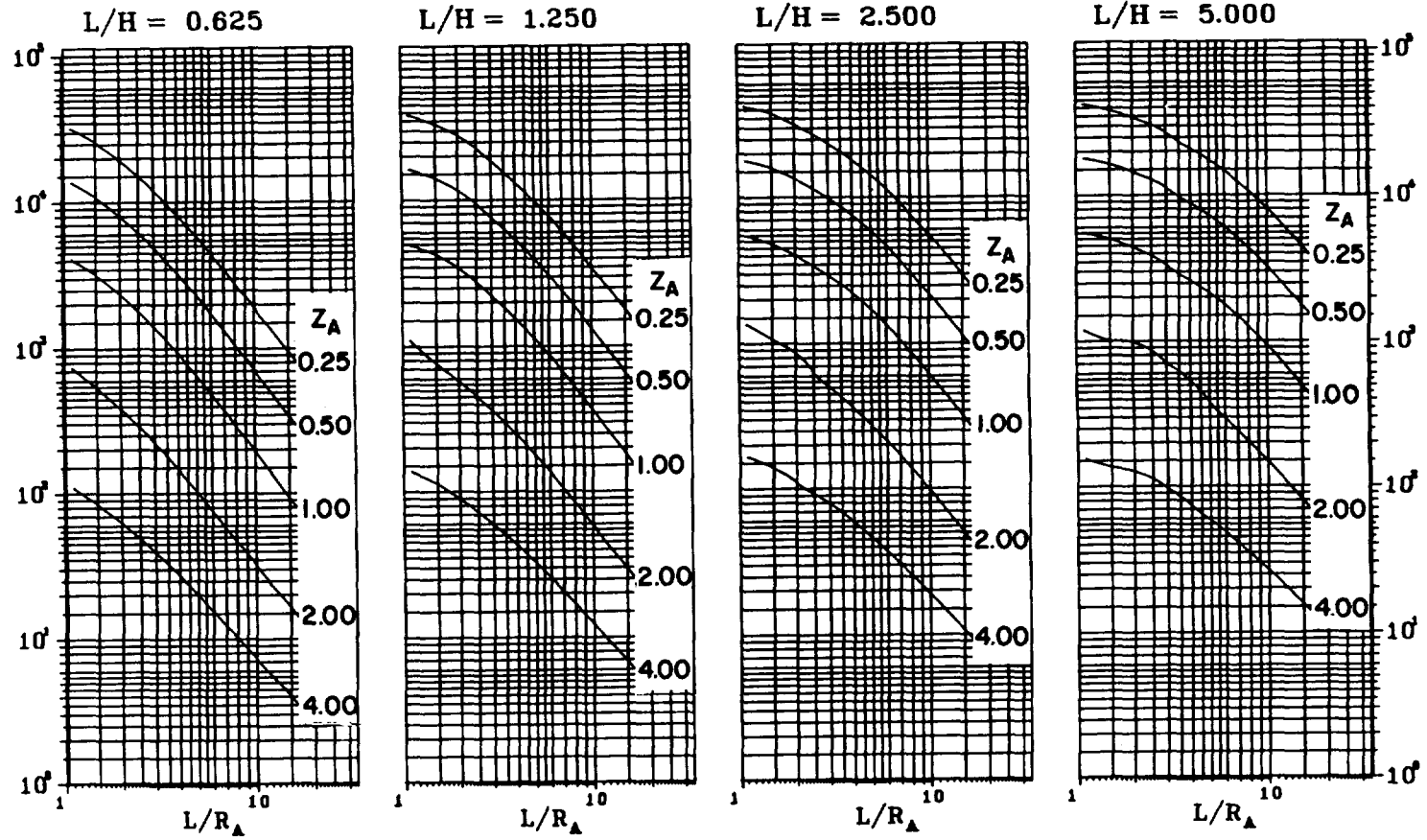


04B

Figure 2-55 Average peak reflected pressure ($N = 1$, $\lambda/L = 0.10$, $h/H = 0.25$)

AVERAGE PEAK REFLECTED

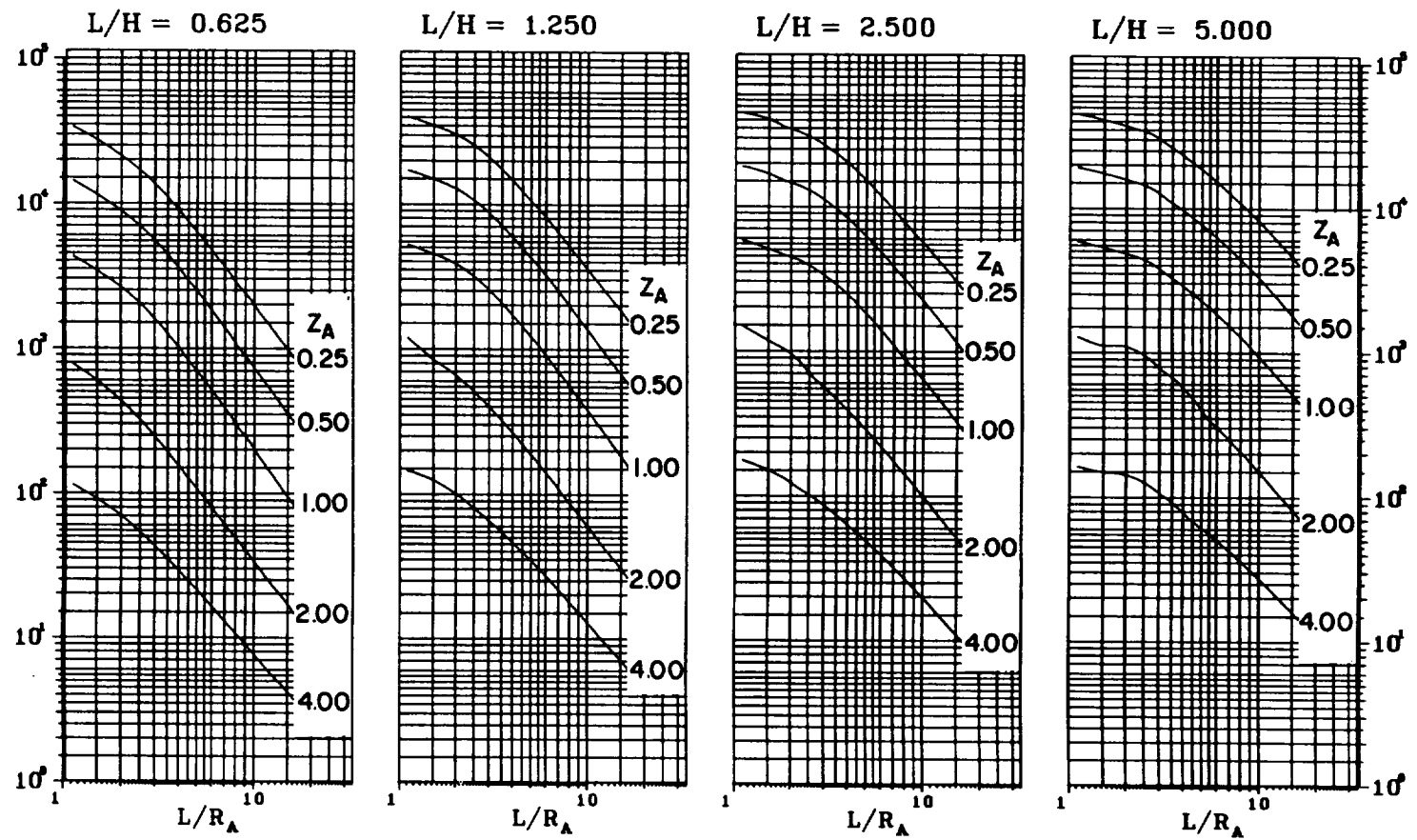
PRESSURE, p_r (psi)



05B

Figure 2-56 Average peak reflected pressure
($N = 1$, $l/L = 0.25$ and 0.75 , $h/H = 0.25$)

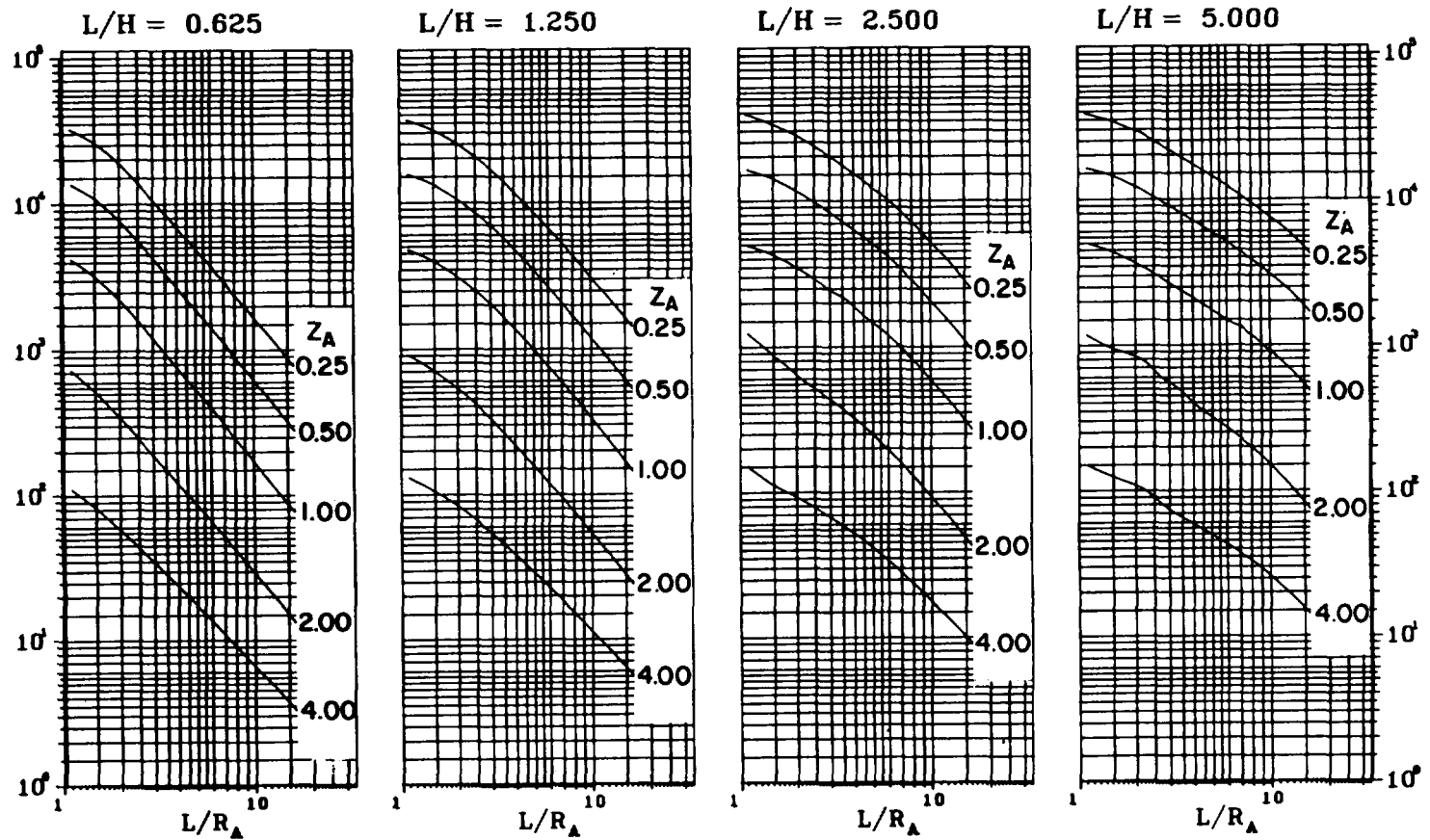
AVERAGE PEAK REFLECTED

PRESSURE, P_r (psi)

06B

Figure 2-57 Average peak reflected pressure ($N = 1$, $l/L = 0.50$, $h/H = 0.25$)

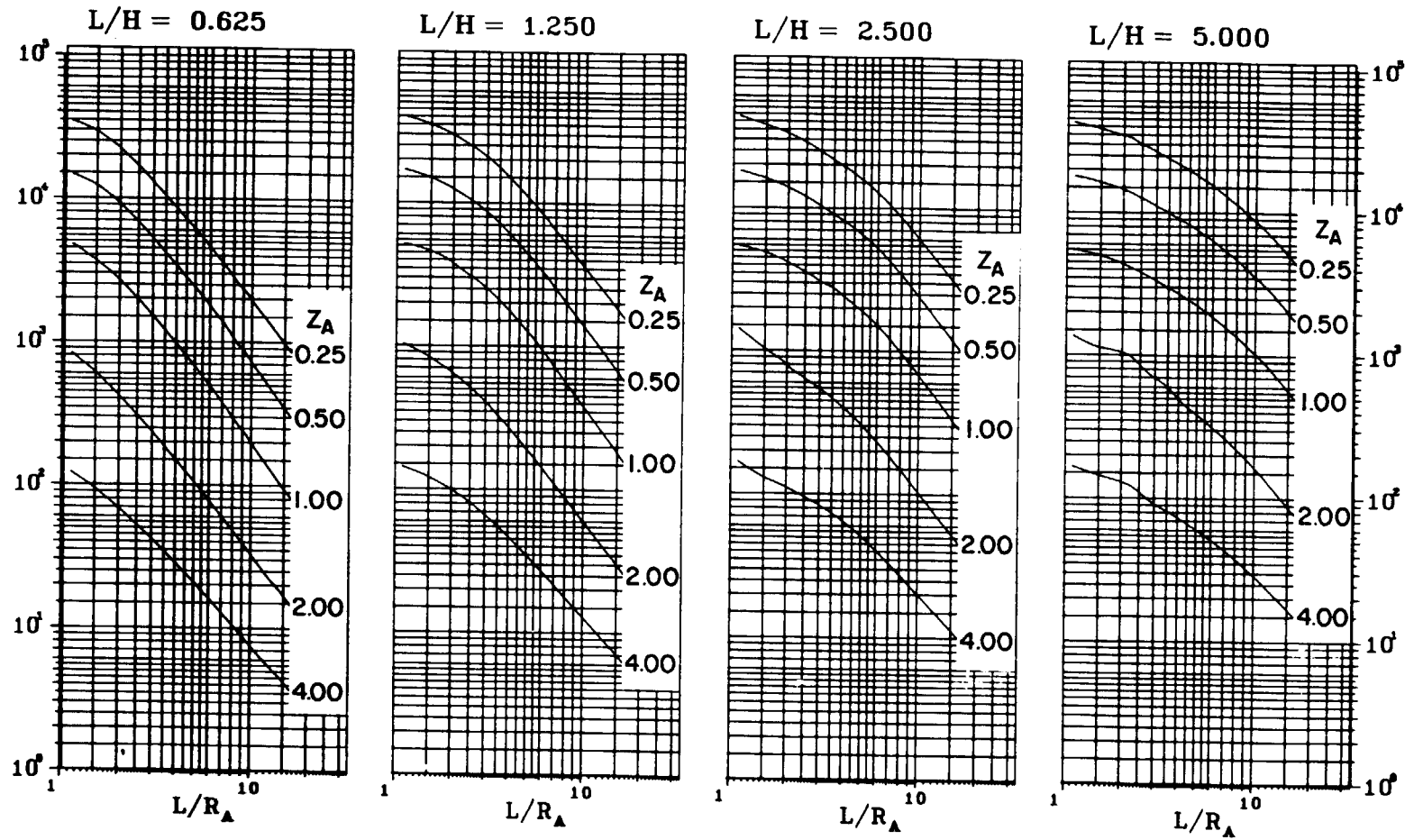
AVERAGE PEAK REFLECTED

PRESSURE, p_r (psi)

07B

Figure 2-58 Average peak reflected pressure ($N = 1$, $\ell/L = 0.10$, $h/H = 0.50$)

AVERAGE PEAK REFLECTED

PRESSURE, p_r (psi)

08B

Figure 2-59 Average peak reflected pressure ($N = 1$, $l/L = 0.25$ and 0.75 , $h/H = 0.50$)

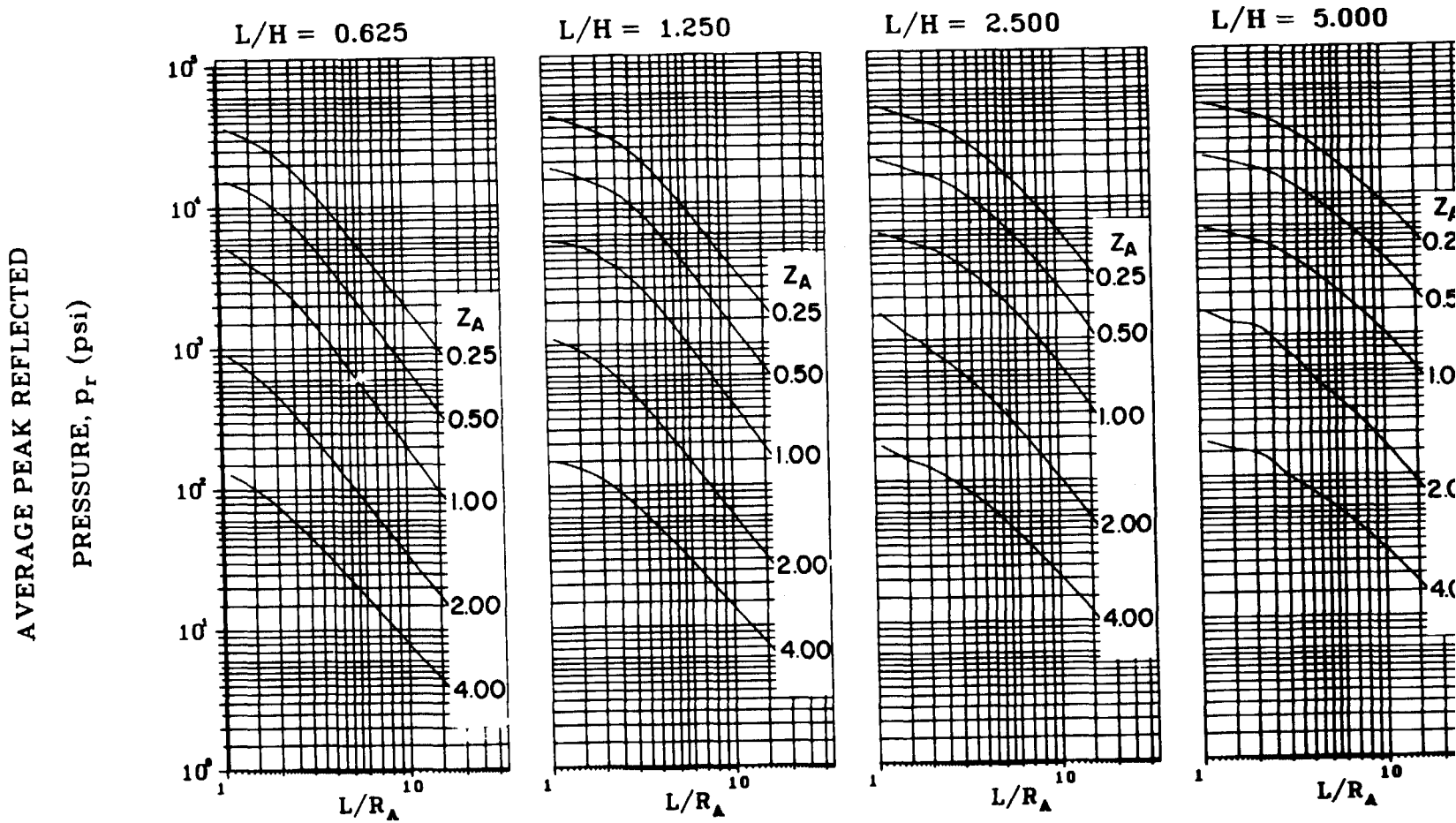


Figure 2-60 Average peak reflected pressure ($N = 1, \rho/L = 0.50, h/H = 0.50$)

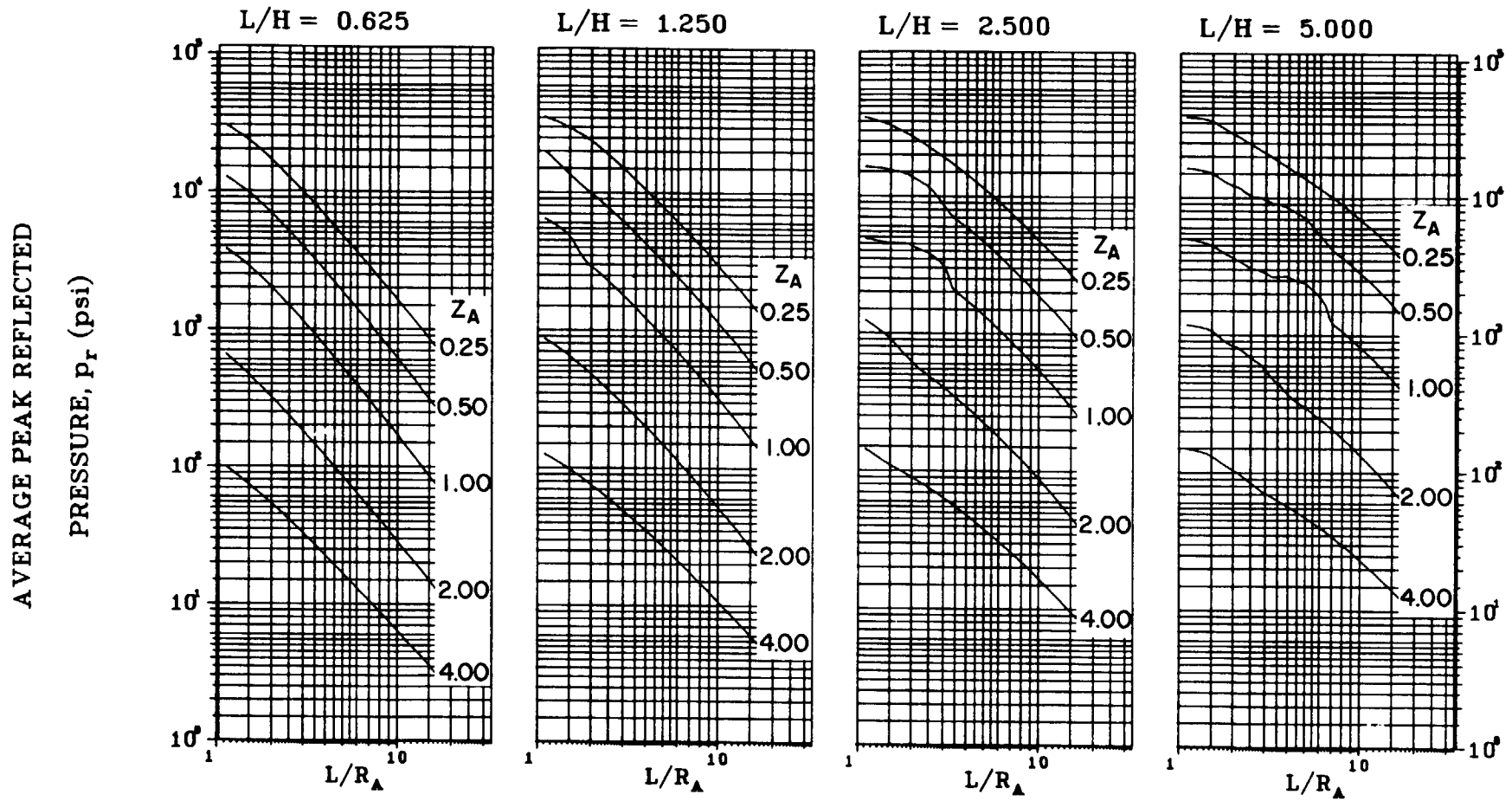
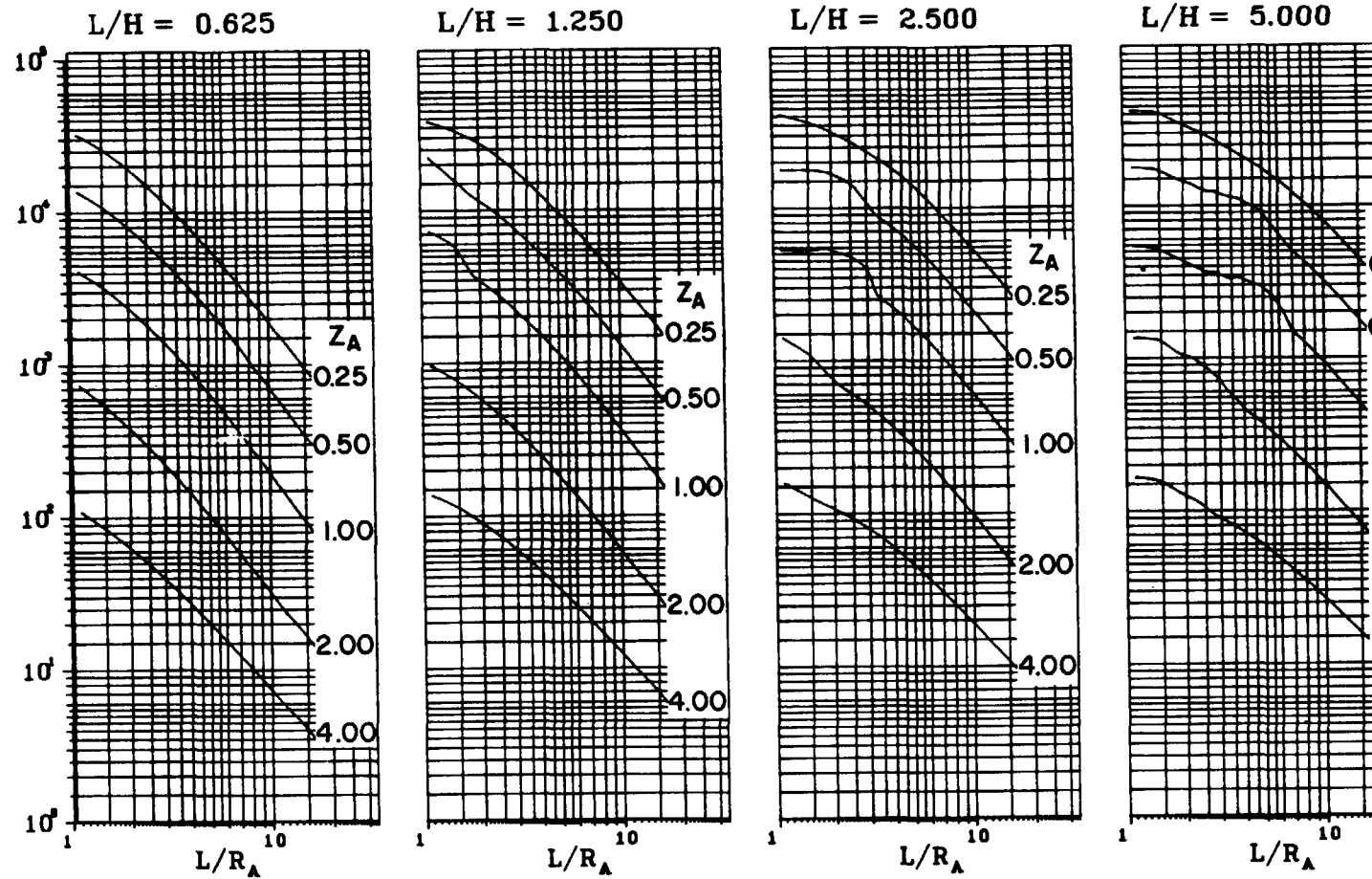


Figure 2-61 Average peak reflected pressure ($N = 1, \ell/L = 0.10, h/H = 0.75$)

AVERAGE PEAK REFLECTED

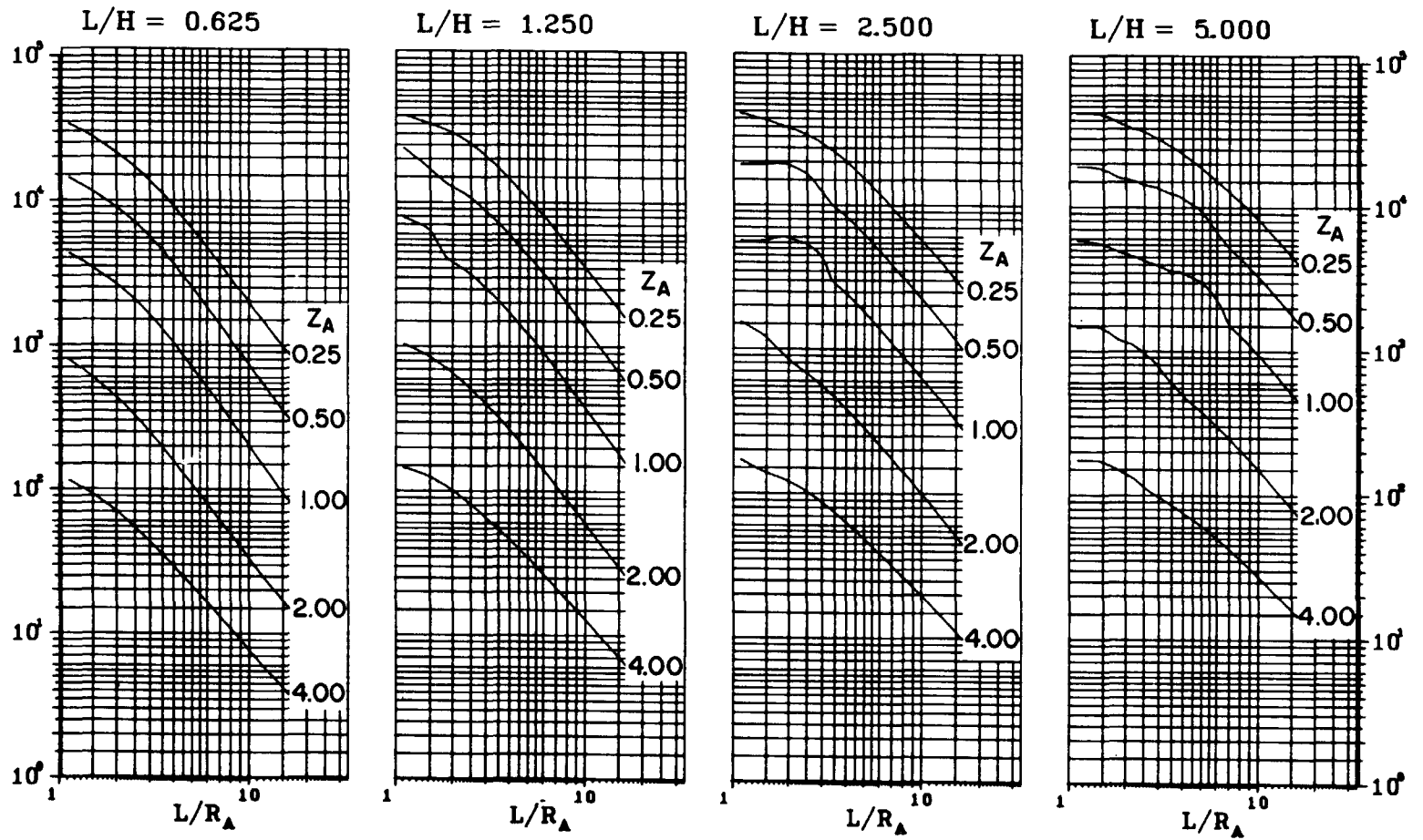
PRESSURE, P_r (psi)

11B

Figure 2-62 Average peak reflected pressure ($N = 1$, $\ell/L = 0.25$ and 0.75 , $h/H = 0.75$)

AVERAGE PEAK REFLECTED

PRESSURE, p_r (psi)



12B

Figure 2-63 Average peak reflected pressure ($N = 1, \rho/L = 0.50, h/H = 0.75$)

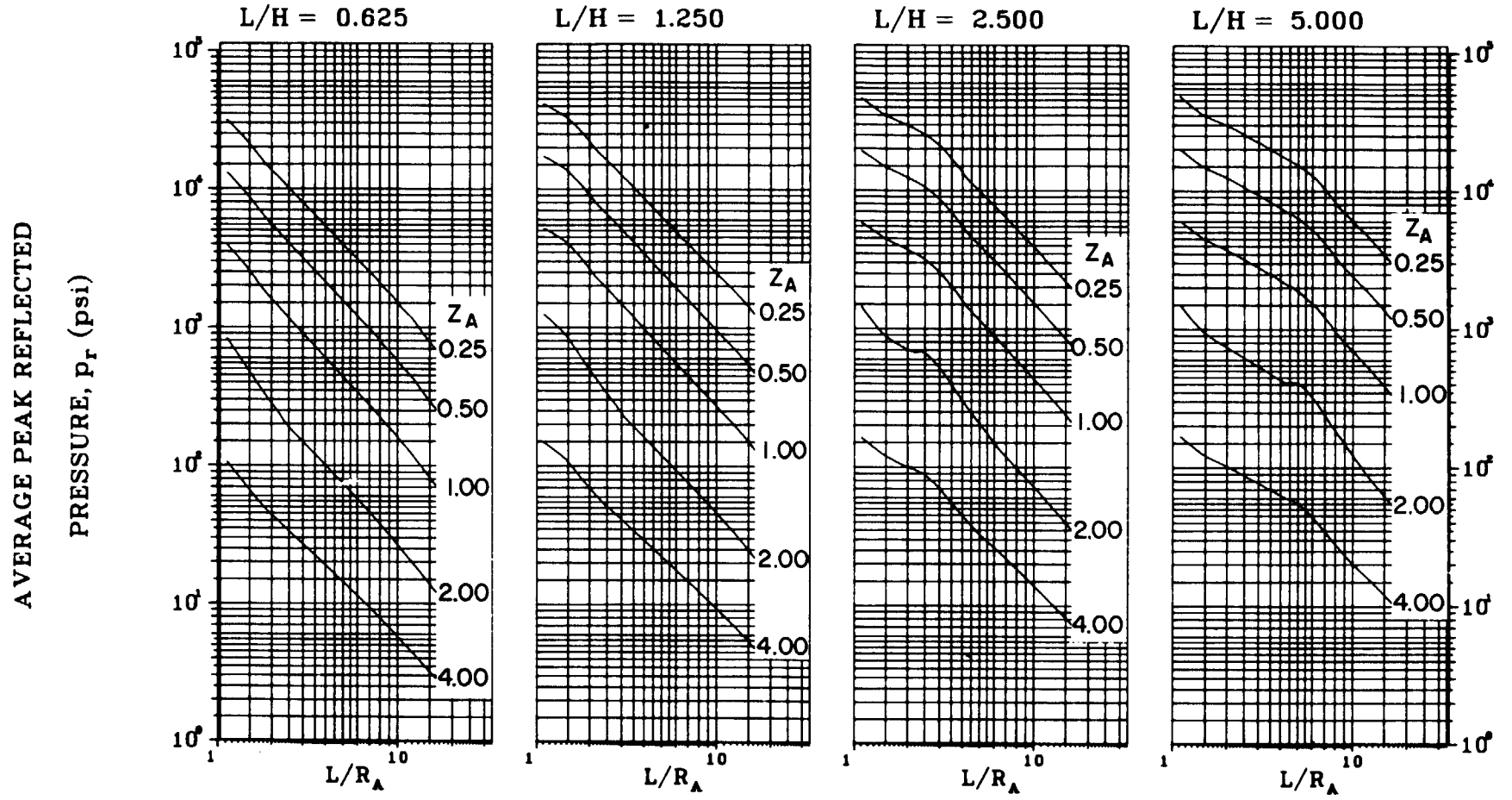


Figure 2-64 Average peak reflected pressure ($N = 2, \ell/L = 0.10, h/H = 0.10$)

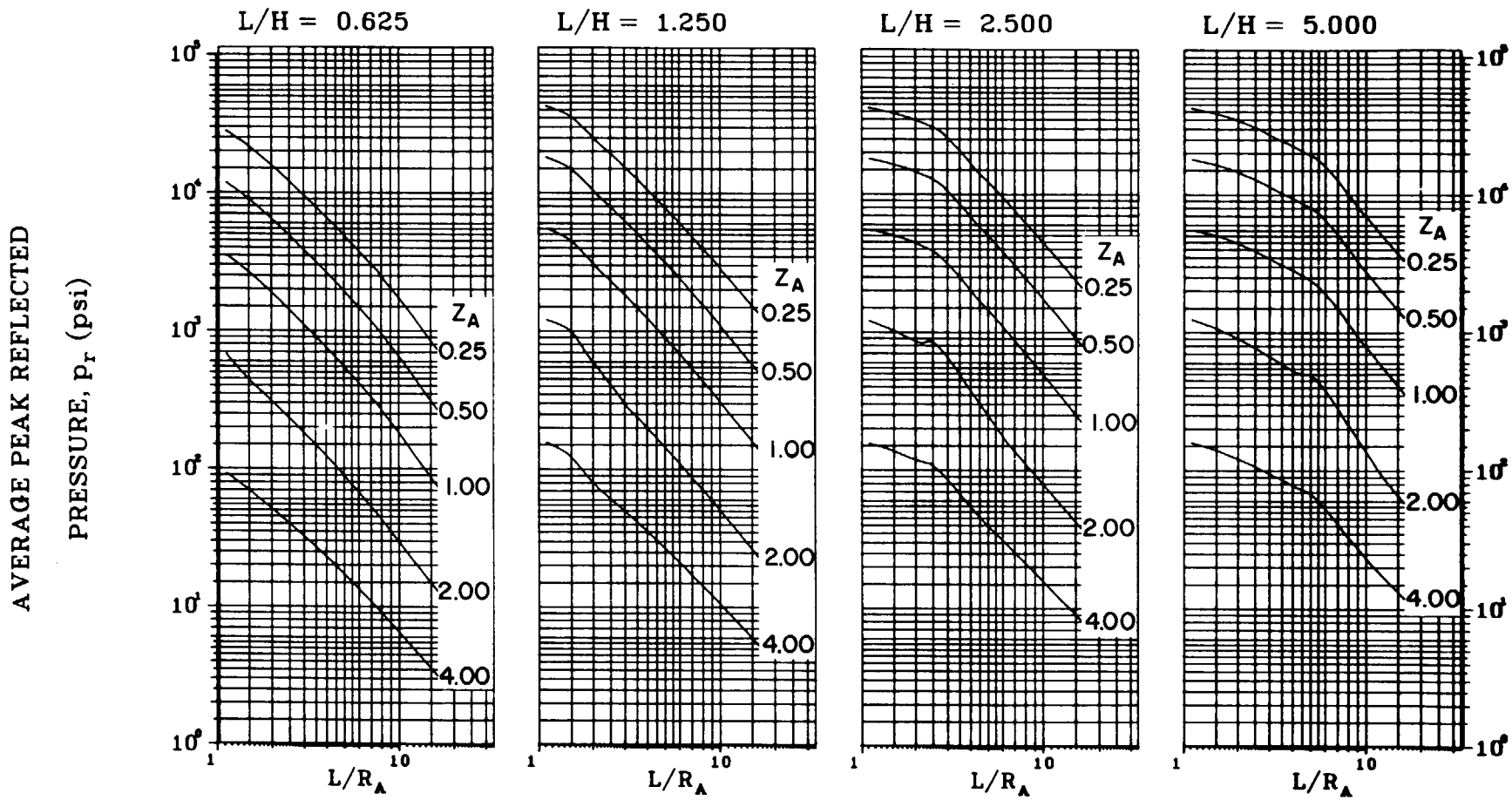
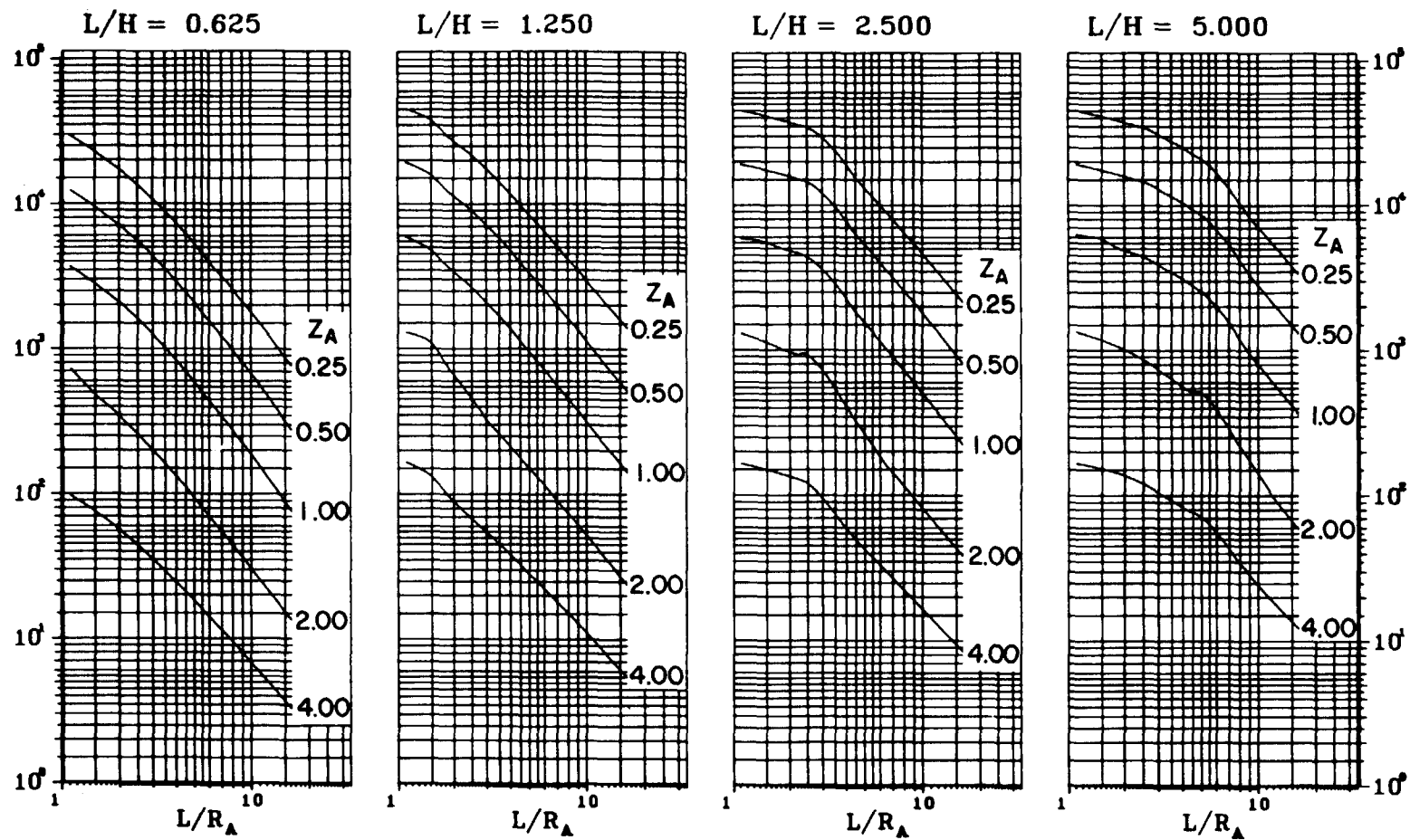


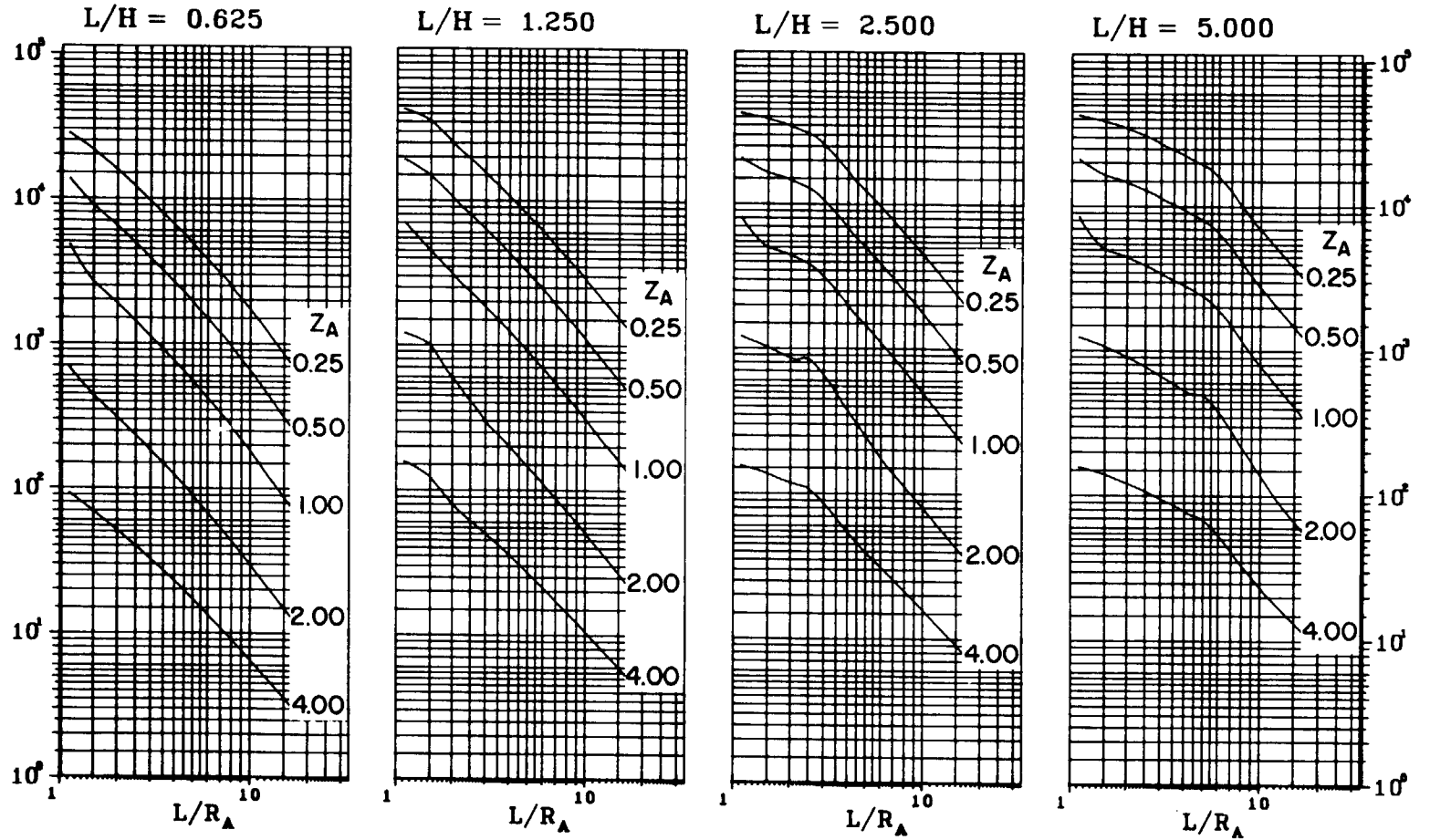
Figure 2-65 Average peak reflected pressure ($N = 2, \ell/L = 0.25, h/H = 0.10$)

AVERAGE PEAK REFLECTED

PRESSURE, p_r (psi)Figure 2-66 Average peak reflected pressure ($N = 2$, $\rho/L = 0.50$, $h/H = 0.10$)

AVERAGE PEAK REFLECTED

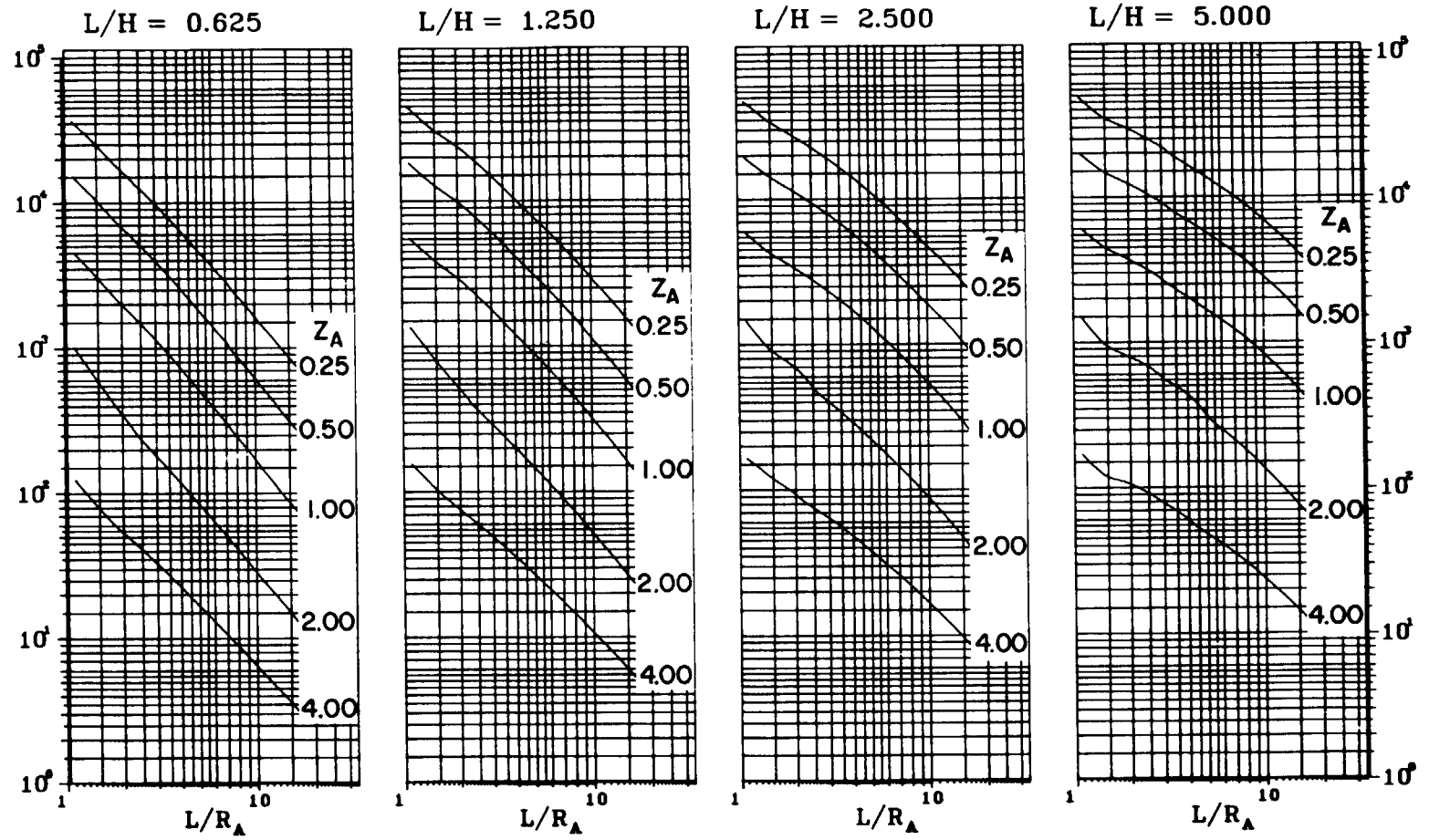
PRESSURE, p_r (psi)



16B

Figure 2-67 Average peak reflected pressure ($N = 2, \ell/L = 0.75, h/H = 0.10$)

AVERAGE PEAK REFLECTED

PRESSURE, p_r (psi)Figure 2-68 Average peak reflected pressure ($N = 2$, $\rho/L = 0.10$, $h/H = 0.25$)

AVERAGE PEAK REFLECTED

PRESSURE, p_r (psi)

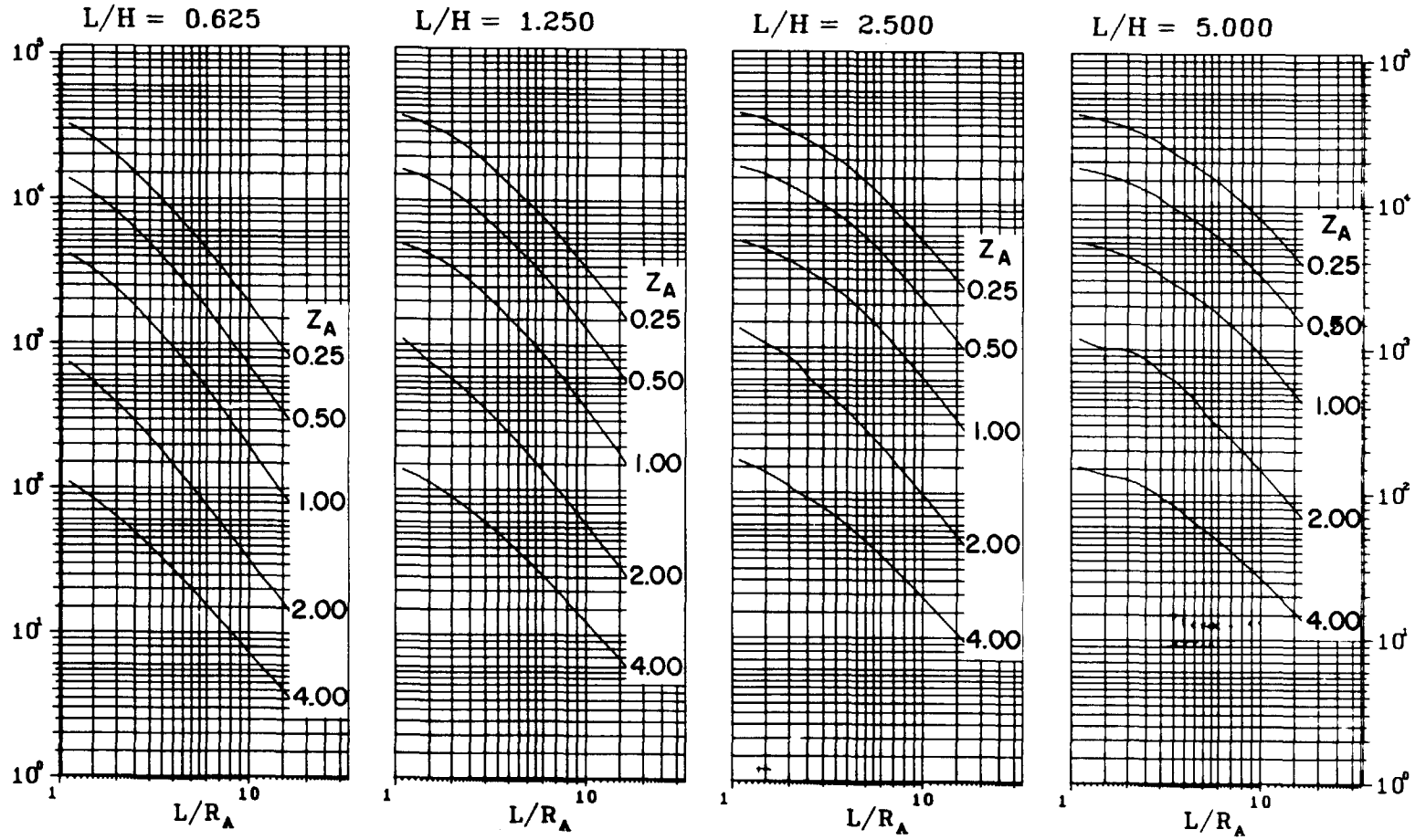


Figure 2-69 Average peak reflected pressure ($N = 2, \ell/L = 0.25, h/H = 0.25$)

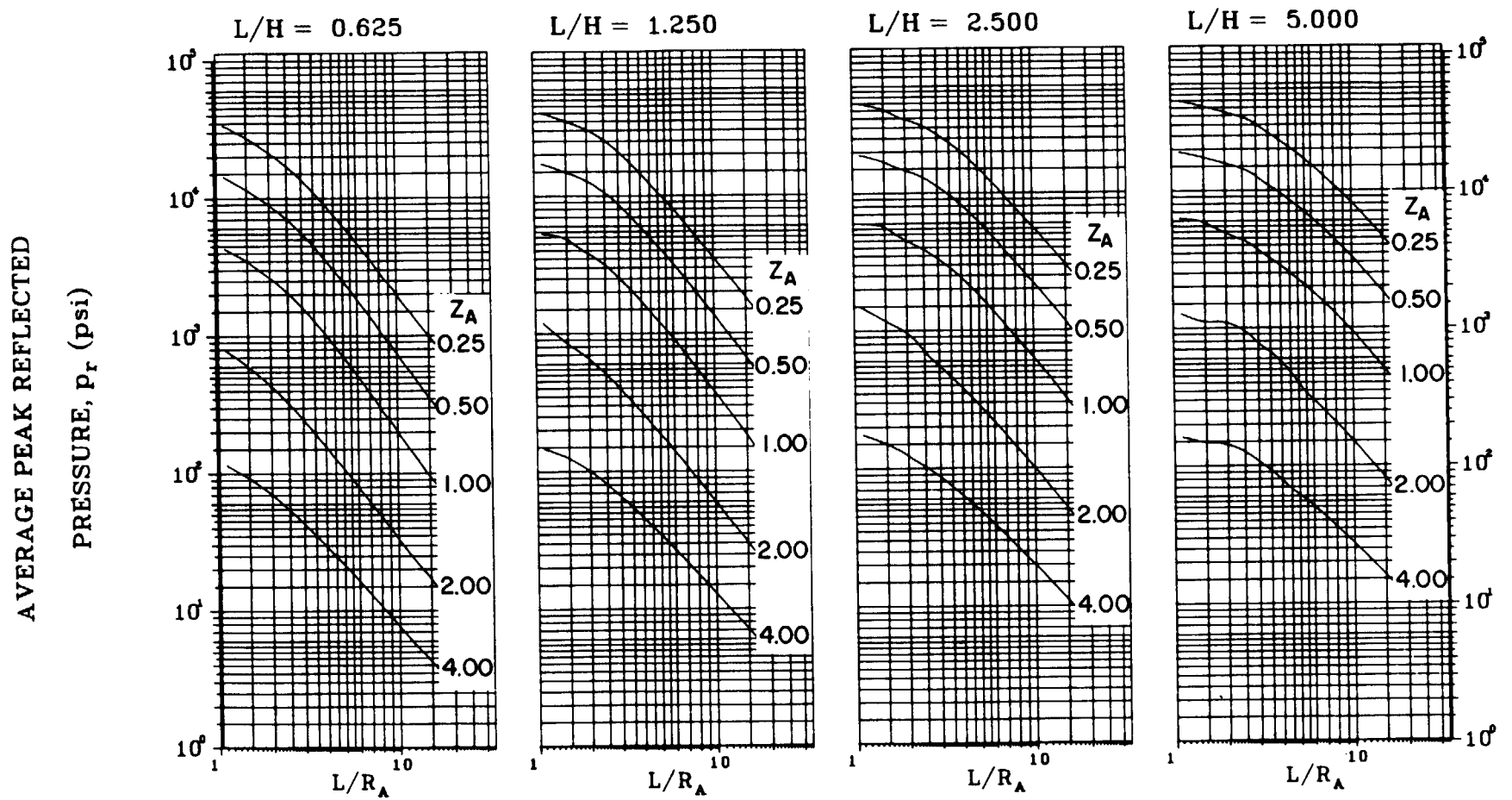


Figure 2-70 Average peak reflected pressure ($N = 2$, $\ell/L = 0.50$, $h/H = 0.25$)

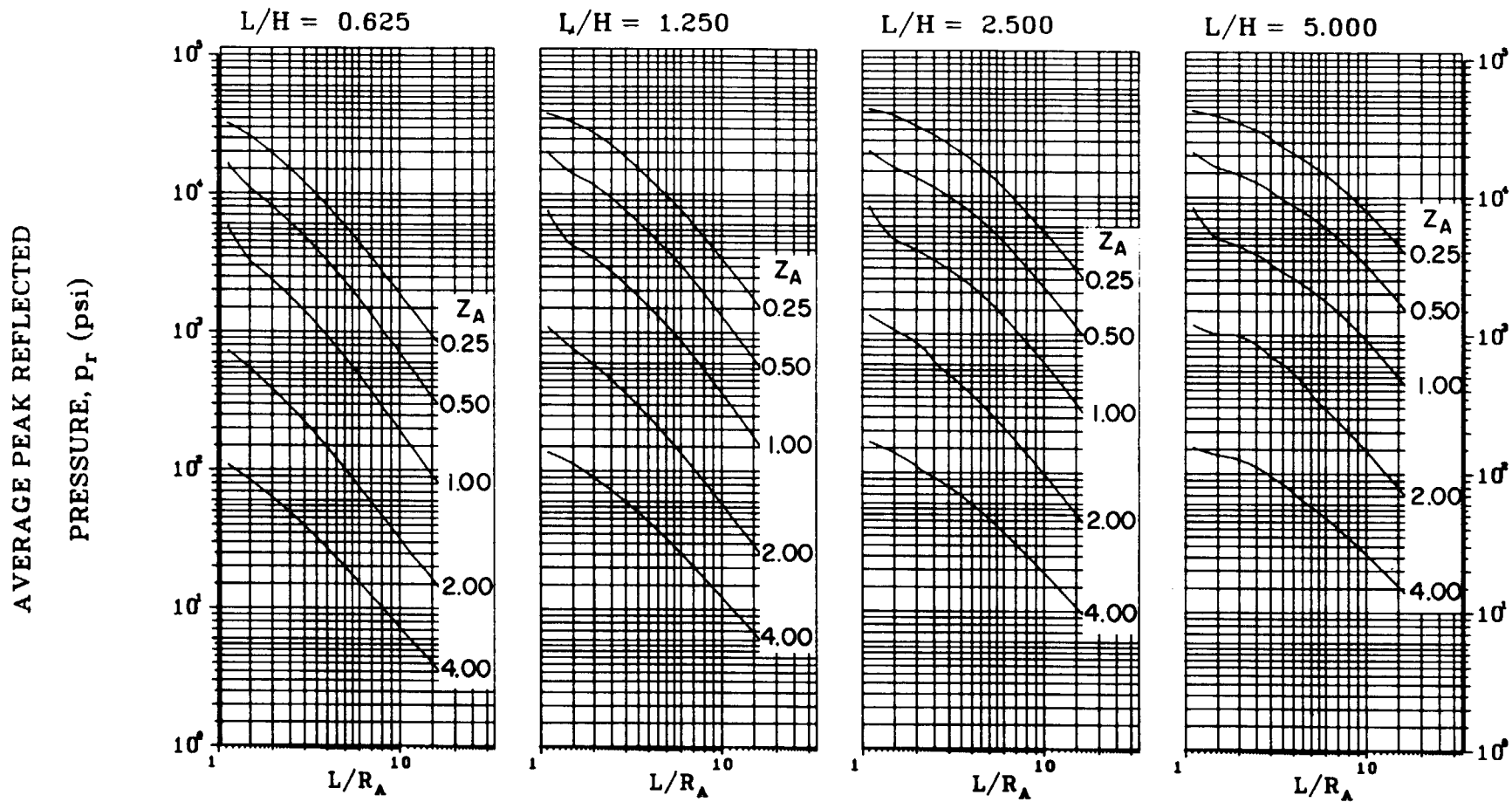


Figure 2-71 Average peak reflected pressure ($N = 2$, $\ell/L = 0.75$, $h/H = 0.25$)

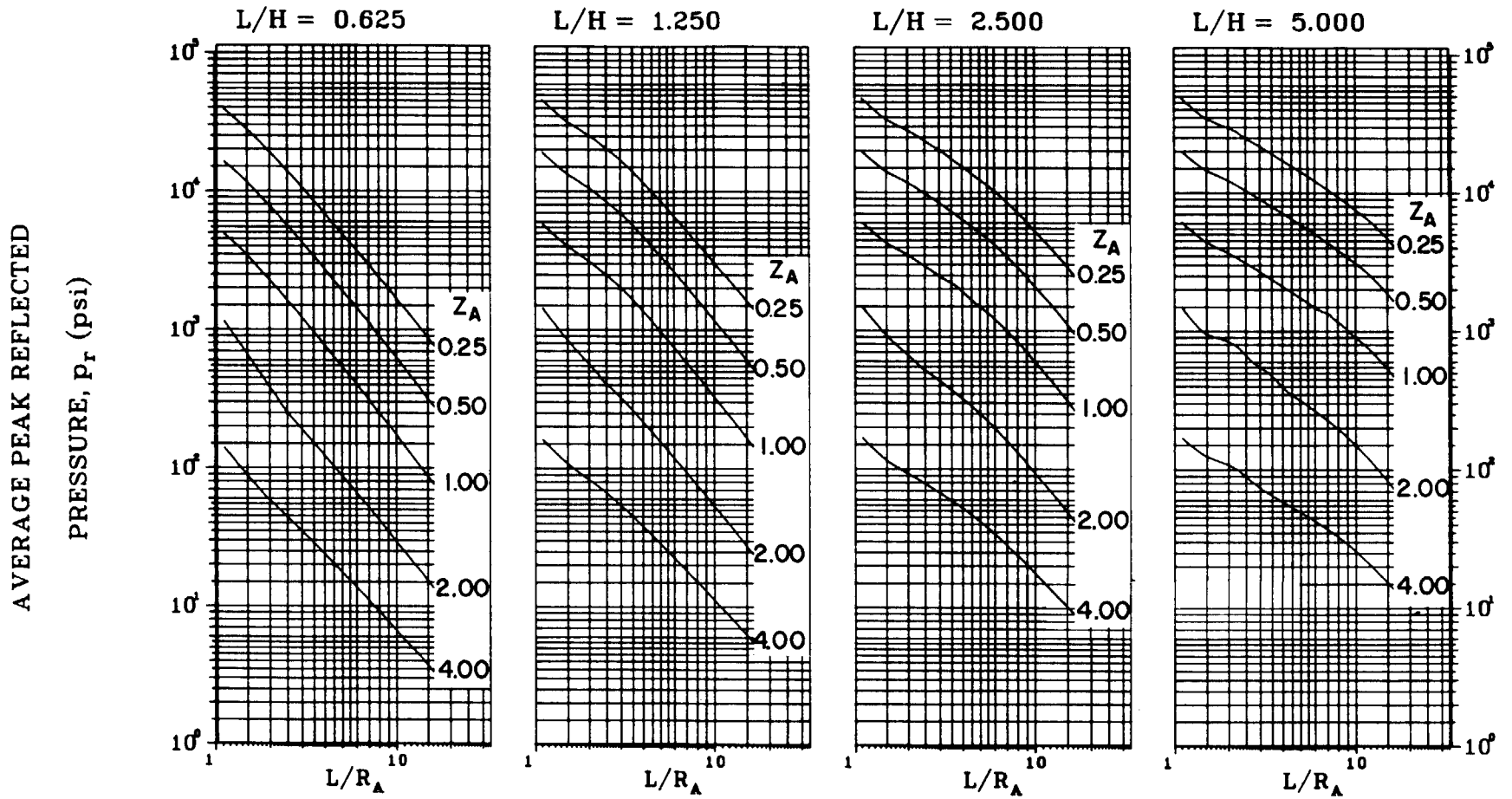
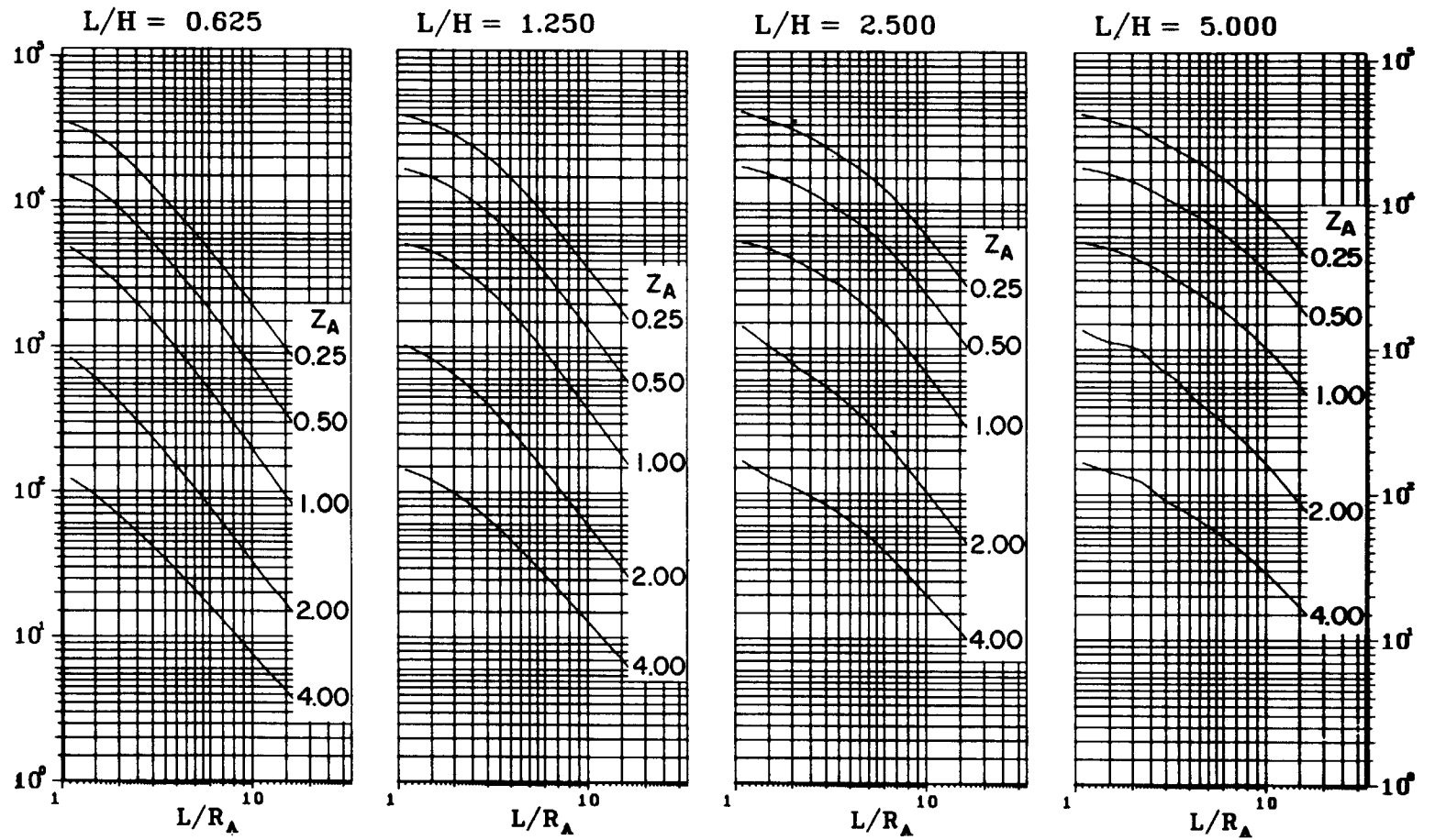


Figure 2-72 Average peak reflected pressure ($N = 2, \ell/L = 0.10, h/H = 0.50$)

AVERAGE PEAK REFLECTED

PRESSURE, P_r (psi)



22B

Figure 2-73 Average peak reflected pressure ($N = 2, \ell/L = 0.25, h/H = 0.50$)

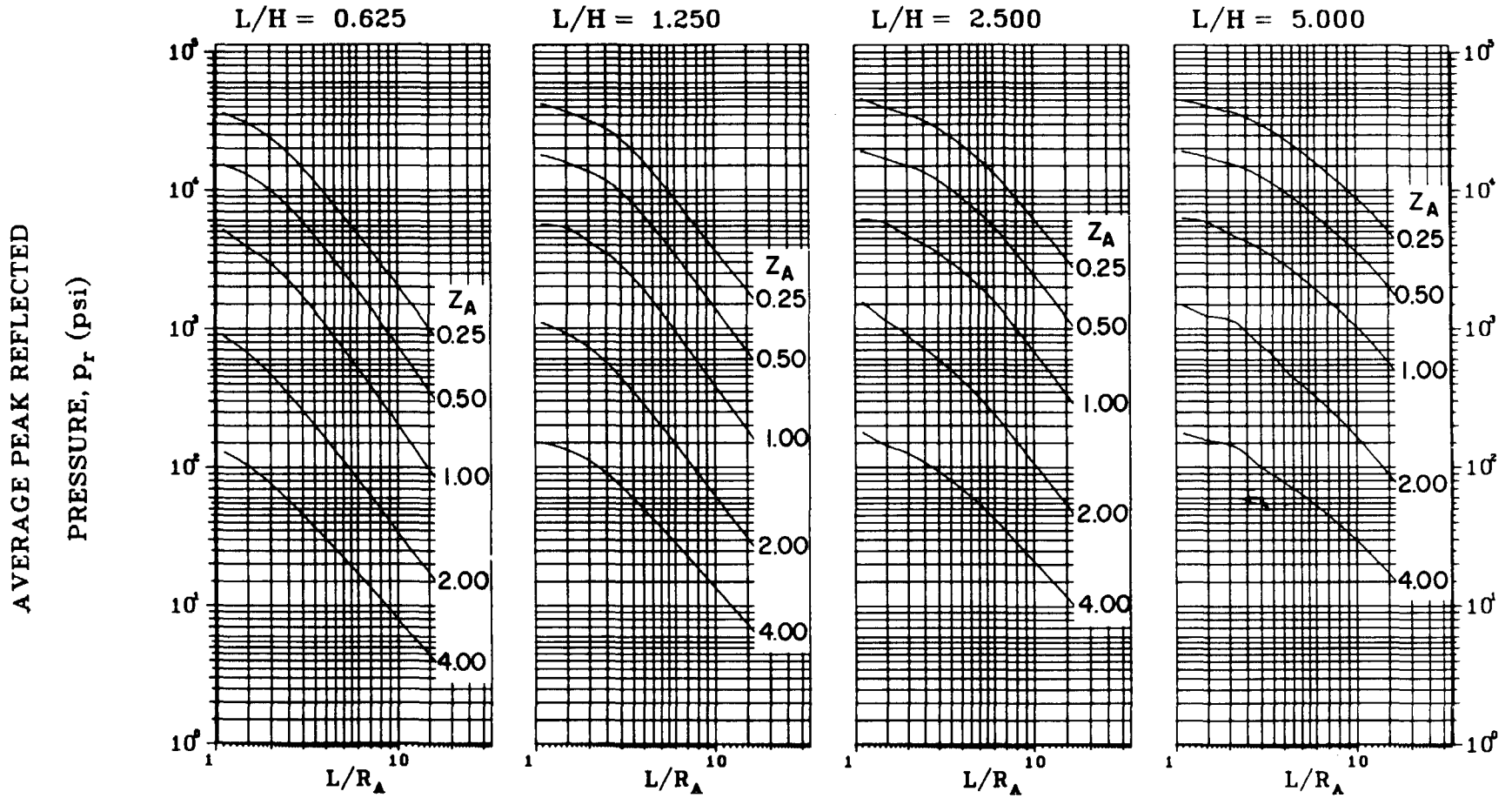
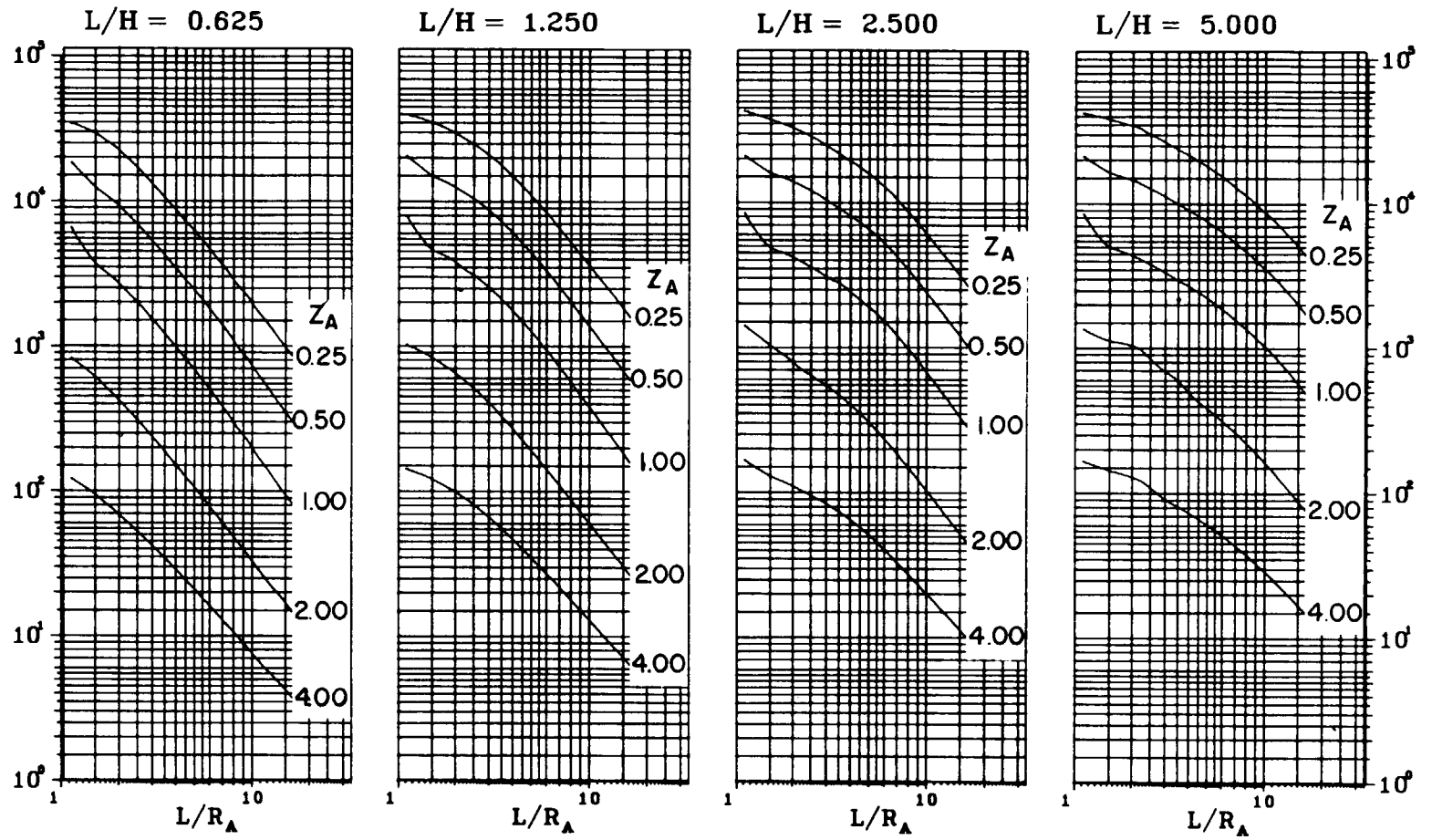


Figure 2-74 Average peak reflected pressure ($N = 2, \ell/L = 0.50, h/H = 0.50$)

AVERAGE PEAK REFLECTED

PRESSURE, p_r (psi)

24B

Figure 2-75 Average peak reflected pressure ($N = 2$, $\ell/L = 0.75$, $h/H = 0.50$)

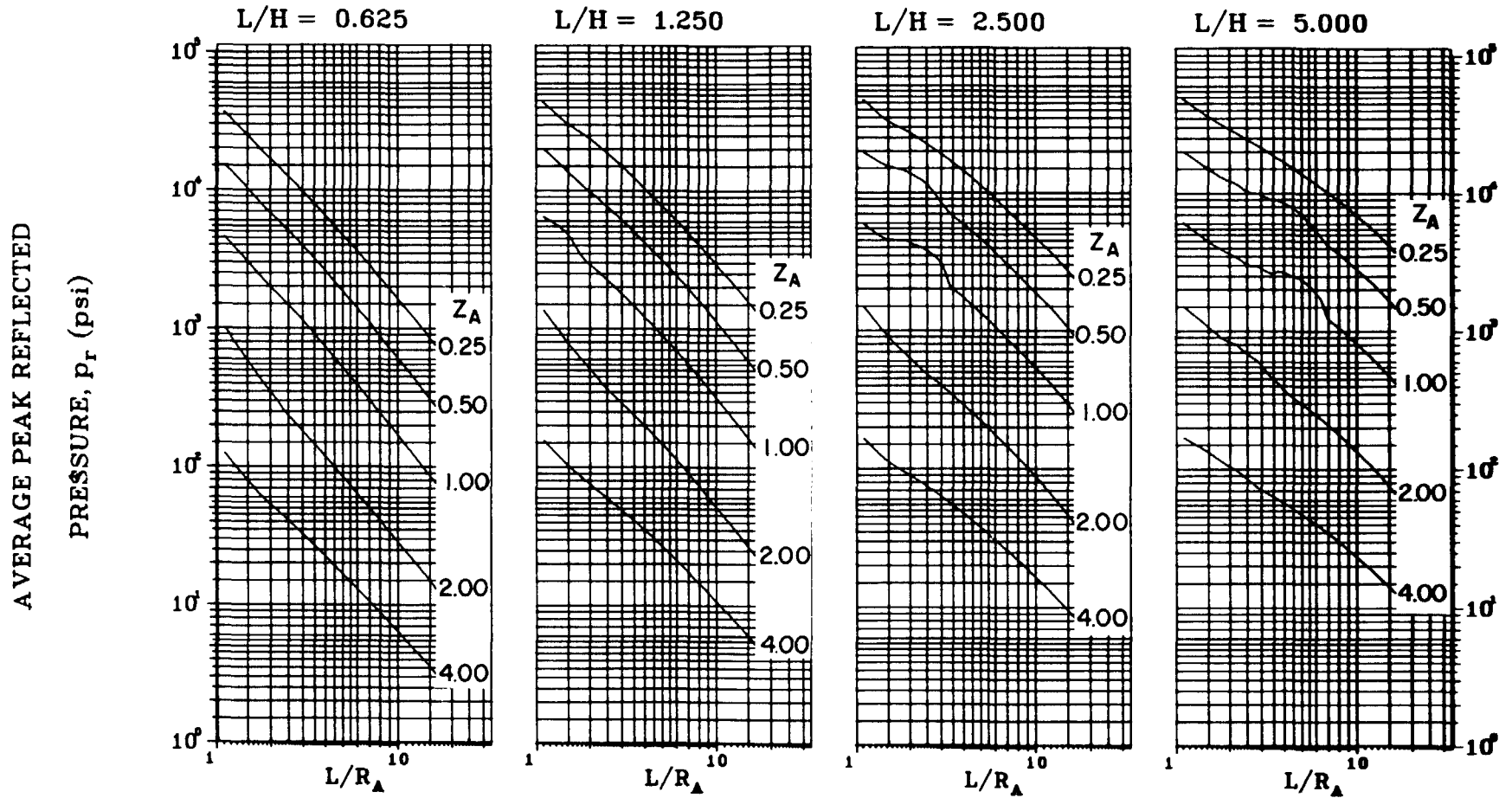


Figure 2-76. Average peak reflected pressure ($N = 2$, $\rho/L = 0.10$, $h/H = 0.75$)

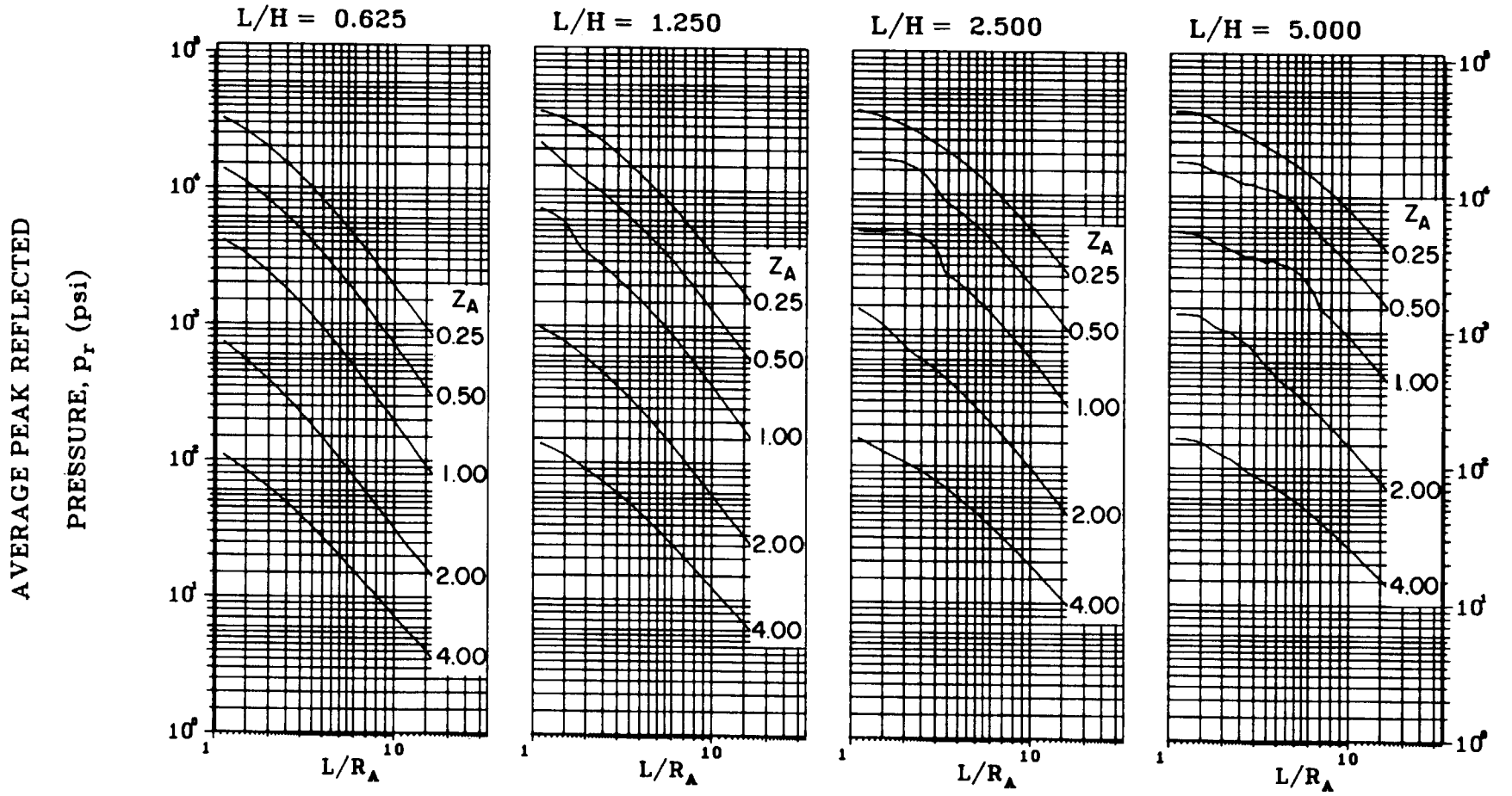


Figure 2-77 Average peak reflected pressure ($N = 2, \ell/L = 0.25, h/H = 0.75$)

AVERAGE PEAK REFLECTED

PRESSURE, p_r (psi)

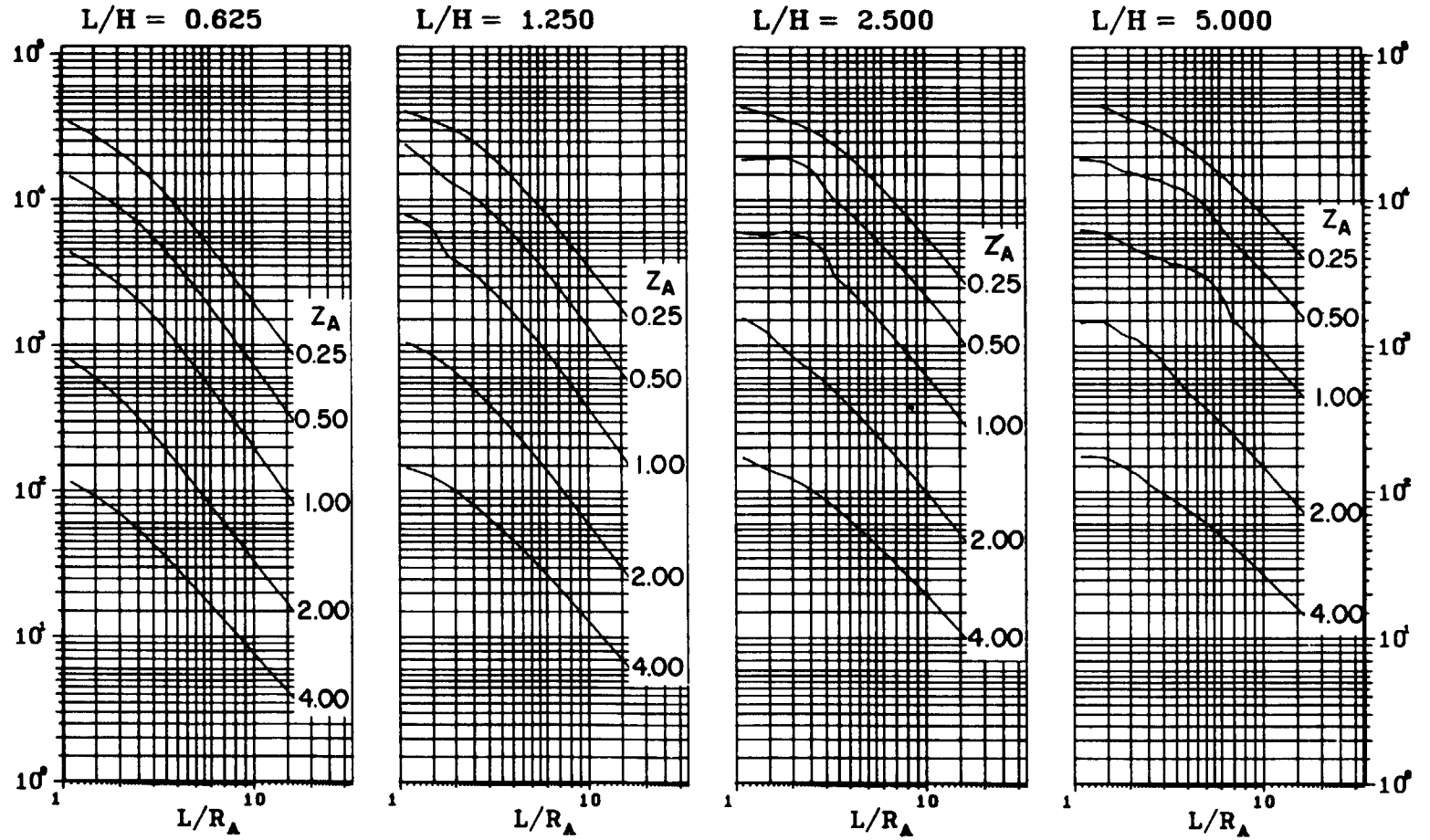


Figure 2-78 Average peak reflected pressure ($N = 2$, $l/L = 0.50$, $h/H = 0.75$)

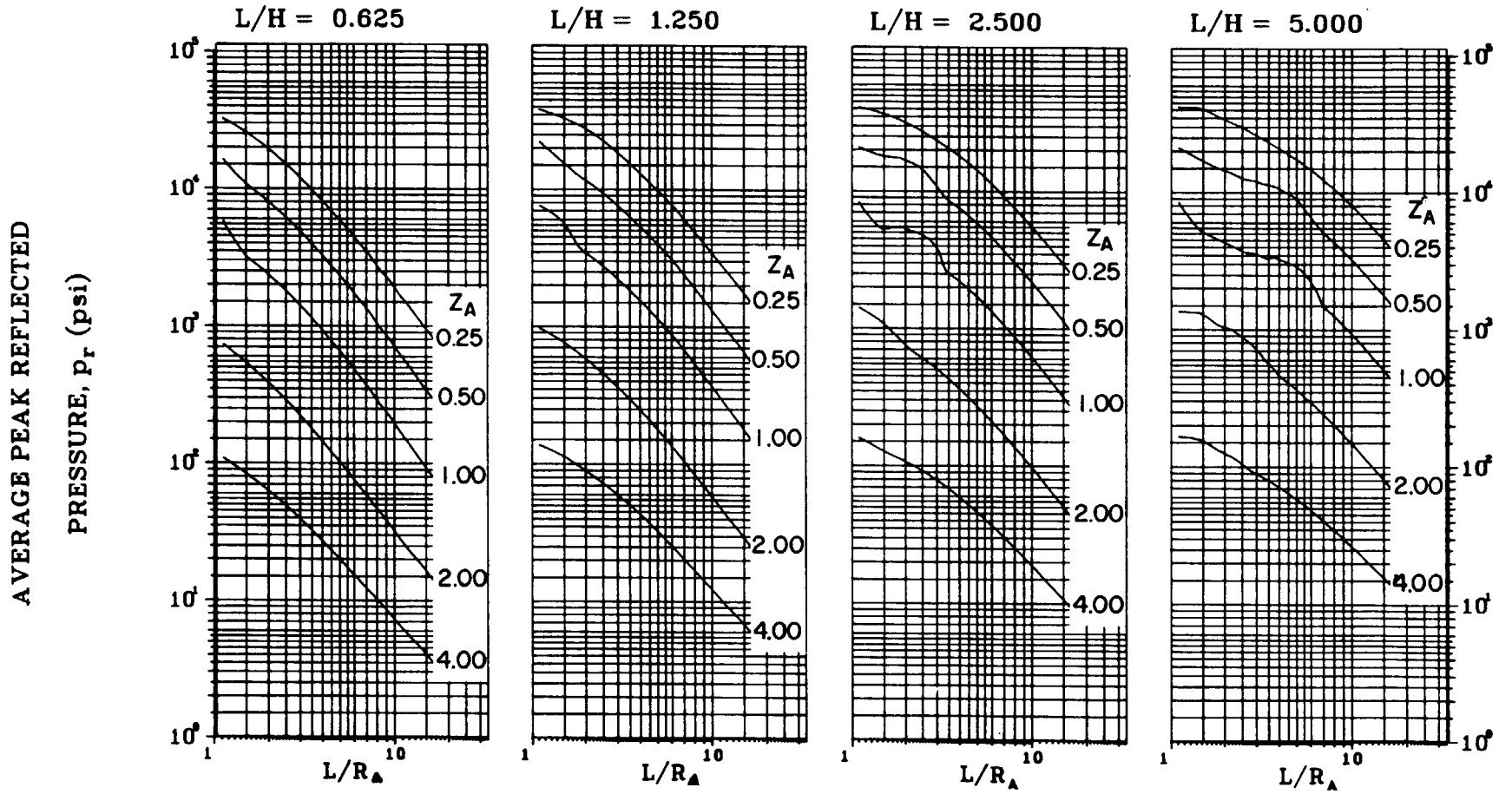


Figure 2-79 Average peak reflected pressure ($N = 2, \ell/L = 0.75, h/H = 0.75$)

AVERAGE PEAK REFLECTED

PRESSURE, p_r (psi)

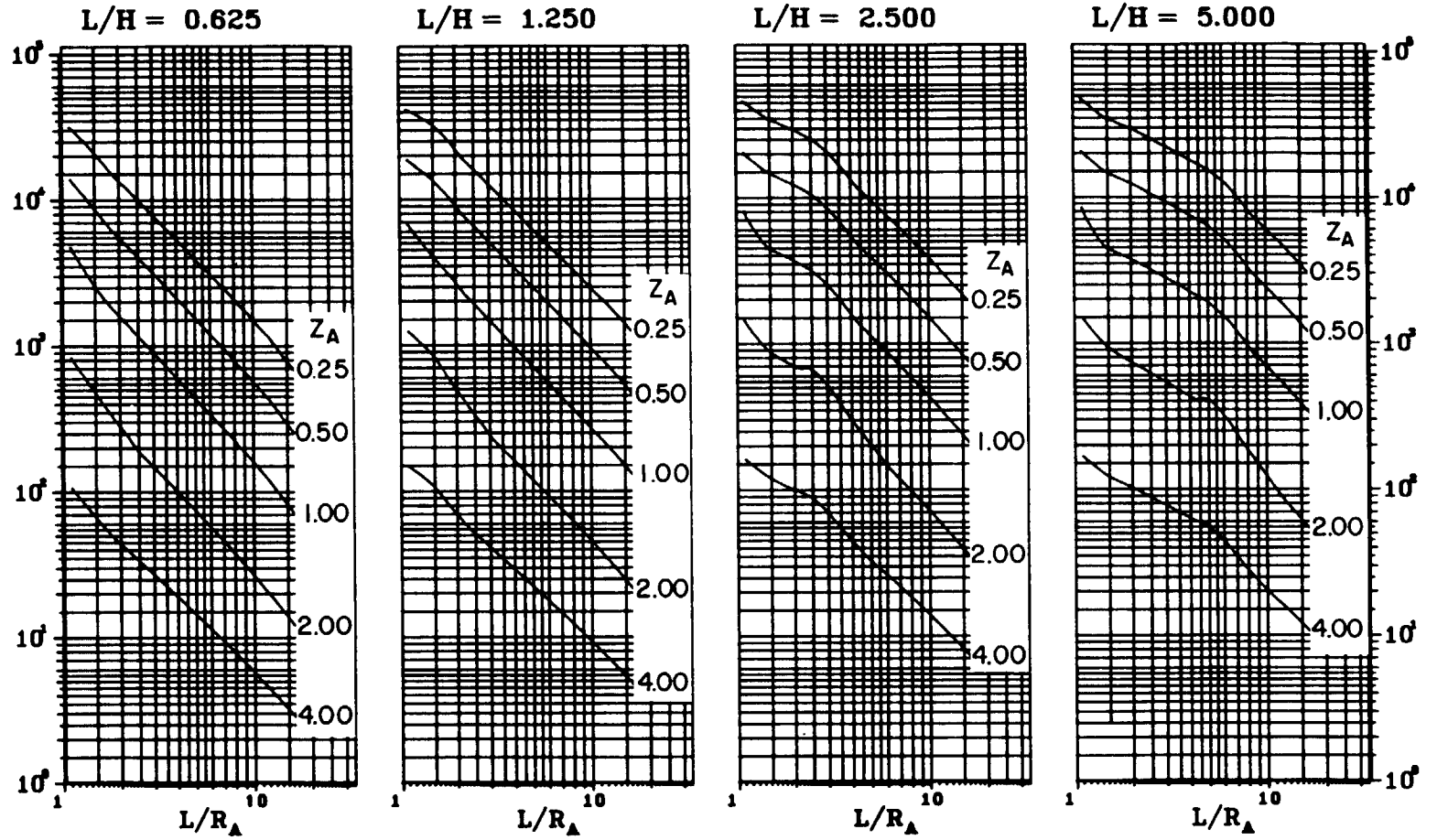


Figure 2-80 Average peak reflected pressure ($N = 3, \ell/L = 0.10, h/H = 0.10$)

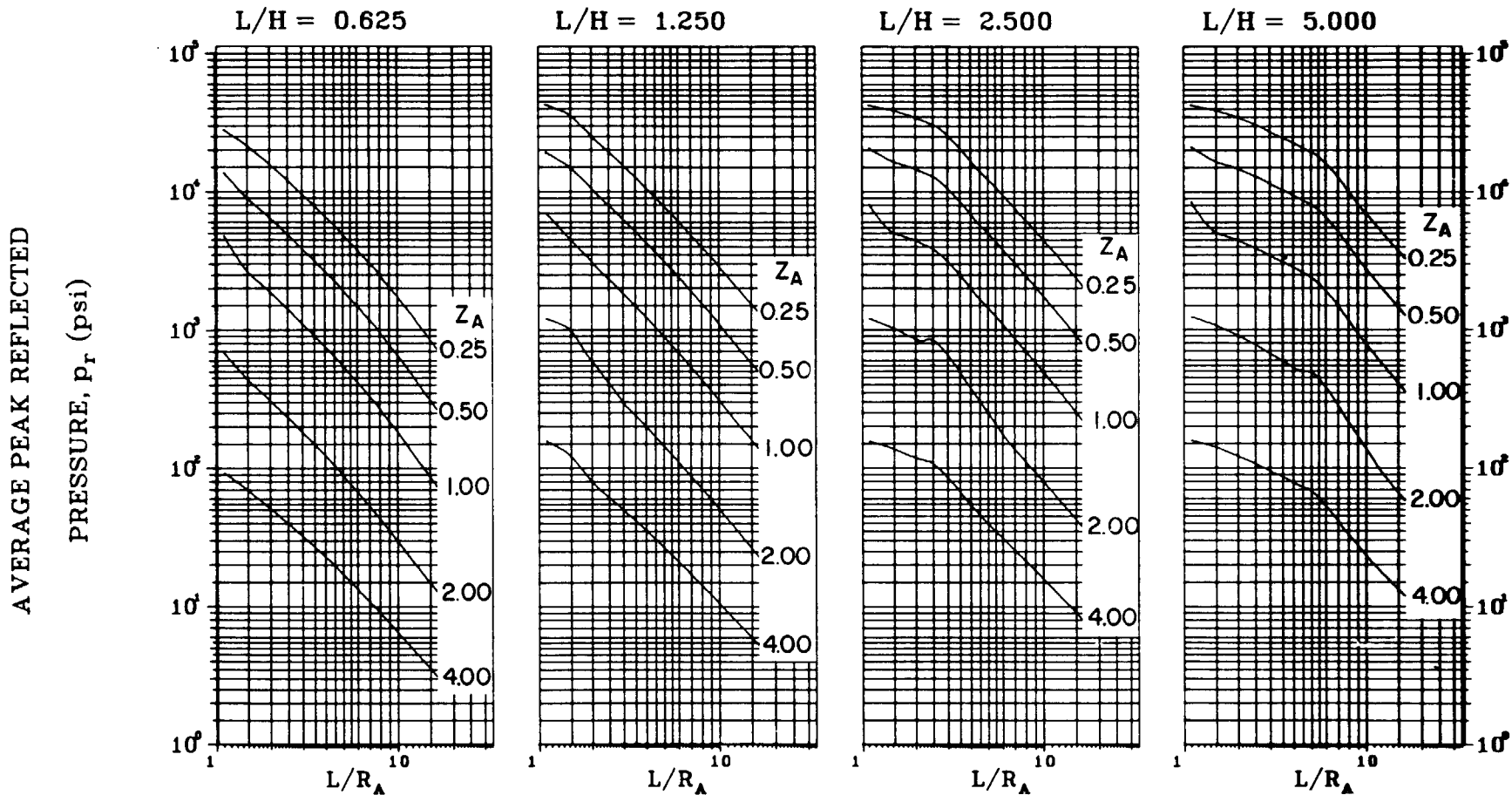


Figure 2-81 Average peak reflected pressure ($N = 3$, $\ell/L = 0.25$ and 0.75 , $h/H = 0.10$)

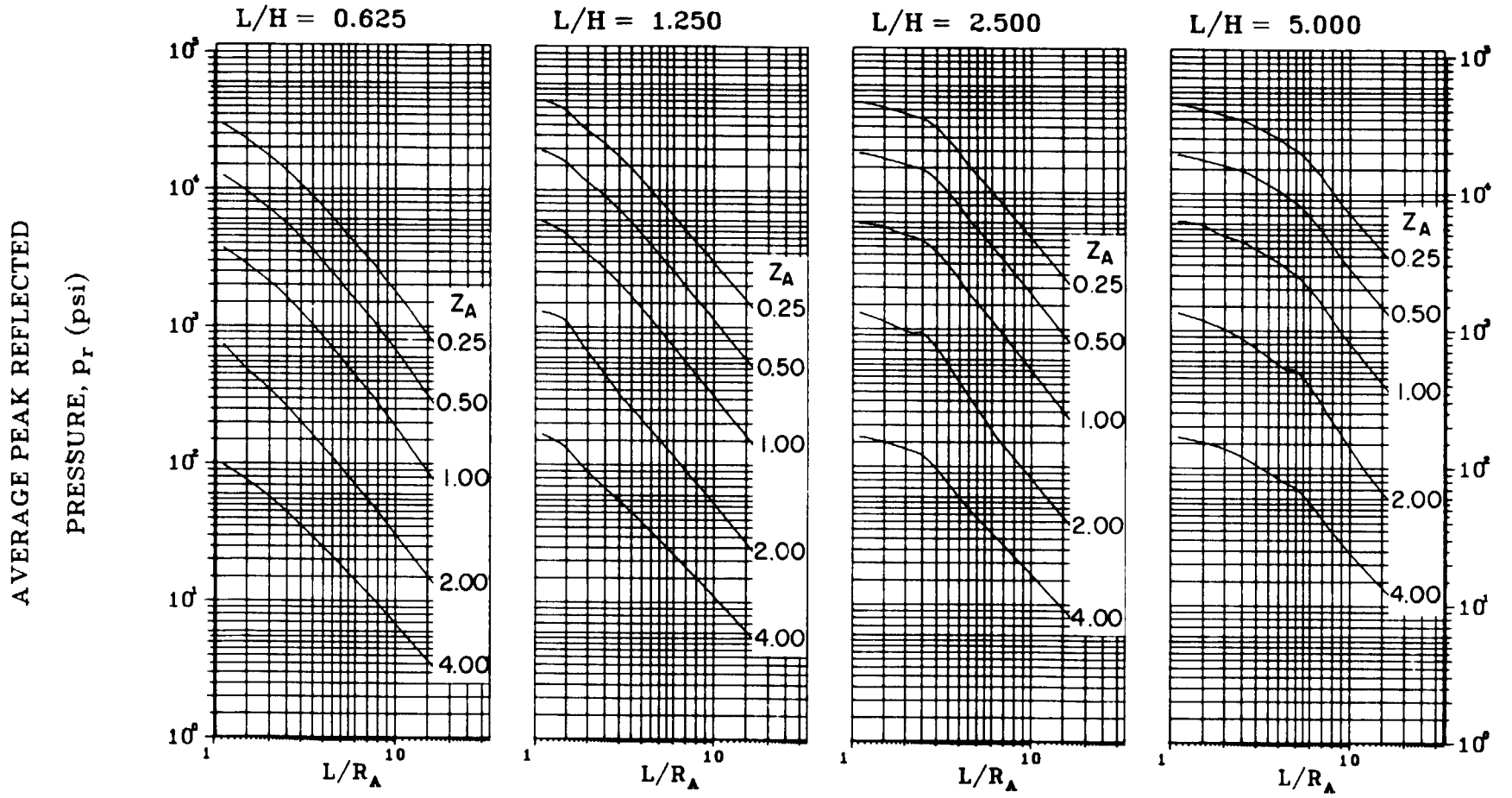


Figure 2-82 Average peak reflected pressure ($N = 3, \ell/L = 0.50, h/H = 0.10$)

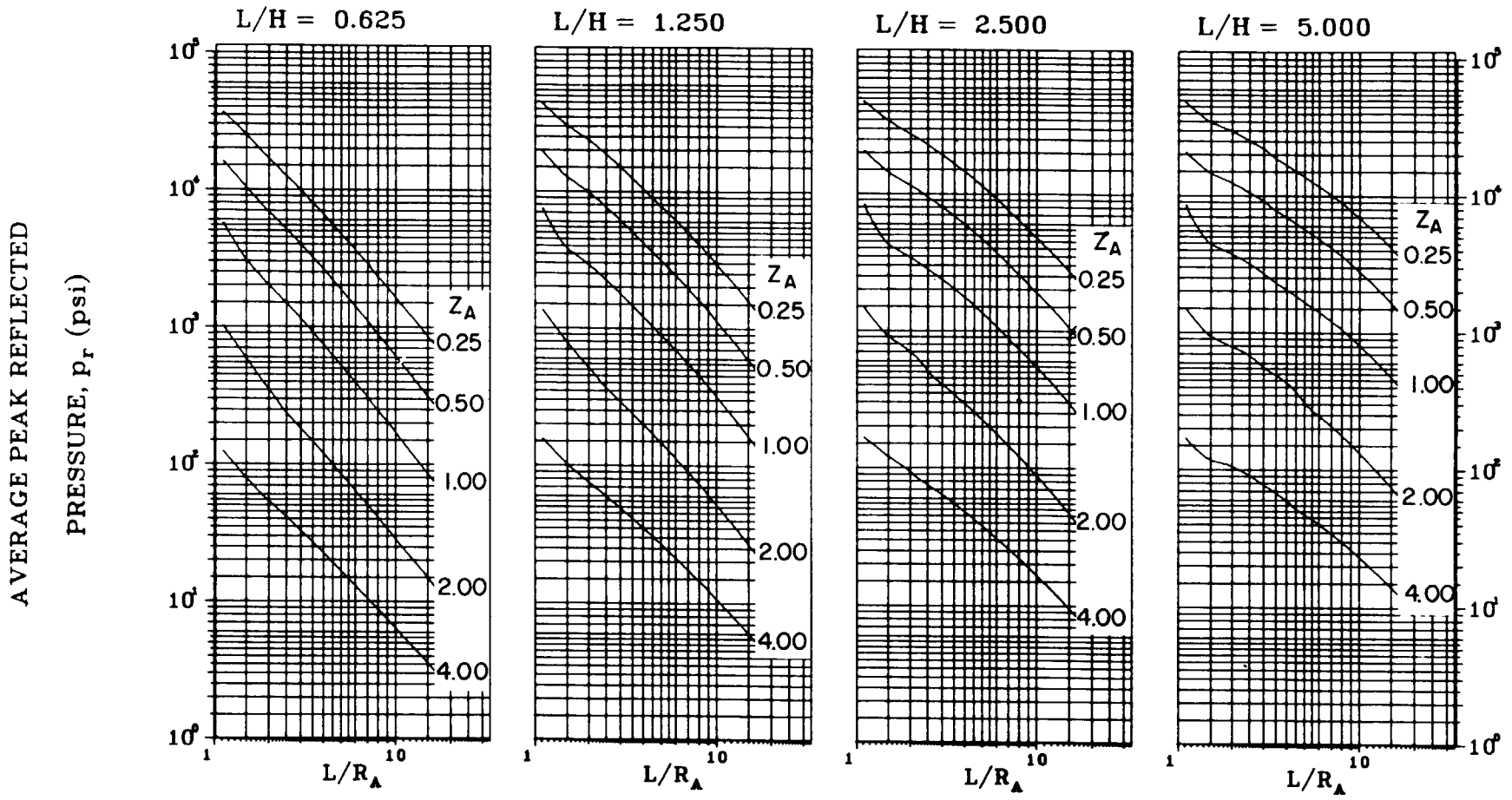
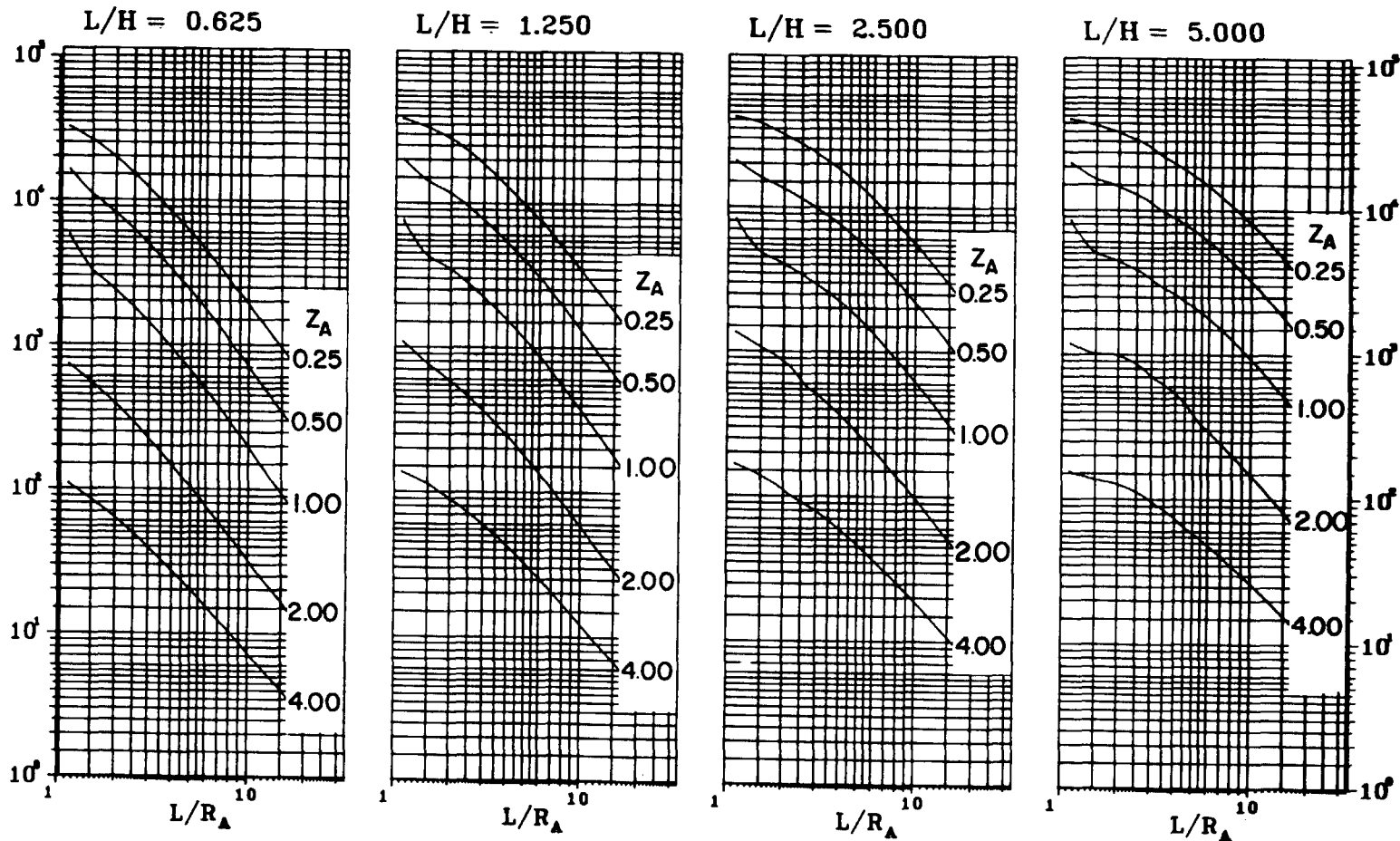


Figure 2-83 Average peak reflected pressure ($N = 3, \ell/L = 0.10, h/H = 0.25$)

AVERAGE PEAK REFLECTED

PRESSURE, p_r (psi)



33B

Figure 2-84 Average peak reflected pressure ($N = 3$, $\ell/L = 0.25$ and 0.75 , $h/H = 0.25$)

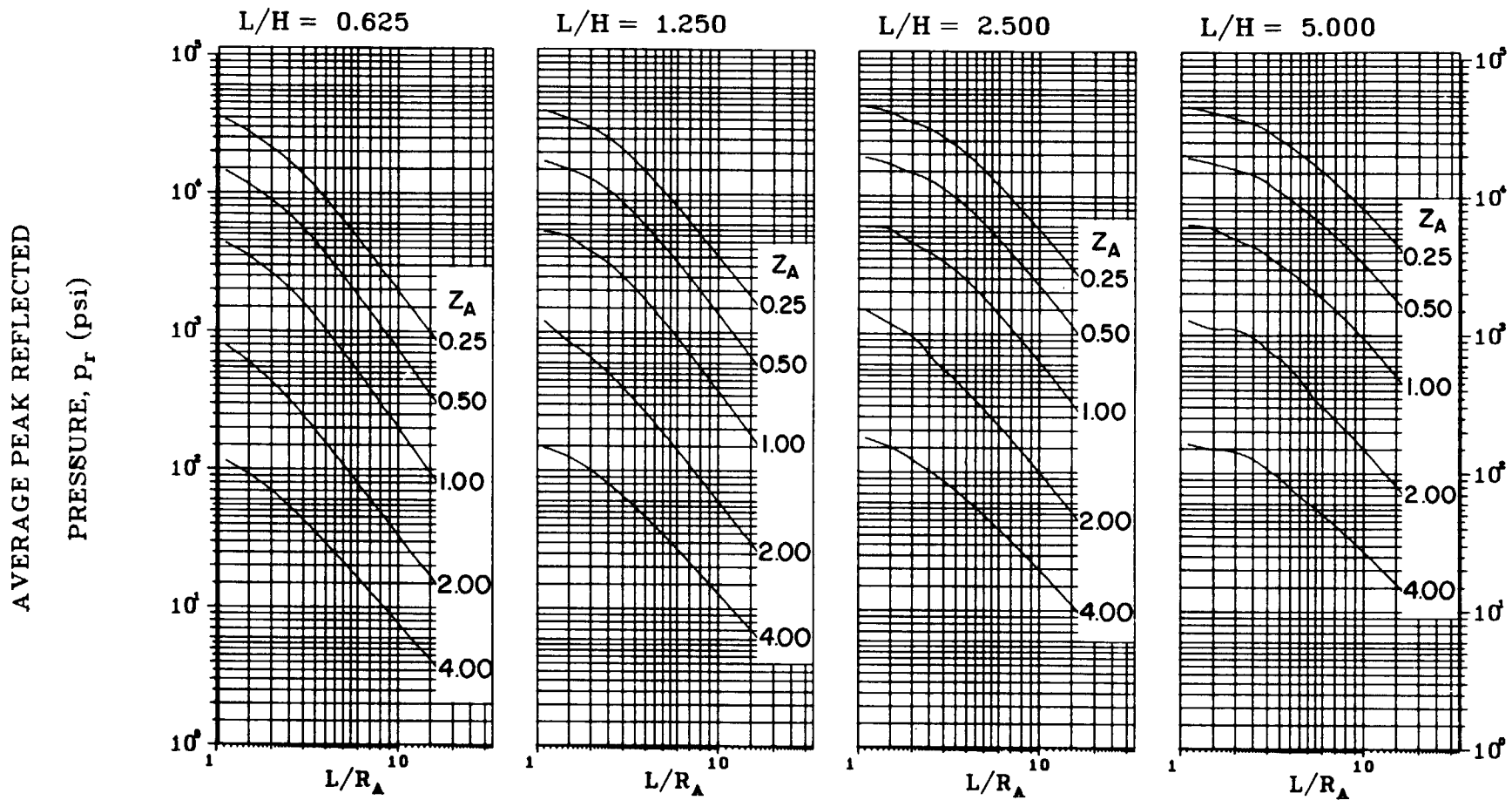


Figure 2-85 Average peak reflected pressure ($N = 3$, $\ell/L = 0.50$, $h/H = 0.25$)

AVERAGE PEAK REFLECTED

PRESSURE, p_r (psi)

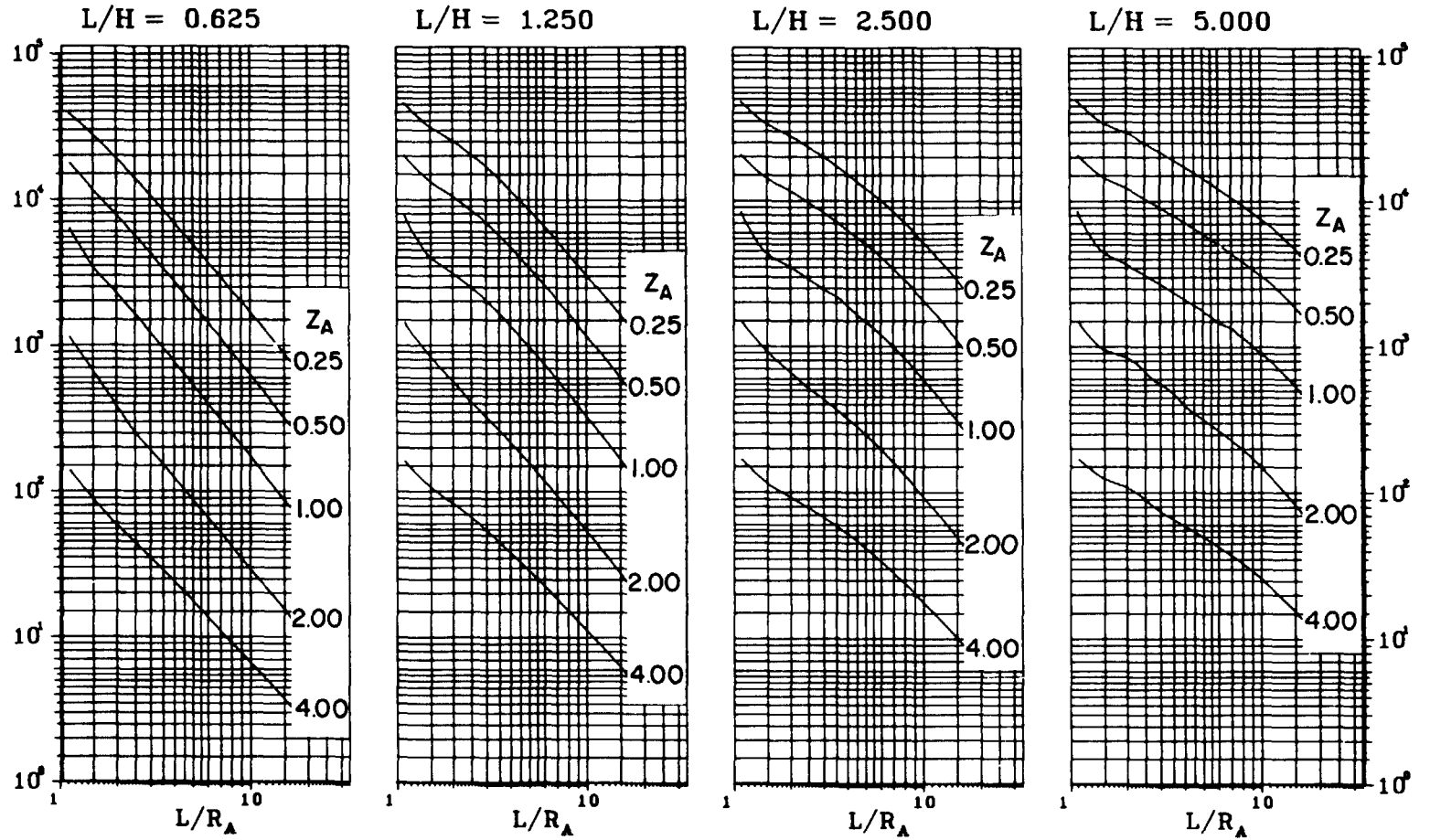
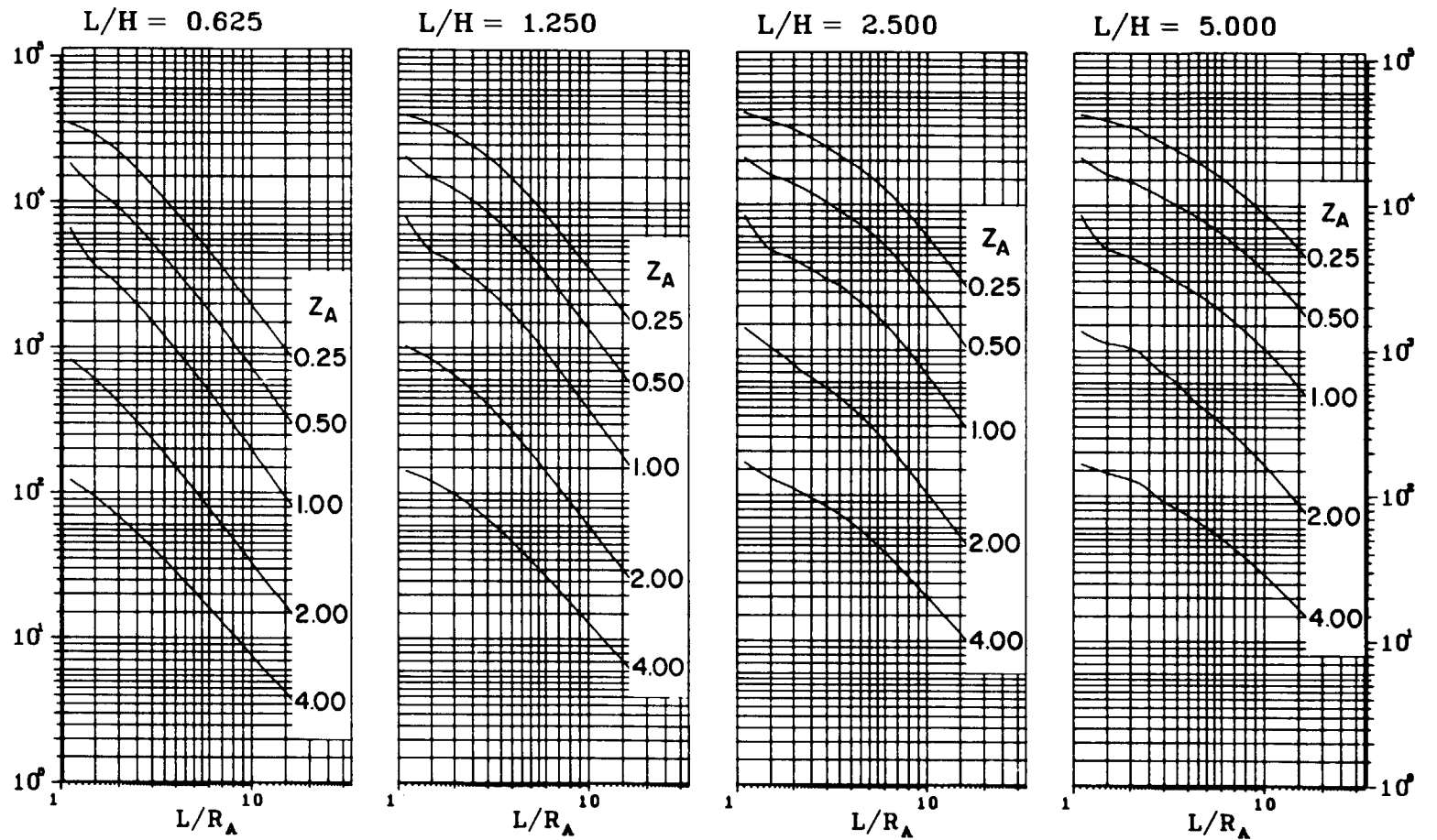


Figure 2-86 Average peak reflected pressure ($N = 3, \ell/L = 0.10, h/H = 0.50$)

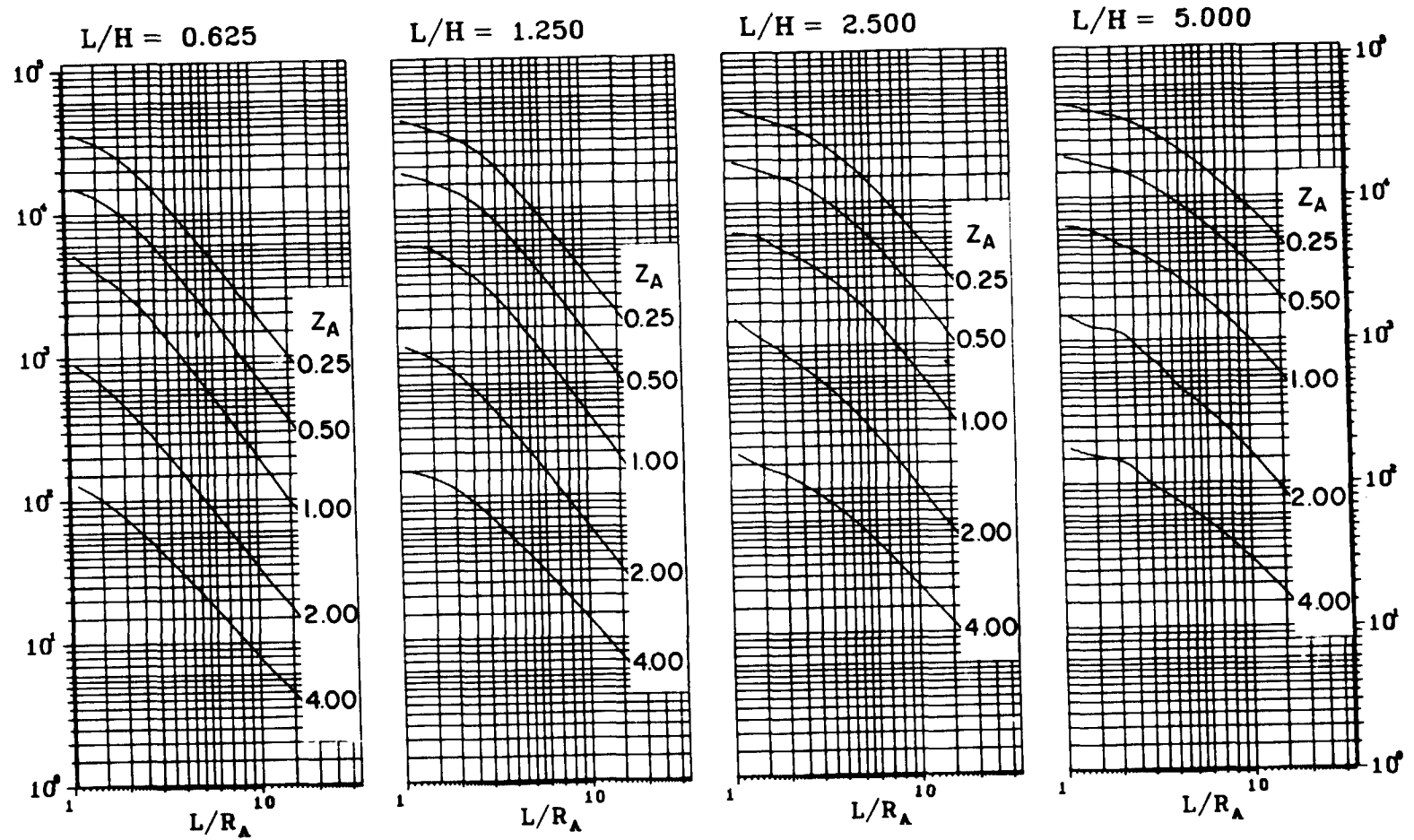
AVERAGE PEAK REFLECTED

PRESSURE, p_r (psi)

36B

Figure 2-87 Average peak reflected pressure ($N = 3$, $\ell/L = 0.25$ and 0.75 , $h/H = 0.50$)

AVERAGE PEAK REFLECTED

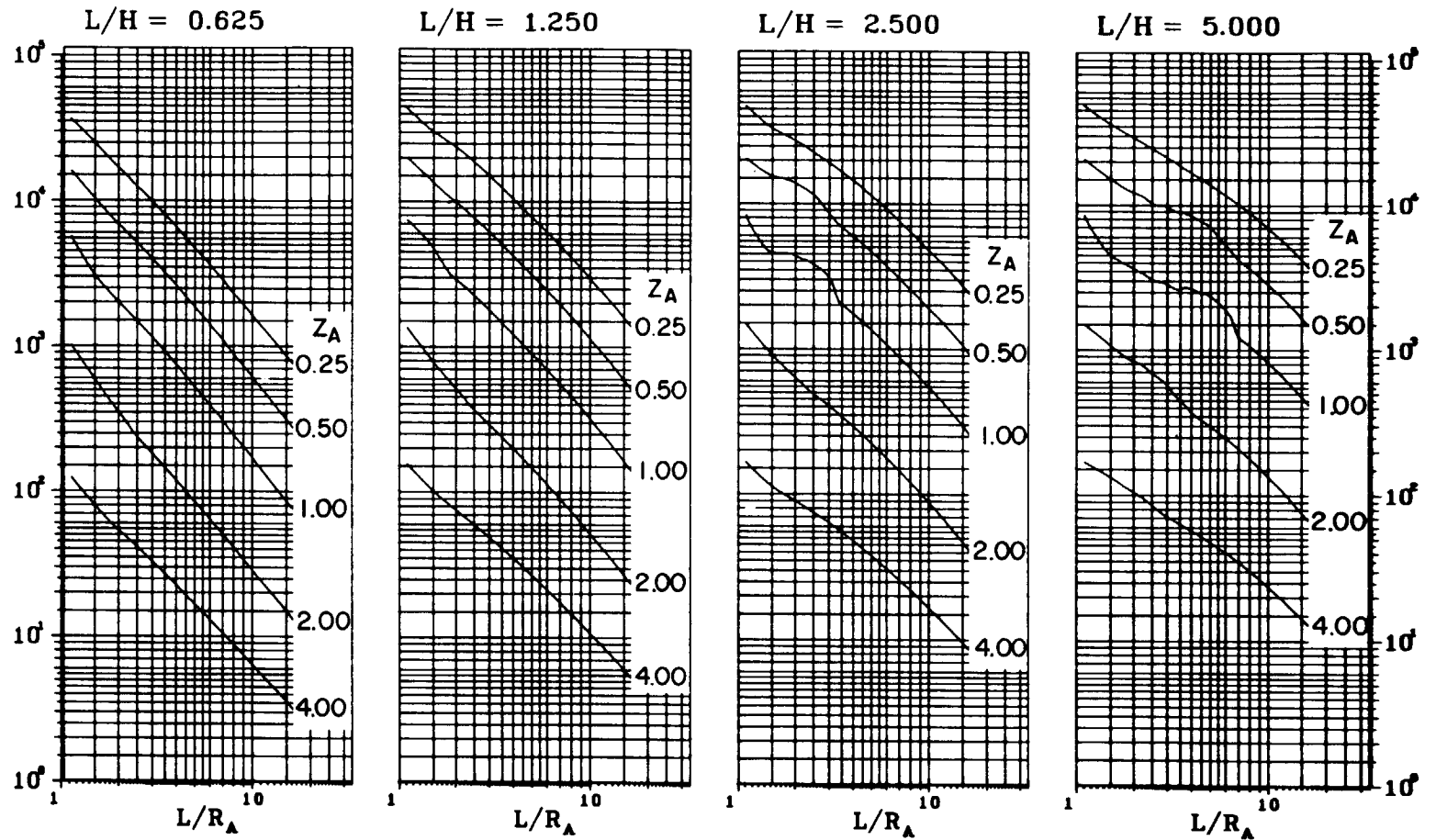
PRESSURE, p_r (psi)

37B

Figure 2-88 Average peak reflected pressure ($N = 3$, $\ell/L = 0.50$, $h/H = 0.50$)

AVERAGE PEAK REFLECTED

PRESSURE, P_r (psi)



38B

Figure 2-89 Average peak reflected pressure ($N = 3, \ell/L = 0.10, h/H = 0.75$)

AVERAGE PEAK REFLECTED

PRESSURE, p_r (psi)

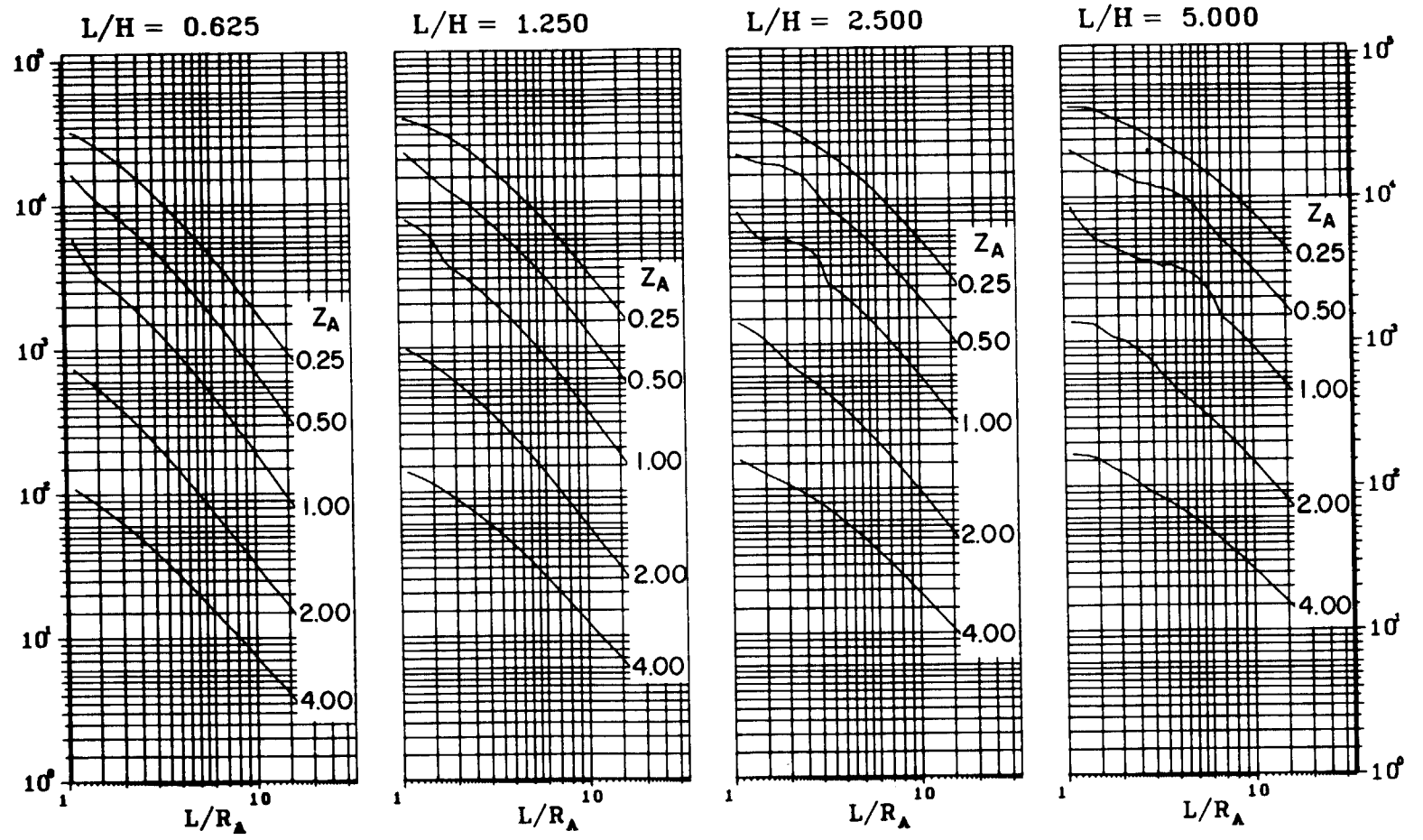


Figure 2-90 Average peak reflected pressure ($N = 3$, $l/L = 0.25$ and 0.75 , $h/H = 0.75$)

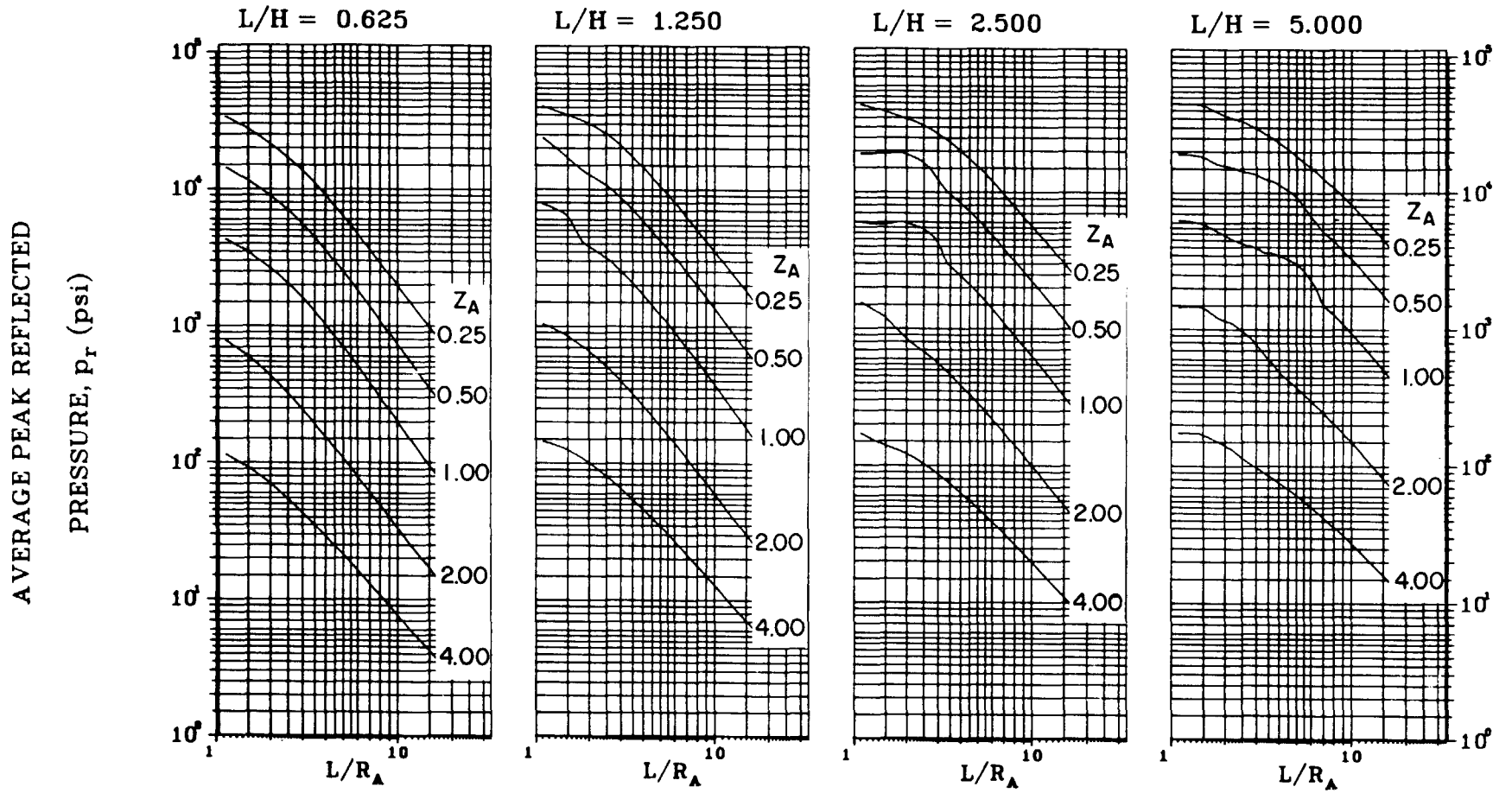
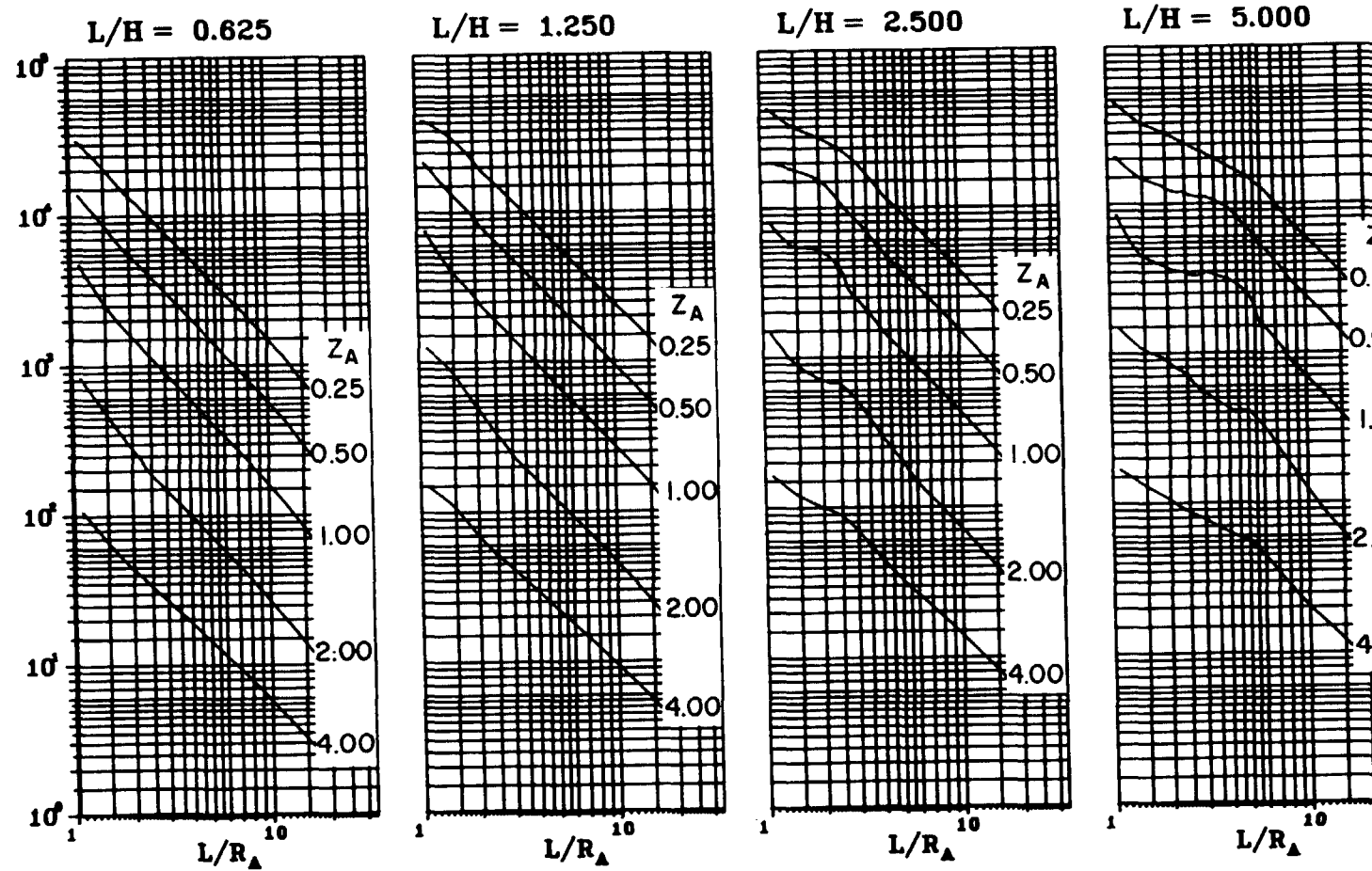


Figure 2-91 Average peak reflected pressure ($N = 3, \ell/L = 0.50, h/H = 0.75$)

AVERAGE PEAK REFLECTED

PRESSURE, p_r (psi)

41B

Figure 2-92 Average peak reflected pressure ($N = 4$, $l/L = 0.10$, $h/H = 0.10$)

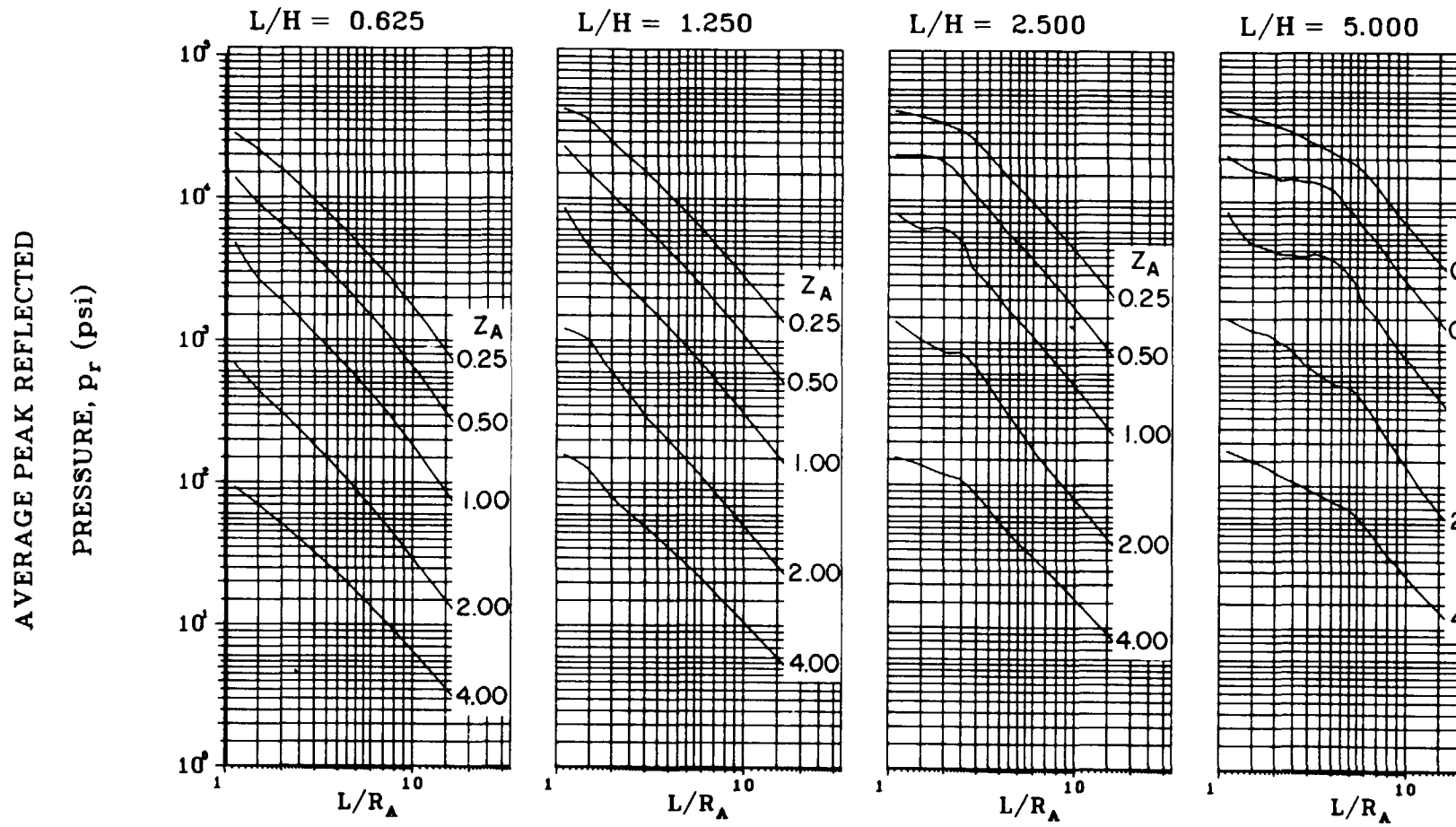
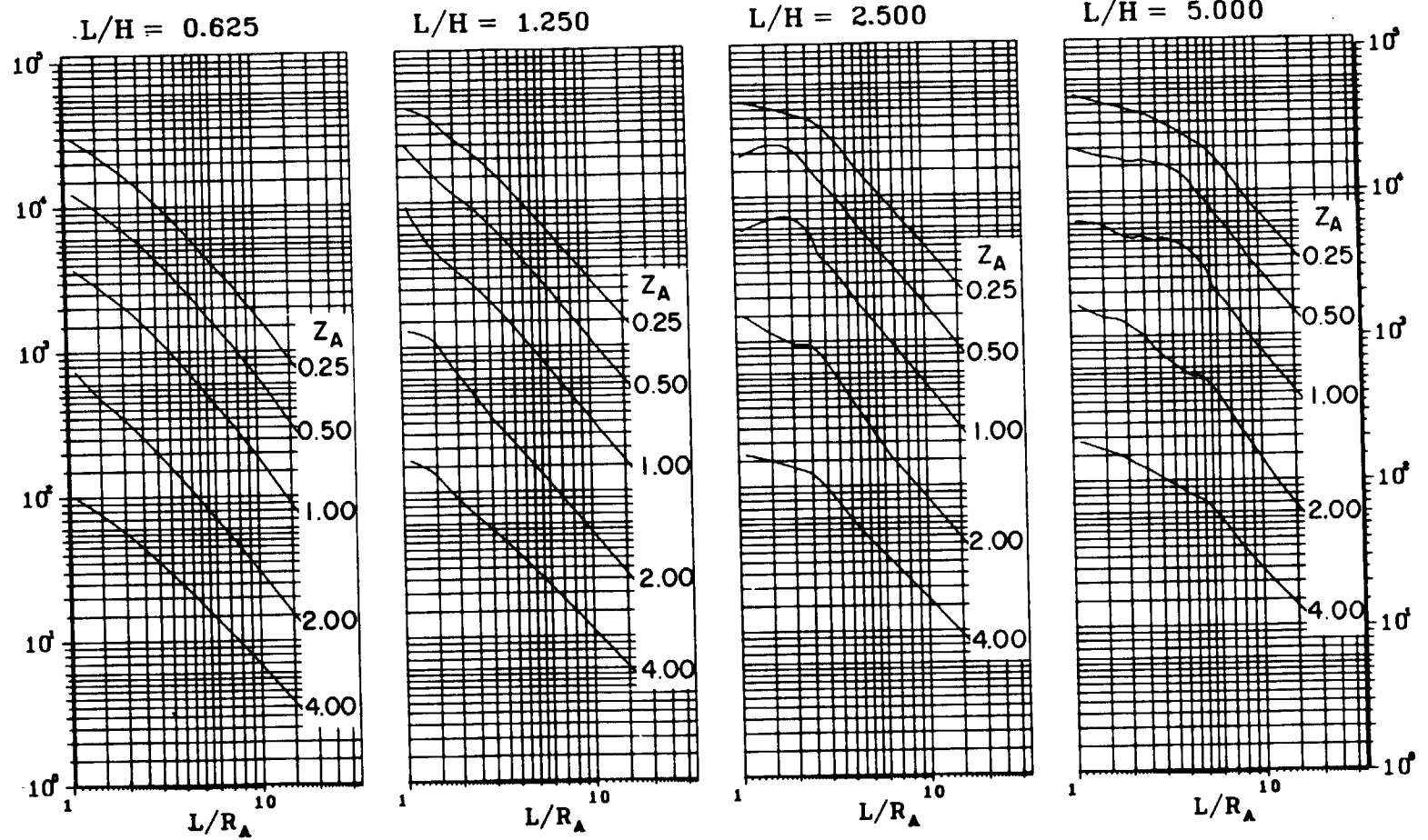


Figure 2-93 Average peak reflected pressure ($N = 4$, $\ell/L = 0.25$ and 0.75 , $h/H = 0.10$)

AVERAGE PEAK REFLECTED

PRESSURE, p_r (psi)

43B

Figure 2-94 Average peak reflected pressure ($N = 4$, $\ell/L = 0.50$, $h/H = 0.10$)

AVERAGE PEAK REFLECTED
PRESSURE, p_r (psi)

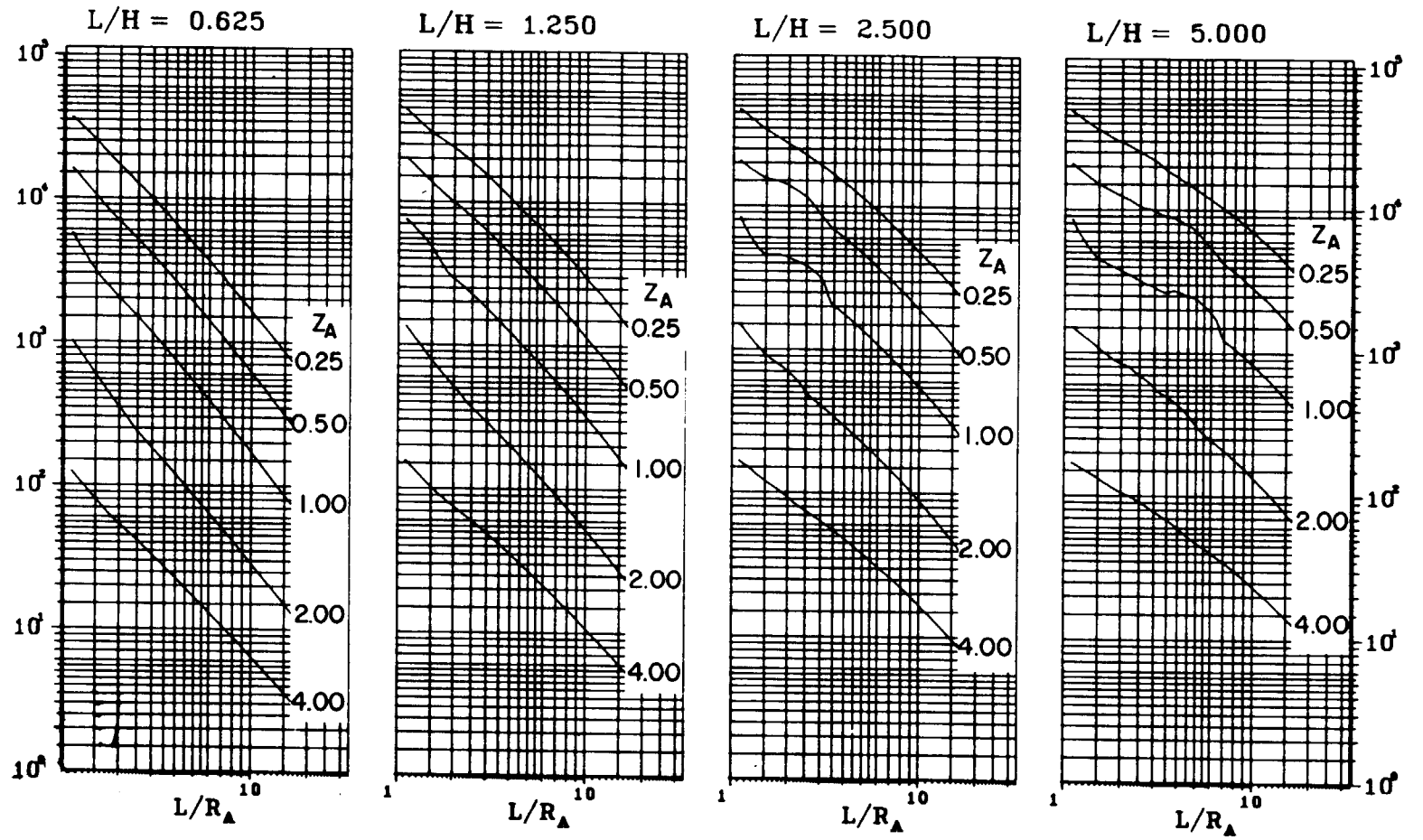


Figure 2-95 Average peak reflected pressure ($N = 4$, $l/L = 0.10$, $h/H = 0.25$ and 0.75)

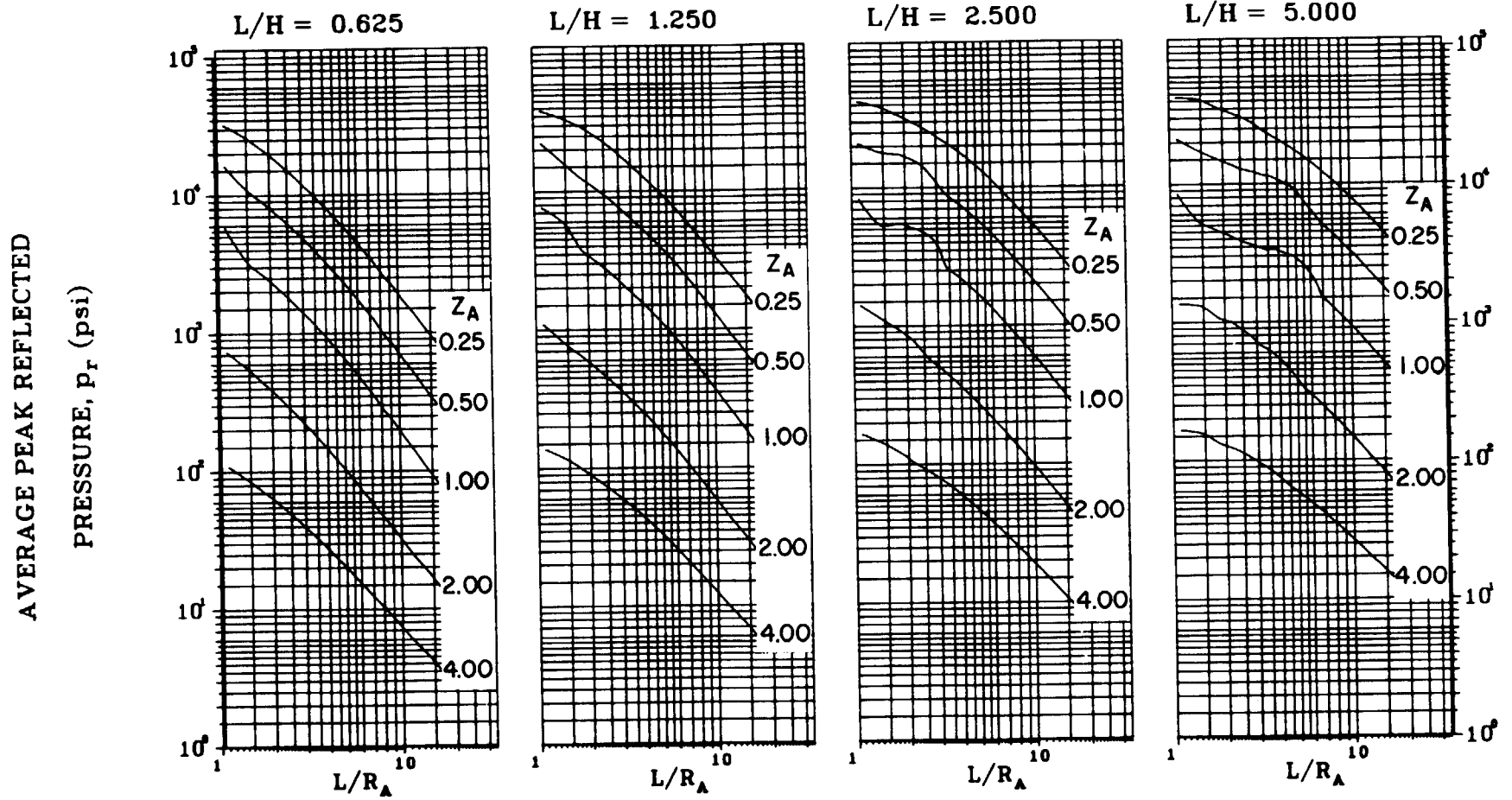


Figure 2-96 Average peak reflected pressure ($N = 4$, $l/L = 0.25$ and 0.75 , $h/H = 0.25$ and 0.75)

AVERAGE PEAK REFLECTED

PRESSURE, p_r (psi)

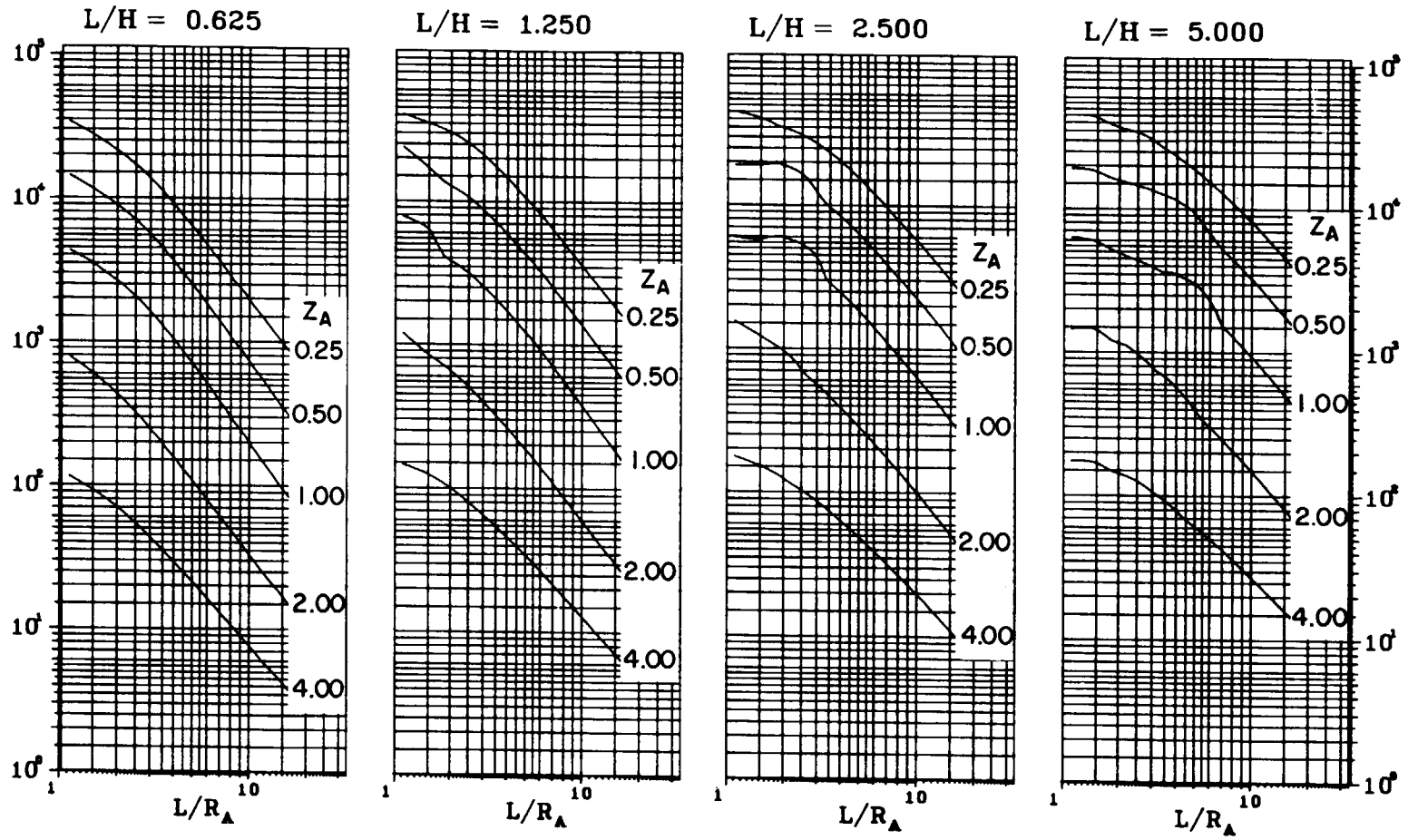


Figure 2-97 Average peak reflected pressure ($N = 4$, $l/L = 0.50$, $h/H = 0.25$ and 0.75)

AVERAGE PEAK REFLECTED

PRESSURE, p_r (psi)

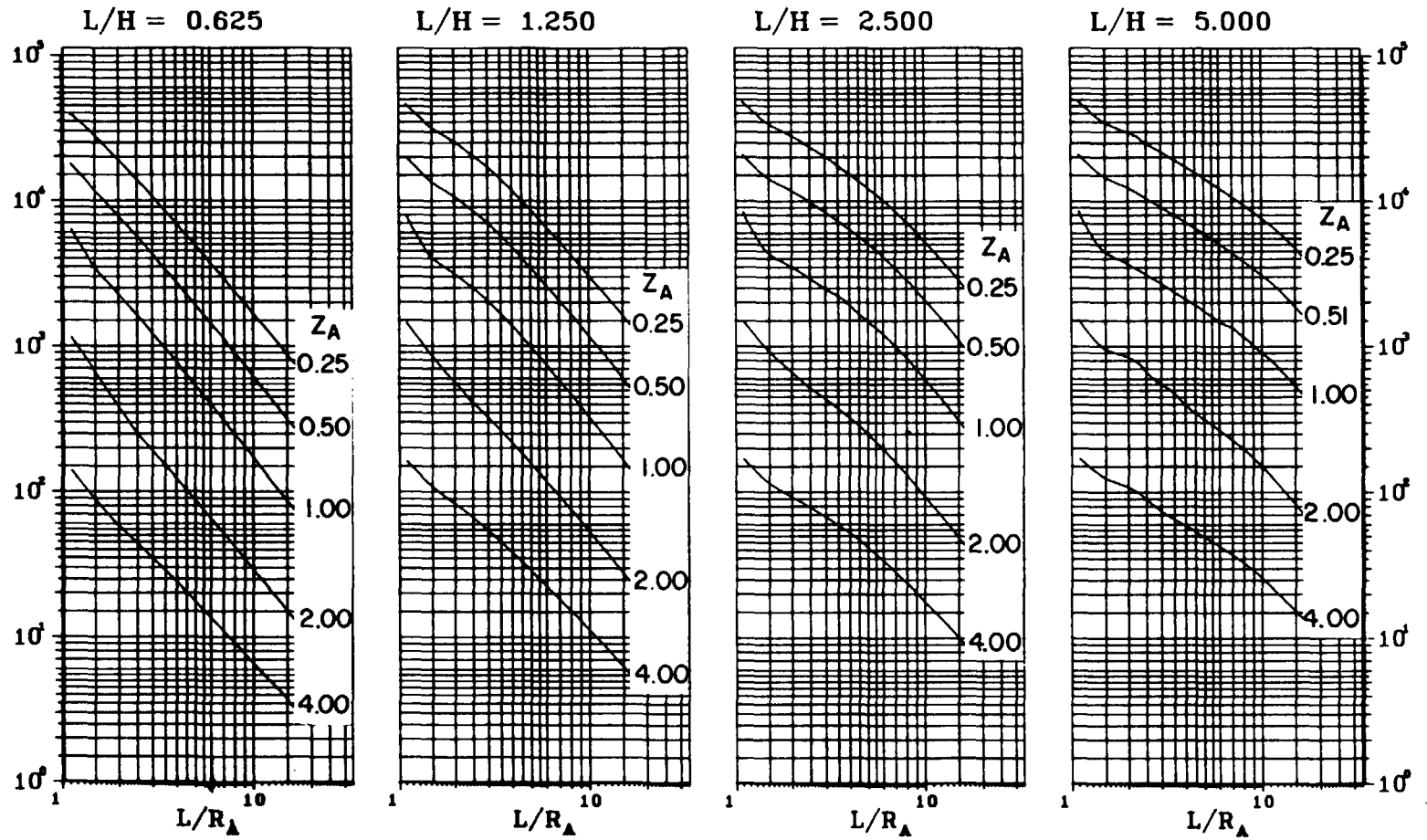


Figure 2-98 Average peak reflected pressure ($N = 4.0$, $\beta = 0.10$, $b/H = 0.50$)

AVERAGE PEAK REFLECTED

PRESSURE, p_r (psi)

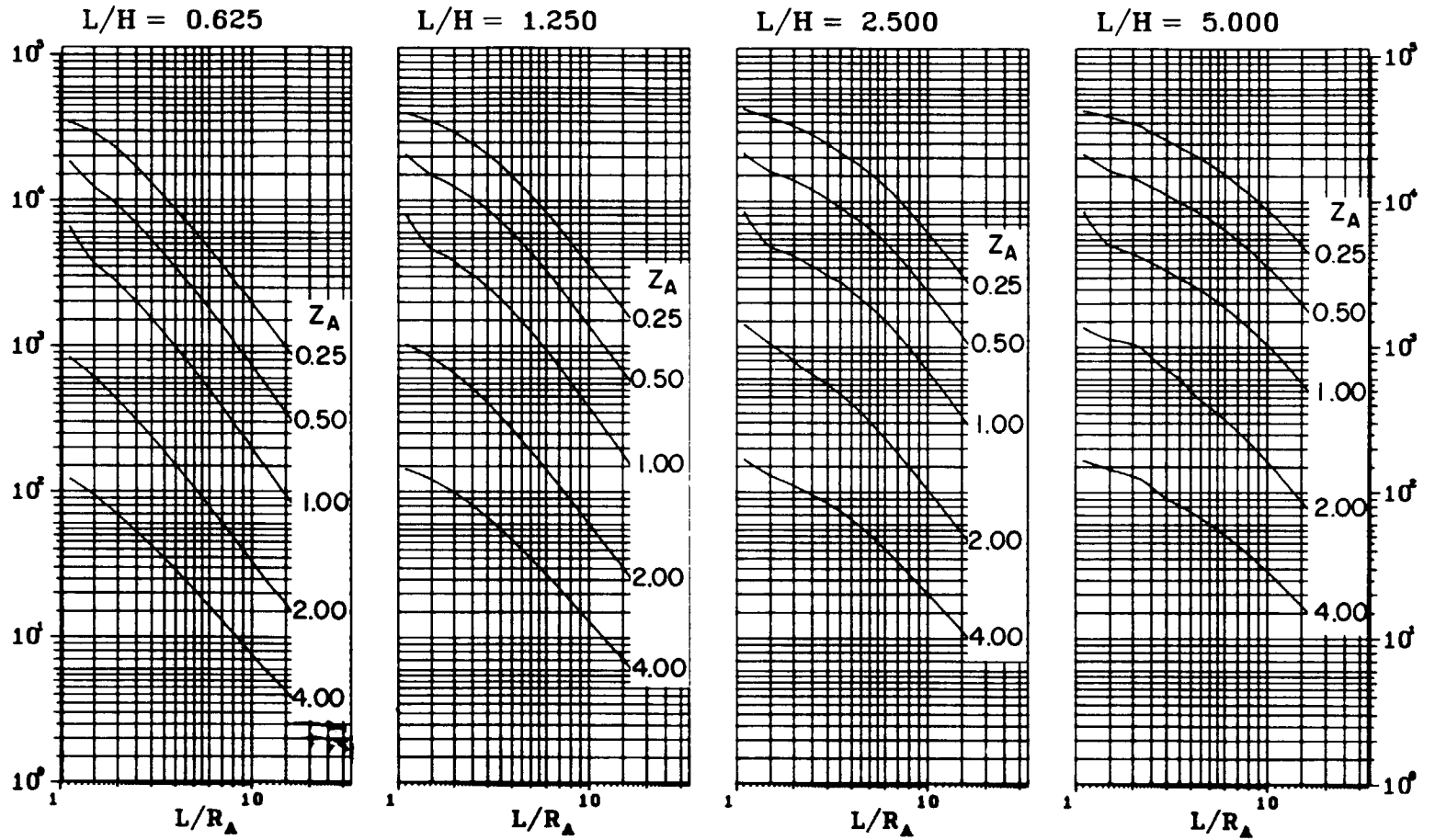


Figure 2-99 Average peak reflected pressure
 ($N = 4$, $l/L = 0.25$ and 0.75 , $h/H = 0.50$)

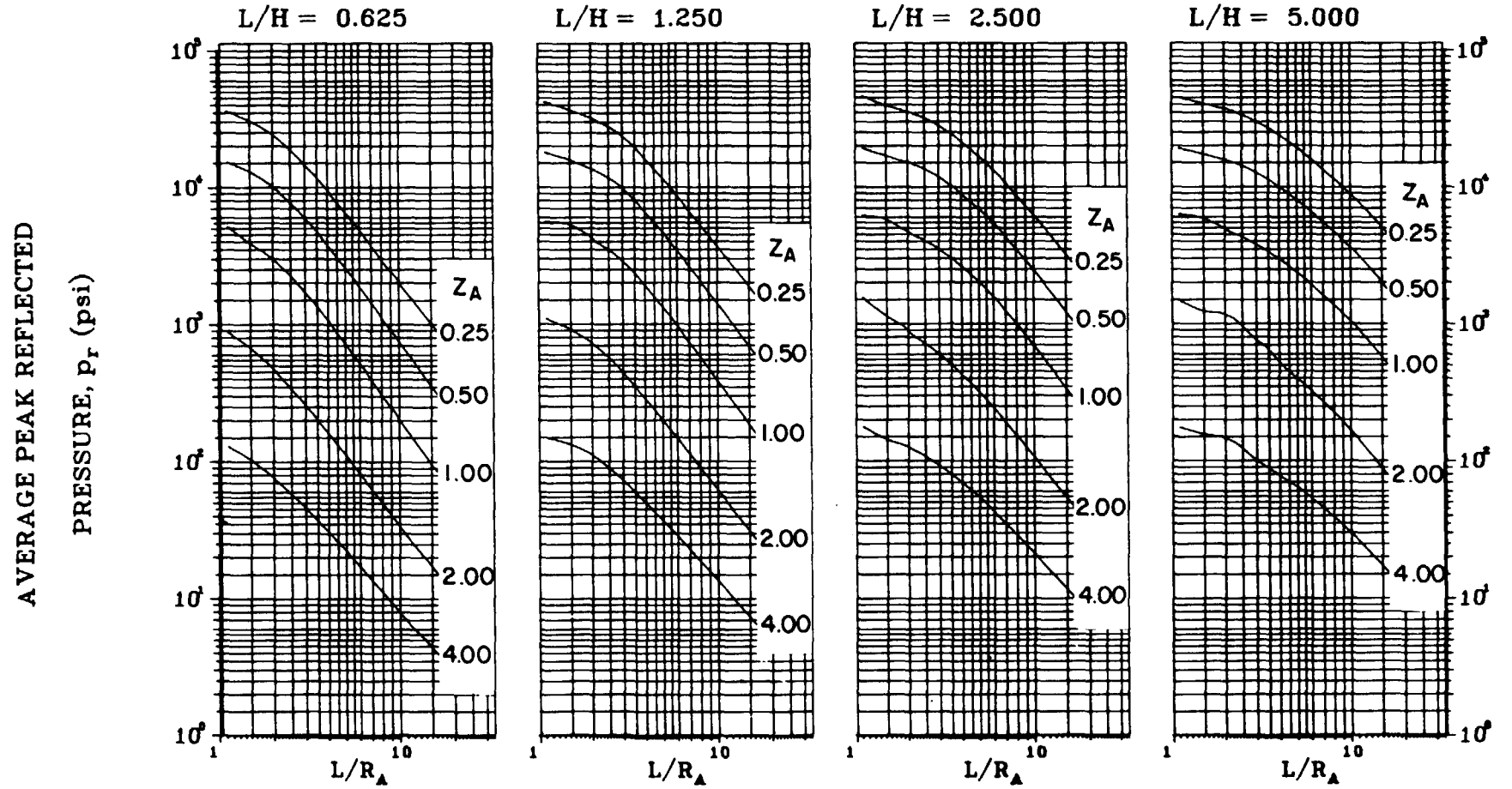


Figure 2-100 Average peak reflected pressure ($N = 4$, $l/L = 0.50$, $h/H = 0.50$)

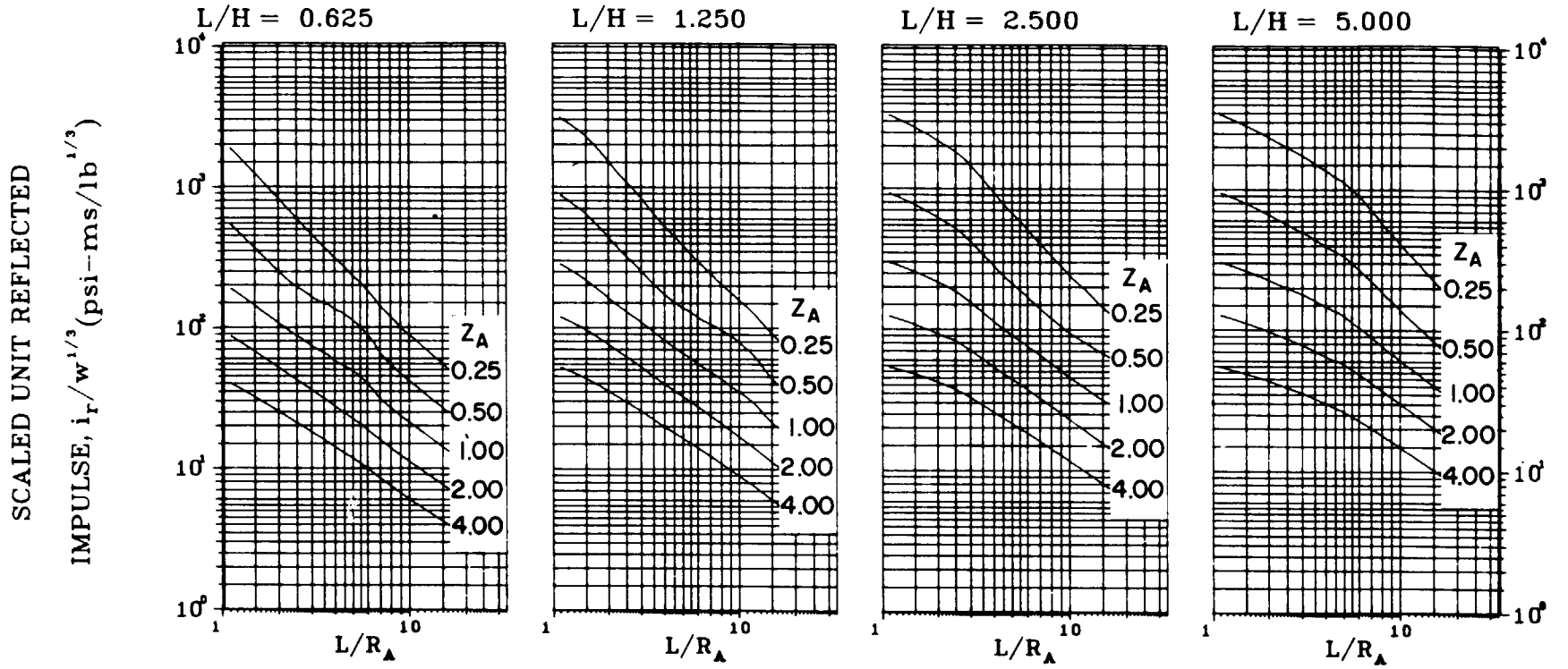
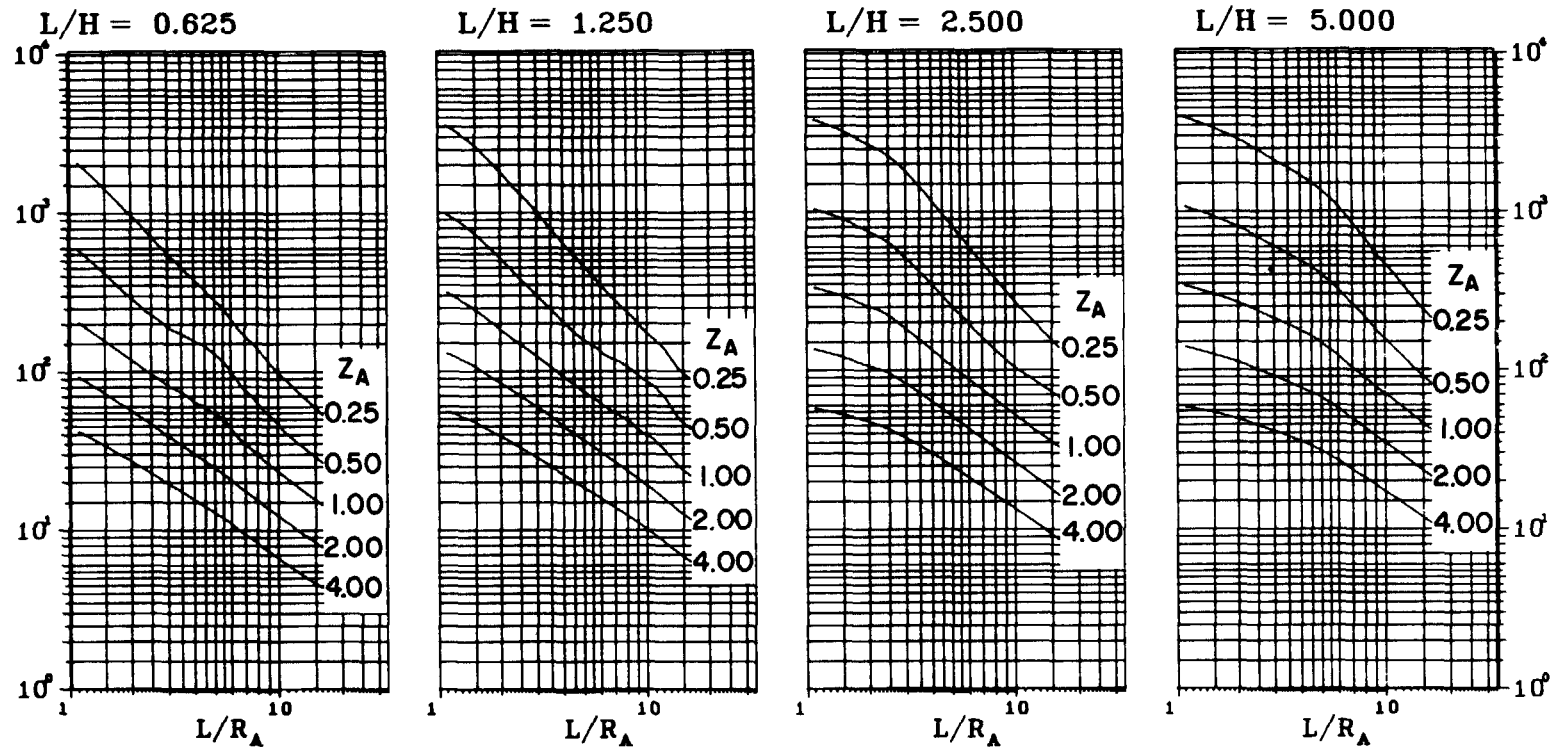


Figure 2-101 Scaled average unit reflected impulse
(N = 1, $\ell/L = 0.10$, $h/H = 0.10$)

SCALED UNIT REFLECTED

IMPULSE, $i_r/w^{1/3}$ (psi-ms/lb^{1/3})



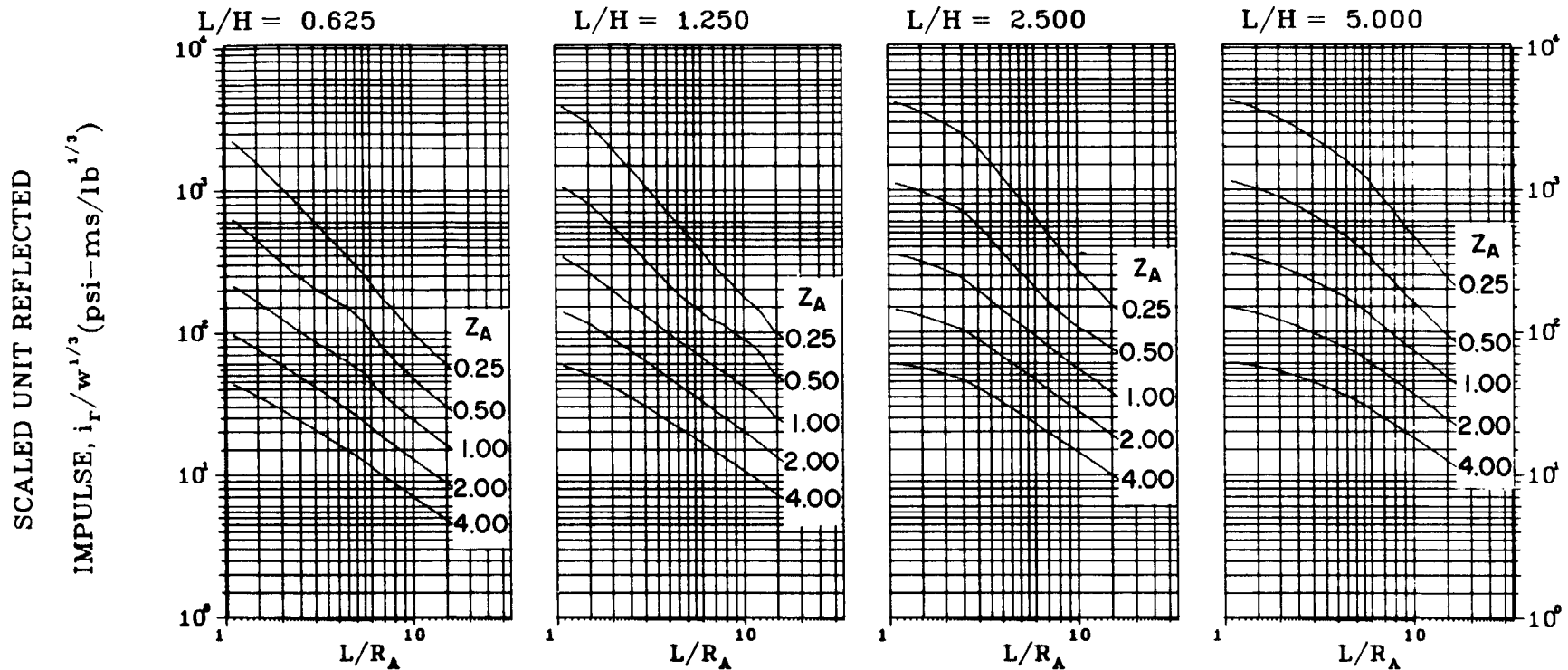


Figure 2-103 Scaled average unit reflected impulse
 ($N = 1, \ell/L = 0.50, h/H = 0.10$)

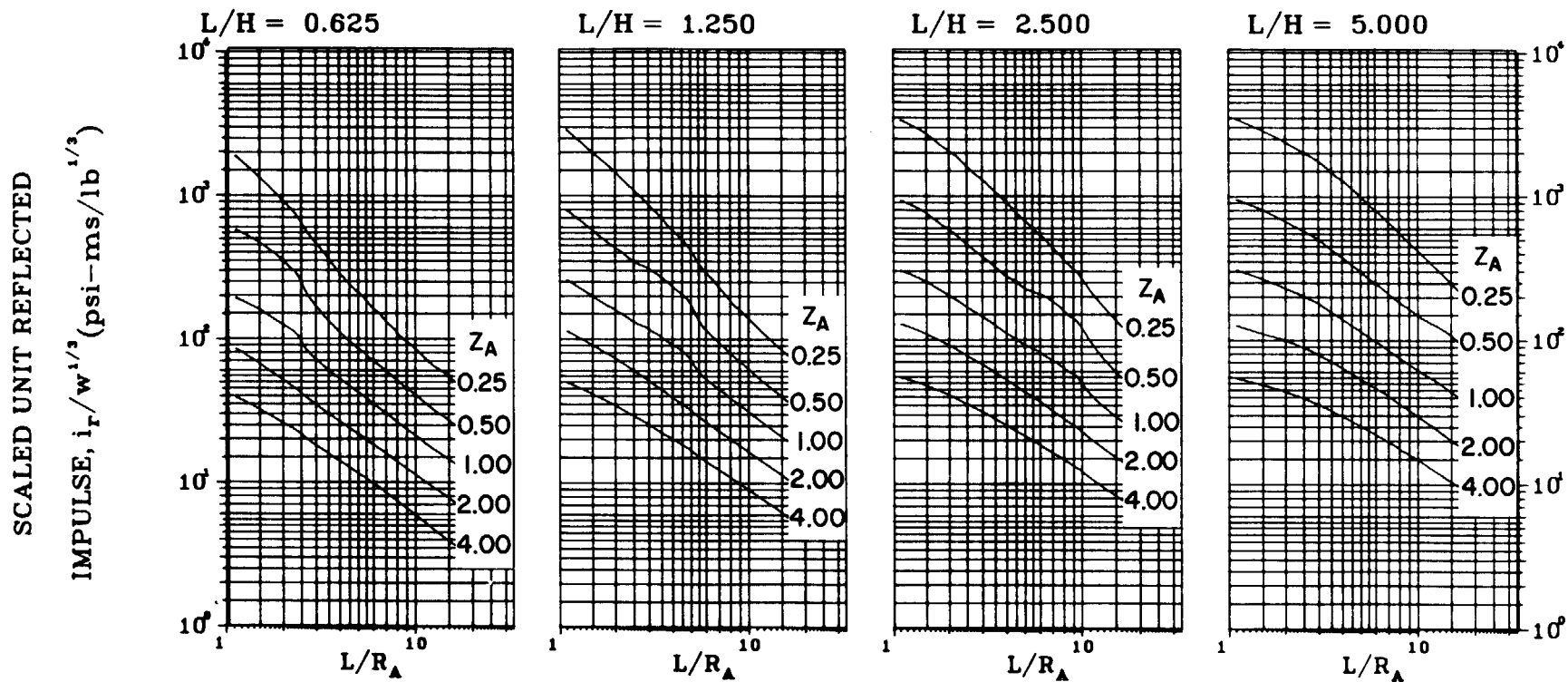


Figure 2-104 Scaled average unit reflected impulse
(N = 1, $\ell/L = 0.10$, $h/H = 0.25$)

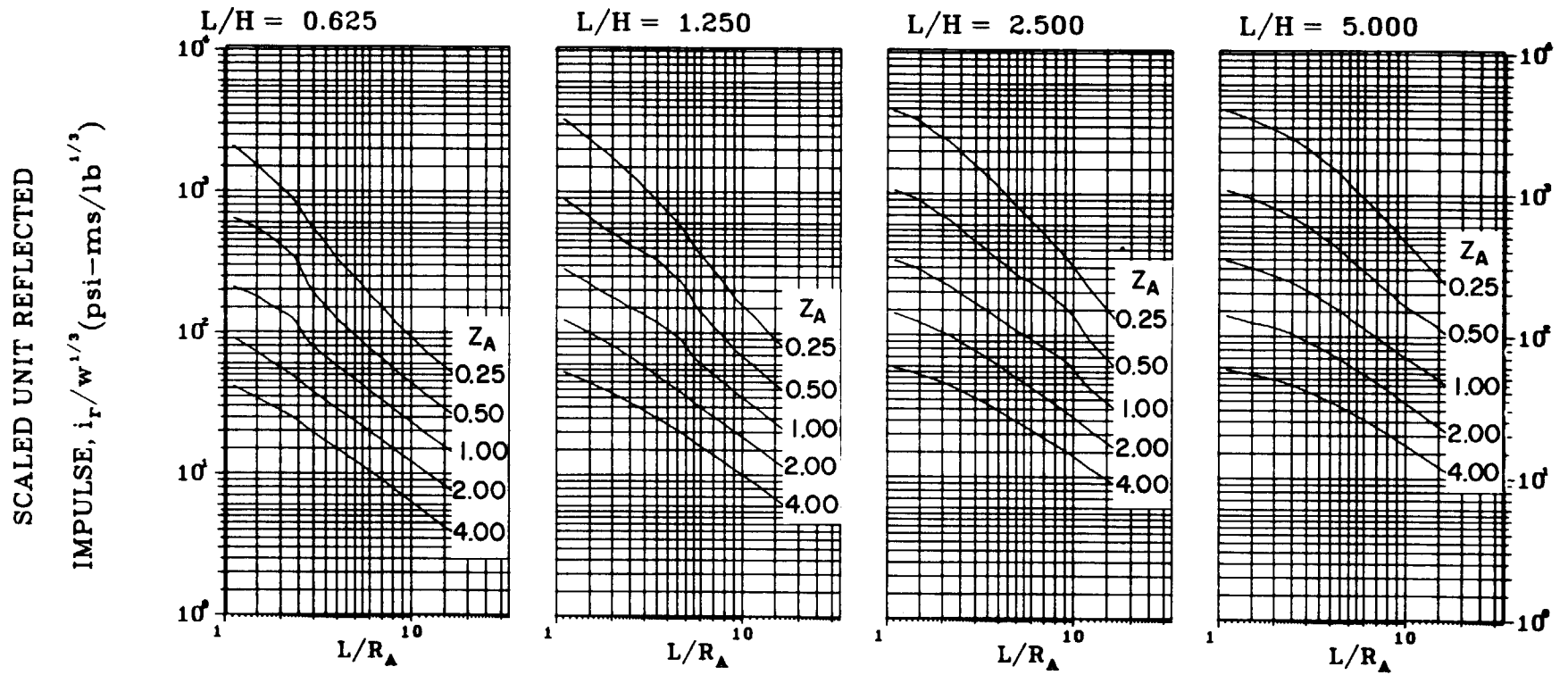


Figure 2-105 Scaled average unit reflected impulse
($N = 1$, $l/L = 0.25$ and 0.75 , $h/H = 0.25$)

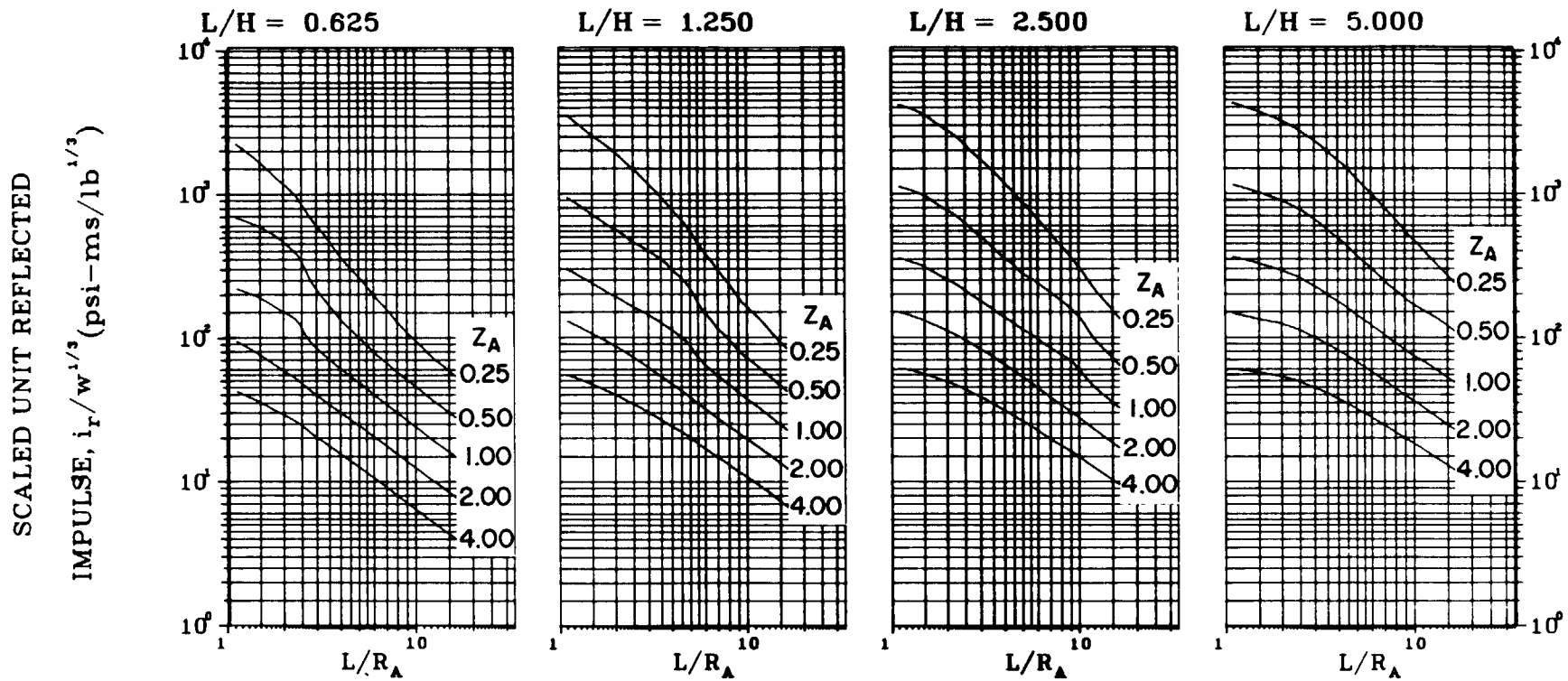


Figure 2-106 Scaled average unit reflected impulse
($N = 1, \ell/L = 0.50, h/H = 0.25$)

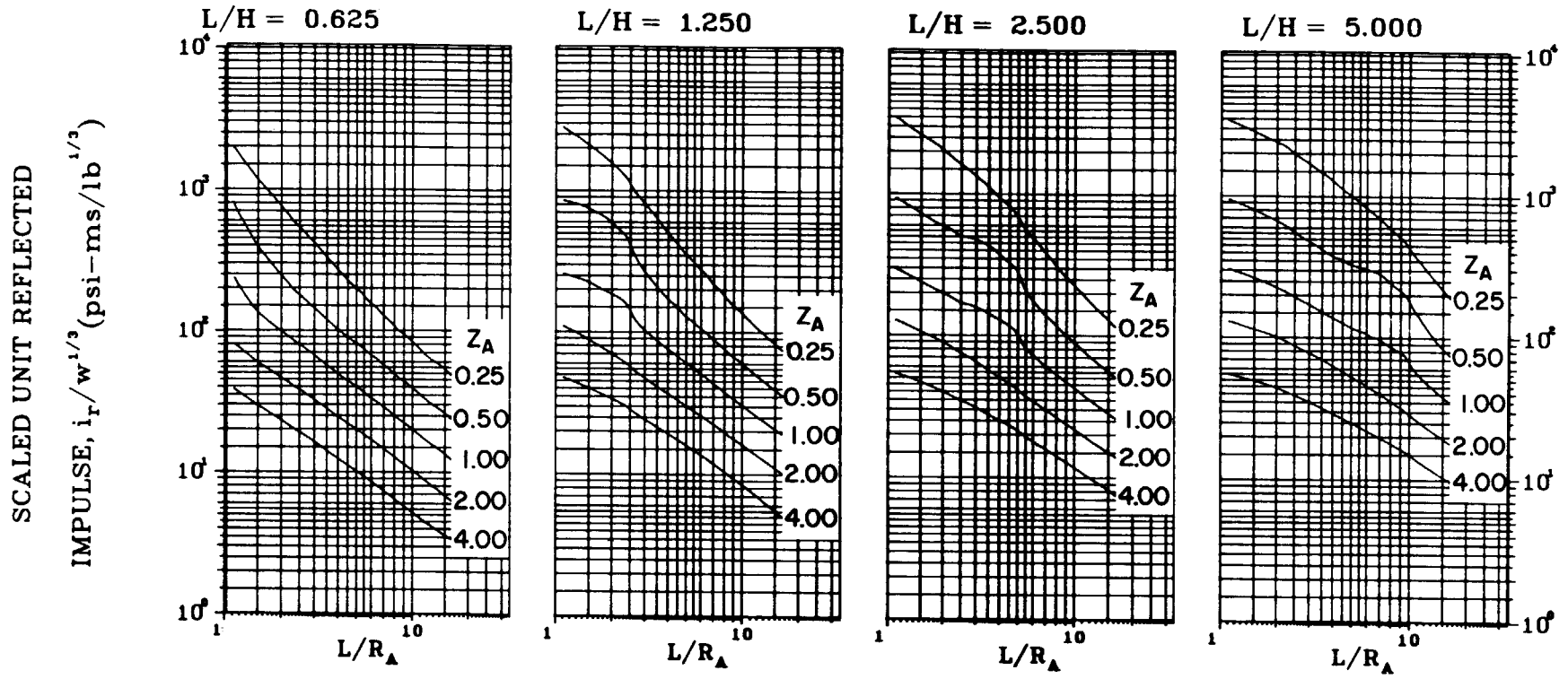


Figure 2-107 Scaled average unit reflected impulse
($N = 1, \ell/L = 0.10, h/H = 0.50$)

SCALED UNIT REFLECTED

IMPULSE, $i_r/w^{1/3}$ (psi-ms/lb^{1/3})

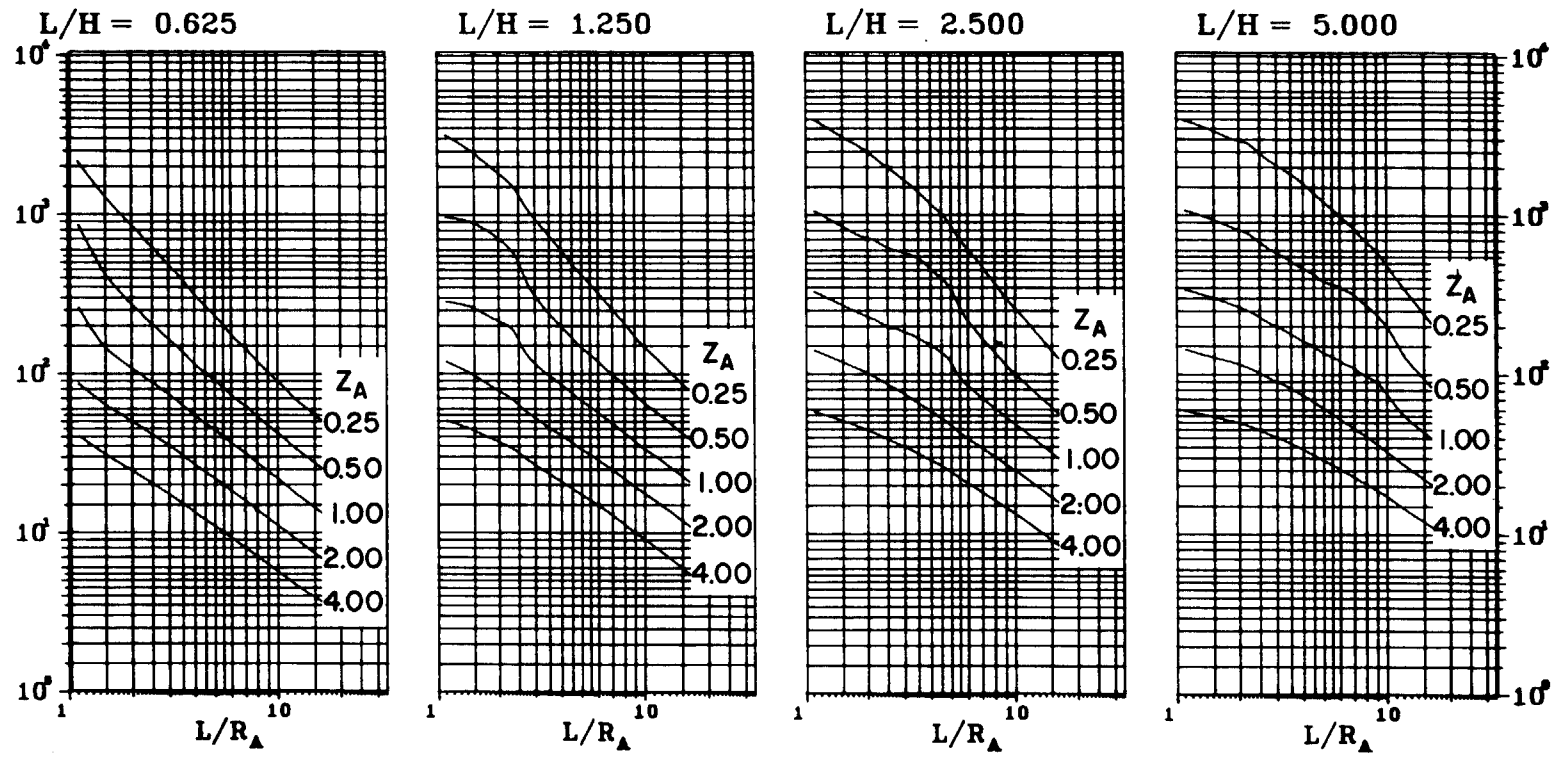


Figure 2-108 Scaled average unit reflected impulse
(N = 1, $\ell/L = 0.25$ and 0.75 , $h/H = 0.50$)

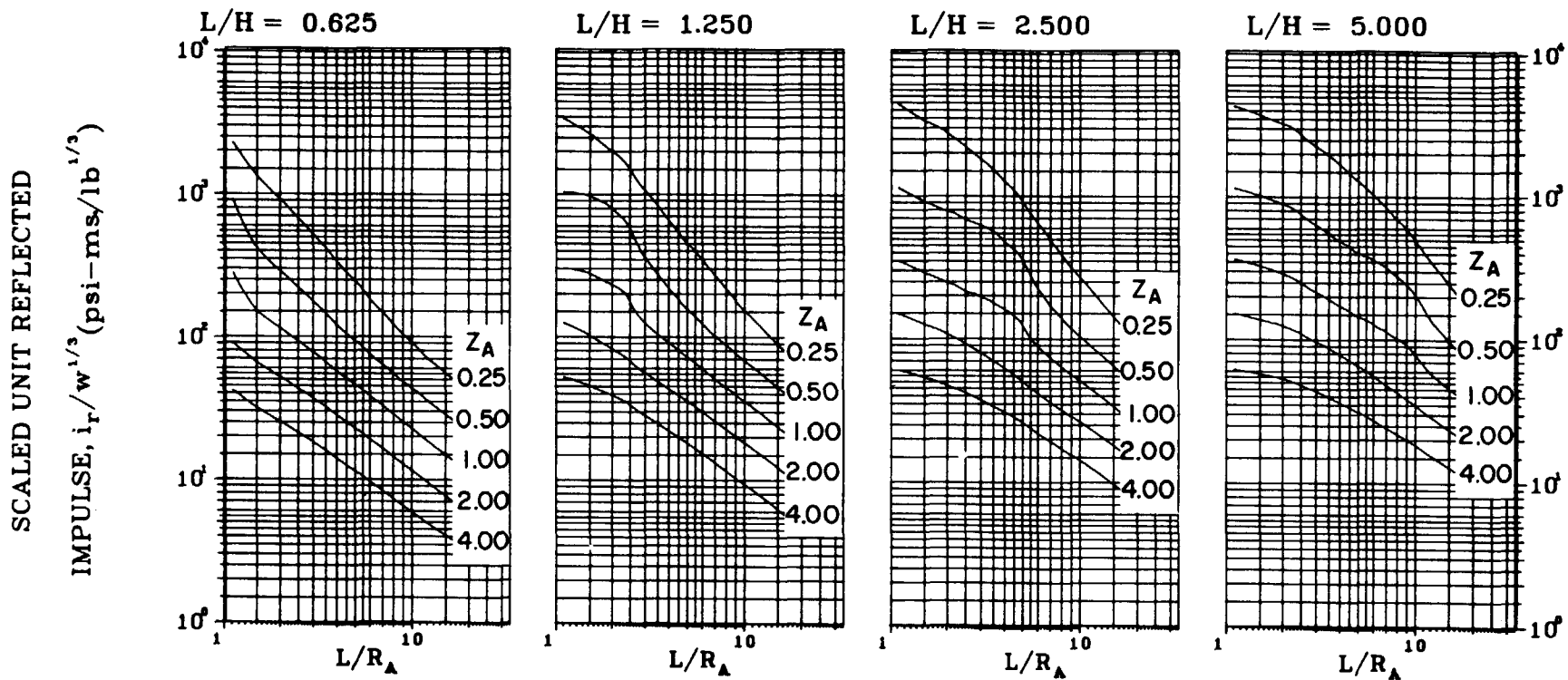


Figure 2-109 Scaled average unit reflected impulse
($N = 1, \ell/L = 0.50, h/H = 0.50$)

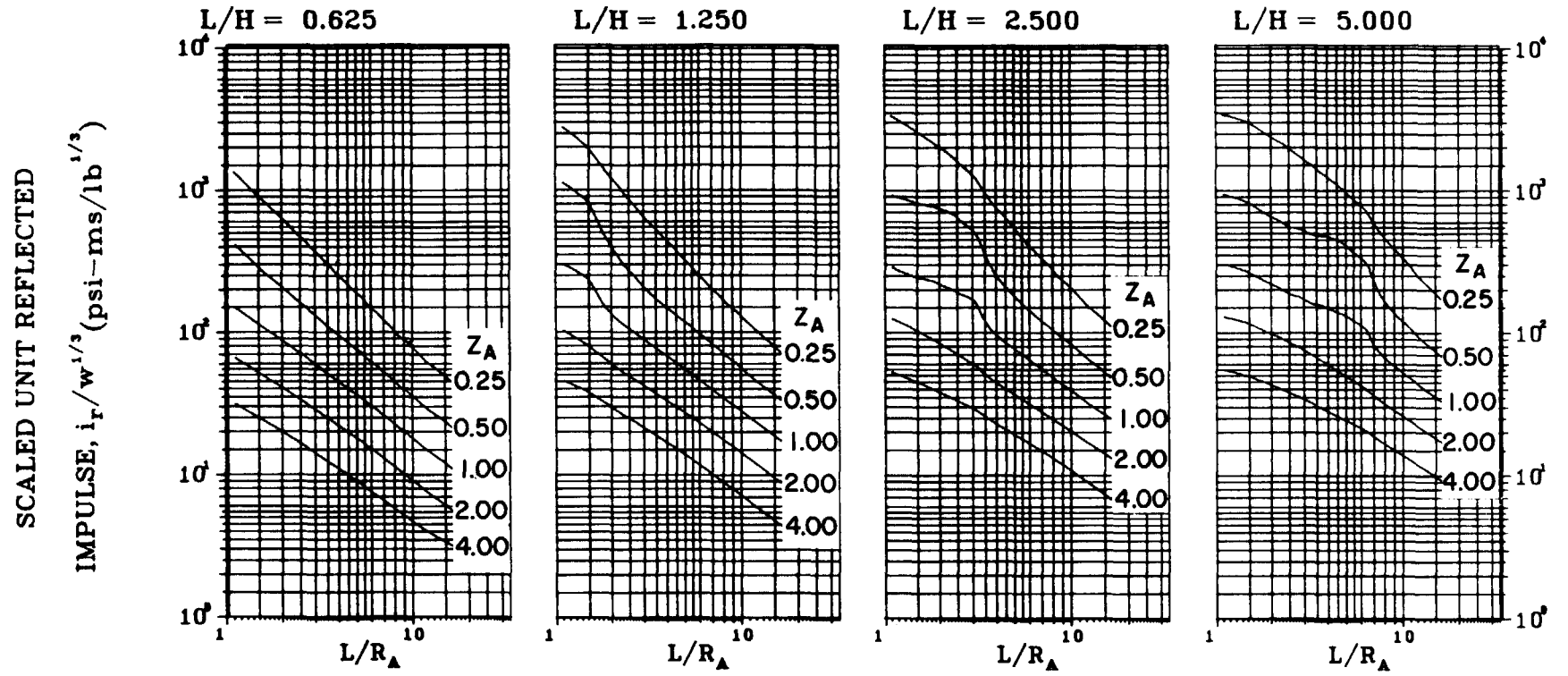


Figure 2-110 Scaled average unit reflected impulse
($N = 1, \ell/L = 0.10, h/H = 0.75$)

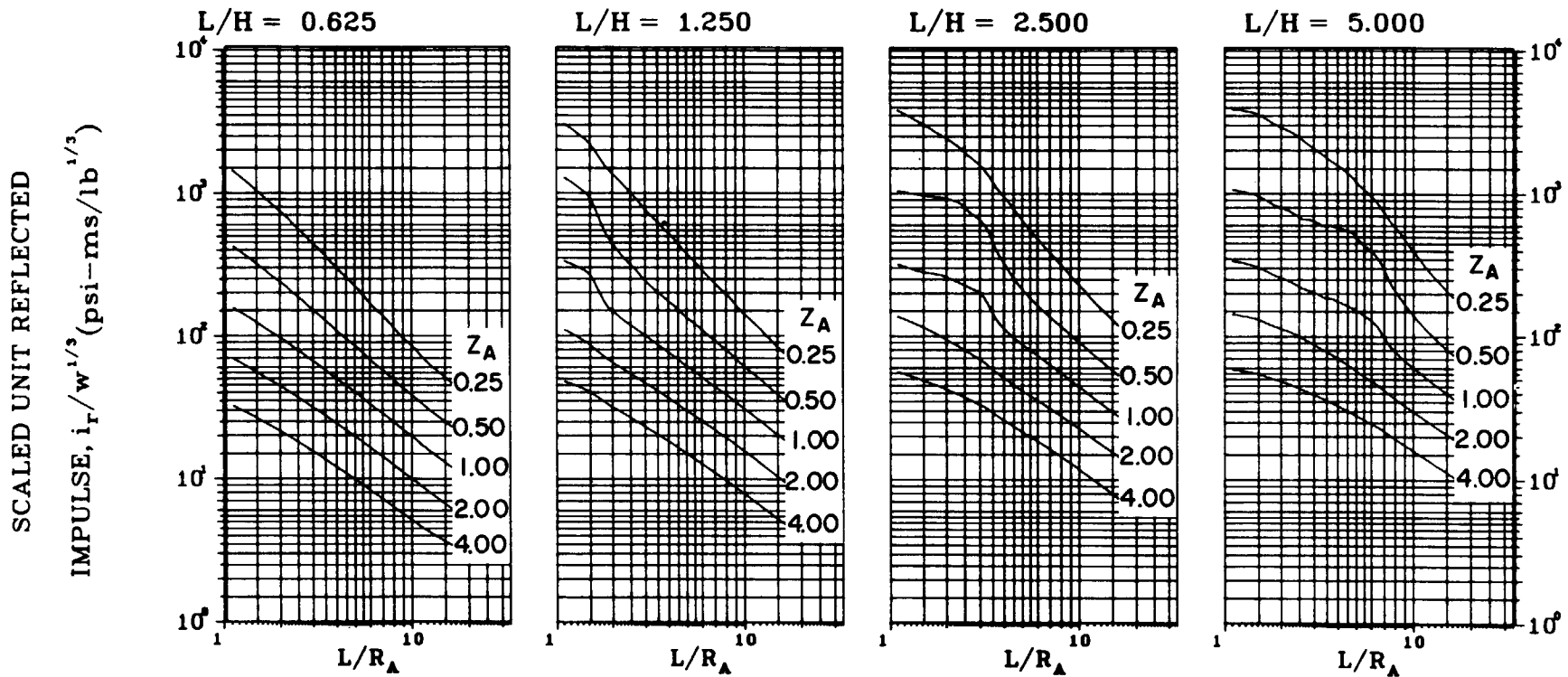


Figure 2-111 Scaled average unit reflected impulse
(N = 1, $\ell/L = 0.25$ and 0.75 , $h/H = 0.75$)

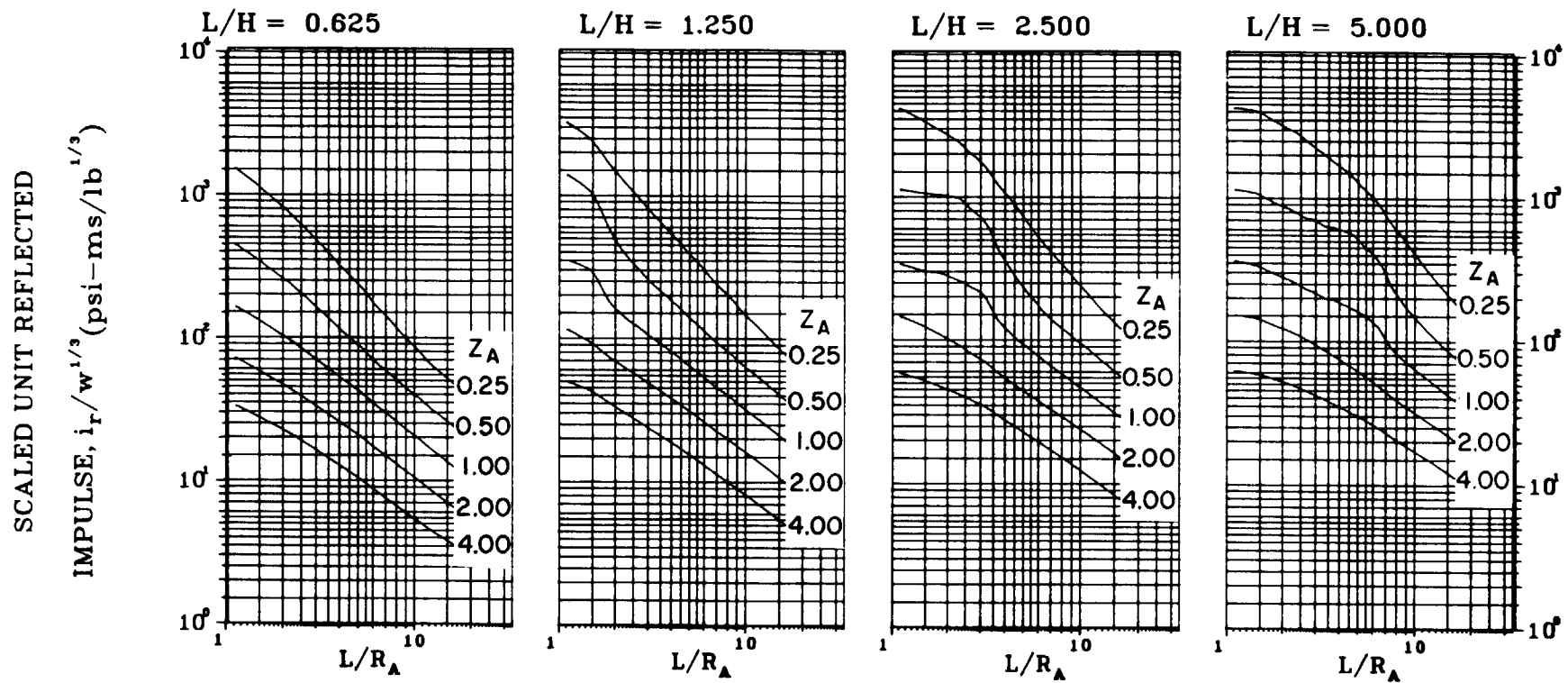


Figure 2-112 Scaled average unit reflected impulse
($N = 1, \ell/L = 0.50, h/H = 0.75$)

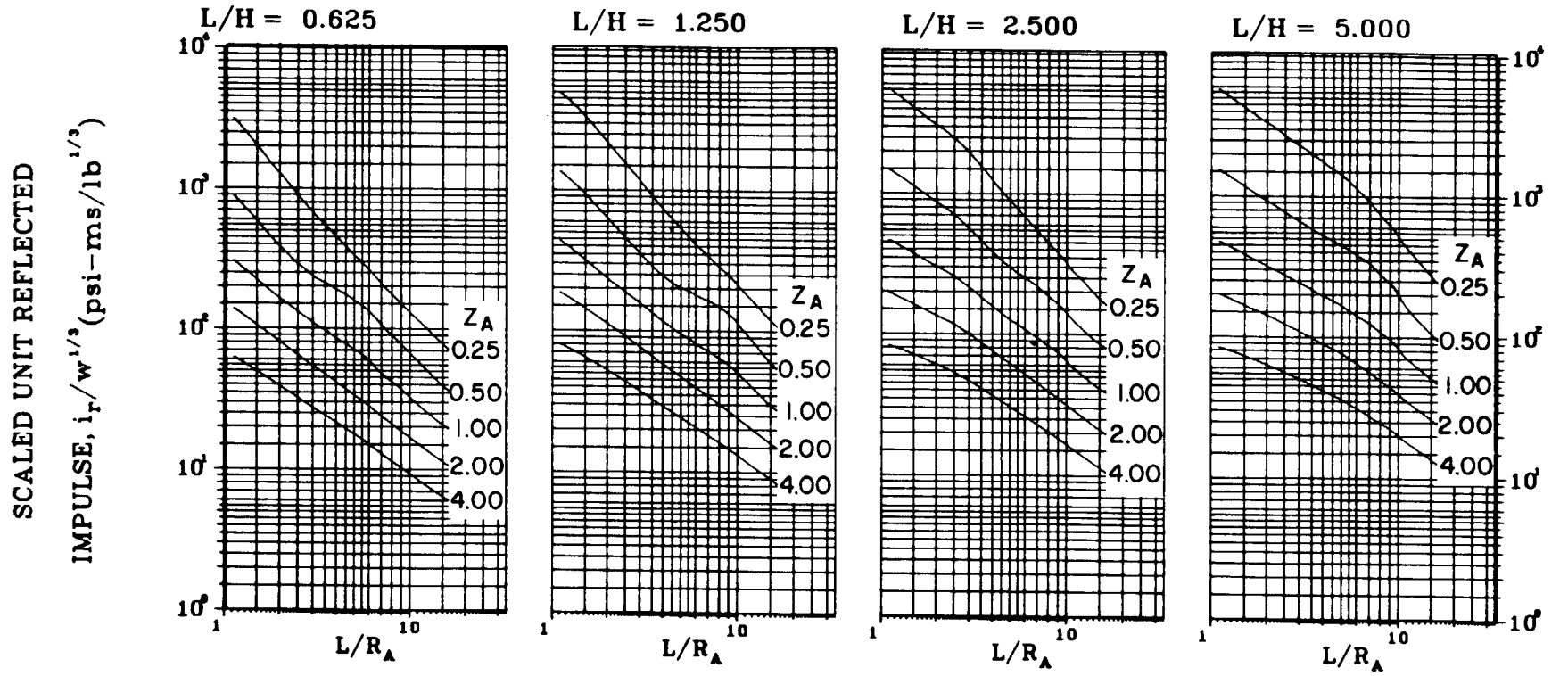


Figure 2-113 Scaled average unit reflected impulse
($N = 2$, $l/L = 0.10$, $h/H = 0.10$)

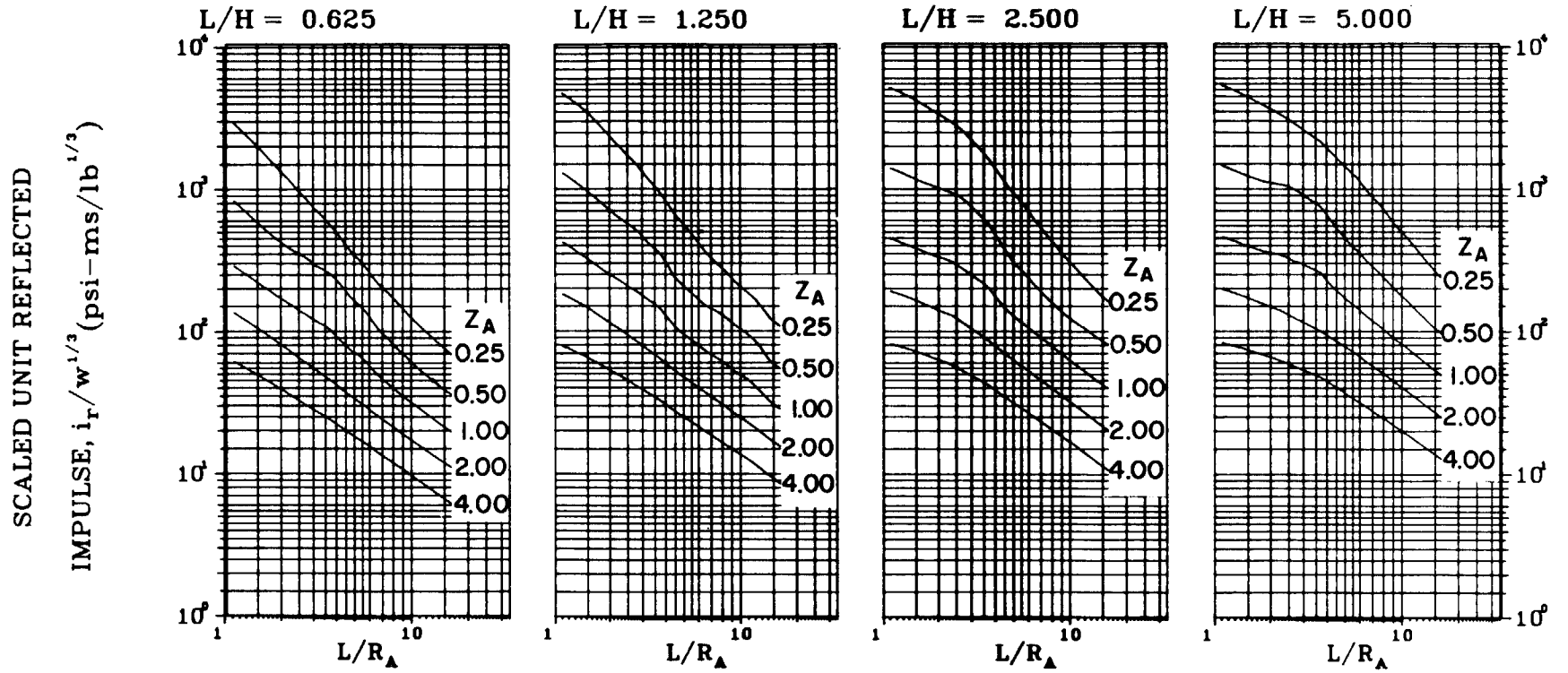


Figure 2-114 Scaled average unit reflected impulse
($N = 2, \ell/L = 0.25, h/H = 0.10$)

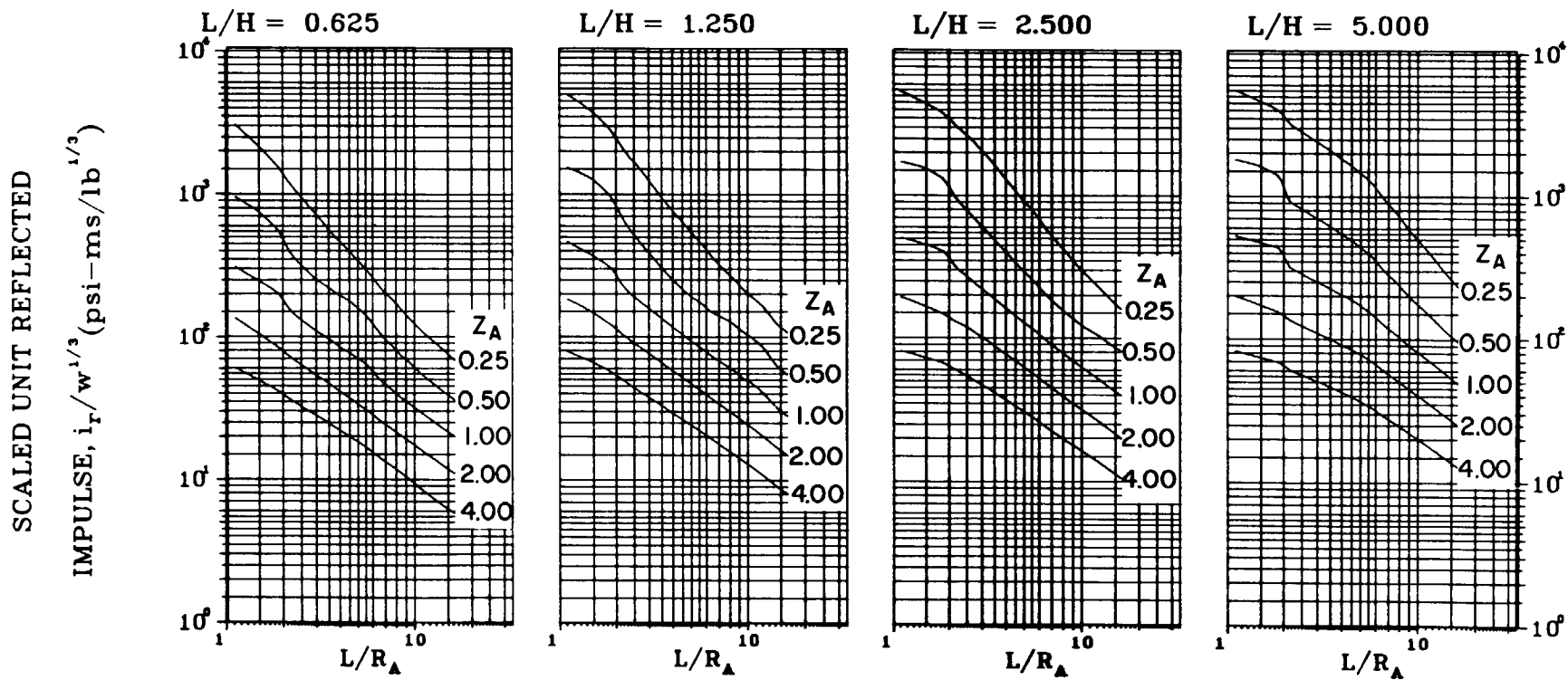


Figure 2-115 Scaled average unit reflected impulse
($N = 2, \ell/L = 0.50, h/H = 0.10$)

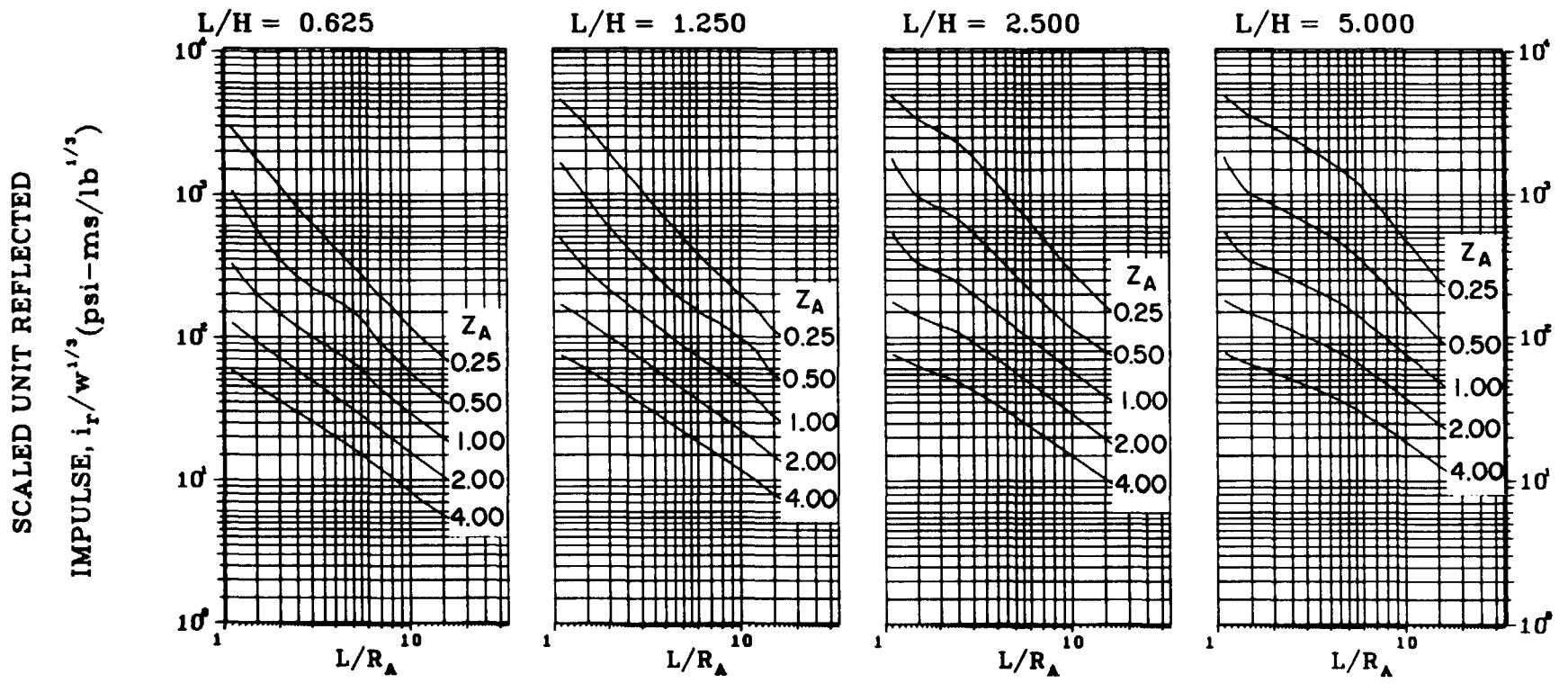
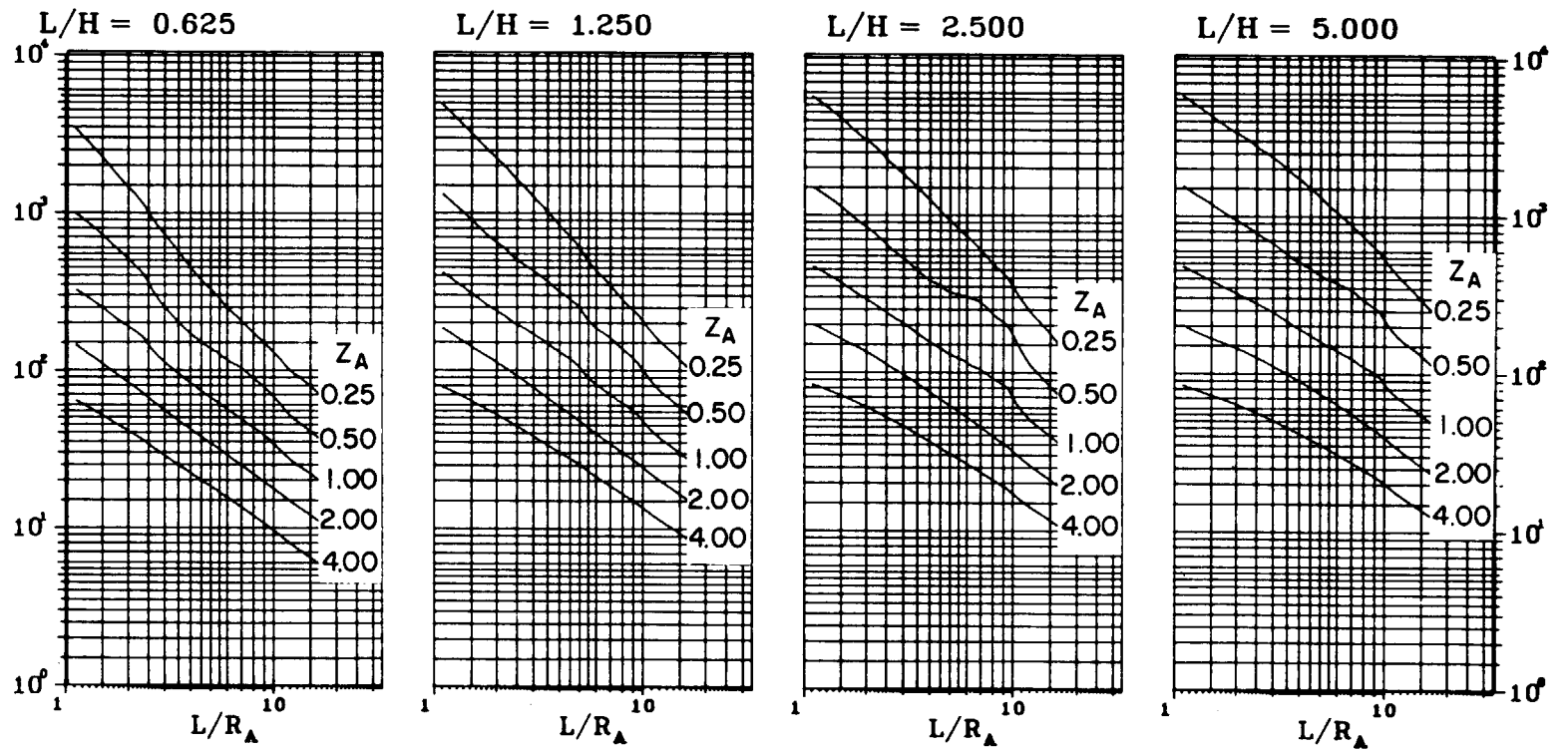


Figure 2-116 Scaled average unit reflected impulse
($N = 2$, $\ell/L = 0.75$, $h/H = 0.10$)

SCALED UNIT REFLECTED

IMPULSE, $i_r/w^{1/3}$ (psi-ms/lb^{1/3})



17A

Figure 2-117 Scaled average unit reflected impulse
(N = 2. $l/L = 0.10$. $h/H = 0.25$)

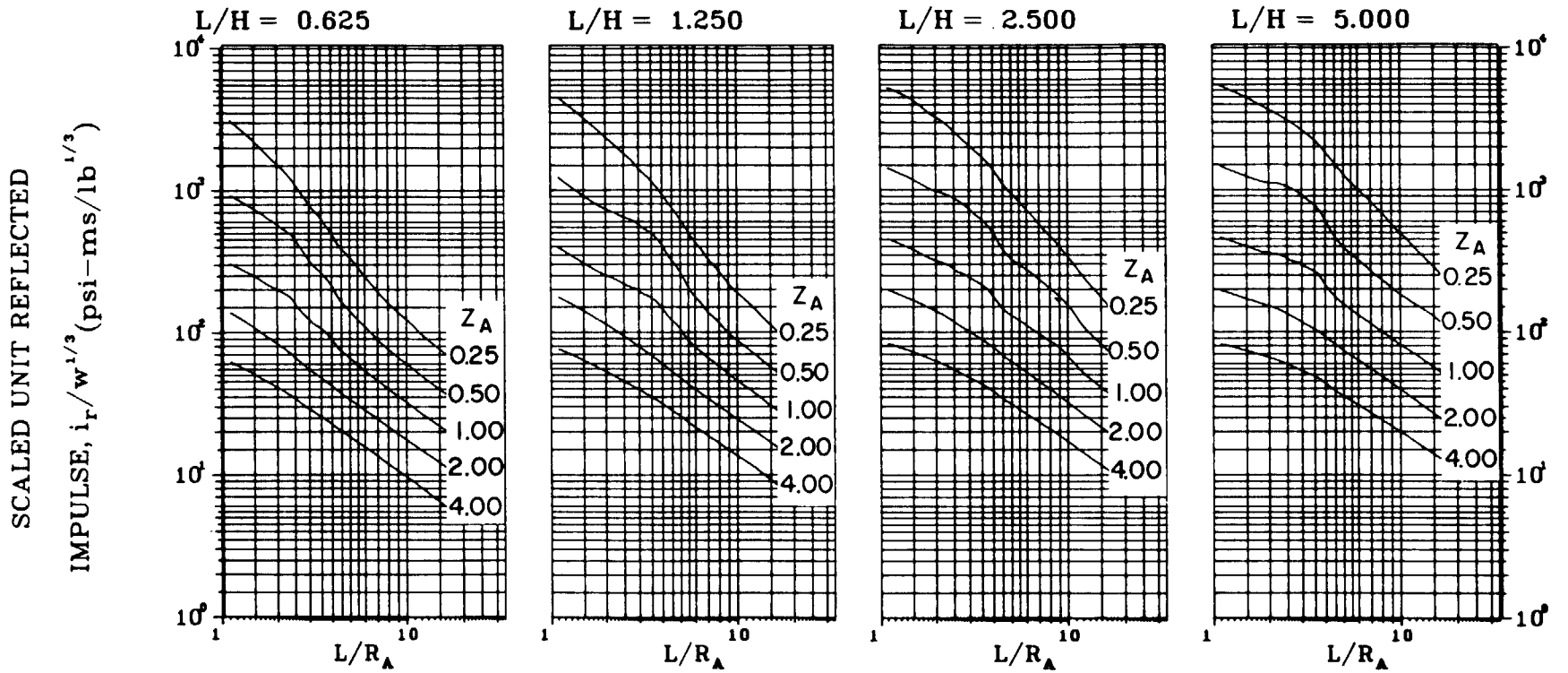


Figure 2-118 Scaled average unit reflected impulse
(N = 2. $\ell/L = 0.25$. $h/H = 0.25$)

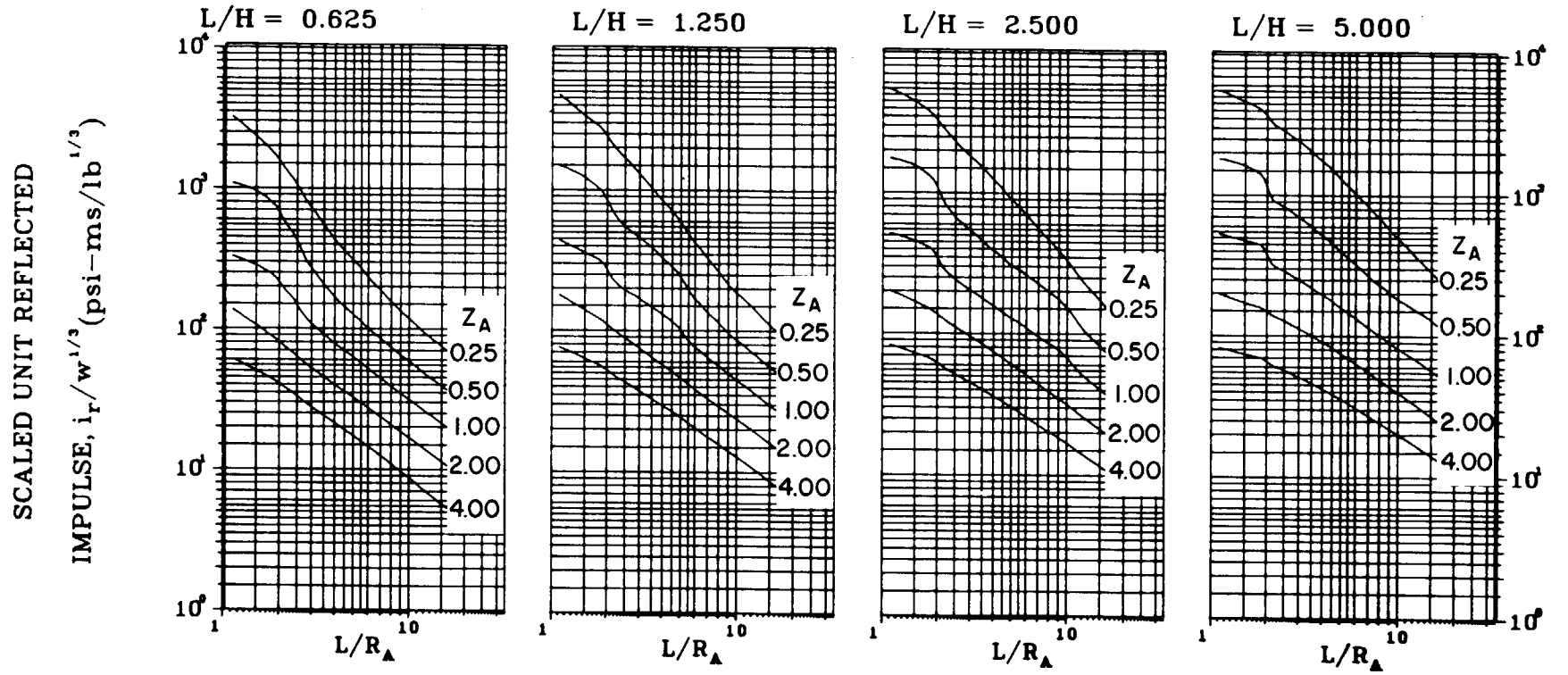
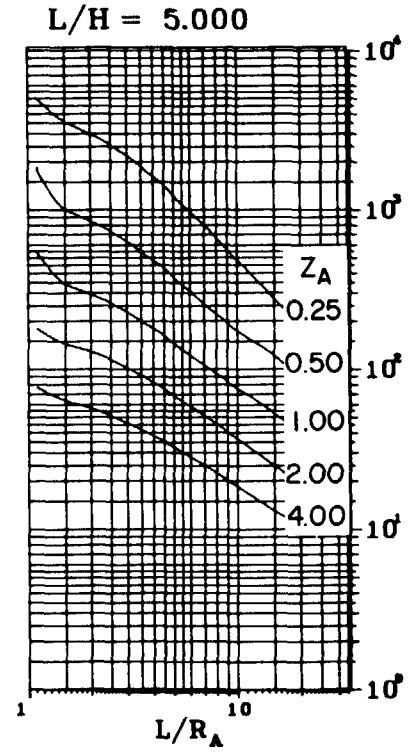
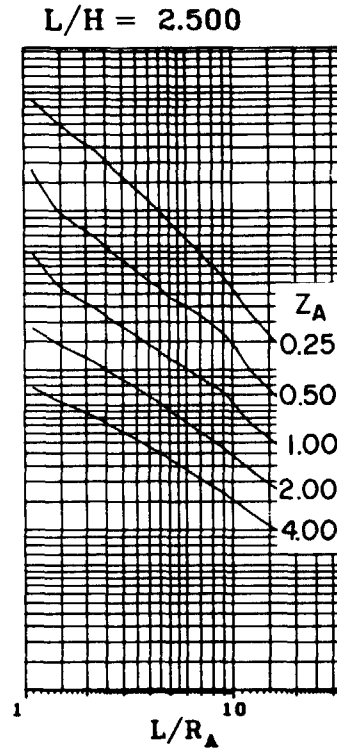
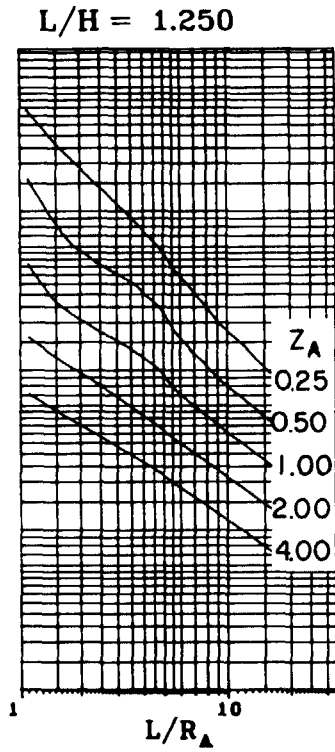
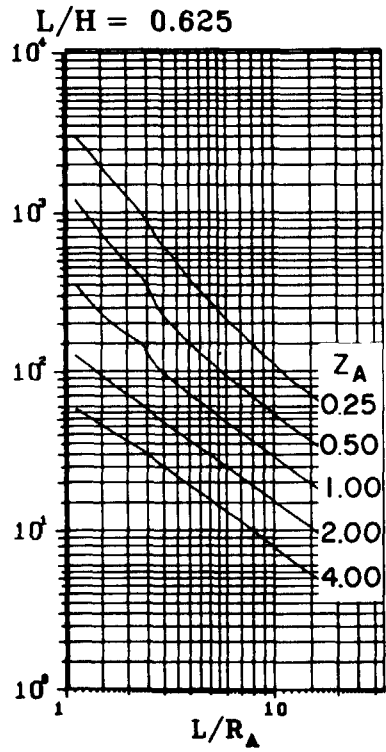


Figure 2-119 Scaled average unit reflected impulse
($N = 2$, $\ell/L = 0.50$, $h/H = 0.25$)

SCALED UNIT REFLECTED

IMPULSE, $i_r/w^{1/3}$ (psi-ms/lb^{1/3})



SCALED UNIT REFLECTED

IMPULSE, $i_r/w^{1/3}$ (psi-ms/lb^{1/3})

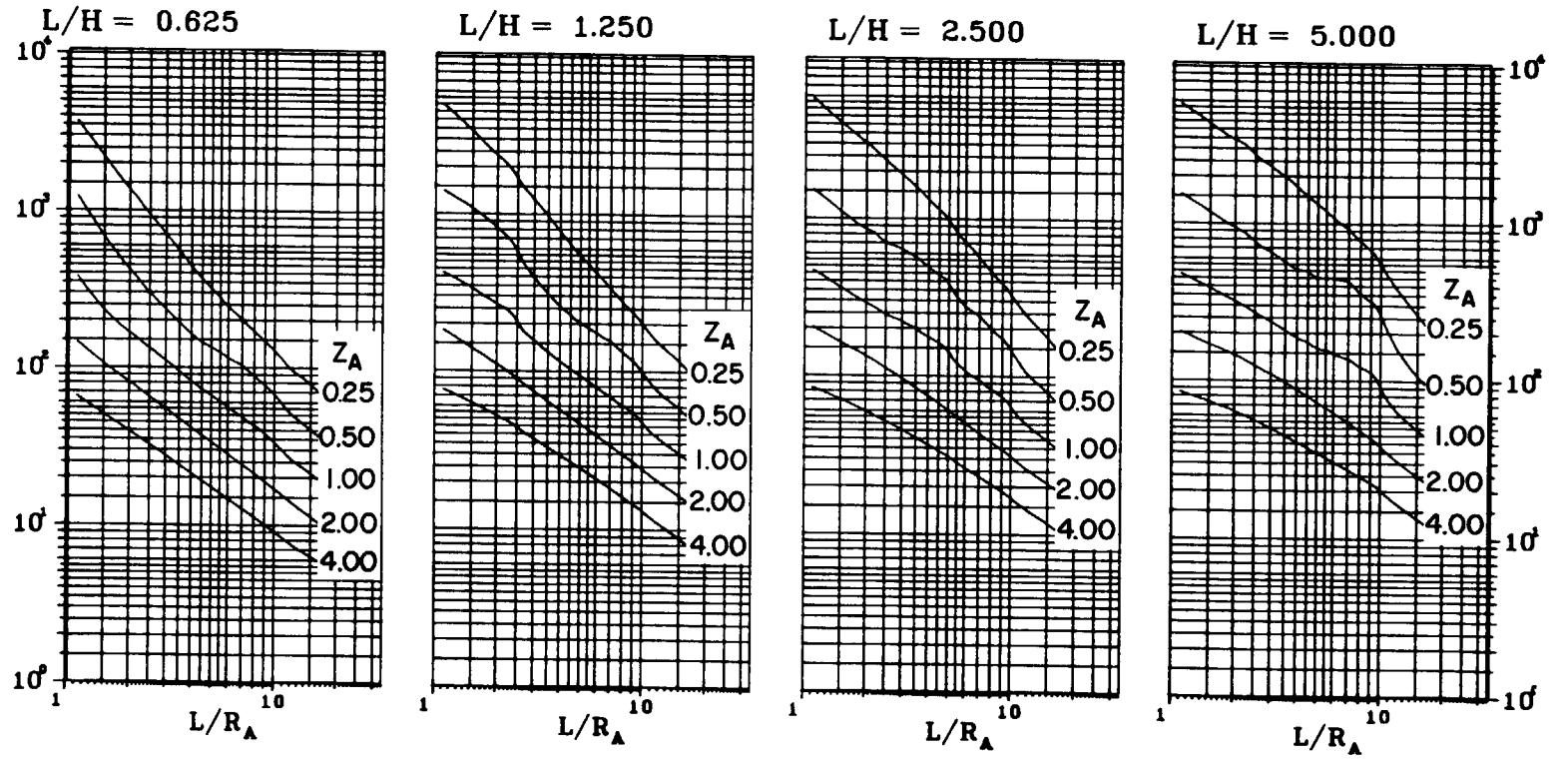
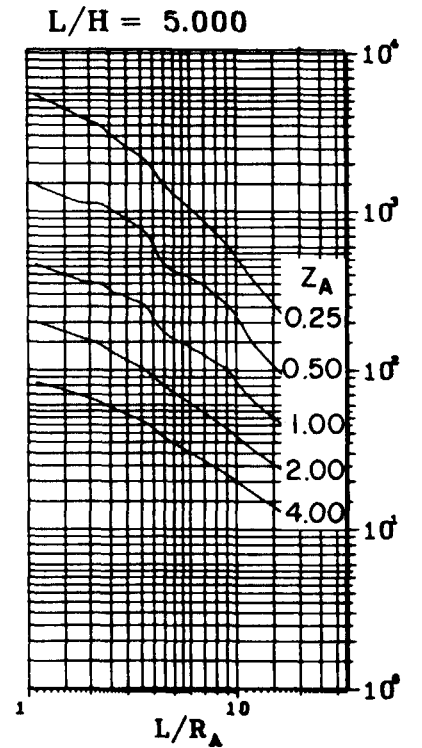
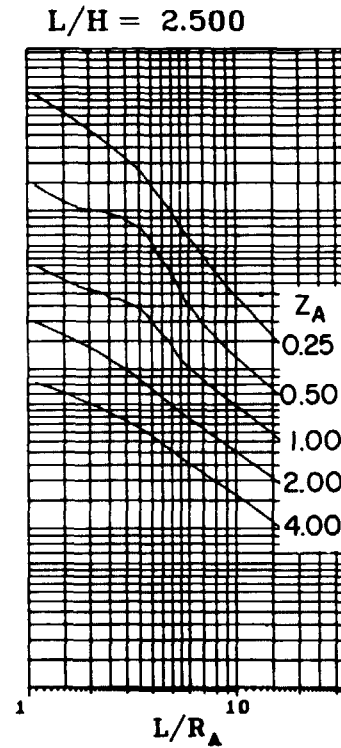
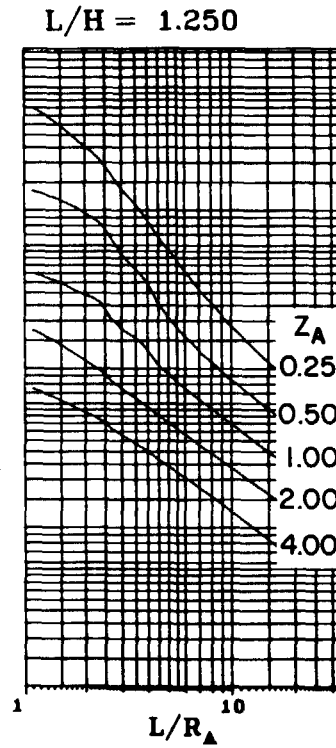
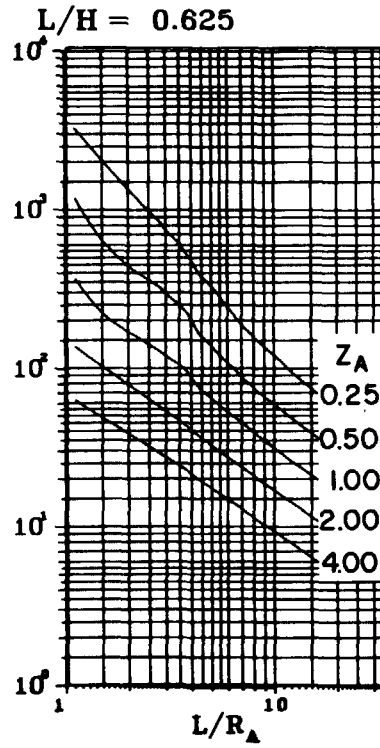


Figure 2-121 Scaled average unit reflected impulse
($N = 2, \ell/L = 0.10, h/H = 0.50$)

SCALED UNIT REFLECTED

IMPULSE, $i_r/w^{1/3}$ (psi-ms/lb^{1/3})



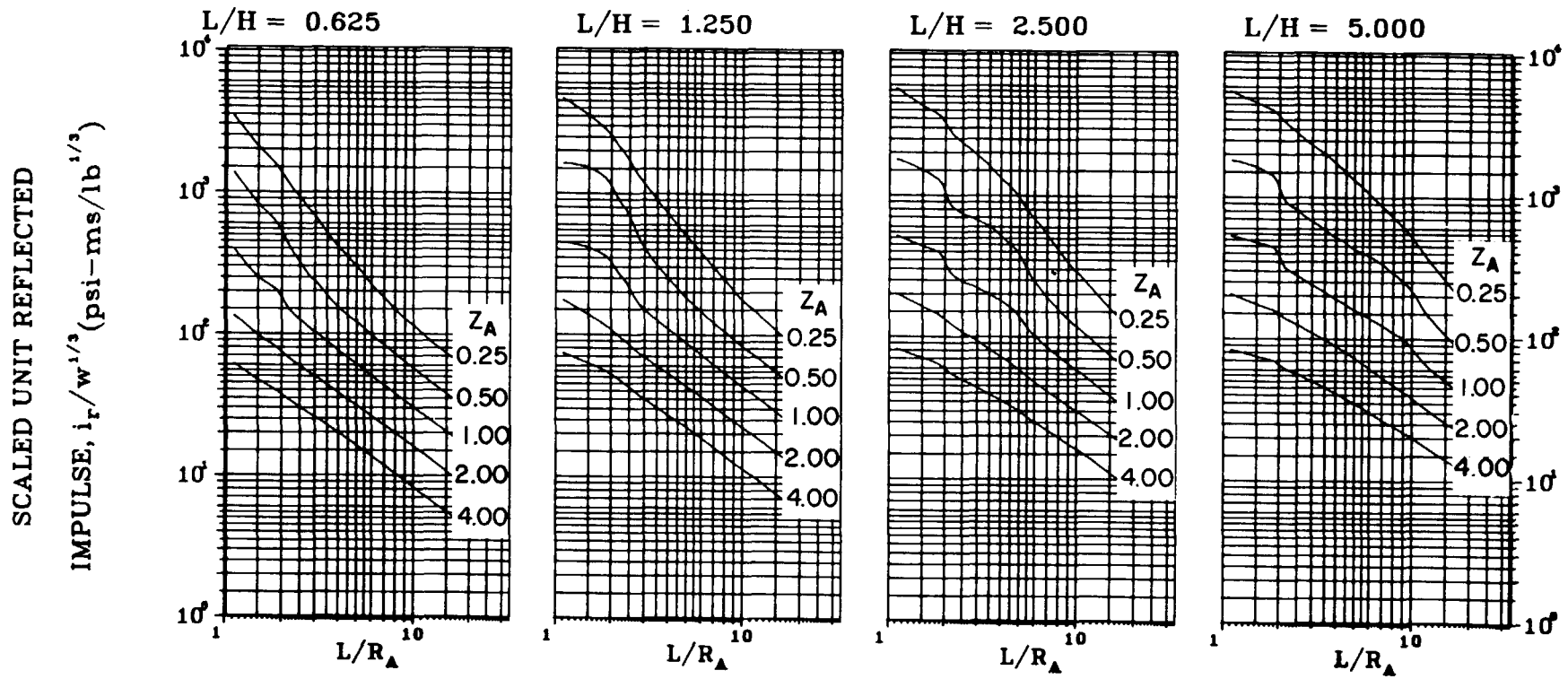
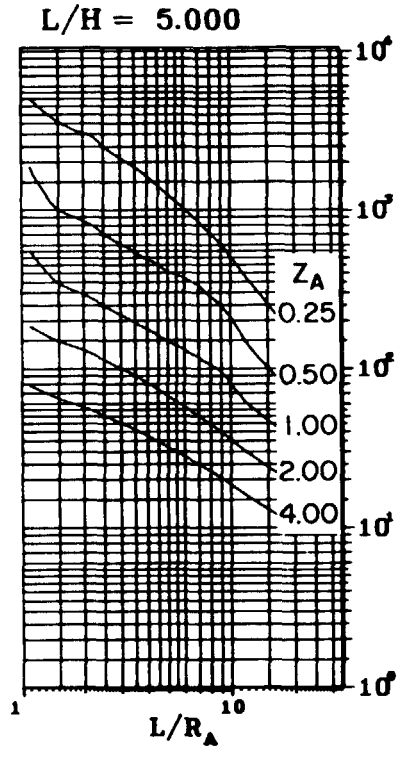
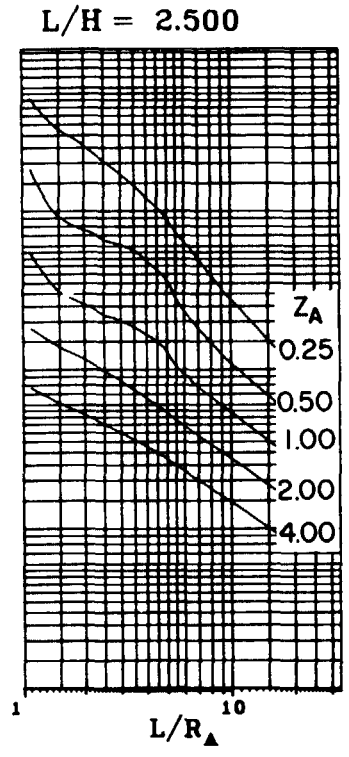
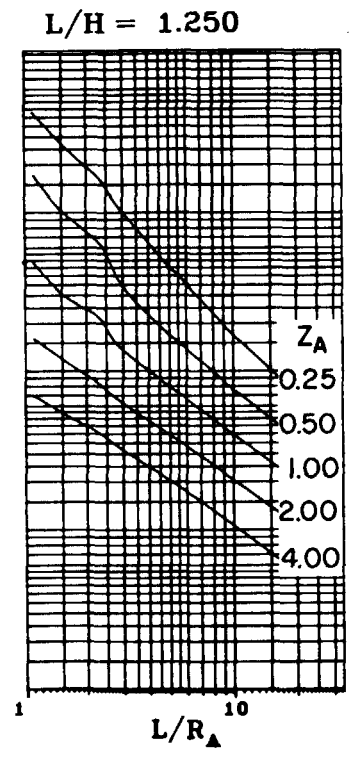
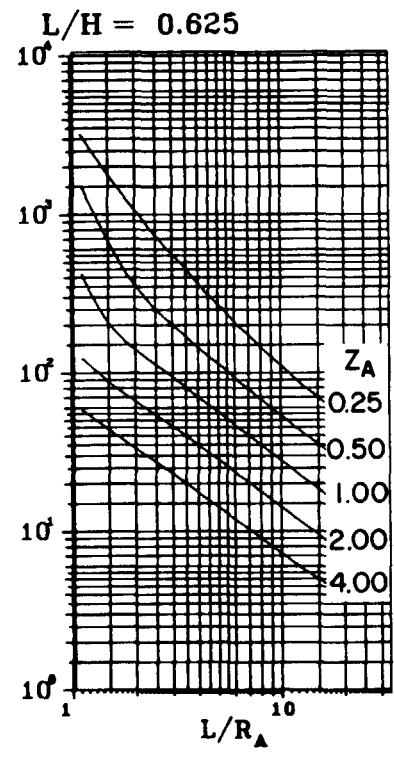


Figure 2-123 Scaled average unit reflected impulse
(N = 2, $\ell/L = 0.50$, $h/H = 0.50$)

SCALED UNIT REFLECTED
 IMPULSE, $i_r/w^{1/3}$ (psi-ms/lb^{1/3})



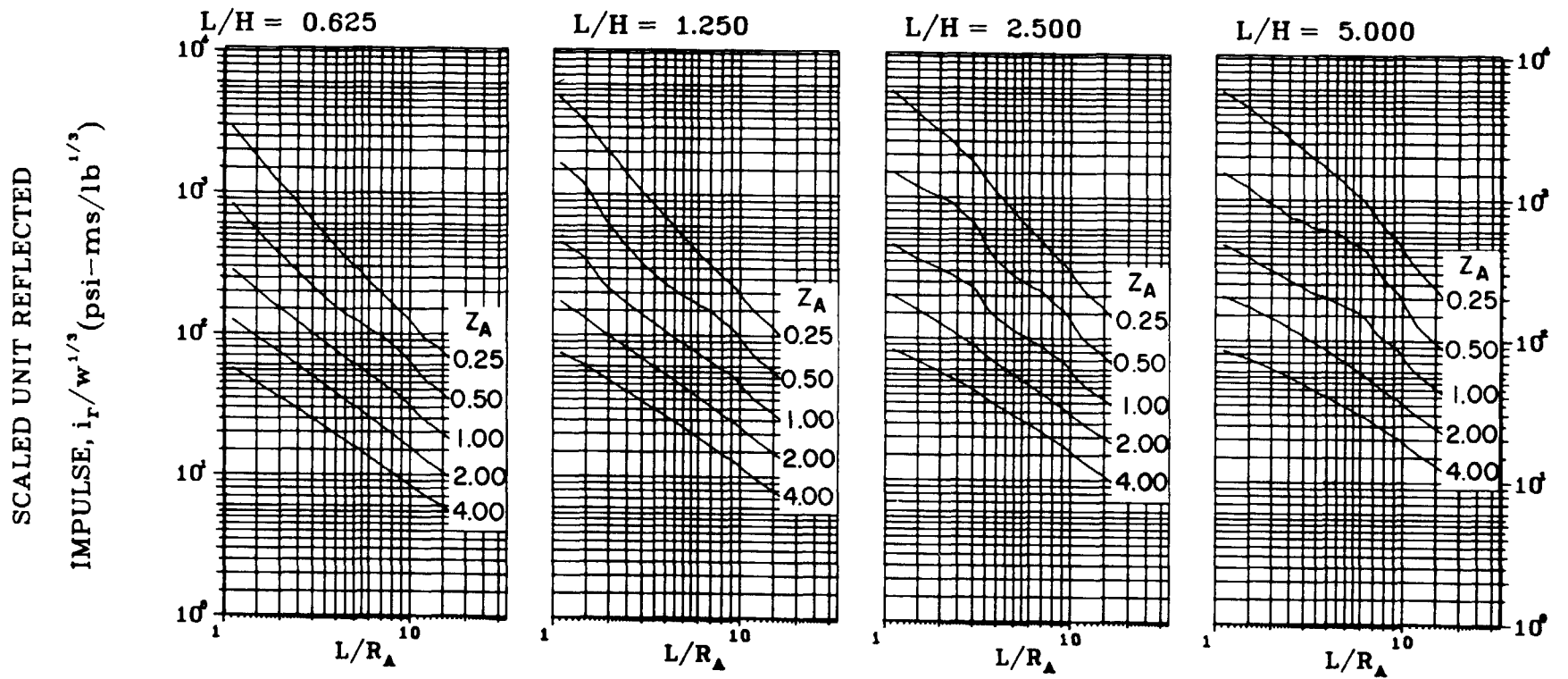
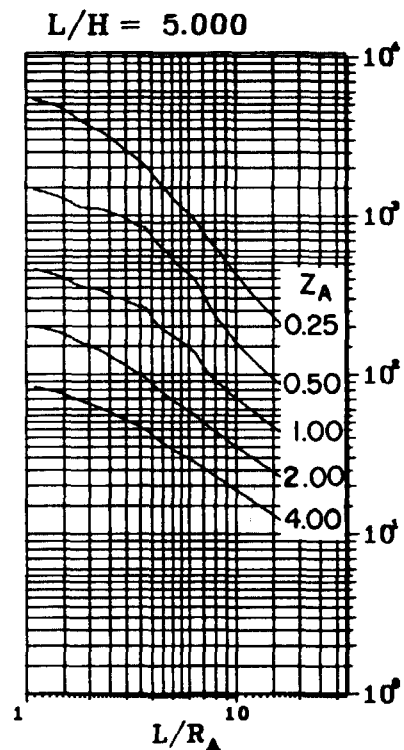
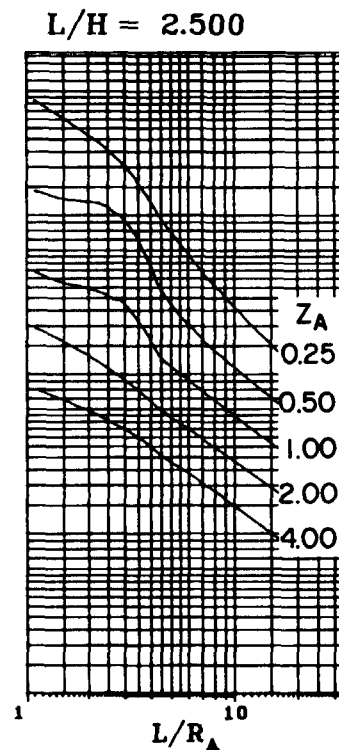
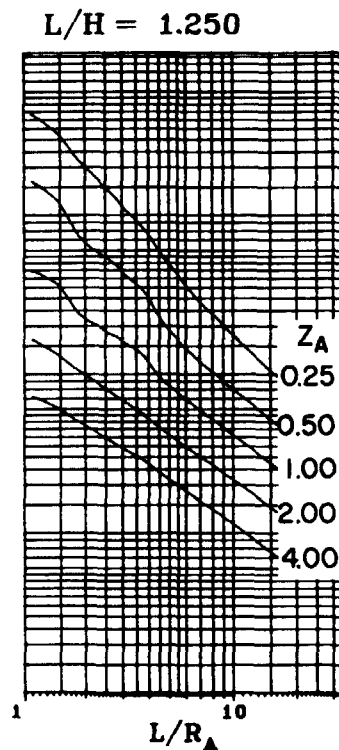
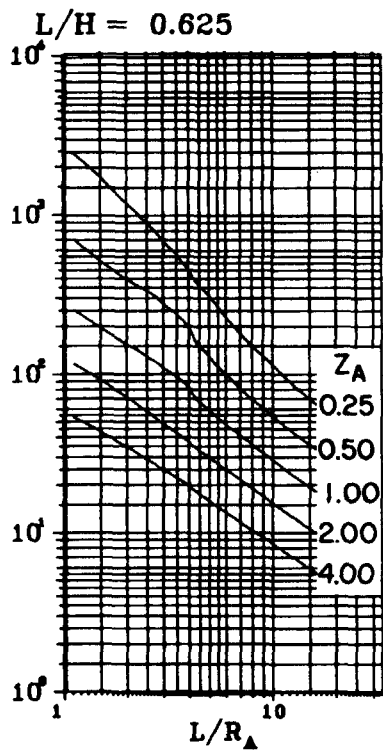


Figure 2-125 Scaled average unit reflected impulse
(N = 2, $l/L = 0.10$, $h/H = 0.75$)

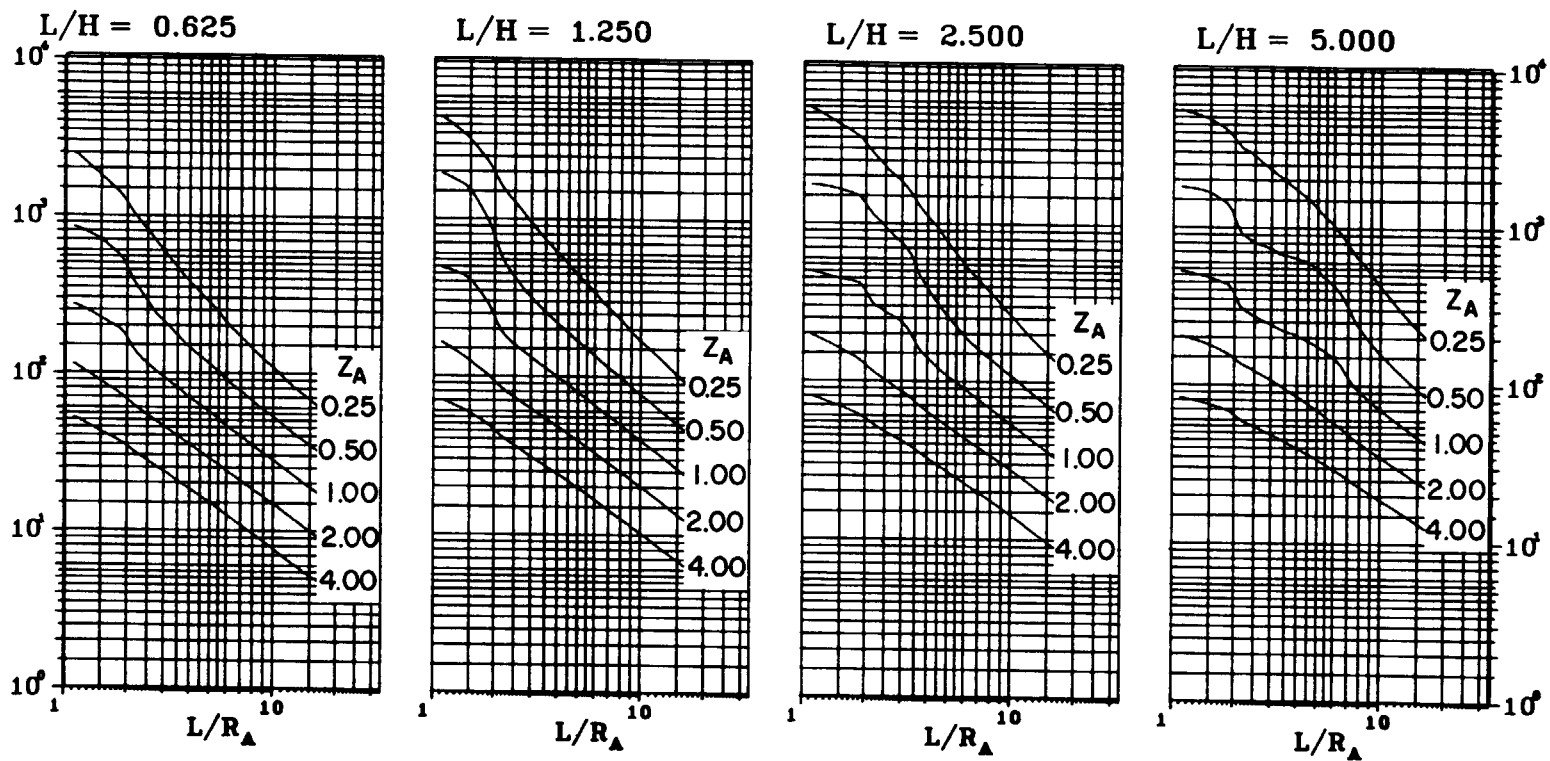
SCALED UNIT REFLECTED

IMPULSE, $i_r/w^{1/2}$ (psi-ms/lb^{1/2})



SCALED UNIT REFLECTED

IMPULSE, $i_r/w^{1/3}$ (psi-ms/lb^{1/3})



27A

Figure 2-127 Scaled average unit reflected impulse
(N = 2, $l/L = 0.50$, $h/H = 0.75$)

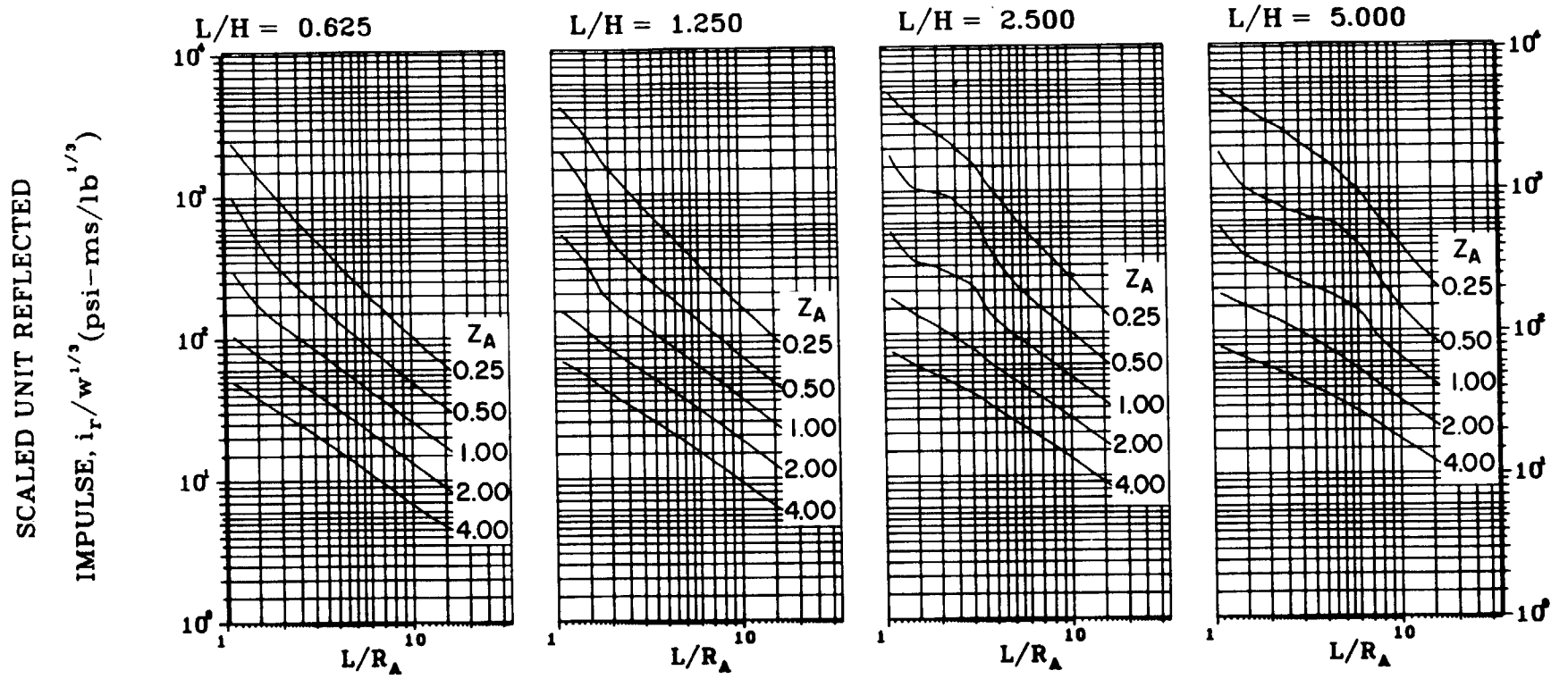


Figure 2-128 Scaled average unit reflected impulse
($N = 2, \ell/L = 0.75, h/H = 0.75$)

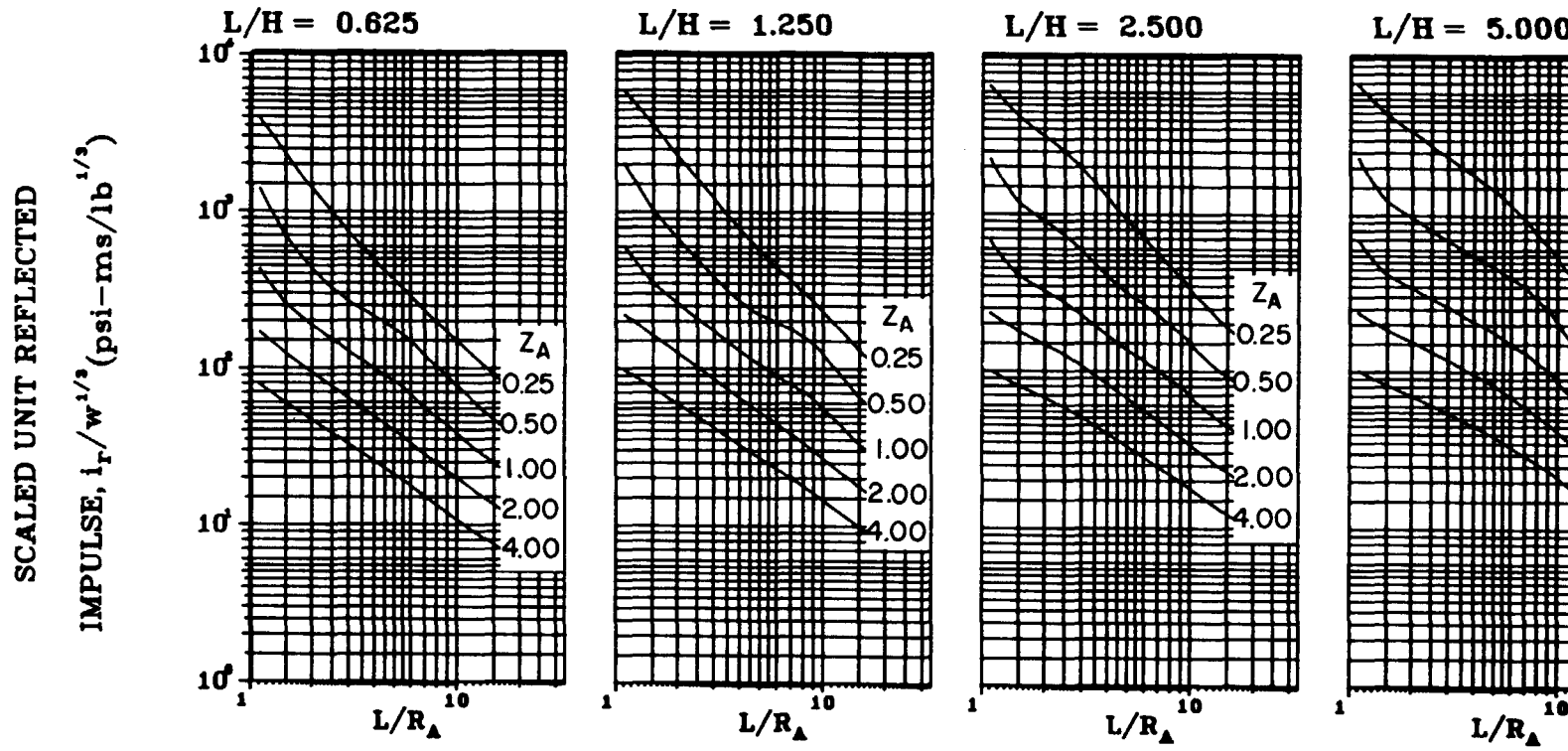


Figure 2-129 Scaled average unit reflected impulse
($w = 2.0$ lb/lb^{1/2}, $\rho = 0.10$ lb/in³, $\mu = 0.10$)

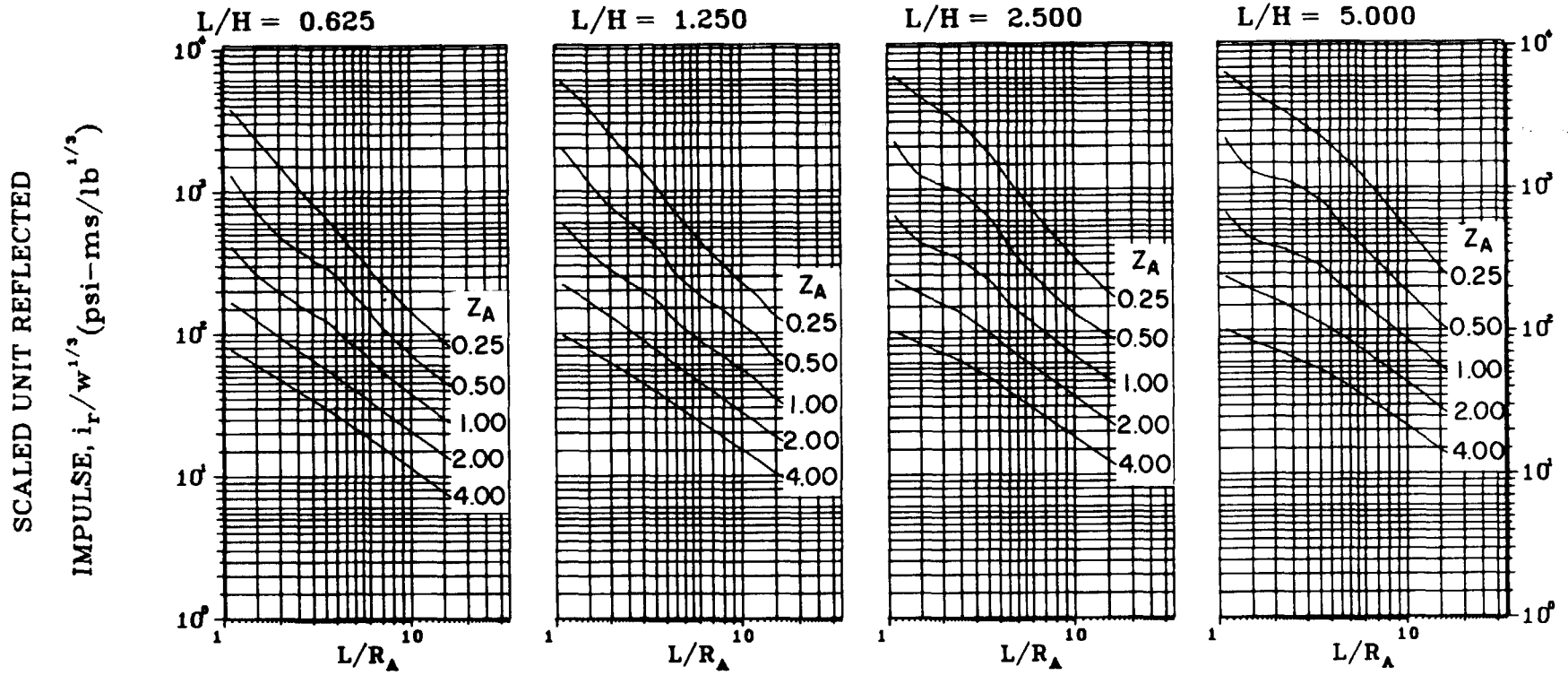


Figure 2-130. Scaled average unit reflected impulse

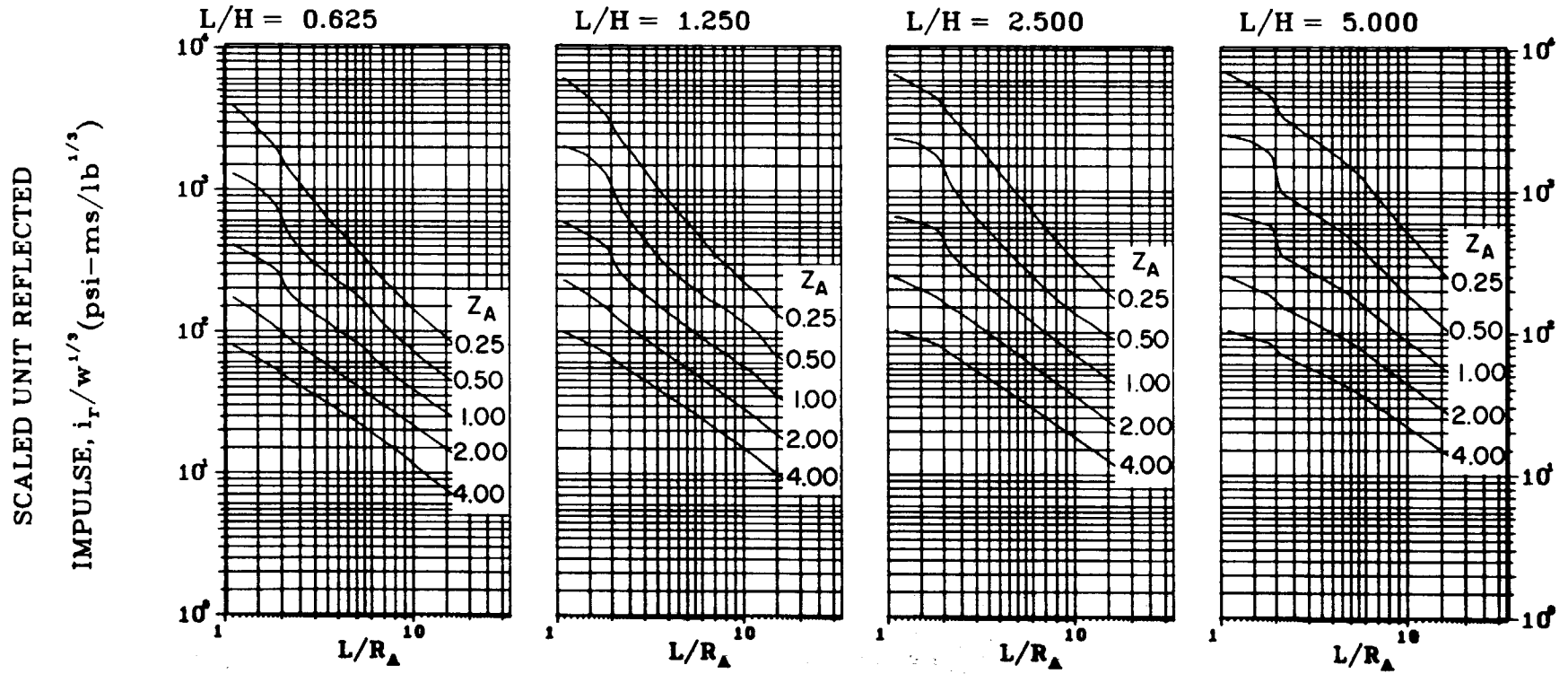
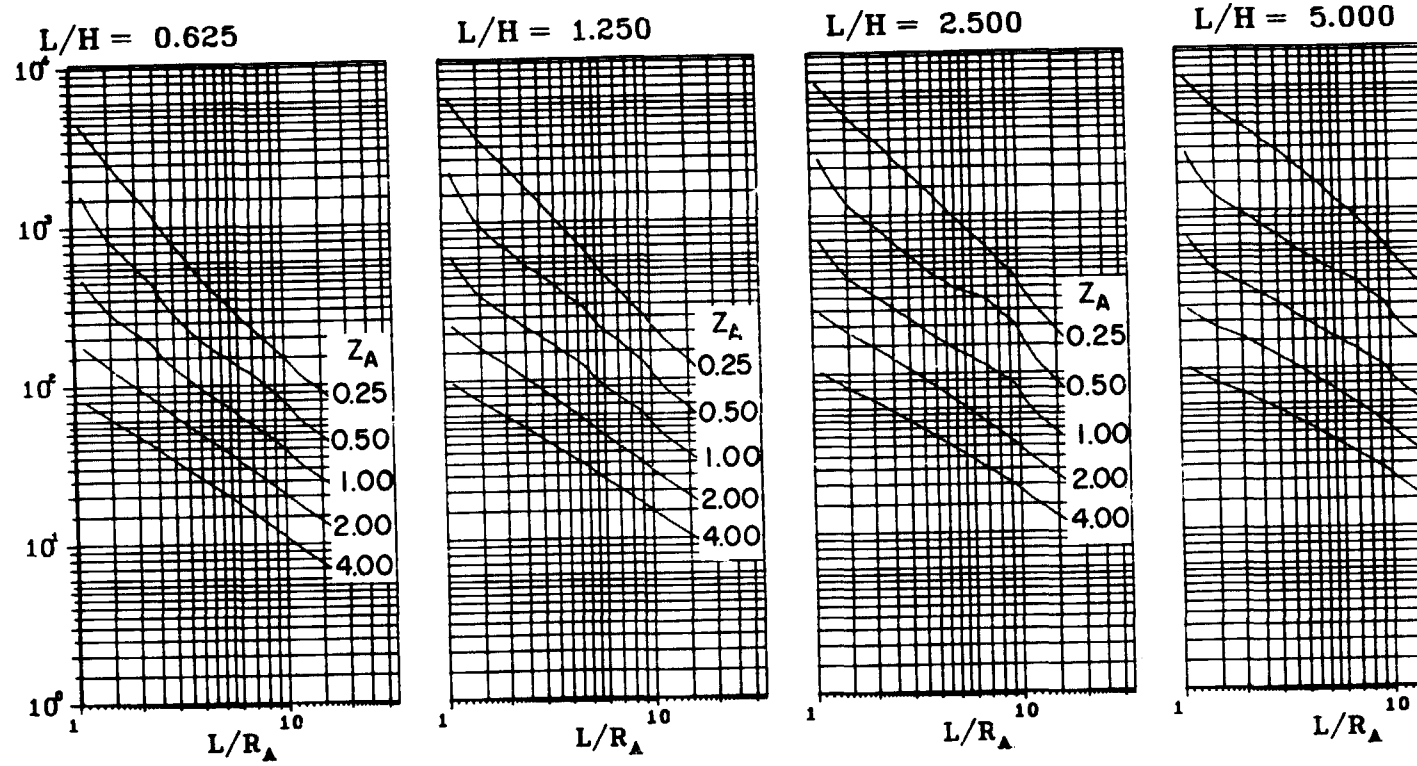


Figure 2-131 Scaled average unit reflected impulse
($N = 3$, $l/L = 0.50$, $h/H = 0.10$)

SCALED UNIT REFLECTED

IMPULSE, $i_r/w^{1/3}$ (psi-ms/lb^{1/3})

32A

Figure 2-132 Scaled average unit reflected impulse
 ($N = 3$, $\ell/L = 0.10$, $h/H = 0.25$)

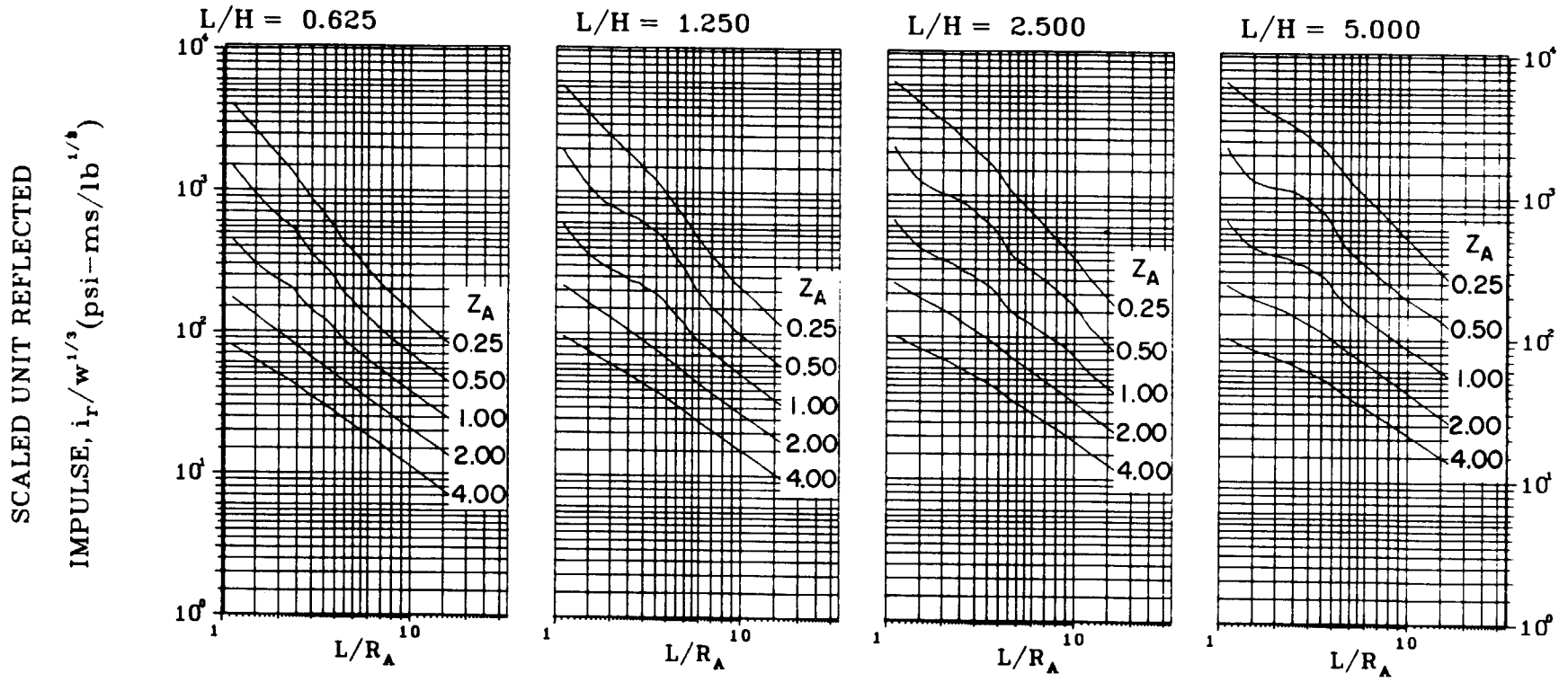
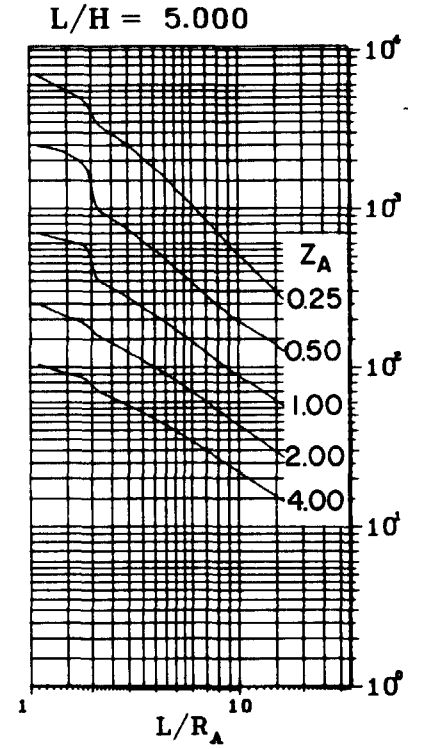
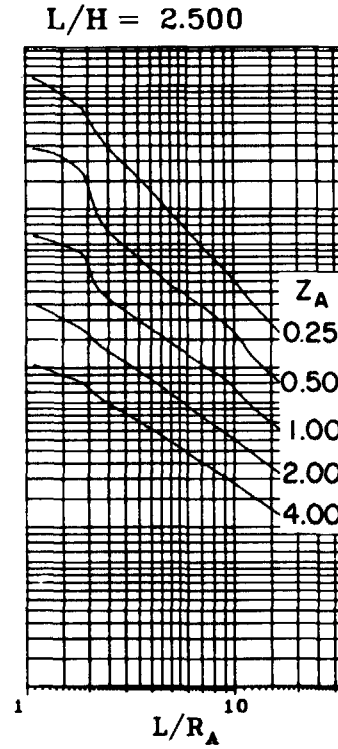
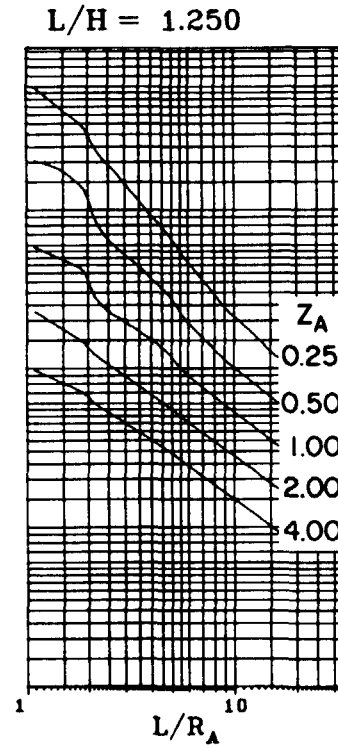
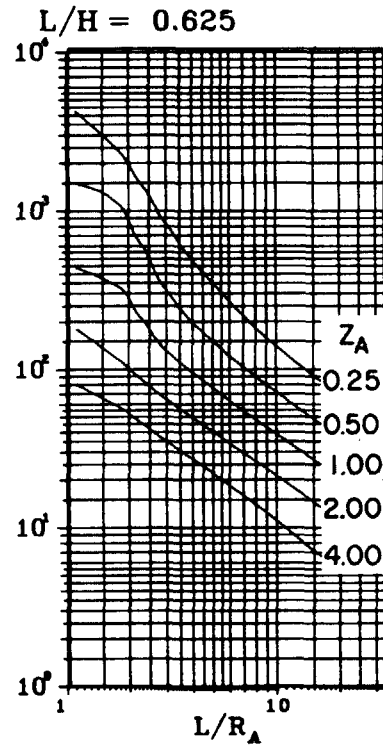


Figure 2-133 Scaled average unit reflected impulse
(N = 3, $l/L = 0.25$ and 0.75 , $h/H = 0.25$)

SCALED UNIT REFLECTED
IMPULSE, $i_r/w^{1/3}$ (psi-ms/lb^{1/3})



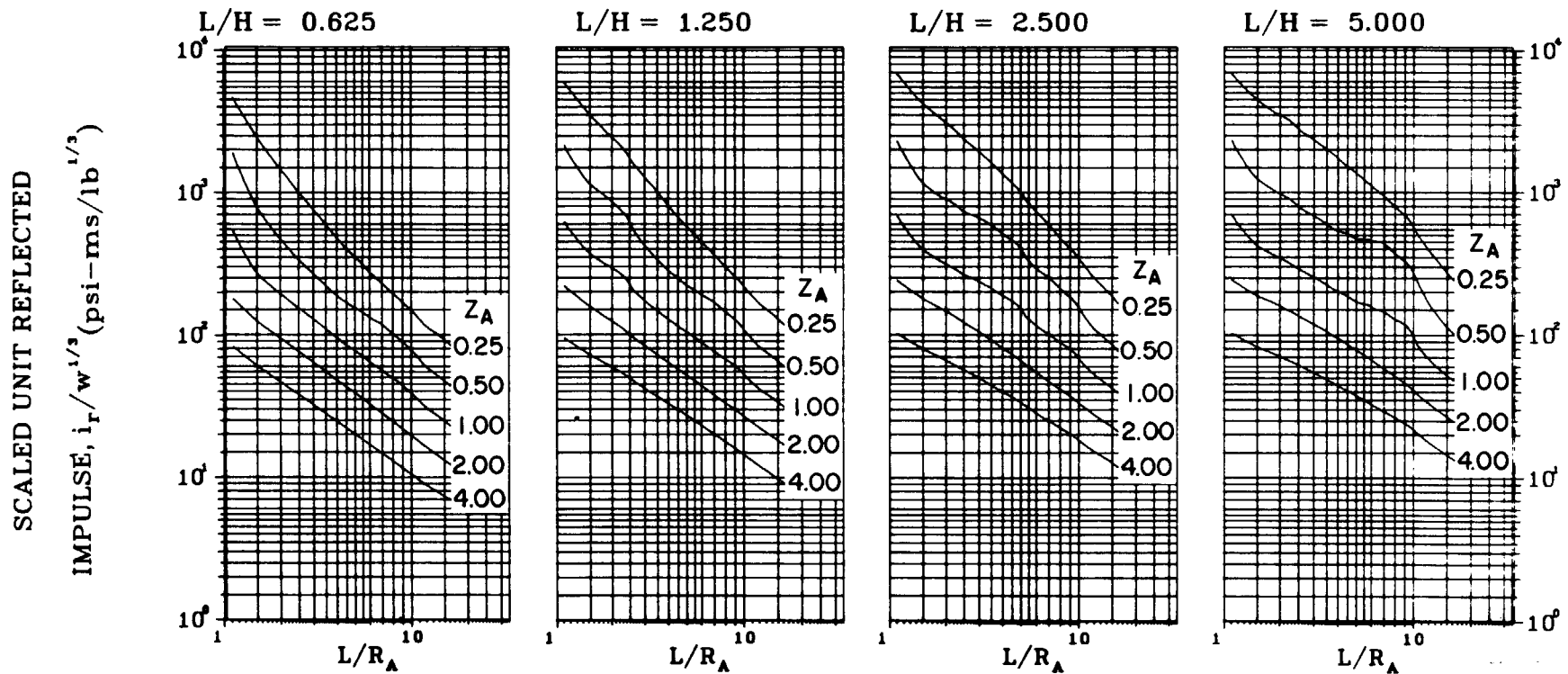


Figure 2-135 Scaled average unit reflected impulse
($N = 3, \ell/L = 0.10, h/H = 0.50$)

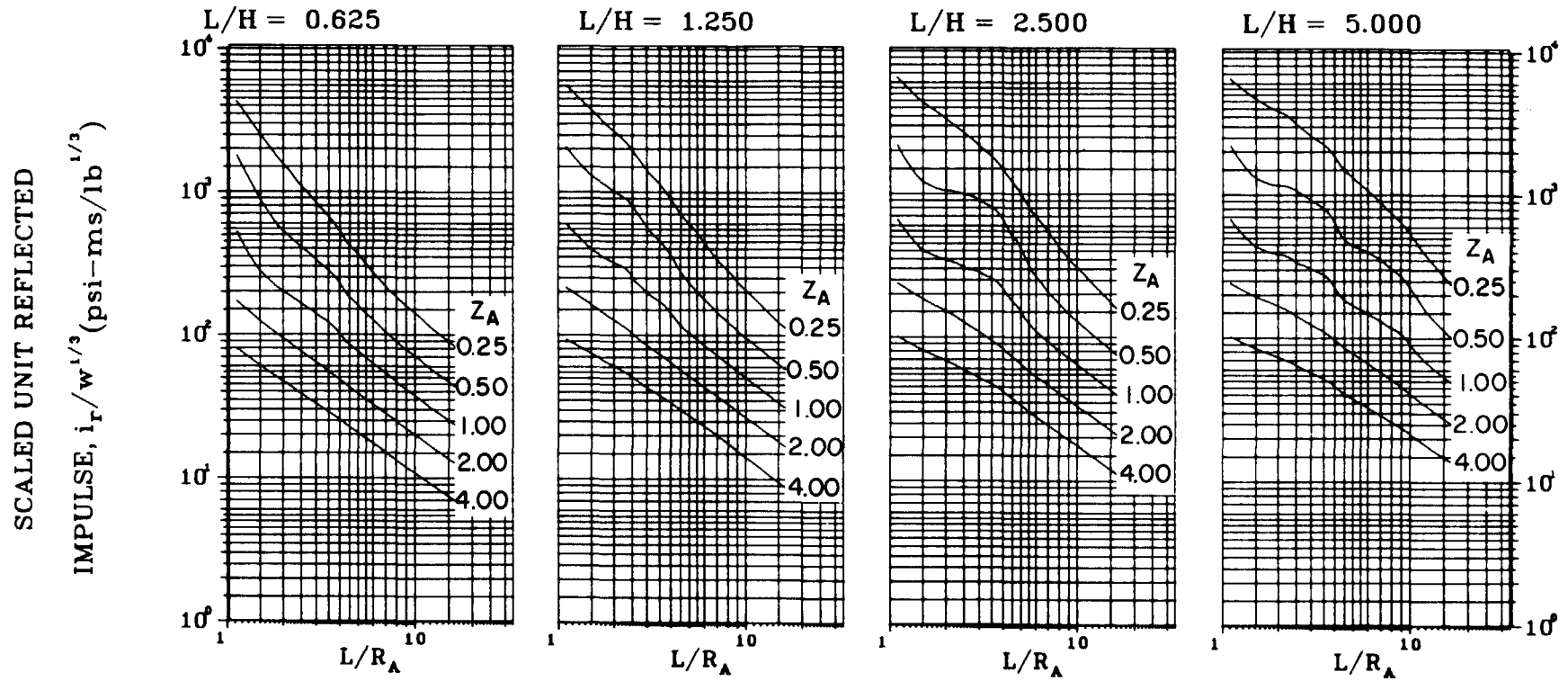


Figure 2-136 Scaled average unit reflected impulse
($N = 3$, $l/L = 0.25$ and 0.75 , $h/H = 0.50$)

SCALED UNIT REFLECTED

IMPULSE, $i_r/w^{1/3}$ (psi-ms/lb^{1/3})

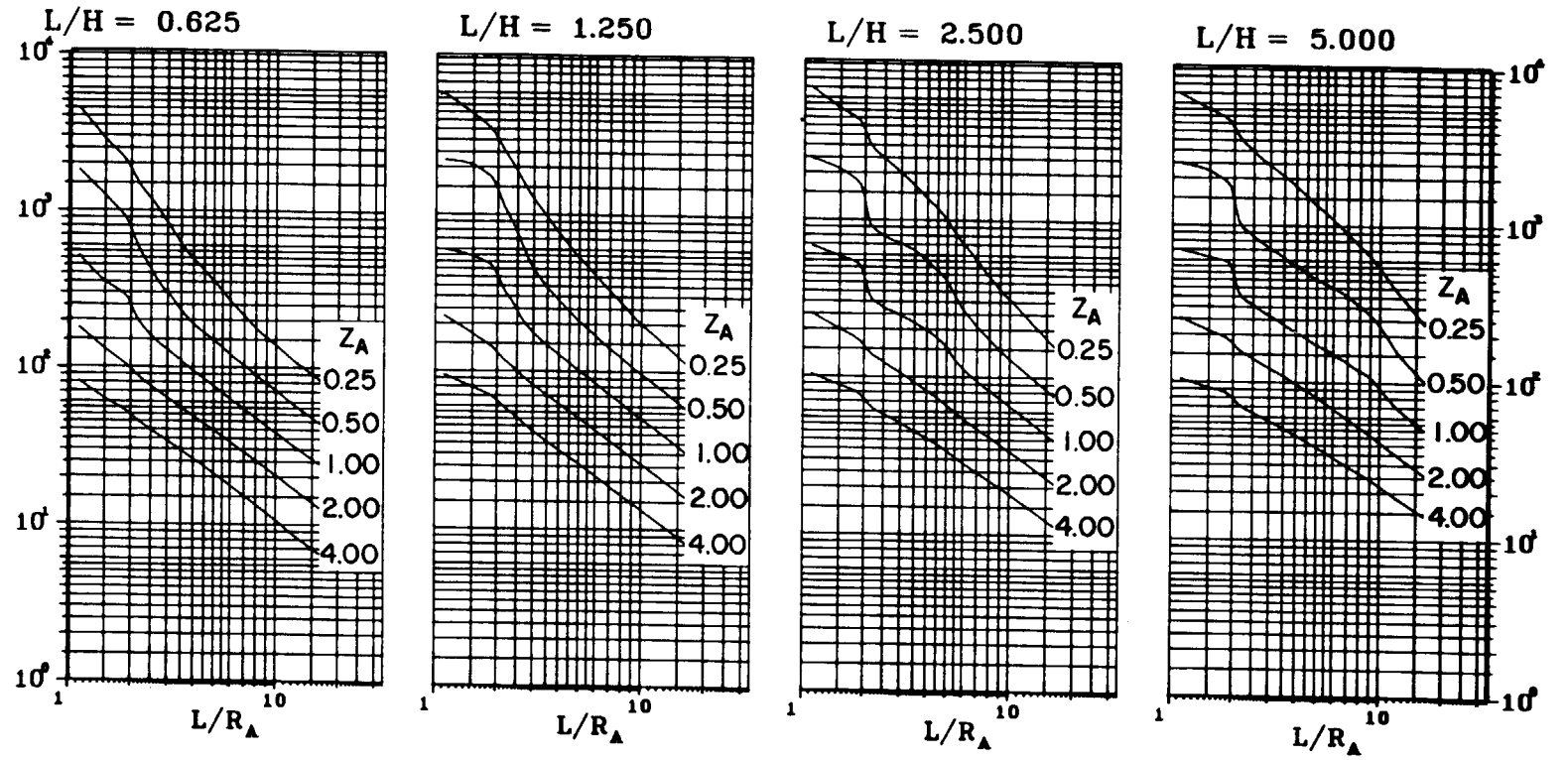


Figure 2-137 Scaled average unit reflected impulse
(N = 3, $\ell/L = 0.50$, $h/H = 0.50$)

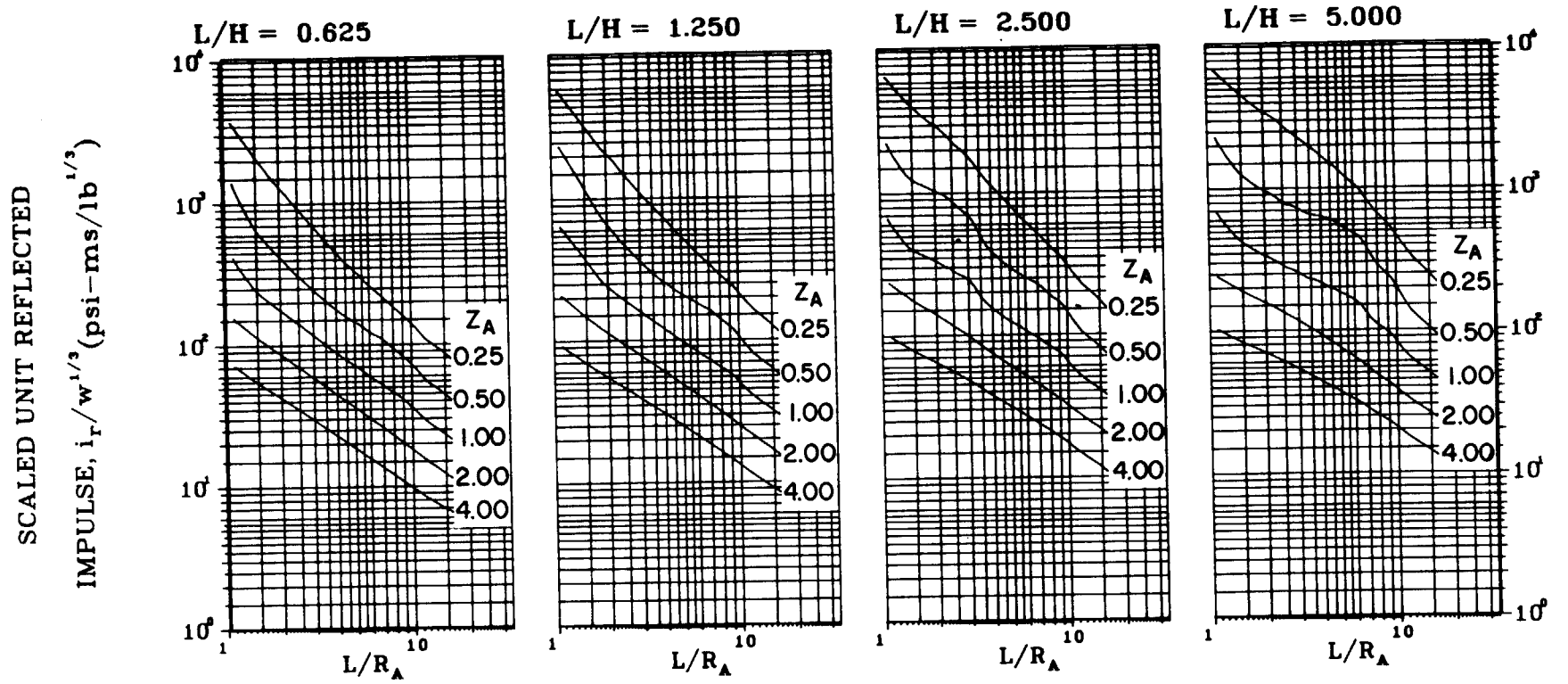


Figure 2-138 Scaled average unit reflected impulse
($N = 3$, $l/L = 0.10$, $h/H = 0.75$)

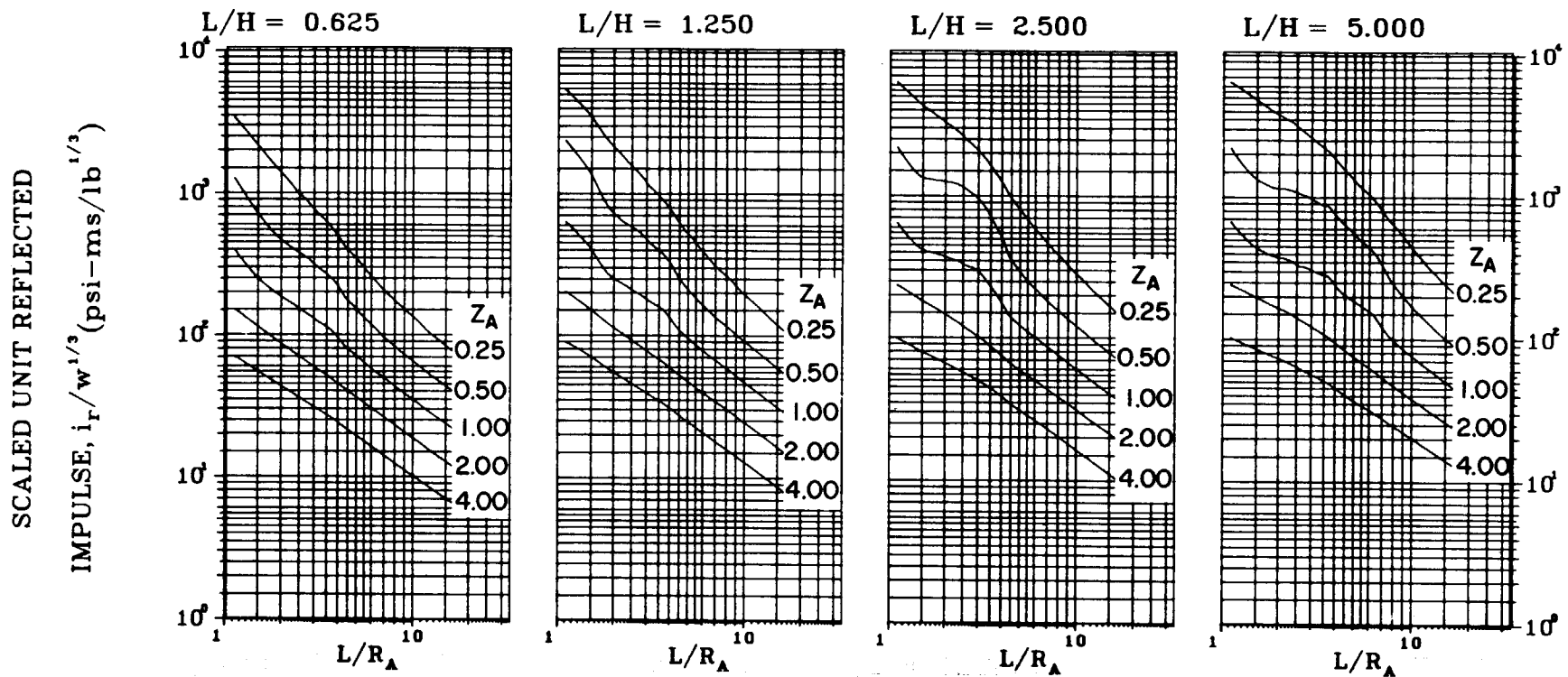


Figure 2-139 Scaled average unit reflected impulse
($N = 3$, $\ell/L = 0.25$ and 0.75 , $h/H = 0.75$)

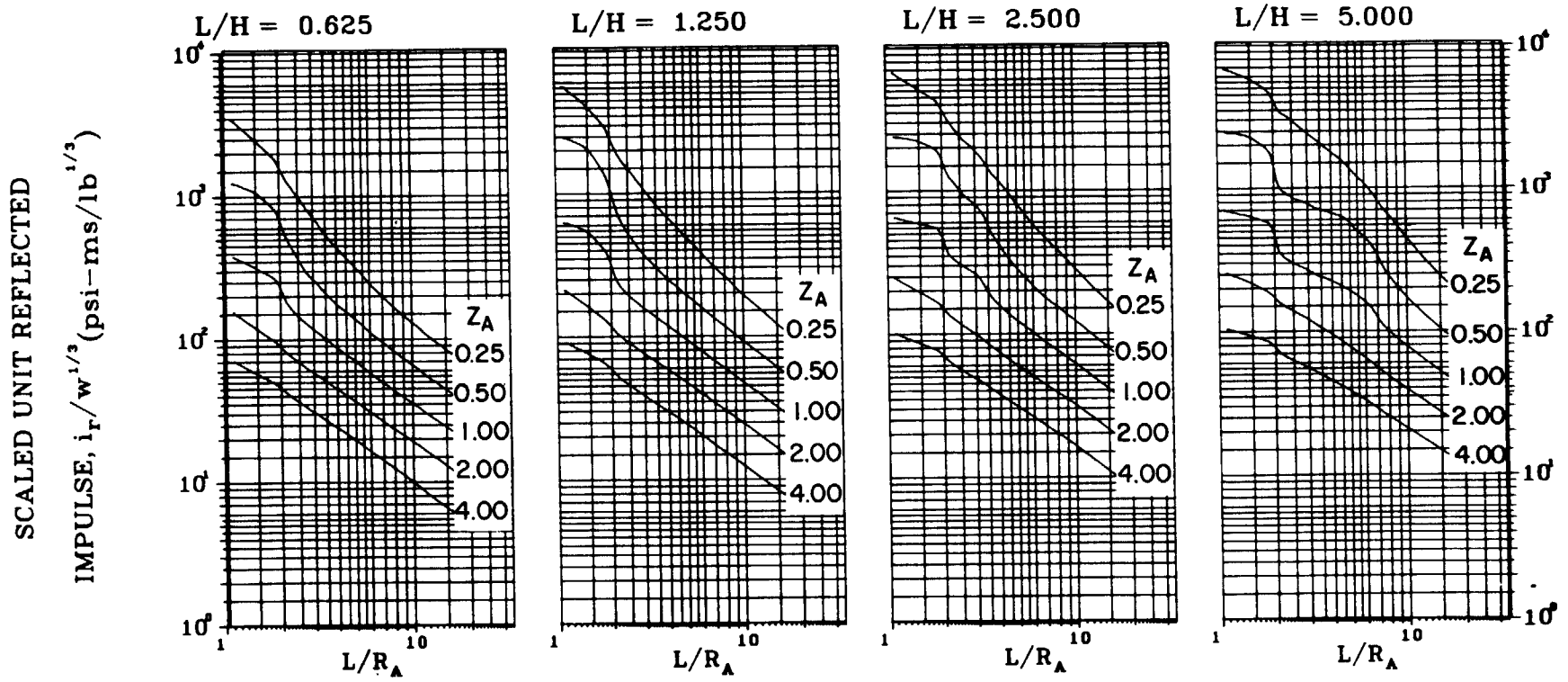


Figure 2-140 Scaled average unit reflected impulse
(N = 3, $\ell/L = 0.50$, $h/H = 0.75$)

SCALED UNIT REFLECTED

IMPULSE, $i_r/w^{1/3}$ (psi-ms/lb^{1/3})

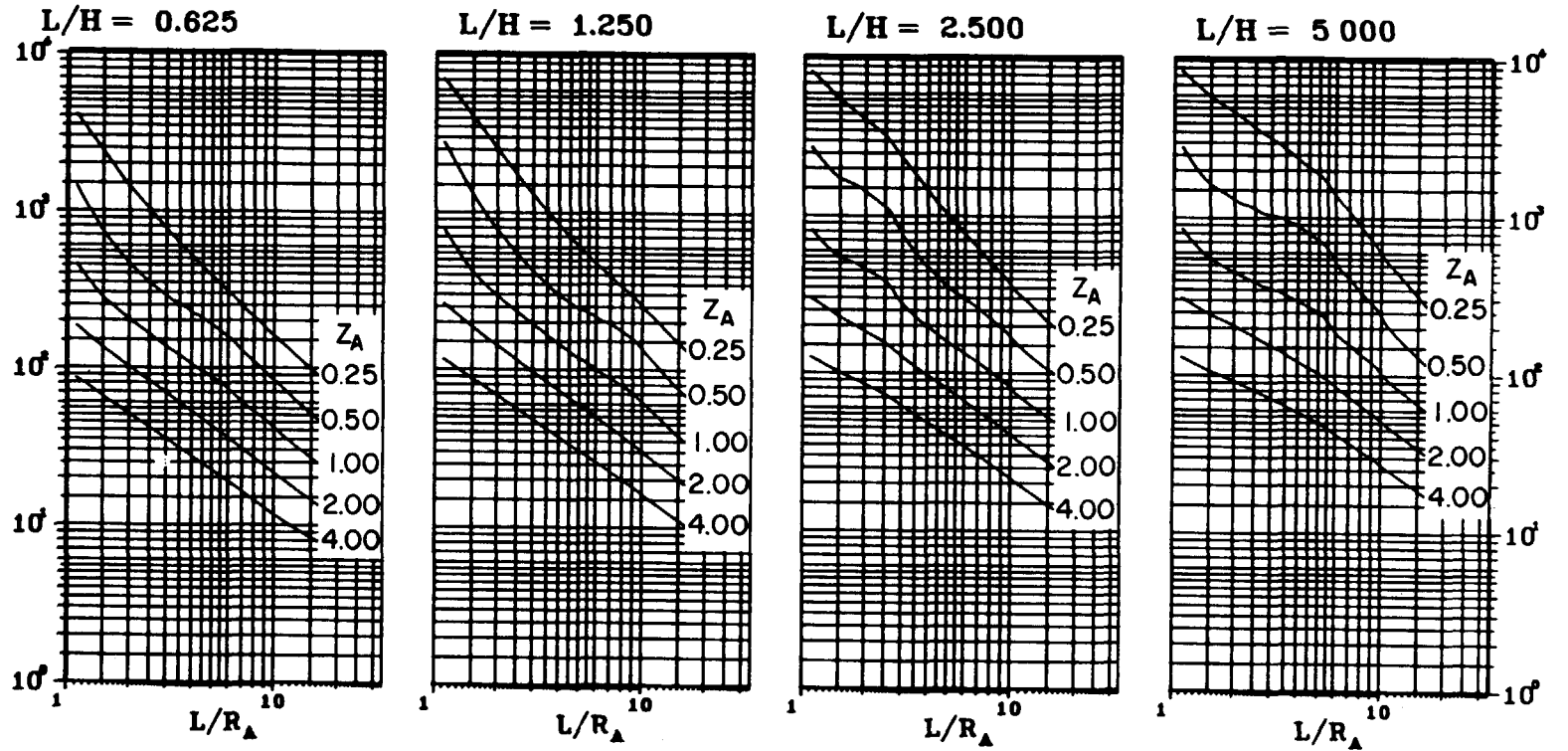


Figure 2-141 Scaled average unit reflected impulse
($N = 4, \ell/L = 0.10, h/H = 0.10$)

SCALED UNIT REFLECTED

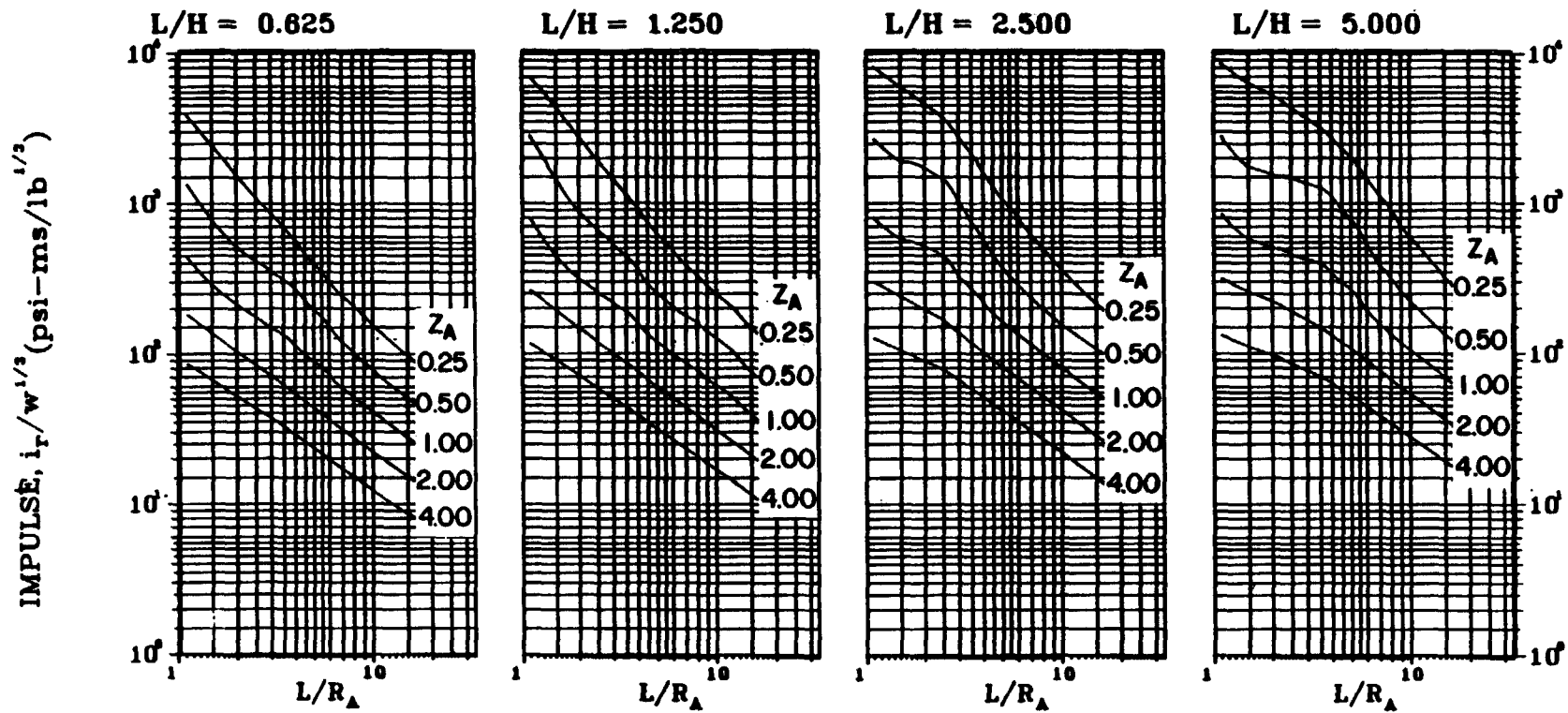


Figure 2-142 Scaled average unit reflected impulse
($N = 4$, $l/L = 0.25$ and 0.75 , $h/H = 0.10$)

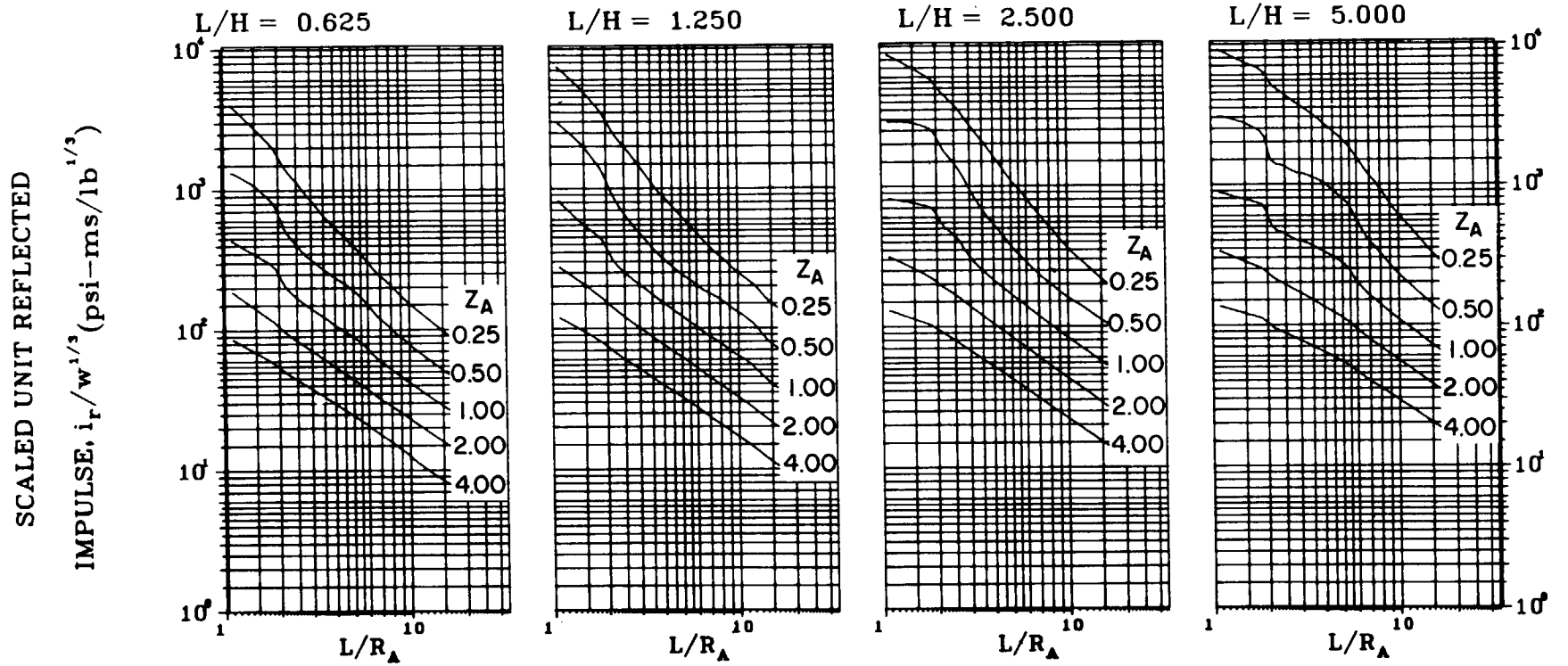


Figure 2-143 Scaled average unit reflected impulse
($N = 4$, $l/L = 0.50$, $h/H = 0.10$)

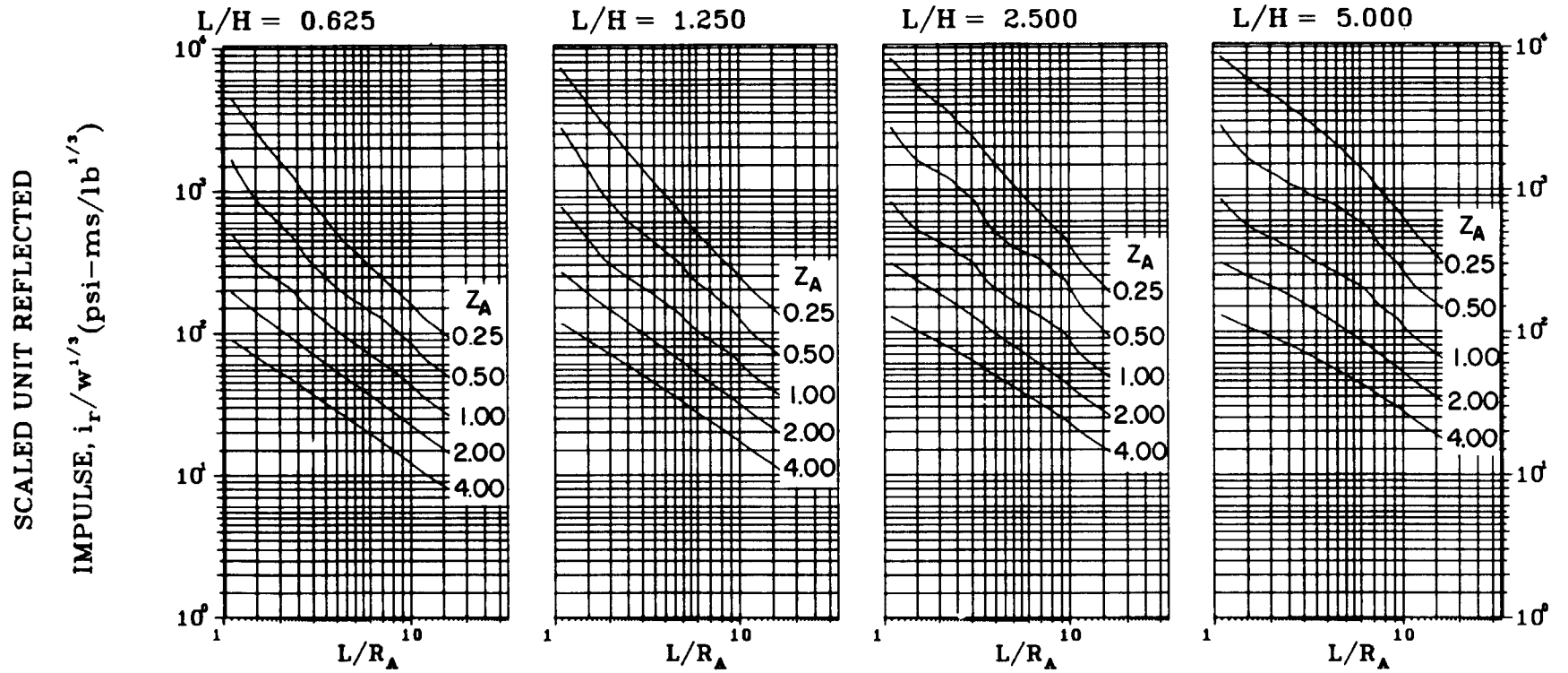


Figure 2-144 Scaled average unit reflected impulse
 ($N = 4$, $l/L = 0.10$, $h/H = 0.25$ and 0.75)

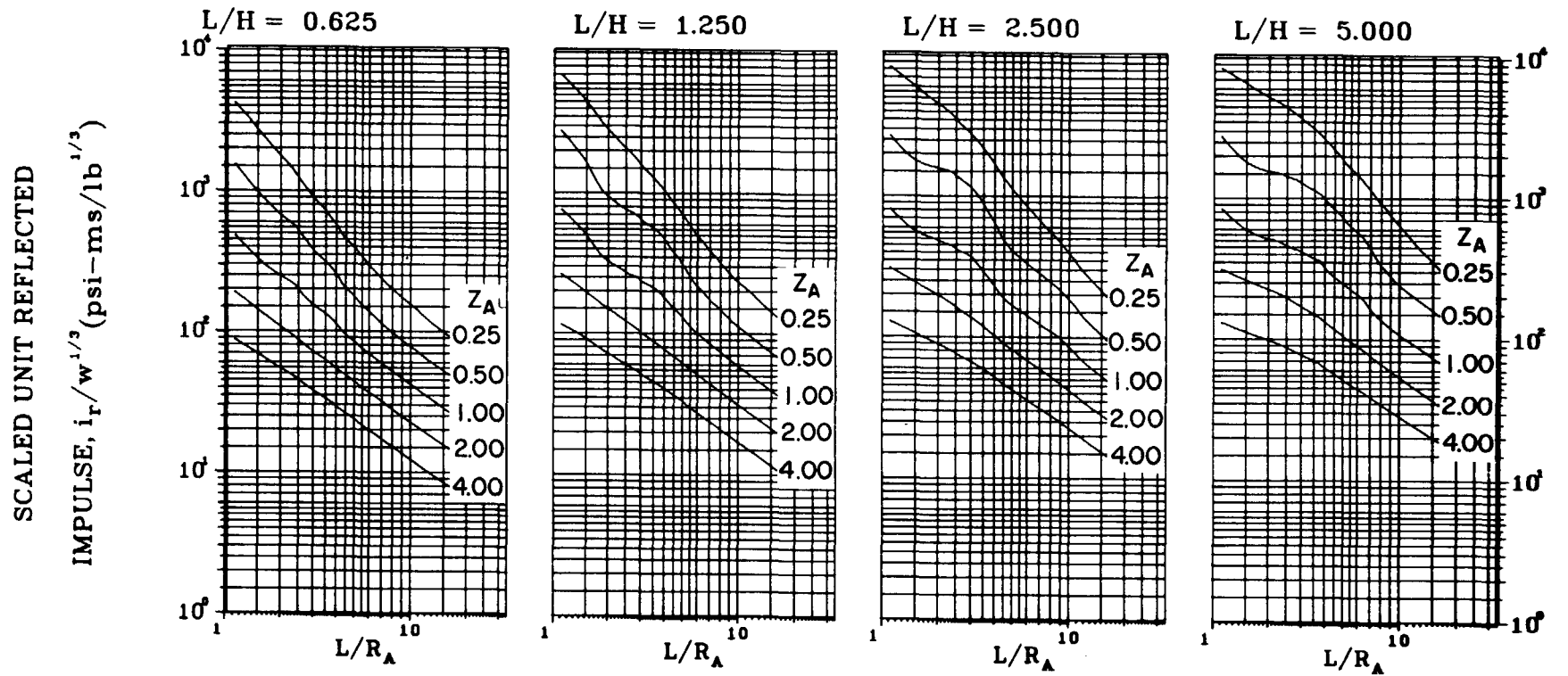


Figure 2-145 Scaled average unit reflected impulse
($N = 4$, $\ell/L = 0.25$ and 0.75 , $h/H = 0.25$ and 0.75)

SCALED UNIT REFLECTED

IMPULSE, $i_r/w^{1/3}$ (psi-ms/lb^{1/3})

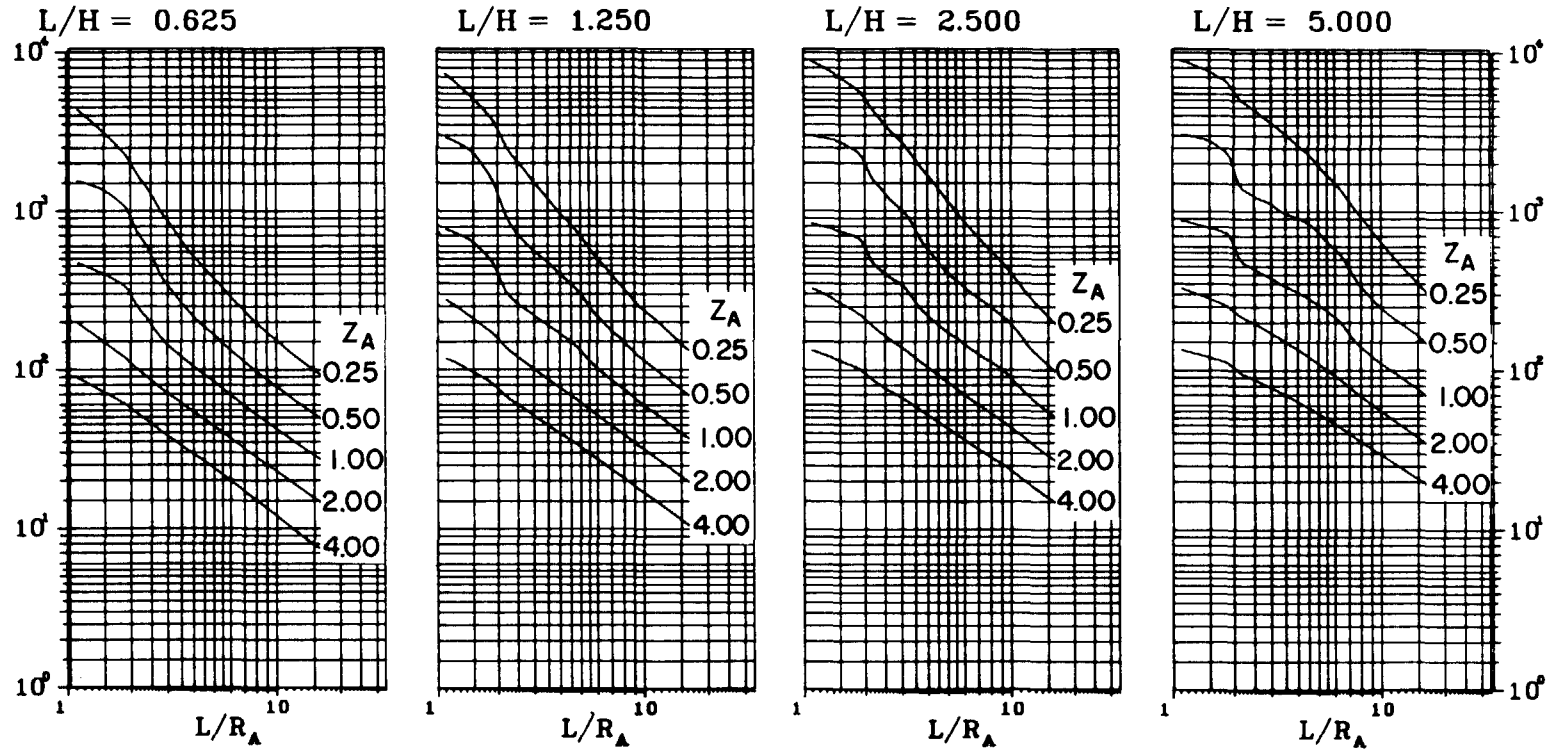


Figure 2-146 Scaled average unit reflected impulse
($N = 4$, $l/L = 0.50$, $h/H = 0.25$ and 0.75)

SCALED UNIT REFLECTED

IMPULSE, $i_r/w^{1/3}$ (psi-ms/lb^{1/3})

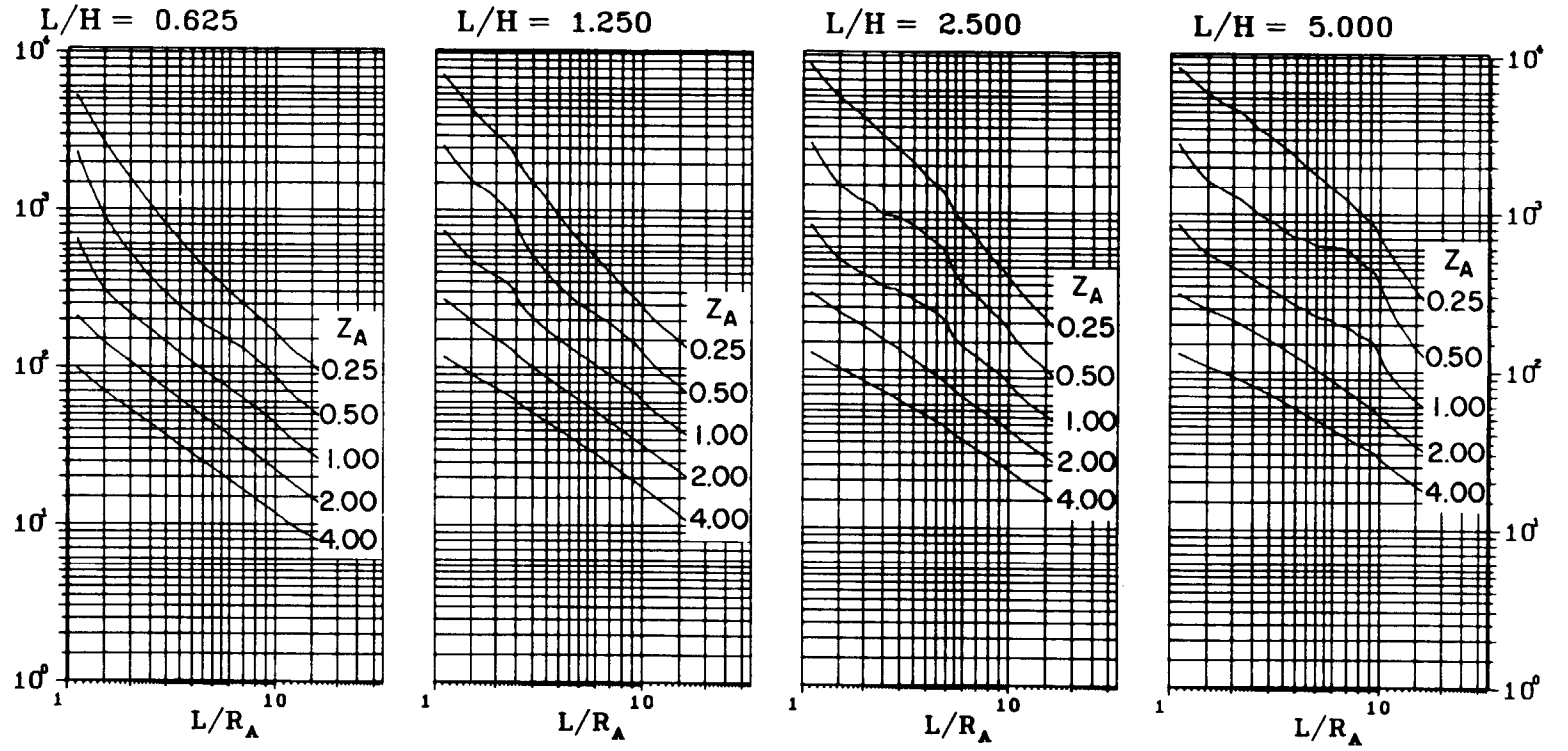


Figure 2-147 Scaled average unit reflected impulse
(N = 4, $\ell/L = 0.10$, $h/H = 0.50$)

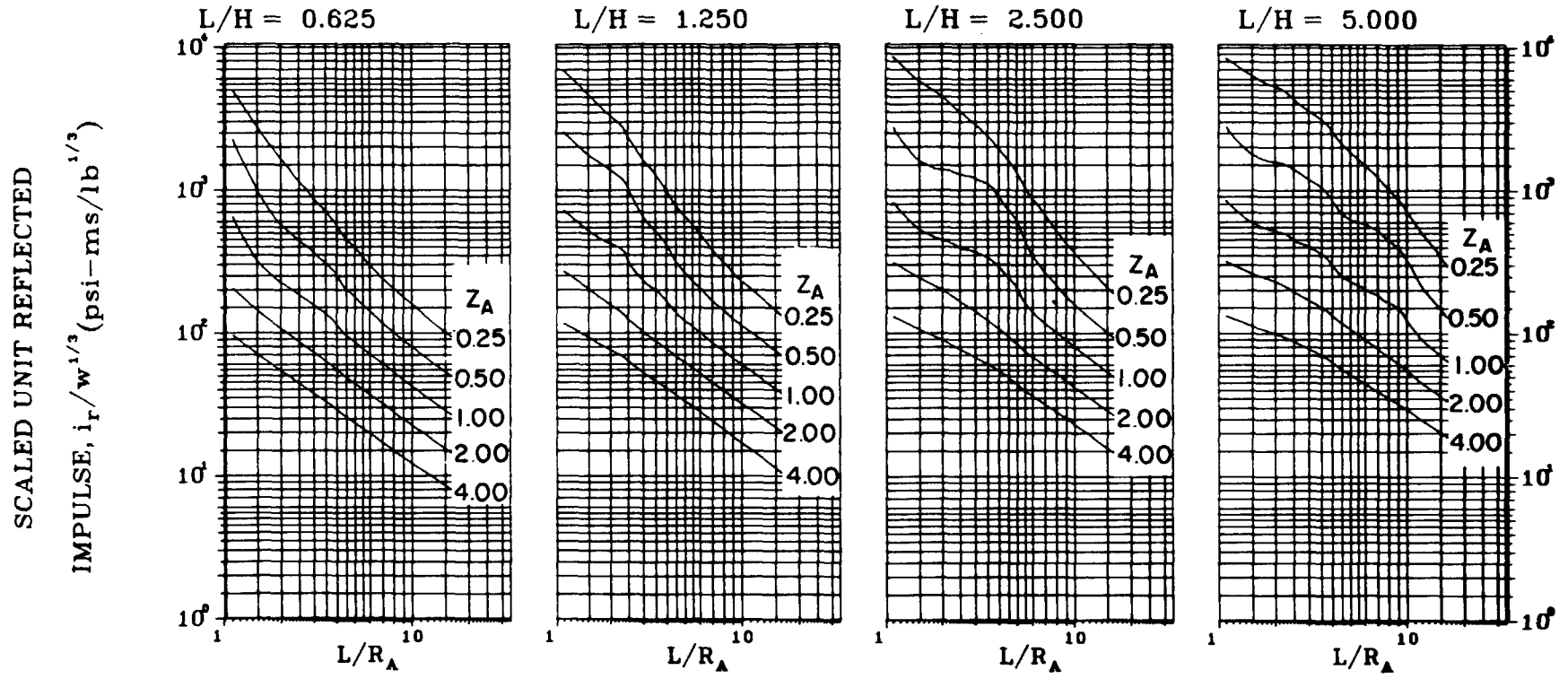


Figure 2-148 Scaled average unit reflected impulse
($N = 4$, $\ell/L = 0.25$ and 0.75 , $h/H = 0.50$)

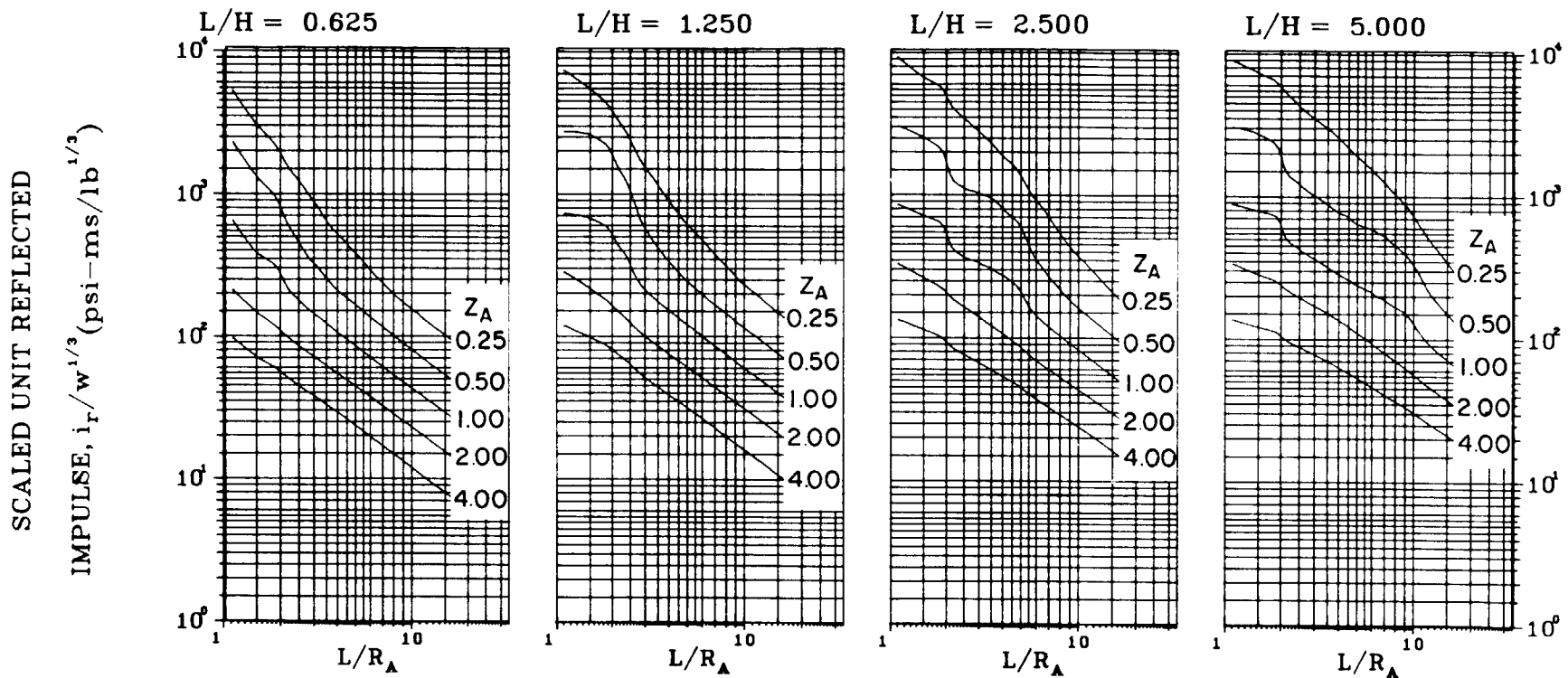


Figure 2-149 Scaled average unit reflected impulse
($N = 4, \ell/L = 0.50, h/H = 0.50$)

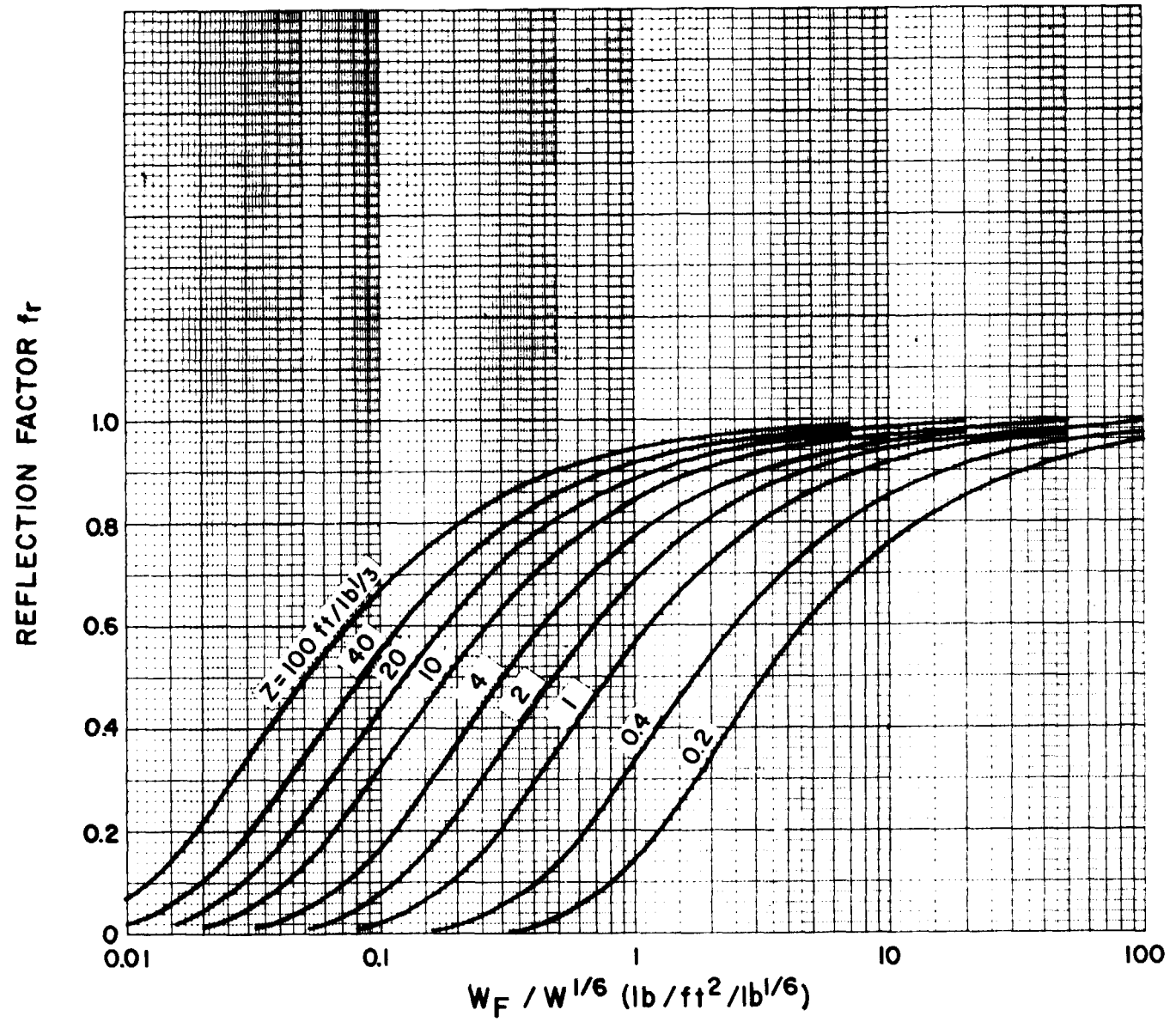


Figure 2-150 Reflection factor for shock loads on frangible elements

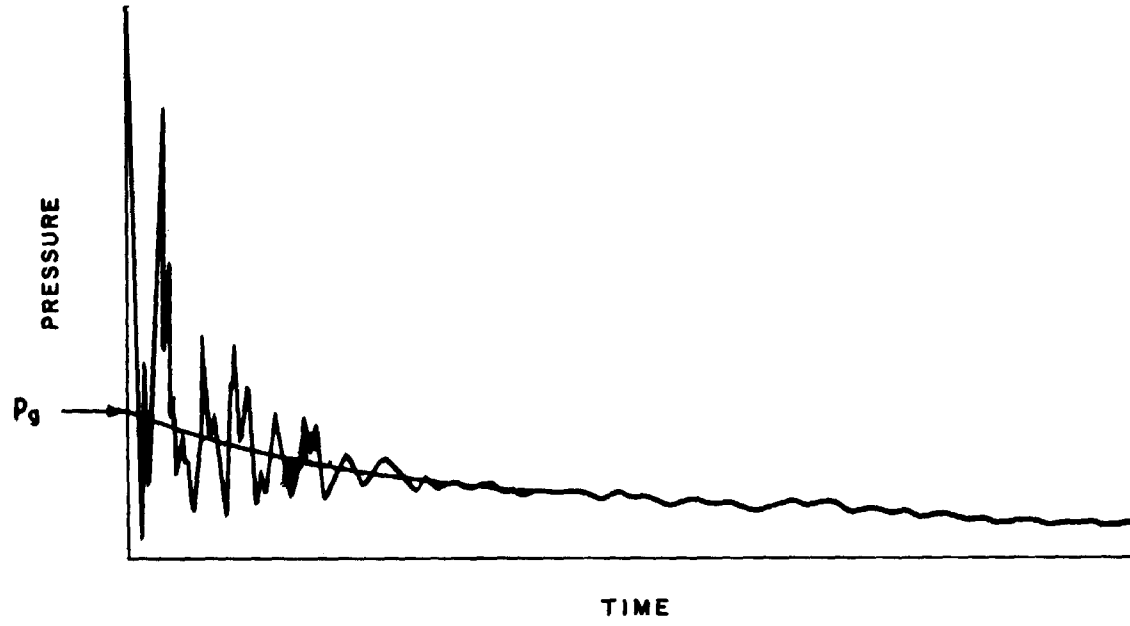


Figure 2-151 Pressure-time variation for a partially vented explosion

2-194

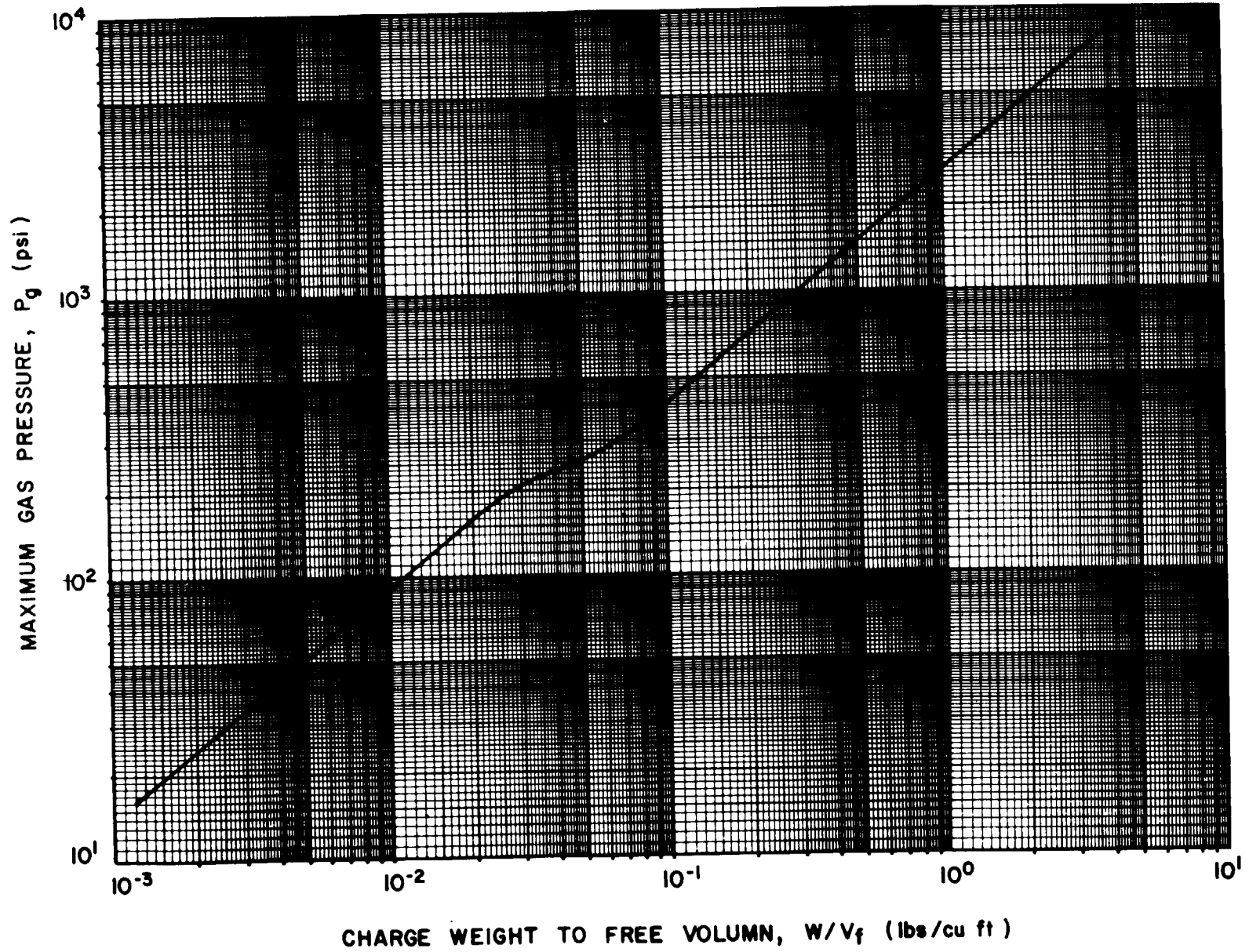


Figure 2-152 Peak gas pressure produced by a TNT detonation in a partially contained chamber

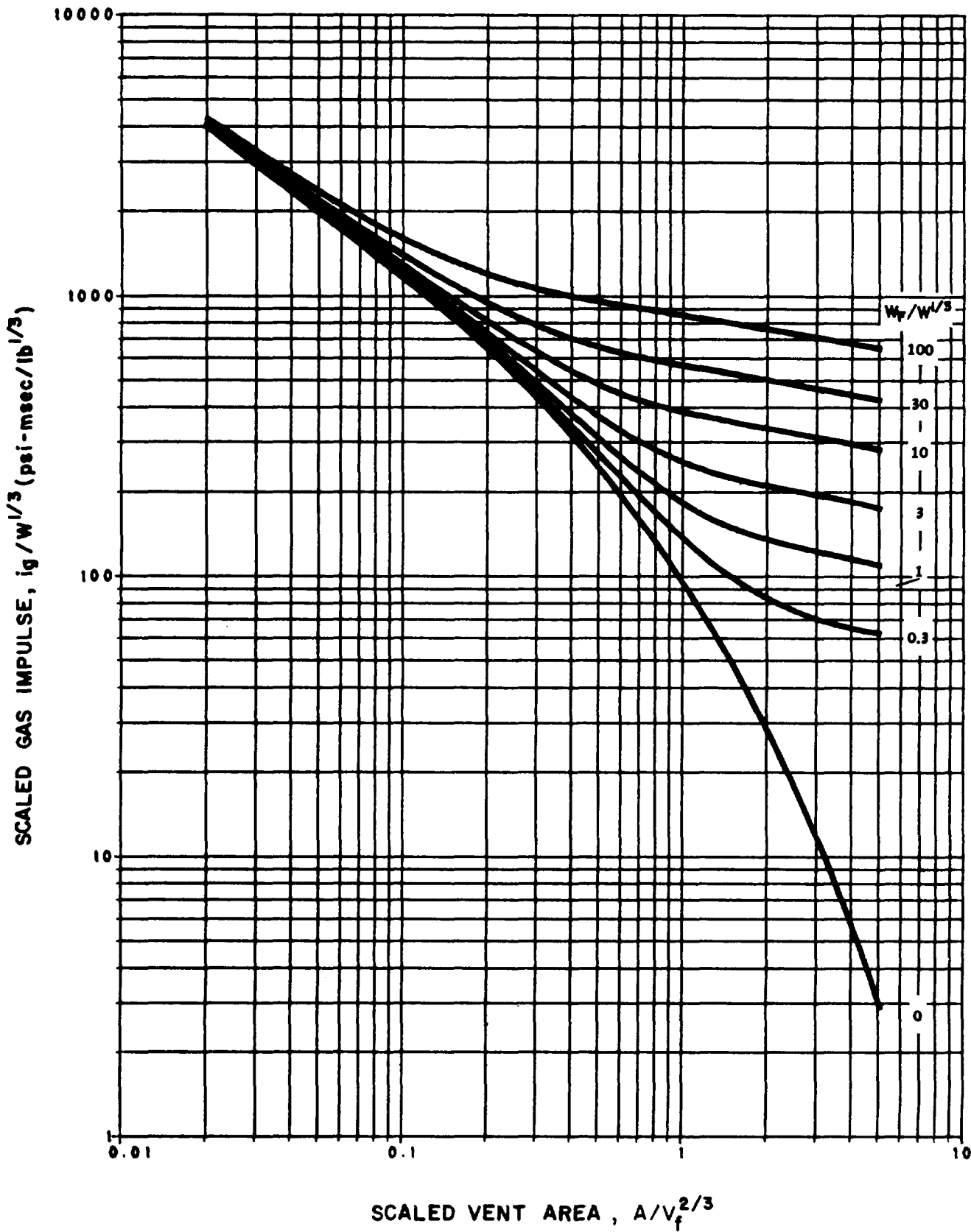


Figure 2-153 Scaled gas impulse ($W/V_f = 0.002$, $i_r/W^{1/3} = 20$)

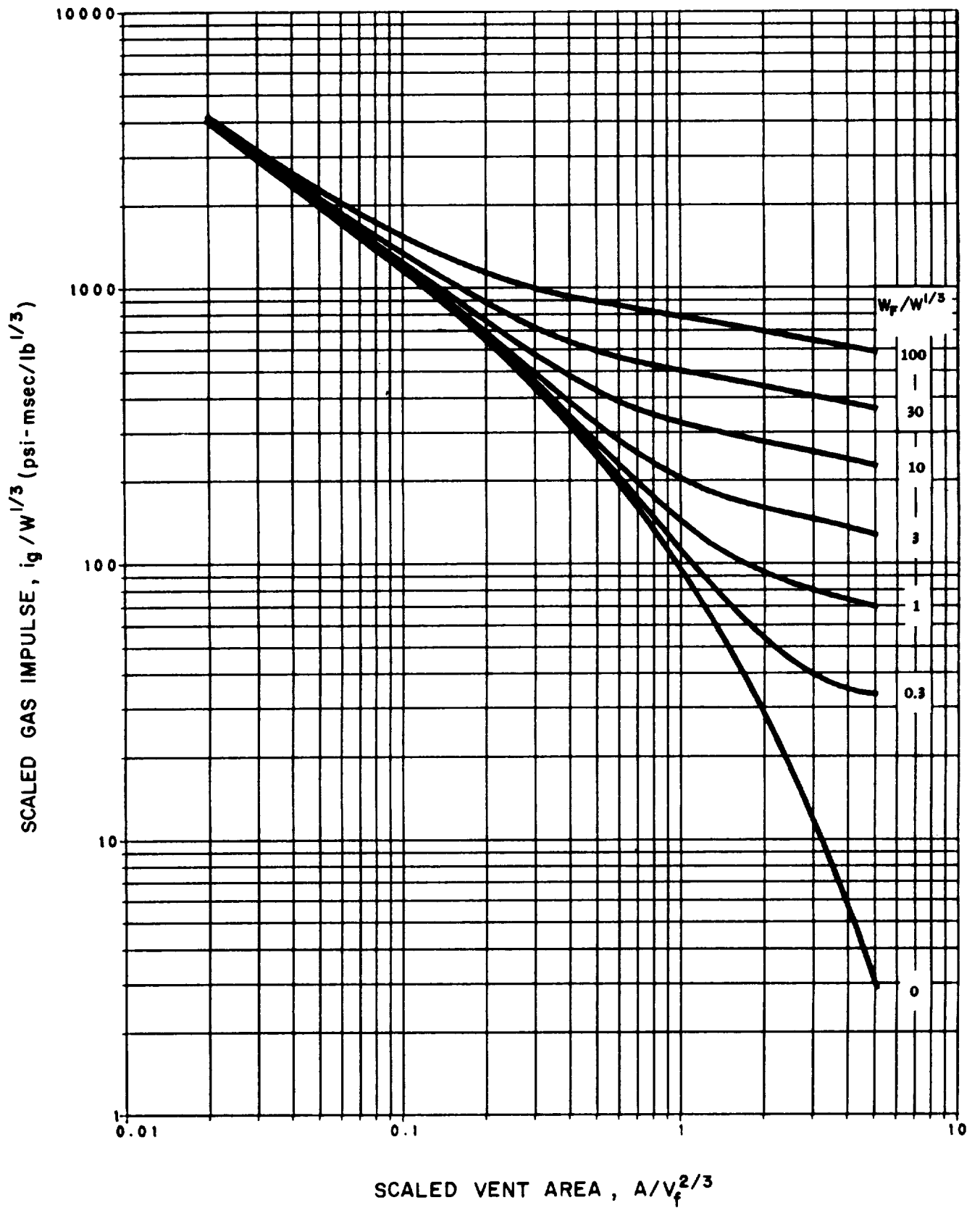


Figure 2-154 Scaled gas impulse ($W/V_f = 0.002$, $i_r/W^{1/3} = 100$)

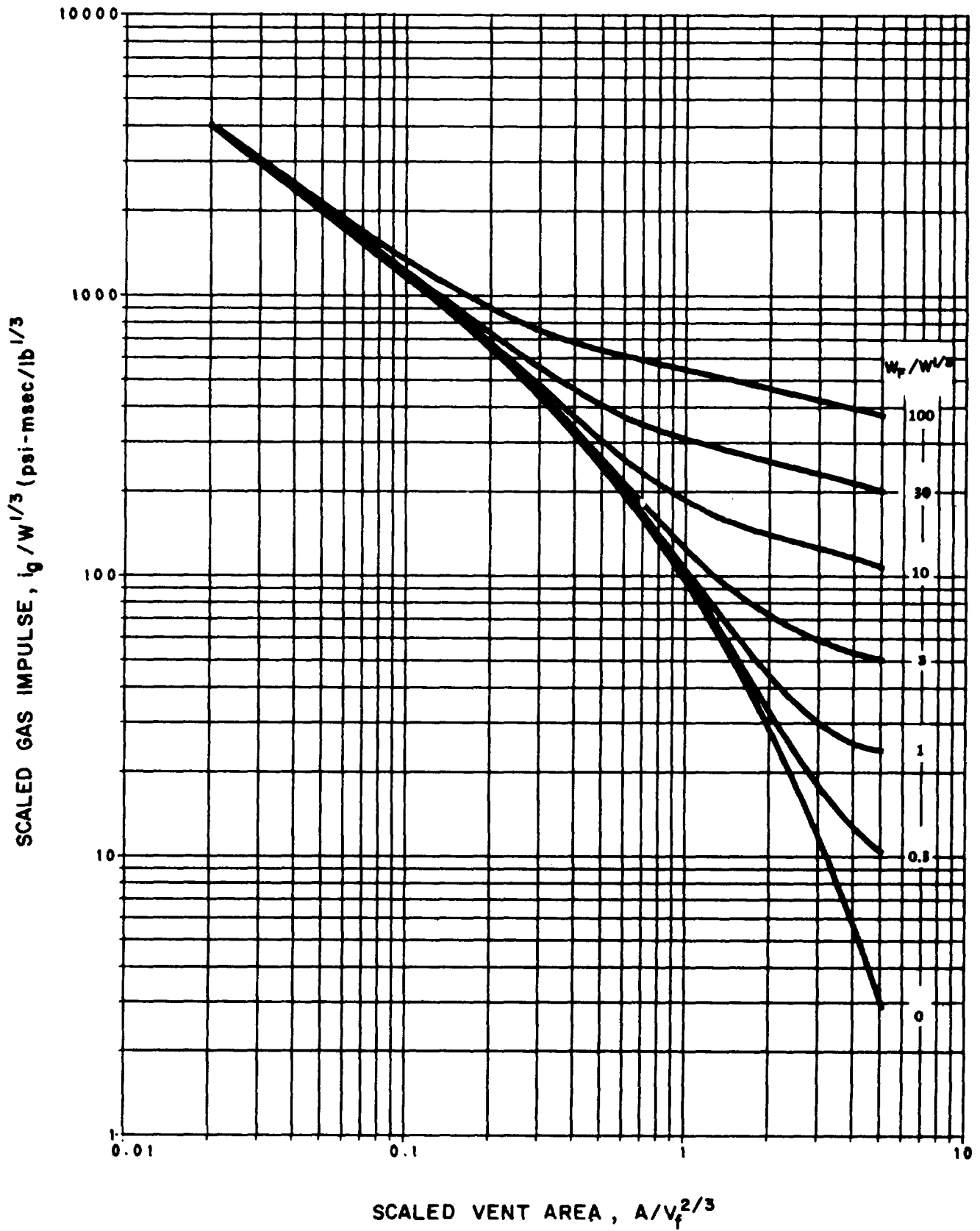


Figure 2-155 Scaled gas impulse ($W/V_f = 0.002$, $i_r/W^{1/3} = 600$)

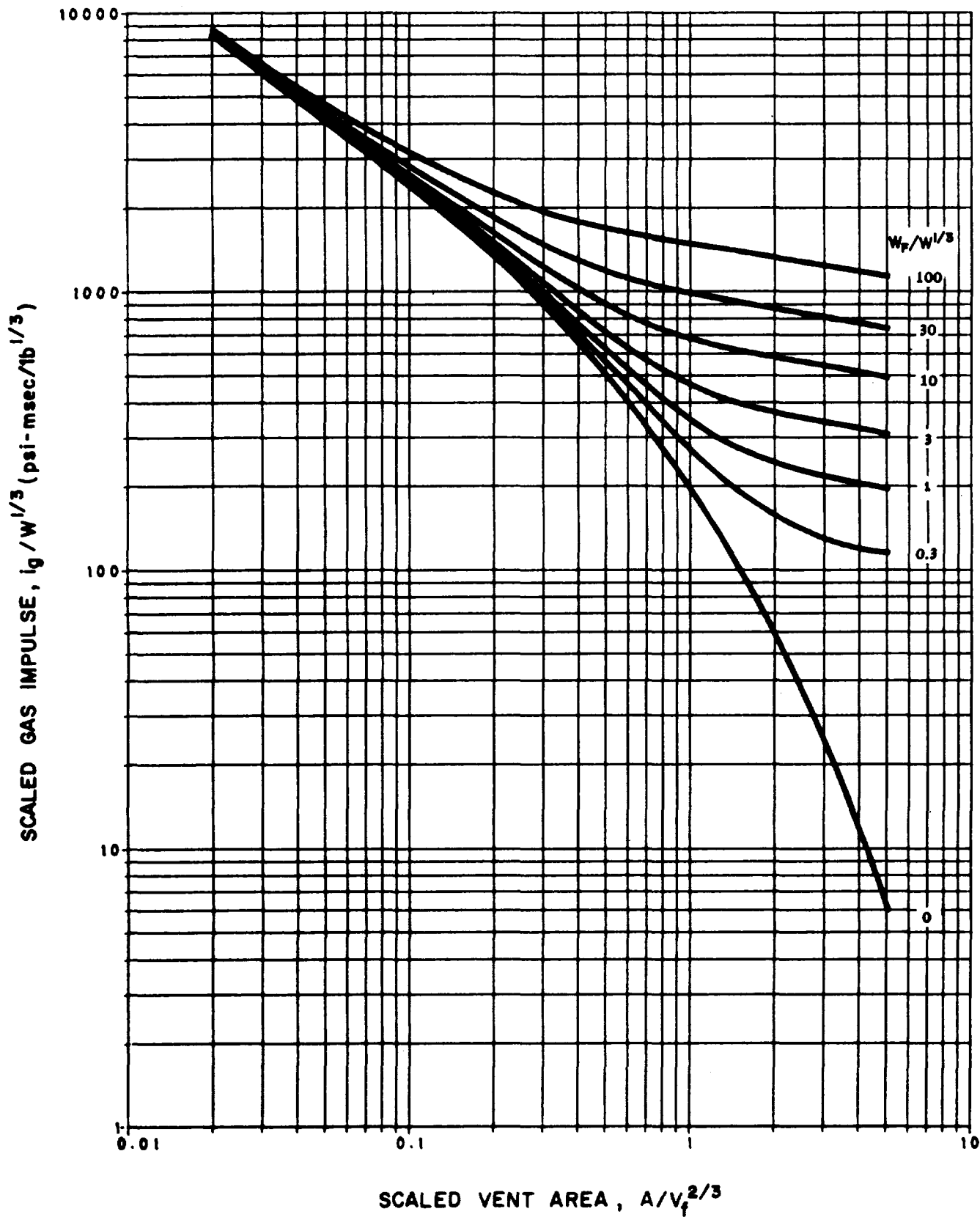


Figure 2-156 Scaled gas impulse ($W/V_f = 0.015$, $i_r/W^{1/3} = 20$)

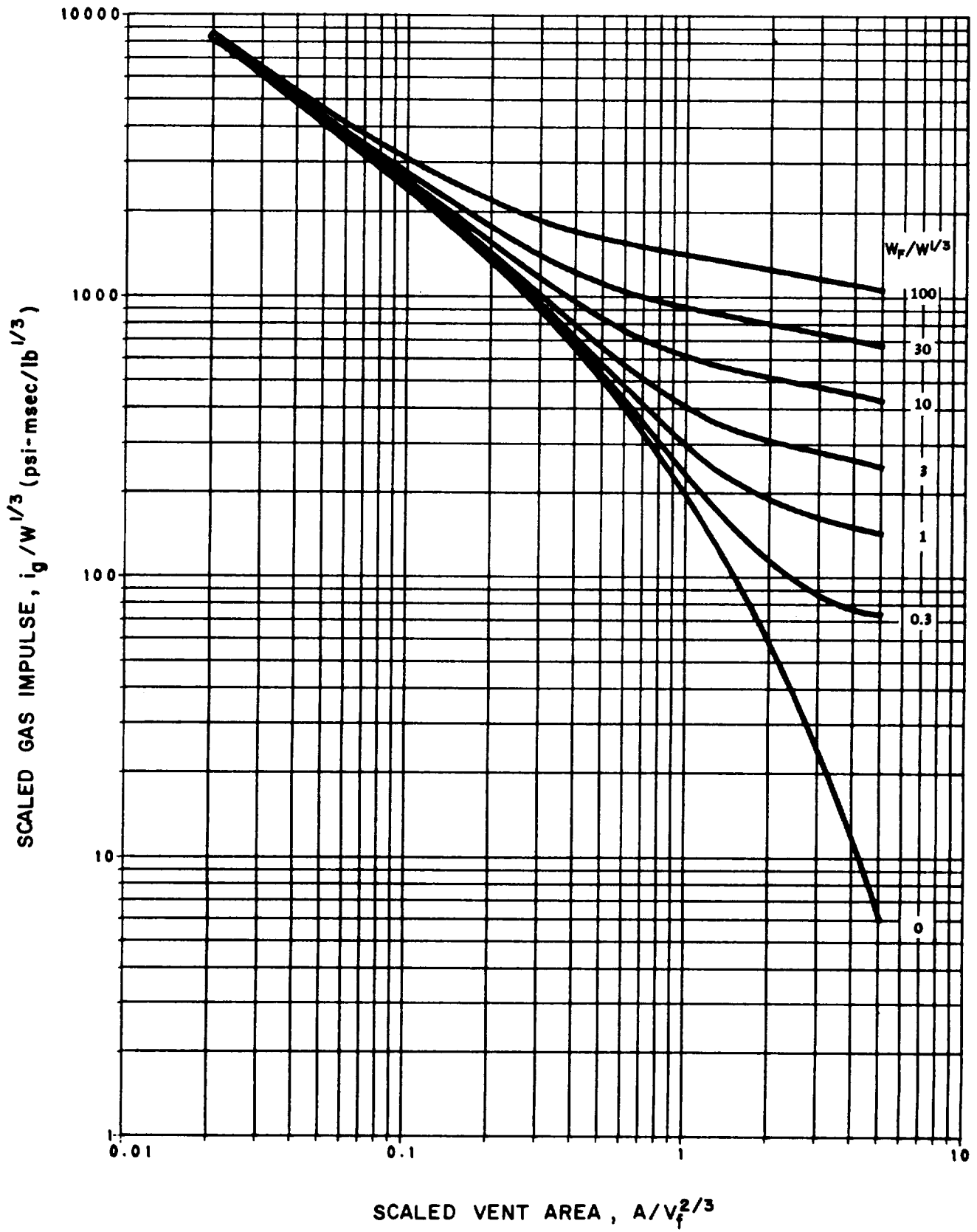


Figure 2-157 Scaled gas impulse ($W/V_f = 0.015$, $i_r/W^{1/3} = 100$)

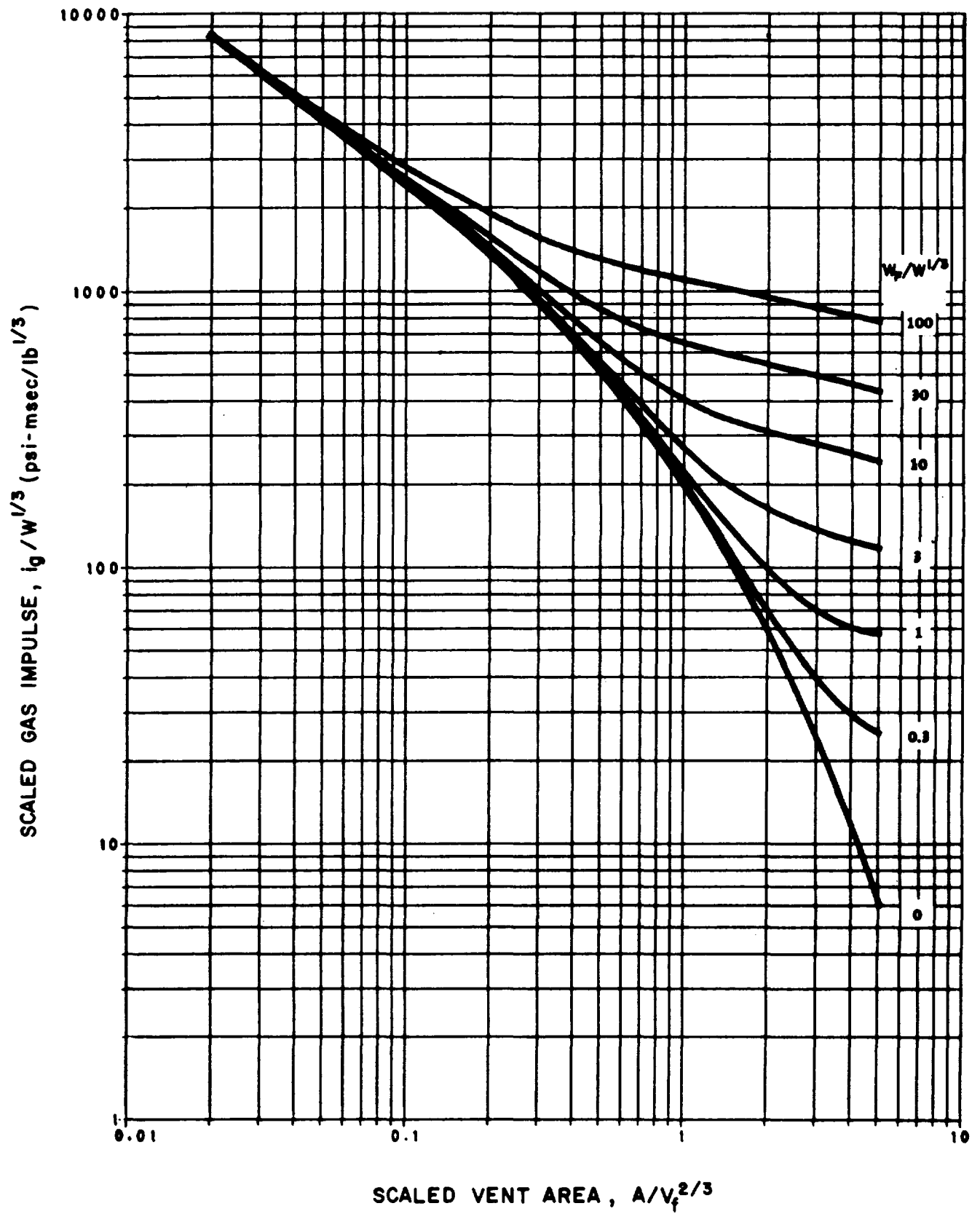


Figure 2-158 Scaled gas impulse ($W/V_f = 0.015$, $i_r/W^{1/3} = 600$)

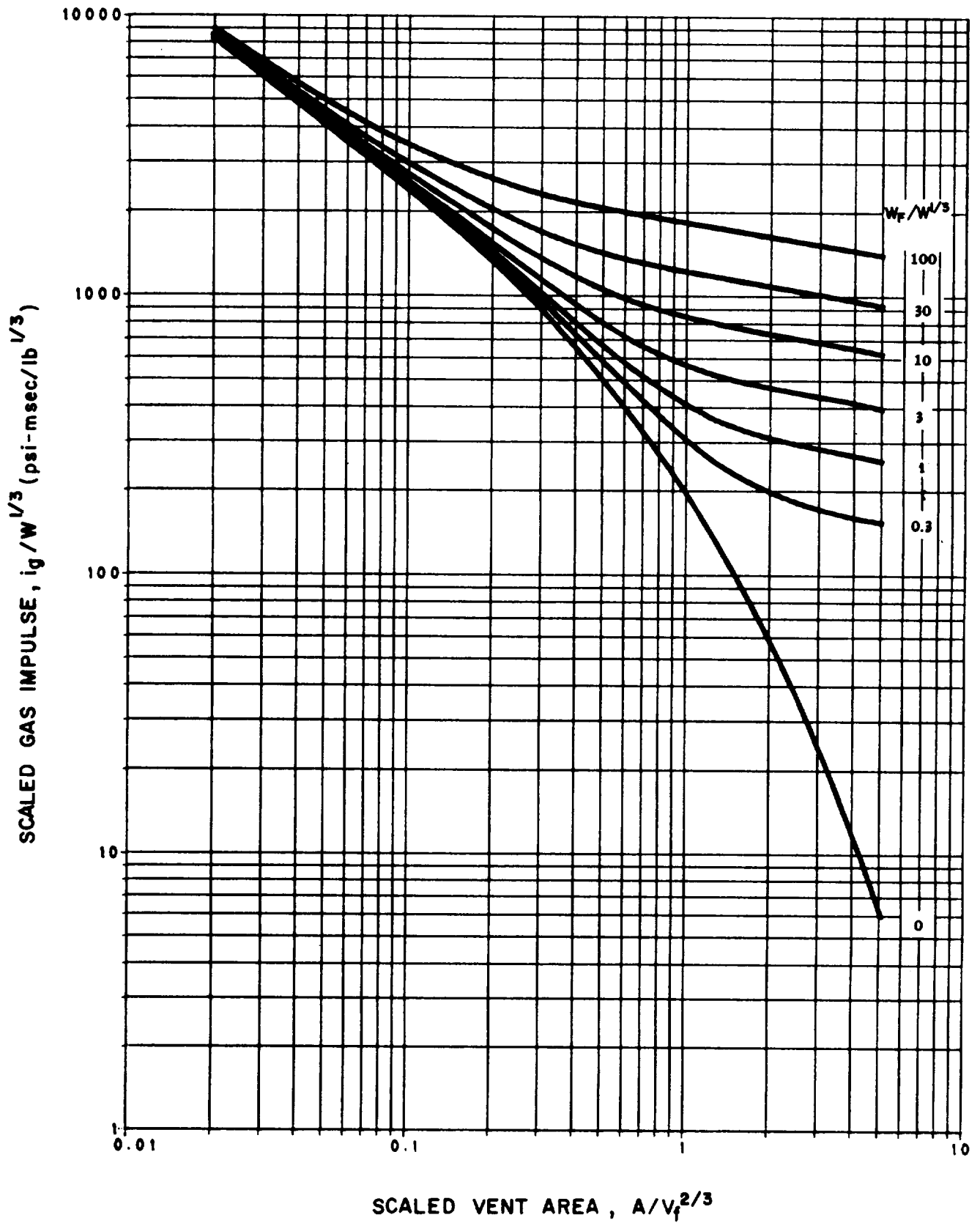


Figure 2-159 Scaled gas impulse ($W/V_f = 0.15$, $i_r/W^{1/3} = 20$)

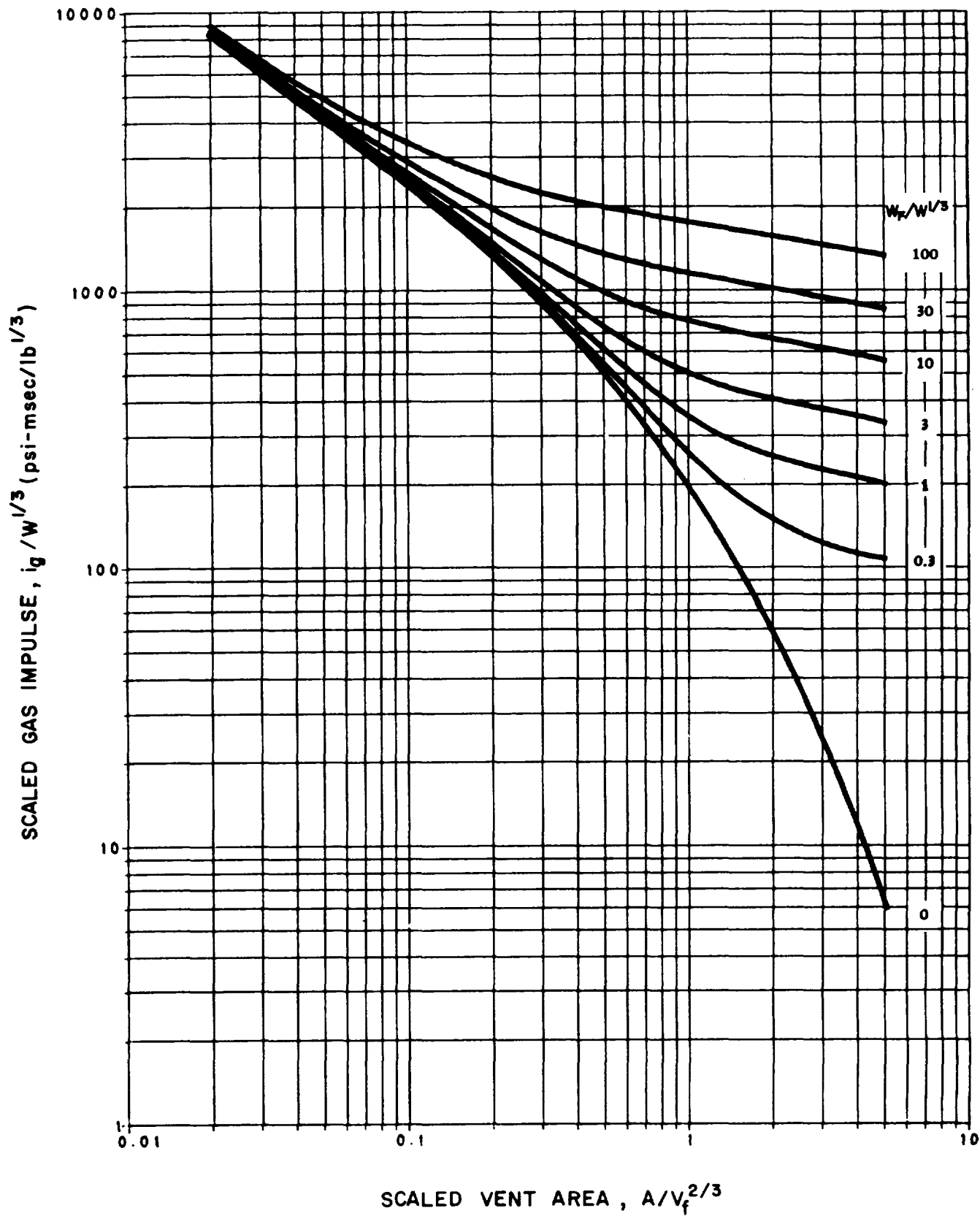


Figure 2-160 Scaled gas impulse ($W/V_f = 0.15$, $i_r/W^{1/3} = 100$)

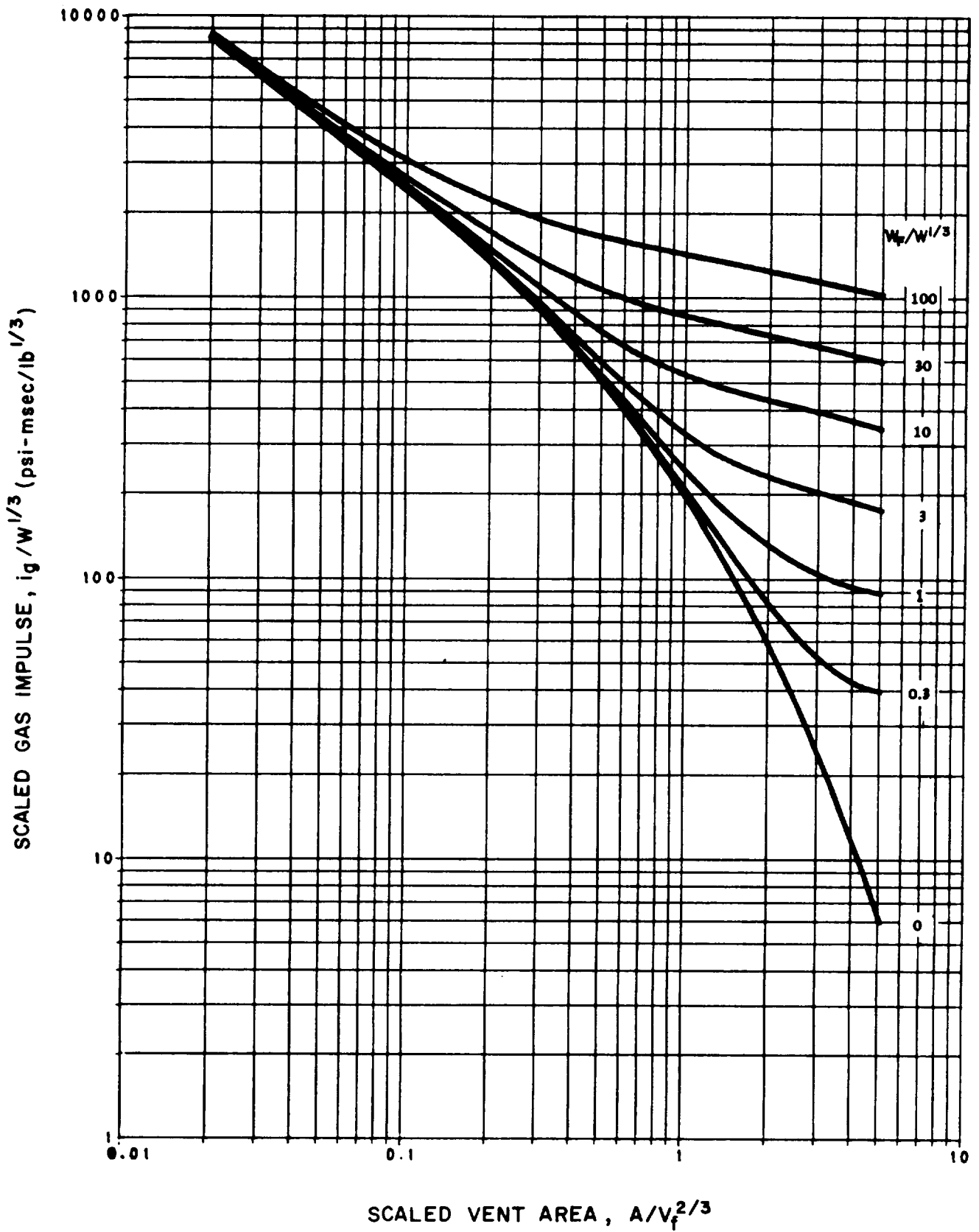


Figure 2-161 Scaled gas impulse ($W/V_f = 0.15$, $i_r/W^{1/3} = 600$)

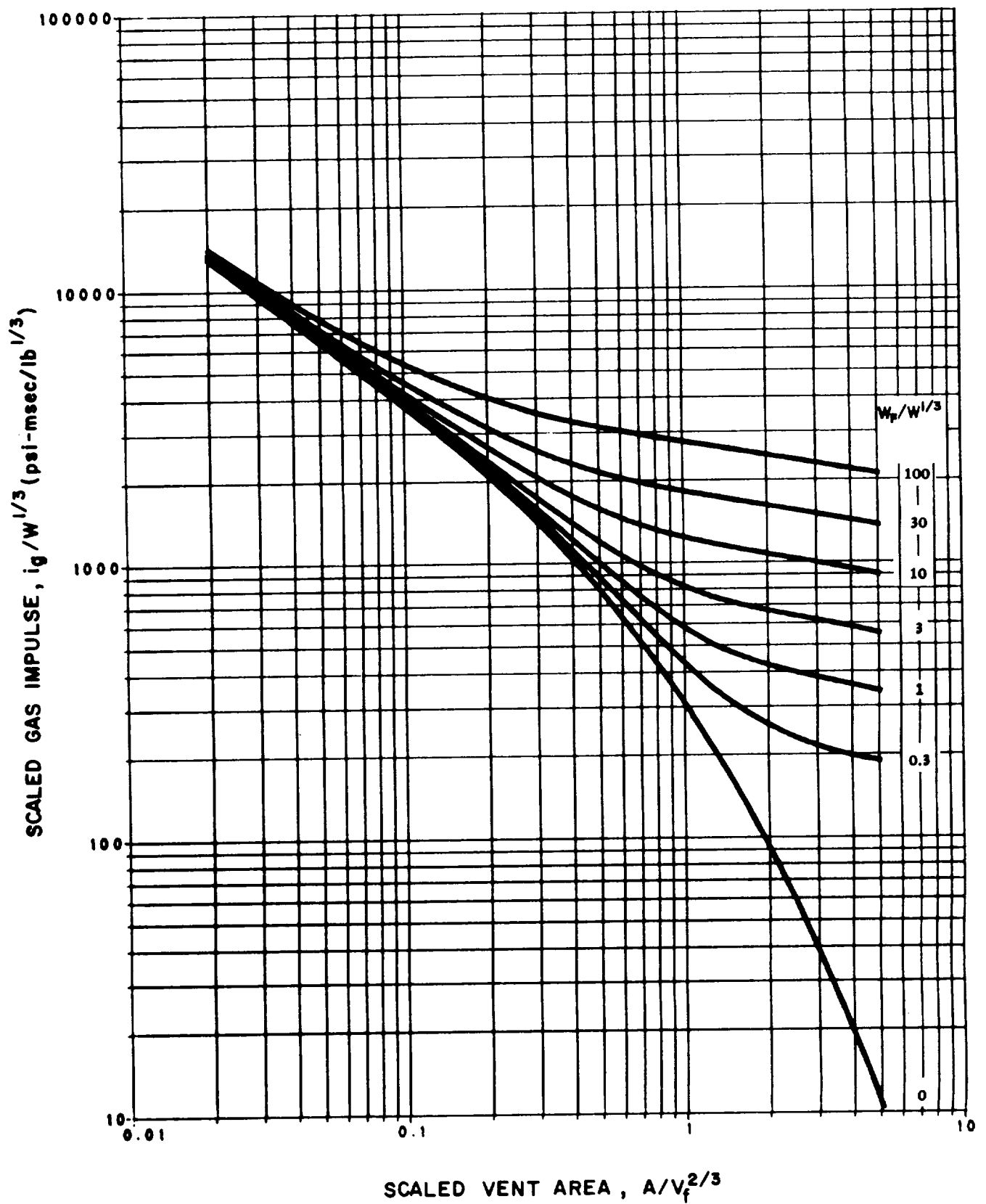


Figure 2-162 Scaled gas impulse ($W/V_f = 1.0$, $i_r/W^{1/3} = 100$)

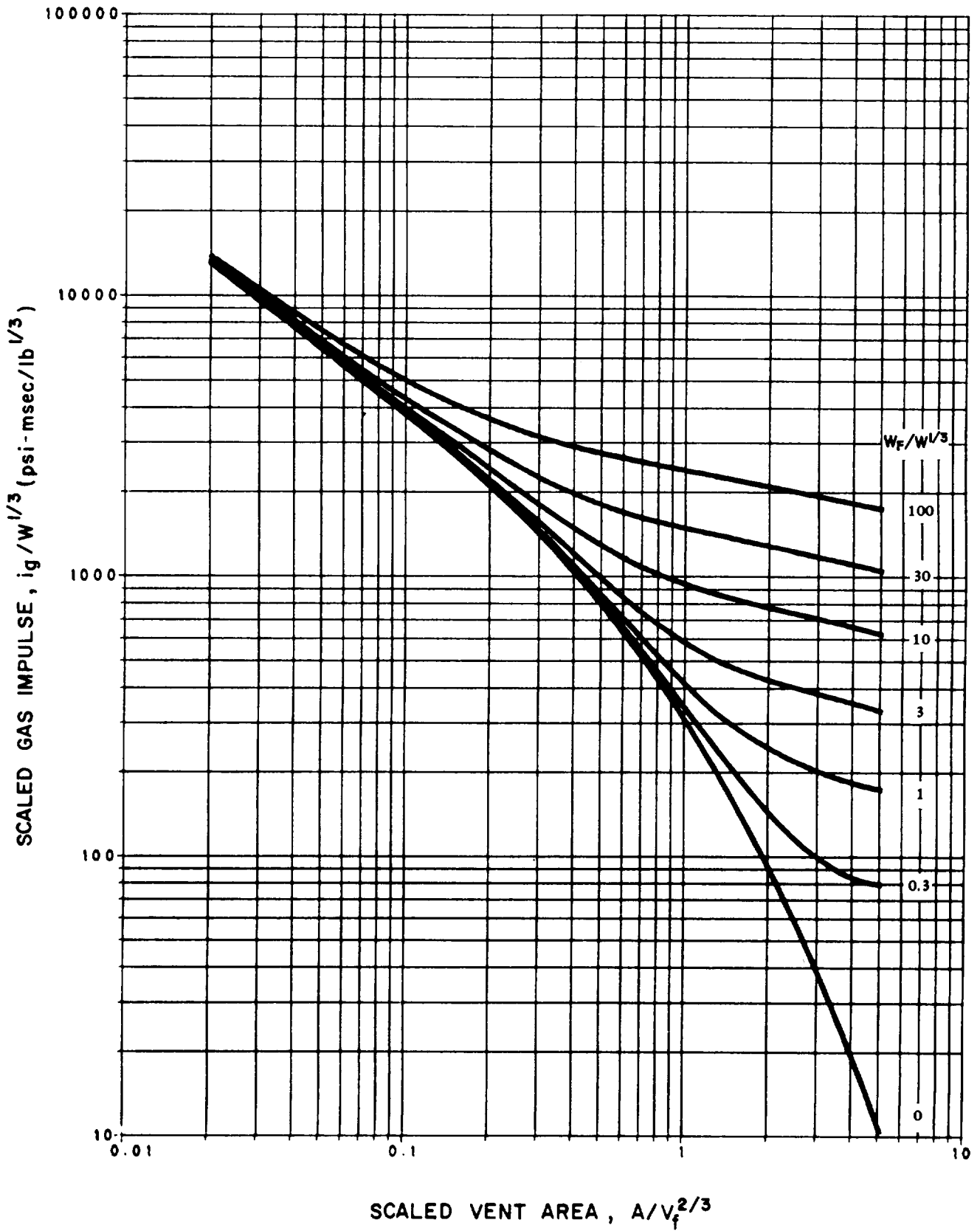


Figure 2-163 Scaled gas impulse ($W/V_f = 1.0$, $i_r/W^{1/3} = 600$)

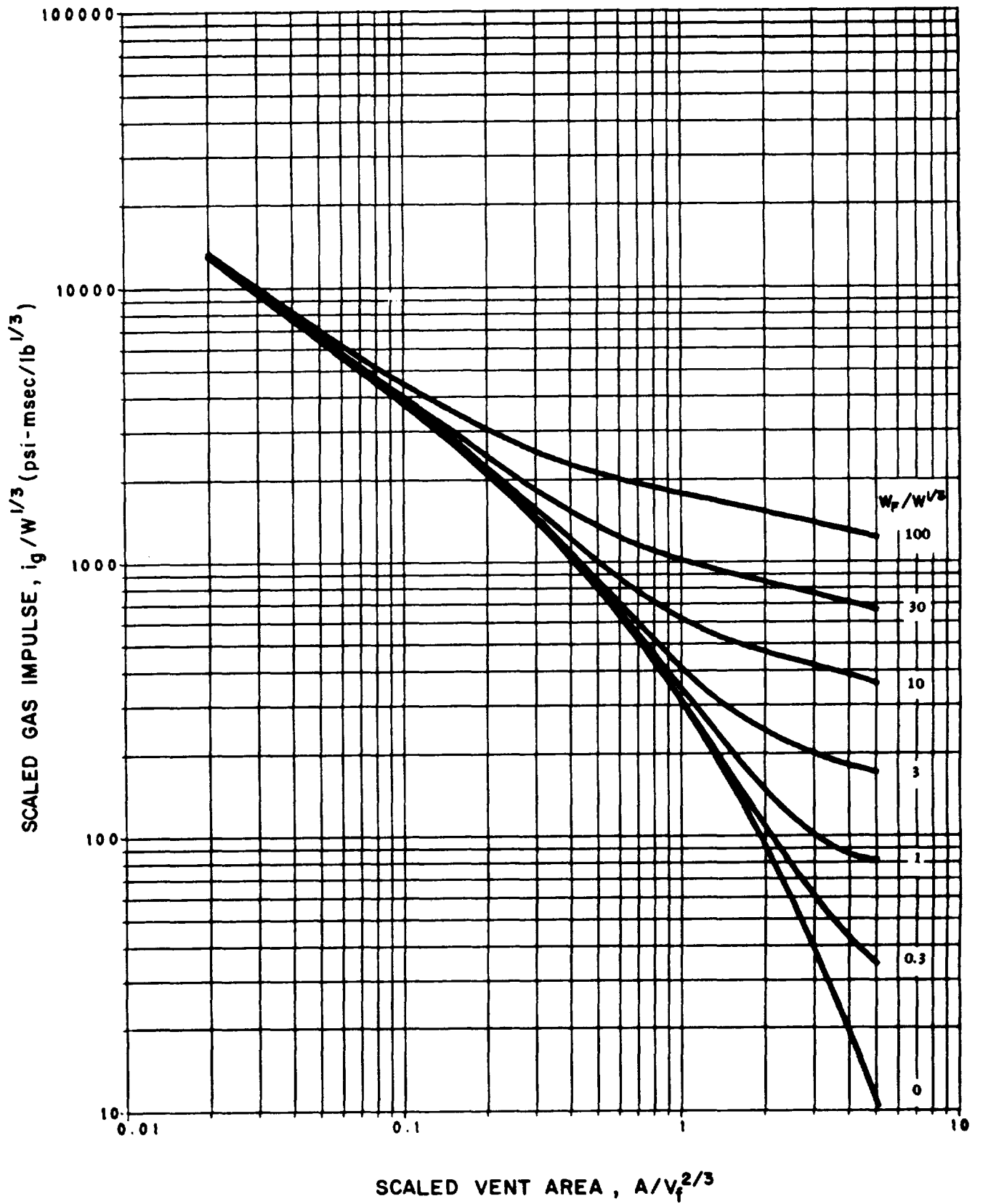
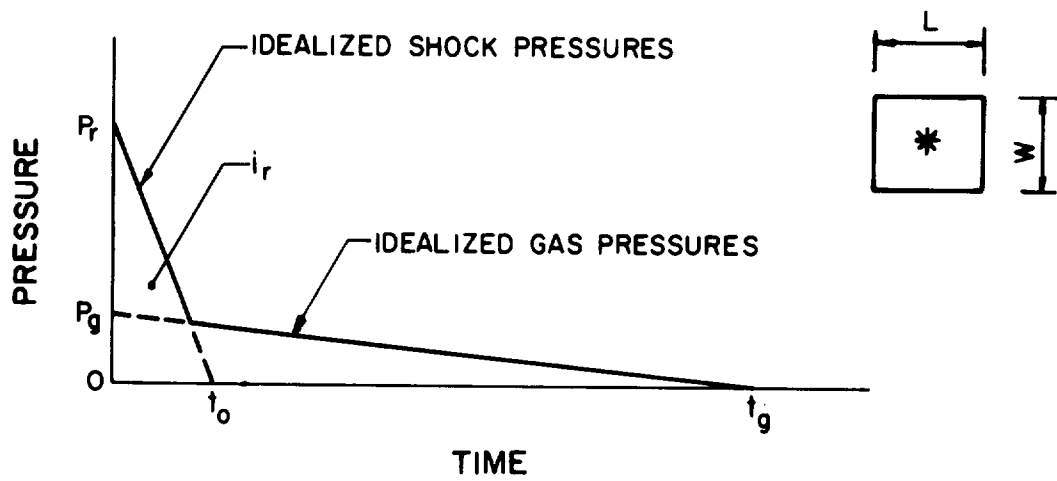
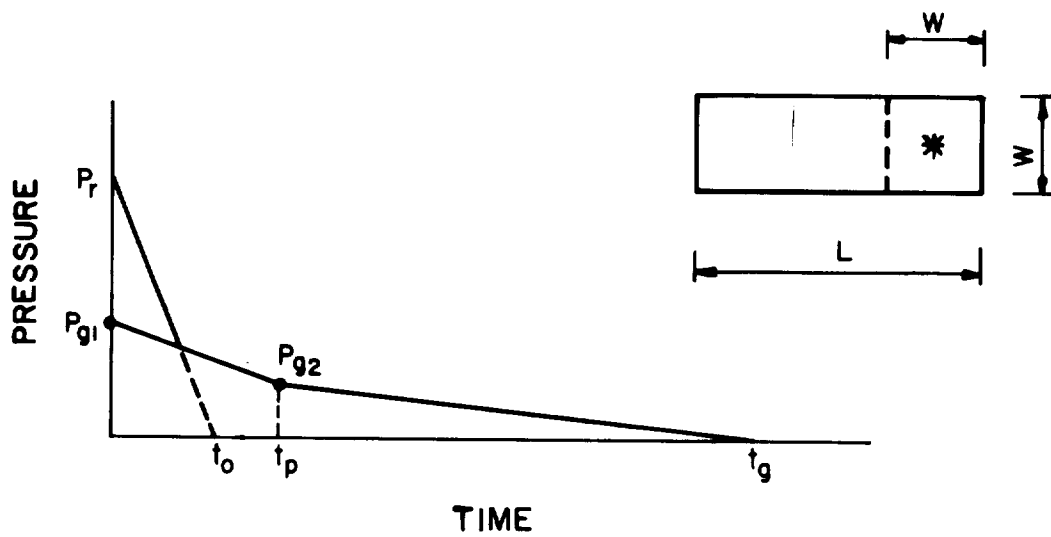


Figure 2-164 Scaled gas impulse ($W/V_f = 1.0$, $i_r/W^{1/3} = 2000$)



a) SMALL AND/OR SQUARE CHAMBER



b) LONG RECTANGULAR CHAMBER

Figure 2-165 Combined shock and gas pressures

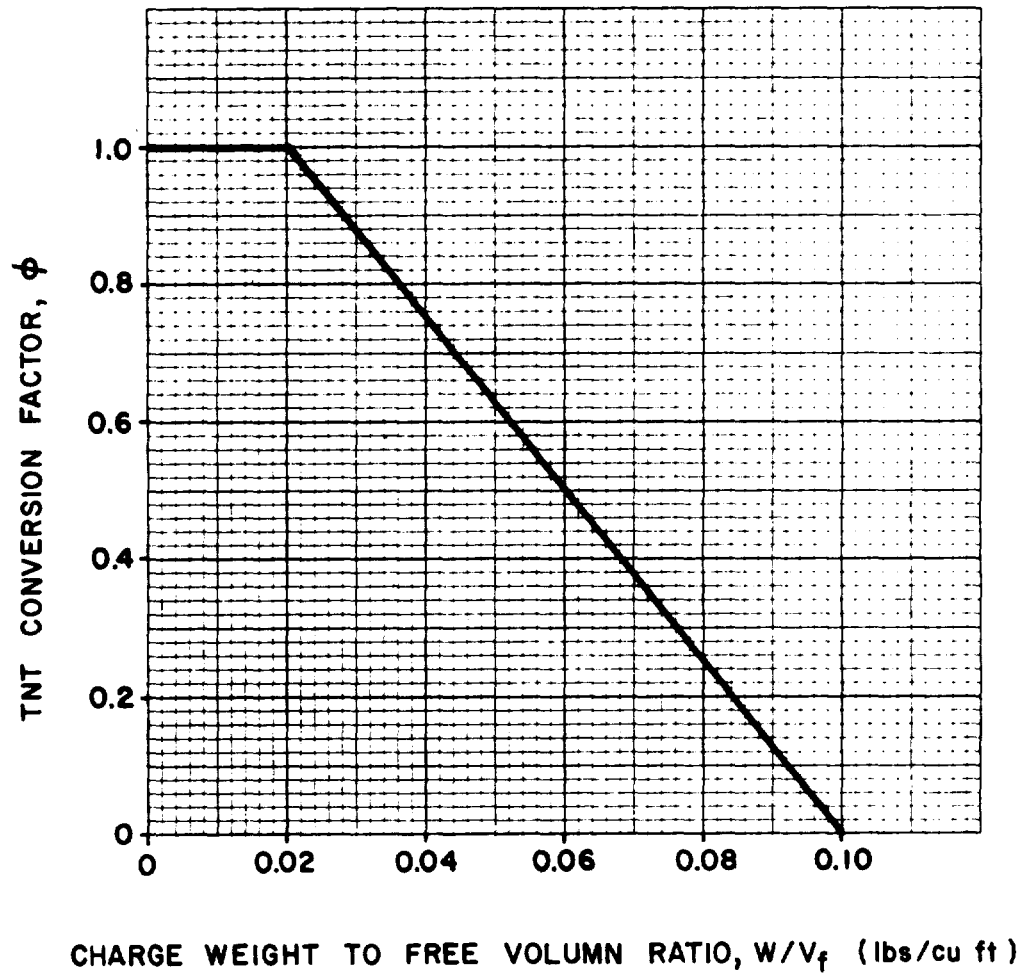
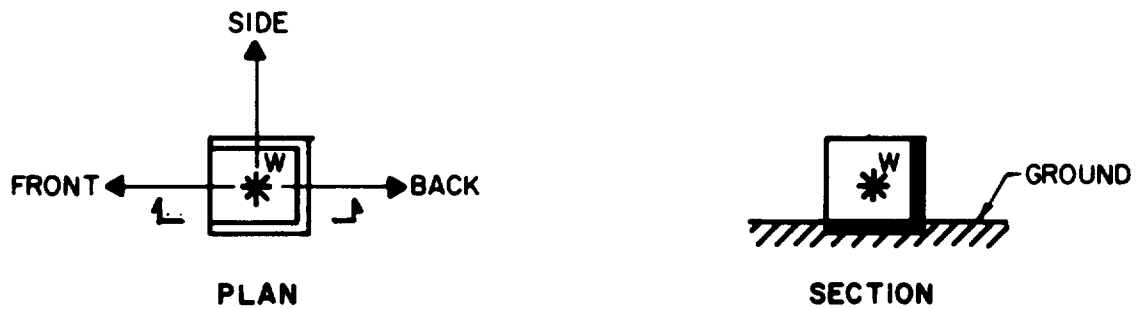
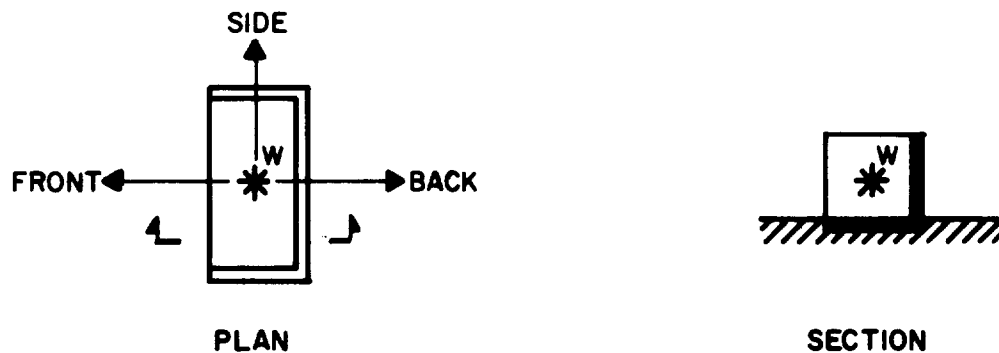


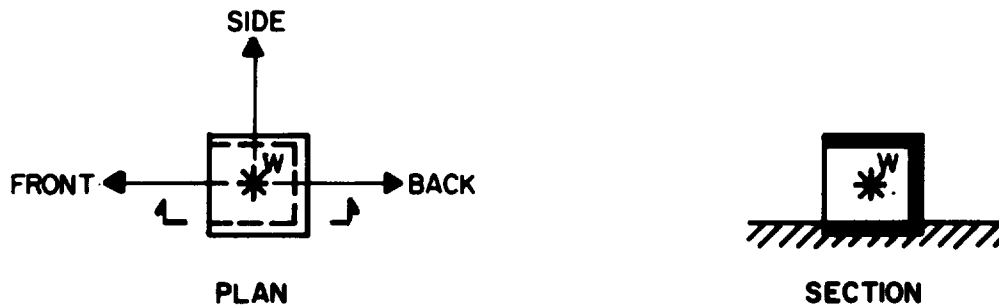
Figure 2-166 TNT conversion factor for charges



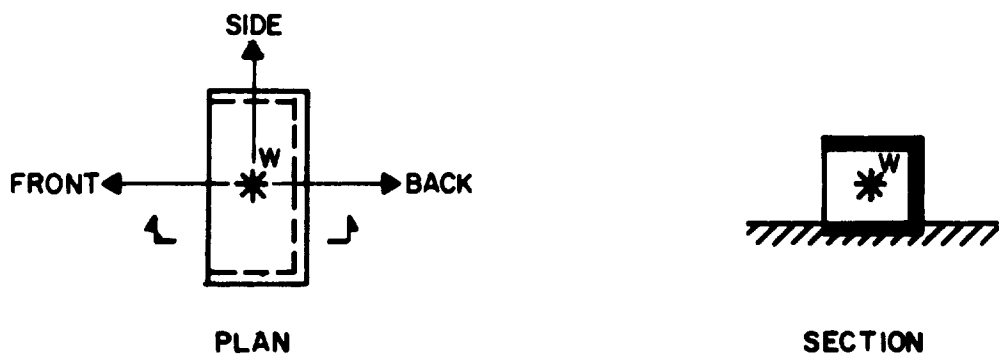
a) CUBIC THREE WALL CUBICLE WITHOUT A ROOF



b) RECTANGULAR THREE WALL CUBICLE WITHOUT A ROOF



c) CUBIC THREE WALL CUBICLE WITH A ROOF



d) RECTANGULAR THREE WALL CUBICLE WITH A ROOF

Figure 2-167 Fully vented three-wall cubicles and direction of blast wave propagation

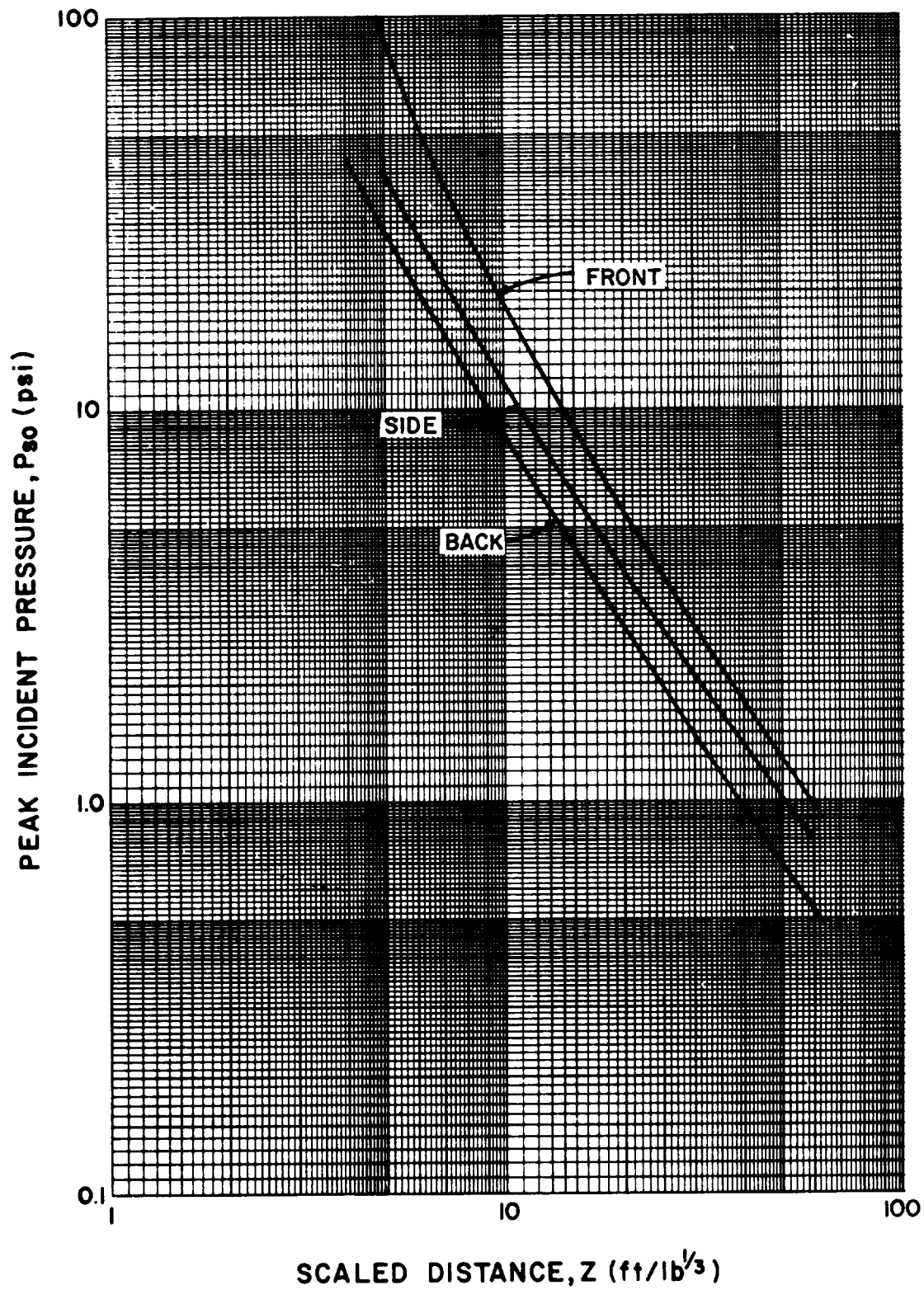


Figure 2-168 Envelope curves for peak positive pressure outside three-wall cubicles without a roof

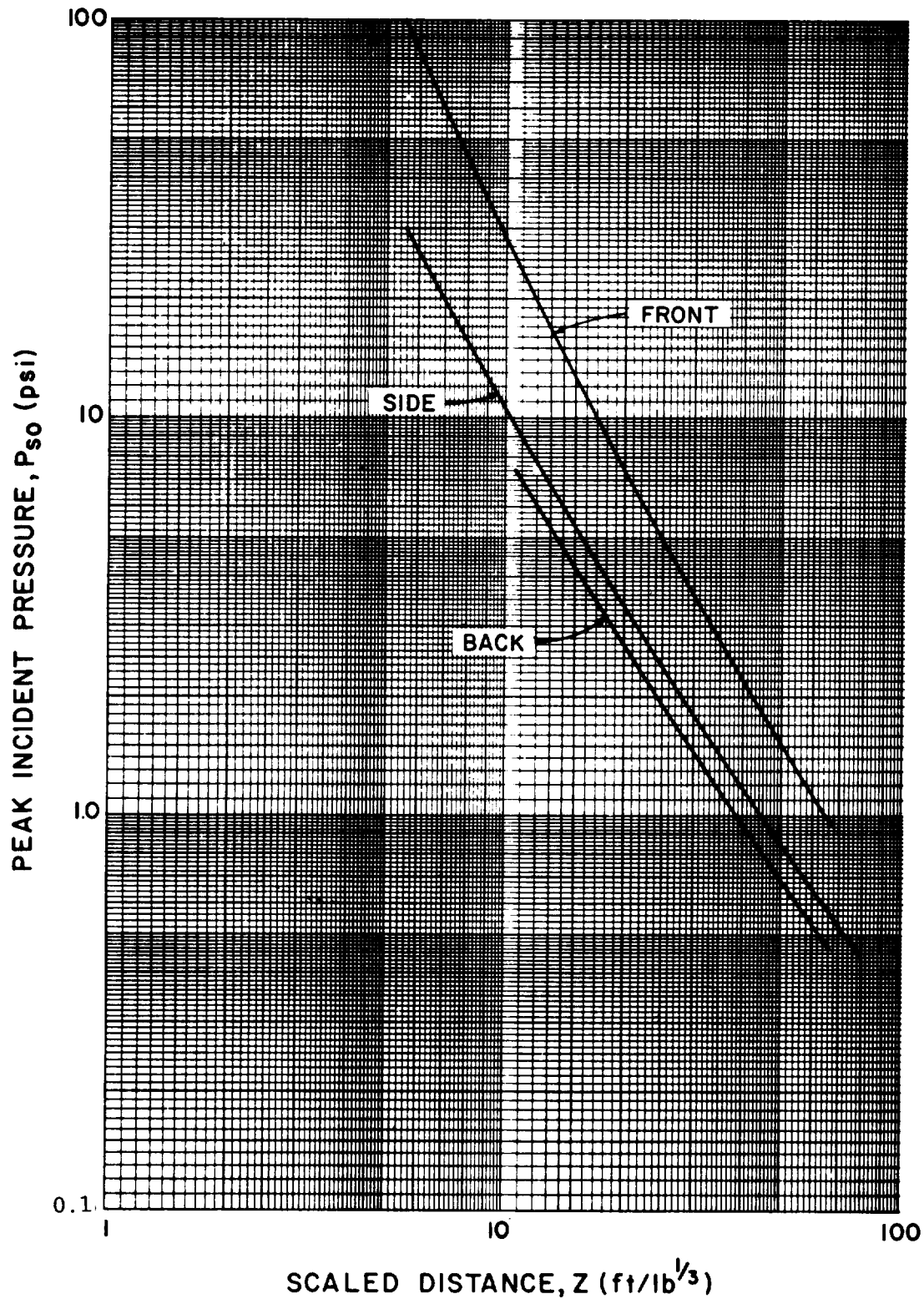


Figure 2-169 Envelope curves for peak positive pressure outside three-wall cubicles with a roof

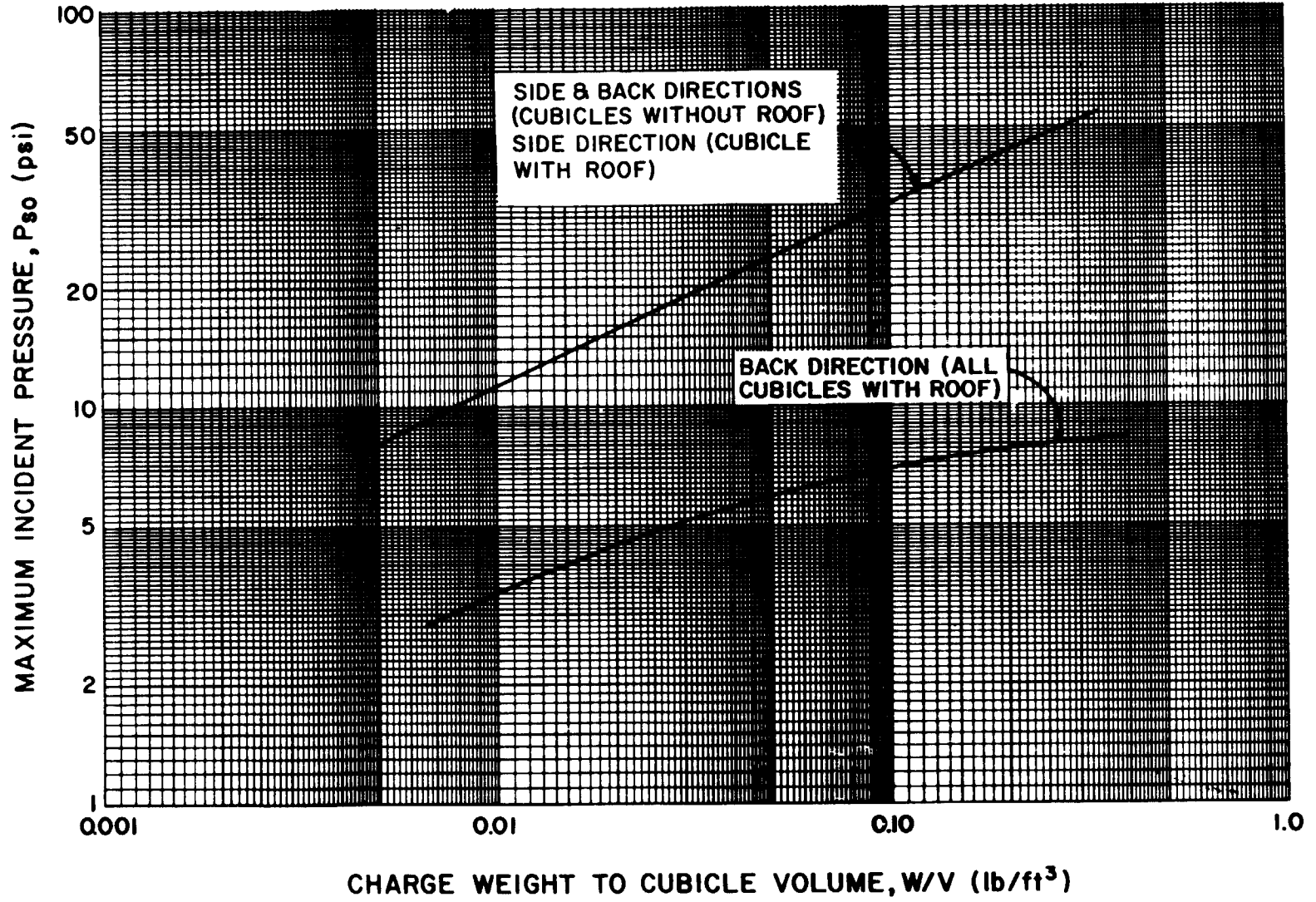


Figure 2-170 Envelope curves for maximum peak pressure outside three-wall cubicles

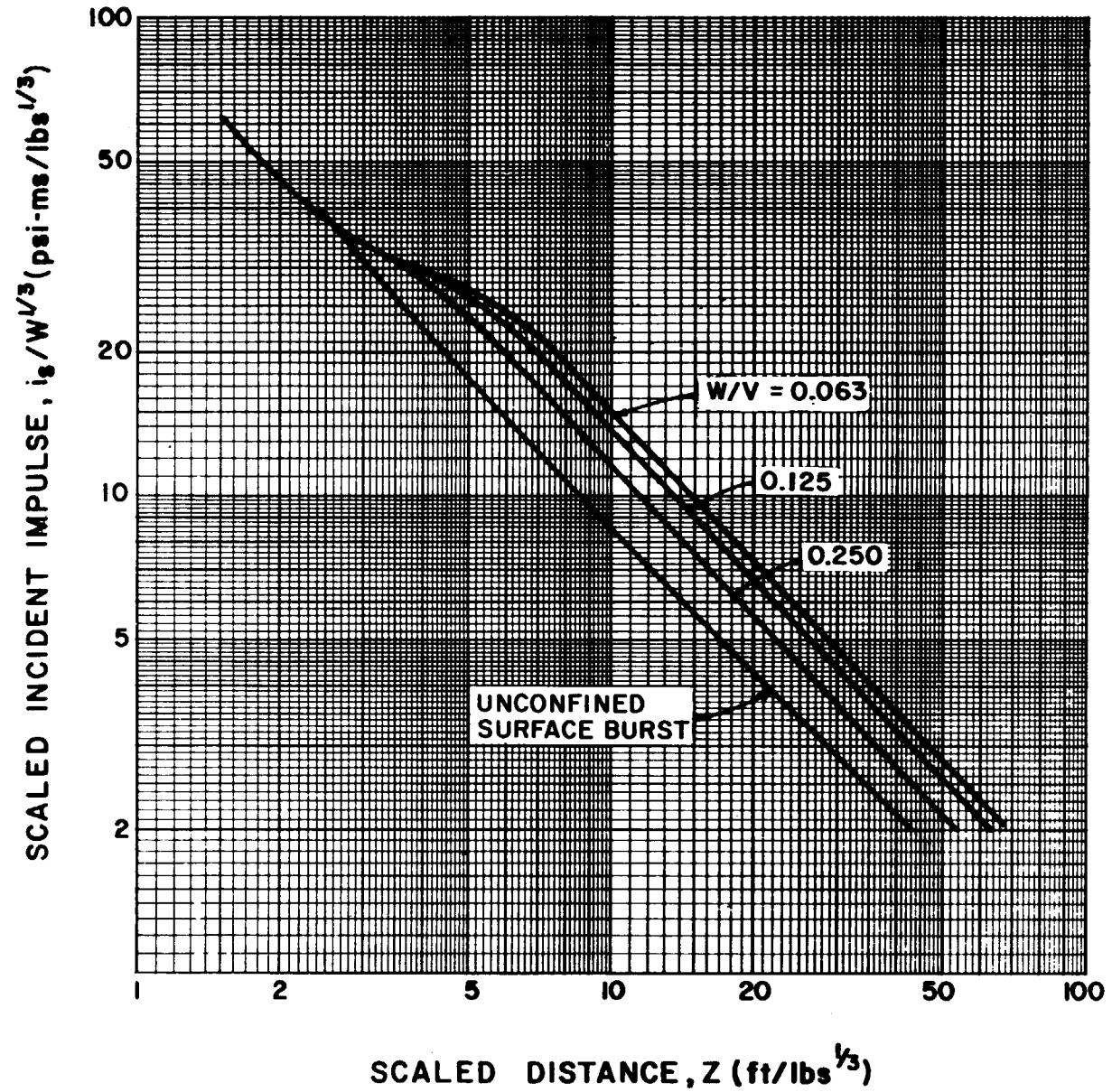


Figure 2-171 Scaled peak positive impulse out the open front of cubic three-wall cubicle without a roof

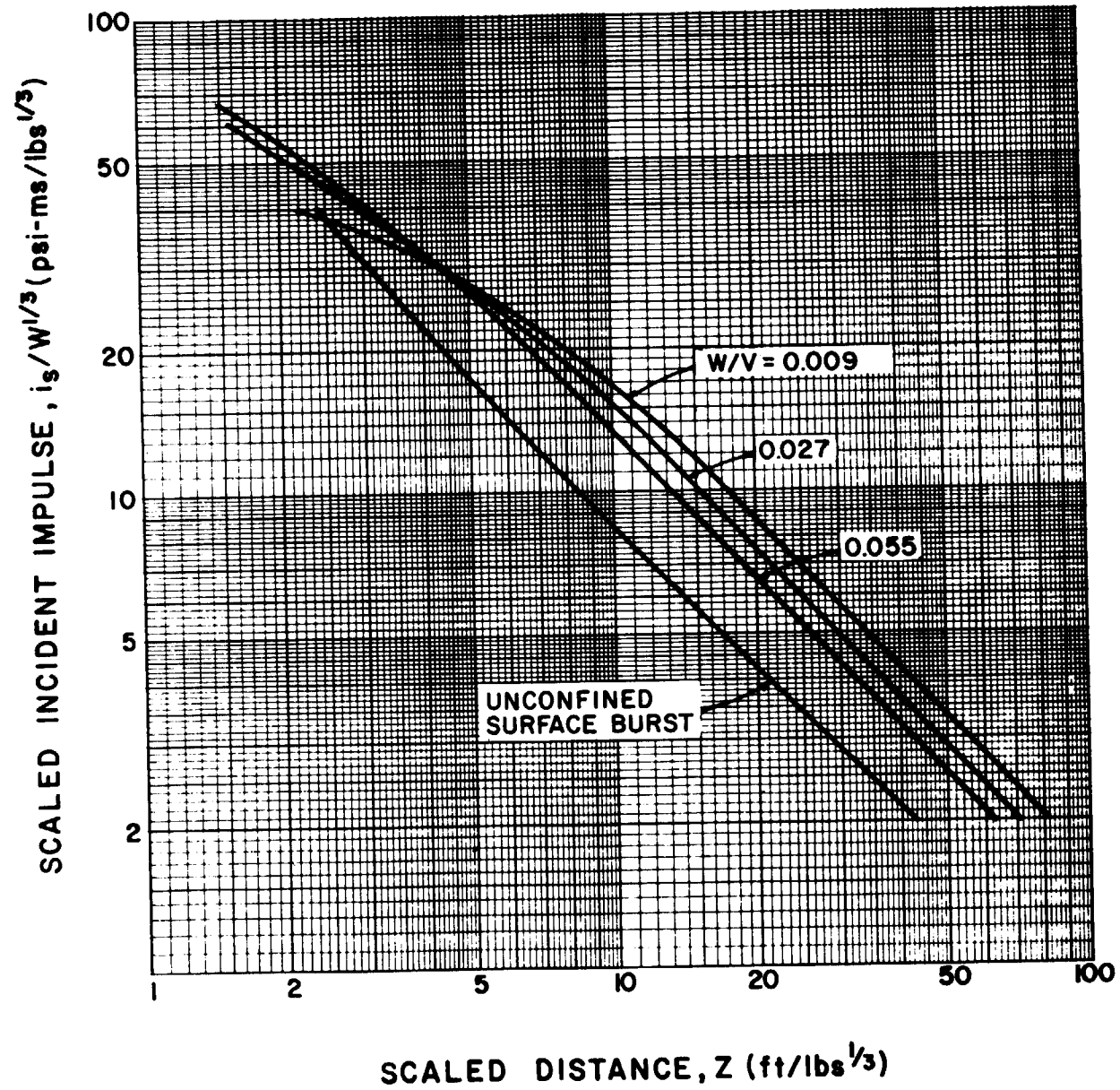


Figure 2-172 Scaled peak positive impulse out the open front of rectangular three-wall cubicle without a roof

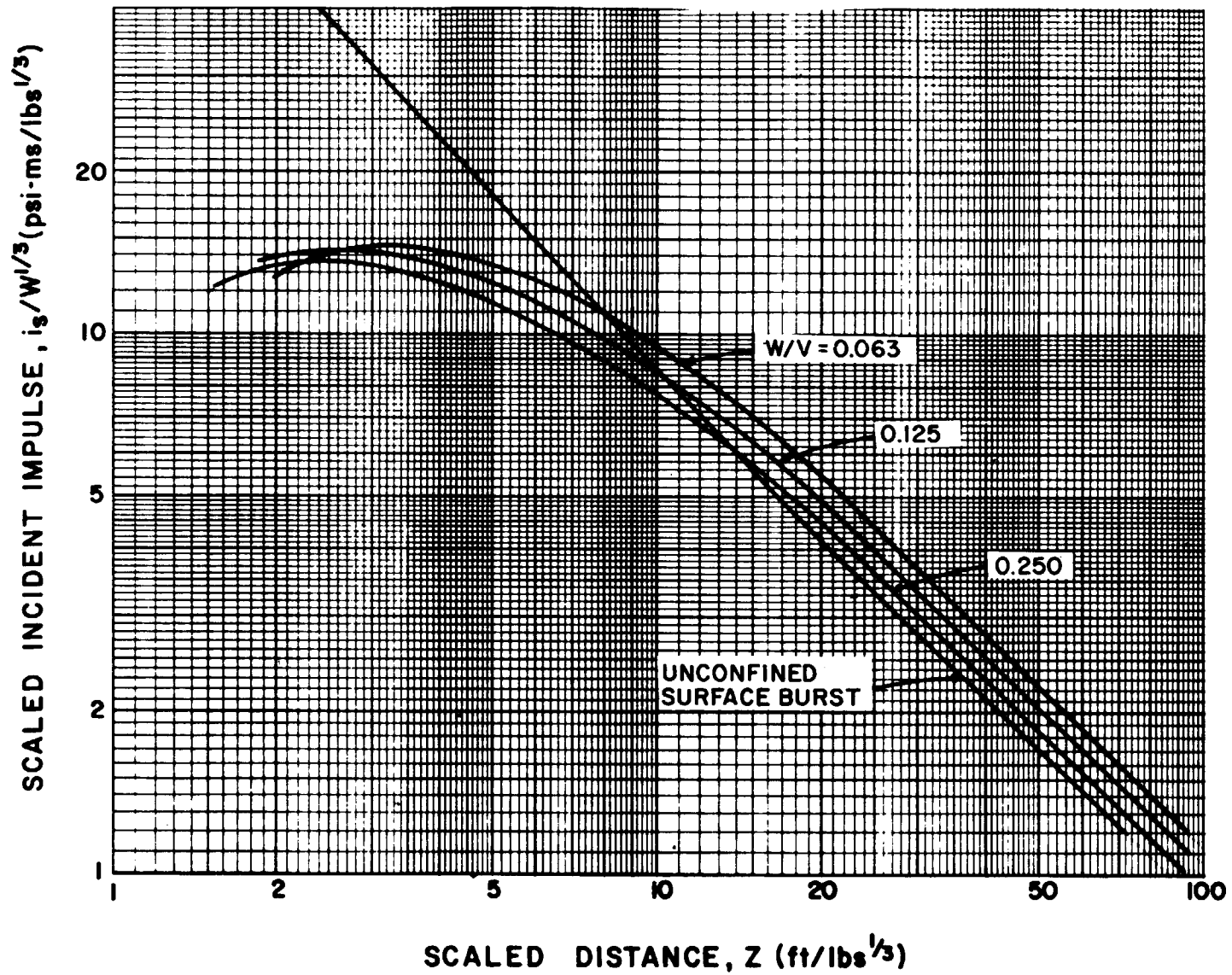


Figure 2-173 Scaled peak positive impulse behind sidewall of cubic three-wall cubicle without a roof

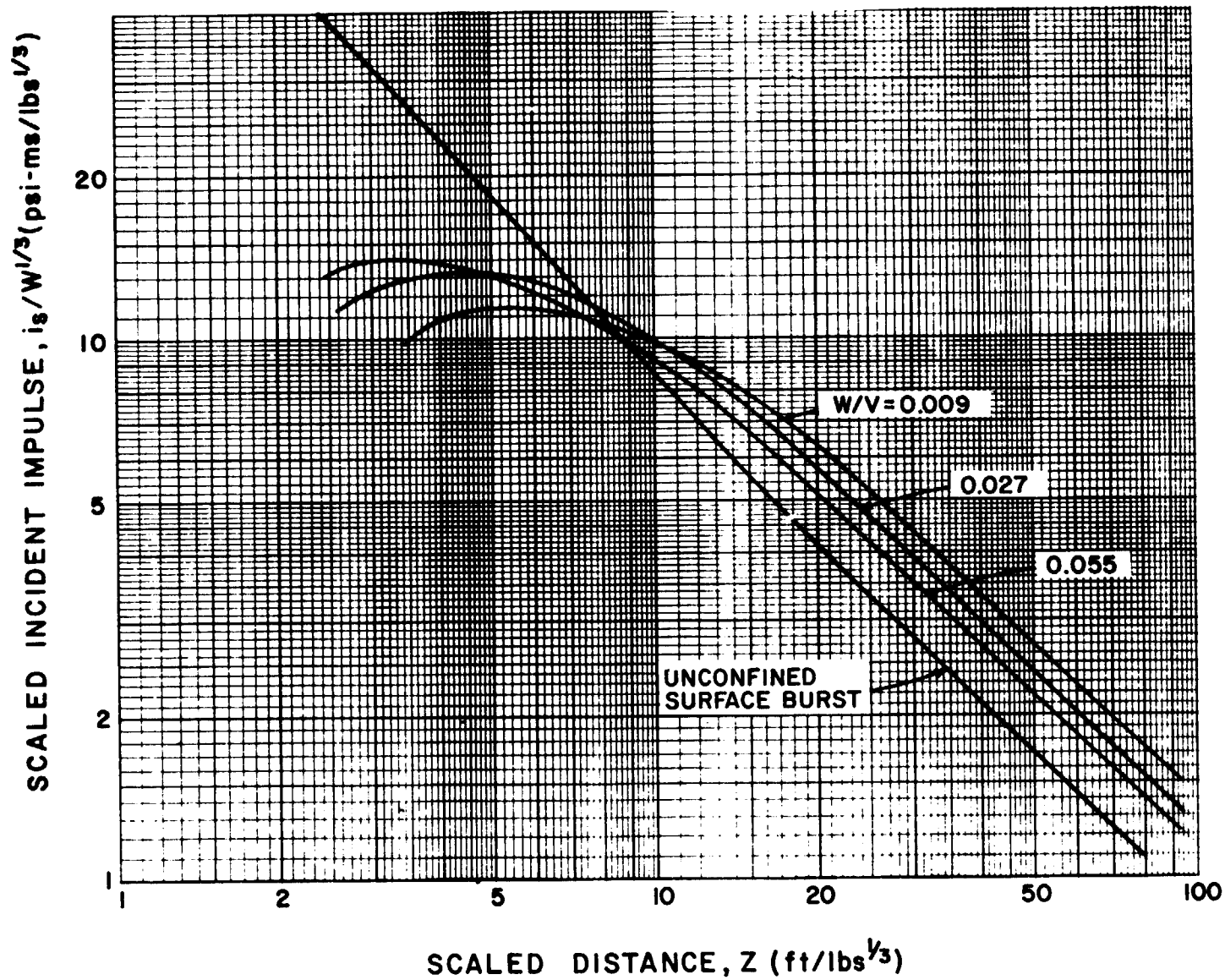


Figure 2-174 Scaled peak positive impulse behind sidewall of rectangular three-wall cubicle without a roof

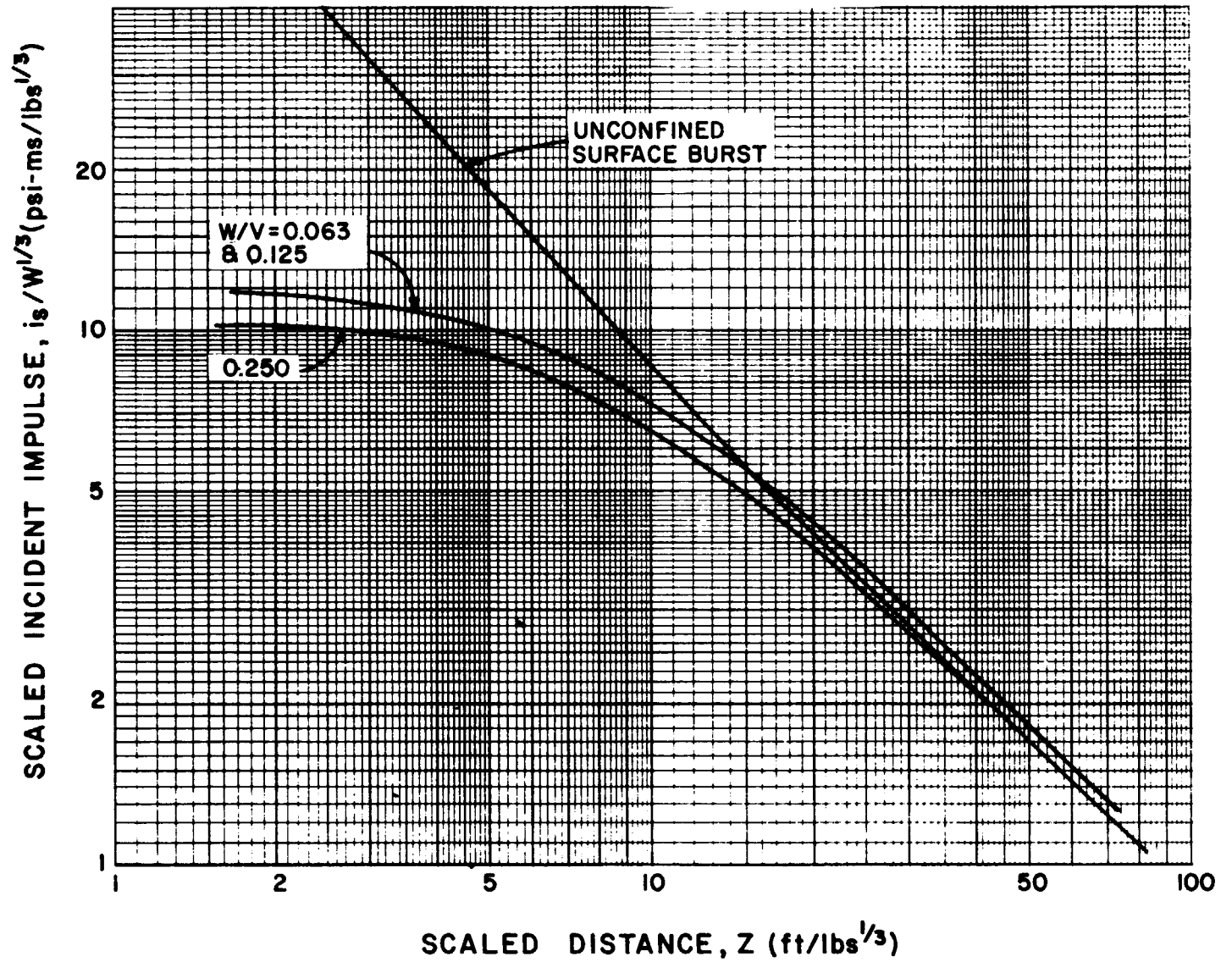


Figure 2-175 Scaled peak positive impulse behind backwall of cubic three-wall cubicle without a roof

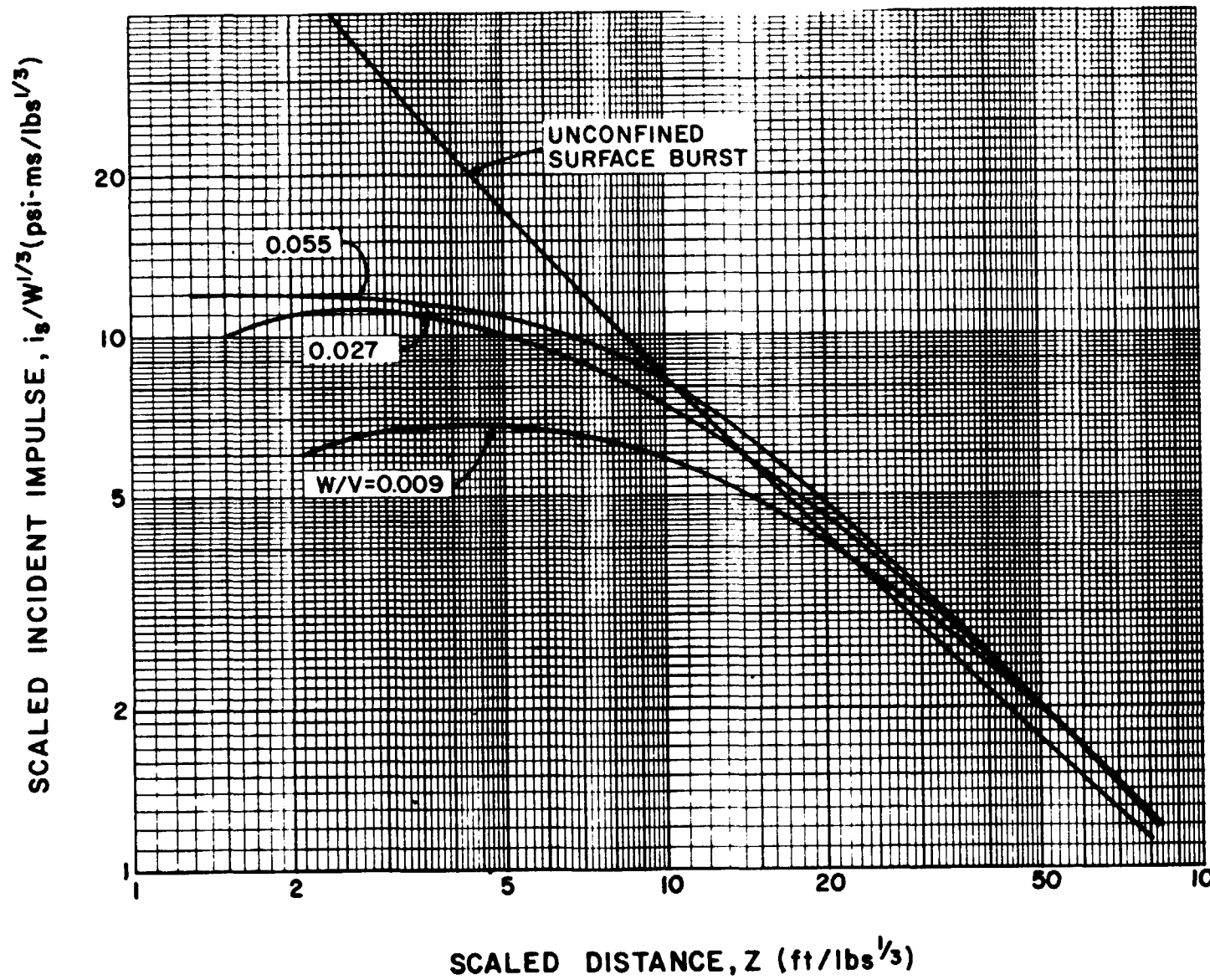


Figure 2-176 Scaled peak positive impulse behind backwall of rectangular three-wall cubicle without a roof

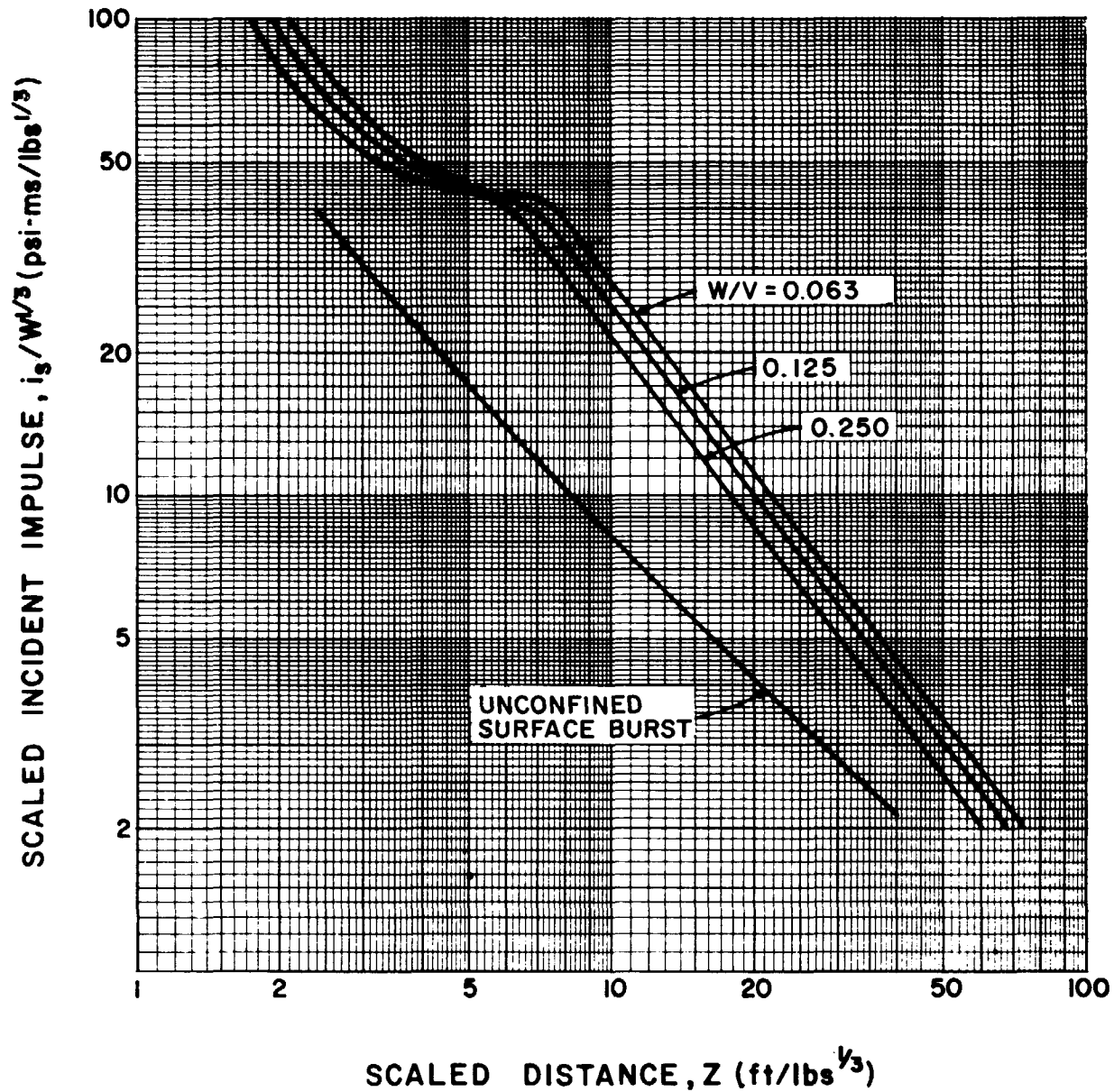


Figure 2-177 Scaled peak positive impulse out the open front of cubic three-wall cubicle with a roof

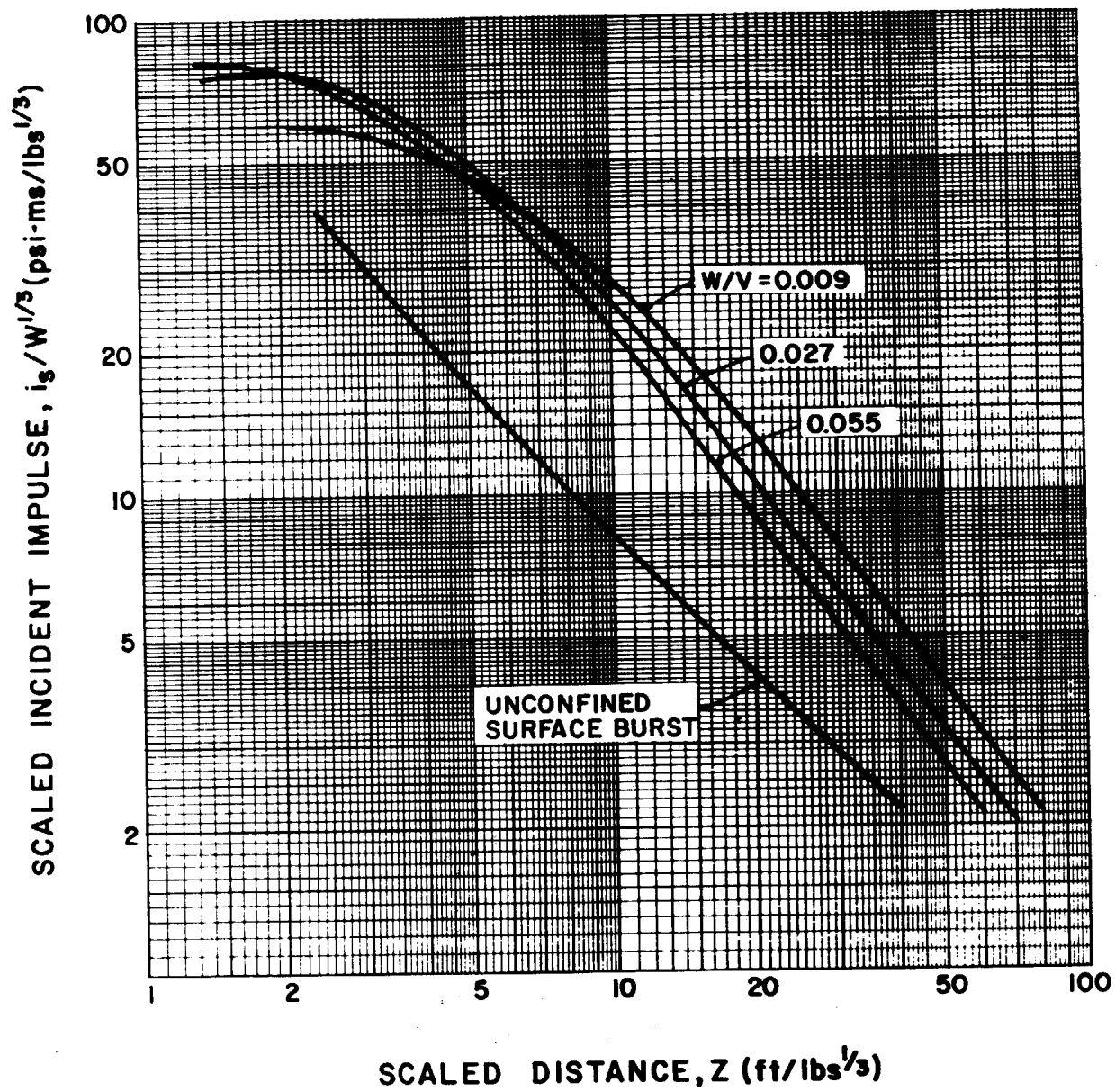


Figure 2-178 Scaled peak positive impulse out the open front of rectangular three-wall cubicle with a roof

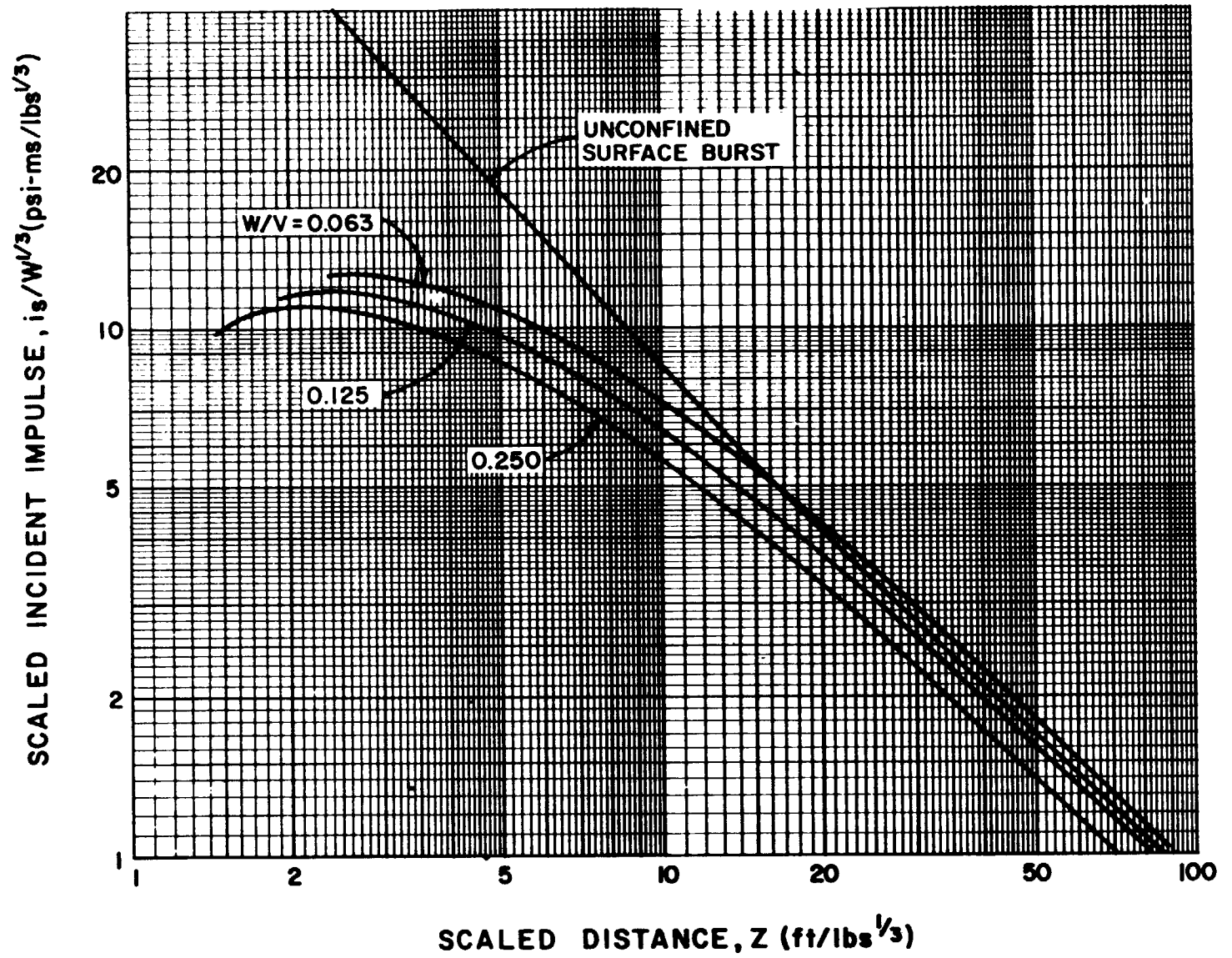


Figure 2-179 Scaled peak positive impulse behind sidewall of cubic three-wall cubicle with a roof

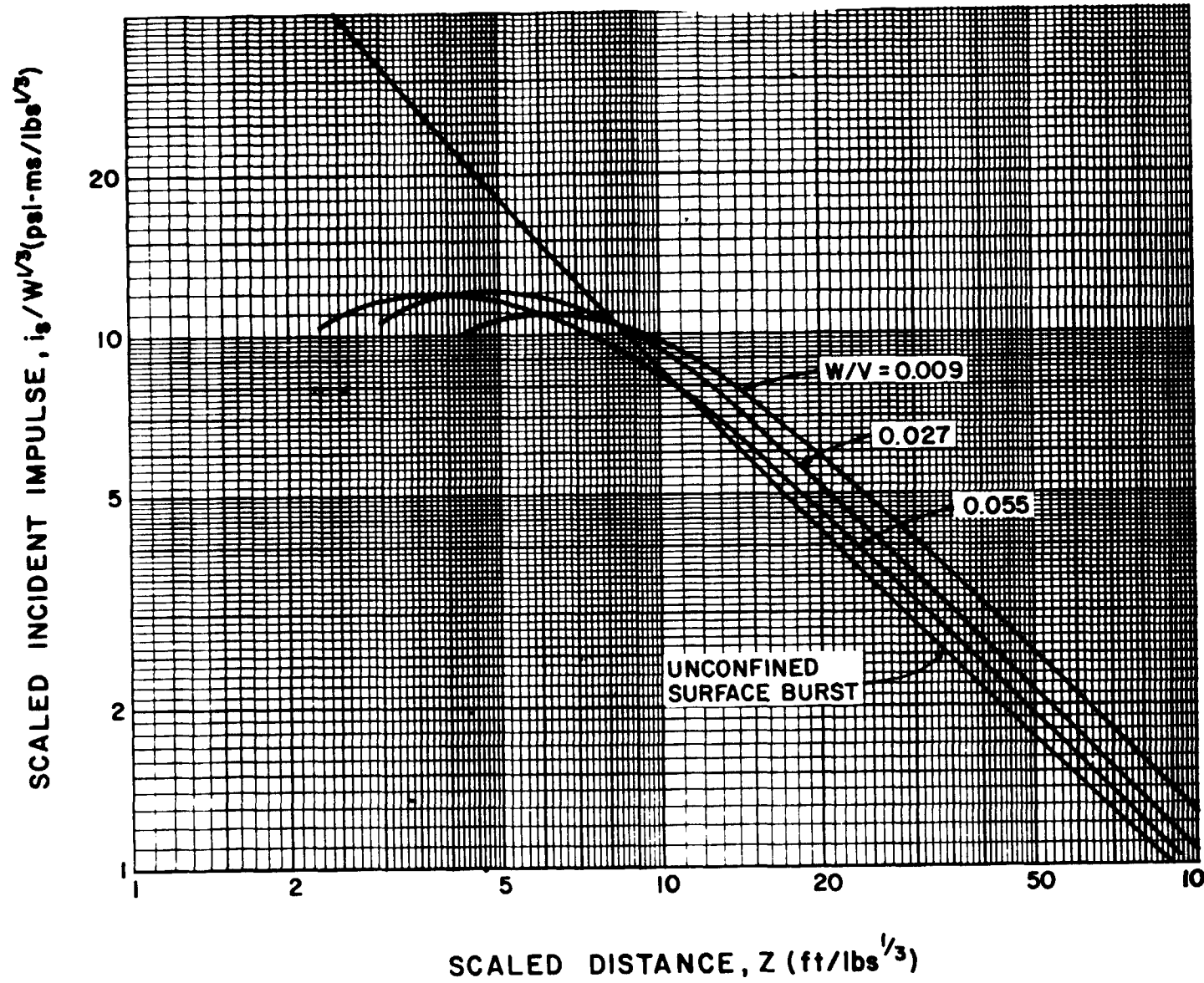


Figure 2-180 Scaled peak positive impulse behind sidewall of rectangular three-wall cubicle with a roof

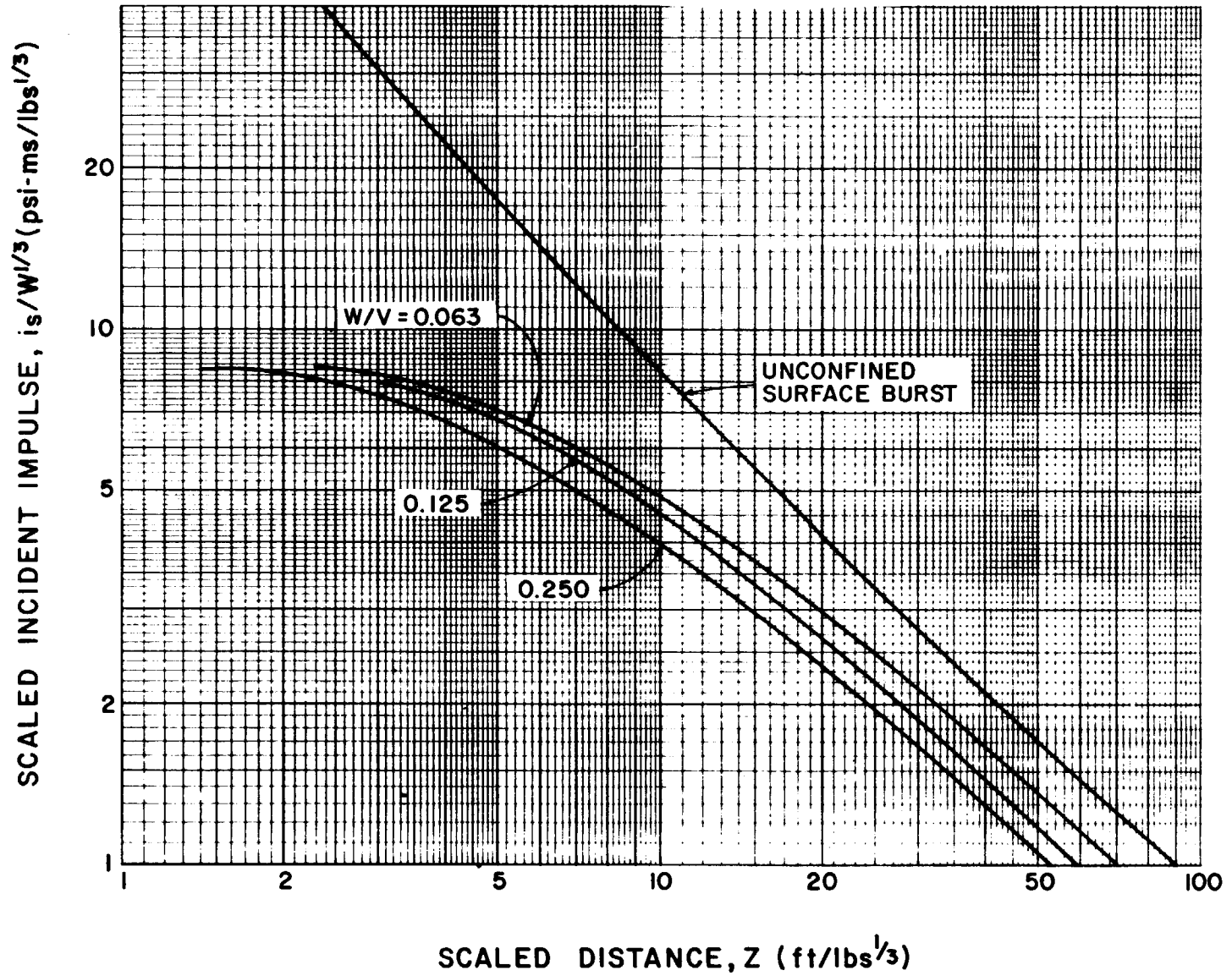


Figure 2-181 Scaled peak positive impulse behind backwall of cubic three-wall cubicle with a roof

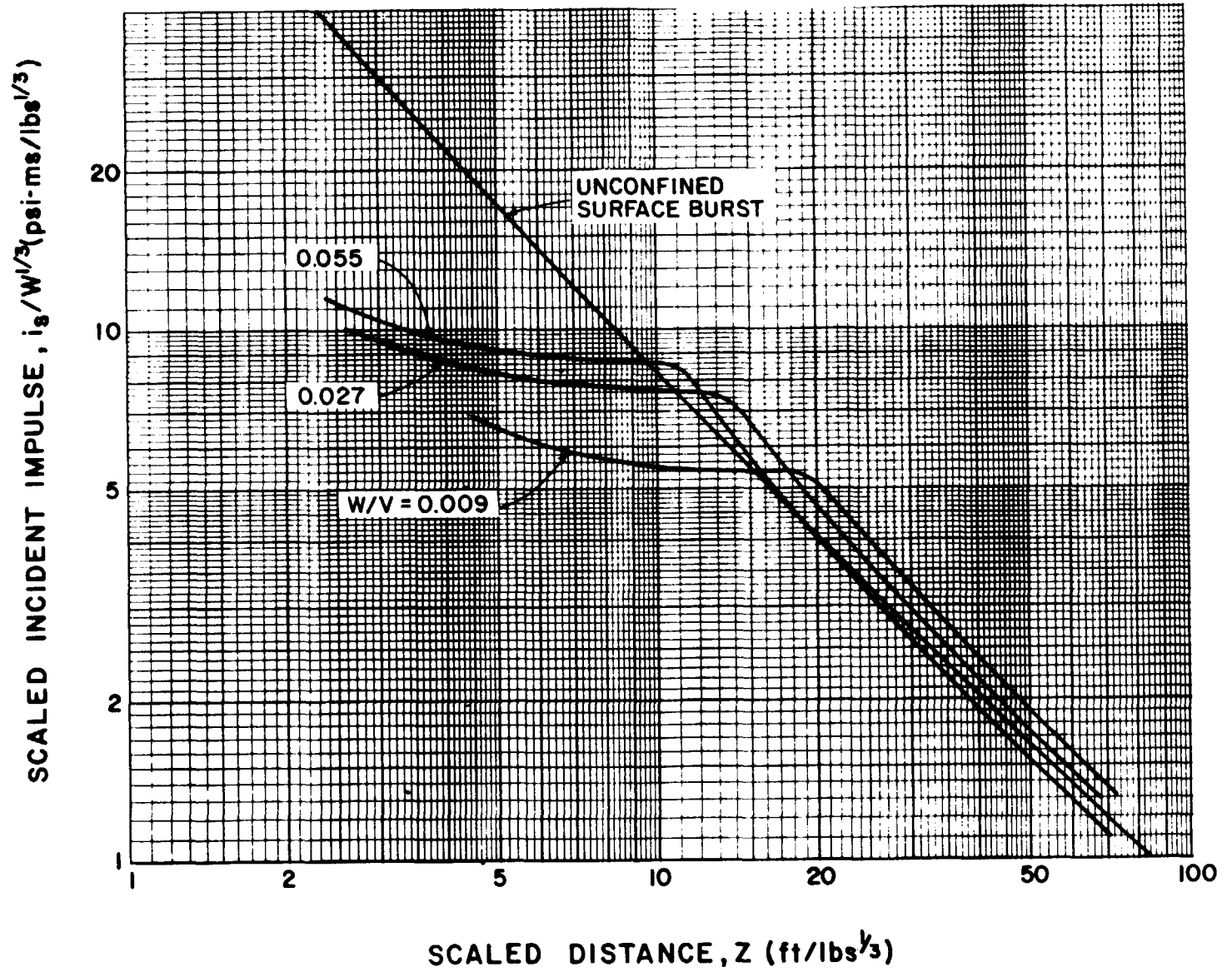
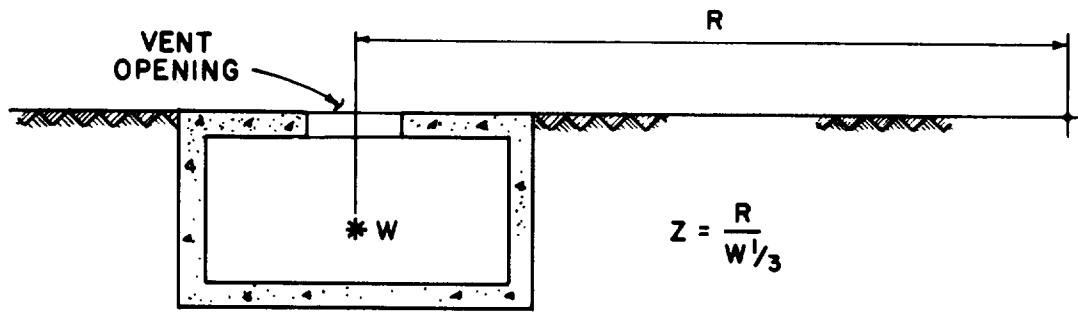
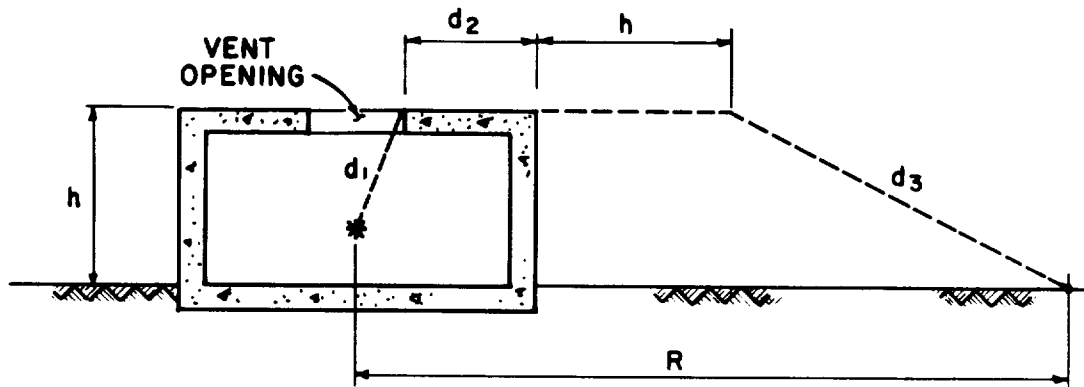


Figure 2-182 Scaled peak positive impulse behind backwall of rectangular three-wall cubicle with a roof



a) BELOW GROUND STRUCTURE WITH ROOF AT GROUND SURFACE



b) ABOVE GROUND STRUCTURE

Figure 2-183 Four wall cubicle vented through its roof

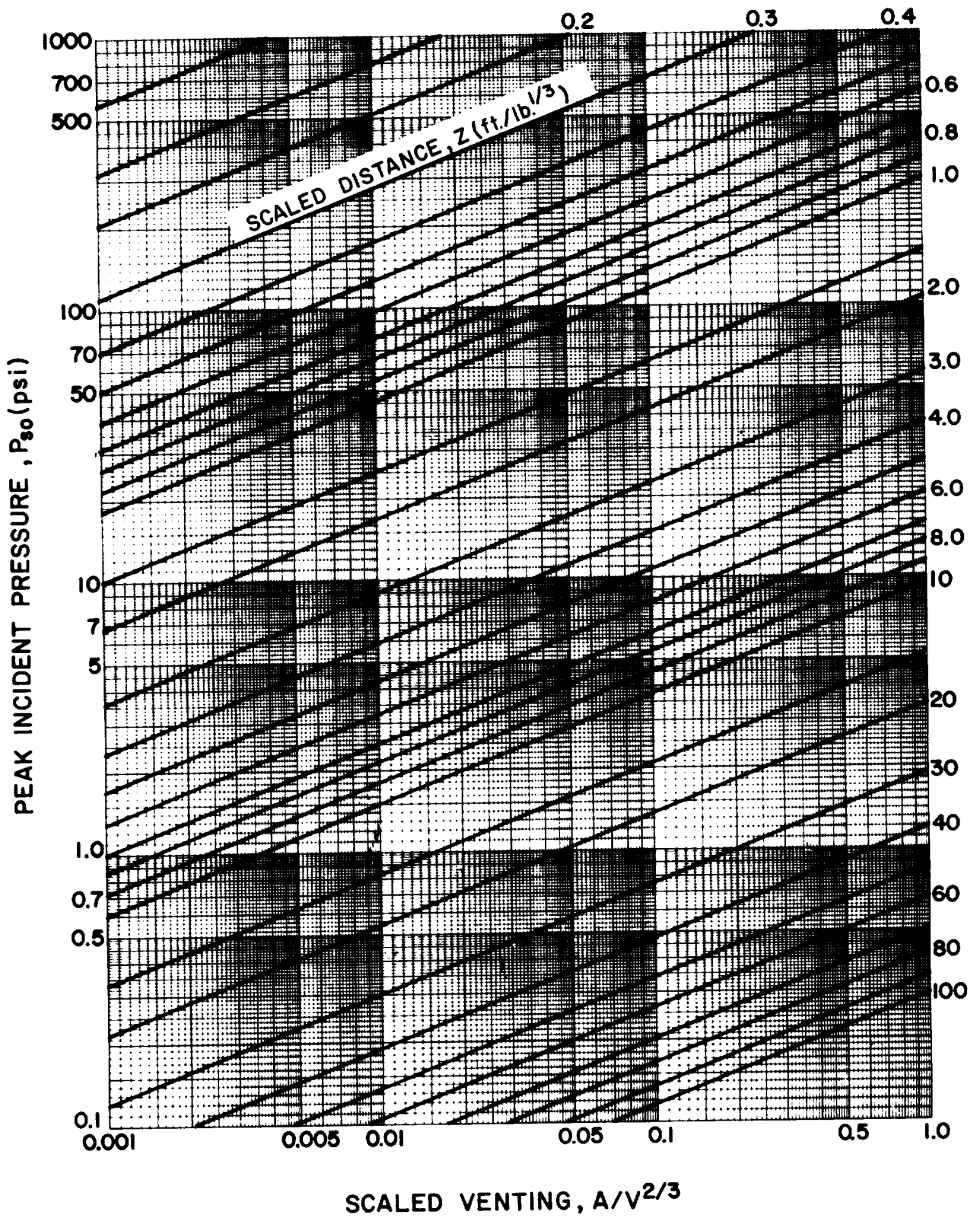


Figure 2-184 Peak positive pressure outside of a four-wall cubicle vented through its roof

2-227

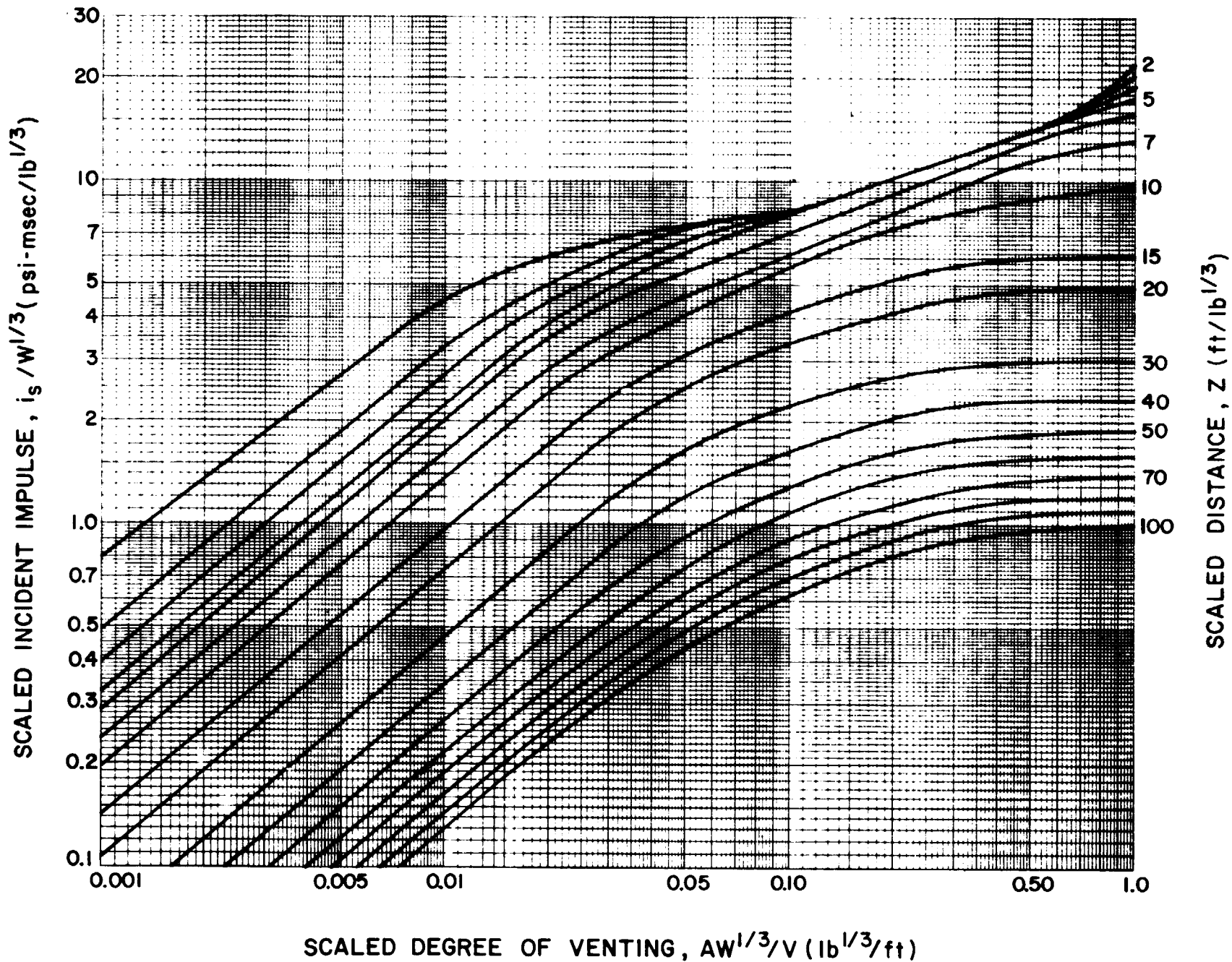
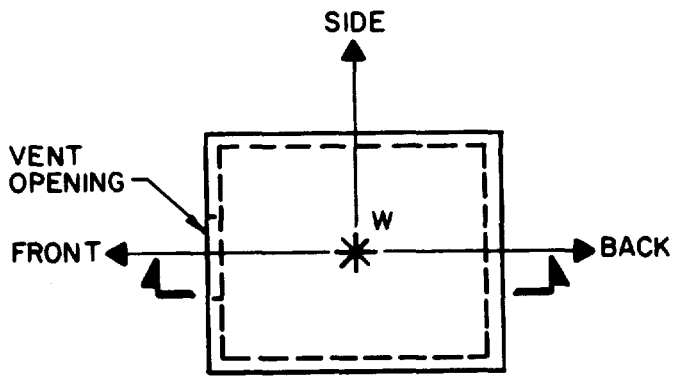
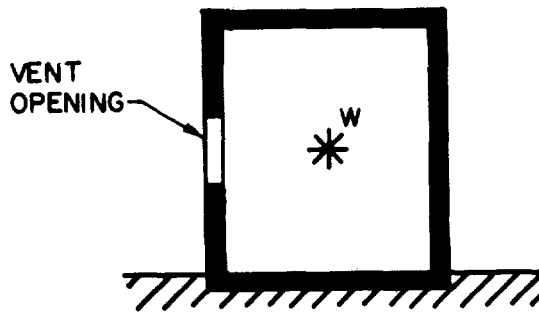


Figure 2-185 Scaled positive impulse outside of a four-wall cubicle vented through its roof



PLAN



SECTION

Figure 2-186 Four wall cubicle vented through a wall and direction of blast wave propagation

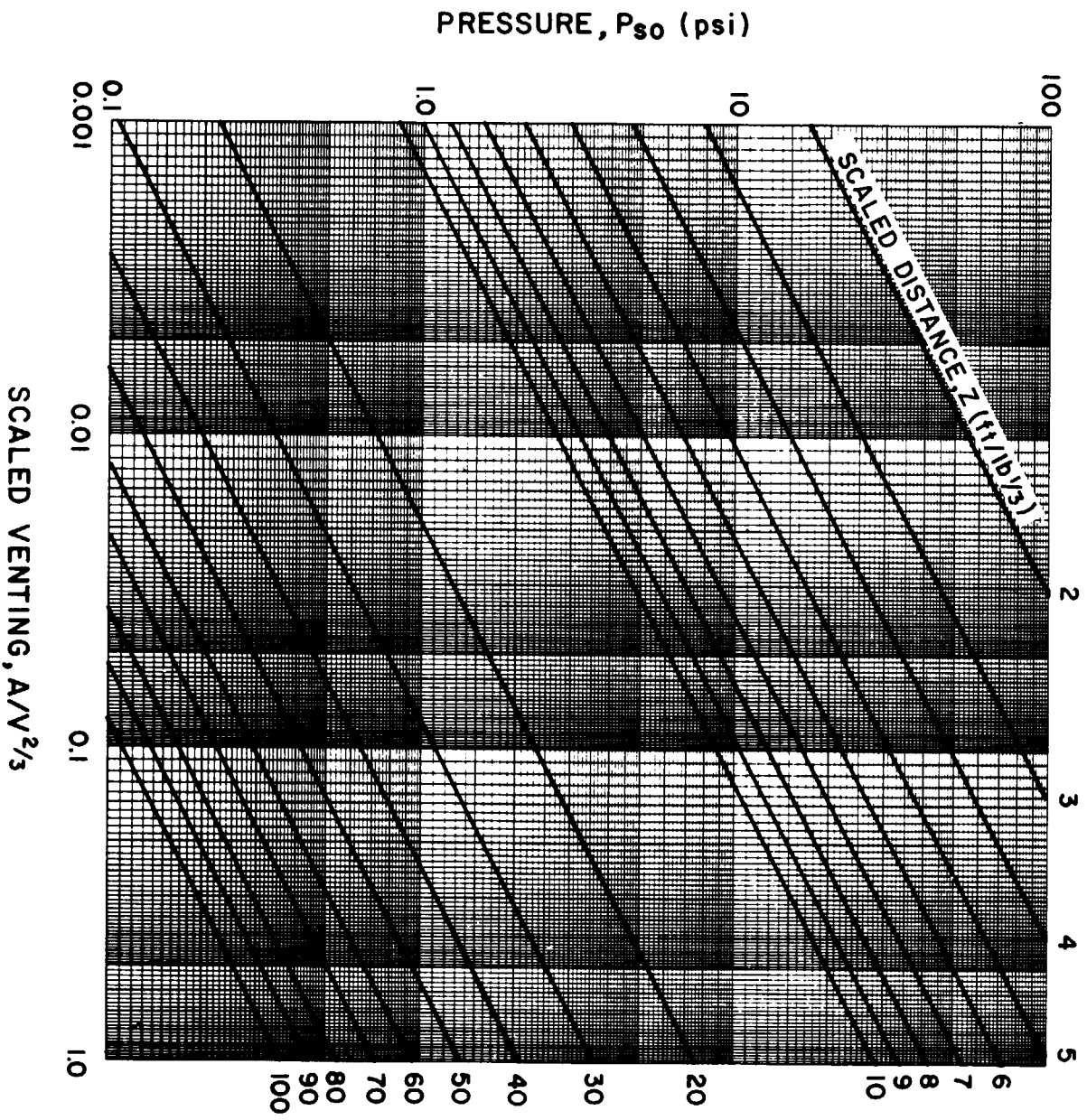


Figure 2-187 Peak positive pressure at the front of a partially vented four-wall cubicle

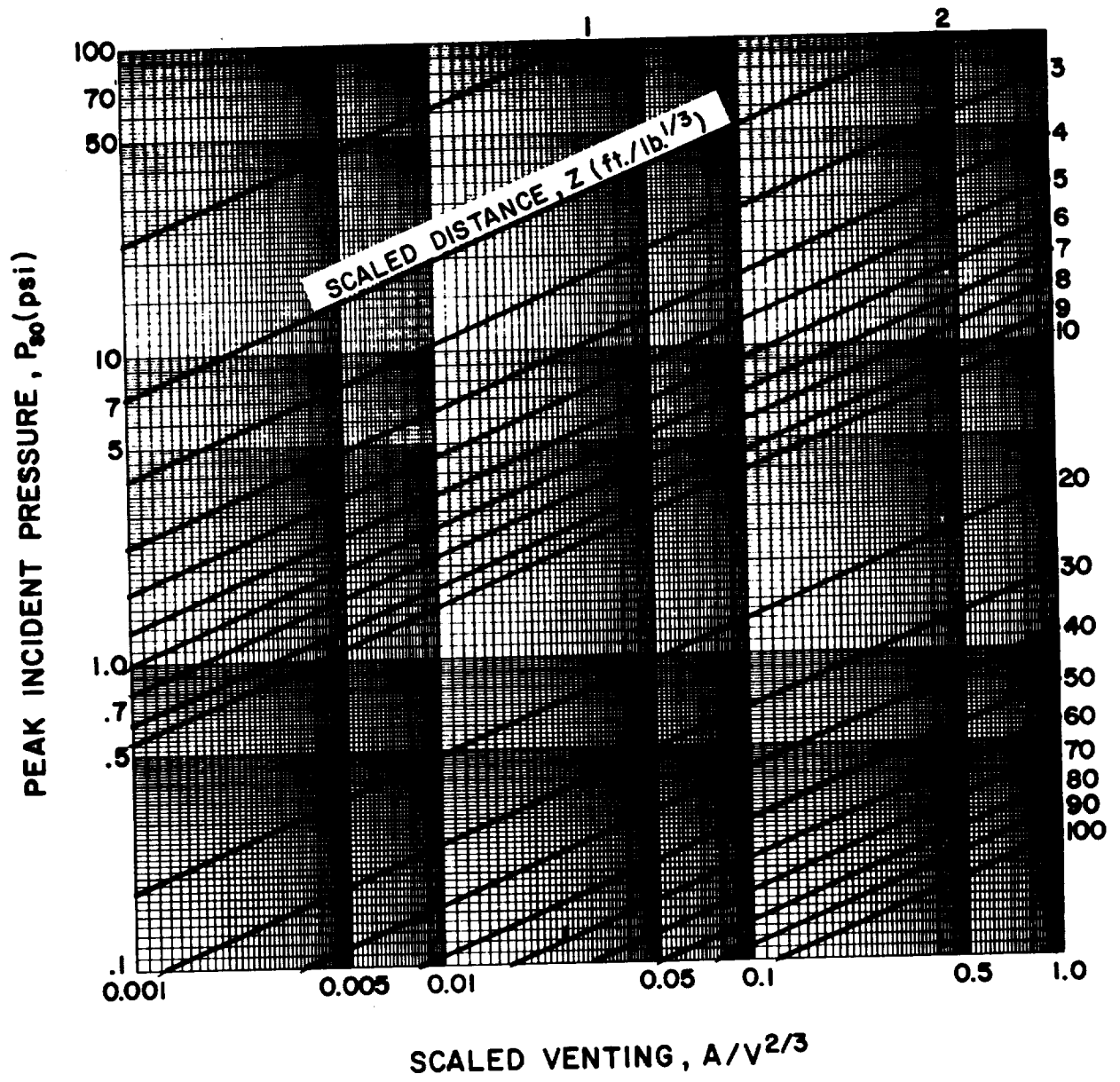


Figure 2-188 Peak positive pressure at the side of a partially vented four-wall cubicle

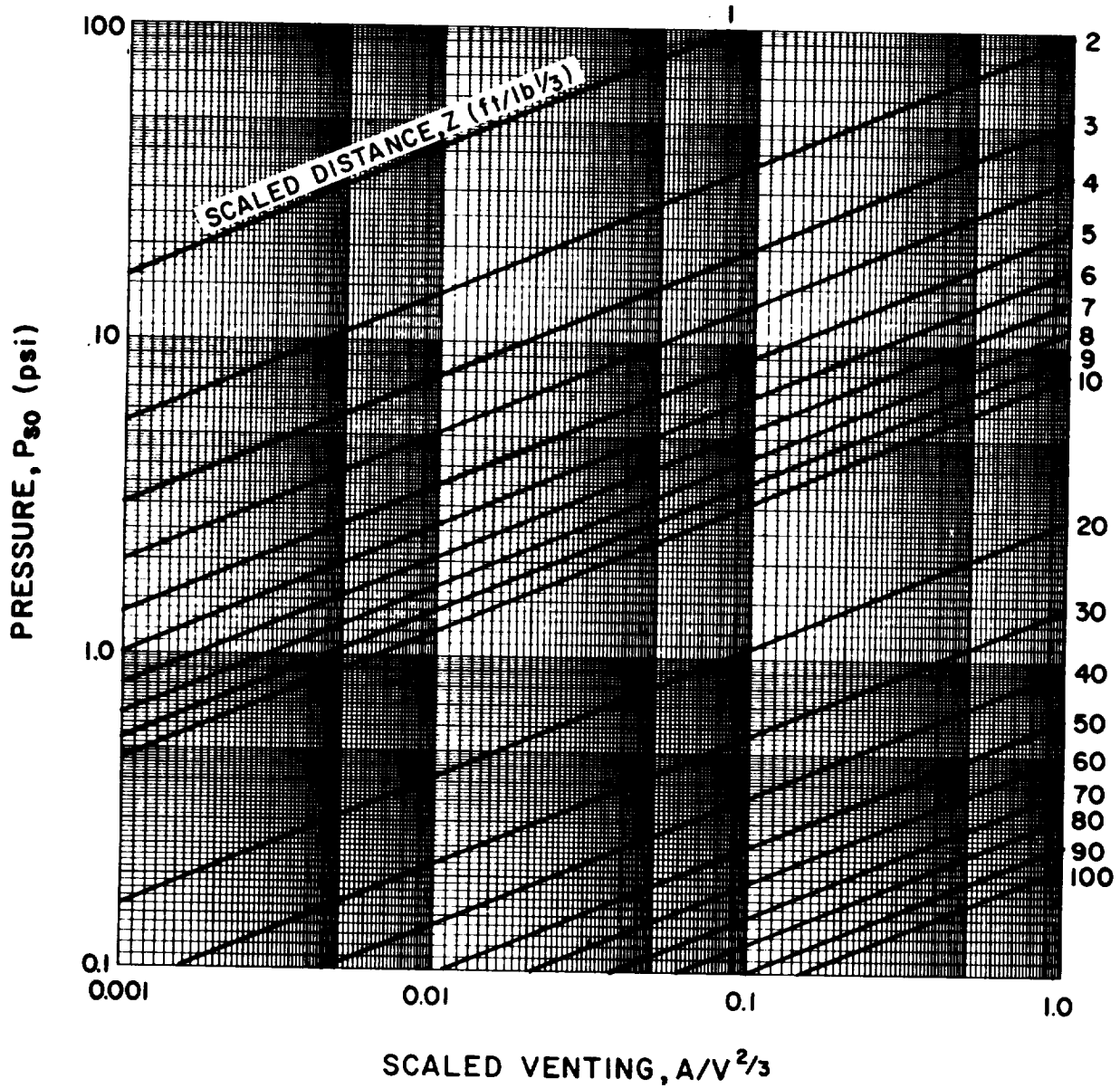


Figure 2-189 Peak positive pressure at the back of a partially vented four wall cubicle

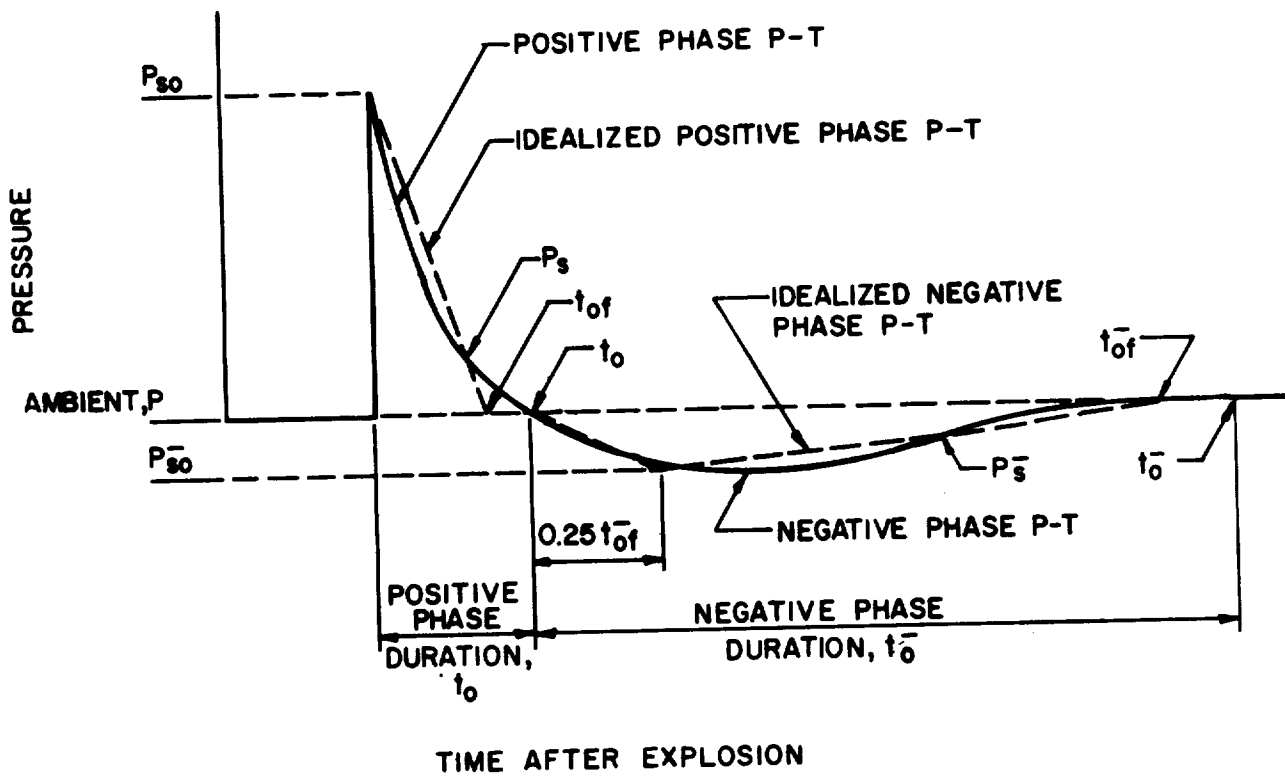
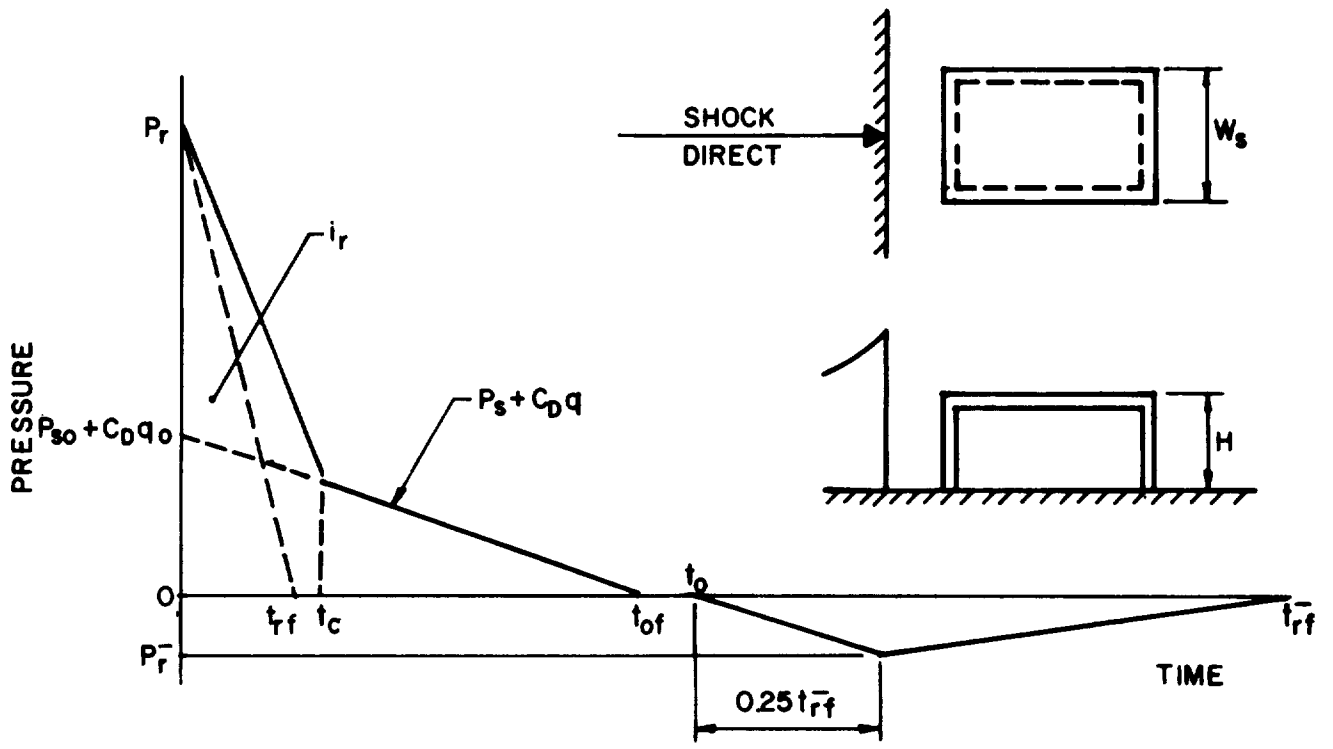
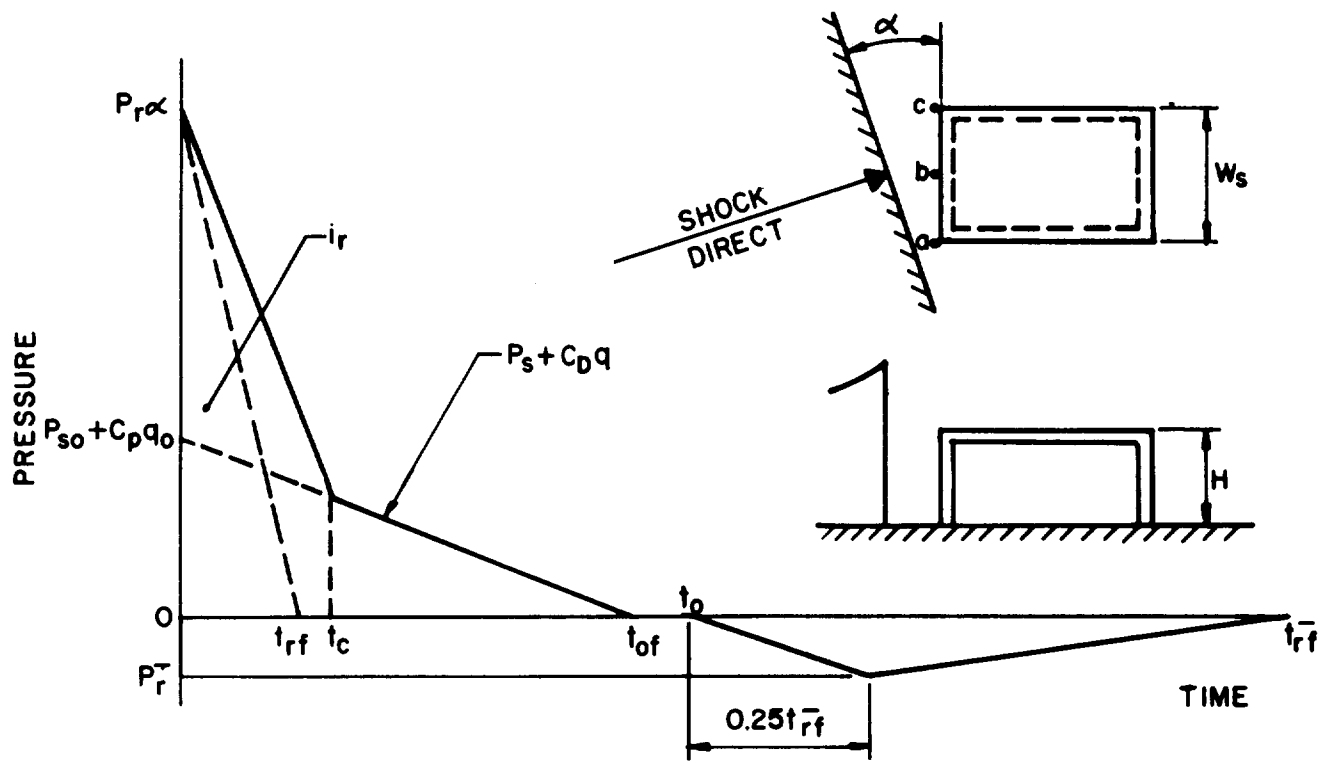


Figure 2-190 Idealized pressure-time variation



a. NORMAL REFLECTION



b. OBLIQUE REFLECTION

Figure 2-191 Front wall loading

2-234

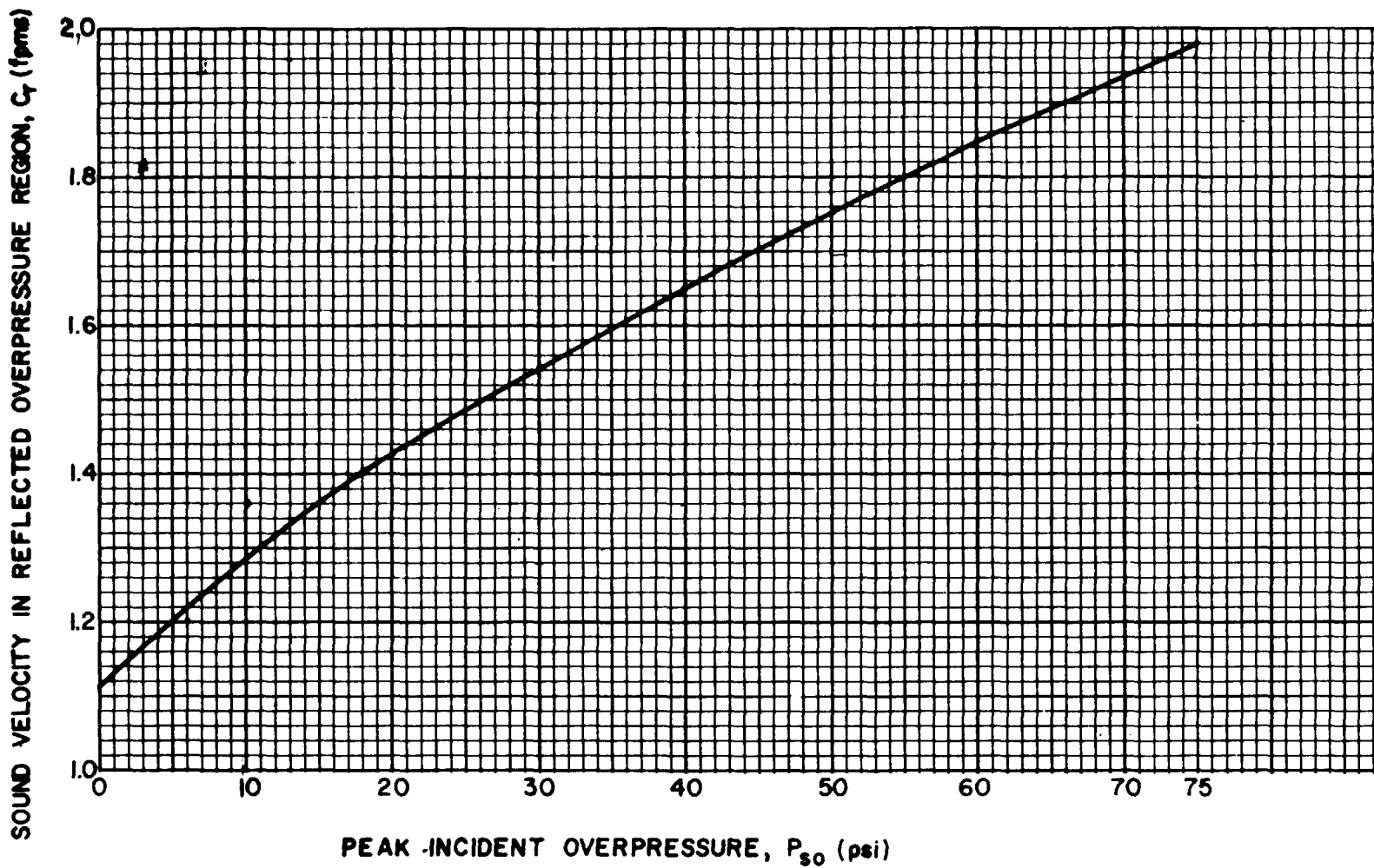


Figure 2-192 Velocity of sound in reflected overpressure region versus peak incident overpressure

2-235

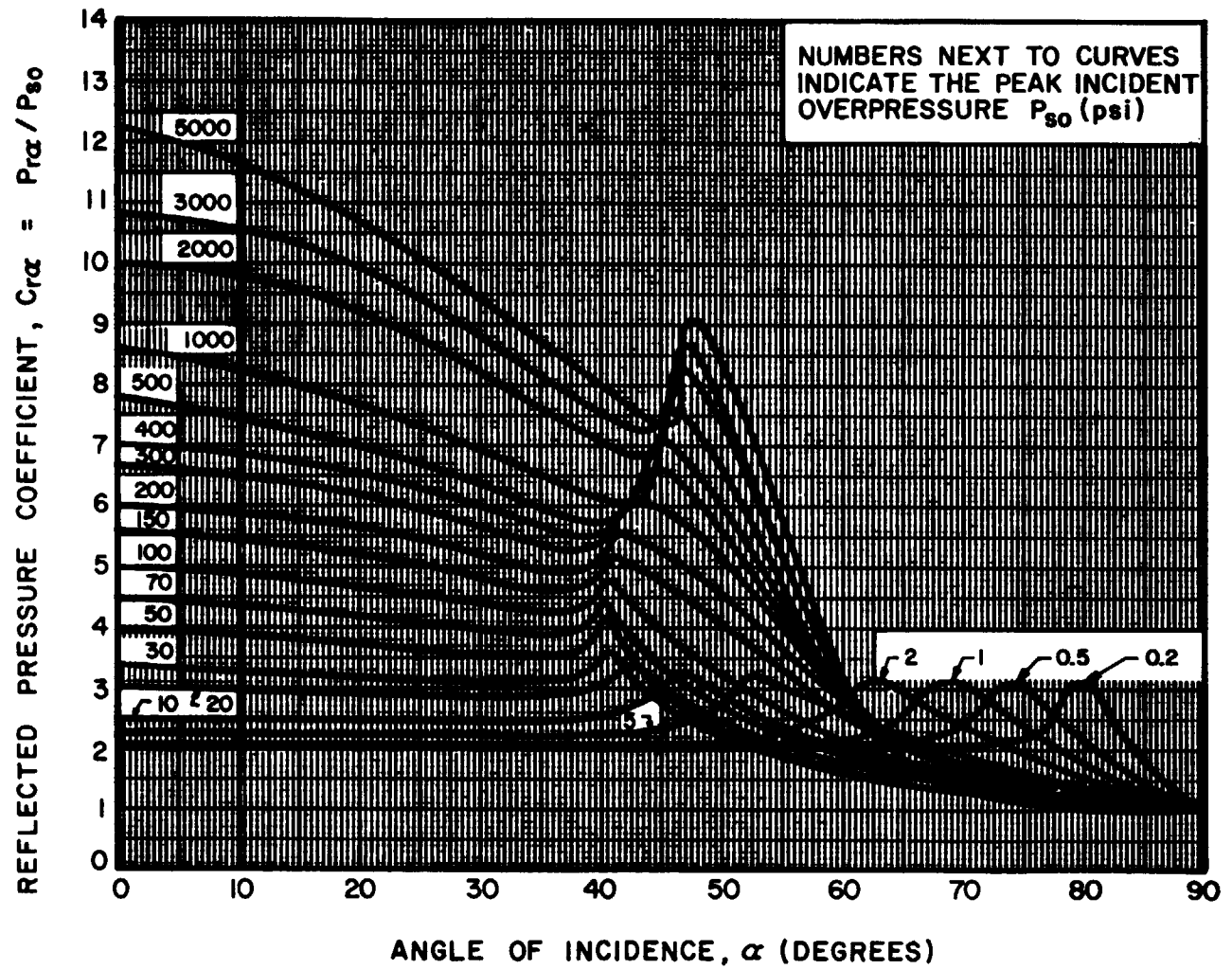


Figure 2-193 Reflected pressure coefficient versus angle of incidence

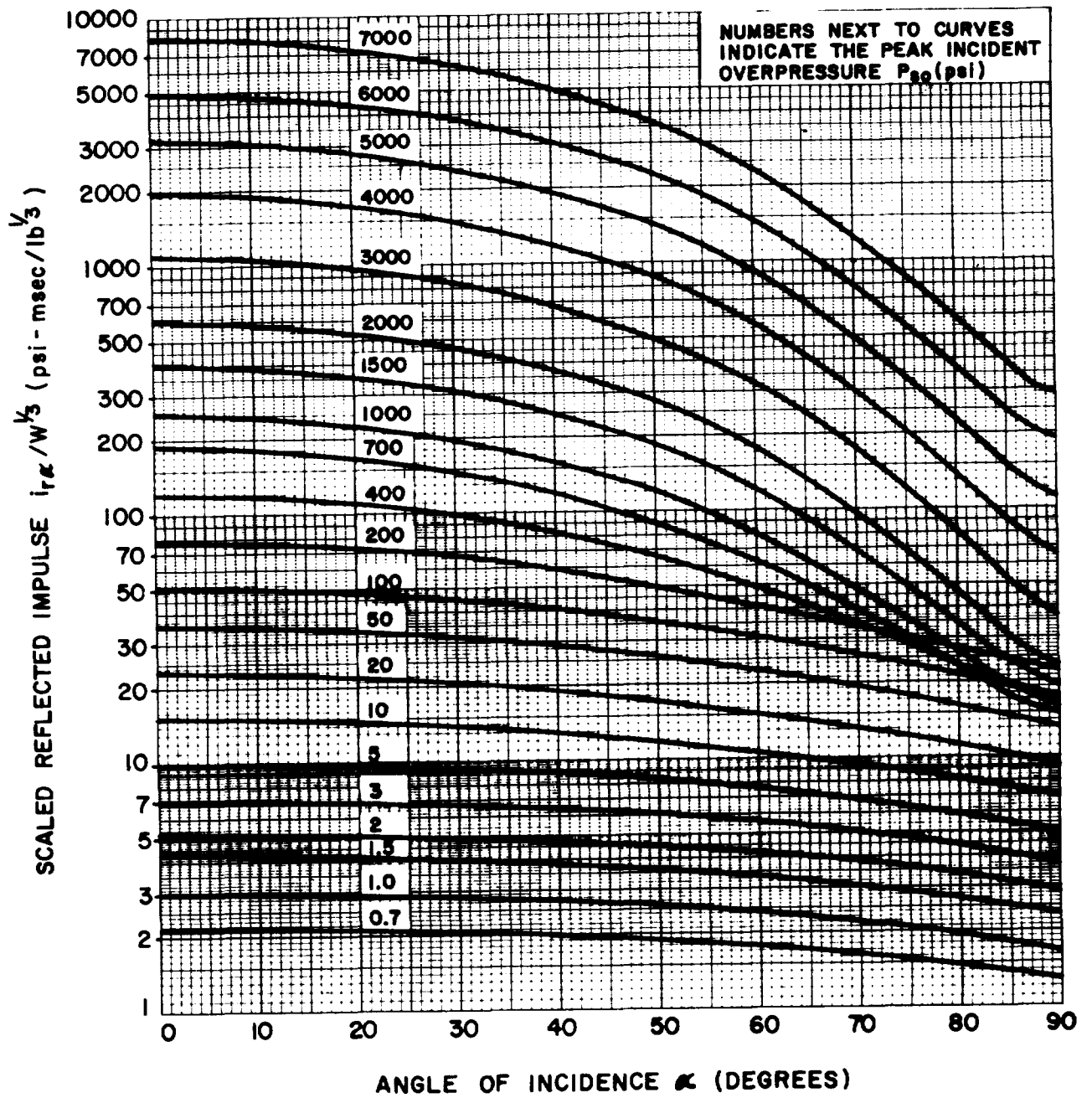
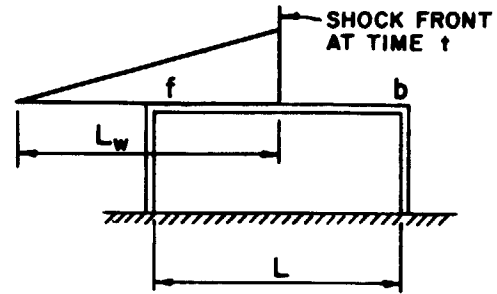
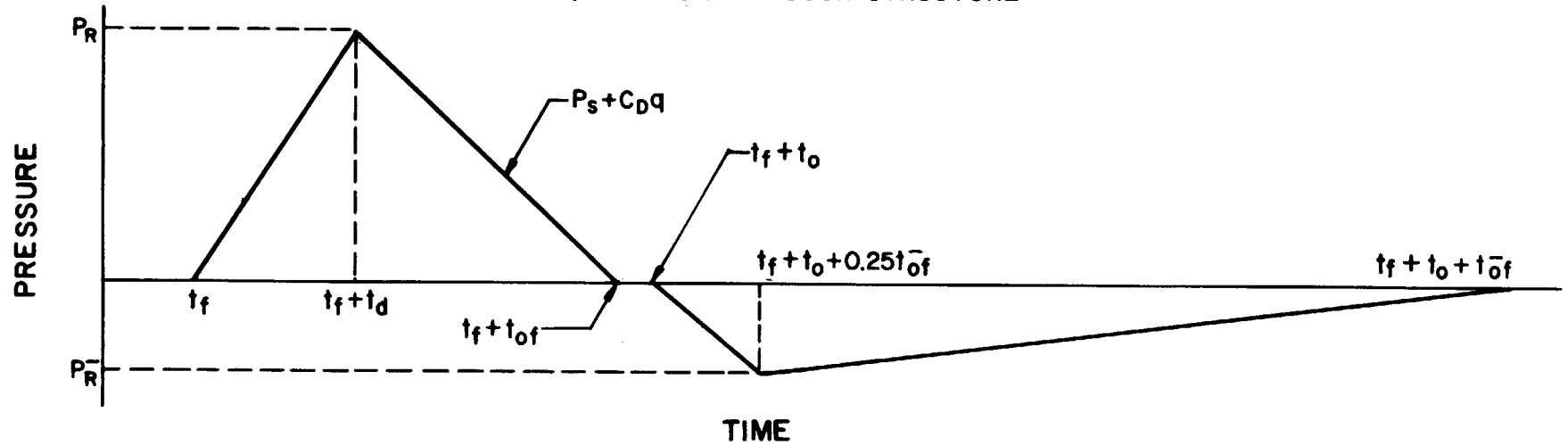


Figure 2-194 Reflected scaled impulse versus angle of incidence



a) SECTION THROUGH STRUCTURE



b) AVERAGE PRESSURE - TIME VARIATION

2-237

Figure 2-195 Roof and side wall loading

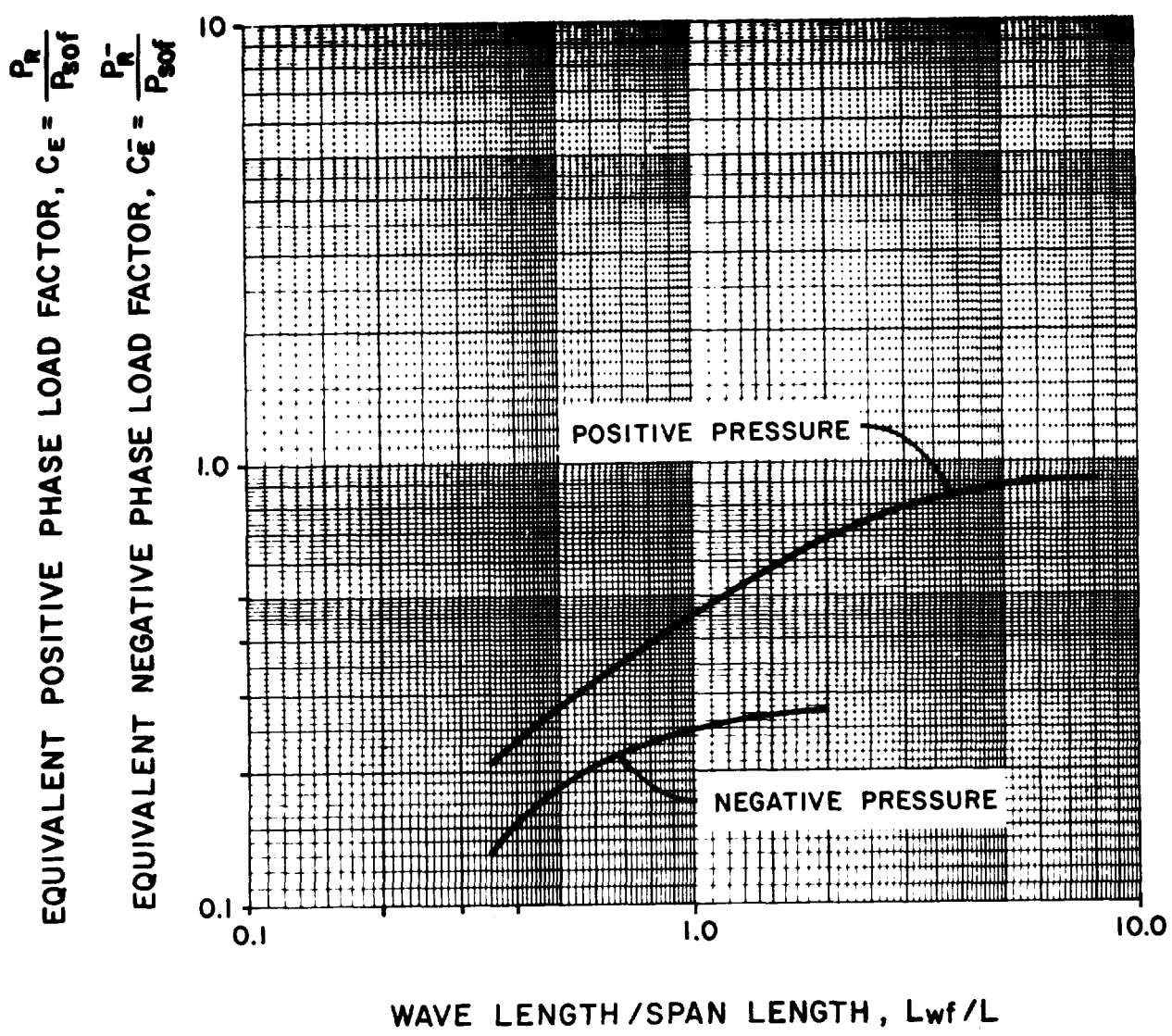
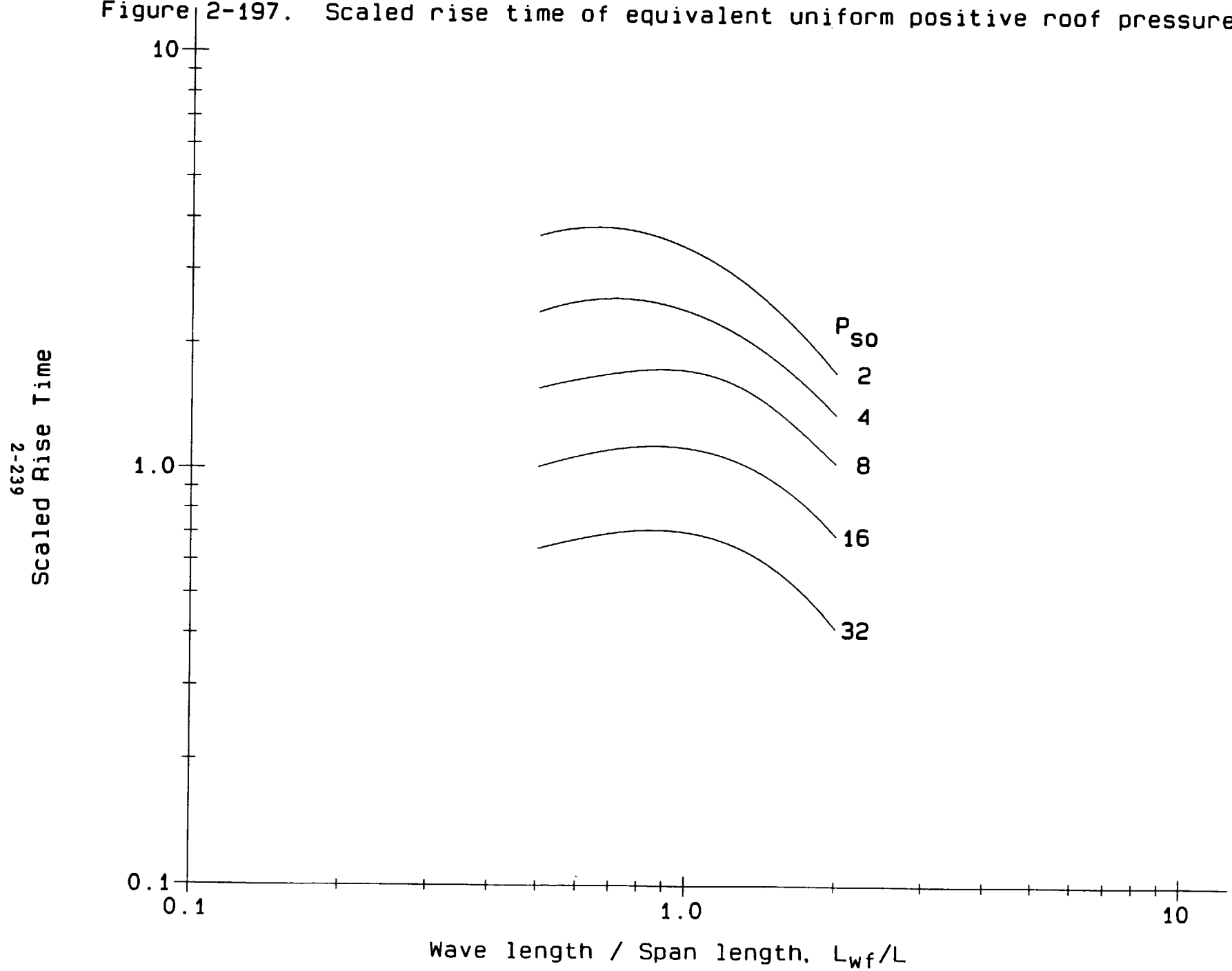


Figure 2-196 Peak equivalent uniform roof pressures

Figure 2-197. Scaled rise time of equivalent uniform positive roof pressures



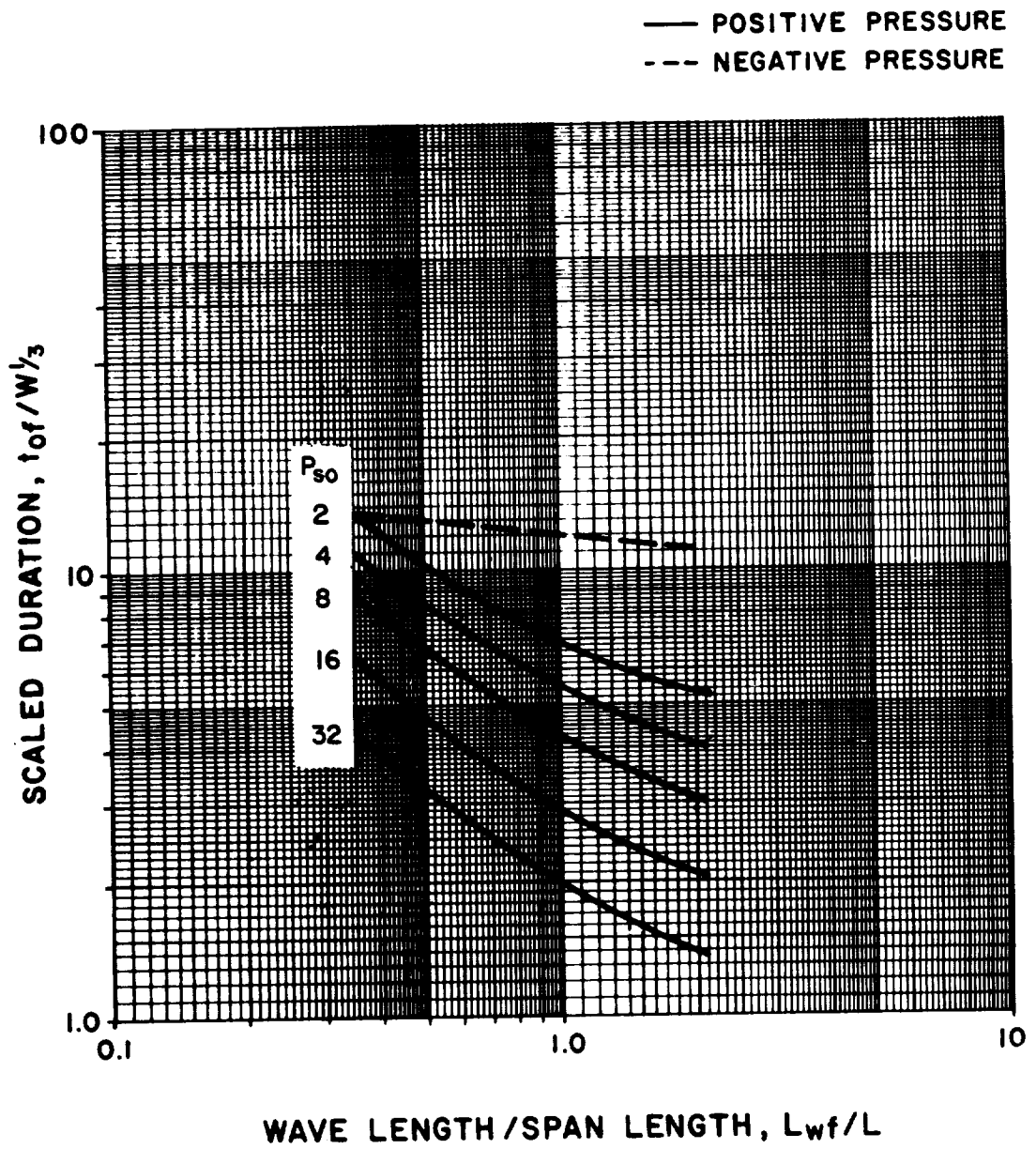
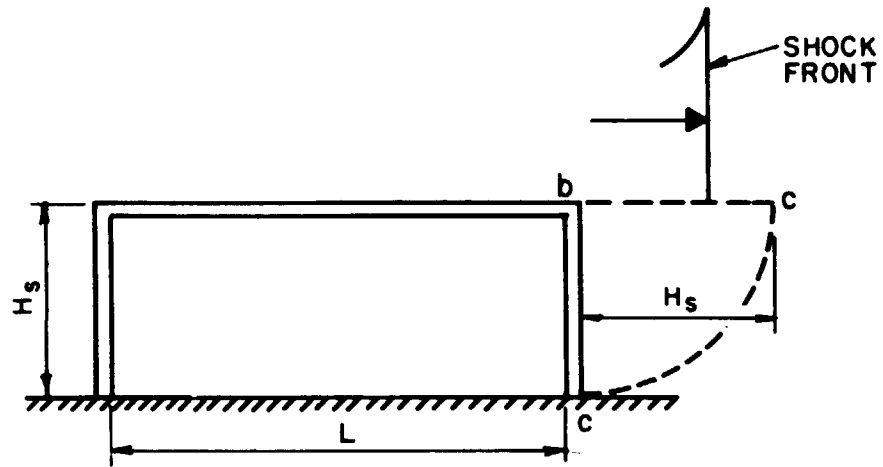
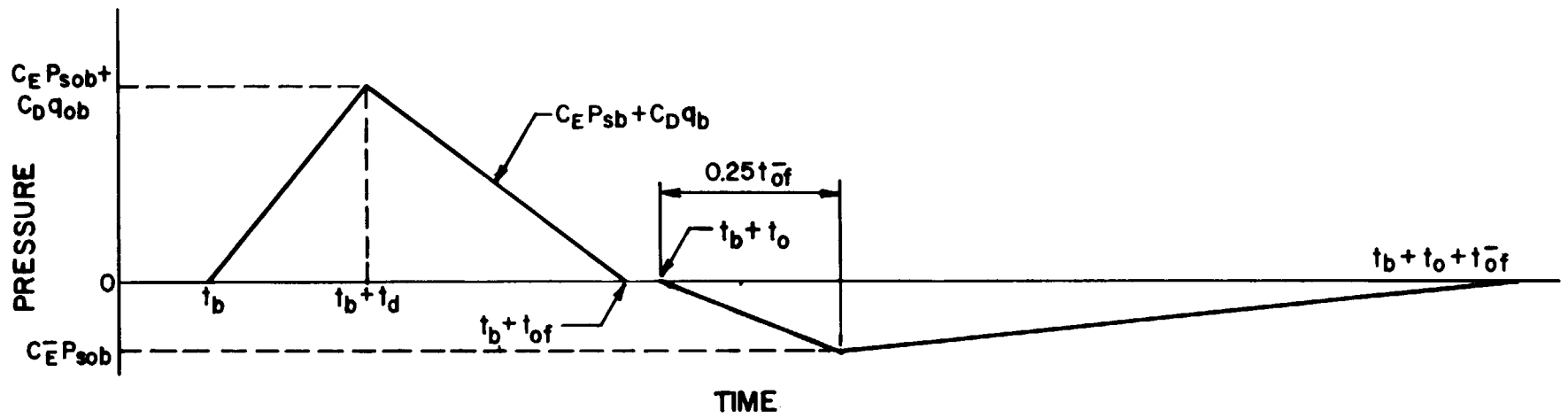


Figure 2-198 Scaled duration of equivalent uniform roof pressures



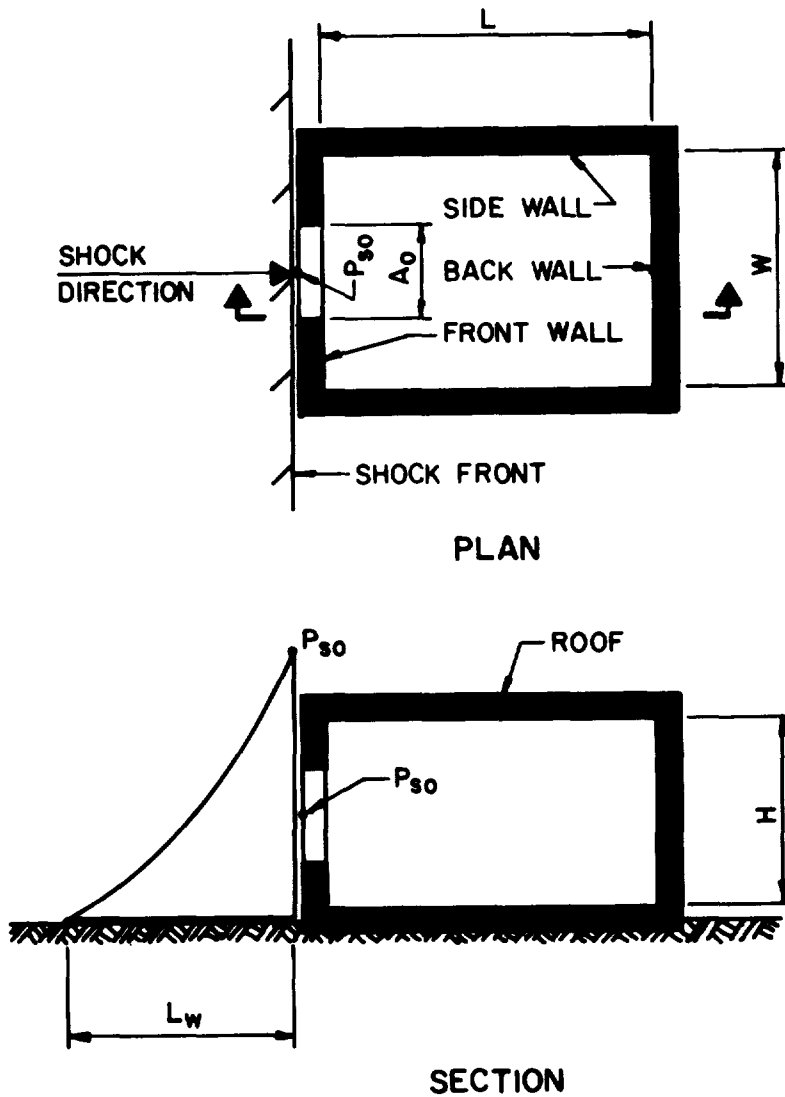
a) SECTION THROUGH STRUCTURE

2-241



b) AVERAGE PRESSURE - TIME VARIATION

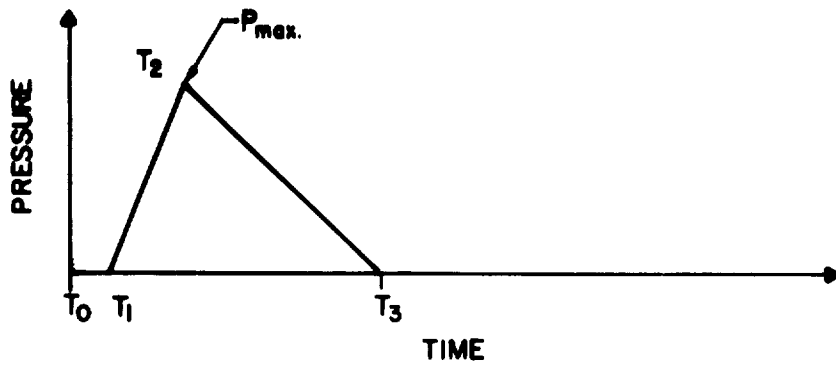
Figure 2-199 Rear wall loading



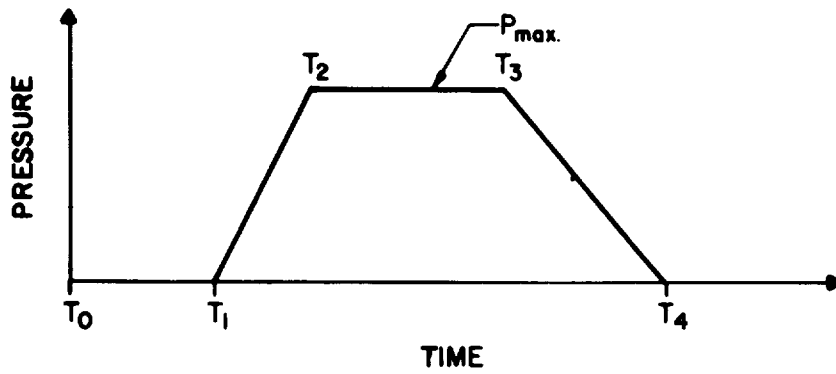
NOMENCLATURE:

- L, LENGTH OF SIDE WALL
- W, WIDTH OF BACK WALL AND FRONT WALL
- H, HEIGHT OF ALL WALLS
- A_0 , AREA OF OPENING IN FRONT WALL
- A_w , AREA OF BACK WALL
- L_w , WAVE LENGTH OF SHOCK WAVE OF INCIDENT PRESSURE, P_{s0} , AT EXTERIOR FACE OF FRONT WALL

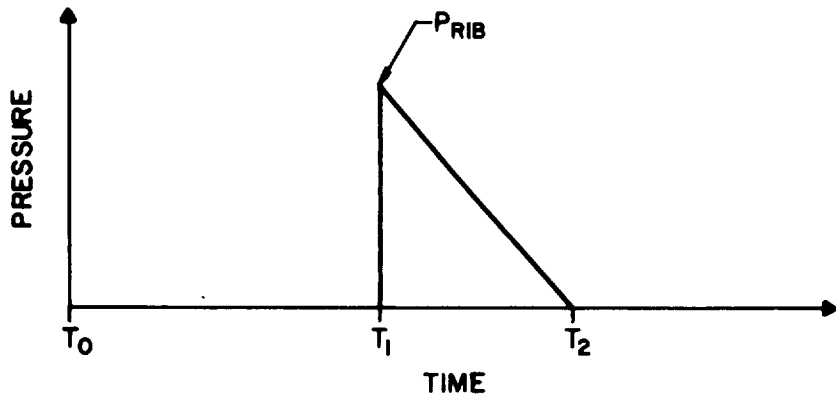
Figure 2-200 Idealized structure configuration for interior blast loads



a. INTERIOR FRONT WALL SURFACE



b. INTERIOR SIDE WALL OR ROOF SURFACE



c. INTERIOR BACK WALL SURFACE

Figure 2-201 Idealized interior blast loads

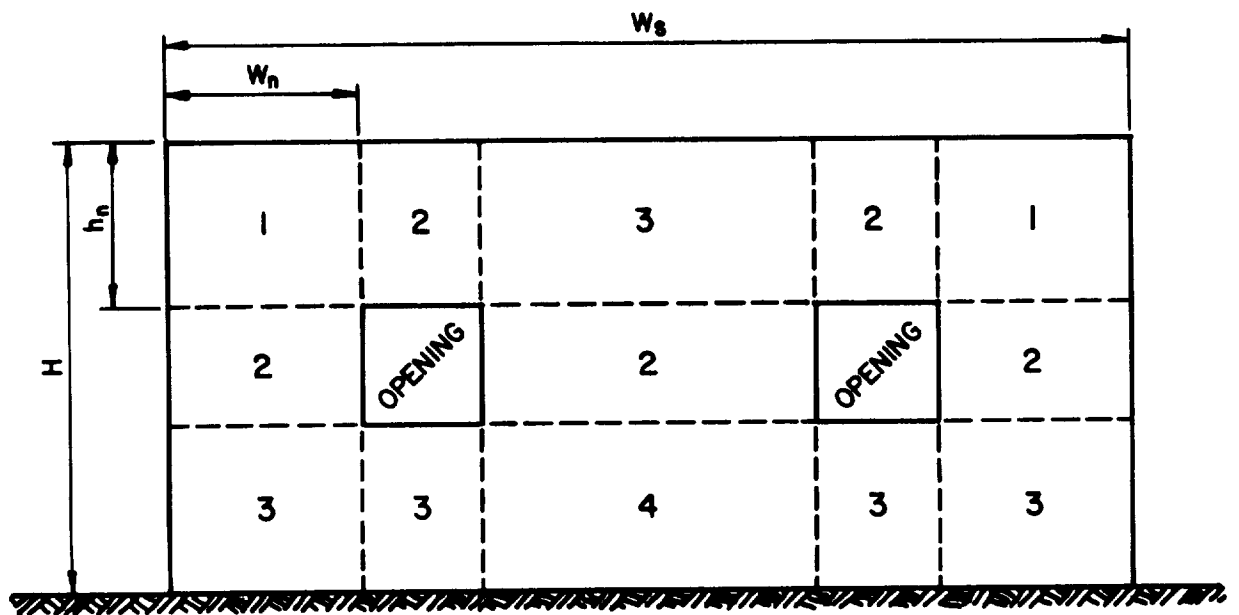
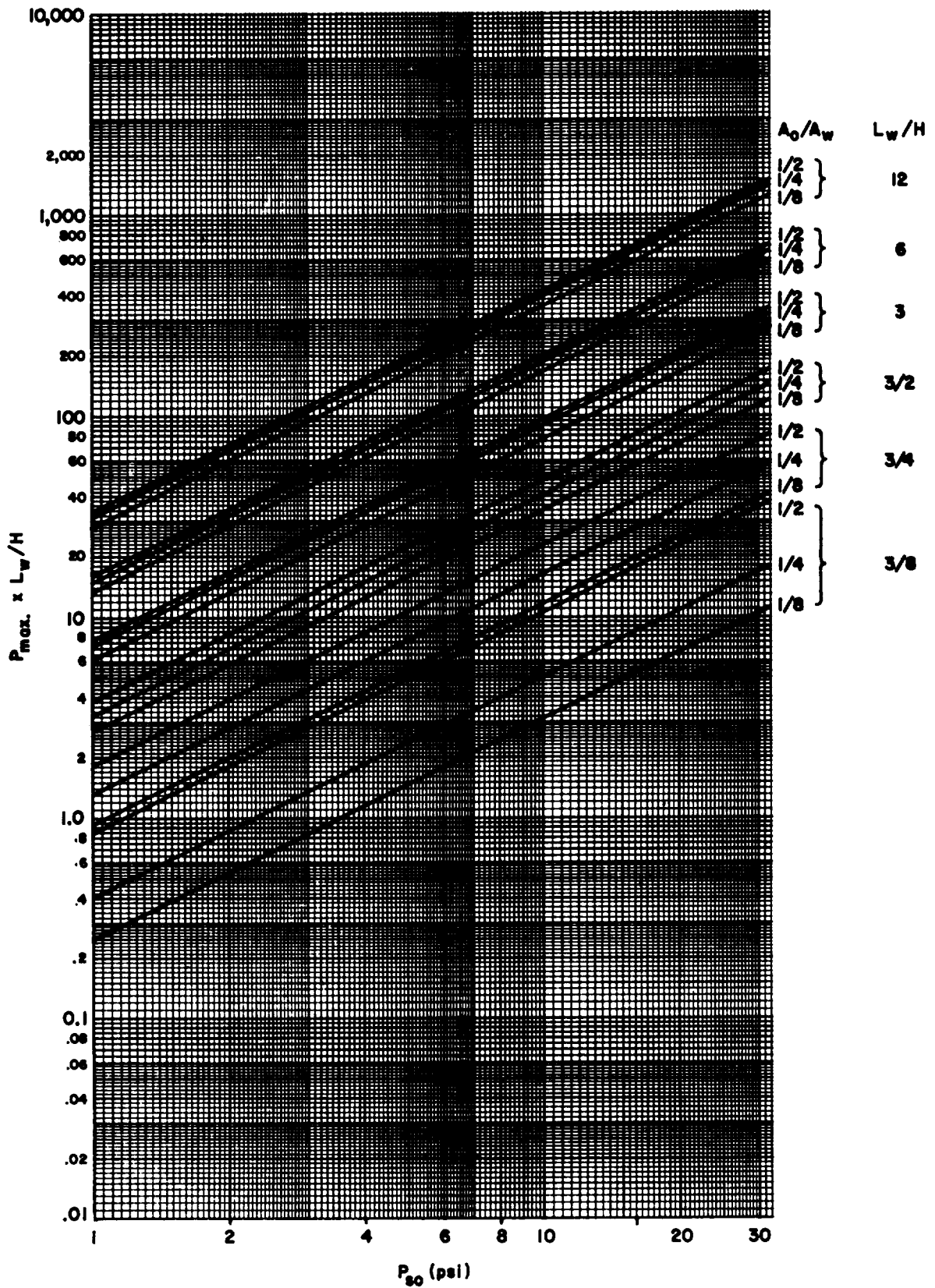
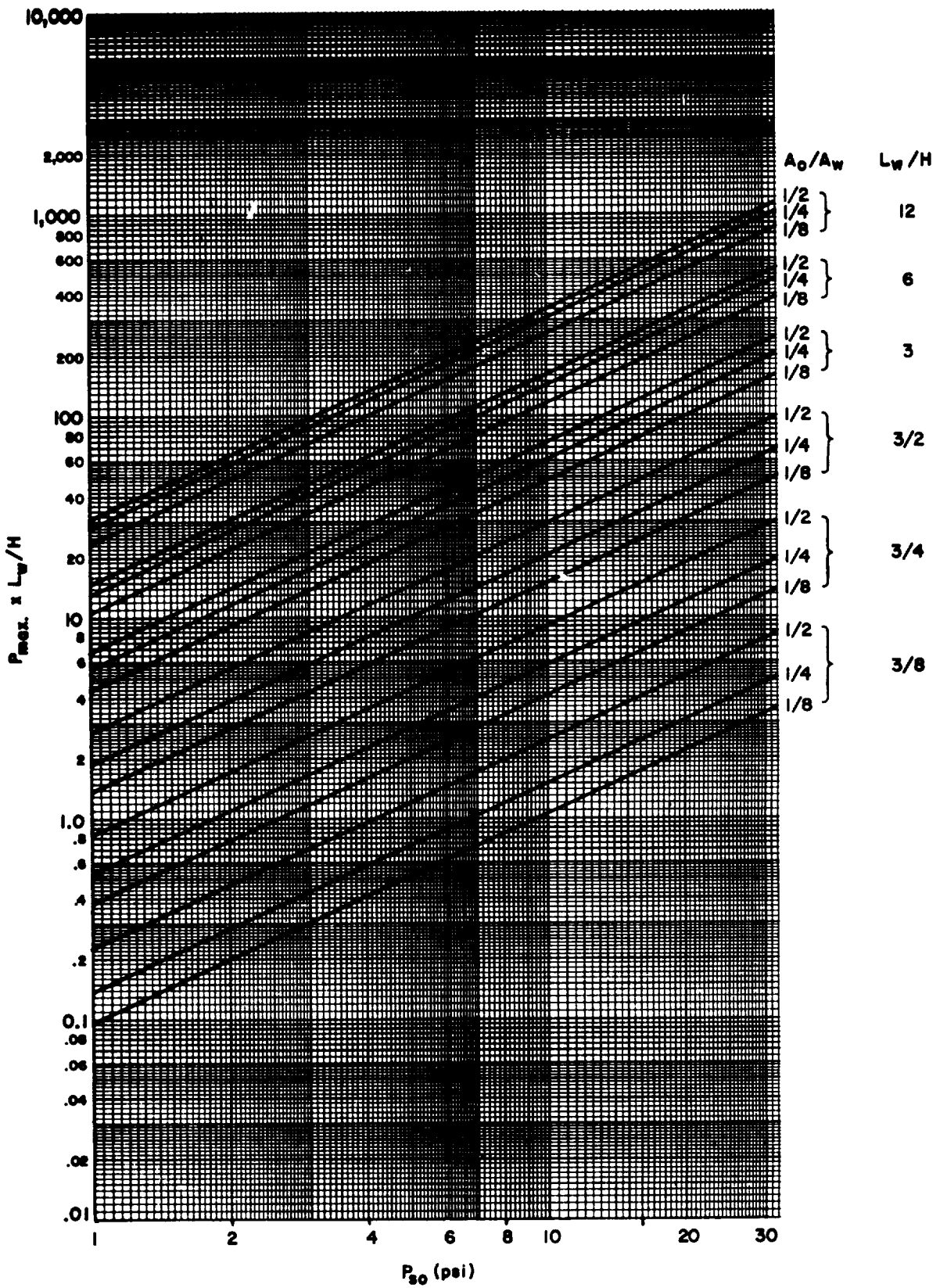


Figure 2-202 Sub-division of typical front wall with openings



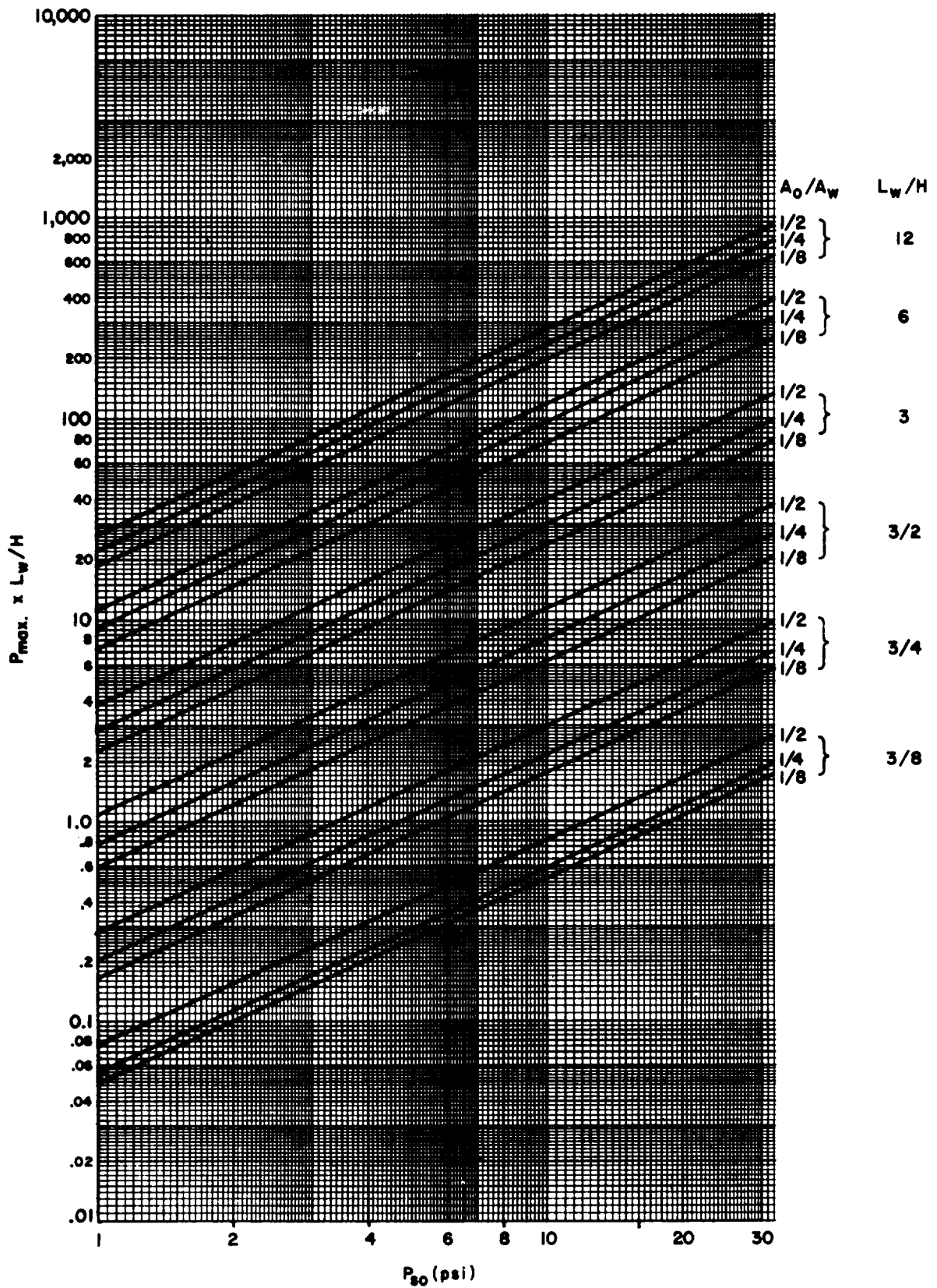
EXTERNAL INCIDENT PRESSURE AT FRONT FACE OF BUILDING, P_{so} (psi)

Figure 2-203 Maximum average pressure on interior face of front wall ($W/H = 3/4$)



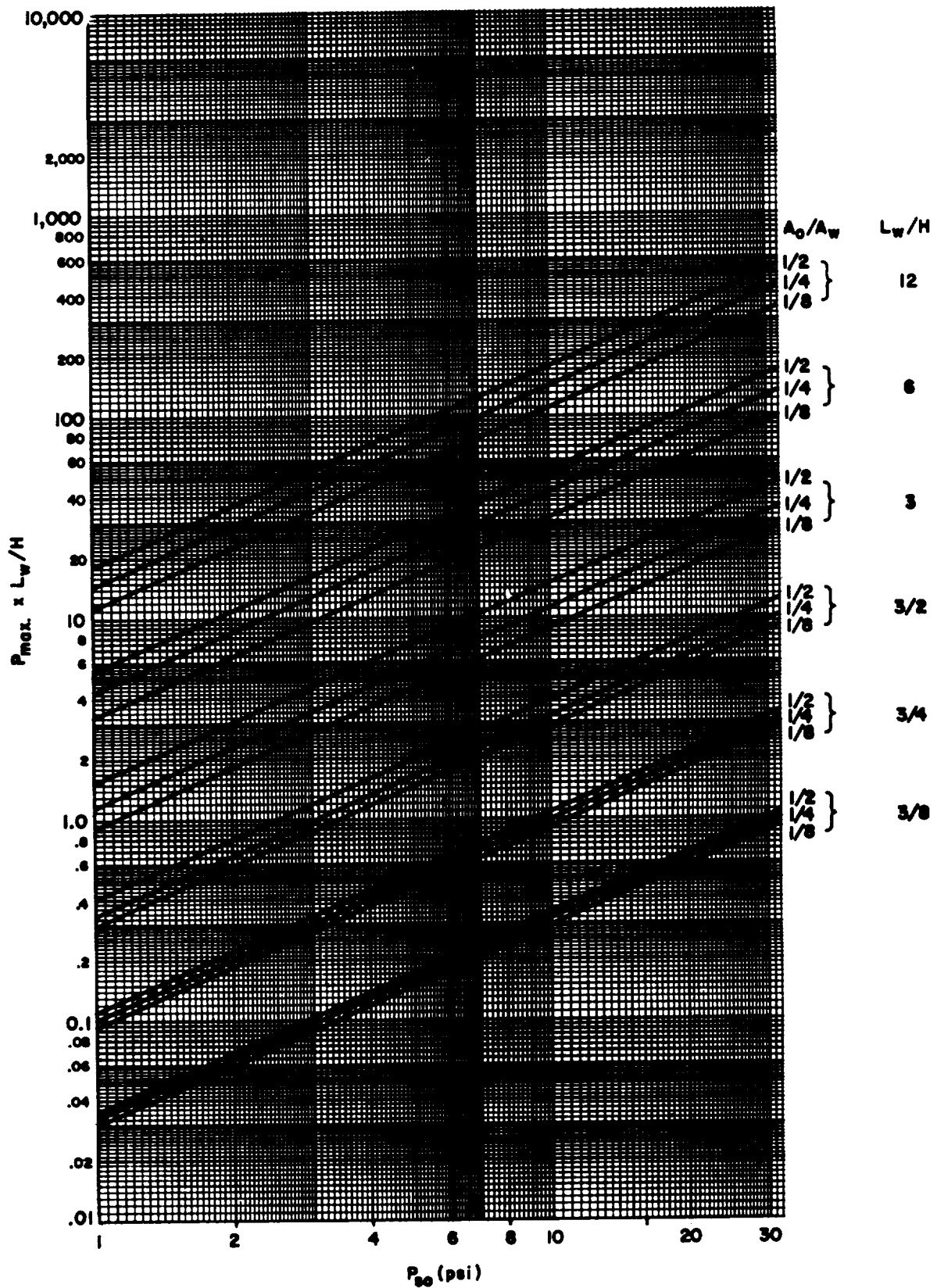
EXTERNAL INCIDENT PRESSURE AT FRONT FACE OF BUILDING, P_{30} (psi)

Figure 2-204 Maximum average pressure on interior face of front wall ($W/H = 3/2$)



EXTERNAL INCIDENT PRESSURE AT FRONT FACE OF BUILDING, $P_{90} (psi)$

Figure 2-205 Maximum average pressure on interior face of front wall ($W/H = 3$)



EXTERNAL INCIDENT PRESSURE AT FRONT FACE OF BUILDING, P_{80} (psi)

Figure 2-206 Maximum average pressure on interior face of front wall ($W/H = 6$)

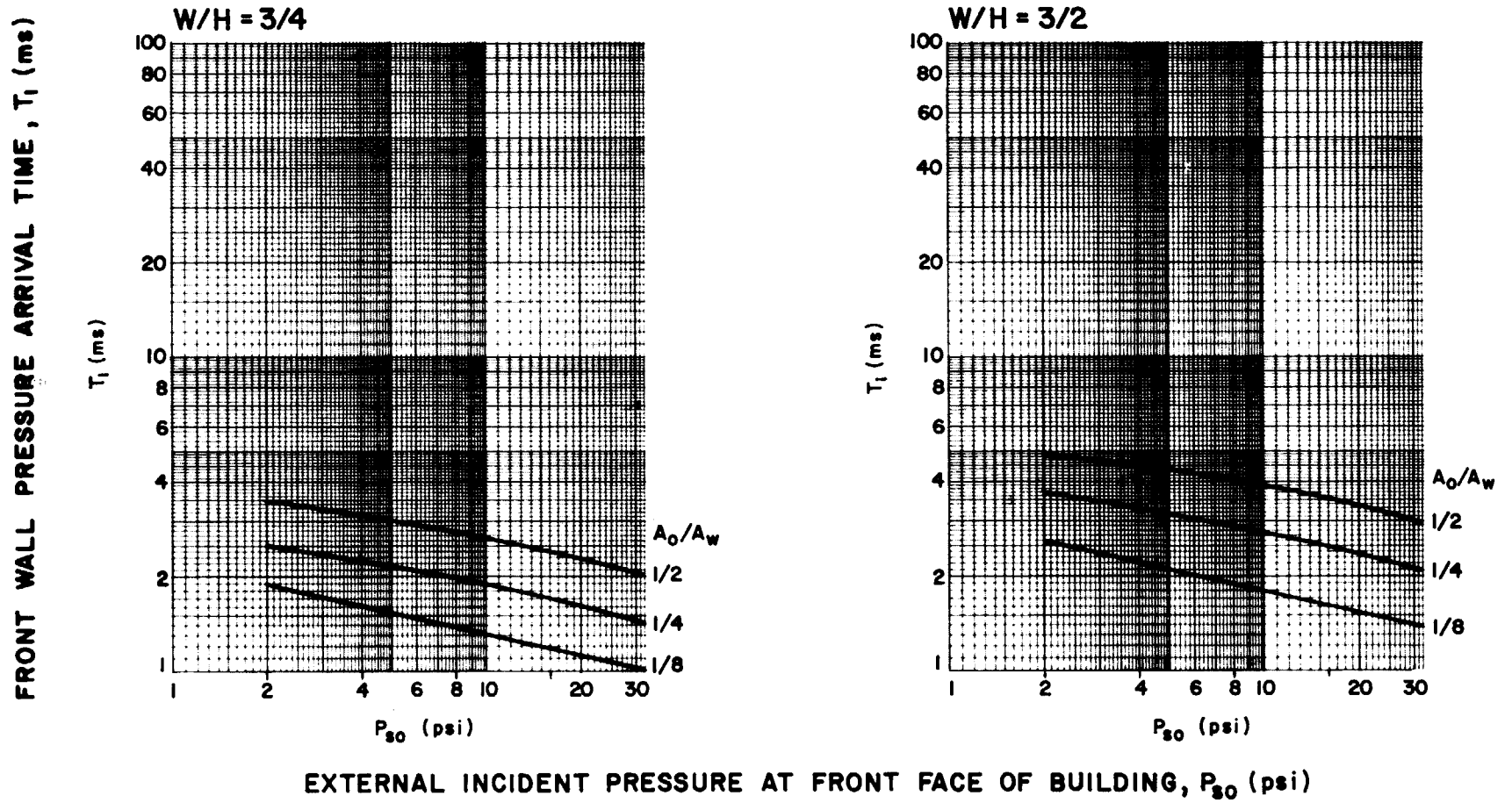
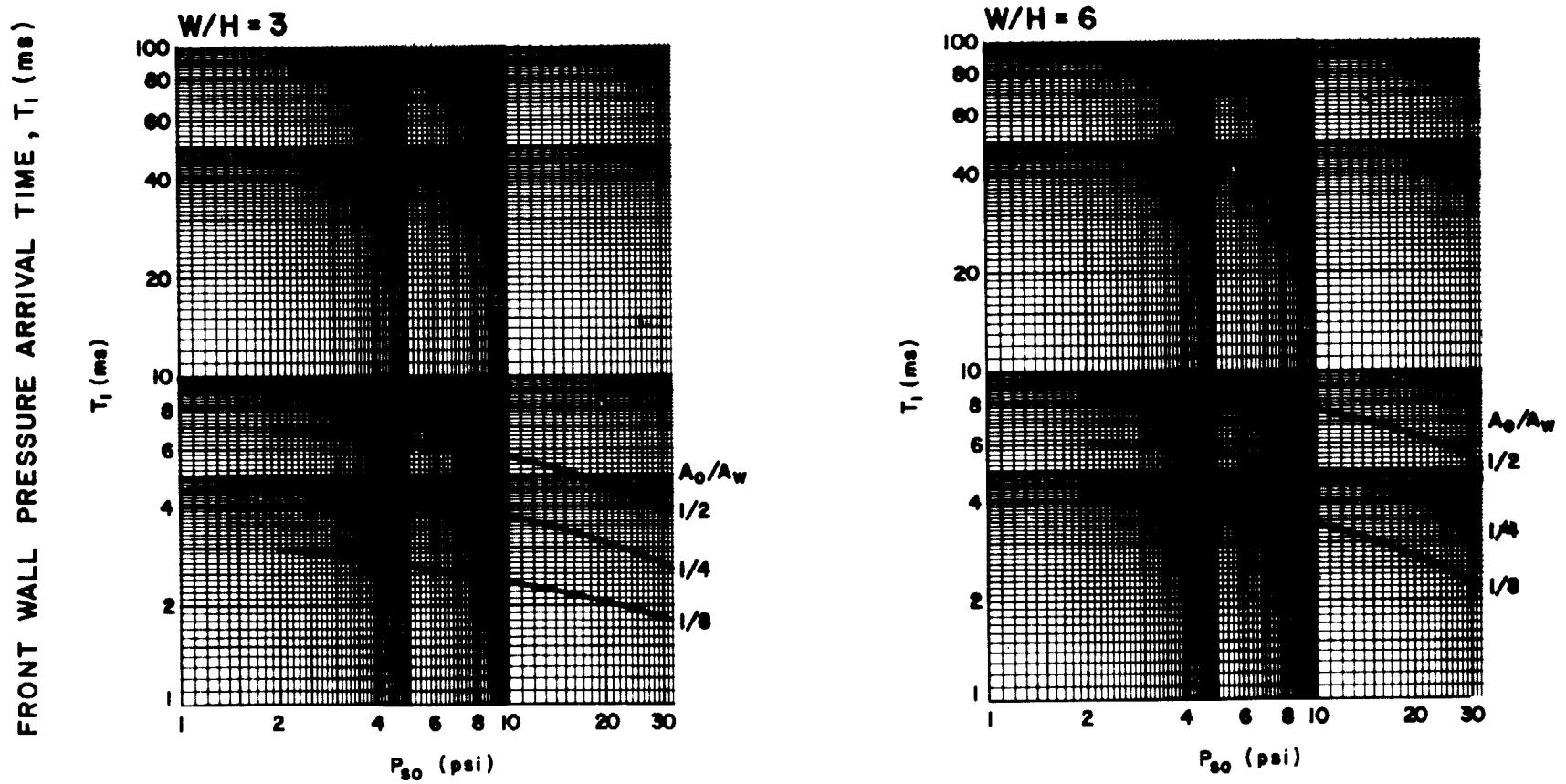


Figure 2-207 Arrival time, T_1 , for interior front wall blast load ($W/H = 3/4$ and $3/2$)



EXTERNAL INCIDENT PRESSURE AT FRONT FACE OF BUILDING, P_{30} (psi)

Figure 2-208 Arrival time, T_1 , for interior front wall blast load (W/H = 3 and 6)

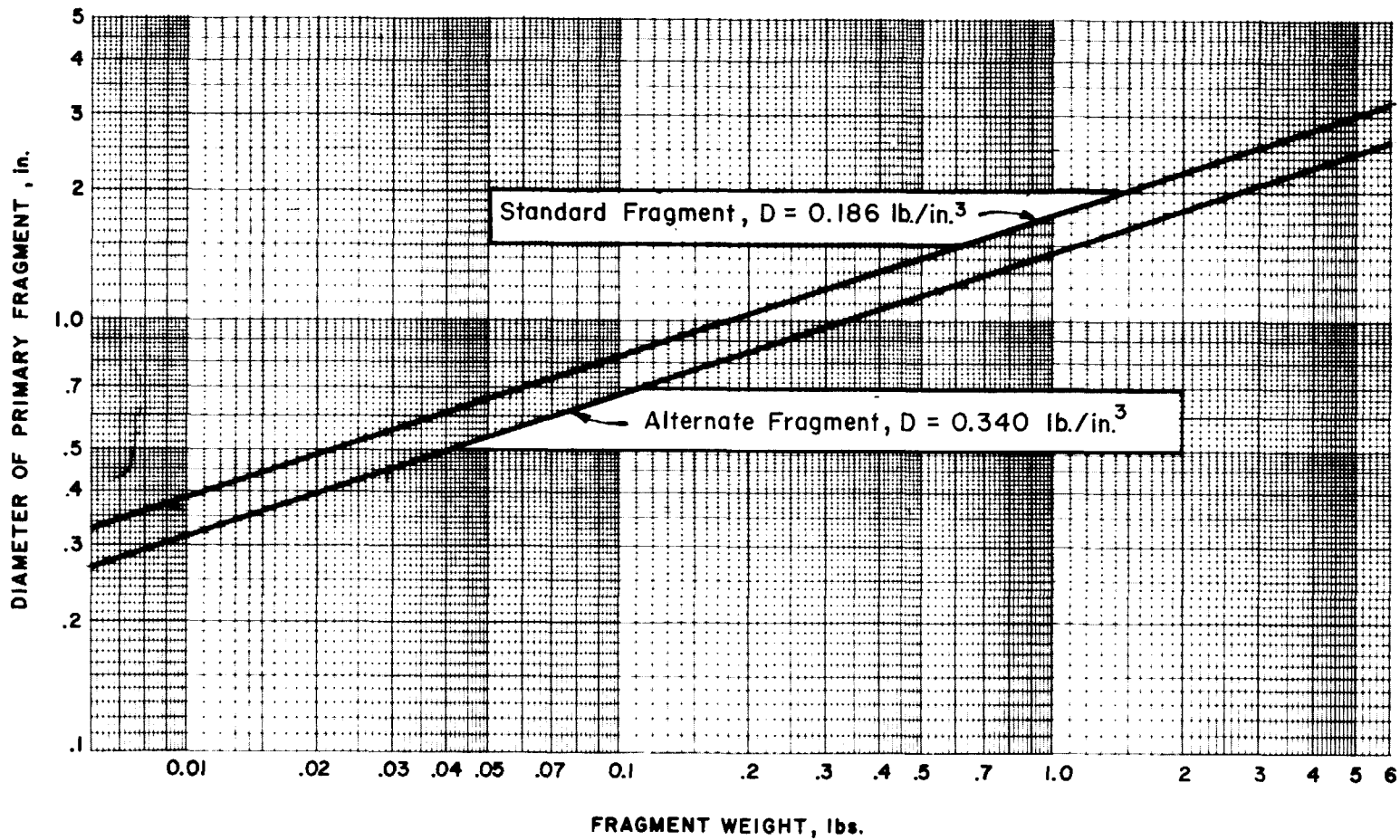


Figure 2-245 Relationship between fragment weight and fragment diameter

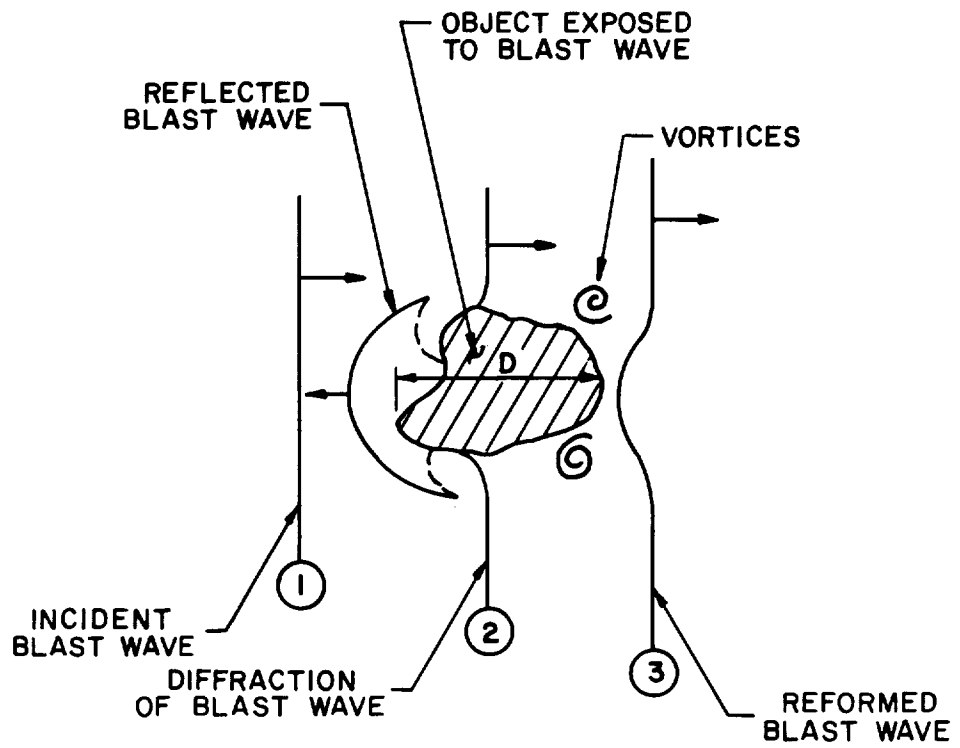


Figure 2-246 Interaction of blast wave with an irregular object

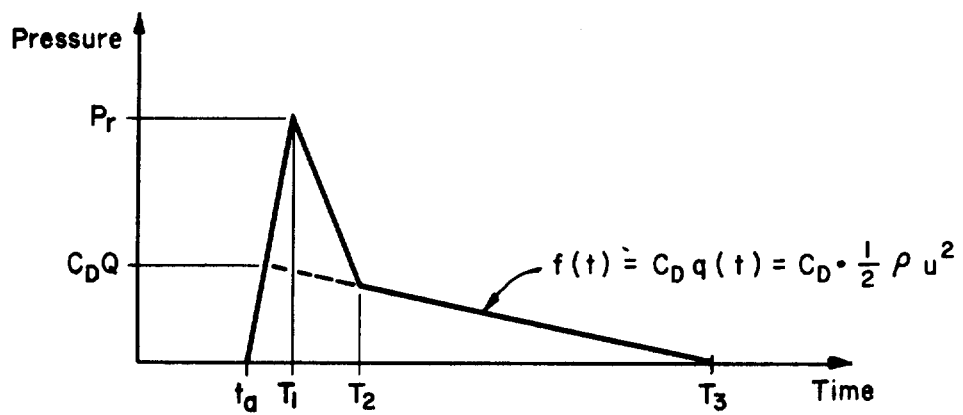


Figure 2-247 Idealized pressure-time loading on an irregular fragment

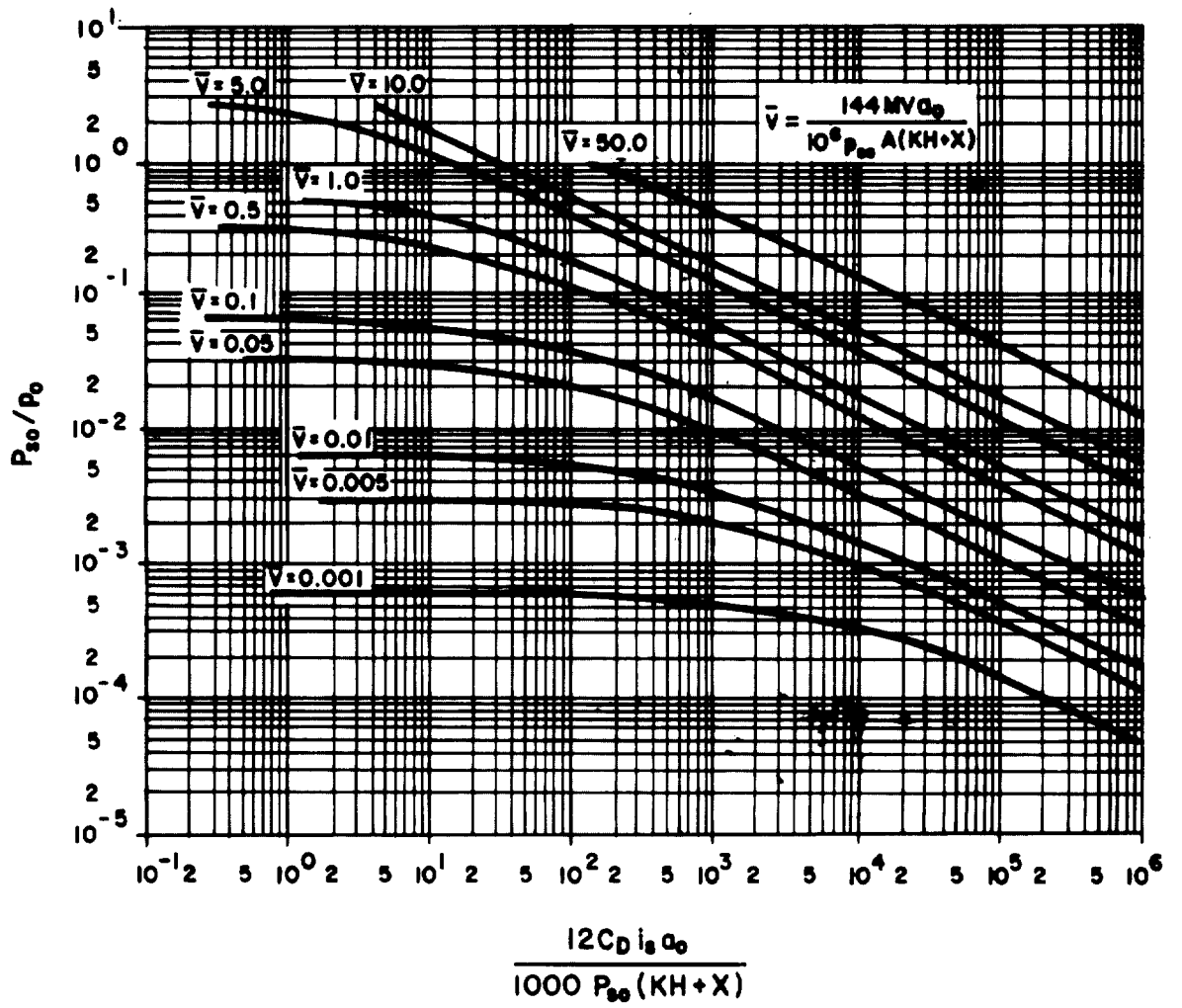
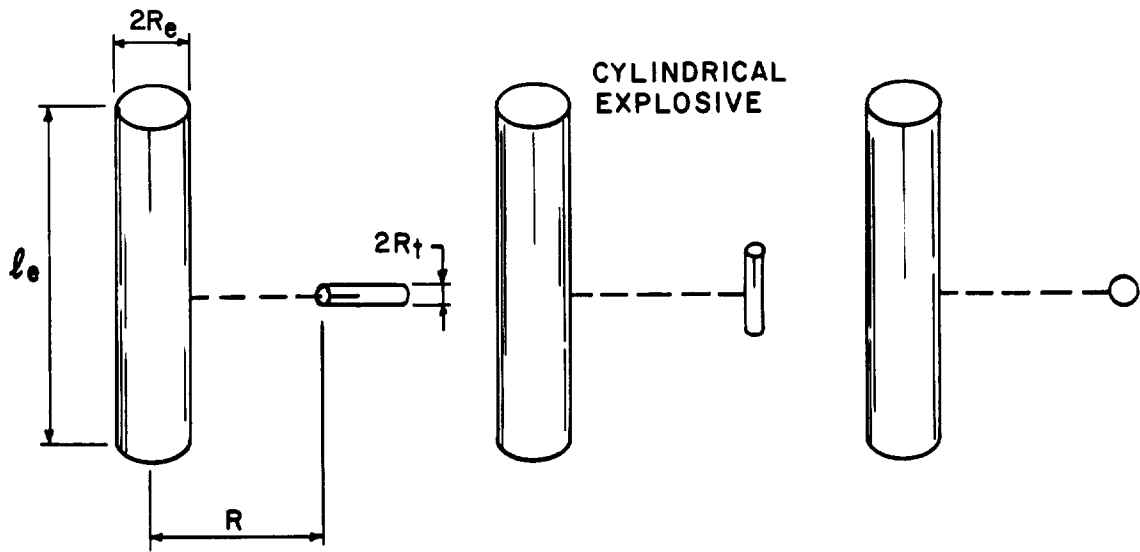


Figure 2-248 Nondimensional object velocity, \bar{V} , as a function of pressure and impulse



(a) EXPOSED FLAT FACE $\beta = 1.0$ (b) EXPOSED CYLINDRICAL SURFACE $\beta = \frac{\pi}{4}$ (c) EXPOSED SPHERICAL SURFACE $\beta = \frac{2}{3}$

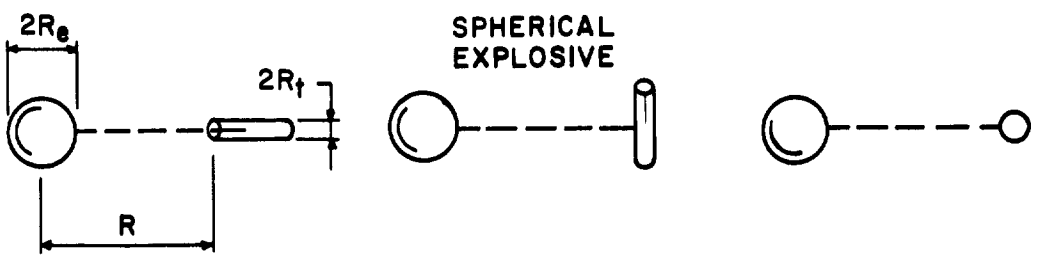


Figure 2-249 Target shape factor for unconstrained fragments

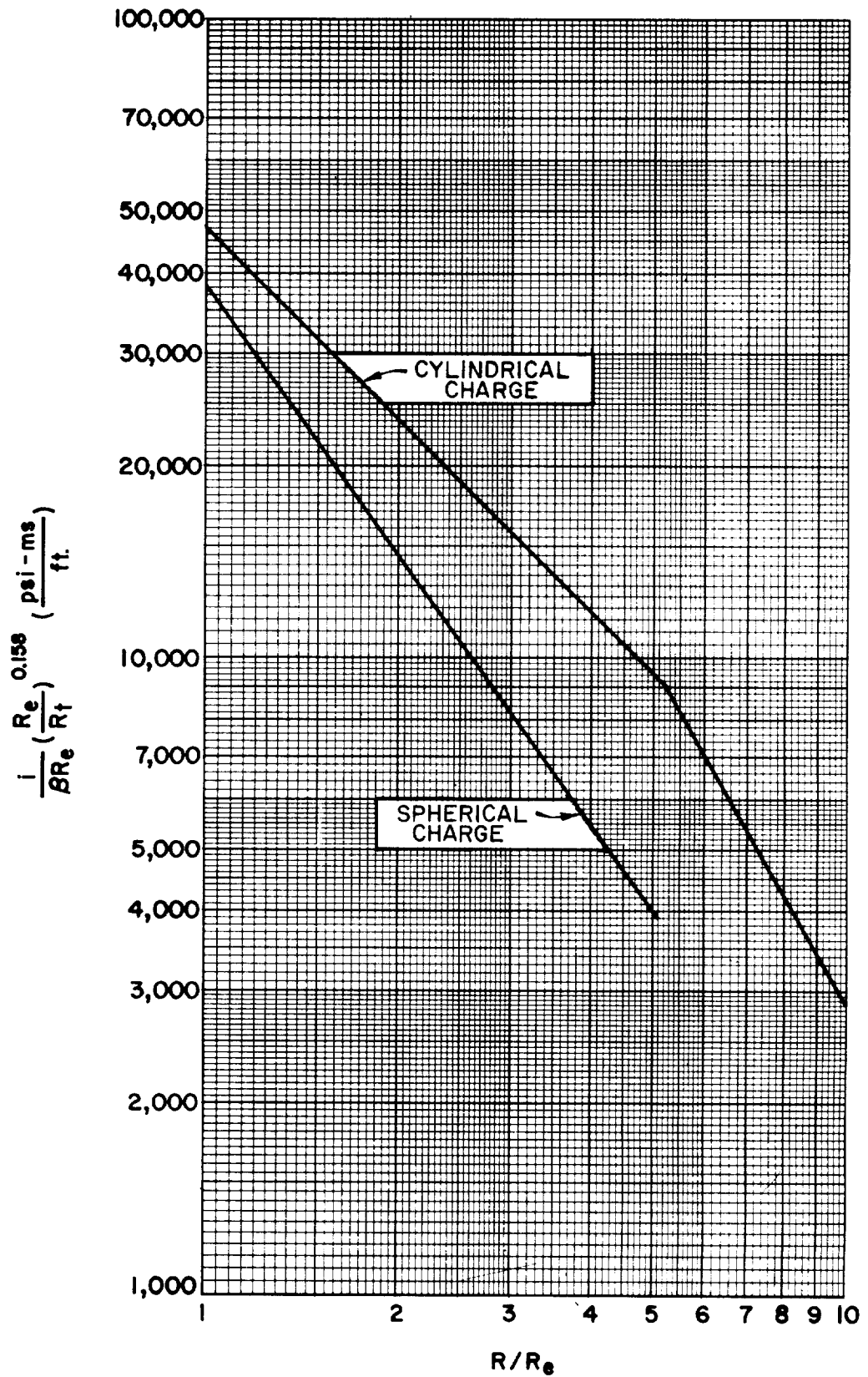


Figure 2-250 Specific acquired impulse versus distance

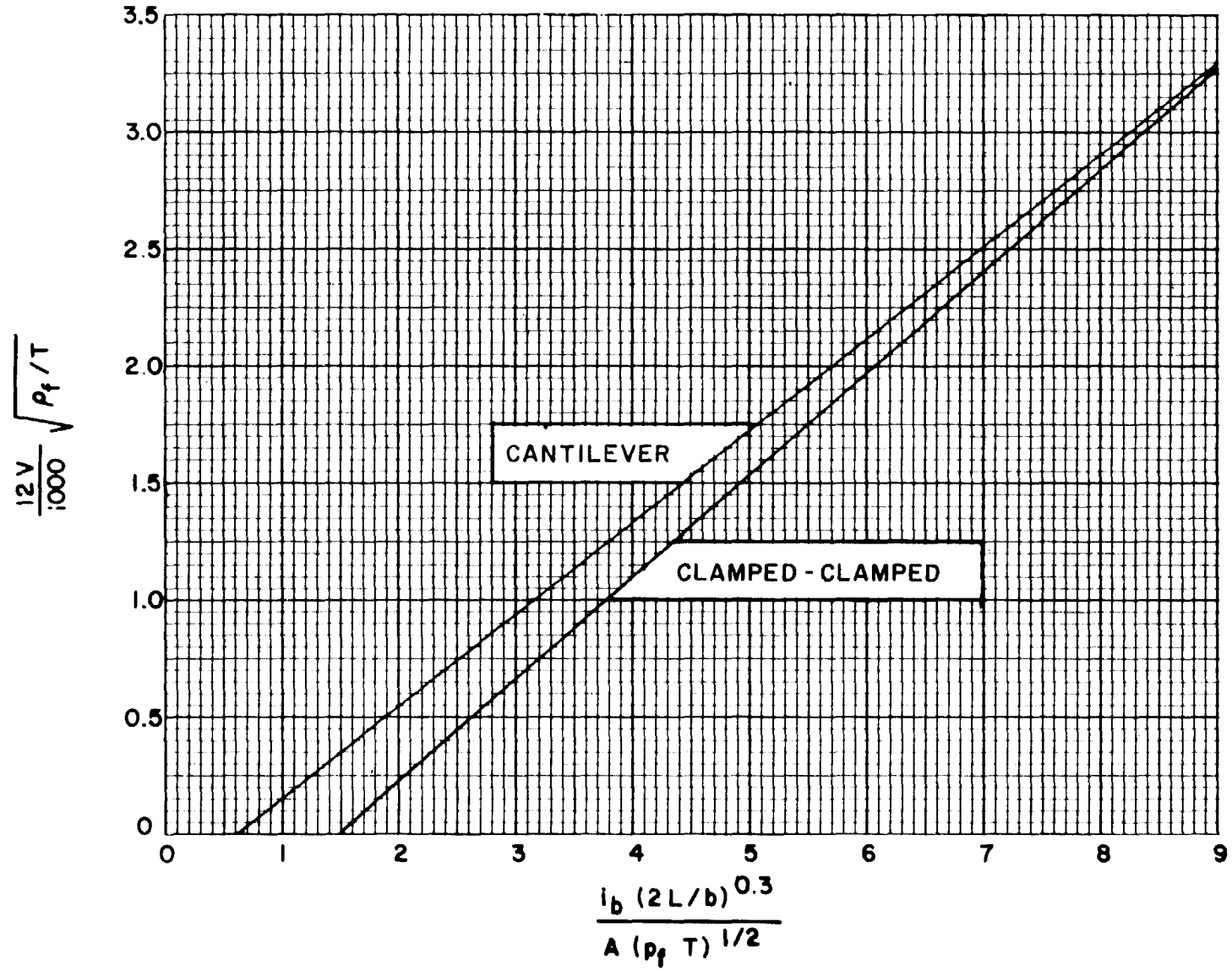


Figure 2-251 Scaled fragment velocities for constrained fragments

2-320

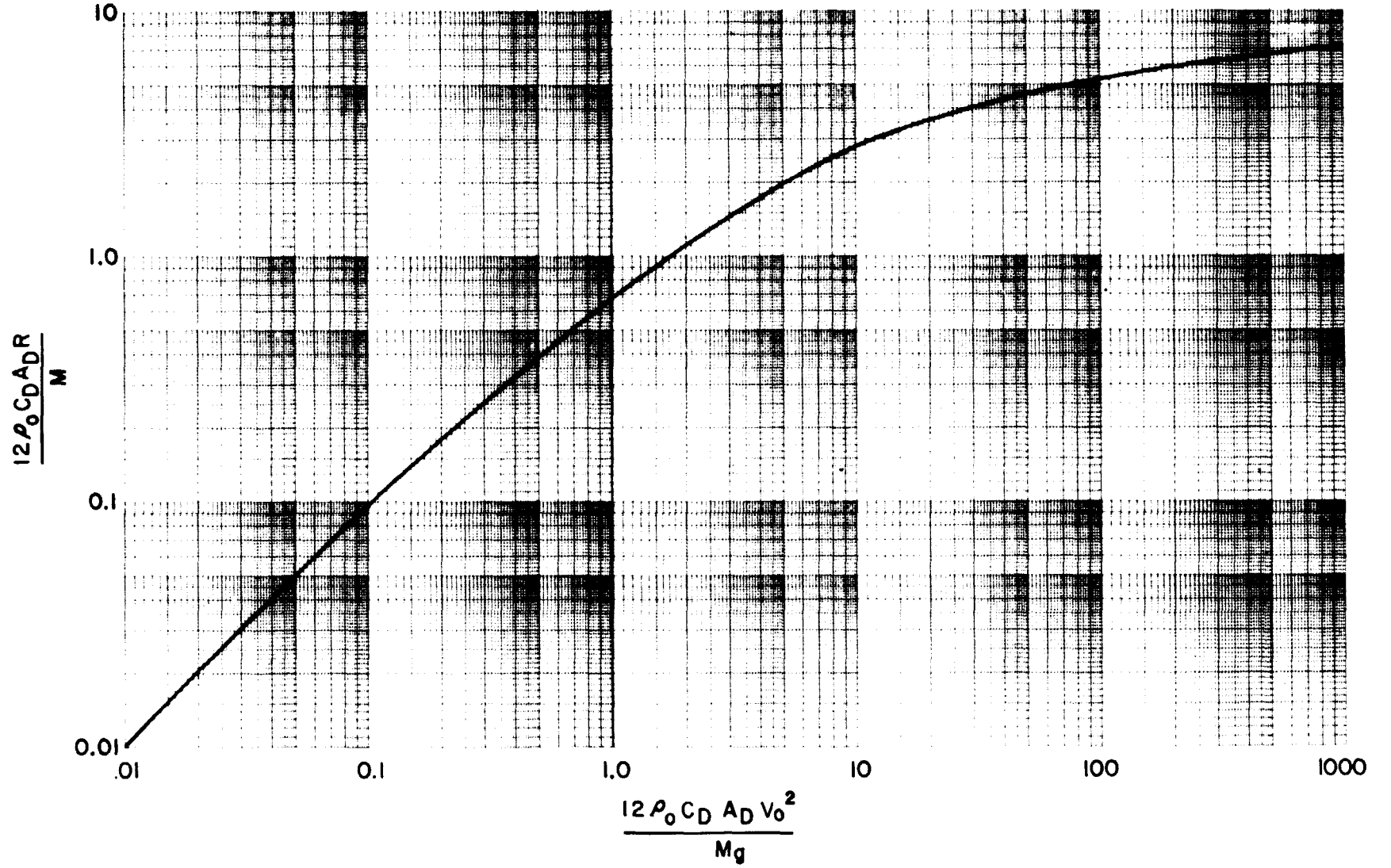
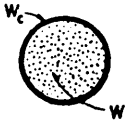
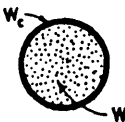
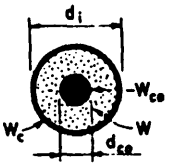
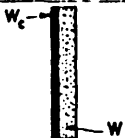

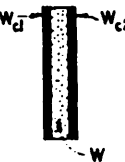


Table 2-5 Specific Weight and Gurney Energy Constant for Various Explosives

Explosive	Specific Weight (lb/in ³)	$\sqrt{2E'}$ (ft/sec)
Composition B	0.0621	9100
Composition C-3	0.0578	8800
HMX	0.0682	9750
Nitromethane	0.0411	7900
PBX-9404	0.0664	9500
PETN	0.0635	9600
RDX	0.0639	9600
TACOT	0.0581	7000
Tetryl	0.0585	8200
TNT	0.0588	8000
Trimonite No. 1	0.0397	3400
Tritonal (TNT/Al = 80/20)	0.0621	7600

Table 2-6 Initial Velocity of Primary Fragments for Various Geometries

Type	Cross-sectional shape	Initial fragment velocity v_0	Maximum v_0	Remarks
Cylinder		$\sqrt{2E'} \left[\frac{\frac{W}{W_c}}{1 + \frac{W}{2W_c}} \right]^{1/n}$	$\sqrt{2E'} \sqrt{3}$	See paragraph 2-17.2
Sphere		$\sqrt{2E'} \left[\frac{\frac{W}{W_c}}{1 + \frac{3W}{5W_c}} \right]^{1/n}$	$\sqrt{2E'} \sqrt{1}$	
Steel cored cylinder		$\sqrt{2E'} \left[\frac{\frac{W}{W_c}}{1 + \frac{(3+a)W}{6(1+a)W_c}} \right]^{1/n}$ where $a = \frac{d_{co}}{1.6d_i}$	$\sqrt{2E'} \sqrt{\frac{6(1+a)}{(3+a)}}$	If the steel core is many times more massive than the explosive, this expression for the initial velocity should be modified by multiplying it by the expression: $\sqrt{1 - \frac{0.02W_{co}}{W}}$ where W_{co} is the weight of the steel core (lbs.).
Plate		$\sqrt{2E'} \left[\frac{\frac{3W}{5W_c}}{1 + \frac{W}{5W_c} + \frac{4W}{5W_c}} \right]^{1/n}$	$\sqrt{2E'} \sqrt{3}$	This expression applies for a rectangular explosive in contact with a metal plate having the same surface area. It is assumed that the entire system is suspended in free air and its thickness is small in comparison to its surface area so that the resulting motions are essentially normal to the plane of the plate.
Hollow cylinder		—	—	Although an expression to predict the velocity of fragments is not available, an upper limit of the initial velocity may be obtained using the expression for a solid cylinder and a lower limit from the expression for a single plate. The ratio of the explosive weight to the casing weight (W/W_c) of the hollow cylindrical charge is used in both expressions.
Sandwich plates		If $W_{c1} = W_{c2}$ $\sqrt{2E'} \left[\frac{\frac{W}{W_{c1} + W_{c2} + \frac{W}{3}(1-g+g^2)}}{\frac{W_{c1} + \frac{W}{2}}{W_{c1} + \frac{W}{2}}} \right]^{1/n}$ where $g = \frac{W_{c1} + \frac{W}{2}}{W_{c1} + \frac{W}{2}}$ If $W_{c1} = W_{c2} = W_c$ $\sqrt{2E'} \left[\frac{\frac{W}{2W_c}}{1 + \frac{W}{6W_c}} \right]^{1/n}$	$\sqrt{2E'} \sqrt{3}$	This expression applies for a rectangular explosive sandwiched between two metal plates having the same surface area as the explosive. It is assumed that the entire system is suspended in free air and its thickness is small in comparison to its surface area so that the resulting motions are essentially normal to the plane of the plates.

Note:
 $W = E =$ Explosive weight
 $W_c = C =$ Casing weight
 W, W_c, W_{c1}, W_{c2} (lbs.)
 d_i, d_{co} (lbs.)
 $v_0, \sqrt{2E'}$ (ft./sec)

Table 2-7 Mott Scaling Constants for Mild Steel Casings and Various Explosives

Explosive	(OZ ^{1/2} ^A in. ^{-3/2})	(OZ ^{1/2} ^B in. ^{-7/6})
Baratol	-	0.512
Composition A-3	-	0.220
Composition B	0.214	0.222
Cyclotol (75/25)	-	0.197
H-6	-	0.276
HBX-1	-	0.256
HBX-3	-	0.323
Pentolite (50/50)	0.238	0.248
PTX-1	-	0.222
PTX-2	-	0.227
RDX	0.205	0.212
Tetryl	0.265	0.272
TNT	0.302	0.312

Table 2-8 Drag Coefficient, C_D , for Various Shapes

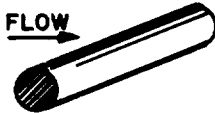


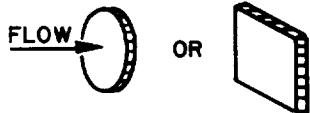
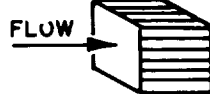
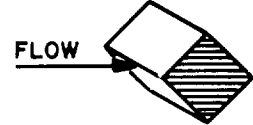



SHAPE	SKETCH	C_D
CIRCULAR CYLINDER (LONG ROD), SIDE-ON		1.20
SPHERE		0.47
ROD, END-ON		0.82
DISC, FACE-ON		1.17
CUBE, FACE-ON		1.05
CUBE, EDGE-ON		0.80
LONG RECTANGULAR MEMBER, FACE-ON		2.05
LONG RECTANGULAR MEMBER, EDGE-ON		1.55
NARROW STRIP, FACE-ON		1.98

Table 2-9 Steel Toughness

Steel	Toughness in-lb/cubic in.
ASTM A 36	12,000
ASTM A 441	15,000
ASTM A514 Grade F	19,000

SHOCK LOADS

2-20. Introduction

The strong air blast waves and high speed fragments are the primary hazards of accidental explosions. The exterior of a protective structure is designed primarily for the blast pressures. In some situations, the fragments may be just as important as the pressures in determining the configuration of a protective facility. While the contents of the structure are protected from the direct effects of blast pressures and fragments by the structure's exterior, the contents are subject to effects of the building's motion. These structure motions can cause injury to personnel, damage to equipment as well as dislodgement of the structure's interior components, including interior partitions, hung ceilings, light fixtures, ductwork, piping, and electrical lines.

Structure motions are caused by what is normally termed shock loads. These are loads which cause transient or short-duration vibratory motions of the ground surface and the structure. They do not cause significant structural damage but instead induce motion which, as stated above, can damage the structure's interior contents.

There are two distinct types of shock loads: ground shock and air shock. Ground shock results from the energy which is imparted to the ground by an explosion. Some of this energy is transmitted through the ground as direct-induced ground shock. Both of these forms of ground shock when imparted to a structure will cause the structure to move in both a vertical and horizontal direction. Air shock results from the blast overpressures striking the building. Vertical, horizontal and overturning motions result from the shock impact. The vertical and overturning motions are usually not significant and can be neglected while the horizontal motions must be considered. Large displacements can result when a structure slides relative to the ground surface.

The net motion of the structure is a combination of the motions due to the air induced and direct-induced ground shock, and the air shock. Curves which describe the ground motion (acceleration versus time, velocity versus time, and displacement versus time curves) are not readily calculated. However, these relationships are not required since the design of protective structures to resist shock loads is based on the peak values of the induced motion rather than the actual motion-time relationships.

The procedures presented in this section are applicable for uniform motions. The shock loads and resulting structure motions apply to rigid concrete structures located at the low- and intermediate-pressure design ranges. At distances corresponding to these pressures, the shock loads are uniform across the structure. A rigid concrete structure acts as a rigid body, that is, all components of the structure have essentially the same motion. The procedures can be applied to structures located close to an explosion and to non-rigid structures. However, the local effects associated with these conditions must be accounted for in the analysis.

2-21. Ground Shock

2-21.1. Introduction

When an explosion occurs at or near the ground surface, ground shock results from the energy imparted to the ground by the explosion. Some of this energy is transmitted through the air in the form of air-induced ground shock and some is transmitted through the ground as direct-induced ground shock.

Air-induced ground shock results when the air-blast shock wave compresses the ground surface and sends a stress pulse into the underlying media. The magnitude and duration of the stress pulse in the ground depend on the character of the air-blast pulse and the ground media. Generally, the air-induced ground motions are downward. They are maximum at the ground surface and attenuate with depth. However, the presence of a shallow water table, a shallow soil-rock interface, or other discontinuities can alter the normal attenuation process. The properties of the incident overpressure pulse and the surface soil layer usually determine the character of air-induced ground shock on above-ground structures.

Direct-induced ground shock results from the explosive energy being transmitted directly through the ground. This motion includes both the true direct-induced motions and cratering-induced motions. The latter generally have longer durations and are generated by the crater formation process in cratering explosions. The induced ground motion resulting from both types have a longer duration than air-blast-induced ground shock and the wave forms tend to be sinusoidal.

The net ground shock experienced by a point on the ground surface is a combination of the air-blast-induced and direct-induced shock. The relative magnitudes and sequencing of the motions are functions of the media (air and soil) through which the shock travels and the distance from the point of detonation. At ranges close to the blast, the highly compressed air permits the air-blast shock front to propagate at speeds greater than the seismic velocity of the ground. In this region, the super-seismic region, the air blast arrives at a given point before the direct-induced ground shock. As the air-blast shock front moves farther from the point of detonation, the shock front velocity decreases, and the direct-induced ground shock catches and "outruns" the air blast. This latter region is called the outrunning region. Wave forms in the outrunning region are generally a complex combination of both types of induced shock. The combined motion can be obtained from consideration of the arrival time of each wave. The arrival time of the air blast is determined from the data presented for unconfined explosions. Whereas, the arrival time of the direct-induced ground shock can be estimated by assuming that the ground shock travels at the seismic velocity of the ground media. The combined ground motion in both the superseismic and outrunning region are illustrated in Figure 2-253.

2-21.2. Air Blast-Induced Ground Shock

One-dimensional wave propagation theory is used to estimate air blast-induced ground shock. For surface structures located on ground media having uniform properties, the expressions to define this motion take very simple forms. Using this approach, the maximum vertical velocity at the ground surface, V_v , can be expressed as

$$V_v = P_{so} / \rho C_p \quad 2-74$$

where

V_V - maximum vertical velocity of the ground surface

P_{SO} - peak positive incident pressure (Fig. 2-15)

ρ - mass density of the soil

C_p - compression wave seismic velocity in the soil

The mass density, ρ , for typical soils and rock are presented in Table 2-10 and the seismic velocities are presented in Table 2-11.

The maximum vertical displacement, D_V , is obtained by integrating the above expression with respect to time. The integral of the pressure with respect to time is simply the total positive phase impulse so that:

$$D_V = i_s / 1,000 \rho C_p \quad 2-75$$

where

D_V - maximum displacement of the ground surface

i_s - unit positive incident impulse (Fig. 2-15)

The maximum vertical acceleration, A_V , is based on the assumption of a linear velocity increase during a rise time equal to one millisecond. The resulting acceleration is increased by 20 percent to account for nonlinearity during the rise time. Accelerations are expressed in multiples of the gravitational constant so that,

$$A_V = 100 P_{SO} / (\rho C_p g) \quad 2-76$$

where

A_V - maximum vertical acceleration of the ground surface

g - gravitational constant equal to 32.2 ft/sec²

The above equation is adequate for predicting the acceleration in dry soil. However, the equation underestimates the acceleration in saturated soils and rock. To approximate the acceleration of saturated soils and rock, it is recommended that the value of the acceleration obtained from the Equation 2-76 be doubled.

The maximum horizontal ground motions are expressed in terms of the maximum vertical motions as a function of the seismic velocity of the soil and the shock wave velocity so that

$$D_H = D_V \tan [\sin^{-1} (C_p / 12,000 U)] \quad 2-77$$

$$V_H = V_V \tan [\sin^{-1} (C_p / 12,000 U)] \quad 2-78$$

$$A_H = A_V \tan [\sin^{-1} (C_p / 12,000 U)] \quad 2-79$$

where U - shock front velocity (Fig. 2-15).

For $(C_p/12,000 U)$ greater than one, horizontal and vertical motions are approximately equal. Therefore, it is recommended that for all values of the

above function greater than one, the horizontal motion is set equal to the calculated vertical motion.

The equations which describe the air-induced ground shock are a function of the density and seismic velocity of the soil. However, a wide range of seismic velocities is given in Table 2-11 for each of the soils listed. In a final design, soil tests are required to accurately determine the density and seismic velocity of the particular soil at the site. In lieu of tests, the mass density given in Table 2-10 may be used. However, since the range of seismic velocities given Table 2-11 is so large, it is recommended that the lower bound value of the velocity be used to produce a conservative estimate of the induced motion.

2-21.3. Direct-Induced Ground Motion

Empirical equations have been developed to predict direct-induced ground motions. The equations apply for TNT detonations at or near the ground surface. Three types of ground media have been considered; dry soil, saturated soil and rock. The ground shock parameters are expressed in terms of the charge weight and distance from the explosion.

The maximum vertical displacement (D_V) of the ground surface for a rock media is given by

$$D_V = 0.025 R_G^{1/3} W^{1/3} / Z_G^{1/3} \quad 2-80$$

in which

$$Z_G = R_G / W^{1/3} \quad 2-81$$

where

R_G = ground distance from the explosion

W = weight of TNT charge

Z_G = scaled distance from the explosion

and the maximum horizontal displacement D_H of the ground surface is equal to one-half of the maximum vertical displacement or

$$D_H = 0.5 D_V \quad 2-82$$

When the ground media consists of either dry or saturated soil, the maximum vertical displacement is given by

$$D_V = 0.17 R_G^{1/3} W^{1/3} / Z_G^{2.3} \quad 2-83$$

while the maximum horizontal displacement D_H is equal to the maximum vertical displacement or,

$$D_H = D_V \quad 2-84$$

The maximum vertical velocity (V_V) for all ground media is given by

$$V_V = 150 / Z_G^{1.5} \quad 2-85$$

and the maximum horizontal velocity (V_H) is equal to the maximum vertical velocity for all ground media or

$$V_H = V_V \quad 2-86$$

Finally, the maximum vertical acceleration (A_V) of the ground surface for all media is given by

$$A_V = 10,000 / (W^{1/3} Z_G^2) \quad 2-87$$

while for dry soil, the maximum horizontal acceleration, A_H , is equal to one-half of the maximum vertical acceleration, or

$$A_H = 0.5 A_V \quad 2-88$$

however, for a wet soil or a rock media, the horizontal and vertical acceleration is equal, or

$$A_H = A_V \quad 2-89$$

2-22. Air Shock

2-22.1. Introduction

When an air blast strikes an aboveground protective structure, motions are imparted to the building. The most severe motion is due to the response of the individual elements which make up the exterior shell of the structure. Procedures for the design of these elements are presented in subsequent chapter of this manual. This section is concerned with the gross motion of the structure on its supporting soil due to the impact of the air blast. This gross motion is in addition to the ground induced motions.

Vertical, horizontal and overturning motions are imparted to the structure by the air blast. However, since the vertical motion of the structure is restricted by the ground which is already compressed due to the dead load of the structure and its contents, vertical motions must necessarily be small and can be safely neglected. Overturning motions are also neglected in this section. These motions are most significant in tall structures with small plan dimensions which are not common in protective construction. This section is concerned solely with horizontal sliding motions which can be quite significant.

Horizontal motion results from an unbalanced blast load acting on the structure. The tendency of the structure to slide is resisted by the friction forces developed between the foundation and the underlying soil. For structures with deep foundations, additional resistance to sliding is afforded by active and passive soil pressures developed at the leeward side of the structure.

2-22.2. Method of Analysis

The gross horizontal motion of a structure is computed in this manual using a method of numerical integration, namely, the acceleration-impulse extrapo-

lation method. This method of dynamic analysis is comprehensively presented in Chapter 3. Briefly, the equation of motion for a single-degree-of-freedom system is given as

$$F - R - D = Ma$$

2-90

where

- F - applied blast load as a function of time
- R - resistance of the system to motion as a function of displacement
- D - damping force as a function of velocity
- M - mass of the single-degree-of-freedom system
- a - acceleration of the system

The numerical method of solving the equation of motion involves a step-by-step integration procedure. The integration is started at time zero where the displacement and velocity are known to be zero. The time scale is divided into small intervals. The values of F, R and M (D is not included) are calculated for each time step. The integration is started by first approximating the acceleration for the first time interval and progresses by successively calculating the acceleration at each time step. The change in velocity and displacement associated with each incremental acceleration is calculated. The accumulated velocity and displacement are obtained for each time step until the maximum values have been obtained.

The first step in the analysis is to describe the blast loads acting on the structure. The pressure-time variation of the blast load is computed as the shock front sweeps across the structure. The unbalanced load in the horizontal direction is computed as a function of the blast loads acting on the front and back walls (windward and leeward walls), respectively. The average blast load action of the roof of the structure is computed as the shock front traverses the building. The procedure used to describe these loading conditions have been presented in previous sections of this chapter.

The second step in the problem is the determination of the resistance of the building to horizontal motion. The tendency of the base of the structure to slide is resisted by friction forces on the foundation and earth pressure at the rear (leeward side) of the structure. For structures with shallow foundations, the resistance to sliding is afforded primarily by friction between the horizontal surfaces of the concrete foundation and underlying soil. The earth pressure resistance at the rear of the structure is small and can be conservatively neglected. For structures with deep foundations, the passive pressure at the rear of the structure is significant and greatly reduces the displacement of the building.

The friction force developed between the horizontal surfaces of the concrete foundation and underlying soil is given by

$$F_f = \mu F_N$$

2-91

where

- F_f - frictional force resisting horizontal motion
- μ - coefficient of friction between concrete and type of supporting soil

F_N = vertical load supported by the foundation

The coefficient of friction μ for the horizontal surface between the concrete foundation and the underlying soil is given in Table 2-12 for various types of soil. The coefficient is not a function of time or displacement. However, the structure must slide a finite amount before the frictional force is generated. The structure should slide approximately one-quarter of an inch before the frictional force is taken into account.

The vertical load F_N supported by the foundation consists of the dead weight of the structure, the weight of the building's interior contents, and the blast load acting on the roof of the structure. Since the blast load is a function of time, the building's resistance to sliding (frictional force F_f) is also a function of time. In addition, the blast load acting on the roof greatly increases the foundation loads, and consequently, significantly increases the building's resistance to sliding.

2-23. Structure Motions

2-23.1. Introduction

The net motion of a structure is a combination of the motions due to the air-induced and direct-induced ground shock, and the air shock. Since the methods of analysis described in this section are applicable to rigid concrete structures located at comparatively large distances from an explosion, the structure motions are taken equal to the ground motions in the vicinity of the building. In the case of air shock, the structure motions are computed directly.

The motion of structures located at comparatively close distances to an explosion as well as the motion of nonrigid structures may be determined. However, the local effects associated with these conditions such as motions due to cratering, fragment impact, etc. must be accounted for in the determination of the structure motions.

2-23.2. Net Ground Shock

The net ground shock associated with an accidental explosion is a combination of the air-induced and direct-induced ground shock. The time at which the shock is felt at adjacent structures and the magnitude and duration of the motion are a function of the quantity of explosives detonating, the absolute distance between the detonation and adjacent structure and the soil media at the site.

The air-induced ground shock is a function of the air blast. Consequently, the arrival time and duration of the ground shock may be taken equal to the arrival time t_A and duration of the air blast. For an explosion occurring at or near the ground surface, the arrival time and duration are obtained from Figure 2-15 for the scaled ground distance Z_G between the explosion and the structure. Figure 2-15 provides the blast parameters associated with the detonation of hemispherical TNT charge located on the ground surface.

The direct-induced ground shock is a function of the soil media. The arrival time of the shock load at the structure is a function of the seismic velocity

in the soil and the distance from the explosion. The arrival time is expressed as

$$t_{AG} = 12,000 R_G / C_p \quad 2-92$$

where t_{AG} - arrival time of the ground shock

R_G - ground distance from the explosion

C_p - compression wave seismic velocity in the soil (table 2-11)

As previously explained, the seismic velocity of the soil should be obtained from soil tests for a final design. In lieu of tests, it is recommended that the entire range of velocities given in table 2-11 be investigated to determine if the direct-induced ground shock can be in phase with the air-induced ground shock.

The actual duration of the shock load is not readily available. However, it is sufficient to realize that the duration is long, that is, many times larger than the duration of the air-induced shock.

The net ground shock is obtained from consideration of the arrival time and duration of each type of induced shock. If $t_A + t_o$ is less than t , the structure is subjected to superseismic ground shock (Fig. 2-253). The air induced ground shock arrives at the structure first and is dissipated by the time that the direct-induced ground shock arrives. The structure feels the effect of each shock separately. If t_A is greater than t_{AG} , the structure is subjected to outrunning ground shock (Fig. 2-253). The direct-induced ground shock arrives at the structure first and, since its duration is long, the air-induced ground shock will arrive at the structure while the direct-induced ground shock is still acting. The structure feels the combined effects of the induced shocks. If t_A is slightly less than t_{AG} and $t_A + t_o$ is greater than t_{AG} , the air-induced ground shock will still be acting when the direct-induced ground shock arrives. For design purposes, this latter case should be treated as an outrunning ground shock.

2-23.3. Maximum Structure Motion

The design of protective structures to resist the effect of shock loads is based on the peak values of the induced motion rather than the actual motion-time relationships. In fact, the actual time history of the motion is not known nor can it be approximated with any degree of accuracy. Consequently, the phasing of the various shocks cannot be accomplished accurately. Therefore, for design purposes the peak values of the in-phase motions are added.

For the case of air-induced ground shock and air shock, the maximum values of horizontal displacement, velocity and acceleration are always added. These shock motions must be in phase since they are caused by the same source, namely, the air blast.

In the case of superseismic ground shock where the air-induced and direct-induced ground shock are completely separated, the maximum motion may be due to either source. The maximum value of displacement, velocity, or acceleration is the numerically larger value regardless of its source.

In the case of outrunning ground, the structure motion results from the combined effect of the air-induced and direct-induced ground shock as well as the air shock. The maximum motions in the vertical and horizontal direction is the algebraic sum of the maximum value of displacement, velocity, and acceleration from each source of motion in the vertical and horizontal directions.

2-24. Shock Response Spectra

2-24.1. Introduction

For the purposes of assessing the effects of shock on structures, one of the simplest interpretations of motion data involves the concept of the response spectrum. A response spectrum is a plot of the maximum response of a simple linear oscillator subjected to a given input motion against frequency. Hence, a response spectrum depicts only maximum response values, not a time-dependent history of the motion of the oscillator. The use of these maximum values is sufficient to ensure a reasonable and safe design for shock loads.

2-24.2. Definition of Shock Spectra Grid

Response spectra are constructed from consideration of the response of a simple linear oscillator. For a protective structure subjected to shock loads, a piece of equipment or any interior component can be considered as the mass of a simple oscillator. The load-deflection properties of the structural system which connects the component to the protective structure determine the spring constant of the oscillator.

The maximum displacement of the mass (building component) relative to the base (protective structure) is called the spectrum displacement (D), and the maximum acceleration of the mass is called the spectrum acceleration (A). The maximum velocity of the mass is approximately equal to the more useful quantity called the spectrum pseudo-velocity (V) which is given by

$$V = 2\pi fD \quad 2-93$$

where V = velocity of the mass
 f = natural frequency of vibration of the oscillator
 D = displacement of the mass

For an undamped system, the displacement and acceleration are related by

$$A = \frac{(2\pi f)^2 Dg}{387} \quad 2-94$$

where A = acceleration of the mass in g's
 g = gravitational constant

When damping is present, the above relationship between acceleration and displacement is approximate. However, the relationship may still be used to develop shock spectra.

Plots of the three quantities, displacement D, velocity V, and acceleration A, against frequency f, are then shock spectra. They may be plotted individually or, more conveniently, on a single plot by means of the type of chart shown in

Figure 2-254. Any point on this logarithmic grid represents a simultaneous solution to Equations 2-93 and 2-94. The log-log grid must be proportioned to satisfy the solution of the equations. The grid is constructed from standard log-log paper on which a second log-log grid is superimposed and rotated 45 degrees. The width of a log cycle on this rotated grid is 0.707 times the width of a cycle on the standard grid.

2-24.3. Response Spectra

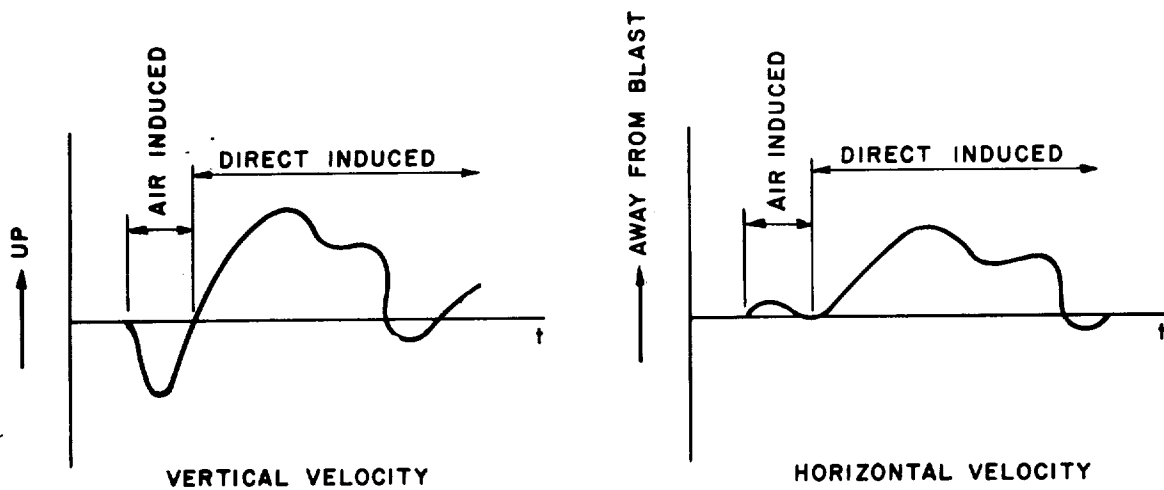
A response spectrum is a plot of the maximum response of a single-degree-of-freedom system to a given input motion. The given input motions are the air shock and the air-induced and direct-induced ground shocks. Since the maximum values of the free-field displacement, velocity, and acceleration (input motion) are used to construct the spectra, a response spectrum envelope is produced. The spectrum takes a trapezoidal shape and is shown in Figure 2-254 by the lines labeled D, V and A. The three sides of this trapezoid can be related to the maximum free-field input motion parameters of displacement, velocity, and acceleration.

Relationships between the spectrum envelope bounds and the characteristics of the time dependent free-field input motions (displacements, velocities, and accelerations) clearly indicate that as the variation of the free-field motion parameters versus time is defined, the definition of the corresponding spectrum envelope can be refined. However, in the general case of blast-induced motions, the variation of the input motions with time cannot visually be described in significant detail. Consequently, it is recommended that for the elastic response of systems, the spectrum be defined by the following three straight lines as illustrated in Figure 2-254.

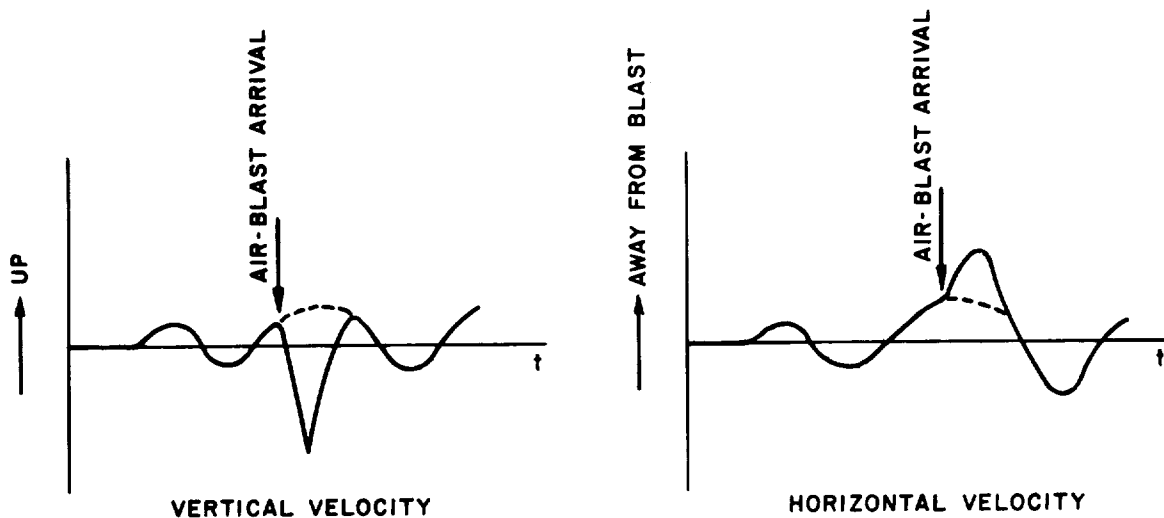
- (1) Line "D" is drawn parallel to lines of constant displacement with a magnitude equal to the maximum free-field (building) displacement.
- (2) Line "V" is drawn parallel to lines of constant velocity (actually pseudo velocity) with a magnitude equal to one and one-half (1.5) times the maximum free-field (building) velocity.
- (3) Line "A" is drawn parallel to lines of constant acceleration with a magnitude equal to two (2) times the maximum free-field (building) acceleration.

A spectrum defined in this manner is clearly an approximation, however, its accuracy is considered to be consistent with the accuracy of the input free-field (building) motions on which it is based. In those cases where the input motions can be defined with greater confidence, the spectrum identified above can be defined to reflect the greater accuracy.

In most cases, interior components of the structure and/or equipment and equipment supports are designed elastically. Therefore, the shock spectra described above will suffice. However, when a very large explosion causes large structure motions, interior systems may require inelastic designs. These conditions will usually not arise for the charge capacities considered in this report. Therefore, methods for calculating inelastic shock spectra have not been presented. It is recommended that the bibliography given at the end of this chapter be consulted for further data on this subject.



(a) SUPERSEISMIC GROUND SHOCK



(b) OUTFRUNNING GROUND SHOCK

Figure 2-253 Net ground motions produced by an explosion at the ground surface

2-337

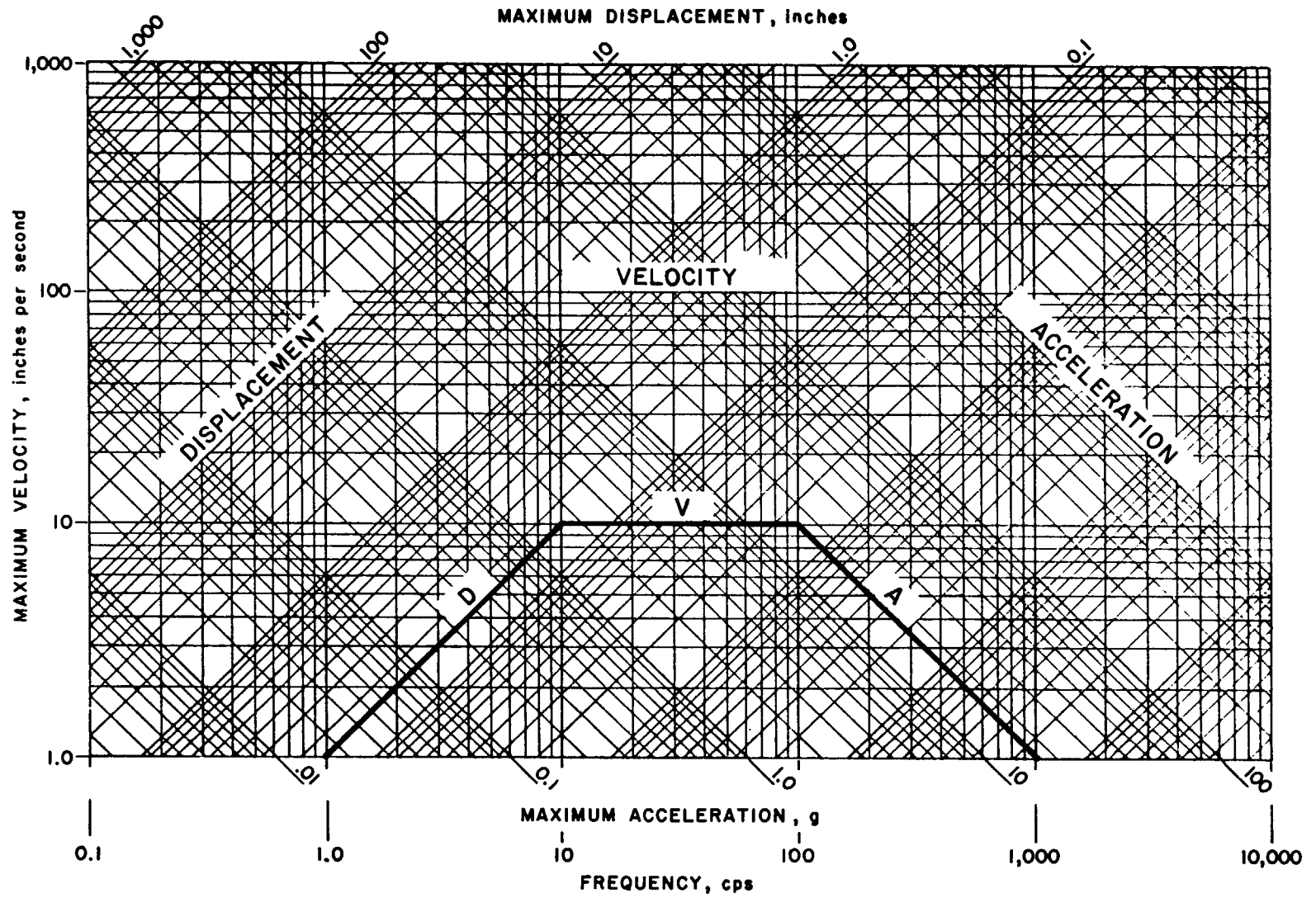


Figure 2-254 Typical response shock spectra

Table 2-10 Mass Density for Typical Soils and Rocks

Material	Mass Density, ρ (lb-sec ²)/in. ⁴
Loose, dry sand	1.42 E-04
Loose, saturated sand	1.79 E-04
Dense, dry sand	1.65 E-04
Dense, saturated sand	2.02 E-04
Dry clay	1.12 E-04
Saturated clay	1.65 E-04
Dry, sandy silt	1.57 E-04
Saturated, sandy silt	1.95 E-04
Basalt	2.56 E-04
Granite	2.47 E-04
Limestone	2.25 E-04
Sandstone	2.10 E-04
Shale	2.17 E-04
Concrete	2.25 E-04

Table 2-11 Typical Seismic Velocities for Soils and Rocks

Material	Seismic Velocity in./sec
Loose and dry soils	7,200 to 39,600
Clay and wet soils	30,000 to 75,600
Coarse and compact soils	36,000 to 102,000
Sandstone and cemented soils	36,000 to 168,000
Shale and marl	72,000 to 210,000
Limestone-chalk	84,000 to 252,000
Metamorphic rocks	120,000 to 252,000
Volcanic rocks	120,000 to 270,000
Sound plutonic rocks	156,000 to 300,000
Jointed granite	9,600 to 180,000
Weathered rocks	24,000 to 120,000

Table 2-12 Coefficient of Friction for Concrete Foundation and Underlying Soils

Soil Material	Coefficient of Friction, μ
Clean sound rock	0.70
Clean gravel, gravel-sand mixture, coarse sand	0.55 to 0.60
Clean fine to medium sand, silty medium to coarse sand, silty or clayey gravel	0.45 to 0.55
Clean fine sand, silty or clayey fine to medium sand	0.35 to 0.45
Fine sandy silt, nonplastic silt	0.30 to 0.35
Very stiff and hard residual or preconsolidated clay	0.40 to 0.50
Medium stiff and stiff clay and silty clay	0.30 to 0.35